
A Comprehensive Approach towards the Phylogeny and Evolution of Cervidae

Nicola Susanne Heckeberg



München 2017

A Comprehensive Approach towards the Phylogeny and Evolution of Cervidae

Dissertation
an der Fakultät für Geowissenschaften
der Ludwig-Maximilians-Universität
München

vorgelegt von Nicola Susanne Heckeberg

aus München
München 2017

München, den 21.03.2017

Erstgutachter: PD Dr. Gertrud E. Rößner

Zweitgutachter: Dr. Robert J. Asher

Tag der mündlichen Prüfung: 12.07.2017

Contents

Acknowledgements	xv
------------------	----

Abstract	xviii
----------	-------

1 Introduction	1
1.1 The Role of Cervidae Today	1
1.2 Artiodactyla and Ruminantia	2
1.2.1 Artiodactyla	2
1.2.2 Ruminantia	2
1.2.3 Systematics within Ruminantia	3
1.3 Cervidae	7
1.3.1 Fossil Record of Cervidae	7
1.3.2 State of the Art in Cervid Systematics	7
1.4 Significance of Cervid Systematics	10
1.5 Objectives	10
1.6 Modus Operandi	11
1.7 Overview of Chapters	14
1.8 List of Abbreviations	16
2 Origination of Antlerogenesis	19
2.1 Introduction	19
2.2 Material and Methods	22
2.2.1 Material	22
2.2.2 Morphological Features	22
2.2.3 Analyses of Antler Characters	22
2.2.4 Introduction of the Term ‘Abscission Area’	22
2.2.5 Taxonomic Issues	23
2.3 Results	23
2.4 Discussion	38
2.4.1 Observations from Investigated Specimens	38
2.4.2 Divergence of Cervidae	41
2.4.3 Ecological Context	43
2.5 Conclusion	44

3	Cervid Systematics based on Morphology	45
3.1	Introduction	45
3.1.1	History of Classification of Cervidae based on Morphology	45
3.1.2	Definition of Morphological Characters	48
3.2	Material and Methods	50
3.2.1	Data Acquisition and Processing	50
3.2.2	Phylogenetic Analyses	52
3.3	Results	59
3.3.1	Morphology	59
3.3.2	Phylogenetic Analyses	72
3.4	Discussion	99
3.4.1	Miocene Cervids	99
3.4.2	Pliocene and Plio-Pleistocene Cervids	110
3.4.3	Pleistocene Cervids	120
3.4.4	Extant Cervids	128
3.4.5	Skull Character Evolution	132
3.4.6	Tooth Character Evolution	136
3.5	Conclusions	140
4	Systematic Relationships of Five Newly Sequenced Cervid Species	143
4.1	Introduction	143
4.2	Material and Methods	145
4.2.1	Material	145
4.2.2	Extraction	145
4.2.3	PCR	147
4.2.4	Alignment	153
4.2.5	Phylogenetic Analyses	154
4.3	Results	157
4.3.1	Extraction, PCR, Sequencing	157
4.3.2	Phylogenetic Analyses	157
4.4	Discussion	160
4.4.1	Phylogenetic Analyses	160
4.4.2	<i>Muntiacus atherodes</i>	161
4.4.3	<i>Rusa marianna</i>	162
4.4.4	Odocoileini	163
4.4.5	<i>Pudu</i>	164
4.4.6	<i>Mazama</i>	164
4.5	Conclusion	167
5	Combined Phylogenetic Analyses and Evolutionary Aspects	169
5.1	Introduction	169
5.2	Material and Methods	170
5.2.1	Molecular Data	170
5.2.2	Combined Molecular and Morphology Analyses	172
5.2.3	Node Calibration Dating	172

5.2.4	Total Evidence Dating	174
5.3	Results	176
5.3.1	Nuclear Genes	176
5.3.2	Mitochondrial Genes	184
5.3.3	Combined Molecular Analyses	188
5.3.4	Combined Molecular and Morphological Analyses	191
5.3.5	Molecular Dating	196
5.4	Discussion	202
5.4.1	General Remarks on Phylogenetic Analyses	202
5.4.2	Systematics of Ruminant Families	208
5.4.3	Extant Cervidae	210
5.4.4	Fossil Cervidae	237
5.4.5	Aspects of Origin, Dispersal and Evolution of Cervidae	241
5.5	Conclusion	249
6	Conclusion and Perspectives	251
6.1	Conclusions	251
6.2	Perspectives	258
	Bibliography	297
	A Extant Cervid Species	299
	B Lists of Extant and Fossil Specimens	303
	C Supplementary Information of Chapter 2	325
C.1	A review on antlerogenesis	325
C.1.1	Antler cycle and histological aspects	325
C.1.2	Physiology and extrinsic control of the antler cycle	326
C.1.3	Ethological role of antlers	327
	D Measurements	337
	E Morphological Description of Extant and Fossil Cervids	343
E.1	Morphology Extant Cervidae	343
E.1.1	Capreolinae	343
E.1.2	Cervini	356
E.1.3	Muntiacini	367
E.2	Morphology Fossil Cervidae	373
E.2.1	Miocene	373
E.2.2	Pliocene	378
E.2.3	Pleistocene	383
	F Adam's Consensus Trees of Chapter 3	389
	G Topologies from SFA Chapter 3	397

H Supplementary Information of Chapter 4	409
H.1 Comments about Ancient DNA Sequencing	417
I Molecular Data of Chapter 5	423

List of Figures

1.1	Controversies in Ruminant Systematics	4
1.2	Classification of Ruminantia	6
1.3	Classification of Cervidae	9
1.4	Overview of all Analyses	13
1.5	Colour Code for Topologies	14
2.1	Antlers of Living Cervids 1	28
2.2	Antlers of <i>Heteroprox</i>	29
2.3	Antlers of <i>Procervulus</i>	30
2.4	Antlers of <i>Dicrocerus</i>	31
2.5	Antlers of <i>Lagomeryx</i> and <i>Paradicrocerus</i>	32
2.6	Antlers of <i>Euprox</i>	33
2.7	Microscopy Images of the area abscissa	34
2.8	Antlers of <i>Ligeromeryx</i> and <i>Palaeoplatyceros</i>	35
2.9	Antlers of Living Cervids 2	36
2.10	Topology of Antler Evolution	37
3.1	Typical Cervid Characters	47
3.2	Age Ranges of Fossil Cervids	51
3.3	Data Completeness	60
3.4	Q	61
3.5	Overview of Upper Dentition	64
3.6	Schematic Overview of Upper Dentition	65
3.7	Overview of Lower Dentition	67
3.8	Schematic Overview of Lower Dentition	68
3.9	Overview of Fossil Dentition	70
3.10	Schematic Overview of Fossil Dentition	71
3.11	Dental Unordered Topology	74
3.12	Dental Ordered Topology	75
3.13	Dental Ordered Extant Topology	76
3.14	Dental Ordered Fossil Topology	77
3.15	BI Dental Topology	79
3.16	ML Dental Topology	80
3.17	Cranial Ordered Extant Topology	82
3.18	BI Cranial Topology	83

3.19	ML Cranial Topology	84
3.20	Combined Unordered Topology	86
3.21	Combined Ordered Topology	87
3.22	Combined Ordered Fossil Topology	88
3.23	Combined Ordered Extant Topology	89
3.24	BI Combined Topology	91
3.25	ML Combined Topology	92
3.26	SFA Summary Topology	97
3.27	EPA Topology	98
4.1	Cervid Classification Chart	144
4.2	Distribution Map of Sampled Species	146
4.3	Overview of Topologies	156
4.4	Topology of Bayesian Analysis	159
5.1	<i>Csn</i> Topology	176
5.2	<i>Lalba</i> Topology	177
5.3	<i>Prkci</i> Topology	178
5.4	<i>Prnp</i> Topology	179
5.5	<i>Sry</i> Topology	181
5.6	Nuclear Combined Topology	183
5.7	Mitochondrial Genome Topology	185
5.8	Mitochondrial Combined BI Topology	186
5.9	Mitochondrial Combined ML Topology	187
5.10	Molecular Combined BI Topology	189
5.11	Molecular Combined ML Topology	190
5.12	Total Evidence BI Topology	192
5.13	Total Evidence ML Topology	193
5.14	Total Evidence MP Topology	195
5.15	Dating Times Overview	196
5.16	Nuclear Node Dating Topology	198
5.17	Mitochondrial Node Dating Topology	199
5.18	Combined Node Dating Topology	200
5.19	Total Evidence Dating Topology	201
6.1	Summarising Topology	253
6.2	Summarising Topology - Detail A	255
6.3	Summarising Topology - Detail B	256
B.1	Correlation of Stage Names	324
D.1	Mandible Measurements Lateral	340
D.2	Skull Measurements Dorsal	341
D.3	Antler Measurements	342
F.1	Dental Ordered All Adam's	390

F.2	Dental Ordered Extant Adam's	391
F.3	Dental Ordered Fossil Adam's	392
F.4	Cranial Ordered Extant Adam's	393
F.5	Combined Ordered All Adam's	394
F.6	Combined Ordered Fossil Adam's	395
G.1	Single Fossil 1	398
G.2	Single Fossil 2	399
G.3	Single Fossil 3	400
G.4	Single Fossil 4	401
G.5	Single Fossil 5	402
G.6	Single Fossil 6	403
G.7	Single Fossil 7	404
G.8	Single Fossil 8	405
G.9	Single Fossil 9	406
G.10	Single Fossil 10	407
H.1	BI-mtG	410
H.2	BI-1140-unpartitioned	411
H.3	BI-1140-partitioned	412
H.4	ML-1140	413
H.5	BI-747-unpartitioned	414
H.6	BI-747-partitioned	415
H.7	BI-569-unpartitioned	416

List of Tables

1.1	Open Questions and Hypotheses	10
2.1	Antler Character Matrix	23
2.2	Antler Character Descriptions	24
3.1	Apomorphies of Cervidae	46
3.2	Overview of analyses - Chapter 3	55
3.3	Consistency Indices	56
3.4	Stepping Stone Sampling Results	72
4.1	GenBank and ENA accession numbers.	148
4.2	Overview of sampled specimens	152
4.3	PCR recipes	153
4.4	Summary of Analyses	155
5.1	Fossil Calibrations for Node Dating	173
5.2	Fossil Calibrations for Total Evidence Dating	175
5.3	Karyotypic Diversity	248
A.1	Info Extant Cervidae	300
B.1	Extant Specimens	304
B.2	Fossil Specimens	309
C.1	Fossil Cervid Antler Specimens	329
C.2	Extant Cervid Antler Specimens	333
D.1	List of Measurements - Mandible	338
D.2	List of Measurements - Cranium	339
H.1	BLAST Results	418
I.1	Molecular Marker Statistics	424

Acknowledgements

First of all I would like to thank my three supervisors Gertrud Rößner, Gert Wörheide, and Robert Asher, who all provided different ideas and input to the project based on their different backgrounds. Thank you for letting me work on such an interesting and diverse project and supporting me throughout all those years.

I would like to thank Gertrud for her attentive supervision, numerous discussions about cervids and ruminants, and for introducing me to many colleagues, who became valuable contacts. Gertrud always supported my pursuits of research and supervised me closely.

Thanks go to Gert, who gave me very useful advice outside the ‘ruminant box’ and got me back on track, when derailed. Thanks a lot for providing me with a great working space (temporally even including a balcony) and the opportunity to work in the Molecular Palaeobiology Lab.

I would like to thank Robert for inviting me to work in the Museum of Zoology in Cambridge for over a year during my PhD. Meetings with Robert were always inspiring with thought-provoking questions, which made me think about my project from different perspectives. I really enjoyed the vibrant atmosphere in the Museum and am indeed grateful to have been part of it.

I thank the Ludwig-Maximilians-Universität München and the SNSB-Bayerische Staatssammlung für Paläontologie und Geologie, which have been my ‘scientific home’ for years and the University of Cambridge for becoming my second scientific home. I appreciated working at both institutions.

Gratefully, I received funding from the German Academic Exchange Service (DAAD; D/11/42358) and the Elitenetzwerk Bayern. The project was further financially supported by the German Research Foundation (DFG; RO 1197/7-1), three SYNTHESYS grants and several smaller travel grants, mostly from the LMU Faculty of Earth Sciences, which was much appreciated.

For this enormous project I visited many European collections; I thank all the following people of various institutions, without whom my work would not have been possible: Dr. Gilla Simon (Museum Mensch und Natur, Munich) for moving huge glass panels, Michael Hiermeier (ZSM Munich) for unlocking and locking doors, Dr. Frank Zachos & Alexander Bibl (Naturhistorisches Museum Wien), Matthew Lowe (UMZC Cambridge) for managing to squeeze the most awkward deer skulls through the narrow staircase and his encouraging invitations to the Tea Room, Jessica McDonald, Emma Bernard, Roberto Portela Miguez, Louise Tomsett (all BMNH London) for access to the impressive fossil mammal collections and the mammal tower, Richard Sabin for the permission to sample from specimens, including type material, and Tracy Heath for mailing the samples to Munich (also both BMNH),

Joséphine Lesur (MNHN Paris) & Christine Argot (MNHN Paris) for tirelessly getting trolley-loads of specimens out of the collections, Patricia Pérez Dios (MNCN Madrid), Lars van den Hoek Ostende (NCB Naturalis), Reinhard Ziegler (SMNS Stuttgart), Loïc Costeur (NMB Basel) for letting me browse through the neverending collections of fossil cervids and also moving huge glass panels, Frieder Mayer & Nora Lange (ZMB Berlin) for access to the fantastic collections and taking and mailing samples to Munich, Thomas Kaiser (ZMH Hamburg), and Andrew Kitchener (NMS Edinburgh) for the access to very rare deer specimens.

Having spent a considerable time in Munich, there are plenty of people from whom I gratefully received help. First I would like to thank Bettina Reichenbacher, who has given me advice on uncountable occasions, who has been my mentor for a decade, and who never gets tired to encourage me. I thank Dirk Erpenbeck for his patient help with stropy sequences and lab frustrations, I thank Gabriele Büttner and Simone Schätzle for assisting me in the lab. Also, all MolPal Lab members, past and present, whom I had the pleasure to meet, for interesting meetings, contributions and feedback, especially Sergio Vargas, Warren Francis, and Martin Dohrmann, the quietest office mate ever, for patiently answering my questions about various programmes. Further, I thank Manuela Schellenberger and Lydia Geißler for helping me with photographs, picture processing and many other graphic design-related questions. I am very grateful to René Neumaier for solving all the computer and cluster problems, for mental support and discussion-rich conversations over coffee. There are also these special people, who became good friends over the years, Melanie Altner, Ann-Marie Schilling, Imelda Hausmann, Astrid Schuster. All of them supported me either simply by their physical presence or by solving and discussing problems, by providing me with chocolate and/or coffee and taking me as I am with all my ups and downs. Especially the efficiency excursions were a valuable change to the daily PhD routine.

Living and studying in two places means you get to know twice as many people. Therefore, there are a lot of people I would like to thank in Cambridge, too: everyone in the Musum of Zoology for giving me a warm welcome and a fantastic time during my visits, for inspiring conversations in the Tea Room, the odd visit to the pub after all the hard work, for taking me to formals, and for the legendary wine and cheese parties. Tom White and Catherine White, I cannot thank them enough for not only giving me a place to life but also a home during my numerous visits to Cambridge; for all the cosy board game evenings, and the amazing cooking skills I got to enjoy. I also thank Tom's and Catherine's parents for their hospitality when inviting me to their homes. Rick Thompson for many fruitful discussions about topologies and phylogenetic methods, for bringing high spirits and sunshine into the crèche every morning. And, of course, Rachel O'Meara for being equally enthusiastic about board games, for planning a dwarf giraffe breeding programme with me, and investigating the systematic affinities of unicorns, and many more fun times. I thank Trisna Tungadi and Luisa Moretto for plenty of hours with the ponies.

I thank Alan and Anthea Gentry for fruitful discussions about cervids and ruminants and a lovely weekend in the country side, Marcus Clauss for a really fascinating day of dissecting, Jeannine Marquardt for all the coffees shared with Dippy, Ellen Schulz-Kornas for her hospitality and collaboration. Thanks go also to Eva Bärman since she is the one to 'blame' for getting me initially interested in working on deer and combined approaches;

thanks a lot for the motivating conversations about ruminants and particularly sheep, and for helping me getting set up in Cambridge. I thank Manuela Aiglstorfer for motivating discussions about ruminants and a great time in Paris. Also, I am grateful to Faysal Bibi and Olaf Bininda-Emonds for sharing their interesting views on ruminant and general phylogenetics.

And, of course, I should thank the deer for being such wonderful and fascinating creatures.

Finally, I am particularly grateful to my family, namely my Mum, Anne Marie Wolf-Heckeberg, my Dad, Hans-Jürgen Heckeberg, my aunt, Ursula Wolf, and Piepmatz, for all their support and hanging in there with me. And thanks to Nico, my fluffy, four-legged loyal companion. Only with all their help was it possible to follow my passion for research.

Abstract

Cervidae (deer) belong to Ruminantia together with Tragulidae (chevrotains), Antilocapridae (pronghorns), Moschidae (musk deer), Giraffidae (giraffes), and Bovidae (cattle, sheep, antelopes). After bovids, cervids are the second most diverse group of ruminants and large herbivores in general. Cervids are natively distributed in the Americas, Europe and Asia inhabiting a broad variety of habitats. Antlers, deciduous, osseous branched outgrowths of the frontal bone, are synapomorphic for all living member of Cervidae except for the Chinese water deer, *Hydropotes inermis*, in which they have presumably been lost. They are unique cranial appendages, which are shed and rebuilt at intervals. The antlerogenic process is controlled by a complex interaction of fluctuating levels of several hormones, most importantly testosterone.

The oldest antler remains are recorded from the early Miocene. These have often been interpreted as non-deciduous appendages in the past, because of supposed permanent skin coverage and the lack of a burr. Extensive comparative morphological analyses of external features of the antler and of the abscission area showed that antlers of all extant and of eight Miocene cervid genera, including those of most of the earliest cervids *Procervulus*, *Ligeromeryx*, and *Lagomeryx* were deciduous. This insight is particularly important for the systematic classification of early Miocene species as Cervidae, because the absence of antler shedding and rebuilding would exclude them from the total group Cervidae.

Cervid systematics has been puzzling researchers for over 150 years. The initial, gross (sub)classifications based on morphology and comparative anatomy are mostly supported by molecular data. In recent decades, molecular systematics has provided new input, but consensus could only be partially reached. Cervids are traditionally subdivided into two subfamilies, Cervinae, consisting of Muntiacini and Cervini, and Capreolinae, consisting of Alceini, Capreolini, Odocoileini, and Rangiferini. While the systematic relationships within Muntiacini and Cervini are, with very few exceptions, resolved, systematic relationships within Capreolinae are much more controversial. The position of Capreolini and Alceini is uncertain and there are many polyphylies within Odocoileini. The latter is the youngest clade of cervids with a quick diversification rate, which makes resolving the systematic relationships more difficult. Also, the rich fossil record of cervids has never been extensively phylogenetically tested concerning potential systematic relationships of fossil representatives to extant cervid taxa.

The aim of this work was to investigate the systematic relationships of extant and fossil cervids using molecular and morphological characters and make implications about their evolutionary history based on the phylogenetic reconstructions.

To achieve these objectives, molecular data were compiled primarily from public data

bases such as GenBank. Some cervid species still lack molecular data because they are difficult to access in the wild. In order to complement the existing data, partial mitochondrial cytochrome b gene sequences from museum specimens of five previously unrecorded species were extracted. The resulting data set was so far the most extensive concerning the taxon sampling for cervids. All molecular data were combined to a data set including 17709 base pairs across five nuclear markers and the complete mitochondrial genome of 50 extant and one fossil cervid species. Several analyses using different data partitions, taxon sampling, partitioning schemes, and optimality criteria were undertaken. Divergence time estimates were undertaken on the molecular data sets using molecular clock node dating.

Additionally, the most extensive morphological character matrix for such a broad cervid taxon sampling was compiled. In total 168 cranial and dental characters of 41 extant and 29 fossil cervid species were scored. Due to the highly conservative morphological features of cervids, solving systematic relationships was challenging for both extant and fossil species. However, it was possible to determine several characters useful to diagnose cervid subclades. The morphological and molecular data were combined for a total evidence approach and other phylogenetic testing. A tip dating analyses was also undertaken on the total evidence data set.

Molecular topologies were partially in conflict with morphological topologies. Nuclear topologies suggested different systematic relationships for some taxa than the mitochondrial topologies. The combined molecular analyses provided robust topologies. The total evidence analyses were less robust and still contained large areas of unresolved taxa. Alternative approaches to combine both data sets and fossil and extant taxa were more useful. The two different divergence time estimate approaches provided differing but feasible results for each approach. The results showed that most of the Miocene cervids were considered to be more closely related to each other than to any other cervid. They were positioned either between the outgroup and all other cervids or as the sister taxon to Muntiacini. Two Miocene cervids were frequently placed within Muntiacini. Plio- and Pleistocene cervids could often be affiliated to Cervini, Odocoileini or Capreolini. Their morphology is more similar to extant cervids than the morphology of most Miocene cervids.

The phylogenetic analyses of this work provide new insights into the evolutionary history of cervids. New systematic relationships were observed, some uncertainties persist and resolving phylogenetic relationships within certain taxa remain challenging. The analyses on the extensive data sets presented here concretised systematic problems and uncertainties, which can now better be targeted with phylogenetic approaches. Several fossil cervids could be successfully related to living representatives, confirming previously assumed affiliations based on qualitative comparisons and introducing new hypotheses. Cervid systematics remains an interesting and fascinating area of research with exciting new results to be expected in the future.

Chapter 1

Introduction

1.1 The Role of Cervidae Today

Deer are iconic animals and most people have a clear image of how a deer looks like. The most conspicuous characteristic of cervids is the presence of antlers, which are popular trophies. As a source of meat and leather, cervids play an important economical, cultural, and environmental role. In contrast to bovids (cattle, goats, sheep, antelopes), cervids have never been domesticated. Only reindeer can be considered as living in semi-domesticated associations with humans in sub-polar/arctic regions.

Deer have played an important role in human life ever since they started coexisting. In prehistoric times, i.e., throughout the last two million years, cervids were important as a source of meat. Their skin was used for clothing and footwear. Particularly the antlers, made of solid bone, were popular for manufacturing tools, as they were robust and easy to process. Deer are culturally important for medical research, trophies, hunting, myths and legend worship (Gentry, 2000; Prothero & Schoch, 2002; Price et al., 2005b; Hall, 2009). Mythological and religious cult associated with deer can be found in many cultures from western Celtic to eastern Shinto. For instance, in several mythologies the deity of hunting is accompanied by or can transform into a deer, e.g., Diana (Roman), Artemis (Greek), Saraswati (Hinduism). Cervids also play an important environmental role shaping actively the landscape by keeping a tree line, which allows more light to lower tiers of the forest, facilitating growth of smaller plants and understorey.

The over 50 living species of Cervidae (Tab. A.1) represent the second-most diverse group of large herbivorous mammals after Bovidae (Groves, 2007). The smallest cervid (*Pudu mephistophiles*, Northern pudu) is 25–35 cm tall and weighs around 5 kg, whereas the largest cervid (*Alces alces*, moose) stands 200 cm high at the shoulders and weighs up to 450 kg. The social structure of cervids ranges from solitary to gregarious. Cervids are natively distributed in Asia, Europe, North and South America, from the tropics to arctic regions and have an extraordinary diversity in habitat use. They inhabit boreal forests and tundra (*Alces alces*, moose), wetlands, marshy habitats, and seasonally flooded areas (*Blastocerus dichotomus*, marsh deer), thick vegetation and scrubland (*Capreolus capreolus*, roe deer), rocky outcrops and alpine grasslands (*Hippocamelus antisensis*, North Andean deer; *Cervus albirostris*, white-lipped deer), (sub)tropical rainforests (*Mazama* spp., brockets), ecotones, open forests, and prairies (*Odocoileus hemionus*, mule deer),

pampas, savannah, and dry grasslands (*Ozotoceros bezoarticus*, pampas deer), open taiga and high Arctic desert (*Rangifer tarandus*, reindeer), alluvial floodplains (*Axis porcinus*, hog deer), dipterocarp forests (*Rusa alfredi*, Philippine spotted deer), and the temperate woodland-grassland interface (*Cervus elaphus*, red deer). More mountainous species (e.g., *Hippocamelus antisensis*, North Andean deer; *Cervus albirostris*, white-lipped deer) can reach altitudes up to 5000 m (Mattioli, 2011).

The diet of cervids is as diverse as their habitats; they are dietary generalists with browsing, grazing, mixed feeding adaptations. Apart from common plant intake, seeds, bamboo, ferns, grass-roughage, bark, twigs, mosses, and lichens form part of their diet as well as flowers, fruits, berries, and aquatic plants. Given the opportunity, carrion (e.g., lemmings, fish), eggs, birds, fish, crabs, and insects may be included in the diet (Mattioli, 2011).

1.2 Artiodactyla and Ruminantia

1.2.1 Artiodactyla

Cervidae belong to the suborder Ruminantia, which is included in the order Artiodactyla (even-toed ungulates). The most prominent shared feature of artiodactyls is that the weight bearing axis of the limbs runs between the third and fourth digit, so called paraxony, in contrast to uneven-toed ungulates (i.e., horses, rhinos, and tapirs) where the weight-bearing axis runs through the third digit (Gatesy & O’Leary, 2001; Mickoleit, 2004).

Molecular and morphological research over the last decades has shown that not only cattle, deer, antelopes, giraffes and similar more evident even-toed ungulates are included within Artiodactyla, but also hippopotamuses, pigs, camels, whales, and dolphins (O’Leary & Gatesy (2008), Hassanin et al. (2012) and references therein). An exhaustive list of shared derived features for artiodactyls is in Mickoleit (2004).

The oldest known Artiodactyla occurred in the early Eocene around 55 million years ago (mya) in North America, Europe, and Asia with *Diacodexis* (Rose, 1996); their ancestors were presumably Palaeocene condylarths (arctocyonids) (Gentry, 2000).

1.2.2 Ruminantia

The first ruminants appeared in North America and Eurasia in the mid Eocene around 50–45 mya. Most extant ruminants have an innovative and efficient digestive system including a four-chambered stomach. The diet is broken down via fermentation by symbiotic microorganisms in the rumen, the first and largest chamber of the stomach. Then several cycles of regurgitating and re-chewing the cud, i.e., rumination, follow (Gentry et al., 1999). This made the digestion of plant fibres very efficient, because cellulose walls could be cracked.

Further, key innovations of ruminant evolution included newly acquired structures such as cranial appendages, hypsodonty, dolichocephaly (= elongated diastema) and adaptations in the postcranial skeleton to a cursorial life style. All these adaptations resulted in performance of new functions, the ability to enter new niches, and a rapid diversification of the group (Janis & Scott, 1988; DeMiguel et al., 2013).

These mid Eocene ruminants were small (<5 kg), forest-inhabiting animals with an omnivorous diet and included for example *Leptomeryx*, *Archaeomeryx*, and *Hypertragulus* (Gentry, 2000; DeMiguel et al., 2013). Further shared derived hard tissue anatomy characters of ruminants comprise the replacement of the upper incisivi with a horny plate, incisiviform lower canines, upper canines vary from extremely elongated forms to complete reduction, loss of the upper first premolar, reduction and eventual loss of the lower first premolar, a fused naviculocuboid, fusion of the capitatum and the multangulum minus, an elongated facial proportion of the lacrimal often including a lacrimal fossa (Mickoleit, 2004; Janis & Theodor, 2014).

The presumably non-homologous cranial appendages represent one of the key innovations of ruminant evolution. They appear suddenly and simultaneously in several lineages during the early Miocene within a very short time span (19.5–17 mya) in North America and Eurasia. It is assumed that climate change, a drop in the global temperature and a first significant increase in seasonality in lower latitudes (0–50°), triggered the development of these structures (DeMiguel et al., 2013). The first cranial appendages were suggested to be metabolic responses to the increased seasonality (Morales et al., 1993; DeMiguel et al., 2013). The origin of headgear is still not entirely known; a single developmental and evolutionary origin from protuberances in a common ancestor has been suggested by Webb & Taylor (1980) and Gentry (1994). However, there are many hypotheses suggesting an independent origin and evolution of the four different types of ruminant headgear (Janis & Scott, 1988; Gentry, 2000; Prothero & Schoch, 2002; Davis et al., 2011; DeMiguel et al., 2013). To test different hypotheses, it is crucial that ruminant phylogenetic relationships are unambiguously resolved (DeMiguel et al., 2013).

1.2.3 Systematics within Ruminantia

Ruminants underwent several parallel radiations during the Neogene and are therefore a taxonomically problematic group, whose systematic relationships are still difficult to solve (Janis & Scott, 1988; Janis & Theodor, 2014). The poor phylogenetic resolution at the base of Pecora (= ‘horned livestock’) most likely reflects a rapid cladogenesis resulting from these rapid adaptive radiations (Bibi, 2014). Figure 1.1 shows different systematic hypotheses based on different character sets over the last few decades (Price et al., 2005b). There is yet no consensus on the ruminant or artiodactyl phylogeny.

Phylogenetic reconstructions of ruminants changed a lot over the last century. In the 1940s Pecora consisted of Cervioidea including giraffids and cervids and Bovoidea including bovids and antilocaprids. Moschidae was the sister taxon to Pecora and Tragulidae was the sister taxon to all of them (Janis & Theodor, 2014). Four decades later, hypotheses of ruminant phylogeny suggested a sister taxon relationship of Moschidae to Antilocapridae plus Cervidae. These three built up Cervioidea, with Giraffidae and Bovidae as polytomous sister taxa; Tragulidae remained the sister taxon to all of them. While another 30 years later phylogenetic reconstructions based on morphological data still resemble those from the 1980s, most molecular topologies look like the one in Figure 1.2 (Janis & Theodor, 2014).

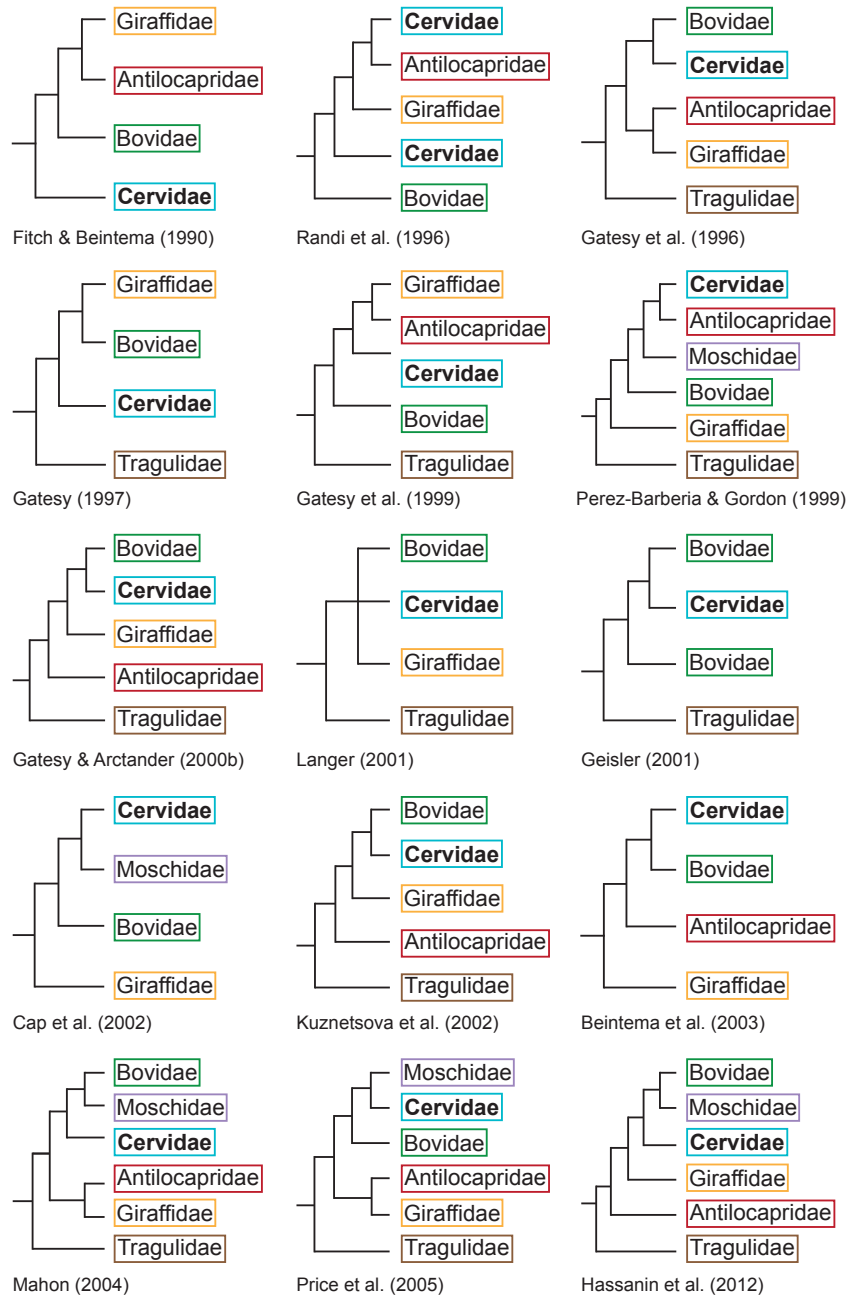


Figure 1.1: This figure shows hypotheses of ruminant phylogeny of the past three decades. It demonstrates that the only consensus about the systematic position of ruminant families reached so far is the position of Tragulidae as the sister taxon to all other ruminant families. Modified after Price et al. (2005b).

Ruminantia comprises six extant families; with the exception of tragulids they are included in the infraorder Pecora, which is generally characterised by the presence of cranial appendages except for Moschidae. Figure 1.2 provides an overview of the six ruminant families.

Members of **Tragulidae** (chevrotains) do not have headgear; instead the upper canines of males are enlarged. Tragulids are minute ruminants with large eyes and a stocky body carried on thin legs. They live in thick vegetation always in close vicinity to water bodies, as they have remarkable diving adaptations, which is part of their predator escape strategy. They natively occur in the tropical forests of Africa, India, and Southeast Asia (Rössner, 2007; Mattioli, 2011). Tragulidae is the sister taxon to Pecora/all other ruminants (Figs 1.1, 1.2).

Moschidae (musk deer) comprises small- to medium-sized ruminants with long ears and strong legs. They do not have headgear; instead, males have elongated upper canines. Moschids inhabit mountainous regions with alpine vegetation (forest, scrub) in palaeartic of Central and East Asia, and Indo-Malayan Regions (Mattioli, 2011). Their systematic position is highly controversial (Figs 1.1, 1.2); recently the taxon is repeatedly placed as the sister taxon to Bovidae (Hassanin & Douzery, 2003; Marcot, 2007; Hassanin et al., 2012), but see Bibi (2014) for a critical assessment of the robustness of this placement.

The monotypic **Antilocapridae** (pronghorns) is endemic to the nearctic regions of North America. Antilocaprids are medium-sized agile ruminants with an elongated trunk on long legs. They are characterised by headgear called pronghorns that consists of a deciduous, bifurcating keratinous sheath on an osseous protuberance originating from the frontal bone. Female antilocaprids develop smaller pronghorns (Davis et al., 2011; Mattioli, 2011). The systematic position of pronghorns is unsolved (Figs 1.1, 1.2).

Bovidae (cattle, goats, sheep, antelopes) comprises small- to large-sized ruminants with diverse body shapes based on their diverse adaptations to different habitats. They are characterised by headgear called horns consisting of a permanent keratinous sheath sitting on an osseous horn core, the os cornu, which fuses to the frontal bone. In some species horns are developed in both sexes. Bovids are natively distributed from the tropics to holarctic regions of North America, Africa, Indo-Malayan regions, and (majorily southern regions of) Eurasia (Davis et al., 2011; Mattioli, 2011). It is not solved yet, whether Bovidae is the sister taxon to Cervidae or Moschidae (Figs 1.1, 1.2).

Giraffidae (giraffes and okapis) comprises large-sized ruminants with elongated necks, long limbs and a sloping back. The headgear of giraffids called ossicones consists of a permanently skin covered bony structure, which fuses to the frontal bone and forms the so called ossicone. They are non-deciduous. Giraffids are patchily distributed in tropic savannahs or rainforests of Africa (Davis et al., 2011; Mattioli, 2011). Their systematic position is controversial (Figs 1.1, 1.2).

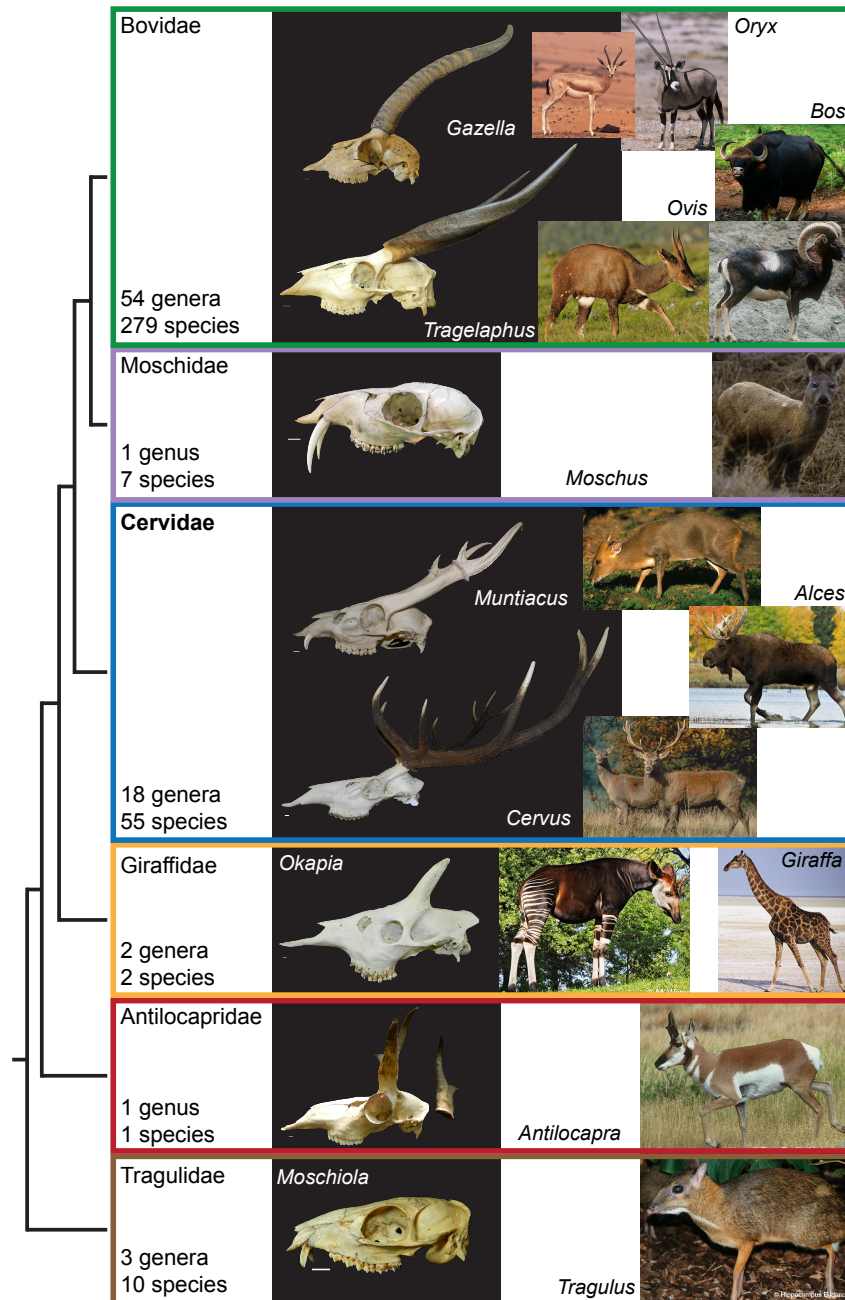


Figure 1.2: This figure provides an overview of all living ruminant families. On the left the number of genera and species is given for each family. Examples of skulls are given in the middle and the pictures of living representatives are given on the right. The topology is modified after Hassanin et al. (2012). (The skull of *Gazella* is taken from the Morphobank Project 352 [https://morphobank.org/index.php/Projects/ProjectOverview/project_id/352] and the copyright is by Eva Bärmann, all other skulls were photographed by me. The pictures of the living animals are taken from www.arkive.org).

Cervidae (deer) comprises small- to large-sized ruminants with long legs. They are characterised by headgear called antlers, osseous outgrowths of the frontal bone, which are shed and rebuilt at regular intervals. Exceptions are the Chinese water deer (*Hydropotes inermis*), which lacks antlers in both sexes, and the reindeer (*Rangifer tarandus*), where females commonly grow antlers as well (Janis & Scott, 1987). Cervids are widely distributed across Eurasia and the Americas; it is unclear whether their North African distribution is native or not (Davis et al., 2011; Mattioli, 2011). Further, it is unclear, whether Cervidae is the sister taxon to Bovidae or Moschidae or Bovidae and Moschidae (Figs 1.1, 1.2).

1.3 Cervidae

1.3.1 Fossil Record of Cervidae

The first fossil cervids are known from the early Miocene of Spain, France, and Germany (Land Mammal Zone MN3, 19.5–17.2 mya; Hilgen et al. (2012)). *Ligeromeryx*, *Procervulus*, and *Acteocemas* are the first representatives (Janis & Scott, 1987; Ginsburg, 1989; Azanza, 1993a; Gentry, 1994; Rössner, 1995; Azanza & Ginsburg, 1997; Rössner, 1997; Gentry et al., 1999; Azanza Asensio, 2000; Ginsburg et al., 2000; Aguilar et al., 2003; Groves, 2007). The relationship of Miocene cervids to extant cervids is controversial (Gentry, 2000).

The rich fossil record of the past 20 million years allows for tracking evolutionary trends and changes over geological time scales. For example, the increase in size and complexity of antlers and the reduction in size and loss of upper canines. These fossils provide the perfect basis for an approach combining morphological and molecular data with fossil and extant cervids towards a phylogenetic reconstruction.

1.3.2 State of the Art in Cervid Systematics

There is an imbalance in extant cervids concerning the data availability and intensity of research on some species. This imbalance is reflected by the data available for assessing the threat status by IUCN (Tab. A.1). Nine species are data deficient, 17 species are least concerned, and 29 species are endangered to some extent. Because of this situation, there are a lot of data available for common and unthreatened species, such as *Cervus elaphus*, *Capreolus capreolus*, *Rangifer tarandus*, and *Odocoileus virginianus* (Hall, 2009). In contrast, only sparse data are available for some of the threatened or data deficient species and access to material and specimens often is limited. This makes it difficult to maintain a balanced taxon sampling.

Solving the systematic relationships of Cervidae has been challenging for the past 150 years. Morphological features were the only available source for a classification for a long time and many of the findings based on comparative anatomy still hold (Chapter 3; Brooke, 1878; Simpson, 1945; Bouvrain et al., 1989). Availability and subsequent use of molecular data greatly improved the understanding of cervid systematics in the past few decades (e.g., Cronin, 1991; Hassanin & Douzery, 2003; Price et al., 2005b; Gilbert et al., 2006; Agnarsson & May-Collado, 2008; Hassanin et al., 2012). However, phylogenetic reconstructions for Cervidae remain ambiguous. There is a broad consensus that Cervidae is monophyletic. A consistent split into two subfamilies, Cervinae and Capreolinae is found since Brooke

(1878) first suggested this classification (referring to ‘Plesiometacarpi’ and ‘Telemetacarpi’, respectively).

Figure 1.3 A shows a topology with current views of systematic relationships of Cervidae (Hassanin et al., 2012). In recent molecular studies the monophyly of Capreolinae is questioned, because Alceini and Capreolini vary in their position, forming sister taxon relationships to Odocoileini and Cervinae or to all cervids. There are two conflicting hypotheses concerning higher hierarchical relationships (Fig. 1.3). In one hypothesis Muntiacini and Cervini are sister taxa, united as Cervinae, and Capreolinae is the sister taxon to Cervinae. The other hypothesis is that Cervini(/-ae) and Capreolinae form a sister taxon relationship and Muntiacini(/-ae) is the sister taxon to both. The majority of topologies reflects the first hypothesis.

Within Odocoileini the genera *Hippocamelus*, *Pudu*, *Odocoileus*, and *Mazama* are polyphyletic and the systematic relationships of the latter are particularly complex. Another long-existing controversy concerns the position of *Hydropotes inermis*. The absence of antlers in this species was long regarded as a primitive condition and therefore it was often placed as the sister taxon to all other cervids (Harrington, 1985; Groves & Grubb, 1987; Janis & Scott, 1987; Hernández Fernández & Vrba, 2005). More recent molecular studies, where *Hydropotes inermis* is consistently positioned as the sister taxon to *Capreolus*, support the hypothesis that the absence of antlers is a secondary loss (Kraus & Miyamoto, 1991; Douzery & Randi, 1997; Randi et al., 1998; Hassanin & Douzery, 2003; Pitra et al., 2004; Hughes et al., 2006; Gilbert et al., 2006; Marcot, 2007; Agnarsson & May-Collado, 2008; Hassanin et al., 2012). For more details of open questions and problems in cervid systematics see Table 1.1.

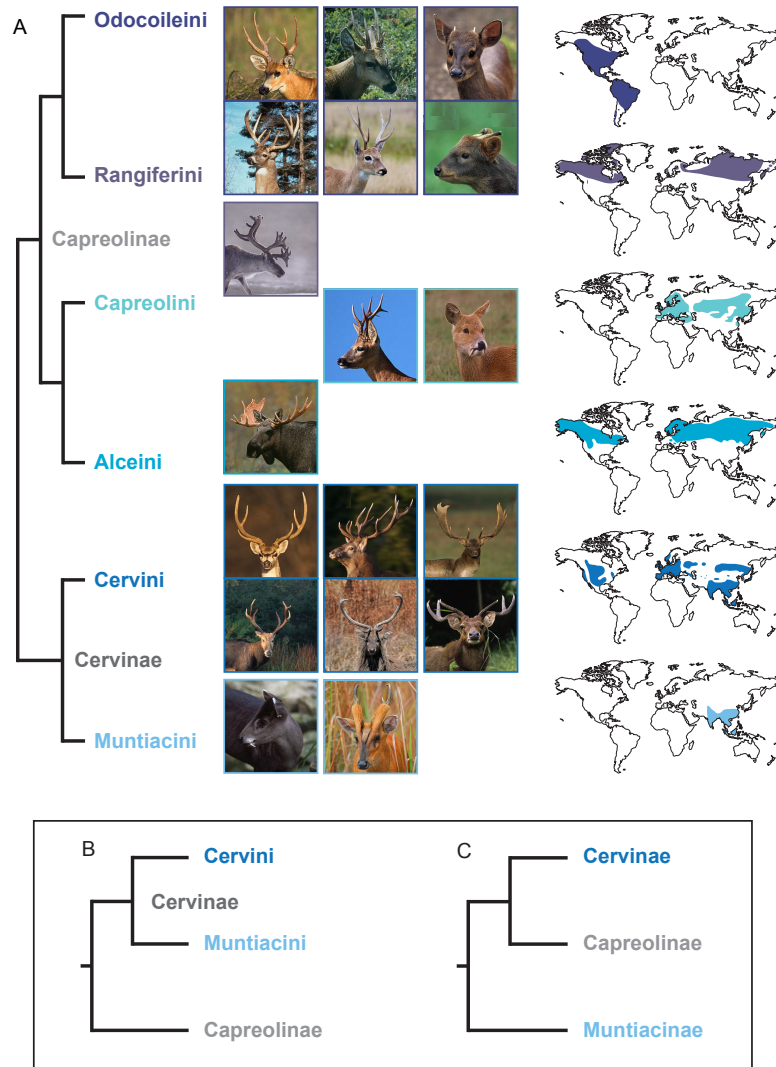


Figure 1.3: Overview of cervid systematics. A) provides an overview of the rough classification of Cervidae modified after Hassanin et al. (2012) indicating higher hierarchical taxa. Each cervid genus is pictured and maps with the distribution of the tribes are shown on the right. From top to bottom and left to right: Odocoileini: *Blastocerus*, *Hippocamelus*, *Mazama*, *Odocoileus*, *Ozotoceros*, and *Pudu*; Rangiferini: *Rangifer*; Capreolini: *Capreolus*, *Hydropotes*; Alceini: *Alces*; Cervini: *Axis*, *Cervus*, *Dama*, *Elaphurus*, *Rucervus*, *Rusa*; Muntiacini: *Elaphodus*, *Muntiacus*. B) and C) show two hypotheses of systematic relationships of Capreolinae and Cervinae including Muntiacini and Cervini. The hypothesis in B) is supported in most recent studies (e.g., Hassanin & Douzery, 2003; Hernández Fernández & Vrba, 2005; Kuznetsova et al., 2005; Price et al., 2005b; Gilbert et al., 2006; Hughes et al., 2006; Hassanin et al., 2012). In C) Muntiacini(/-ae) and Cervini(/-ae) are considered as subfamilies rather than tribes (Marcot, 2007; Azanza et al., 2013). (sources of figures: *Ozotoceros*: www.flickr.com/photos/cdtimm/9263379481/; all others: www.arkive.org).

Table 1.1: Open questions, problems, and hypotheses to be tested, partly collected from the literature (Randi et al., 1998; Meijaard & Groves, 2004).

The position of Muntiacini and Cervini as sister taxa in the clade Cervinae.
There is still molecular data missing for some cervid species.
The relationships within <i>Cervus</i> (and <i>Przewalskium</i>).
The systematic position of <i>Elaphurus davidianus</i> .
The genus <i>Rucervus</i> is potentially polyphyletic.
The relationships of Philippine <i>Rusa</i> and Indonesian and mainland <i>Rusa</i> are uncertain.
Is Capreolinae monophyletic?
Is Alceini the sister taxon of Capreolini?
What is the systematic position of Alceini and Capreolini?
Are <i>Hydropotes</i> and <i>Capreolus</i> sister taxa?
The position of all taxa within Odocoileini is not unambiguously solved.
There are polyphyly in <i>Mazama</i> , <i>Pudu</i> , and <i>Hippocamelus</i> .
How are the systematic relationships between living and extinct cervids?
Are there any direct descendants of fossil cervids among extant cervids?
Is there a distinct stem group of early cervids?
Why are there no cervids in Africa?

1.4 Significance of Cervid Systematics

Apart from the systematic value, the significance of further investigation of cervid (and ruminant) systematics lies within the cultural and economic importance of these animals for humans and is therefore of general interest (Price et al., 2005b). Correct systematics of Cervidae have another critical aspect in conservation, because only an accurate taxonomy allows for delimiting, identifying, and protecting endangered species. New insights into cervid systematics will shed light on the evolutionary history of the taxon and the relationships between fossil and living cervids.

1.5 Objectives

Many of the existing discrepancies between palaeontological and neontological approaches stem from differences in character choice and scoring of both disciplines (Bibi, 2014). A shortcoming of separate morphological and molecular analyses is that living and extinct taxa are rarely combined in the dataset.

My thesis aims at bridging the gap between palaeontological and neontological approaches towards a total cervid phylogeny. This will eventually contribute towards an all-encompassing ruminant phylogeny. The objective was to combine morphological and molecular information of fossil and extant cervids in an interdisciplinary and comprehensive phylogenetic approach for the first time and to reconstruct the evolutionary history

of cervids. Incorporating as much information as possible potentially compensates the disadvantages of each type of data and a total evidence approach is the only possibility to link extinct and living species.

1.6 Modus Operandi

A morphological and a molecular data matrix are required for a total evidence approach. The morphological matrix can be either obtained from the literature or characters need to be scored directly from the specimens. The problem with many earlier studies using morphological characters is that the character (state) descriptions are often too cryptically written to reproduce the scoring. Another hindrance of morphological character scoring is that it can be subjective depending on how clearly delimited the thresholds of character states are. A character may be considered ‘small’ by one researcher, but may be considered as ‘medium’ by the next. To avoid this, the character and character state descriptions must be given as unambiguously as possible to allow for objective and reproducible scoring. In my work I used detailed and explicit character (state) descriptions and clear character state delimitations.

The morphological matrix of my dissertation is stored at Morphobank under the project ID 1021 and comprises 168 characters (<http://morphobank.org/permalink/?P1021>). This platform was established for using, sharing, and providing morphological character matrices. Several characters were obtained from Eva Bärmann’s morphobank project 352 on systematics of Antilopini, which were partly modified, some characters were compiled from the literature and some characters were defined by me (for details see <http://morphobank.org/permalink/?P1021>).

The morphological data collection here focused on cranial and dental characters, because they more likely bear evolutionary signal than postcranial material. The extant diversity was broadly sampled with 41 cervid species; the 29 scored fossil cervids represent a substantial proportion of their past diversity concerning the generic coverage. European cervids were more broadly sampled because of their availability and accessibility in European collections than Asian (5), North (1) or South American (1) cervids. Most of the Miocene genera could be scored, which are the key to understanding the early evolutionary history of Cervidae. In total, over 200 extant and over 500 fossil specimens were scored (Tabs B.1, B.2).

Molecular data often yield robustly supported topologies, solving the systematic relationships of extant taxa. However, these molecular phylogenetic reconstructions provide bare topologies only, without any possibility to track character evolution. Secondly, only extant species can be included, because apart from a few exceptions, there are no molecular data available for fossil species. Also, the sampling is far from complete and the number of molecular markers for most cervid species is still limited and the same sequences get repeatedly analysed yielding - not surprisingly - similar results.

In my project, I compiled the most complete molecular data set for cervids to date comprising the mitochondrial genome, including the most commonly sampled cytochrome b, and five nuclear markers for a total of 50 species (not all markers are available for all species).

Additionally, molecular data was complemented by sequencing five cervid species, which had no molecular record previously. This extensive data set was analysed in various subsets, using different optimality criteria, Maximum Parsimony, Maximum Likelihood, and Bayesian Inference and experimenting with different models and other analysis parameters. Further two approaches to estimate divergence times were undertaken, molecular clock node dating and total evidence dating. See Figure 1.4 for an overview of all analyses. The plethora of topologies were investigated for systematic congruences and incongruences. The phylogenetic reconstructions allowed for interpretations of the evolutionary history of cervids. Figure 1.5 shows the colour code that is consistently used in all topologies.

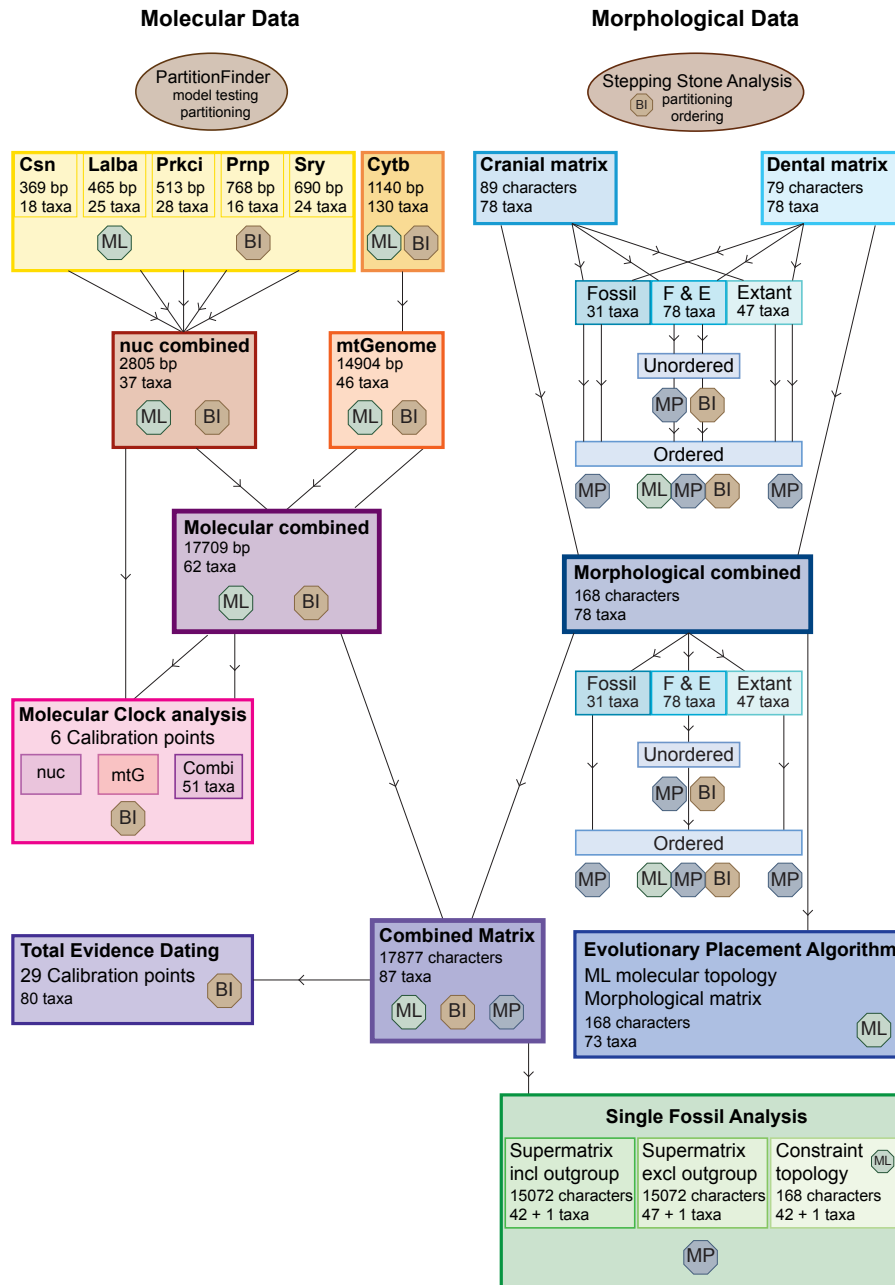


Figure 1.4: This overview shows all analyses undertaken and the optimality criteria under which they were run. The left boxes mainly refer to the molecular analyses, while the right boxes mainly refer to the morphological analyses. The bottom boxes contain different combined approaches of the data set. For abbreviations see 1.8 List of Abbreviations.

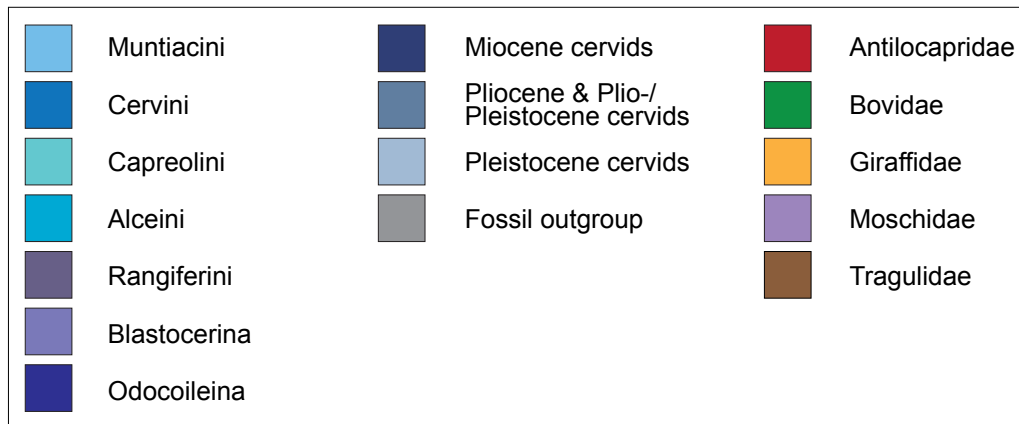


Figure 1.5: This is the colour code indicating the different taxa and is used for all topologies throughout.

1.7 Overview of Chapters

The dissertation consists of six chapters. **Chapter 1** and **Chapter 6** frame my thesis with a thorough Introduction to the topic and a summarising Conclusion.

Chapter 2 – Origination of Antlerogenesis deals with identifying the earliest member of Cervidae, which already possessed deciduous antlers. Because some of the early Miocene cervids, e.g., *Lagomeryx*, *Ligeromeryx*, and *Procervulus*, were long assumed to have permanent antlers, they were not diagnosed as Cervidae *sensu strictu*, but were regarded as cervoids. However, material of certainly shed antler specimens, partly not previously published, provides evidence that these early cervids already were able to shed their antlers. This has critical consequences for cervid systematics and molecular dating approaches.

Citation: Heckeberg NS (2017). Origination of antlerogenesis. *Journal of Morphology*, **278**(2), 182– 202. DOI: 10.1002/jmor.20628. One of the main text figures was used as the cover image.

<http://onlinelibrary.wiley.com/doi/10.1002/jmor.20628/full>

Chapter 3 – Cervid Systematics based on Morphology provides an overview of the most important morphological features of extant and fossil cervids. It also presents the results of extensive morphological analyses, experimenting with character and taxa subsets, with ordering and different optimality criteria. This chapter mainly aimed at identifying characters carrying phylogenetic signal and placement of fossil cervids in relation to extant cervids. Further analyses using constraint molecular topologies were undertaken.

Chapter 4 – Systematic Relationships of Five Newly Sequenced Cervid Species shows the results of sequencing thirteen museum specimen samples of five cervid species, including three holotypes, which were without any molecular record previous to our study. Analysing the most comprehensive data set for cervids in terms of taxon sampling using the mitochondrial marker cytochrome b, answered many systematic questions, but also pointed to new issues, particularly within South American cervids.

Citation: Heckeberg NS, Erpenbeck D, Wörheide G, Rössner GE (2016). Systematic relationships of five newly sequenced cervid species. *PeerJ*, 4:e2307. DOI: 10.7717/peerj.2307. <https://peerj.com/articles/2307/>

Author Contributions: Nicola S. Heckeberg conceived and designed the experiments, performed the experiments, analysed the data, wrote the paper, prepared figures and/or tables, reviewed drafts of the paper. Dirk Erpenbeck, Gert Wörheide and Gertrud E. Rössner conceived and designed the experiments, contributed reagents, materials, analysis tools, reviewed drafts of the paper.

Data Deposition: DNA sequences: European Nucleotide Archive: LT546647–LT546659. All alignments and analyses information are deposited at Open Data LMU DOI: 10.5282/ubm/data.96.

Chapter 5 – Combined Phylogenetic Analyses and Evolutionary Aspects contains results from molecular analyses based on individual markers and combined data sets, combined morphological and molecular approaches, and divergence time estimates. Topologies of Chapter 3 and Chapter 5 were compared to investigate the systematic relationships of fossil cervids in relation to extant cervids. Two approaches to estimate divergence times, molecular node dating and total evidence dating, were undertaken.

The raw data and supplementary information of Chapter 2 and 4 are accessible via the link to the publications, the raw data and supplementary information for Chapter 3 and 5 is available via the LMU library server for electronic dissertations (<https://edoc.ub.uni-muenchen.de/view/autoren/index.H.html>).

1.8 List of Abbreviations

Collections

MNCN	Museo Nacional de Ciencias Naturales Madrid, Spain
MNHN	National d'Histoire Naturelle Paris, France
MNN	Museum Mensch und Natur, Munich, Germany
NHM/BMNH	Natural History Museum London, UK
NHMW	Naturhistorisches Museum Wien, Austria
NMB	Naturhistorisches Museum Basel, Switzerland
NMS	National Museum Scotland Edinburgh, UK
RGM	Naturalis Leiden, The Netherlands
SMNS	Staatliches Museum für Naturkunde Stuttgart, Germany
SNSB-BSPG	Bayerische Staatssammlung für Paläontologie und Geologie, Munich, Germany
UMZC	University Museum of Zoology Cambridge, UK
ZMB	Museum für Naturkunde Berlin, Germany
ZMH	Zoologisches Museum Hamburg, Germany
ZSM	Zoologische Staatssammlung München, Germany

Molecular Data

<i>Lalba</i>	α -lactalbumin
<i>Prkci</i>	protein kinase C iota
<i>Sry</i>	sex determining region on the Y-chromosome
<i>Csn</i>	κ -casein
<i>Prnp</i>	prion protein
<i>Cytb</i>	Cytochrome b
mtG	mitochondrial genome
mt	mitochondrial
nuc	nuclear

Analyses

BI	Bayesian Inference
ML	Maximum Likelihood
MP	Maximum Parsimony
ND	Node Dating
TE	Total Evidence
TED	Total Evidence Dating
PP	Posterior Probability
BS	Bootstrap
HKY	Hasegawa-Kishino-Yano model
GTR	General Time Reversible model
F	Fossil
E	Extant

Dentition

i	Lower incisors
c	Lower canines
p	Lower premolars
m	Lower molars
C	Upper canines
P	Upper premolars
M	Upper molars

Chapter 2

Origination of Antlerogenesis

2.1 Introduction

Antlers are the only mammalian appendages that can undergo complete regeneration (Goss, 1983, 1990; Goss et al., 1992; Price et al., 2005b; Davis et al., 2011) and are the shared derived feature of cervids (e.g., Geist, 1998) and references therein. Horns of Bovidae and ossicones of Giraffidae are epiphyseal cranial appendages, in which an osseous horn core develops individually and later fuses with the frontal bone. Bovid horns are characterised by a keratinous sheath, while giraffid ossicones are skin-covered (Davis et al., 2011). In contrast, cervid antlers and pronghorns of Antilocapridae are apophyseal appendages. In these groups, a part of the frontal bone protrudes to form the pedicle, from which the deciduous antler beam originates in cervids; in antilocaprids, the frontal protrusion is covered by a deciduous, keratinous sheath (Goss, 1983; Davis et al., 2011).

Cervid antlers are osseous, branched outgrowths of the frontal bone, which are shed and regenerated at intervals throughout the lifetime of an individual (Janis & Scott, 1987; Bubenik, 1990; Geist, 1998). This process of antlerogenesis is controlled intrinsically by fluctuating hormone levels, which in turn are dependent on extrinsic photoperiodicity, resulting in an annual antler cycle with distinct seasonality at higher latitudes (Goss, 1983). Antlers are usually restricted to male individuals (except in the case of reindeer, *Rangifer tarandus*; (e.g., Geist, 1998) and play a crucial role in socio-reproductive behaviour (e.g., Brown, 1980; Clutton-Brock, 1989; Caro et al., 2003). The size and/or morphological complexity of antlers are species specific, increasing with successive generations of the appendages until the animal reaches its prime (Geist, 1998); there is no simple linear correlation between body size and relative antler size (Lemaître et al., 2014). Only repeated shedding allows for growing larger and/or more complex antlers with the next set of antlers. Interspecific variety in antler size ranges from barely 1 cm up to 150 cm in length (Mattioli, 2011). The branching pattern varies from single spikes or simple bifurcated or trifurcated to complex multibranched or palmated forms. Furthermore, antlers show a high intraspecific variability (e.g., Goss, 1983; Geist, 1998). The large antlers of genera such as *Alces*, *Cervus*, and *Rangifer* represent the fastest growing hard tissues known, attaining average growth rates of 1.7 cm/day and peak growth rates of up to 10 cm/day (Goss, 1983).

Antler shedding is triggered by the necrosis of antler bone, which is in turn brought on by severance of the blood supply; this process induces the growth of a new set of antlers

(Goss, 1983). With declining testosterone levels, osteoclasts (cells specialised for bone resorption) appear directly below the burr or on top of the pedicles (Goss et al., 1992) and spread centripetally. Small impressions of osteoclasts and cavities can be seen on the surface of the abscission area after resorption (Goss, 1983; Goss et al., 1992). Around these cavities, connective tissue remains as a source for antler bud formation; a scab that forms after blood vessel rupture protects this delicate connective tissue (Goss et al., 1992; Price et al., 2005a). A highly vascularised skin covers the centripetally growing mesodermal tissue, and osteoblasts (cells specialised for bone formation) appear. An antler regeneration bud (blastema) develops instead of a normal scar (Goss, 1983; Goss et al., 1992).

The internal bone of the antler is cancellous, allowing for rich vascularisation, surrounded by more compact bone; the rich vascularisation is important for the high growth rate of the antler tissue (Brown, 1980; Goss, 1983). During growth, antlers are covered in a specialised skin known as velvet, owing to its resemblance to the fabric of the same name (Goss, 1983).

The cycle of antlerogenesis is controlled by several interacting hormones. Testosterone plays the most important role for antler mineralisation; high levels of testosterone prevent shedding, decreasing levels induce shedding, and low levels allow continued antler growth without full mineralisation (Bubenik, 1990). In regions that experience high levels of seasonality, photoperiodicity imposes an additional control over testosterone levels. In such regions, the antler cycle and other life events (such as birth times, rutting season, etc.) are optimally timed and synchronised between individuals and populations (Lason et al., 2001). By contrast, in areas without seasonal changes such as the tropics there is no synchronisation between individuals/populations and the antler cycle sometimes lasts longer than a year. The regular shedding and regeneration of antlers requires immense physiological effort; the evolutionary advantage is predicated on intraspecific display and reproductive success (Goss, 1983; Geist, 1998). Because antlers are relatively ineffective as weapons, it is likely that they evolved primarily for display purposes rather than combat (Brown, 1980; Goss, 1983; Gilbert et al., 2006). Their role in establishing a social ranking of individuals may be more important than their role in sexual behaviour or intraspecific fighting (Brown, 1980). There is little to support a correlation of antler morphology and environmental factors; it is more likely that antler morphology is mainly driven by female preference (Caro et al., 2003). A detailed review of antlerogenesis is in Appendix C.

The evolutionary history of antlerogenesis is documented in the fossil record, which reveals the successive appearance of features characteristic to modern antlers from the early Miocene onwards. However, the range of branched headgear in the fossil record is diverse, and some fossils lack the complete character suite of modern antlers. This led to controversies about which fossil cranial appendages represent true antlers and which do not (e.g., Pilgrim, 1941; Simpson, 1945; Bubenik, 1990; Azanza, 1993a,b; Gentry, 1994; Azanza & Ginsburg, 1997; McKenna & Bell, 1997; Gilbert et al., 2006; Azanza et al., 2011). The coronet or burr, a circular osseous protuberance around the base of the antler, has been considered to be crucial for antler shedding and critical for the identification of potentially shed antler-like headgear (Hensel, 1859; Stehlin, 1937; Dehm, 1944; Thenius, 1948; Bubenik, 1990; Azanza, 1993a,b; Gentry, 1994; Azanza & Ginsburg, 1997; Azanza et al., 2011). In living cervids, the burr is located close to the area of bone resorption between the perennial pedicle and deciduous antler (Goss, 1983). This led to the assump-

tion that the mechanism of antler shedding and regeneration is only possible when a burr is present; therefore, burrless, antler-like appendages from the early and middle Miocene of Eurasia have often been interpreted as non-deciduous headgear (Stehlin, 1937; Simpson, 1945; Thenius, 1950; Vislobokova et al., 1989; Bubenik, 1990; Azanza, 1993a; Gilbert et al., 2006; Groves, 2007). It is important to note that there is evidence for deciduous antlers in genera that were previously assumed to have had permanent antlers, such as *Lageromeryx* Roger 1904, *Heterocemas* Young 1937, *Ligeromeryx* Azanza & Ginsburg 1997, and *Procervulus* Gaudry 1877 (Ginsburg, 1985; Ginsburg & Azanza, 1991; Rössner, 1995; Azanza & Ginsburg, 1997). However, earlier X-ray and histological studies on fossils of *Ligeromeryx* and *Dicrocerus* Lartet 1837 indicated different modes in the ontogeny of these cranial appendages in comparison with extant genera (Bubenik, 1990; Azanza & Ginsburg, 1997; Azanza et al., 2011). These different modes include shedding of appendages still connected to the blood supply, and centrifugal ossification (from the centre to the periphery). These discrepancies raised the question of when the earliest ‘true’ antler arose (i.e., the first fossil antler that underwent the same antlerogenic processes as observed in extant species). Identifying the first ‘true’ antler, together with all of the features indicative of antlerogenesis, also diagnoses the first member of total group Cervidae.

In extant cervids ornamentation of antlers can be smooth (*Rangifer*, *Dama*), nodose (i.e., covered in numerous, small, rounded protuberances) predominantly at the antler base (*Blastocerus*, *Odocoileus*, *Ozotoceros*), ridged across almost the whole antler (*Mazama*, *Muntiacus*, *Pudu*), or a combination of these (*Cervus*, *Rucervus*, *Rusa*). Palmated elements of antlers sometimes show imprints of blood vessels and innervation (e.g., *Rangifer*, *Dama*). Furthermore, the occurrence of ornamentation can vary in coverage of the antler (whole antler or only parts of it) and in intensity (weak vs. strong).

The appearance of the burr in younger individuals is often more nodose and less continuous, consisting of scattered knobs; in adult individuals (e.g., *Blastocerus*, *Cervus*, *Elaphurus*, *Muntiacus*, *Ozotoceros*, *Rucervus*) the burr forms a continuous, distinct, indented ring around the base of the antler. In some species, the burr is broader and thicker, often irregular and less clearly indented, and more nodose throughout, sometimes with a smooth transition to the nodose ornamentation of the beam. In *Rangifer*, the burr is rather inconspicuous, with an irregular outline consisting of a series of individual knobs. In *Capreolus*, the thick, nodose ornamentation on the burrs can cause the proximal parts of the left and right antler beam to fuse together.

This study seeks to identify features indicative of antlerogenesis in extant species in the fossil record. Fossils representing eight Miocene cervid genera were studied and compared with living species in an extensive comparative morphological study of external phenotypic characters of antlers. The results are discussed in the context of cervid systematics, environmental and behavioural evolution.

These analyses also enabled the following hypotheses to be tested: 1) that the burr represents a by-product of repeated antler shedding and regeneration, 2) that antler shedding is independent of antler ornamentation, 3) that permanently skin-covered antlers have never existed, and 4) that the concavity of the abscission area has changed as antlers have evolved.

2.2 Material and Methods

2.2.1 Material

Antler material representing 138 fossil and 136 extant cervid specimens was studied from 12 European Museum collections. A complete list of the fossil and extant specimens including their origin and collection numbers is given in the Appendix C Tables C.1 and C.2. The studied material included eight widely distributed European early and middle Miocene cervid genera with 13 species (Tab. C.1). For comparison, 16 genera of extant cervids, represented by 43 species, were also studied (Tab. C.2). Some of the fossil and living specimens have never been published before.

2.2.2 Morphological Features

The proximal antler surface (abscission area, see below) of fossil and extant antlers was studied in detail based on comparative morphology; in addition, the external features of the cortical bone, burr or burr-like structures, and the overall morphology were macroscopically investigated and documented by photographs. Some specimens were also scrutinised using a light microscope. Terminology for antler morphology follows Bubenik (1990). Accordingly, the antler itself consists of a shaft (proximal part of the antler, below the first bifurcation), a beam (part of the apophysis with potential to develop branches/bifurcations above the shaft), and tines (branch-offs from beam). A more detailed classification of these features and a distribution of their different states across taxa are provided in Tables 2.1 and 2.2.

2.2.3 Analyses of Antler Characters

The character matrix containing data from 25 taxa and 18 antler characters (Tab. 2.1) was used as the basis for two maximum parsimony analyses using PAUP* v.4.0 beta 4a147 (Swofford, 2002). The first of these included all taxa, while the second included all eight fossil taxa and three extant taxa (*Cervus*, *Muntiacus*, and *Odocoileus*). These analyses were performed using a heuristic search with 1000 random sequence addition replicates. Rearrangements were obtained via tree-bisection and reconnection; polymorphic characters were treated as true polymorphisms. If more than one most parsimonious tree was found, the strict consensus of these trees was calculated. Bootstrap values were calculated using 1000 pseudoreplicates under the same heuristic search criteria as described above (1000 random sequence addition replicates per pseudoreplicate). *Procervulus* was used as the outgroup taxon. It is important to note that because there is a lot of homoplasy in the character set, these analyses represent a reconstruction of antler evolution rather than a systematic phylogeny of Cervidae.

2.2.4 Introduction of the Term ‘Abscission Area’

A crucial anatomical structure in the context of the antler cycle is the proximal surface of the base of the antler, which is shaped by resorption phenomena prior to and during shedding. Bubenik (1990) suggested the term ‘seal’ for this particular structure, but this has not been widely used in subsequent literature and has therefore not become established

Table 2.1: Character matrix of the morphological features of living and fossil cervid species.

Taxon	1	2	3	4	5	6	7	8	9	10	11	12	13	14	15	16	17	18
<i>Alces</i>	1	1	1	1	6	2	4	1	1	1	2	2	1	1	2	1	1	2
<i>Azis</i>	1	1	1	1	3	2	4	1	1	1,2	1,2	1,2	1	1	1	0	1	2
<i>Blastocerus</i>	1	1	1	1	4	2	4	1	1	1	1	1	1	1	2	1	1	1
<i>Capreolus</i>	1	1	1	1	3	2	4	1	1	1	1	1	1	0,1	2	0	1	1
<i>Cervus</i>	1	1	1	1	4	2	4	1	1	1	1	1	1	1	1	1	1	2
<i>Dama</i>	1	1	1	1	6	2	1	2	1	1	1	1	1	1	1	1	1	2
<i>Elaphodus</i>	1	1	?	?	1	2	2	1	1	2	2	2	0	0	—	—	1	0
<i>Elaphurus</i>	1	1	1	1	4	2	2	1	1	1	1	1	1	1	1	1	1	3
<i>Hippocamelus</i>	1	1	1	1	2	2	3	1	1	1	1	1	1	1	1	0	1	2
<i>Mazama</i>	1	1	1	1	1	2	2	1	1	2	2	2	0	0	—	—	1	0
<i>Muntiacus</i>	1	1	2	2	2	2	2	2	1	2	2	2	0	0	1	—	1	0
<i>Odocoileus</i>	1	1	1	1	4	2	3	1	1	1	2	1	0,1	1	2	0,1	1	2
<i>Ozotoceros</i>	1	1	1	1	3	2	3	1	1	1	2	1	1	1	2	1	1	1
<i>Pudu</i>	1	1	1	1	1	2	2	1	1	2	1	2	1	0	—	—	1	0
<i>Rangifer</i>	3	1	1	1	6	2	1	2	1	1	1	1	1	1	1	1	1	3
<i>Rucervus</i>	1	1	1	1	4	2	4	1	1	1	1	1	1	0	1	1	1	3
<i>Rusa</i>	1	1	1	1	3	2	4	1	1	1	2	1	1	1	1	0	1	2
<i>Dicrocerus</i> †	1	2	2	2	2	3	2	2	1	0	2	0	0	0	1	0	—	0
<i>Euprox</i> †	1	1	1	1	2	2	2	1	1	2	2	2	0	1	1	—	1	0
<i>Heteroprox</i> †	1	1	2	2	2	1	2	1	1	1	2	0,1	0	1	0	—	0	0
<i>Lagomeryx</i> †	1,2	2	2	2	5	1	1	2	1	0	2	0	?	1	0	—	0	?
<i>Ligeromeryx</i> †	1	2	2	2	5	1	1,2	2	2	0	2	0	0	1	0	—	0	?
<i>Palaeoplatyceros</i> †	1	1	?	?	6	2	2	1	1	0	2	0	1	0	2	—	0	0
<i>Paradicrocetus</i> †	1,2	2	2	2	5	1	2	1	1	?	2	1	?	1	0	—	?	?
<i>Procervulus</i> †	1	1	2	2	2	1	1,2	2	2	0	2	0	0	0	1	—	0	0

as a technical term. Because of the importance of this structure, the introduction of the term ‘area abscissa’ or ‘abscission area’ (derived from the Latin ‘abscindere’ = *lit.* to cut away, more freely: separating) is hereby proposed, in order to facilitate future communication. Abscission, most commonly used as a botanical term describing the mechanism of leaf shedding, can be seen in numerous similar examples of fragmentation, detachment, and shedding in animals (Addicott, 1982). This phenomenon is especially common in invertebrates, particularly within the protostome superclade Ecdysozoa, all of which moult, but also occurs in vertebrates (e.g., tail shedding in reptiles, seasonal fur moulting in some mammals). The term ‘abscission line’ has been occasionally used to refer to the zone of separation between antler and pedicle (Goss et al., 1992).

2.2.5 Taxonomic Issues

Because of unresolved taxonomic discussions, *Heteroprox* is used in this study instead of the proposed senior synonym *Procervulus*; see synonymised use in Van der Made (2003) and discussion in Rössner (2010). In addition, *Paradicrocetus* is used instead of the junior synonym *Stehlinoceros* (excluded from *Stephanocemas* by Azanza & Morales (1989) see also Böhme et al. (2012)).

2.3 Results

Among the fossil specimens, several antler fragments were characterised by a regular, concentric topology and transverse proximal surface (abscission area) observed in the shed antlers of living cervids and linked to bone resorption processes (Fig. 2.1 A–D, F, H, I) Price et al. (2005a). The abscission area of naturally shed antlers is characterised by a regular surface with a granular, rugose, and porous texture with a concentric topology and is surrounded by a definite border (Figs. 2.1, 2.2 A, D, E, 2.3 C, H, J, L, 2.4 C, D, 2.5 B, D,

Table 2.2: Detailed list of antler character and character states and descriptions.

- 1 – Shape of the area abscissa
 - 1) round/oval
 - 2) elongated
 - 3) irregular
- 2 – Diameter of the area abscissa compared to the diameter of the antler shaft
 - 1) approximately equal
 - 2) much smaller
- 3 – Topology of the area abscissa
 - 1) convex
 - 2) concave
- 4 – Transition of the area abscissa to antler base
 - 1) indentation
 - 2) sharp edge
- 5 – Antler morphology
 - 1) single spike
 - 2) bifurcated
 - 3) trifurcated
 - 4) multibranched
 - 5) coronate
 - 6) palmated
- 6 – Burr
 - 1) absent
 - 2) present
 - 3) burr-like thickening
- 7 – Antler ornamentation
 - 1) smooth
 - 2) furrows/ridges
 - 3) nodose
 - 4) combination
- 8 – Distribution of the antler ornamentation
 - 1) more prominent on proximal parts
 - 2) equally prominent
- 9 – External antler to pedicle transition
 - 1) obvious
 - 2) not obvious
- 10 – Antler position/origination in lateral view
 - 0) antler base directly dorsal to orbit
 - 1) antler base posterior to orbit
 - 2) antler base far posterior to orbit

Table 2.2: Continued

- 11 – Pedicle position in frontal view
 - 0) pedicles very close together (entirely over braincase)
 - 1) pedicles at same distance between midline and lateral borders of the skull/orbit (partially over braincase)
 - 2) pedicles far apart (mostly or entirely outside braincase)
- 12 – Inclination of the pedicle to horizontal plane
 - 0) upright, $>60^\circ$
 - 1) inclined, $41-60^\circ$
 - 2) extremely inclined, $<40^\circ$
- 13 – Cross section of the pedicles (\varnothing med-lat/ \varnothing ant-post)
 - 0) mediolaterally compressed (<0.9)
 - 1) round ($0.9-1.1$)
 - 2) anteroposteriorly compressed (>1.1)
- 14 – Pedicles in dorsal view
 - 0) \pm parallel
 - 1) divergent
- 15 – Development of the antler shaft
 - 0) broad antler base base, no shaft
 - 1) small antler base, bifurcation close to burr
 - 2) small antler base, bifurcation far from burr, long shaft
- 16 – Angle between the ‘brow tine’ and the main beam
 - 0) $<90^\circ$
 - 1) $>90^\circ$
- 17 – Origination of the pedicles in lateral view
 - 0) directly above orbita
 - 1) well behind orbita
- 18 – Adult antler length divided by the average pedicle length
 - 0) <5
 - 1) $5-15$
 - 2) $16-30$
 - 3) >30

F, 2.6 A, E, 2.7 A, C, E). The shape of the abscission area reflects the outline of the pedicle cross-section and is predominantly oval or round. Furthermore, it indicates preceding concentric resorption of bone trabeculae. The concentric topology and centripetal (from the periphery toward the centre) expansion of osteoclasts is indicative of antler shedding. Conversely, taphonomically or mechanically fragmented specimens are characterised by an irregular, non-concentric abscission area, with a rough texture and sharp breaking edges; often parts of the pedicle are still attached to the antler. Breakages do not appear in the same plane due to the impact of unidirectional external forces. Unnatural areas of rupture show no clear border or a clear concave/convex indication (Fig. 2.6 C, D).

According to these selection criteria, 37 fossil specimens could be identified as naturally shed. These specimens exhibit an abscission area, which occurs in a transverse plane between the antler and the pedicle. The main difference between shed antler fragments of early fossil and modern cervids is the burr, which is present in all living species and in Pliocene and Pleistocene cervids. In burr-bearing antlers, the burr is positioned surrounding the most proximal part of the antler, directly dorsal and external to the abscission area (e.g., Figs. 2.1 A, 2.6 B, D, F, 2.8 A).

The abscission area is convex in most extant species (Fig. 2.1 A–D; contrast to the concave abscission area evident in early fossil cervids in Figs. 2.2 A, D, E, 2.3 D, 2.4 A, 2.5 D, F, 2.7 A). The concave abscission area of *Muntiacus* is an exception among living cervids (Fig. 2.1E–I). Compared to the diameter of the whole base of the antler (proximal view) the diameter of the abscission area appears relatively small in some of the Miocene cervids (e.g., *Paradicrocerus*, *Dicrocerus*; qualitative observations; Figs. 2.4 C, D, 2.5 F). *Lagomeryx*, *Ligeromeryx*, *Dicrocerus*, and *Paradicrocerus* have a unique antler morphology, lacking a shaft and with bifurcation/ branching starting directly from the base (Figs. 2.4 A–D, 2.5, 2.7). The abscission area appears to be as large as the antler diameter (excluding the burr) in antlers with a developed shaft, as is the case in extant cervids, but always reflects the approximate diameter of the pedicle (e.g., Figs. 2.1 A, 2.2 B, 2.9). Above the abscission area, the antler either smoothly initiates directly from bases of varying size, sometimes with burr-like thickening (e.g., *Dicrocerus*; Fig. 2.4 A–D) or, as in more modern cervids, a burr forms from which the antler shaft initiates (Figs. 2.1 A, 2.8 A).

Investigations of the abscission area using a digital light microscope support the similarities found in shed fossil (Fig. 2.7 A–D) and extant antlers (Fig. 2.7 E–G). In Figure 2.7 A, D, the concentric and concave nature of the abscission area can be seen; Figure 2.7 D in particular shows the difference between the more compact external cortical bone and the more cancellous internal bone. In all parts of Figure 2.7, tiny round depressions are visible; the trabeculae connecting and surrounding these tiny holes are rounded and show no sharp edges indicating resorption (see Fig. 2.7 B, E, G, in which these rounded trabeculae can be seen clearly). In Figure 2.7 E, the sharp transition between the burr and the area abscissa, typical for extant cervids, is shown.

The character matrix and the list of characters provide an overview of all morphological structures (Tabs 2.1, 2.2). The overall branching pattern of antlers is species specific (e.g., Geist, 1998). The antlers of most Miocene cervids studied here, except for *Euprox furcatus*, *Heteroprox larteti*, and *Palaeoplatyceros hispanicus*, are characterised by the lack of a shaft; the antler usually bifurcates directly above the abscission area or forms a small, multibranched crown (Figs. 2.3–2.8 C–E). *Euprox*, *Heteroprox*, and *Palaeoplatyceros* are

the earliest known fossil cervids that show a very short shaft before the first bifurcation (Figs. 2.2 B, C, F, 2.6, 2.8 A–B).

The topology resulting from the analysis of the antler character matrix shows a clear distinction of burr-bearing antlers and antlers without a burr (Fig. 2.10). This does not represent current systematic relationships of cervids, but shows the phenotypic classification of cervids based on antler morphology only. However, it demonstrates the important steps in antler evolution. The schematic figures of the antlers of each genus show the broad diversity of shapes in extant and fossil cervids (Fig. 2.10). *Procervulus* is the sister taxon to all other cervids. The four cervids with broad antler bases are in a clade; within that clade *Dicrocerus* with bifurcated antlers is the sister taxon to the three genera with a coronate antler morphology, *Lagomeryx*, *Ligeromeryx*, and *Paradicrocerus*. *Heteroprox* is the sister taxon to those taxa with a broad antler base and the clade with these five fossil taxa is the sister taxon to all burr-bearing cervids (Fig. 2.10). The extinct *Euprox* and *Palaeoplatyceros* with burr-bearing antlers are in a clade with all living cervids, which means that they are stem-representatives of crown Cervidae. Extant taxa with a simple antler morphology, *Muntiacus*, *Elaphodus*, *Pudu*, *Mazama*, and *Euprox* and *Palaeoplatyceros* are in a polytomy with the clade uniting all extant genera with multi-tined, more complex antlers. All extant taxa within this clade are in a polytomy except for *Dama* and *Rangifer*, which form a clade of cervids characterised by ramified palmated antlers, in contrast to the palmated antlers of *Alces*, which have no or only very little ramification.

Because the number of taxa is higher than the number of characters, the topology including all taxa lacks resolution; however, the analysis including the eight fossil and three extant taxa did not lead to a better resolution within fossil genera. Results from this comparative analysis allowed for differentiation of represented structures (Tabs 2.1, 2.2); with this differentiated classification, it was possible to assess the grade of similarity of morphological features of antlers with and without a burr. Fundamental physiological phenomena associated with antlerogenesis could be inferred for fossil antlers and are discussed in the following section.

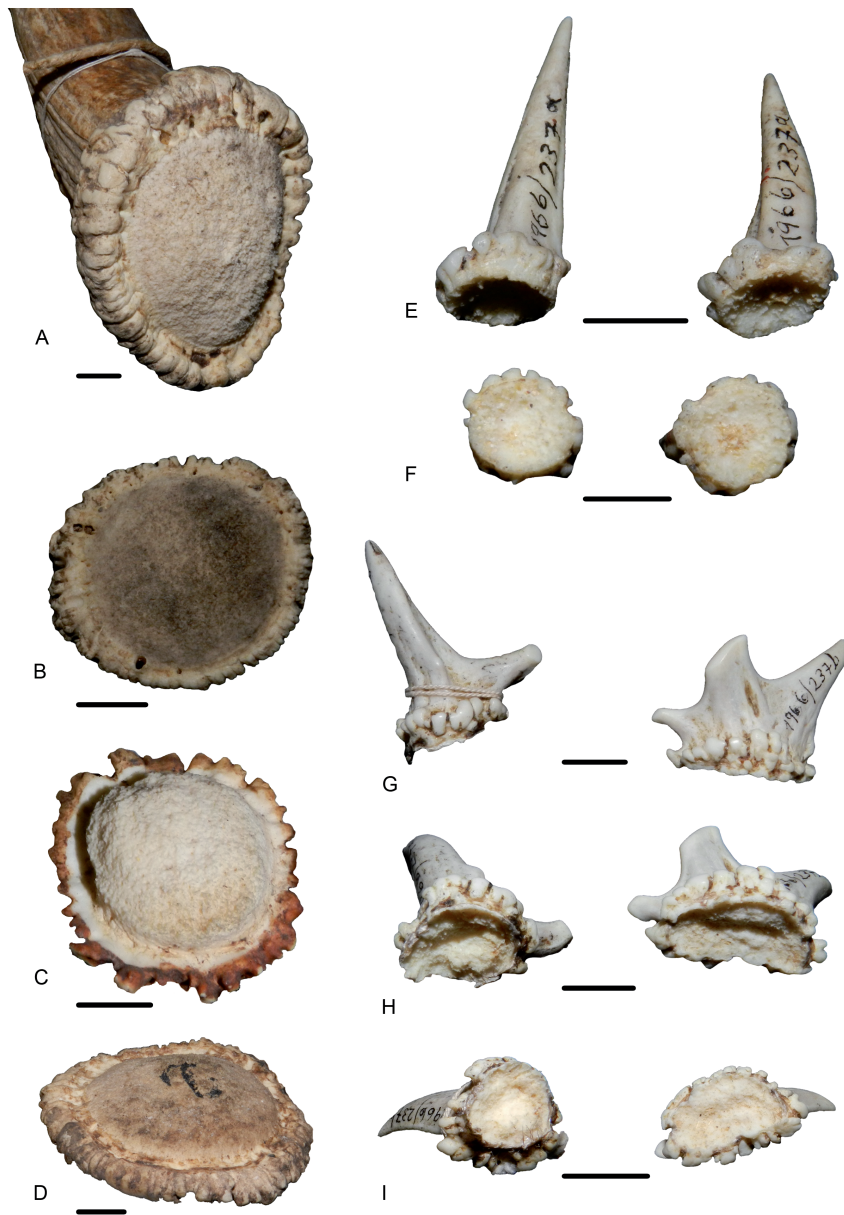


Figure 2.1: Examples of shed antlers and abscission areas of living cervids. A) ZSM 1964/222 *Dama dama* abscission area in semiproximal view showing the properties of the abscission area and the distinct border between the abscission area and the burr. B) ZSM 1954/253 *Dama dama* abscission area in proximal view. C) ZSM 1971/555 *Odocoileus virginianus* abscission area in proximal view. D) ZSM 1954/235 *Rucervus duvaucelii* abscission area in semi-proximal view. E) ZSM 1966/237a *Muntiacus muntjak* two shed antlers in lateral view. F) ZSM 1966/237a *Muntiacus muntjak* two shed antlers in proximal view. G) ZSM 1966/237b *Muntiacus muntjak* two shed antlers in lateral view. H) ZSM 1966/237b *Muntiacus muntjak* two shed antlers in semi-proximal view. I) ZSM 1966/237b *Muntiacus muntjak* two shed antlers in proximal view. Scale bars equal 1 cm.



Figure 2.2: Three clearly cast antler fragments of *Heteroprox larteti*, showing the typical features of the abscission surface. A) SNSB-BSPG 1881 IX 654 *Heteroprox larteti* ventral view. B) SNSB-BSPG 1881 IX 654 *Heteroprox larteti* in lateral view. C) SNSB-BSPG 1881 IX 55 *Heteroprox larteti* in lateral view. D) SNSB-BSPG 1881 IX 55 *Heteroprox larteti* in ventral view. E) SNSB-BSPG 1959 II 5258 *Heteroprox larteti* in ventral view. F) SNSB-BSPG 1959 II 5258 *Heteroprox larteti* in lateral view. Scale bars equal 1 cm.

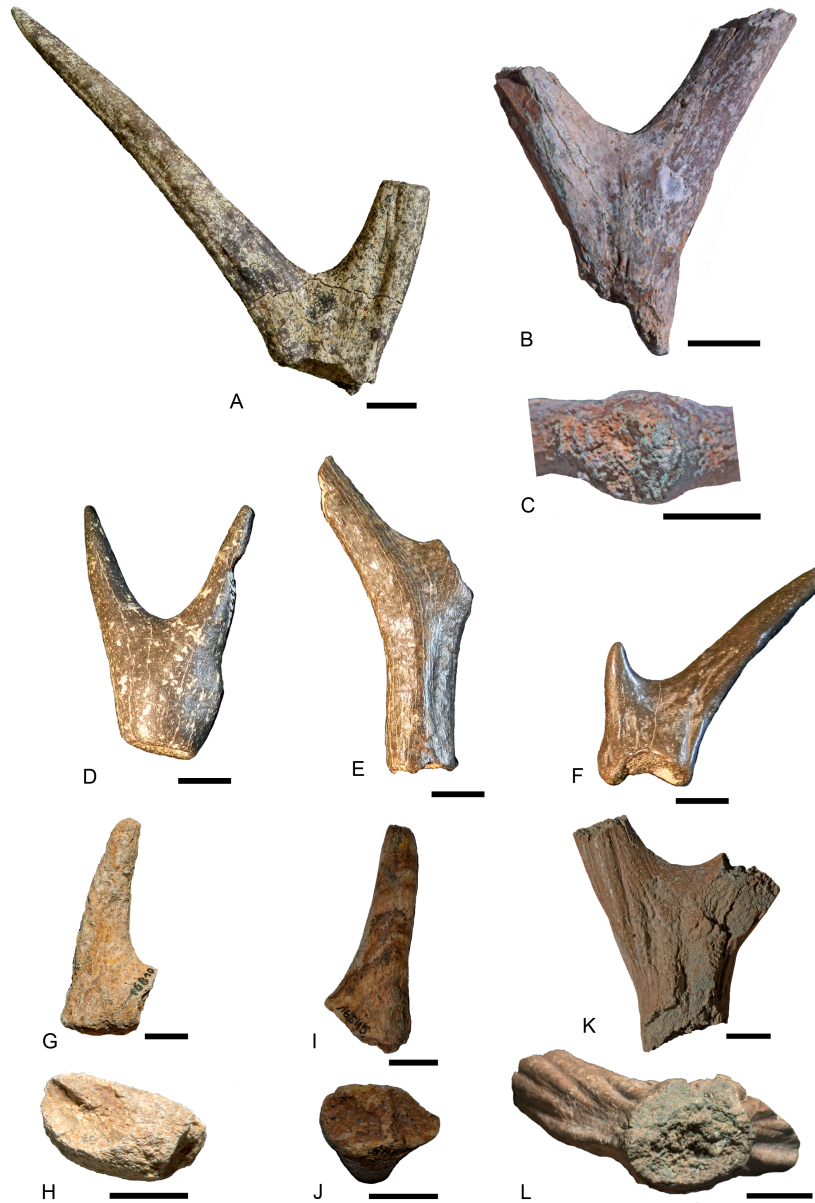


Figure 2.3: Antler specimens of *Procervulus*. A) MNHN Ba 836 *Procervulus dichotomus* in lateral view. B) SNSB-BSPG 1937 II 16804 *Procervulus aureliensis praelucidus* in lateral view. C) SNSB-BSPG 1937 II 16804 *Procervulus aureliensis praelucidus* in ventral view. D) MNHN FS 286 *Procervulus dichotomus* in lateral view. E) MNHN FS 1401 *Procervulus dichotomus* in lateral view. F) MNHN FS 5123 *Procervulus dichotomus* in lateral view. G) SNSB-BSPG 1937 II 16810 *Procervulus aureliensis praelucidus* in lateral view. H) SNSB-BSPG 1937 II 16810 *Procervulus aureliensis praelucidus* in ventral view. I) SNSB-BSPG 1937 II 16845 *Procervulus aureliensis praelucidus* in lateral view. J) SNSB-BSPG 1937 II 16845 *Procervulus aureliensis praelucidus* in ventral view. K) SNSB-BSPG no no. *Procervulus dichotomus* Langenau in lateral view. L) SNSB-BSPG no no. *Procervulus dichotomus* Langenau in ventral view. Scale bars equal 1 cm.

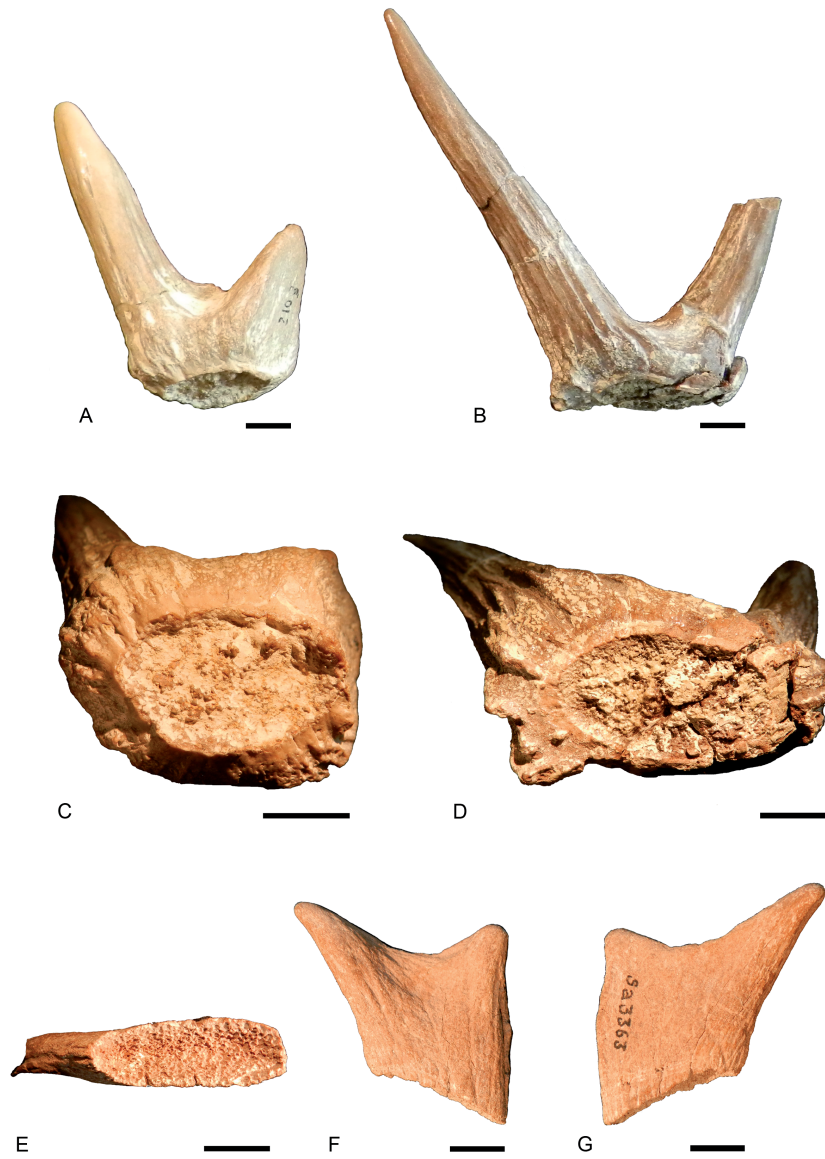


Figure 2.4: Shed antler specimens of *Dicrocerus elegans*. The specimen E)–G) probably represents juvenile antlers. A) MNHN Sa 3327 *Dicrocerus elegans* in lateral view. B) MNHN Sa 10333 *Dicrocerus elegans* in lateral view. C) MNHN Sa 3327 *Dicrocerus elegans* in ventral view. D) MNHN Sa 10333 *Dicrocerus elegans* in ventral view. E) MNHN Sa 3363 *Dicrocerus elegans* in ventral view. F) MNHN Sa 3363 *Dicrocerus elegans* in right lateral view. G) MNHN Sa 3363 *Dicrocerus elegans* in left lateral view. Scale bars equal 1 cm.

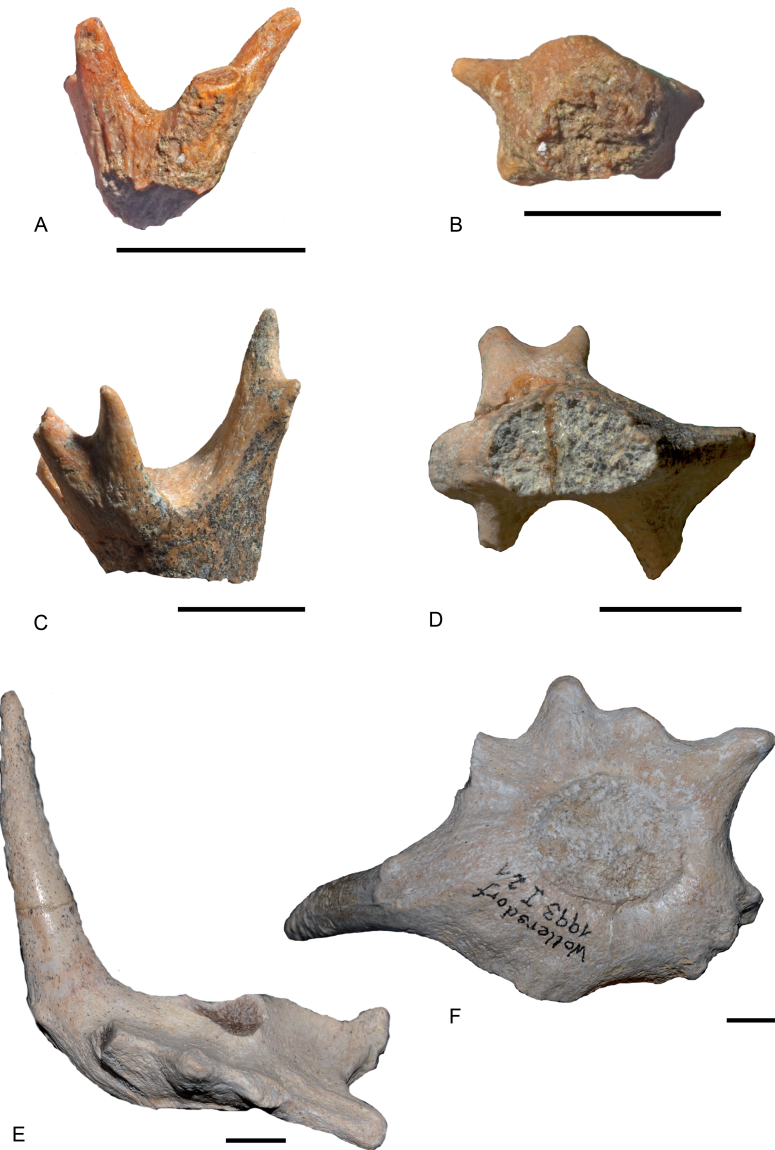


Figure 2.5: Shed antler specimens of *Lagomeryx* and *Paradicrocerus elegantulus*. A) SNSB-BSPG no no. *Lagomeryx* (Upfkofen) in lateral view. B) SNSB-BSPG no no. *Lagomeryx* (Upfkofen) in ventral view. C) SNSB-BSPG no no. *Lagomeryx* (Niederaichbach) in lateral view. D) SNSB-BSPG no no. *Lagomeryx* (Niederaichbach) in ventral view. E) SNSB-BSPG 1993 I 21 *Paradicrocerus elegantulus* in lateral view. F) SNSB-BSPG 1993 I 21 *Paradicrocerus elegantulus* in ventral view. Scale bars equal 1 cm.

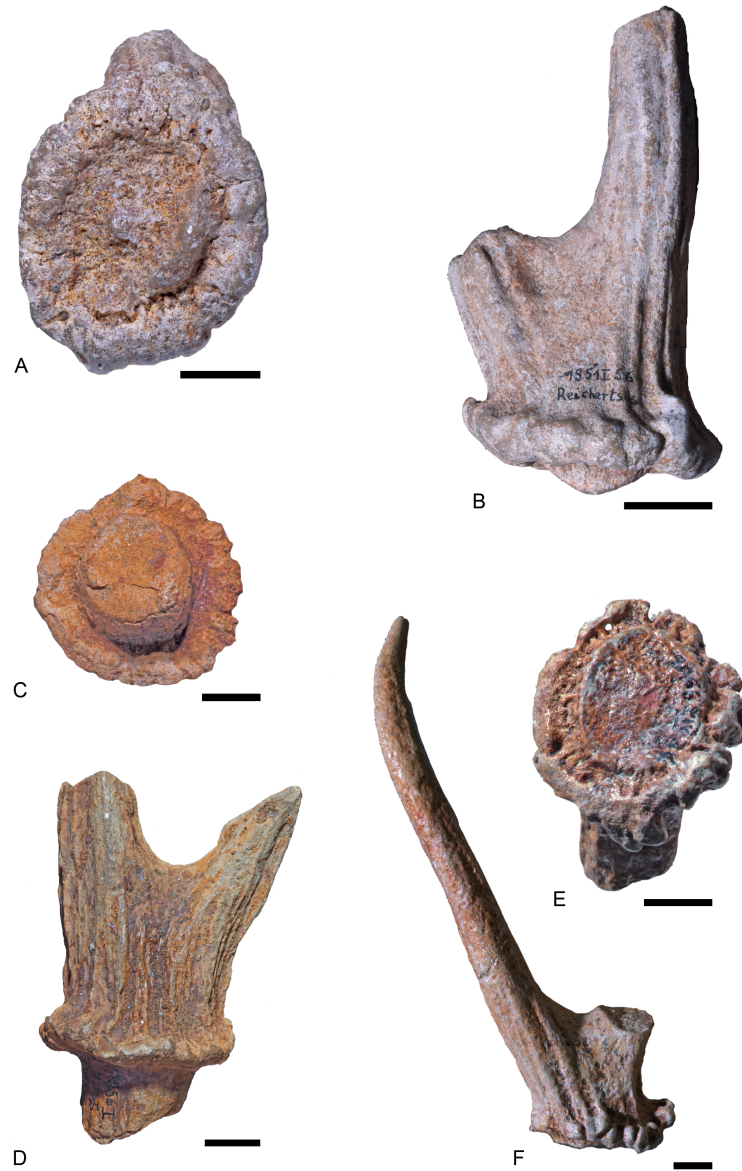


Figure 2.6: Antler specimens of *Euprox furcatus*. A)–B) & E)–F) are cast antler fragments, exhibiting typical features of the abscission surface, whereas C)–D) is an example of a broken specimen. The fracture occurred approximately 1 cm below the burr, involving the pedicle. The area of fracture is rough and uneven. A) SNSB-BSPG 1951 I 56 *Euprox furcatus* in ventral view. B) SNSB-BSPG 1951 I 56 *Euprox furcatus* in lateral view. C) SNSB-BSPG 1956 I 404 *Euprox furcatus* in ventral view. D) SNSB-BSPG 1956 I 404 *Euprox furcatus* lateral in view. E) SNSB-BSPG 1966 XIV 34 *Euprox furcatus* in ventral view. F) SNSB-BSPG 1966 XIV 34 *Euprox furcatus* in lateral view. Scale bars equal 1 cm.

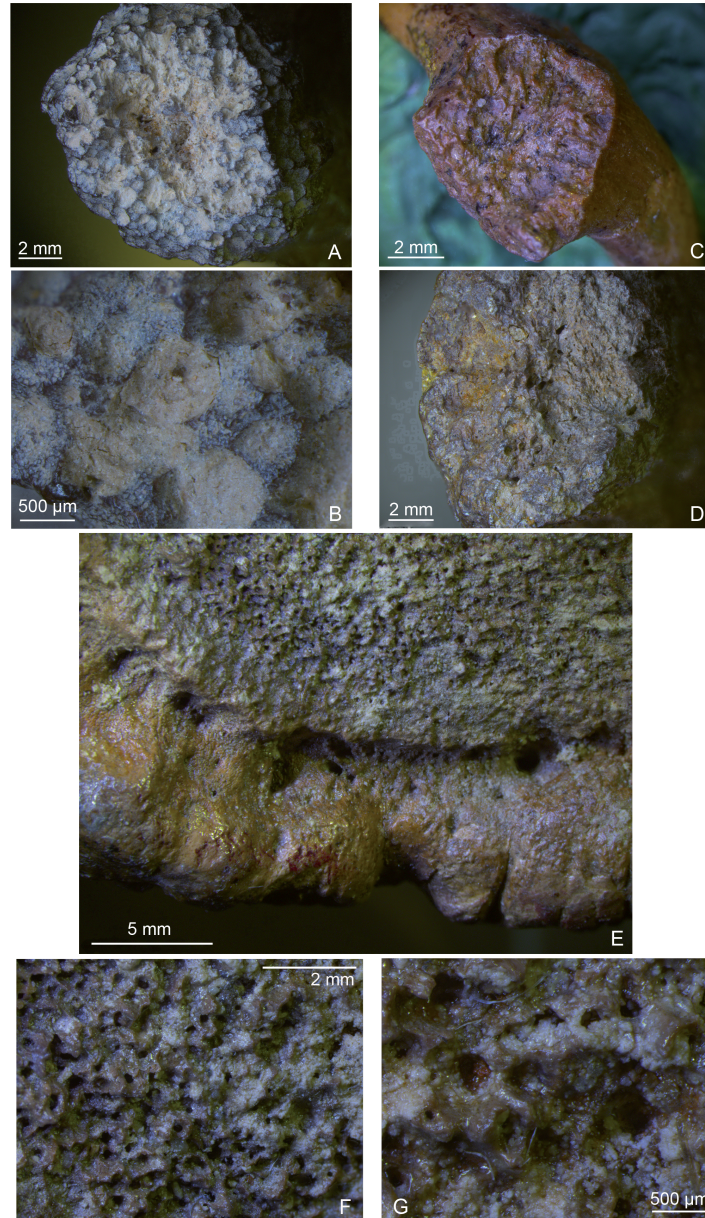


Figure 2.7: Close up light microscopy images of the abscission area of fossil *Heteroprox larteti*, *Lagomeryx parvulus*, and living *Cervus elaphus*. A) SNSB-BSPG 1959 II 5258 *Heteroprox larteti* abscission area. B) SNSB-BSPG 1959 II 5258 *Heteroprox larteti* abscission area close up. C) SNSB-BSPG 1959 II 7803 *Lagomeryx parvulus* abscission area. D) SNSB-BSPG 1959 II 5268 *Heteroprox larteti* abscission area. E) SNSB-BSPG 1955 I 513 *Cervus elaphus*, sub-recent, transition of the abscission area to the burr in ventral view. F) SNSB-BSPG 1955 I 513 *Cervus elaphus*, sub-recent, abscission area. G) SNSB-BSPG 1955 I 513 *Cervus elaphus*, sub-recent.

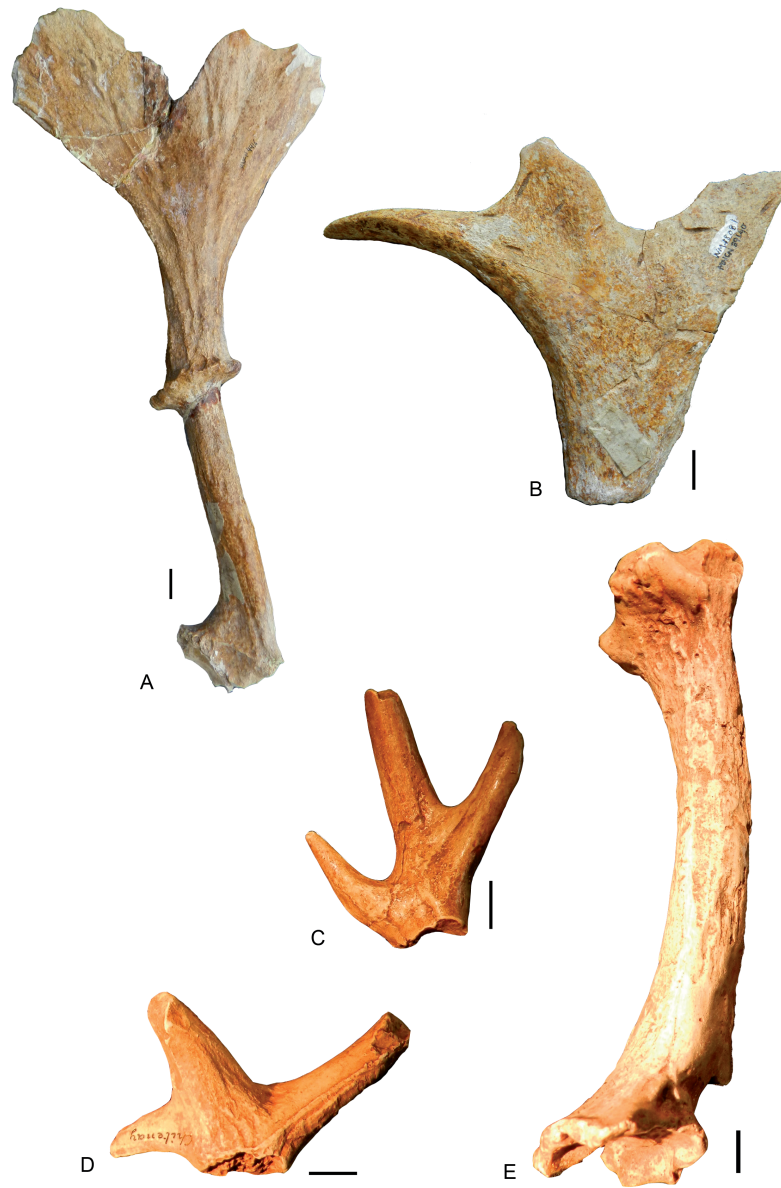


Figure 2.8: Antler fragments of *Ligeromeryx praestans* and *Palaeoplatyceros hispanicus*. A) MNCN 4416 *Palaeoplatyceros hispanicus* in lateral view. B) MNCN 39140 *Palaeoplatyceros hispanicus* shed antler in lateral view. C) MNHN 1938-9 *Ligeromeryx praestans* shed antler in lateral view. D) MNHN 1938-10 *Ligeromeryx praestans* shed antler in lateral view. E) MNHN 1938-8 *Ligeromeryx praestans* pedicle with antler in lateral view. Scale bars equal 1 cm.

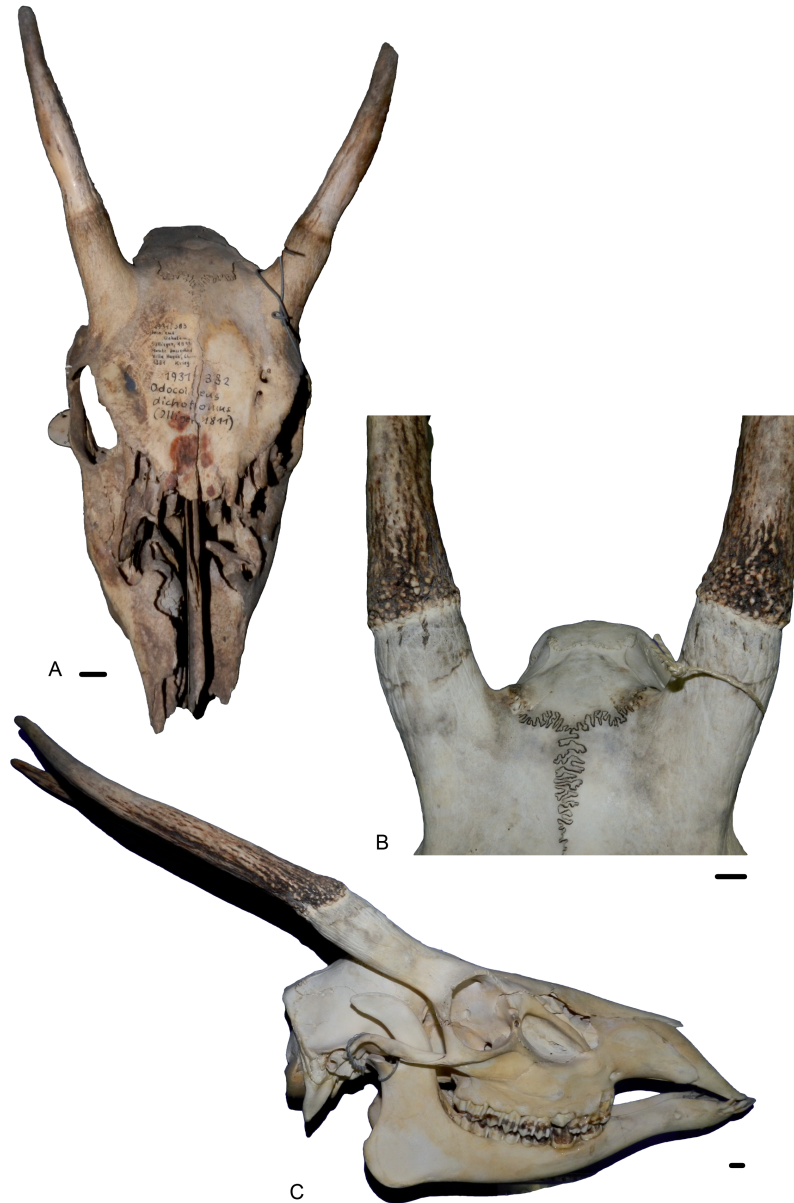


Figure 2.9: The first set of antlers of two living cervids, *Blastocerus dichotomus* and *Rusa unicolor* demonstrating the burr-less condition in yearlings. A) ZSM 1931/382 *Blastocerus dichotomus* in dorsal view. First set of antlers without burrs. B) ZMH 9398 *Rusa unicolor* in dorsal view. Close up of the pedicle to antler transition showing the absence of burrs, but instead a nodose ornamentation in the position of the future burrs. C) ZMH 9398 *Rusa unicolor* in lateral view. First set of antlers (note the erupting P4). Scale bars equal 1 cm.

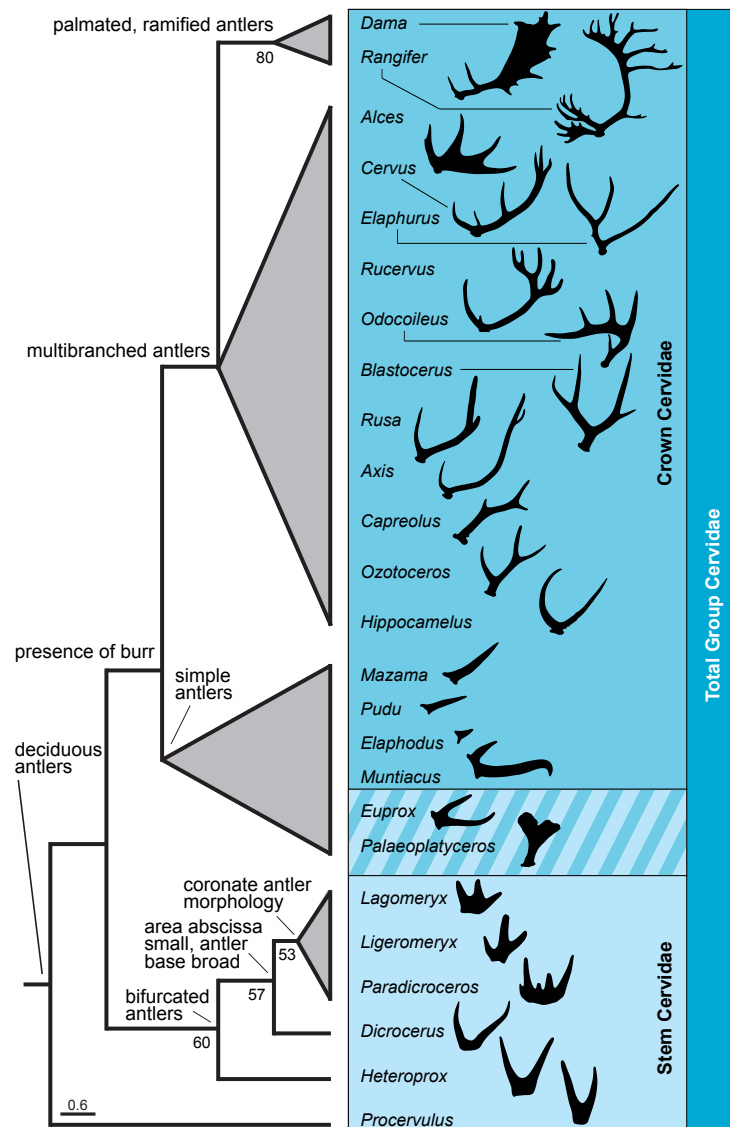


Figure 2.10: Topology from the maximum parsimony analysis based on the small antler character set. The topology does not reflect the systematic relationship of cervids, but provides a phenotypic classification of the taxon based on antler morphology. The numbers next to the nodes represent bootstrap support values. The major morphological changes in antler evolution are indicated by comments. The first antlers were bifurcating or coronate without a burr. The development of a burr is first observed in *Euprox* and *Palaeoplatyceros*. *Muntiacus* shows a similar antler morphology as *Euprox*. The antlers of *Mazama*, *Pudu*, and *Elaphodus* are single spikes and in the case of *Mazama* and *Pudu* most likely represent secondary adaptations. *Hippocamelus* shows derived bifurcating antlers, sometimes with a tiny accessory tine. All other living cervids possess three-tined or more complex, sometimes palmated, antlers.

2.4 Discussion

2.4.1 Observations from Investigated Specimens

Early fossil cervids

The classification of morphological structures of shed antlers (Tabs 2.1, 2.2) demonstrates the number of shared and differing characteristics in crown and stem cervids. Concentricity of the abscission area and centripetal expansion of osteoclasts are crucial features, with which the connection between morphology and physiology can be made. This allows for implications from fossil morphology to physiological processes in the past.

The first antler morphotypes were small, simply forked or multi-pointed, sitting on long pedicles protruding from the part of the frontals which formed the orbit roof and always co-existing with enlarged upper canines in males (Gentry, 1994; Rössner, 1995; Azanza Asensio, 2000). Most recent sources of the chronological occurrence of early fossil cervids include Gentry (1994), Gentry et al. (1999), Azanza Asensio (2000), Böhme et al. (2012) for Europe, as well as Vislobokova (1990) and Vislobokova (1997) for Asia. The oldest known cervids, as defined by the presence of antler-like branched frontal protuberances, have been found in the early Miocene (Land Mammal Zone MN3, 19.5–17.2 mya; Hilgen et al. 2012). They include *Procervulus* Gaudry 1877 from Spain, France, and Germany, *Acteocemas* Ginsburg 1985 from France and *Ligeromeryx* Azanza & Ginsburg 1997 from France (Ginsburg, 1989; Azanza, 1993a; Gentry, 1994; Rössner, 1995; Azanza & Ginsburg, 1997; Rössner, 1997; Gentry et al., 1999; Azanza Asensio, 2000; Ginsburg et al., 2000; Aguilar et al., 2003; Böhme et al., 2012). There are three morphotypes of early antlers: *Procervulus* with dichotomously forked antlers (Rössner, 1995), *Ligeromeryx* with multi-pointed, crown-like antlers (Azanza & Ginsburg, 1997), and *Lagomeryx* and *Paradicrocerus* with coronate, shaft-less antlers (Azanza & Ginsburg, 1997).

In particular, *Procervulus*, *Lagomeryx*, and *Paradicrocerus* have long been regarded as possessing antler-like appendages that were not shed, and it was assumed that their appendages were permanently skin covered (Azanza & Ginsburg, 1997). The theory of non-deciduous antlers in *Procervulus* was further strengthened by the absence of a burr (Dehm, 1944; Azanza, 1993b; Groves, 2007). For *Lagomeryx* and *Paradicrocerus*, a sufficient number of shed antler fragments has been found, confirming the hypothesis that these fossil cervids had deciduous antlers.

The antlers of *Procervulus* are smooth to weakly ridged and bifurcating; they do not possess burrs or thickening of the antler around the abscission area (Fig. 2.3). Figure 2.3 A, D–J shows *Procervulus* antler fragments with a concave, regular, planar abscission area; therefore, these fragments are considered to have been shed. Figure 2.3 B–C, K–L in contrast shows broken antler fragments. There is no evidence for a link between a smooth surface and permanent skin coverage, as some living cervid species have a very smooth antler surface (e.g., *Rangifer*) but do not have permanent skin coverage and shed their antlers. Additionally, the presence of a burr has never been proven necessary for antler shedding (see above). Based on this, the *Procervulus* specimens presented here (Fig. 2.3 A, D–J) are clearly shed antler fragments.

The antlers of *Heteroprox* are characterised by a relatively smooth to furrowed surface, are bifurcated, and have a concave abscission area; the burr is absent (Fig. 2.2). All

specimens in Figure 2.2 show clear evidence for shedding. In addition, several shed antler specimens and different ontogenetic stages in *Heteroprox* noted in the literature indicate antler shedding (Fig. 2.2; Stehlin, 1928; Azanza, 1993b).

The antlers of *Lagomeryx*, *Ligeromeryx*, and *Paradicrocerus* are coronate; that is, several times (normally 3–7) originate directly from the antler base (Figs. 2.5 and 2.8 C–E). This morphology is unique and not present in any Pliocene, Pleistocene or extant cervid. Shed antler fragments of *Lagomeryx*, *Paradicrocerus*, and *Ligeromeryx* can be seen in Figures 2.5 A–D, E–F, and 2.8 C–D, respectively.

As was the case for *Procervulus* (see above), the smooth antler surface and the absence of a burr (Azanza & Ginsburg, 1997) led to the assumption that lagomerycid antlers were permanently skin-covered. It was concluded that they must have been either non-deciduous (Stehlin, 1937; in the case of *Lagomeryx complicidens*: Young, 1964) or that they were shed while still connected to the blood supply, which seems very unlikely. Wang et al. (2009) suggested a special position in the transition from non-deciduous to deciduous antlers for *Stephanocemas* (= *Paradicrocerus*), hypothesising shedding for that species and *Lagomeryx*. Due to the peculiar coronate antler morphology, the base of the antler in *Paradicrocerus* is very broad and largely exceeds the pedicle diameter (Stehlin, 1937). Stehlin (1937) refers to one particular specimen (the holotype to Roger, 1898, Pl. H, Fig. 2.2; specimen stored in the Museum Augsburg), which shows a tendency for developing burr-like grooves and perforations. He also points out that the abscission area of *Paradicrocerus* is concave surrounded by a sharp edge in contrast to extant cervids (Fig. 2.5 E–F). The shed antler specimens of *Lagomeryx* (Fig. 2.5 A–D), *Paradicrocerus* (Fig. 2.5 E–F), and *Ligeromeryx* (Fig. 2.8 C–D) indicate that shedding was possible in these species at least in irregular intervals.

The similar antler morphology suggests that *Stephanocemas* (= *Paradicrocerus*) is closely related to *Lagomeryx*-related artiodactyls (Wang et al., 2009). Vislobokova et al. (1989) pointed out that the systematic position of *Lagomeryx*-related artiodactyls is controversial and that they possibly form a unique branch of cervoids. *Lagomeryx*-related artiodactyls possessed deciduous antlers based on our results and should be included within the total group Cervidae, presumably representing a separate clade of stem Cervidae indicated by their peculiar coronate antler morphology and supported by the topology of antler evolution presented here (Fig. 2.10).

Dicrocerus has strongly furrowed, normally bifurcating antlers with a medial burr-like structure on the base of the antler (Ginsburg & Azanza, 1991; Fig. 2.4 A–D). Figure 2.4 shows three shed antler fragments of *Dicrocerus*; Figure 2.4 E–G most likely represents the first ontogenetic stage of antlers in *Dicrocerus* characterised by the continuation from the pedicle with a moderate fork at the end Ginsburg & Azanza (1991).

My observations confirm the ability of antler shedding in *Dicrocerus* (Fig. 2.4; Azanza, 1993a; Groves, 2007). Changes in size and complexity with age observed from numerous shed antler fragments of *Dicrocerus* was used plausibly as an argument for shedding by Azanza et al. (2011), whereas the same evidence was used by Lartet (1837) to argue against shedding. Azanza (1993b) hypothesised antler presence (and shedding) in both sexes of *Dicrocerus* based on size bimodality. However, the bimodality could be equally likely produced by other causes, such as different subspecies, other ecological reasons or simply by different ontogenetic stages. The only cervid species to exhibit antlers in both

sexes is the reindeer (*Rangifer tarandus*), which is one of the most derived and specialised living cervids. Therefore, the presence of antlers in both sexes as the primitive condition of cervids, as suggested in Ginsburg & Azanza (1991) remains speculative. According to Bubenik (1990), testosterone plays a less important role in *Rangifer* and it is assumed that some adrenal androgens, which can substitute for testosterone, are responsible for antler growth in female *Rangifer*. In contrast to other living cervid species, both male and female castrated *Rangifer* are able to shed and re-grow their antlers in regular cycles (Ginsburg & Azanza, 1991).

Euprox is the first fossil species with a clearly developed burr (Stehlin, 1928, 1939; Fig. 2.6); its antlers are similar to those of modern *Muntiacus*, bifurcated, and moderately ornamented (Fig. 2.6). Shed antler fragments are shown in Figure 2.6 A–B and E–F, whereas a broken, not shed fragment can be seen in Figure 2.6 C–D. Similarly, the slightly younger *Palaeoplatyceros* has a clearly developed burr (Fig. 2.8 A–B); its antlers are palmated and flattened medio-laterally, a unique morphology not known from any other cervid species. The contemporaneous *Amphiprox* also shows definite burrs (Stehlin, 1939). *Procapreolus* and *Lucentia* were the first members of Cervidae that developed a more than dichotomous antler pattern from the forked antler morphotype (Korotkevich, 1965; Böhme et al., 2012).

Comparative morphology

The results of this study reveal that observed fossil antlers of all early cervids, bifurcated, coronate or palmated, contained definitely deciduous examples; these antlers also have a relatively broad base or very short shaft; the development of a longer shaft, a burr, and a long main beam evolved with the antlerogenic process (Tab. 2.1, Fig. 2.10). To diagnose members of Cervidae, it is crucial to distinguish taphonomically broken from shed fossil antlers.

The abscission area, a crucial feature of shed fossil and extant antlers, shows clear evidence for resorption as described above. The rugose surface with residual bone spiculae indicates successive osteoclastic activity resorbing bone material (Goss et al., 1992). In Figure 2.7 B, F, G, the smooth surface of the trabeculae is evidence for bone resorption. Furthermore, the concentric and concave abscission area clearly visible in Figure 2.7 A and also indicated in Figure 2.7 C–D supports that these antlers were shed. However, the differing concavity of the abscission area (convex in most extant, concave in most fossil cervids) indicates a possibly different spatial dispersion of osteoclasts in antlers with a convex abscission area compared to antlers with a concave abscission area. The reason why *Muntiacus* has a concave abscission area may be that it is, as it is widely agreed on, a more ancestral member of crown group Cervidae, and therefore, its abscission area morphology may resemble more that of early stem cervids. However, the properties of the abscission area are not sufficiently enough understood to make inferences about why there obviously has been a shift from a concave to a convex morphology.

The burr or coronet is an enigmatic structure. In the literature, a burr is often referred to as a compulsory prerequisite to recognise antler shedding (e.g., Ginsburg & Azanza, 1991; DeMiguel et al., 2013); thus, the mechanism of antler shedding has been assumed to be absent in some early cervids based on the lack of burrs on their antlers (Stehlin, 1937; Dehm,

1944; Simpson, 1945; Thenius, 1950; Vislobokova et al., 1989; Bubenik, 1990; Azanza, 1993a). It is not known where this statement/assumption originated. Antlers without a burr or a burr-like structure have been referred to as ‘protoantlers’ (e.g., Bubenik, 1990; Azanza et al., 2011). This study has shown that early burr-less antlers were shed, therefore representing true antlers, and should be referred to as such. The term ‘protoantler’ is therefore obsolete and should not be used.

The extensive review of the literature on the antlerogenic process (Brown, 1980; Goss, 1983; Bubenik, 1990; Goss et al., 1992), and examination of extant and fossil cervid antlers in the present study did not reveal evidence of a primary causative relation of the presence of a burr and antler shedding. Furthermore, the first set of antlers of a modern deer does not possess burrs at all (Bubenik 1990; this study, Fig. 2.9). It is likely that the development of a burr might be a side effect from the repeated exaggerated bone apposition and intensified ossification proximal of the zone of resorption prior to shedding (Goss, 1983). The underlying function of the burr needs more thorough investigation. The first clear burrs are known from middle Miocene *Euprox minimus* from Austria (Böhme et al., 2012).

The wide range of surface texture of antlers in modern cervids, ranging from entirely smooth to furrowed (Tabs 2.1, 2.2), shows that antler shedding is independent of ornamentation. A smooth antler surface does not indicate permanent skin coverage, as has been suggested for *Procervulus* and *Lagomeryx*. Thus, antlers that are permanently skin covered are very unlikely to occur. Based on evidences for regular shedding and regeneration, shed antler specimens were identified for all early Miocene cervids investigated. Thus, the very first deciduous antlers most likely adhered to the same physiological mechanisms as observed in living cervids. A mechanism that involves growing antlers under skin coverage, which is later shed to expose a fully grown set of antlers. The antlers die and are eventually shed, inducing the regeneration of a new set of antlers.

The complex antler shedding mechanism is unique and a fundamental component in cervid evolution. However, the antler cycle, as it appears in modern cervids, and the anatomical differences between early and modern antlers reflect physiological modifications, which have appeared since the origin of cervids.

2.4.2 Divergence of Cervidae

The total group Cervidae is diagnosed by the presence of antlers, which again are defined as deciduous, osseous outgrowths of the frontal bone (Janis & Scott, 1987). In living cervids, antlers are present in males of all species with the exception of *Hydropotes inermis*. The absence of headgear in this species has long been assumed to be a primitive condition; however, more recent morphological investigations and molecular studies show that it is more likely to represent secondary loss (e.g., Pitra et al., 2004; Hassanin et al., 2012). If the early Miocene taxa were not able to shed their antlers, their systematic position within the total group Cervidae would be incorrect, if the monophyly of Cervidae were based on the synapomorphy ‘presence of antlers’. Since the early cervids investigated here were able to shed their antlers, they are positioned as stem cervids (Fig. 2.10).

The analysis based on the antler character set presented here shows that most Miocene cervids are placed in a stem position. Only the two Miocene species that possessed antlers

with burrs (*Euprox*, *Palaeoplatyceros*) were put within the crown group more closely related to living than fossil Cervidae. The topology does not represent current cervid systematics, but it shows the important steps throughout antler evolution (Fig. 2.10). The first antlers were dichotomous, with moderate or no ornamentation, lacking both burr and shaft. There was a trend toward a more complex, coronate antler morphology in *Lagomeryx*, *Ligeromeryx*, and *Paradicrocerus*, but all of them became extinct by the end of Miocene. The first antlers with burrs and a short to moderately long shaft are known from *Euprox* and *Palaeoplatyceros*. *Muntiacus* shows a similar antler morphology to *Euprox*. There are three extant genera that have single-tined antlers, *Mazama*, *Pudu*, and *Elaphodus*; all other extant genera have at least three-tined or even more complex multibranched or palmated antlers. An exception is *Hippocamelus*, which mostly has bifurcated antlers (Fig. 2.10).

Controversies concerning the ability of antler shedding led to differing opinions for a long time on which species represents the first true cervid. Several suggestions have been made for the earliest known cervid over the past few decades: *Dicrocerus* (middle Miocene, Eurasia) and *Stephanocemas* (= *Paradicrocerus*) (middle Miocene, Eurasia) were suggested by Goss (1983) and Janis (1990); *Lagomeryx* (MN3, early Orlanian, early Miocene, Western Europe) was proposed as earliest member of Cervidae by Janis & Scott (1987) and Groves (2007); Pitra et al. (2004) and Di Stefano & Petronio (2002) suggested *Cervocerus novorossiae* (late Miocene) as the most primitive deer. Several studies regarded *Procervulus*, *Ligeromeryx*, and *Acteocemas* as the earliest known cervids (early Miocene, Western Europe) (Ginsburg & Azanza, 1991; Azanza, 1993b; Gentry, 1994; Rössner, 1995; Gentry et al., 1999; Azanza Asensio, 2000; Böhme et al., 2012), followed by *Paradicrocerus* and *Dicrocerus* in the middle Miocene. These early cervids all became extinct by the late Miocene.

The earliest evidence of cervids from the early Miocene has been challenged by interpretations of recent molecular clock analyses, which suggest a maximum divergence time of the cervid stem lineage at the middle/late Miocene boundary. This would mean that all early and middle Miocene genera assigned to cervids by palaeontologists are not included in the total group Cervidae (Gilbert et al., 2006; Hassanin et al., 2012). Molecular clock calculations and divergence time estimates are dependent on calibration points representing the first appearance of a representative of a clade; therefore, calibration point selection is crucial for the best results. In Gilbert et al. (2006) and Hassanin et al. (2012), earliest crown cervids were chosen as calibration points. Hassanin et al. (2012) used *Cervavitus shanxiensis* and *Muntiacus noringenensis* as calibration points for the split between Cervini and Muntiacini (961 mya). The divergence time estimations provided an age of 11.5–10.7 mya for the divergence of Cervidae from other ruminants. This is much younger than what is found in the fossil record, where the first representative of cervids appears at least in the early Miocene, as the shed antler specimens in this study demonstrate. Gilbert et al. (2006) used the ‘oldest fossil cervid’ (20±2 mya; Ginsburg, 1988) as calibration point for the Cervidae-Ruminantia split; however, their analyses provided a divergence time estimate for this split of 18–16.5 mya, which is slightly too young and contradicts clear evidence from the fossil record. Their ancestral state reconstruction for a male resulted in a tall (shoulder height > 65 cm) last common ancestor with distinct sexual dimorphism, normal-sized canines, bearing three-tined antlers, and inhabiting open habitats (Gilbert et al., 2006). The information that can be obtained and inferred from the fossil record contradicts all

these features of the presumed common ancestor. All early Miocene cervids have tusk-like, enlarged upper canines and none of them shows a three-tined antler morphology. Based on the overall small size (with a shoulder height < 65 cm), it is assumed that females and males were monomorphic regarding their body size/mass, as is the case in smaller extant cervid species.

2.4.3 Ecological Context

The climate in higher latitudes of Eurasia during the early Miocene (23–16 mya) was humid and warm and Europe was covered with tropical forests with a diverse fauna (Fortelius et al., 2014). Assuming that the early Miocene cervids originated in these forests, their simple antler morphology is easily interpreted (in comparison with the antler morphology of extant *Mazama*, *Pudu*, and *Muntiacus*, which live in heavily vegetated habitats), as it would have enabled them to move quickly through this environment. Presumably, the next evolutionary step was to incline the pedicles (including antlers) to allow for a more streamlined appearance, facilitating moving through vegetation.

The transition from high temperatures to cooling was during the Middle Miocene Climatic Transition (MMCT 14.2–13.8 mya [minimum temperatures around 13.9 mya]; Shevenell et al., 2004; Holbourn et al., 2005). With the drier climate and utilisation of new habitats, that is, ecotone regions, more open grassland, or temperate forests with less dense understorey, antlers grew larger and some of them developed a more complex morphology, that is, an increasing number of tines (Bubenik, 1990).

From around 10 million years ago onwards, western Europe was affected by increased seasonality, especially with low winter temperatures, which resulted in replacement of evergreen subtropical woodlands by deciduous forests (Fortelius et al., 2014). This change in vegetation would have been crucial for animals depending on browse that is available year round and this change may have triggered synchronisation of the reproductive cycle with the seasons. A detailed description of the climatic development during the Miocene and Pliocene can be found in Fortelius et al. (2014).

The presence of an antler cycle is confirmed for the early Miocene cervids. As indicated above, the climate across Eurasia during the early Miocene was humid and warm with little or no seasonality (Fortelius et al., 2014); therefore, antler cycles in early cervids were most likely not yet influenced by seasonality and antler shedding in those early cervids presumably occurred at intervals that were more irregular and were not synchronised, similar to the condition today in tropical cervids. However, intrinsic factors, such as hormones, presumably already drove shedding of antlers in early Miocene cervids. Most likely, the strict seasonal cycle developed with the change of climate and environmental factors. Repeated shedding is the prerequisite for growing larger and/or more complex antlers during the next growing cycle.

Azanza et al. (2011) indicate differences in the histology of procervulines and lagomerycids compared to other shed antlers from radiographic evidence, which would need further scrutiny with visualisation techniques allowing for higher resolution and a larger sample size.

2.5 Conclusion

This review of antlerogenesis demonstrates that it is a complex process and involves a number of physiological phenomena that are dependent on extrinsic factors. In living cervids, the antler cycle comprises successive growth from the pedicle, ossification, necrosis, and sequestration. All phases include histological specifics (Brown, 1980). The morphological traits of abscission, indicating bone resorption, are identical or similar in early fossil cervids compared to extant cervids. This provides evidence that the process of antlerogenesis, antler shedding and rebuilding, was already present in the first early Miocene cervids.

Detailed scrutiny of shed antler fragments from early cervids shows that all species discussed in this study were able to shed their antlers, even in absence of a burr.

It, therefore, follows that antler shedding was already present in *Procervulus*, *Lagomerix*, *Ligeromeryx*, and *Paradicrocerus*, where it was assumed that the antler shedding mechanism was absent due to the lack of burrs. Although the burr is a typical feature of extant antlers, is not required in order for shedding to occur. It is more likely that this feature evolved as a by-product of repeated bone apposition and intensified ossification in modern antlers. Furthermore, the ability to shed antlers is independent of antler ornamentation shown by the partly rich and diverse ornamentation in antlers of modern cervids. Presence of modern antlers with a smooth surface that are not permanently skin-covered rule out that a smooth surface can be used as evidence for permanent skin cover. Thus, the existence of permanently skin covered antlers has not so far been established.

The systematic position of all these Miocene taxa is within the total group of Cervidae. Thus, the oldest known members of Cervidae are *Procervulus praelucidus* (Germany), *Acteocemas* (France), and *Ligeromeryx* (France) all from the early Miocene (MN3). From the late Miocene onward, several evolutionary trends in antler development can be observed. These include the concavity of the abscission area, which is almost always concave in early cervids and almost always (with the exception of *Muntiacus*) convex in extant cervids, the development of a burr, the development of a longer shaft pushing the first bifurcation more distally, and the development of a long main antler beam. Furthermore, the branching patterns in antlers became more complex, pedicles became shorter, and the upper canines became smaller.

Chapter 3

Cervid Systematics based on Morphology

3.1 Introduction

3.1.1 History of Classification of Cervidae based on Morphology

The first classification of Cervidae based on morphological characters was done by Brooke (1878). The classification was based on differences in the metacarpals. Modifications of the metapodials include the complete fusion of the third and fourth metapodials to the so-called cannon bone and the loss of the first metapodial. While the metatarsus consists of the cannon bone only, the metacarpus possesses rudiments of the second and fifth metacarpals. The slender and short metacarpals have articular surfaces, but are detached from the cannon bone and situated posterior to the cannon bone, one on each side (Fig. 3.1; Brooke, 1878). These rudimentary metacarpal bones can have two different positions; at the proximal end of the cannon bone, which is called the plesiometacarpal condition, or at the distal end of the cannon bone, which is called the telemetacarpal condition. Brooke's gross division of cervids into two groups, Telemetacarpi (= Capreolinae) and Plesiometacarpi (= Cervinae), still holds today. *Muntiacus* is further characterised by the absence of the phalanges of the second and fifth digits.

In this early work, a suite of characters was listed, which distinguishes cervids from bovids. However, apart from character 11 none of them is exclusively found in cervids (Tab. 3.1). The combination of characters 2, 3, 4, and 5 is present in all Cervidae, while this combination is never found in Bovidae (Fig. 3.1; Brooke, 1878).

Antlers are the most striking feature of cervids; they are defined as deciduous, osseous, branched, apophyseal outgrowths of the frontal bones, which are shed and re-built regularly, generated by periosteum induced endochondral ossification (Janis & Scott, 1987, 1988). Antlers represent a strong sexual dimorphism, as they are only present in males with the exception of *Hydropotes inermis*, which does not grow antlers and *Rangifer tarandus*, in which males and females grow antlers. A detailed description on the antler cycle and early evolution of antlers is in Chapter 3.

Plesiometacarpi include also the following characters: an undivided nasal cavity, contact of the praemaxilla with the nasals, and presence of a tuft on the outside of the

Table 3.1: Apomorphies of Cervidae modified after Brooke (1878).

No.	Character
1	Antlers = osseous, deciduous outgrowths from cylindrical processes of the frontals in males only (exceptions: <i>Hydropotes</i> , <i>Rangifer</i>)
2	Two lacrimal orifices on or inside orbit
3	Presence of lacrimal fossa
4	Presence of ant- or praeorbital vacuity
5	m1 and M1 brachyodont in all species
6	C in both sexes for most species except for <i>Capreolus</i> , <i>Axis</i> , <i>Dama</i> , ‘ <i>Cariacus</i> ’ (= <i>Odocoileus</i>), <i>Blastocerus</i> , <i>Pudu</i> , <i>Alces</i> , some <i>Rusa</i>
7	Distal ends of lateral metacarpals present in some species
8	Presence of 1 st and 2 nd phalanges of lateral digits except for <i>Muntiacus</i>
9	Parieto-squamosal suture closer to the upper border of the temporal fossa than to the lower border
10	Navicular, cuboid, and ectocuneiform fused in some species
11	Placenta with few cotyledons
12	Absence of gall bladder

metatarsals, which is always absent on the inside. Plesiometacarpi or Cervinae consists of *Muntiacus*, *Elaphodus*, *Cervus*, *Rusa*, *Rucervus*, *Elaphurus*, *Axis*, and *Dama* (Brooke, 1878).

Telemetacarpi is subdivided into two groups. Taxa of the first group have an undivided nasal cavity and a tuft on the outside of the metatarsals and comprise *Alces*, *Capreolus*, and *Hydropotes* (Groves, 2007). The second group of Telemetacarpi or Capreolinae have a vomer dividing the nasal cavity, a praemaxilla, which is not in contact with the nasals, and a tuft on the outside of the metatarsals, which is often also present on the inside. Taxa with this suite of characters include *Odocoileus*, *Hippocamelus*, *Blastocerus*, *Ozotoceros*, *Mazama*, *Pudu*, and *Rangifer* (Brooke, 1878; Randi et al., 1998).

Apart from the division into Telemetacarpi and Plesiometacarpi, Bouvrain et al. (1989) presented several characters, which can be used to further classify cervids. The foramina palatina are in a medial position between the midline of the palate and the tooth row, variable in size, but almost always on the maxillopalatine suture (Bouvrain et al., 1989). In the Plesiometacarpi (Cervinae), the temporal foramina, which are the openings for the canal temporalis, are separated by a complete bone bar and are situated entirely within the squamosal. In all Telemetacarpi (Capreolinae) this bar is incomplete and partly formed by the petrosal (Bouvrain et al., 1989; Groves, 2007).

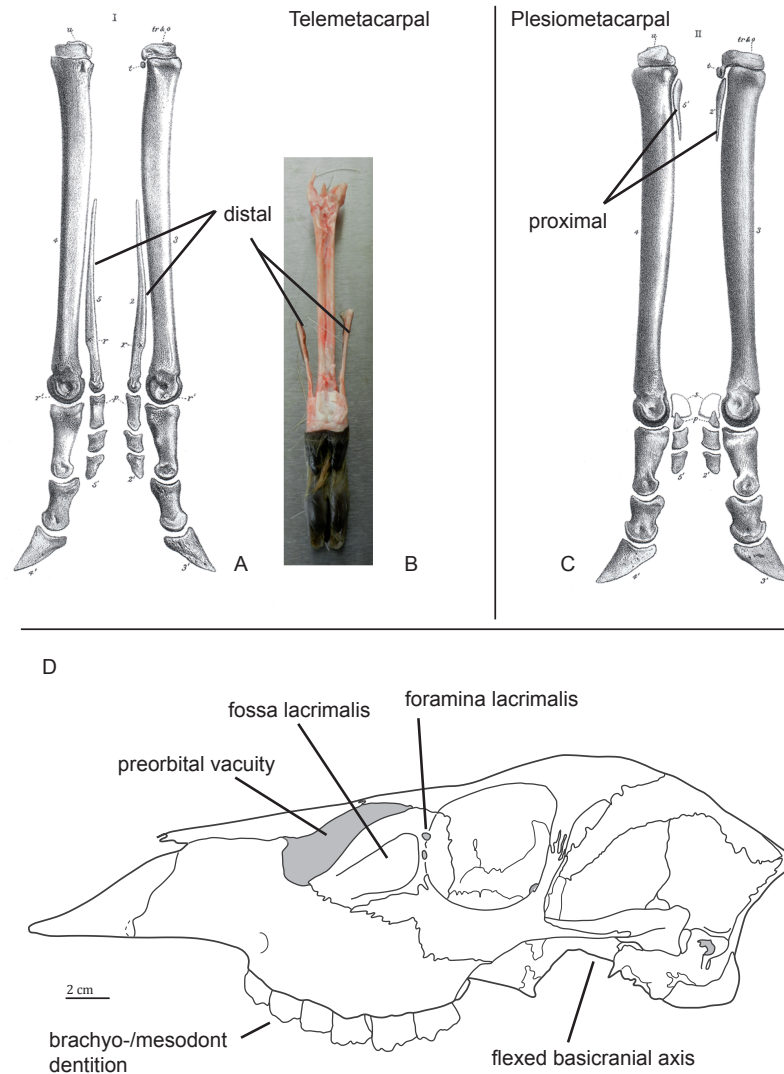


Figure 3.1: (A) Lateral aspect of the front limbs of *Capreolus capreolus* showing the telemetacarpal condition, where the metacarpals are in a distal position, modified after Brooke (1878). (B) Posterior aspect of the left front limb of *Hydropotes inermis* showing the telemetacarpal condition. (C) Lateral aspect of front limbs of *Cervus elaphus* showing the plesiometacarpal condition, where the metacarpals are in a proximal position, Brooke (1878). (D) Lateral aspect of the skull of a female *Blastocerus dichotomus* showing five typical cervid cranial characters.

Subsequent literature listed the following characters diagnosing Cervidae: presence of a fossa lacrimalis, brachyodont to mesodont dentition, metapodials not elongated, partial retention of metapodials II and V, and the absence of the gall bladder (Janis & Scott, 1987, 1988). In Mickoleit (2004) two lacrimal foramina, a lacrimal with elongated facial proportion, osseous antlers, a flexed basicranial axis, praeorbital vacuity, plesio- or telemetacarpal condition, few cotyledones in placenta, and two pairs of teats are listed as characters, which diagnose Cervidae.

This split into Capreolinae and Cervinae is also confirmed by behavioural characters (Cap et al., 2002; Groves, 2007) and both subclades share an antlered common ancestor (Cronin, 1991). Further subdivision solely based on morphological features is difficult and almost impossible, because cervid characters are highly conservative, phylogenetically uninformative and/or prone to convergence because of ecological adaptation (Groves & Grubb, 1987; Janis & Scott, 1987; Lister, 1996; Wada et al., 2007). However, there are a few phenotypic features, which unite some species to groups; these features include the morphology of antlers (albeit antler morphology has to be considered with caution, see Chapter 2), the general skull shape, coat colour, cutaneous glands, or the external outline of the body (Brooke, 1878). Further, the morphology of p4, especially the degree of closing of the anterior valley, the postprotocristae of the upper molars, RNA of the pancreas, variation of chromosome numbers are useful to distinguish groups of cervid species (Bouvrain et al., 1989; Cronin, 1991). These natural group patterns of cervids are important to gain insights into their evolutionary history (Brooke, 1878).

3.1.2 Definition of Morphological Characters

Defining morphological characters is not trivial; there are three major difficulties: First, character change is continuous not discrete, but discrete character states are scored, which are more prone to subjectivity. Second, parallel evolution/convergence is possible and even highly likely to occur. Third, the distribution of certain character states do not line up with the distribution of other character states or other taxon groups as it is the case in molecular data (Gentry, 2000). Ideally, characters show variation between terminal units, but not within terminal units. Creating smaller invariant units, excluding variable characters or coding polymorphisms are solutions to deal with that sort of variation (Wiens, 2000). Variation is ubiquitous in morphological data and therefore, it is necessary to explicitly state how variation was dealt with in terms of the way of coding and exclusion or inclusion of certain characters. Different coding methods can differ greatly in accuracy (Wiens, 2000).

Polymorphic characters are more homoplastic than fixed characters, but may contain useful phylogenetic information and therefore, unless certain characters can be convincingly identified as misleading, should be included. It has been found that analyses including polymorphic characters are consistently more accurate than analyses excluding them (Poe & Wiens, 2000). Polymorphisms are variations within individuals of comparable age and sex of the same species and evolve from population genetic processes and must be distinguished from interspecific variation, which results from different evolutionary processes (Wiens, 2000).

Selection criteria for choosing or rejecting characters should be operational and objec-

tive and have to be explicitly explained and discussed. This *modus operandi* is crucial, because it increases the rigour of morphological systematics and reduces or at least explains subjectivity. Further, the level of homoplasy and the polarity of characters should be discussed (Poe & Wiens, 2000). If all of these precautions are considered, morphological characters can be justifiably used for phylogenetic reconstructions.

In contrast to historically early phylogenetic reconstructions, which were generally consistent with the temporal distribution of fossil species, this temporal order is rarely considered in today's phylogenetic studies. Stratigraphic data can be used to estimate phylogeny, examine the congruence between the fossil record and phylogeny, examine models of fossil preservation, and to root phylogenetic trees (Huelsenbeck & Rannala, 2000). The perception of fossils has changed over the last decades. Before the access to molecular data and more explicit phylogenetic methods, palaeontologists were the main practitioners of phylogenetics/cladistics and fossils were regarded as essential for reconstructing accurate topologies. The attitude changed with increasing molecular data, because the latter outweigh morphological data, which are often regarded to be less useful for resolving relationships (Huelsenbeck & Rannala, 2000). There is a widespread but largely unsubstantial opinion that morphological data are more subject to homoplasy than molecular data (de Queiroz, 2000).

Taxa containing a lot of missing data do not need to be excluded *a priori*, as it has been shown that incorporating even highly incomplete taxa of up to 75 % missing data can increase overall accuracy of the analysis (Poe & Wiens, 2000; Wiens, 2003, 2006; Pattinson et al., 2015). Inclusion of fossils into phylogenetic reconstruction can be critical and may change the interpretation of character evolution. It was found that inclusion of more fossils is more useful for phylogenetic reconstructions than adding more extant taxa (Huelsenbeck, 1991; Huelsenbeck & Rannala, 2000). Further, fossils are important because they often combine plesiomorphic and apomorphic characters and these combinations are often unique. Fossils also serve as a test for the fit of estimated fossils to the fossil record and to assess the uncertainty of calibration times (Huelsenbeck & Rannala, 2000).

Considering all these aspects of morphological characters is important for the objectivity of morphological phylogenetic hypotheses and facilitates comparability of topologies, of different types of characters, and of morphological features between taxonomic groups (Poe & Wiens, 2000). The morphological character sets and analyses in this chapter have all taken these potential biases and peculiarities into account. Despite a potentially high level of homoplasy in the data set inclusion of morphological data is the key to solve systematic relationships of fossils among each other and to their living relatives.

This is the first time that a comprehensive morphological data set of this size including many fossil and extant cervid taxa was analysed. The data set focused on cranial and dental characters. Several analyses were undertaken on the individual partitions (cranial, dental) and the combined data set analysing fossil and extant taxa separately and together, and under different optimality criteria. Additionally, analyses using a molecular and morphological supermatrix or a constraint topology including only one fossil at a time were undertaken. The data were also analysed under the Evolutionary Placement Algorithm (EPA). All these analyses aimed at investigating the strength of morphological characters to reconstruct a cervid phylogeny, the systematic position of fossil cervids, and the influence of data partitioning and varying taxon sampling on the phylogenetic signal. The

latter aspect was important in order to critically evaluate the systematic positions of taxa, especially fossils. The results provide new and intriguing insights into how fossil cervids are related to extant cervids.

3.2 Material and Methods

3.2.1 Data Acquisition and Processing

In total, 41 extant cervid species, 29 fossil cervid species, six non-cervid extant ruminants, and two non-cervid fossil ruminants were measured using 45 distances, documented by photographs and character-coded into the morphological matrix. The extant species were studied on 232 specimens (Tab. B.1), the fossil species were studied on 504 specimens (Tab. B.2). Most of the fossil species consist of fragments of several individuals. The fossils ranged from the Miocene until the Holocene and their temporal ranges are shown in Figure 3.2.

Measurements of each specimen were taken with a digital calliper with an accuracy of 0.1 mm. Where the range of the calliper was not sufficient, measuring tape was used with an accuracy of 0.5 mm. All measuring distances are listed in detail in Tables D.1 and D.2 and shown in Figures D.1, D.2, and D.3. The measurements are stored on the LMU library server for electronic dissertations (<https://edoc.ub.uni-muenchen.de/view/autoren/index.H.html>), as specified in Chapter 1. To decrease errors, measuring distances are direct, i.e., along the skull, not interpolated, and were taken in a consistent manner. Generally, measurements follow the anatomical terms, e.g., length refers to the anterior-posterior extension, width to the medial-lateral or lateral-lateral extension, and height to the dorsal-ventral extension. Exceptions from this rule are anatomical structures, which resemble geometrical objects, such as the auditory bulla, the lacrimal fossa, and the praeorbital vacuity, because their orientation can deviate from the strict anatomical orientation. In these structures the length refers to the maximal extension and width/height to the minimal extension. Each distance was measured once in each individual or fragment. Ratios of the measurements served as source for discrete quantitative characters for the morphological matrix.

Photographs were taken in dorsal, lateral (dextral and sinistral), anterior, posterior, and ventral view and are stored on morphobank (<http://morphobank.org/permalink/?P1021>). The dentition was photographed in separate close-ups. Ideally, characters were directly coded from the specimens in the collections. Sometimes the photographs of specimens had to be used for character coding. Character matrices and the character state lists are available on morphobank (<http://morphobank.org/permalink/?P1021>). Several characters were taken from Bärmann (2012) (https://morphobank.org/index.php/Projects/ProjectOverview/project_id/352). However, some of the character states had to be modified, as they resulted in constant coding for cervids. Several characters were newly defined and are used for the first time in this study. If only a few specimens per species were available for investigation, variable characters were difficult to score. Here, I coded these variant characters as polymorphic. One of the states was assigned a posteriori by the phylogenetic reconstruction algorithm (Wiens, 2000).

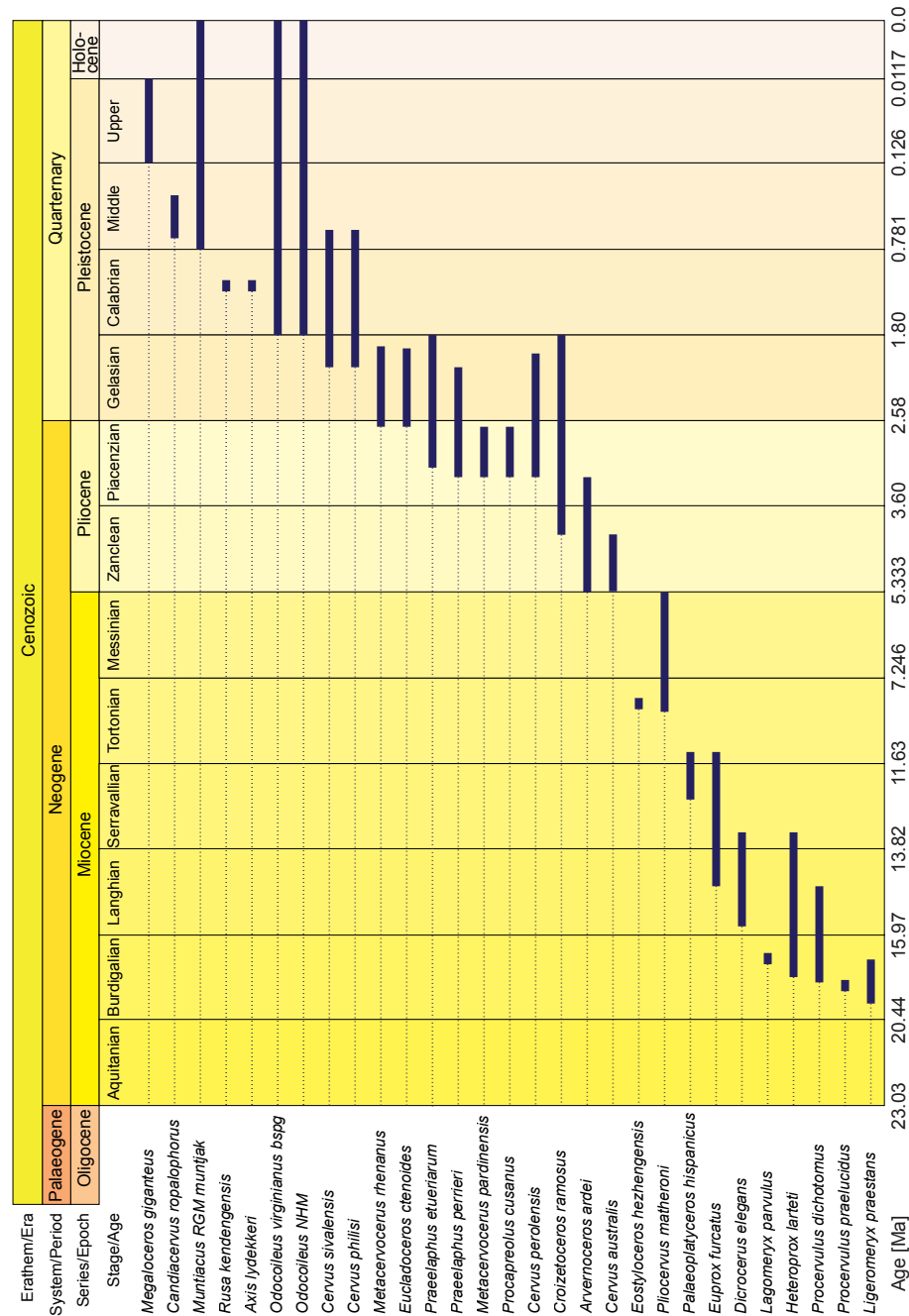


Figure 3.2: Age Ranges of Fossil Cervids. Fossil cervids are arranged from the oldest first appearance datum on the bottom to the youngest first appearance datum on the top. The stage column widths are not correlated with time. The dates were compiled from the literature (Gentry et al., 1999; Steininger, 1999; Böhme et al., 2012; Hilgen et al., 2012; Cohen et al., 2013; Croitor, 2014) and databases (NOW: www.helsinki.fi/science/now/, PBDB: www.paleobiodb.org)

I divided all morphological characters into seven partitions: upper, lower, and other dentition, mandible, viscerocranium, neurocranium, and antlers. Pattinson et al. (2015) developed Q as a measure of how balanced partitions are sampled within a taxon. Q is the sum of the product of the proportions of n partitions pairwise combined with each other and divided by the number of products. Q is between 0 and 1; the more evenly sampled a taxon is the closer Q is to 1, when only one partition is sampled Q is 0. With the seven partitions in this data set the number of summands in the numerator was 21. Q is displayed on a logarithmic scale, as it does not increase linearly with increasing completeness of partitions.

The anatomical nomenclature used here is according to standard text books, such as König & Liebich (2015) and Nickel et al. (2004). Instead of rostral and caudal, anterior and posterior has been used throughout. The Latin spelling of the prefix ‘prae-’ is used for anatomical terms throughout with exception for the dental terminology, which strictly follows Bärmann & Rössner (2011). Mostly, simplified anatomical terms are used, i.e., maxilla instead of os maxillare, for a better reading flow.

3.2.2 Phylogenetic Analyses

Data Sets

Dental Character Set. The dental character set included 78 taxa, 41 extant cervid species, 29 fossil cervid species, 6 non-cervid extant ruminant species, and 2 fossil non-cervid ruminant species. In total 79 characters were coded, 8 characters are based on measurements, 35 characters cover the upper dentition, 39 characters cover the lower dentition, 5 characters cover upper canines and lower incisors and canines. 11 characters were suitable for ordering (6–8, 14, 21, 32, 40, 51, 59, 64, 72).

Cranial Character Set. The cranial character set included 78 taxa, 41 extant cervid species, 29 fossil cervid species, 6 non-cervid extant ruminant species, and 2 fossil non-cervid ruminant species. In total 89 characters were coded, 17 characters are based on measurements, 7 characters cover the mandible, 65 cover the cranium, and 17 cover antlers and pedicles. 23 characters were suitable for ordering (2, 4, 5, 8–12, 14, 15 17–20, 23, 61, 74–79, 89).

Combined Morphological Data Set. The combined morphological data set included 78 taxa, 41 extant cervid species, 29 fossil cervid species, 6 non-cervid extant ruminant species, and 2 fossil non-cervid ruminant species. This data set consisted of 168 characters, of which 34 were suitable for ordering (see above).

Stepping Stone Analyses

Unlike for molecular data, there are no sophisticated programmes to determine the model distribution or partitioning scheme of morphological data sets. Therefore, it was tested which model distribution and partitioning scheme best fits the present morphological character sets by comparing the Bayesian marginal likelihoods of the different possibilities. Up until recently there have been two methods to estimate marginal likelihoods of BI analyses,

the harmonic mean and the thermodynamic integration (Xie et al., 2011). Because the first approach often overestimated the marginal likelihood and the second was computationally costly, Xie et al. (2011) introduced the more accurate and efficient stepping stone (SS) sampling. This approach uses importance sampling to estimate each ratio in a series, bridging posterior and prior distributions and comes at low computational costs. The marginal likelihood measures the average fit of a model to the given data; traditionally, these approaches (e.g., Likelihood Ratio Test, Akaike Information Criterion) are based on the fit of each competing model at its best and none of them takes the priors into account (Xie et al., 2011). The Bayes Factor (BF) is calculated as the ratio of the marginal likelihood of one model to the marginal likelihood of the competing model; BFs can then be used as the relative evidence in the data that favours one hypothesis in that respect that it predicts the observed data better than the competing hypotheses (Xie et al., 2011).

To test the combined morphological data set for the most suitable partitioning scheme, ordering scheme (unordered vs. ordered), and model distribution choice (gamma vs. not gamma), SS analyses were undertaken. First, the data set was tested for the partitioning scheme with an analysis of an unpartitioned data set, a maximally, and a minimally partitioned data set. Afterwards, the data set, applying the resulting partitioning scheme, was tested for the gamma (Γ) distribution (Yang, 1994), and for ordering characters.

Each SS analysis was run for 21.5 million generations, with a diagnostic frequency of 1000 and a sample frequency of 500 and had 40 steps in total. The general settings are the same as for a normal BI analysis with MrBayes (Ronquist et al., 2012). However, there is an initial burnin of samples that is discarded and an additional burnin in each step of the SS sampling. The aforementioned importance distributions are called power posterior distributions and are sampled via the Metropolis Coupled Monte Carlo Markov Chain (MC³) run (Ronquist et al., 2012). Its definition is:

$$\text{prior} * \text{likelihood}^\beta$$

Beta ranges from 0 (= prior) to 1 (= posterior). In MrBayes this parameter is called alpha and was left as the default setting of 0.4, because in empirical studies it was found that the accuracy is maximal with an alpha value between 0.3 and 0.5 (Ronquist et al., 2012).

MrBayes input:

```
ssp ngen=21500000 diagnfreq=1000 samplefreq=500 nsteps=40 append=no;
ss;
```

After the completed stepping stone sampling, the BFs of the summary of the marginal likelihoods of all 40 steps were calculated and compared with each other to decide for the favoured hypothesis.

Standard Phylogenetic Analyses

The three data sets were analysed each under MP with character ordering and taxon sampling including fossil taxa, extant taxa, and fossil and extant taxa and with unordered characters including fossil and extant taxa, under BI with and without character ordering including fossil and extant taxa, and under ML without character ordering including fossil and extant taxa (Tab. 3.2).

Table 3.2: Overview of all analyses undertaken mainly based on the morphological character matrix. Dent=Dental, Cran=Cranial, UnO=unordered, O=ordered, N=No, Y=Yes; Opt. Crit.=Optimality Criterion, CI=consistency index, HI=homoplasy index, RI=retention index, RC=rescaled consistency index, E=Extant, F=Fossil.

Analysis ID	Opt. Crit.	Data Set	Charac- ters	Taxa	Ordered	CI	HI	RI	RC	Tree Length
Dent_UnO_FE	MP	dental	79	78	N	0.2559	0.9006	0.4786	0.1225	1016
Dent_O_FE	MP	dental	79	78	Y	0.1848	0.9285	0.2116	0.0391	1412
Dent_O_E	MP	dental	79	78	Y	0.2567	0.8850	0.2982	0.0766	861
Dent_O_F	MP	dental	79	78	Y	0.3520	0.7458	0.4036	0.1420	358
Dent_MB_UnO	BI	dental	79	78	N	-	-	-	-	-
Dent_MB_O	BI	dental	79	78	Y	-	-	-	-	-
Dent_MB_ML	ML	dental	79	78	N	-	-	-	-	-
Cran_UnO_FE	MP	cranial	89	78	N	-	-	-	-	-
Cran_O_FE	MP	cranial	89	78	Y	-	-	-	-	-
Cran_O_E	MP	cranial	89	78	Y	0.2186	0.8357	0.4329	0.0946	773
Cran_O_F	MP	cranial	89	78	Y	-	-	-	-	-
Cran_MB_UnO	BI	cranial	89	78	N	-	-	-	-	-
Cran_MB_O	BI	cranial	89	78	Y	-	-	-	-	-
Cran_MB_ML	ML	cranial	89	78	N	-	-	-	-	-
Combi_UnO_FE	MP	combined	168	78	N	0.2216	0.8825	0.4312	0.0956	2017
Combi_O_FE	MP	combined	168	78	Y	0.1597	0.9155	0.1653	0.0264	2806
Combi_O_E	MP	combined	168	78	Y	0.2583	0.8503	0.4335	0.1120	1510
Combi_O_F	MP	combined	168	78	Y	0.3238	0.7350	0.1556	0.0504	698
Combi_MB_UnO	BI	combined	168	78	N	-	-	-	-	-
Combi_MB_O	BI	combined	168	78	Y	-	-	-	-	-
Combi_MB_ML	ML	combined	168	78	N	-	-	-	-	-

Table 3.3: Summary of the experiments on the consistency indices. * indicates indices based on the character set excluding parsimony uninformative characters. CI=Consistency Index, HI=Homoplasy Index, RI=Retention Index, RC=Rescaled Consistency Index

Analysis Name	Tree Length	CI	HI	CI*	HI*	RI	RC
Dent.UnO_FE	979	0.2503	0.8958	—	—	0.4735	0.1185
Dent.O_FE	1402	0.1748	0.9272	—	—	0.1765	0.0308
Dent.UnO_E	714	0.3081	0.8613	0.3072	0.6928	0.4405	0.1357
Dent.UnO_F	376	0.2926	0.7606	0.2672	0.7328	0.2672	0.0782
Cran.UnO_E	737	0.2185	0.8331	0.2153	0.7847	0.4234	0.0925
Combi.UnO_FE	1975	0.2131	0.8825	0.2116	0.7884	0.4094	0.0873
Combi.O_FE	1939	0.2171	0.8804	0.2155	0.7845	0.4359	0.0946
Combi.UnO_F	533	0.3617	0.6817	0.3037	0.6963	0.2676	0.0968
Combi.UnO_E	1530	0.2490	0.8549	0.2471	0.7529	0.3895	0.0970
Combi.UnO_E.exCI	931	0.3222	0.8367	0.3193	0.6807	0.3652	0.1177

In addition, five MP analyses were undertaken on an earlier version of the combined morphological data set consisting of 166 characters and 76 taxa, experimenting with consistency indices, ordering characters and taxon sampling 3.3.

The selection of the outgroup taxon is important and the topology may change depending on the distance of relation of the outgroup to the ingroup (Huelsenbeck & Rannala, 2000). Here, tragulids were chosen as the outgroup for all analyses; some programmes include the outgroup information in the tree building process, some programmes do not. In the latter cases the outgroup criterion was set after the analysis when the topology was edited.

All MP analyses including bootstrap analyses were undertaken using PAUP* v.4.0b (Swofford, 2002) and the following settings:

```
BEGIN PAUP;
outgroup <outgroup taxon>;
set autoclose=yes;
set criterion=parsimony;
set maxtrees=100 increase=auto;
pset mstaxa=polymorph;
ctype ord:<no. of characters>;
hsearch swap=tbr addseq=random nreps=1000;
savetrees file=<filename>.tre;
contree all/strict = yes file=<filename>.tre;
cleartrees nowarn=yes;
bootstrap nreps=1000;
hsearch addseq=random nreps=1000 swap=tbr;
```

```
savetrees from=1 to=1 file=<filename>.tre format=altnex brlens=yes
savebootp=NodeLabels MaxDecimals=0;
END;
```

The analyses used a heuristic search running 1000 replicates. An exhaustive search and branch and bound search was ruled out by the large number of taxa. Sequences were added randomly using the tree-bisection-reconnection (TBR) algorithm. Polymorphisms were treated as real polymorphisms. Of all sampled trees, the strict consensus was calculated, which summarises all splits common to a certain percentage of all trees generated during the tree search process. Additionally, the Adam's consensus tree was calculated, which, in contrast to the strict consensus tree, shows those splits, which were not contradicted within all generated trees. Because of this, Adam's consensus topologies are usually better resolved (which is, of course, not necessarily the better topology). For all analyses bootstrap analyses were undertaken. Consistency indices and a detailed apomorphy list (see supplementary information <https://edoc.ub.uni-muenchen.de/view/autoren/index.H.html>) were calculated for the strict consensus trees of all MP analyses using the command

```
describe tree/apolist.
```

The BI analyses were undertaken using MrBayes 3.2.4 (Ronquist et al., 2012) and ran for 50 million generations with two runs à four chains at a temperature of 0.35; trees were sampled at every 5000th generation. The MrBayes block was used with the following settings:

```
BEGIN MRBAYES;
set autoclose=yes nowarn=yes;
outgroup <outgroup taxon>;
lset applyto=(all) rates=gamma coding=inf;
prset applyto=(all) symdirihyperpr=fixed(infinity);
unlink statefreq=(all) revmat=(all) shape=(all);
ctype ord:<no. of characters>;
mcmcp ngen=50000000 relburnin=yes burninfrac=0.25 printfreq=5000 temp=0.35
diagnfreq=50000 samplefreq=5000 nchains=4 savebrlens=yes stoprule=yes
stopval=0.01;
mcmc;
sump;
sumt;
END;
```

All ML analyses started at a random number seed and were run under the Mk-model (Lewis, 2001) with the Γ model rate of heterogeneity without invariant sites. The analyses also included a rapid bootstrap search of 100 replicates starting at a random number seed. The output topology represents the best tree (= most likely tree) instead of a consensus as the summary of the tree search. The ML analyses were undertaken using RAxML v.8.0.26 (Stamatakis, 2014) with the following specifications:

```
-f a -m MULTIGAMMA -q MLMorphpartitions.txt -K MK -p 12345 -x 12345 -# 100
-s MLMorph.phy -n MLMorph.out
```

Single Fossil Analyses (SFA)

In order to reduce missing data and noise in the data set, three sets of analyses were run, which included only one fossil taxon at a time. The first approach included the entire morphological data set and was combined with the complete mitochondrial genome (including cytochrome b (*Cytb*) only for taxa without a complete mitochondrial genome) to facilitate tree search. The data set comprised 78 taxa and 15072 characters in total. In each analysis 47 extant and one fossil species were included. The second approach was on the same data set, but excluding the 5 non-cervid ruminants; it consisted of 73 taxa and 15072 characters. In each analysis 42 extant and one fossil species were included. The third approach was based on the morphological character matrix and a constraint topology. This constraint topology was generated in an analysis of the combined molecular data (see Chapter 5) including only those taxa, for which morphological data were available. The third SFA data set comprised 73 (excluding 5 non-cervid ruminants) taxa and 168 morphological characters. In each analysis only 42 extant and one fossil species were included. All SFA analyses were run with the same PAUP* specifications as listed above.

Evolutionary Placement Algorithm (EPA)

Berger et al. (2011) introduced an algorithm implemented in RAxML, which improves accurate placement of morphology-based fossils in a tree. The EPA analysis is a two step process. The first step is a morphological weight calibration, where a molecular tree is provided alongside with the morphological matrix. All taxa have to entirely overlap in this step, therefore, only extant taxa are included. The second step invokes the actual evolutionary placement algorithm using the same molecular tree as in step one, the morphological matrix, this time including extant and fossil taxa, and the weight vector output from step one.

The molecular tree used here was specifically generated in RAxML based on a data set including only the 41 cervid species for which morphological data is available and *Hymoschus aquaticus* as outgroup and 17709 base pairs (nuc and mtDNA). The morphological matrix for step one contained 42 species and 168 morphological characters. The morphological weight calibration was undertaken using the following command:

```
raxmlHPC -f u -m MULTIGAMMA -t moleculartree.tre -s morphomatrix.phy
-p 12345 -n output
```

The second step of the EPA analysis used the same molecular tree, the morphological matrix now containing 73 taxa, and a file named RAxML_weights.out obtained from the first step. The command is:

```
raxmlHPC -f v -m MULTIGAMMA -t molecular.tree.tre  
-s completemorphomatrix.phy -a weights.out -n output
```

3.3 Results

3.3.1 Morphology

General

The overview of the character completeness 3.3 shows that even Miocene taxa are represented by relatively well sampled species. All fossil taxa are sampled for at least three partitions. The most incomplete fossil is *Eostyloceros hezhengensis* sampled from the literature with 70 % missing data followed by *Ligeromeryx praestans* with 68 % missing data. The most complete fossil cervids are *Megaloceros giganteus* with 0 % missing data and *Candiacervus ropalophorus* with 6 % missing data. Most of the other fossil taxa have around 50 % missing data.

Figure 3.4 shows Q plotted against the completeness of all fossil taxa. There is no trend of higher Q-values in more recent fossils; instead, fossils of the Miocene, Pliocene and Pleistocene are evenly distributed. However, there is a trend that the more complete a taxon is the more evenly the sampling is spread across partitions. This can be observed on the seven taxa with the highest Q-values, *Dicrocerus elegans*, ‘*Cervus*’ *philisi*, *Axis lydekkeri*, *Procervulus dichotomus*, *Eucladoceros ctenoides*, *Candiacervus ropalophorus*, and *Megaloceros giganteus*, which are also those taxa that are most complete.

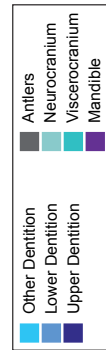


Figure 3.3: Diagram of the characters available for each cervid species. Extant species are arranged in alphabetical starting from the left, fossil cervids and the two non-cervid fossils are arranged from the youngest to the oldest starting from the last extant taxon to the right. Morphological characters were divided into seven partitions. The y-axis shows the absolute number of characters present in a particular taxon.

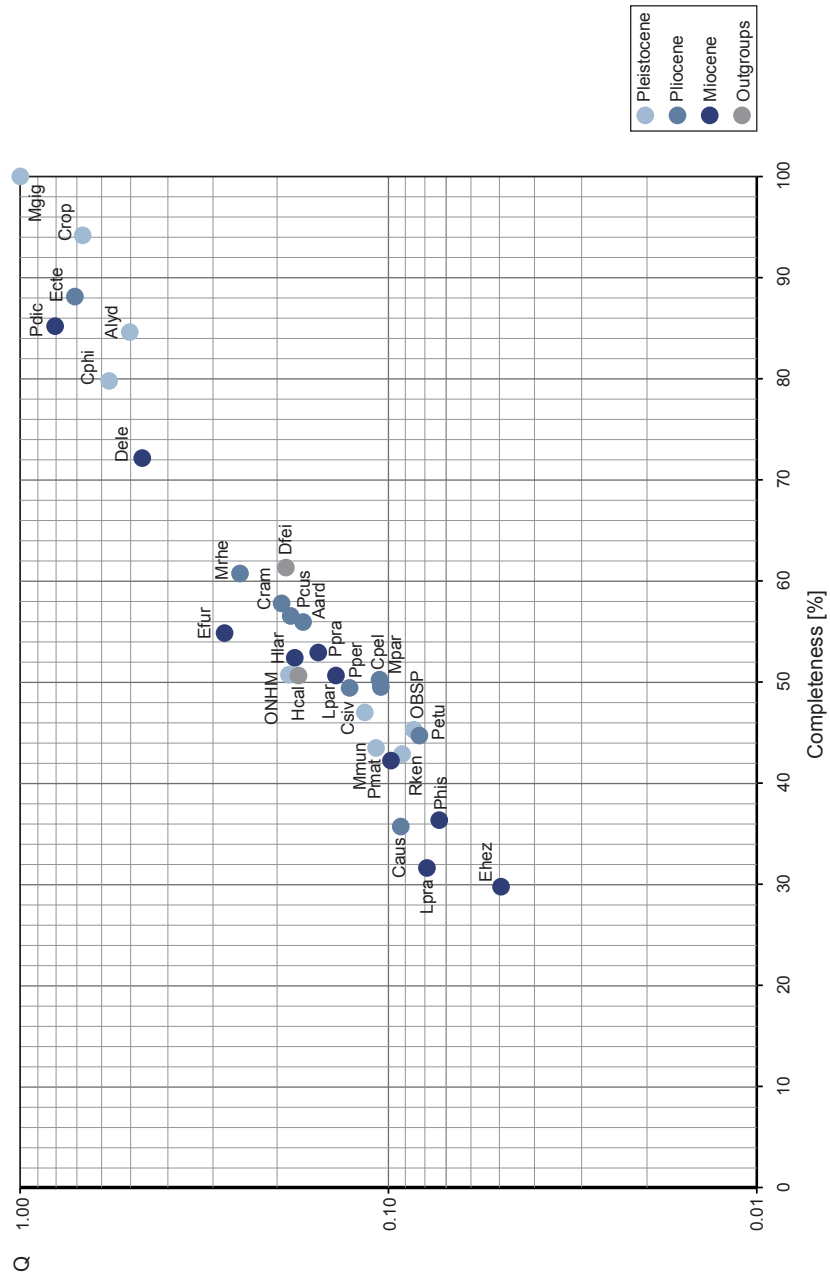


Figure 3.4: In this diagram, Q-values are on a logarithmic scale as a representation of how well balanced each fossil is sampled across the seven partitions and are plotted against the completeness (= relative number of characters present) of each fossil. There is no trend for higher Q-values in more recent species. The abbreviations are the first letter of the genus and the first three letters of the species epithet.

Cranium

Some morphological characters in ruminants are likely to have evolved convergently and bear therefore high levels of homoplasy, which may cause difficulties in reconstructing phylogenetic relationships (Bouvrain et al., 1989; Douzery & Randi, 1997).

Particularly cervids have a highly conservative cranial morphology (Lister, 1996; Merino & Rossi, 2010). Osteological morphological differences between two species are often mainly based on body measurements or the antler morphology. Since antlers mostly have more distinctive, generic features than other anatomical characters, classifications of cervids, especially fossils, are often based on those traits (Kurtén, 1968; Fry & Gustafson, 1974). However, this method has shown to be inadequate and thus, the validity of some fossil cervid taxa is doubtful (Merino & Rossi, 2010).

All cervids share the typical anatomical features, such as two lacrimal foramina, a praeorbital vacuity, and a lacrimal fossa. In lateral view the dorsal outline is characterised by a convex braincase, which makes a transition to the concave fronto-nasal line, continuing in a straight nasal line. The anterior extension of the snout is moderate depending on the overall size of the cervid species. The basicranial outline in lateral view is flexed. There is a detailed, species-specific description in Appendix D.

Some variation within these cervid specific features was observed. The praeorbital vacuity varies in size and form, the lacrimal fossa ranges from deep and round, covering a large proportion of the facial aspect of the skull, to shallow, almost absent (particularly in females). There were consistently two lacrimal foramina, but their position on the orbit rim and to each other varied. The most anterior part of the praemaxillae is moderately tapering in most cervids; in some cervids, the praemaxillae taper more considerably and some species have small mediad pointing protrusions at the anteriormost end of the praemaxillae.

Almost all cervids have two palatine foramina, only in a few specimens four palatine foramina were observed. Considerable differences were observed in the extension of the vomer and the closing of the bar between the temporal foramina. The auditory bullae are oval and only weakly inflated in most cervids; they often have one prominent medial protrusion, some bullae have additional smaller protrusions. In a few cervids the bullae are more inflated, with a weak protrusion. The direction of the meatus acusticus externus can be oriented laterally or posterolaterally. There is variation in the development of the basioccipital tuberosities.

Most cervids have a weakly to moderately posteriad extending protuberantia occipitalis. Only in *Alces*, this structure strongly protrudes posteriad. The development of a sagittal crest is present in some Miocene cervids, but absent in all other cervids. The pedicle contains several characteristics for distinguishing fossil cervids and/or groups of living cervids. One feature is the insertion point of the pedicle which is directly above the orbit in early fossil cervids, but moves more posterior in more recent cervids. Another feature is the inclination of the pedicle, which is upright in most Miocene cervids and more declined in more recent cervids. Muntiacini, *Euprox* and *Eostyloceros* have long and considerably inclined pedicles. The third remarkable difference in the pedicles is the length. Pedicles are very long in Muntiacini and most Miocene cervids and are short in all other cervids.

There is a lot of inter- and intraspecific variation in antlers, which has been covered in detail in Chapter 2. The antler morphology of *Palaeoplatyceros* and lagomerycids is unique;

the antlers of other Miocene cervids is characterised by a simple bifurcating pattern, in which rarely more than two tines are present. Also, the length of the antlers is relatively short in early cervids. From the late Miocene onwards, more complex branching patterns developed and the length of antlers increased. In extant cervids, short and simple antlers and long and more complex or palmated antlers are present. Many extant cervids develop exactly three tines.

Dentition

Upper premolars and molars. Figure 3.5 provides an overview of the occlusal morphology of the upper post-canine dentition of extant cervid species and Figure 3.6 is a schematic representation of how cones are connected via crests and walls. The occlusal morphology and schematic representation of the upper dentition of fossil cervids is in Figures 3.9 and 3.10.

P2 The P2 has a simple morphology with at least one central fold; it is triangular and normally longer than the P4 in Miocene cervids, while the P2 is usually similar in length to or shorter than the P4 in Plio-, Pleistocene or extant cervids. In many extant species it can also be triangular. Sometimes the P2 has a separate anterolingual and posterolingual cone.

P3 The P3 is in most cases horseshoe-shaped with at least one central fold. Sometimes the antero- and posterolingual cone are separate. In a few fossil species a lingual cingulum is developed.

P4 The P4 is horseshoe-shaped with at least one central fold. Several fossil species have a well developed lingual cingulum. The lingual cone is sometimes separated into an antero- and posterolingual cone. In some species there are additional smaller central folds in addition to the main central fold; this could be observed in all premolar positions, but most often in P4. Sometimes the main central fold is serrated. *Rangifer* is the only cervid without any central folds on the upper premolars.

Upper molars. All upper molars have a similar morphology and are quadrangular. In M3 the posterior lobe is sometimes distinctively smaller than the anterior lobe. Entostyles are variably present on one to three molars, but are absent in some species or specimens. In some species the entostyle(s) has/have a λ -shaped morphology, especially in later wear. Several species have an anterior cingulum. Several fossil cervids have a lingual cingulum. The protocone and metaconule folds are variably present. In a few species the premetaconulecrista is serrated.

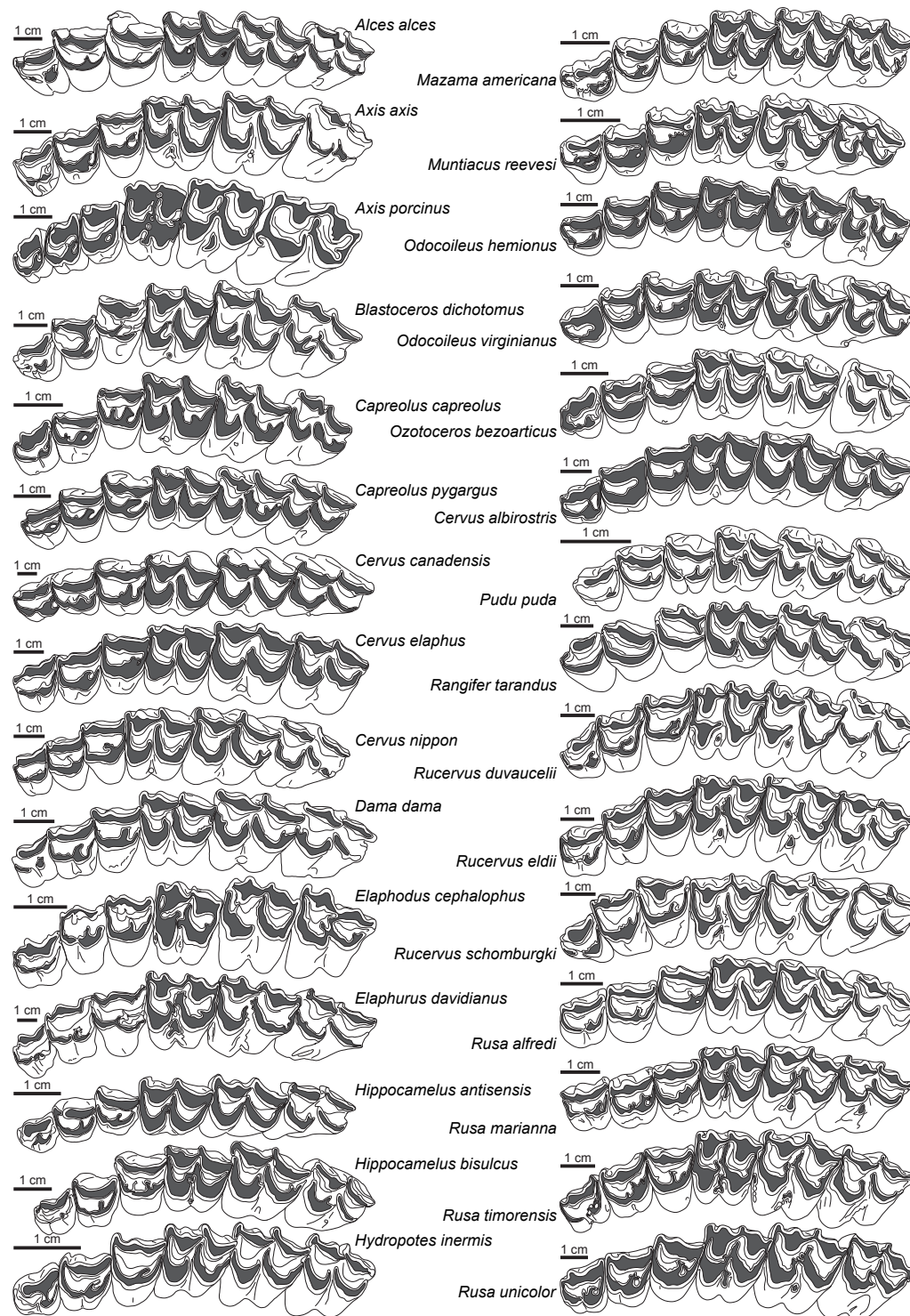


Figure 3.5: Overview of the upper post-canine dentition of 30 extant cervid species in occlusal view.

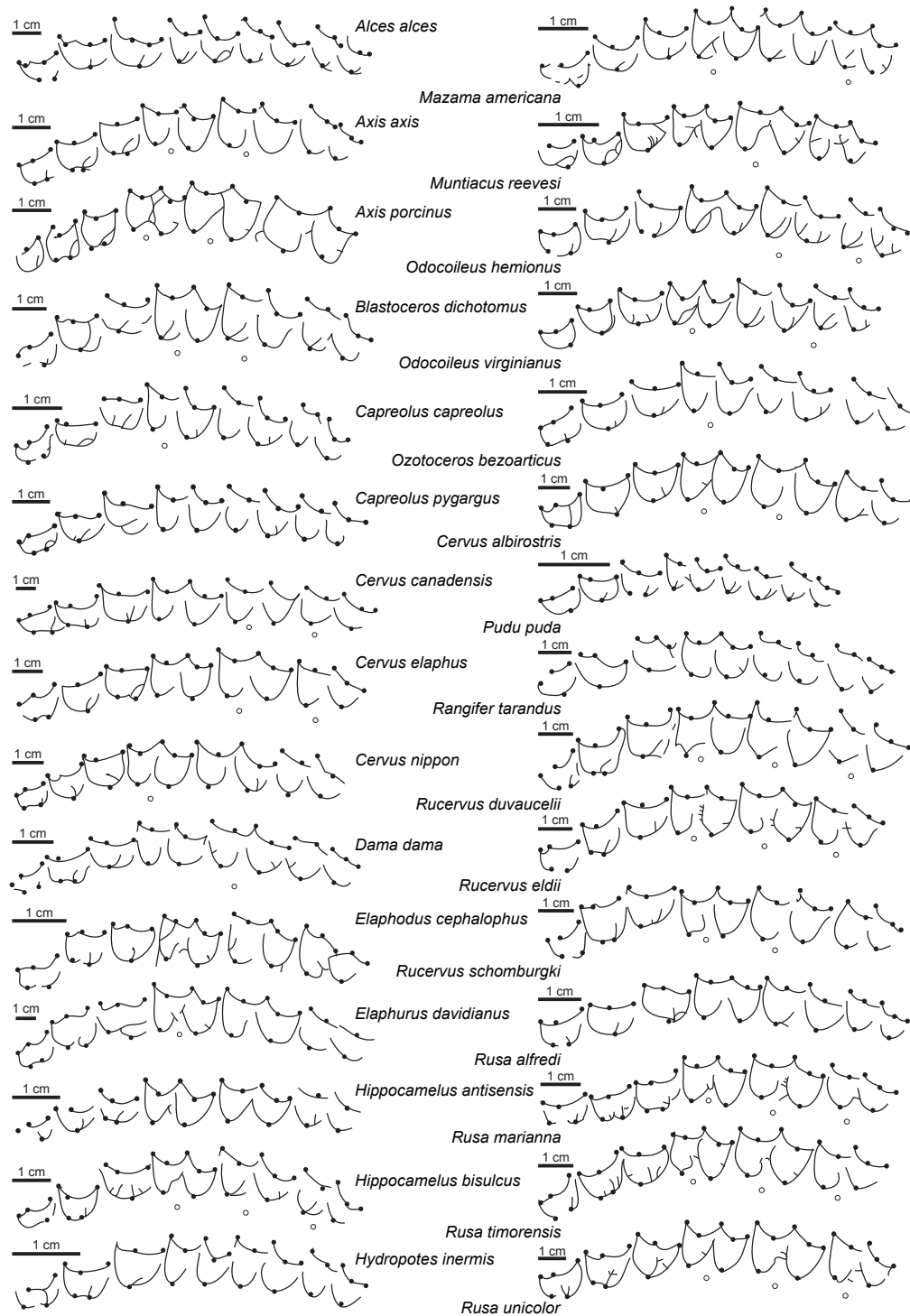


Figure 3.6: Schematic overview of the upper post-canine dentition of 30 extant cervid species in occlusal view. Only cristae (lines) and cones (dots) are shown.

Lower premolars and molars. Figure 3.7 provides an overview of the occlusal morphology of the lower post-canine dentition of extant cervid species and Figure 3.8 is a schematic representation of how conids are connected via crests and walls. The occlusal morphology and schematic representation of the lower dentition of fossil cervids is in Figures 3.9 and 3.10. The p1 is usually absent in cervids.

p2 The p2 generally has a simple morphology with two conids (mesolabial conid, posterolabial conid); most often the posterolingual conid is present and a posterior stylid and cristid. The transverse cristid is often present and the anterior conid is sometimes present. In some species there is a labial incision. A strong reduction in length could be observed in *Mazama* and particularly in *Ozotoceros*. In a few specimens the p2 is missing.

p3 Almost all tooth elements are usually present in p3. An anterior conid and anterior stylid are present in almost all cases. While the mesolingual conid is commonly present, the mesolingual cristids are absent in most species. The p3 is not molarised except for in *Alces* and *Rangifer*, where the mesolingual cristids are well developed and form an initial closing of the anterior valley.

p4 The p4 is the most variable tooth in cervids. The morphology ranges from simple without developed mesolingual cristids (e.g., *Axis axis*, *Procervulus*, *Dicrocerus*) and sometimes without an anterior stylid to highly molarised. The molarised p4 have either only the anterolingual cristids closing the anterior valley, e.g., *Cervus*, *Dama*, or have a restructured tooth morphology as in *Alces* and *Rangifer*.

Lower molars. All lower molars have a similar morphology; m1 and m2 are two-lobed, m3 is three-lobed. Ectostylids are variably present on one to three molars, sometimes they are absent. In most Miocene cervids external postprotocristids are present on all molars. Anterior cingulids are present in several species, usually more prominent on the more anterior molar position(s). The metastylids can be bent labiad in some species; this is particularly well developed in *Alces*. The third lobe on m3 is variable; most often the hypoconulid and entoconulid are connected via the postento- and posthypoconulidcristids and form a crescent-shaped structure. Sometimes, especially in later wear, the preentoconulidcristid fuses with the entostylid. The third lobe of m3 may also only consist of one conulid, mostly the hypoconulid. Rarely, there is a fold protruding from the hypoconulid into the back fossa of m3.

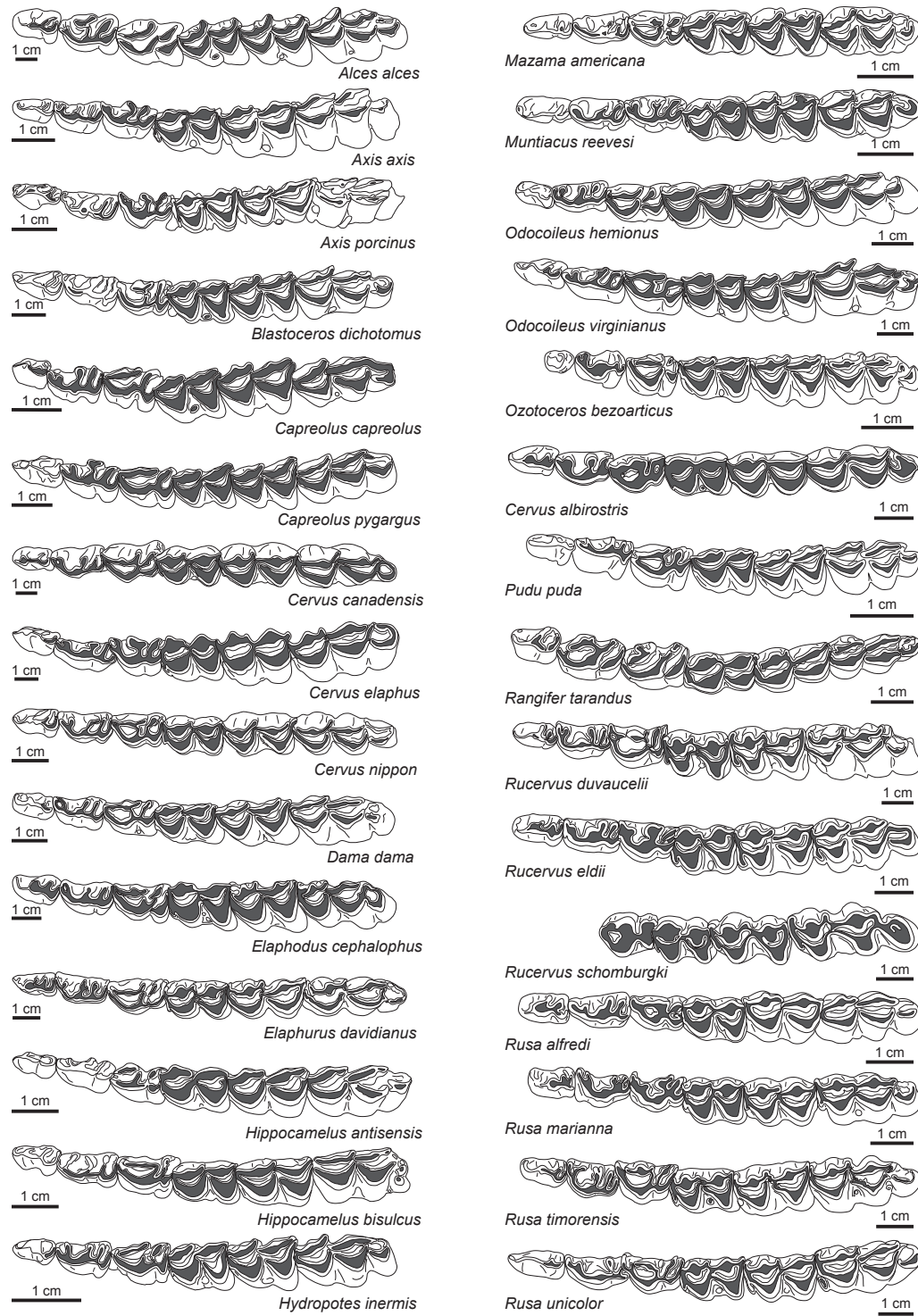


Figure 3.7: Overview of the lower dentition of 30 extant cervid species in occlusal view.



Figure 3.8: Schematic overview of the lower dentition of 30 extant cervid species in occlusal view. Only cristids (lines) and conids (dots) are shown.

Other dentition

Upper canines The upper canines are enlarged in all Miocene cervids, similar to those in *Muntiacus* today, and curved posteriad. From the Pliocene onwards they become strongly reduced in size and are lost in some species. Most extant cervines have small upper canines, a few lack upper canines. In extant capreolines upper canines are usually absent or sometimes represented as tiny deciduous upper canines. All extant muntiacines have enlarged upper canines and *Hydropotes* has strongly elongated, sabre-tooth-like upper canines.

Lower incisors and canines The lower incisors, i1–i3, have a simple spatulate morphology. The crown width decreases from i1 to i3, i.e., i1 typically is distinctively broader than i2 and i3. This also is already observed in fossil cervids. Exceptions are *Alces*, *Hippocamelus*, and *Pudu*, where i1 is only a little broader than i2. Particularly in some small cervid species, e.g., *Mazama*, *Muntiacus*, and *Elaphodus*, the i1 is extremely broad compared to the other incisors. In some cervids the i3 is reduced in width to a pointed crown. In *Elaphurus davidianus* the lower incisors and canines have a strong crest on the lingual side from the base to the crown and some additional small protrusions at the base. All lower canines in Cervidae are incisiform and are almost indistinguishable from i3. In some specimens they may be slightly more pointy than the incisors. It was observed that the lower incisors and canines are strongly procumbent in aged individuals, while they are relatively upright in adults.

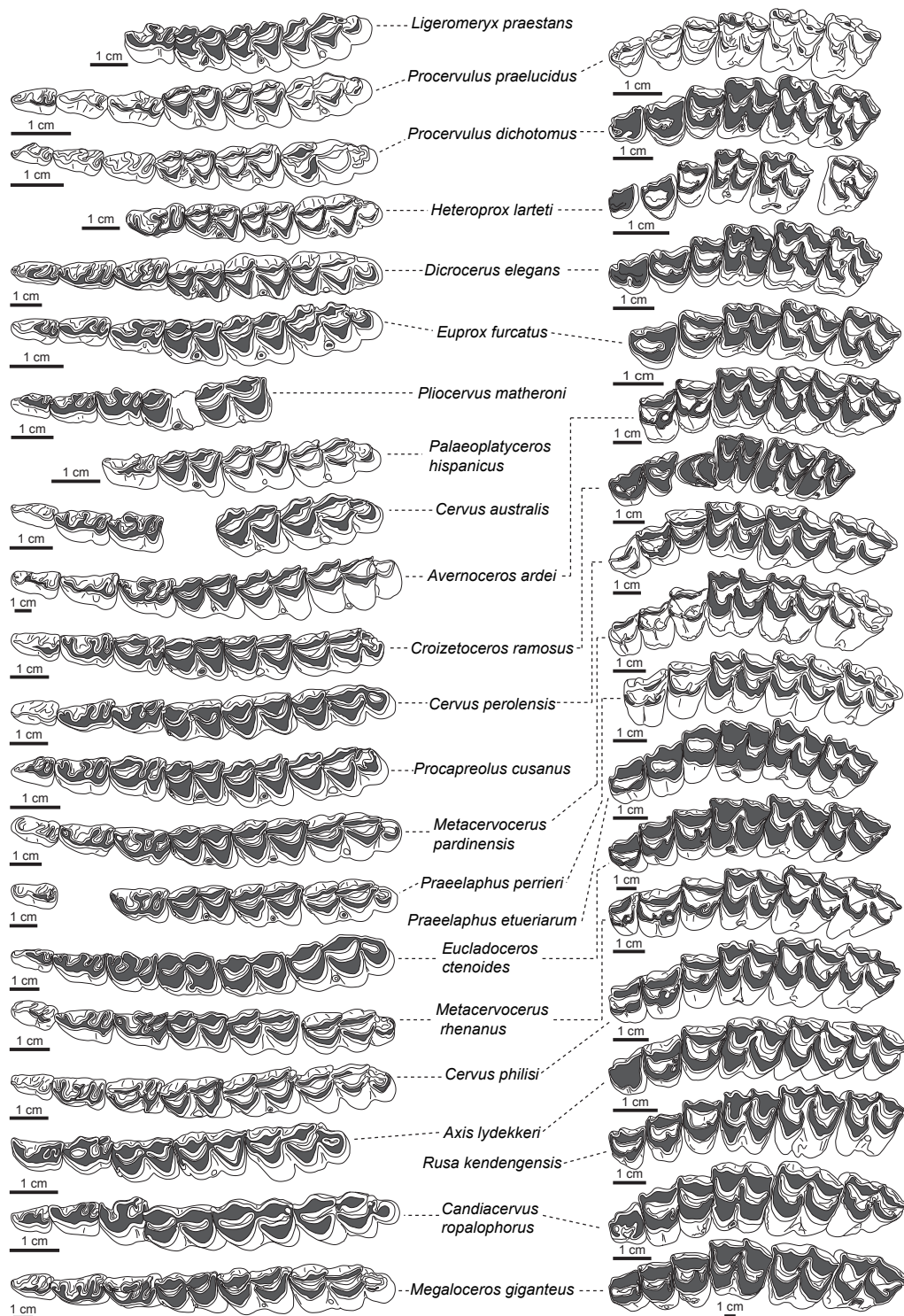


Figure 3.9: Overview of lower (left) and upper (right) dentition of the fossil cervids studied in occlusal view.

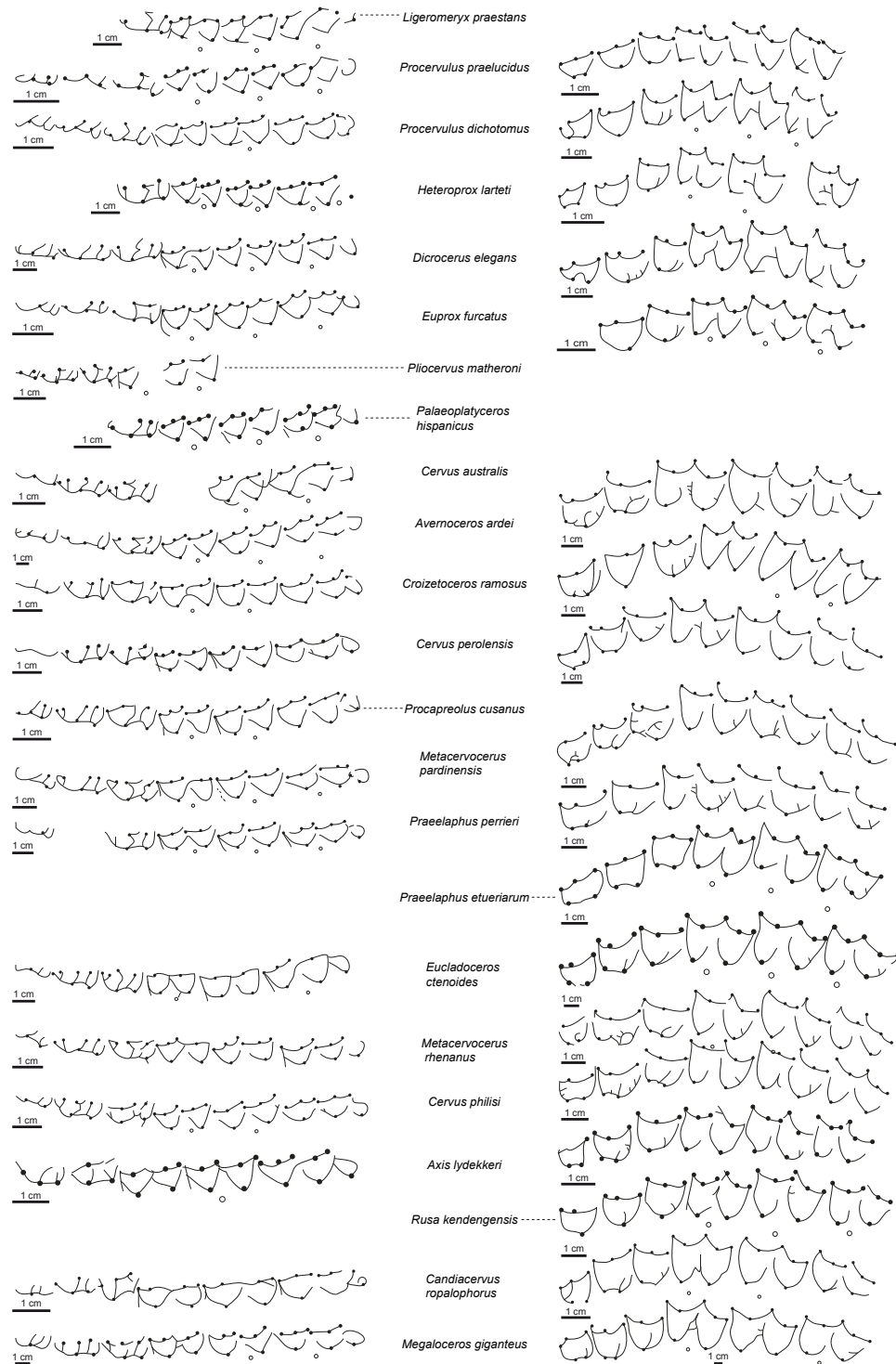


Figure 3.10: Schematic overview of lower (left) and upper (right) dentition of the fossil cervids studied in occlusal view. Only cristids/cristae (lines) and conids/cones (dots) are shown.

3.3.2 Phylogenetic Analyses

Stepping Stone Analyses

In total, five SS sampling analyses were undertaken; the first set of three analyses was used to determine the partitioning scheme, running one analysis with an unpartitioned, unordered data set with the Γ distribution, one with a minimal partitioning scheme, dividing the data set into a cranial and dental character set. The third data set was run with the maximal possible partitioning scheme, dividing the data set into, upper cheek dentition, lower cheek dentition, other dentition, mandible, viscerocranium, neurocranium and antler characters. The fourth analysis was run with the unordered, unpartitioned data set, without the Γ distribution, and the fifth analysis was run with an ordered, unpartitioned data set with Γ distribution. The decision for one hypothesis is based on the Bayes Factor

$$BF_{01} = \log \text{Hypothesis}_0 - \log \text{Hypothesis}_1$$

If $BF > 0$ hypothesis 0 is favoured, if $BF < 0$ hypothesis 1 is favoured. Comparing BF's of the three analyses testing the partitioning scheme (Tab. 3.4) showed that the data set is best analysed unpartitioned, as in both cases tested against maximal and minimal partitioning, the BF's of the unpartitioned data set were favoured. Testing the use of a Γ distribution and ordering showed that Γ distribution should be used and ordering characters is better than not ordering characters. This shows that the data is best represented when run unpartitioned, with character state ordering, where applicable, and with a Γ distribution. However, BI and MP analyses were run unordered and ordered for each character set for comparison. See Table 3.2 for details.

Table 3.4: Results from the Stepping Stone Sampling analyses. Values represent mean Bayes Factors calculated from the mean of the sum of the marginal likelihoods of the two runs of each analysis.

	Unpart ordGam	Un- ordGam	PartMin	PartMax	UnPart NoGam	UnPartOrd
UnpartUnord Gam	—		-18,792119	-22,391951	-69,252349	4,000185
PartMin	18,792119		—	-3,599831	—	—
PartMax	22,391951		3,599831	—	—	—
UnPartNo Gam	69,252349		—	—	—	—
UnPartOrd	-4,000185		—	—	—	—

Standard Phylogenetic Analyses

Dental Character Set The strict consensus and the Adam's consensus tree resulting from the MP analysis including all taxa and unordered character states are very similar to each other and relatively well resolved (Fig. 3.11). The main difference between those two topologies is a clade consisting of six Miocene cervids in the Adam's consensus tree, which was unresolved in the strict consensus tree. Most clades consist of mixed capreoline, cervine, and non-cervid taxa. The *Elaphurus-Rucervus-Rusa*-clade was recovered with both *Axis* species as the sister taxon to it, and *Cervus elaphus* as the sister taxon to all of them. There was also a clade containing *Dama dama*, *Arvernoceros ardei*, *Metacervocerus pardinensis*, and *Metacervocerus rhenanus*. Except for *Muntiacus feae* and *Elaphodus cephalophus* Muntiacini formed a clade including the fossil *Muntiacus muntjak* and *Dicrocerus elegans*. Unfortunately, no bootstrap values could be obtained from this analysis.

In the MP analysis using character state ordering on the full taxon sampling, the strict consensus tree recovered only a few nodes (Fig. 3.12); the *Elaphurus-Rucervus-Rusa*-clade with both *Axis* species as the sister taxon, a *Muntiacus*-clade consisting of six taxa, and a few sister taxon relationships. In both topologies *Lagomeryx parvulus* and *Palaeoplatyceros hispanicus* were placed between the outgroup and all remaining taxa. In the Adam's consensus tree more nodes were resolved (Fig. F.1), but apart from the two clades already mentioned above, cervine, capreoline, and non-cervid taxa were mixed. Unfortunately, the bootstrap analysis of this data set crashed before completion; therefore, only interim bootstrap values were available and should be interpreted with caution. Only a few nodes are poorly supported.

The strict consensus tree of the MP analysis on the extant only taxon sampling was largely unresolved, the Adam's consensus tree recovers more nodes (Figs 3.13, F.2). A few clades were supported by relatively weak bootstrap values. There is a clade consisting of *Rucervus*, *Rusa*, *Elaphurus*, and *Axis*. The sister taxon relationship of the two *Axis*-species and *Capreolus*-species were recovered. All other clades or polytomies consisted of mixed capreoline, cervine, and outgroup taxa.

In the MP analysis on the fossil only data set with ordered character states *Hypotragulus calcaratus* was used as outgroup. The strict consensus tree contained several polytomies, the Adam's consensus tree was better resolved (Figs 3.14, F.3). A bootstrap analysis weakly supported the sister taxon relationship of *Heteroprox larteti* and *Euprox furcatus*. Miocene, Pliocene, and Pleistocene taxa were distributed across the tree, none of them formed a distinct clade.

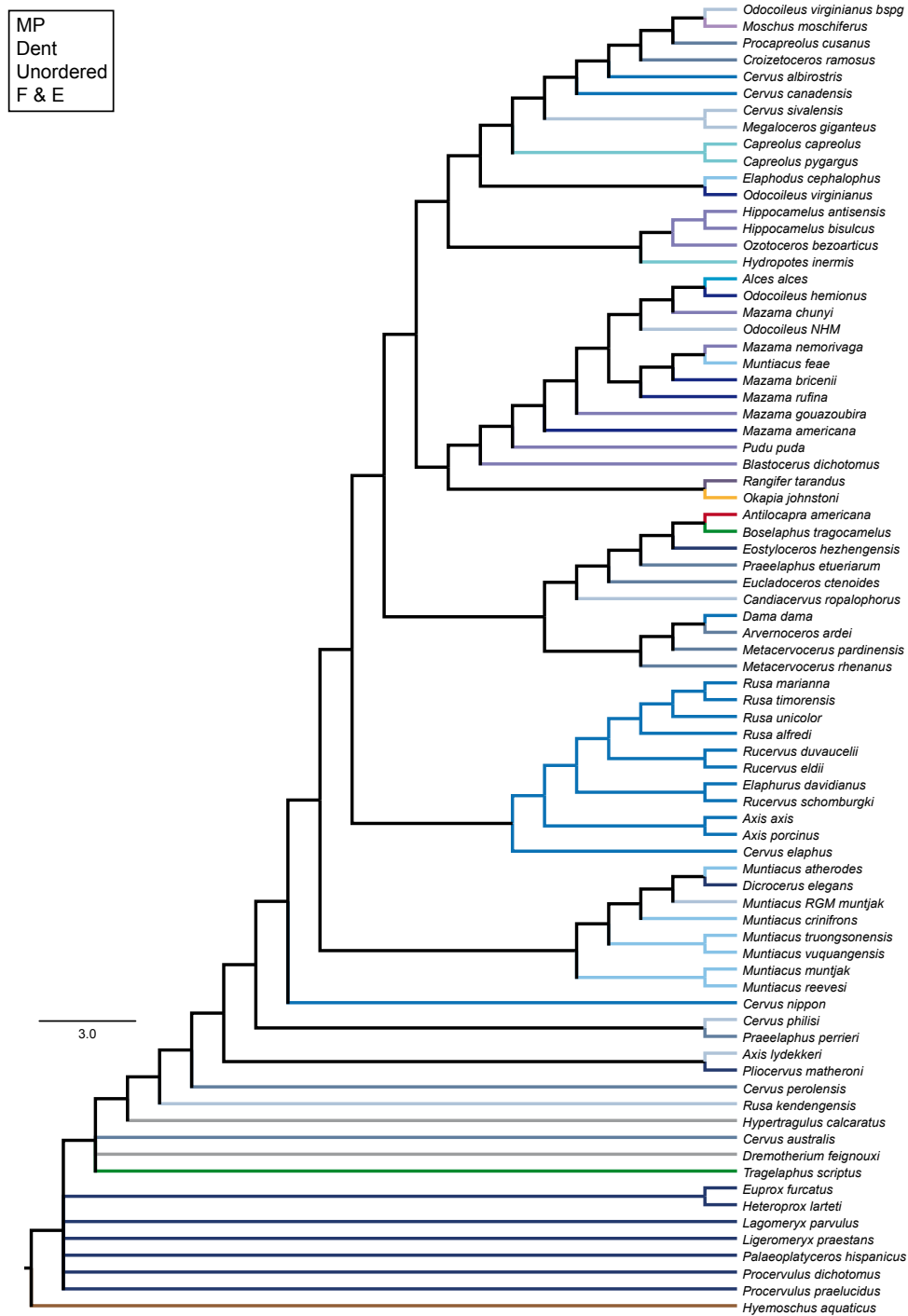


Figure 3.11: Consensus topology of the MP analysis based on the unordered dental character set for fossil and extant taxa.

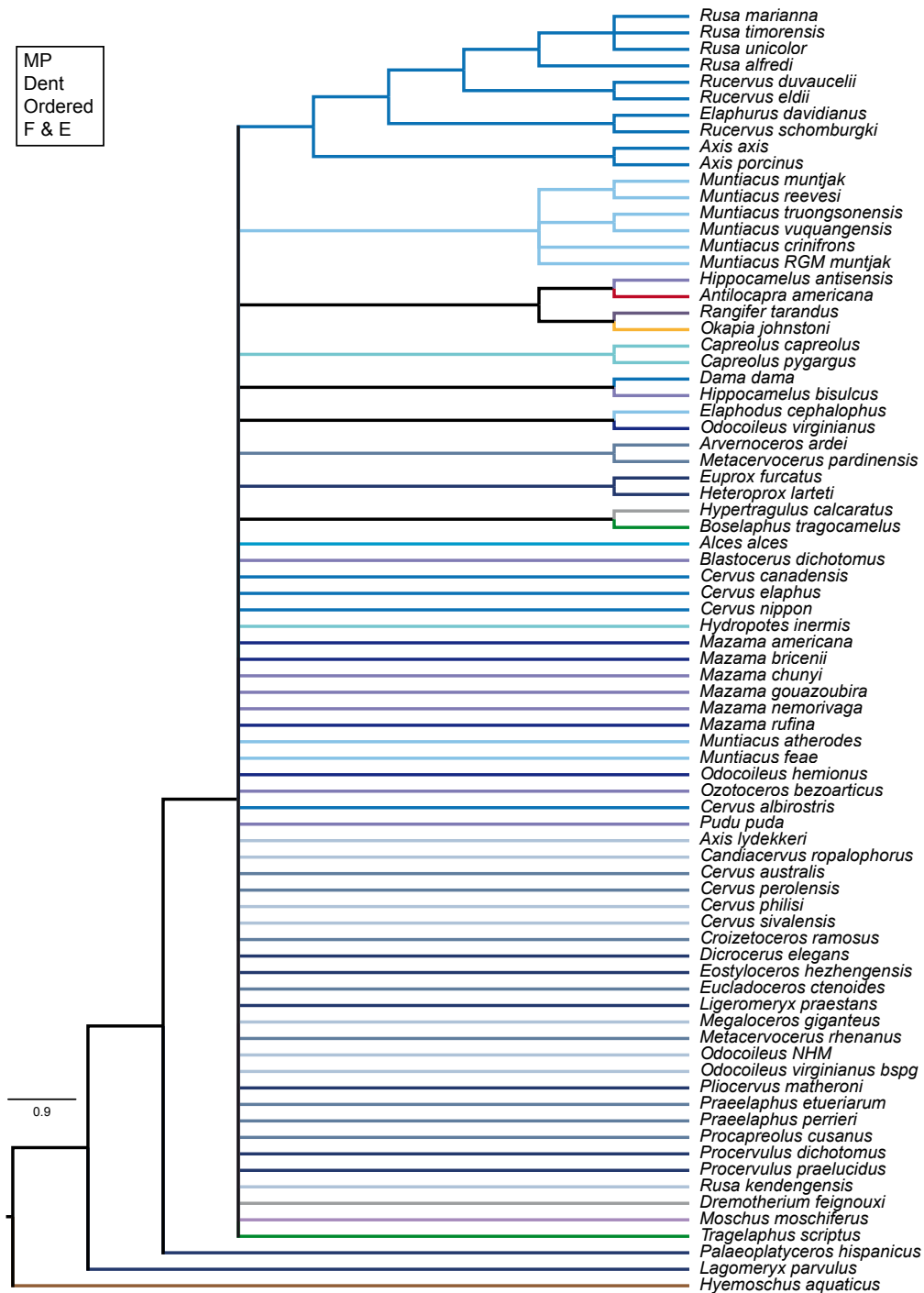


Figure 3.12: Consensus topology of the MP analysis based on the ordered dental character set for fossil and extant taxa.

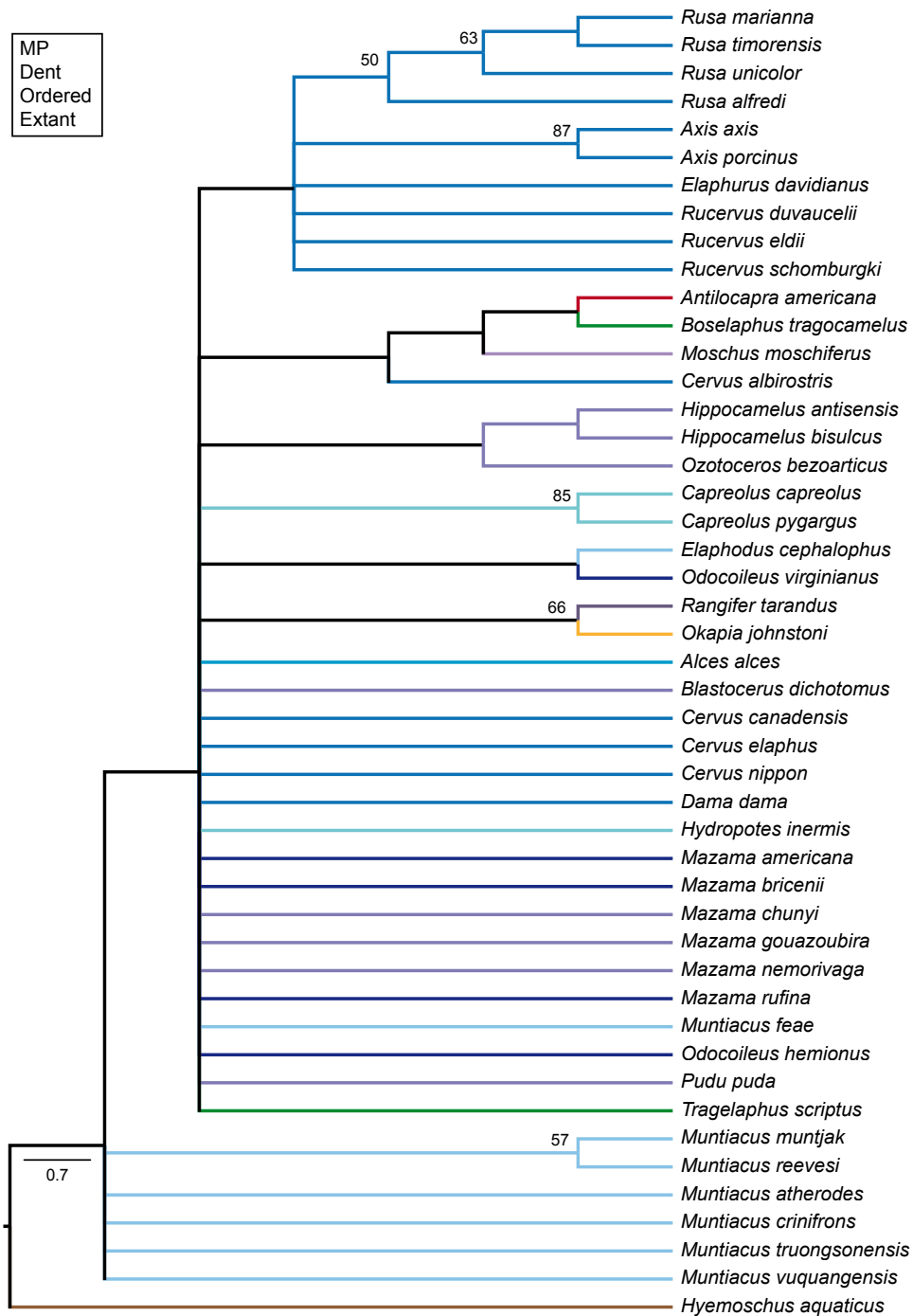


Figure 3.13: Consensus topology of the MP analysis based on the ordered dental character set for extant taxa.

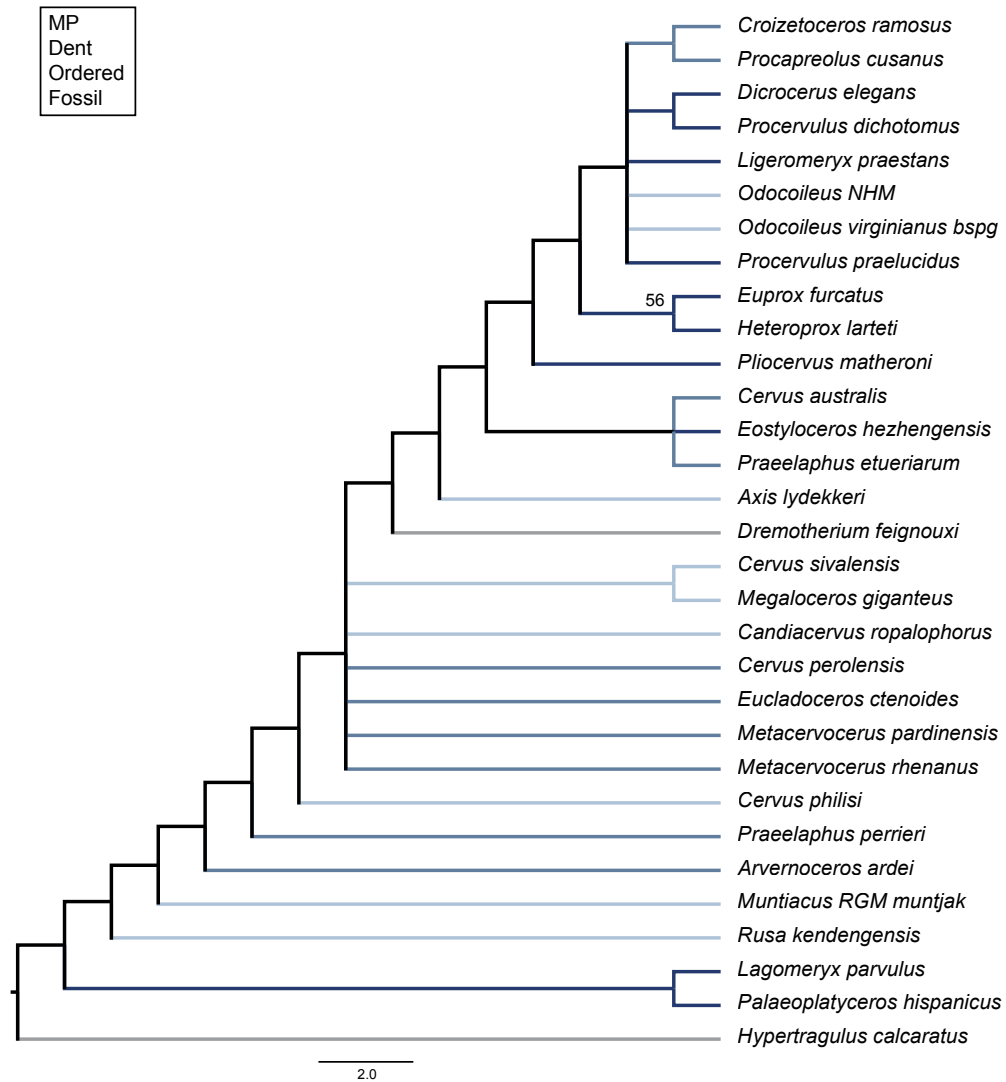


Figure 3.14: Consensus topology of the MP analysis based on the ordered dental character set for fossil taxa.

The ordered and unordered BI analyses of the dental character set resulted in congruent and largely unresolved topologies (Fig. 3.15). The posterior probabilities differed slightly in both topologies. Only a few taxa formed clades mostly with poor support. Sister taxon relationships existed between *Axis axis* and *Axis porcinus*, *Capreolus capreolus* and *Capreolus pygargus*, *Okapia* and *Rangifer tarandus*, *Muntiacus truongsongensis* and *Muntiacus vuquangensis*, and *Dicrocerus elegans* and *Procervulus dichotomus*. There was one relatively well supported clade consisting of *Elaphurus* as the sister taxon to *Rucervus* and *Rusa*; within that clade all four *Rusa* species formed a monophyletic group, all three *Rucervus* species were unresolved sister taxa to the *Rusa*-clade. There was a clade unit-

ing all taxa except for *Lagomeryx parvulus*, *Palaeoplatyceros hispanicus*, and the outgroup unresolved in a big polytomy together with the mentioned clades.

In the ML topology bootstrap support values are largely low (Fig. 3.16). Nine Miocene cervid taxa and *Cervus australis* were placed between the outgroup and all other taxa, six living muntjacs and the fossil *Muntiacus muntjak* formed a clade, the *Elaphurus-Rucervus-Rusa*-clade was recovered including both *Axis* species between *Elaphurus davidianus* and the rest of the clade; the highest support values were within that clade. The sister taxon relationship between both *Capreolus* species was supported. The majority of taxa formed mixed cervine, capreoline, and non-cervid taxa clades.

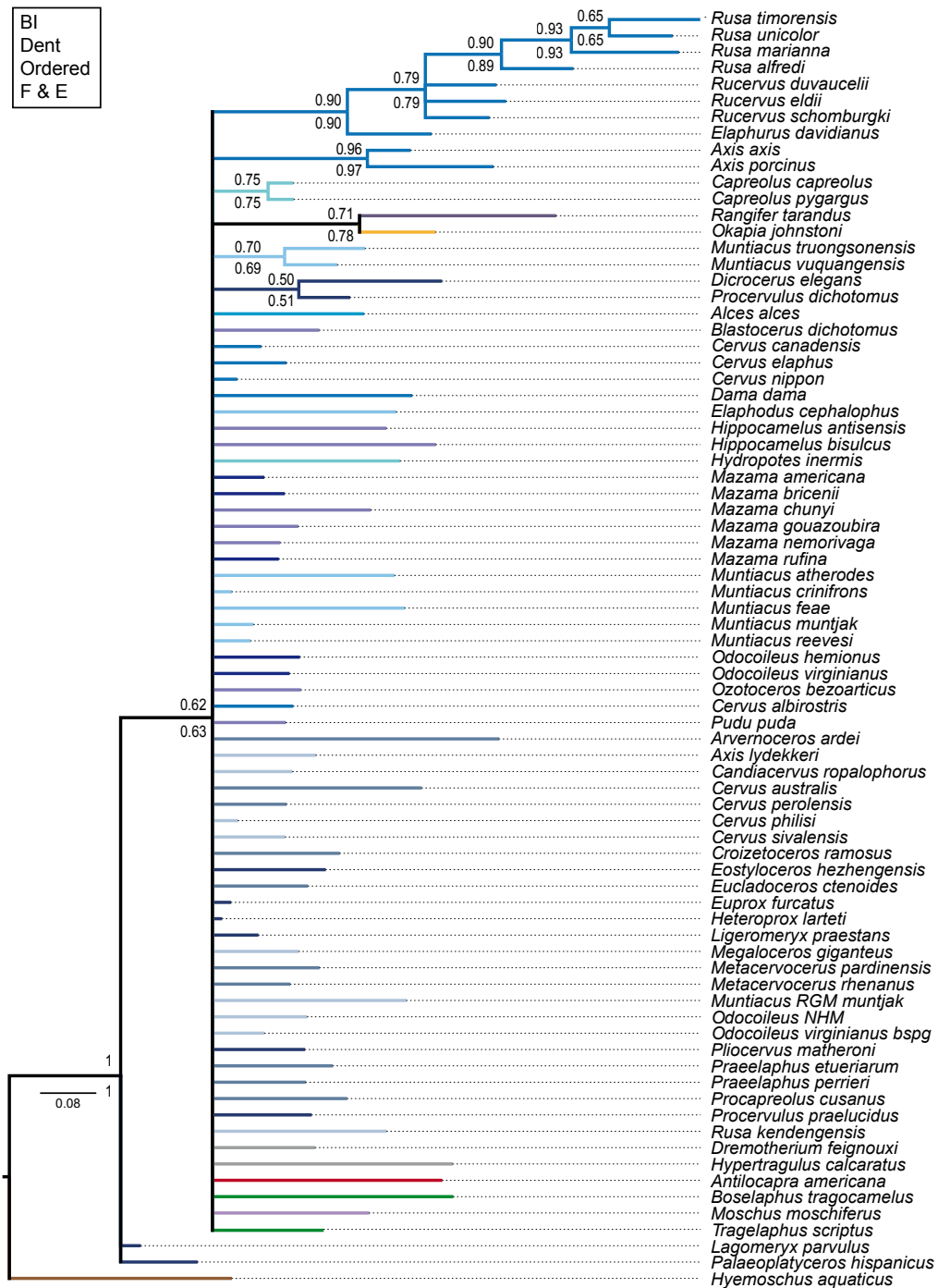


Figure 3.15: Consensus topology of the BI analysis based on the ordered dental character set for fossil and extant taxa. Posterior probabilities of this analysis are above the respective branch, the posterior probabilities of the unordered analysis are below the branches.

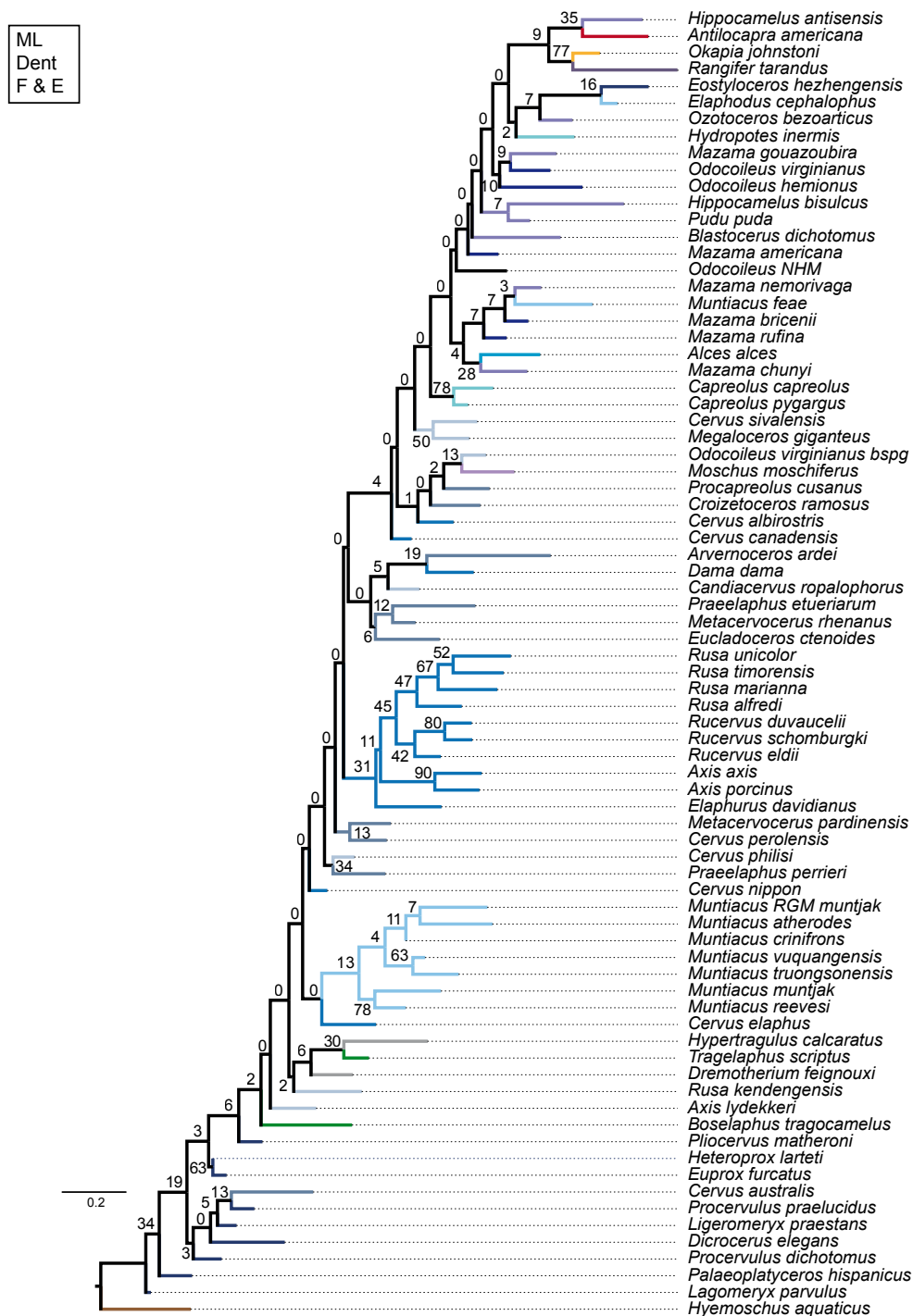


Figure 3.16: Best tree of the ML analysis based on the dental character set for fossil and extant taxa. Bootstrap support values are shown.

Cranial Character Set Unfortunately, the unordered and ordered MP analyses of the cranial data set with the fossil and extant taxon sampling and the ordered MP analysis of the fossil only taxon sampling of the same data set were not successful. The tree search process did not proceed further than the first replicate in all three analyses. The low character to taxon ratio and the conservative nature of cervid skulls prevented the tree search replicates from finishing under the MP framework.

The MP analysis of the ordered extant only data set was successful including a bootstrap analysis. There were several polytomies in the strict and the Adam's consensus tree (Figs 3.17, F.4). All muntiacines were in a clade, *Blastocerus dichotomus*, and both *Hippocamelus*-species formed a clade, and *Rusa timorensis*, *Rusa unicolor*, and *Rucervus schomburgki* were in a clade; the other taxa formed mixed capreoline-cervine-outgroup taxa-clades. The only weakly supported clade of the bootstrap analysis was *Rusa alfredi* and *Rusa marianna*. All small-sized cervids, i.e., *Mazama*, *Pudu*, *Muntiacus*, and *Elaphodus* were in a clade.

The unordered and ordered BI analyses of the cranial data set were congruent and differ only in minor differences in the posterior probabilities (Fig. 3.18). Both topologies had a poor resolution, resolving only a few sister taxon relationships with weak support. *Muntiacus atherodes*, *Muntiacus vuquangensis*, and *Muntiacus feae* formed a clade. Sister taxon relationships existed between *Rangifer tarandus* and *Megaloceros giganteus*, *Rusa alfredi* and *Rusa marianna*, *Rusa timorensis* and *Rusa unicolor*, *Cervus canadensis* and *Elaphurus davidianus*, *Procervulus dichotomus* and *Procervulus praelucidus*, *Muntiacus truongsongensis* and *Muntiacus crinifrons*, and *Hippocamelus bisulcus* and *Cervus australis*. All these clades were in a big polytomy with all other taxa exclusive of the outgroup.

The ML topology based on the cranial data set was poorly supported by bootstrap values (Fig. 3.19). Members of Muntiacini formed a clade including *Euprox furcatus*, *Eostyloceros hezhengensis*, but excluding the fossil *Muntiacus muntjak*. There was a clade uniting seven of the Miocene cervids. All other clades consisted of mixed cervine, capreoline, and non-cervid taxa.

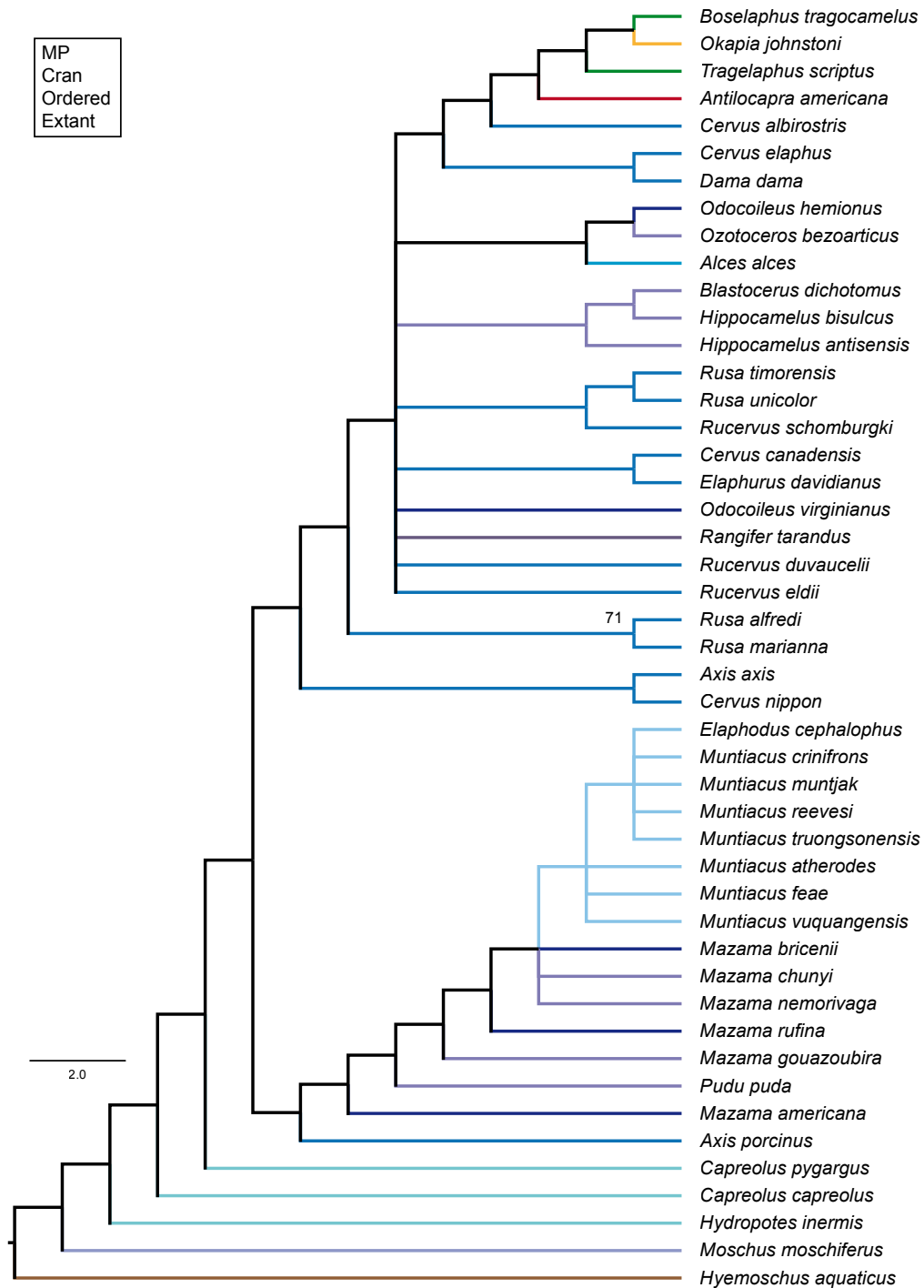


Figure 3.17: Consensus topology of the MP analysis based on the ordered cranial character set for extant taxa.

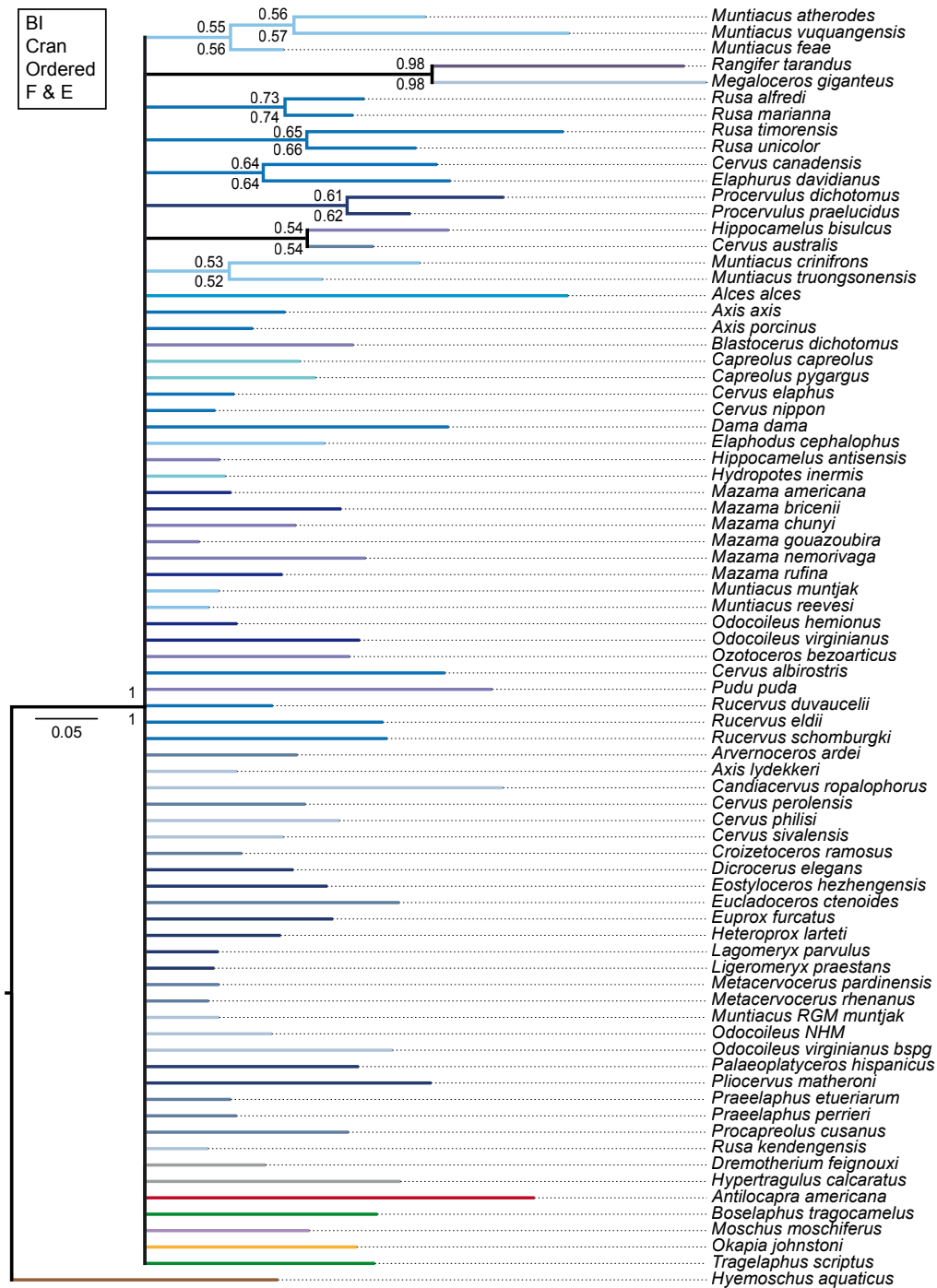


Figure 3.18: Consensus topology of the BI analysis based on the ordered cranial character set for fossil and extant taxa. Posterior probabilities of this analysis are above the respective branches, posterior probabilities of the unordered analysis are below the branches.

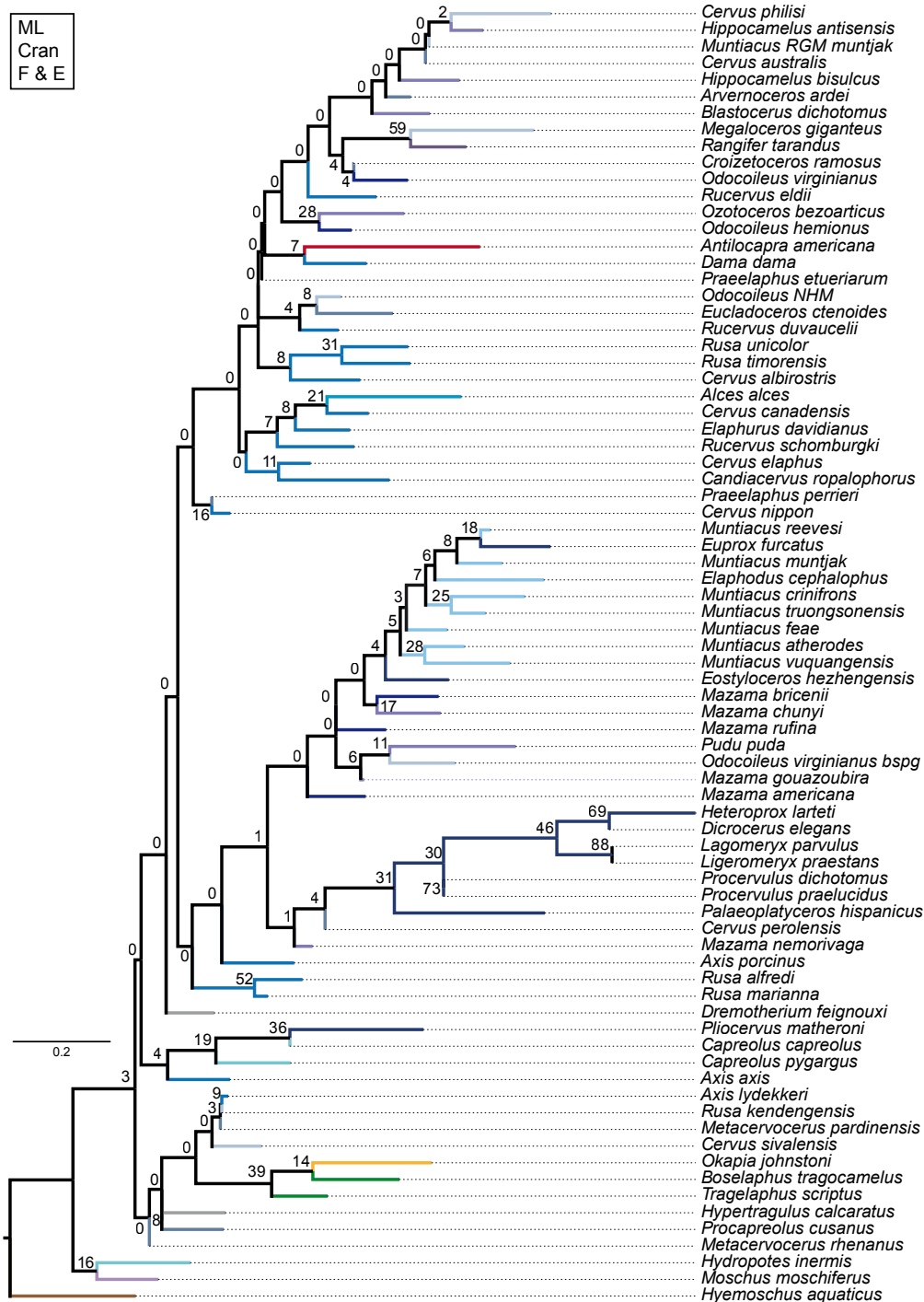


Figure 3.19: Best tree of the ML analysis based on the cranial character set for fossil and extant taxa. Bootstrap support values are shown.

Combined Character Set The strict consensus tree and the Adam's consensus tree of the MP analysis including all taxa and unordered character states were largely congruent with each other and contained only a few polytomies. The *Elaphurus-Rucervus-Rusa*-clade is recovered and sister taxon to a clade that majorily consists of cervine taxa and fossil species, which are most likely cervines, too (Fig. 3.20). All small-sized deer, i.e., *Mazama*, *Pudu*, and Muntiacini formed a clade. All Muntiacini formed a clade including all extant species, the fossil *Muntiacus muntjak*, and *Eostyloceros hezhengensis*. Both *Capreolus* species were sister taxa to *Hydropotes inermis*; this clade was the sister taxon to the clade of small-sized deer. Nine Miocene taxa and *Hypertragulus calcaratus* were placed between the outgroup and all other taxa. The bootstrap analysis supported the sister relationship of both *Axis*-species, three sister taxon relationships within the *Elaphurus-Rucervus-Rusa*-clade were supported, *Muntiacus reevesi* and *Muntiacus muntjak*, and both *Capreolus*-species.

The strict consensus tree of the MP analysis of the ordered combined data set was largely unresolved. The *Elaphurus-Rucervus-Rusa*-clade and Capreolini are recovered. A few sister taxon relationships were resolved, the remaining taxa were in a polytomy (Fig. 3.21). The Adam's consensus tree had a better resolution (Fig. F.5). The *Elaphurus-Rucervus-Rusa*-clade, Capreolini, and a clade consisting majorily of extant cervines and presumed fossil cervines were recovered, and similar to the unordered topologies, a clade with all extant small-sized deer (*Mazama*, *Pudu*) and Muntiacini including the fossil *Muntiacus muntjak* and *Eostyloceros hezhengensis* was present. Most Miocene cervids and non-cervid ruminants were placed between the outgroup and remaining taxa. The bootstrap analysis supported the same nodes as in the analysis based on unordered characters, but with partly higher values.

The strict consensus tree of the MP analysis with the complete morphological data set including only the fossil taxa resulted in a largely unresolved topology (Fig. 3.22). Both fossil *Odocoileus* specimens are sister taxa in a clade with *Croizetoceros ramosus* and *Procapreolus cusanus*. *Cervus australis*, the fossil *Muntiacus muntjak*, and *Rusa kendengensis* form a clade. *Dicrocerus elegans*, *Procervulus dichotomus*, and *Metacervoceros pardinensis* form also a clade. There is a sister taxon relationship between '*Cervus*' *philisi* and *Praeclaphus perrieri*. All other taxa are in a polytomy with the described clades. In the Adam's consensus tree more nodes are recovered (Fig. F.6). The seven Miocene taxa form a clade and all Miocene cervid taxa except for *Eostyloceros hezhengensis* are placed between the outgroup and the remaining taxa. In addition to the clades recovered in the strict consensus tree, several more nodes were recovered. The bootstrap analysis did not find support for any of the clades.

The strict and Adam's consensus tree of the MP analysis including only extant taxa on the complete morphological data set were almost congruent (Fig. 3.23). All small-sized deer were in one clade. Within that clade Muntiacini formed a monophyletic group. Capreolini were sister taxon to the clade with small-sized deer. The *Elaphurus-Rucervus-Rusa*-clade here includes also *Axis* as the sister taxon to two *Rusa* species. All non-cervid ruminants were placed between the outgroup and Cervidae. The bootstrap analysis found support for the sister taxon relationship of *Muntiacus muntjak* and *Muntiacus reevesi*, *Capreolus capreolus* and *Capreolus pygargus*, both *Axis*-species, *Rusa alfredi* and *Rusa marianna*, *Rusa timorensis* and *Rusa unicolor*, and *Rucervus duvaucelii* and *Rucervus eldii*.

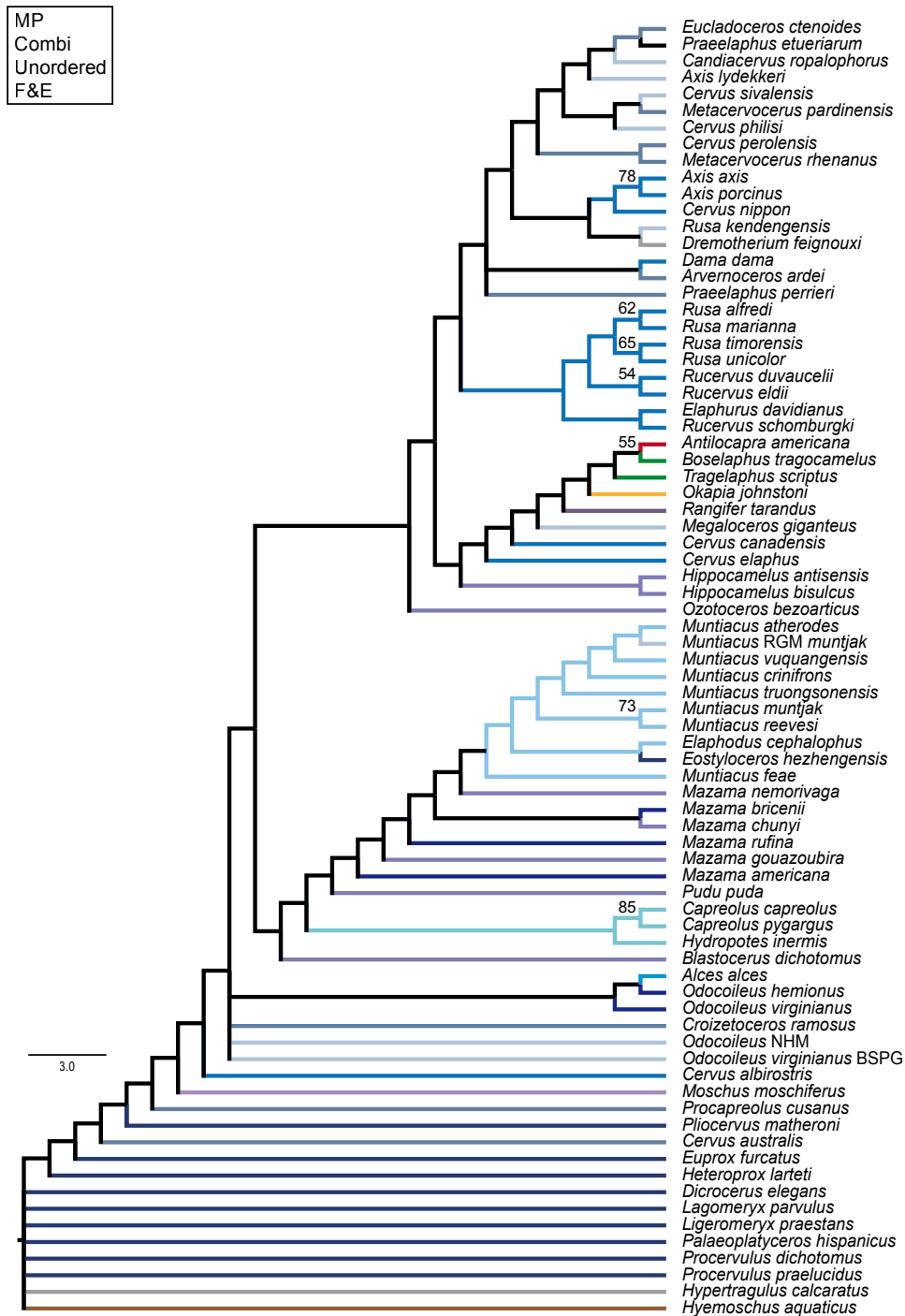


Figure 3.20: Consensus topology of the MP analysis based on the unordered combined character set for fossil and extant taxa.

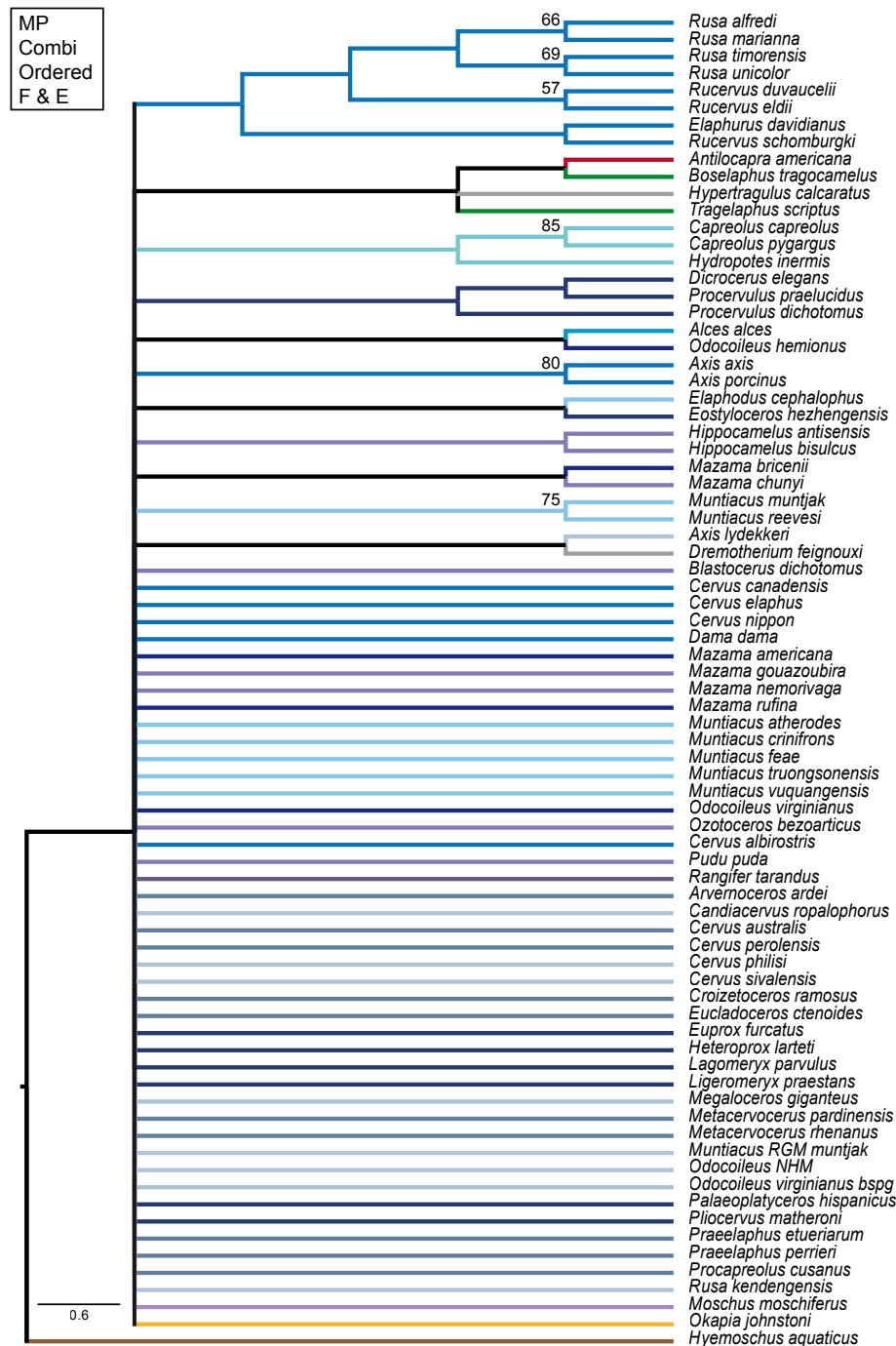


Figure 3.21: Consensus topology of the MP analysis based on the ordered combined character set for fossil and extant taxa.

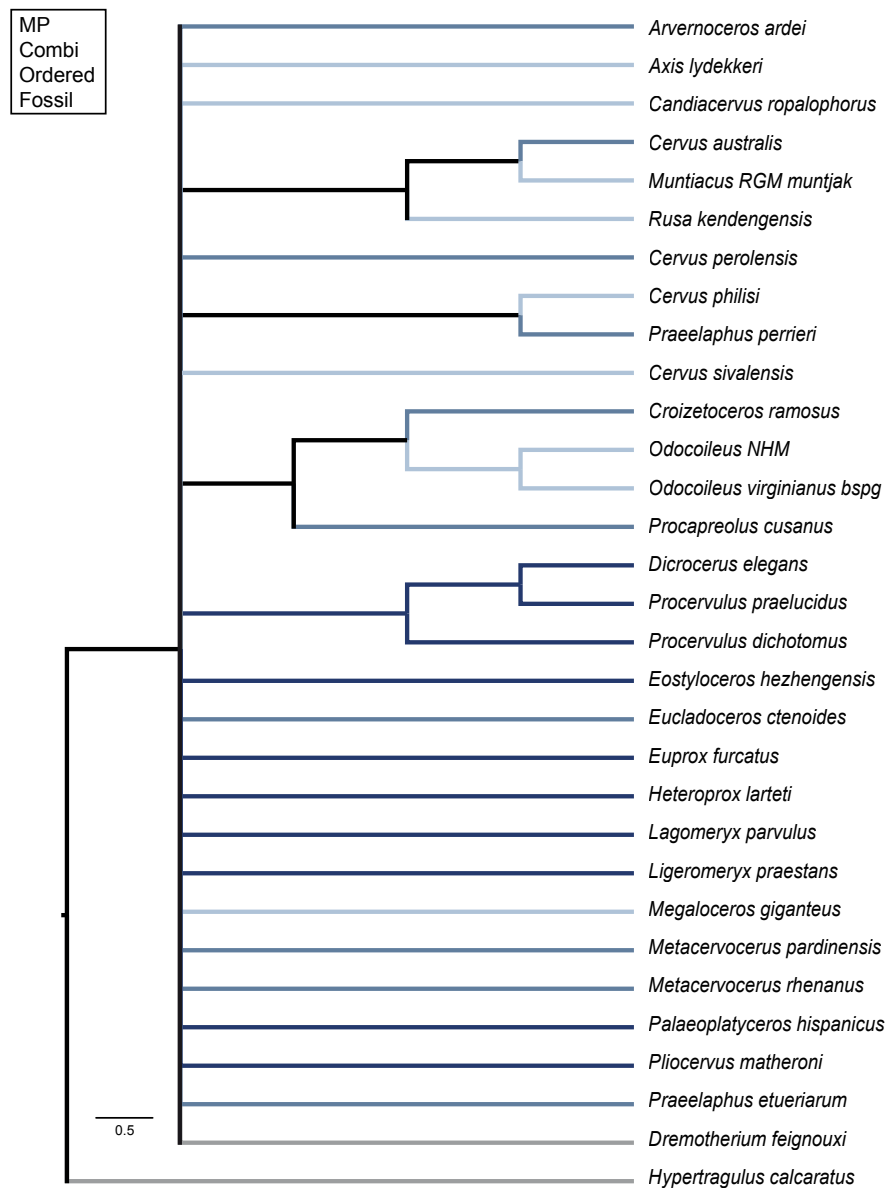


Figure 3.22: Consensus topology of the MP analysis based on the ordered combined character set for fossil taxa.

The unordered and ordered BI analyses of the combined data set were congruent apart from minor differences in the posterior probabilities. Both topologies were largely unresolved (Fig. 3.24). Most of the nodes were poorly supported; the majority of those were within the *Elaphurus-Rucervus-Rusa*-clade. This makes statements about the placings of the other taxa very speculative. All Miocene taxa except for *Eostyloceros hezhengensis* and *Pliocervus matheronis* were placed as the sister taxa to all other taxa, but were not

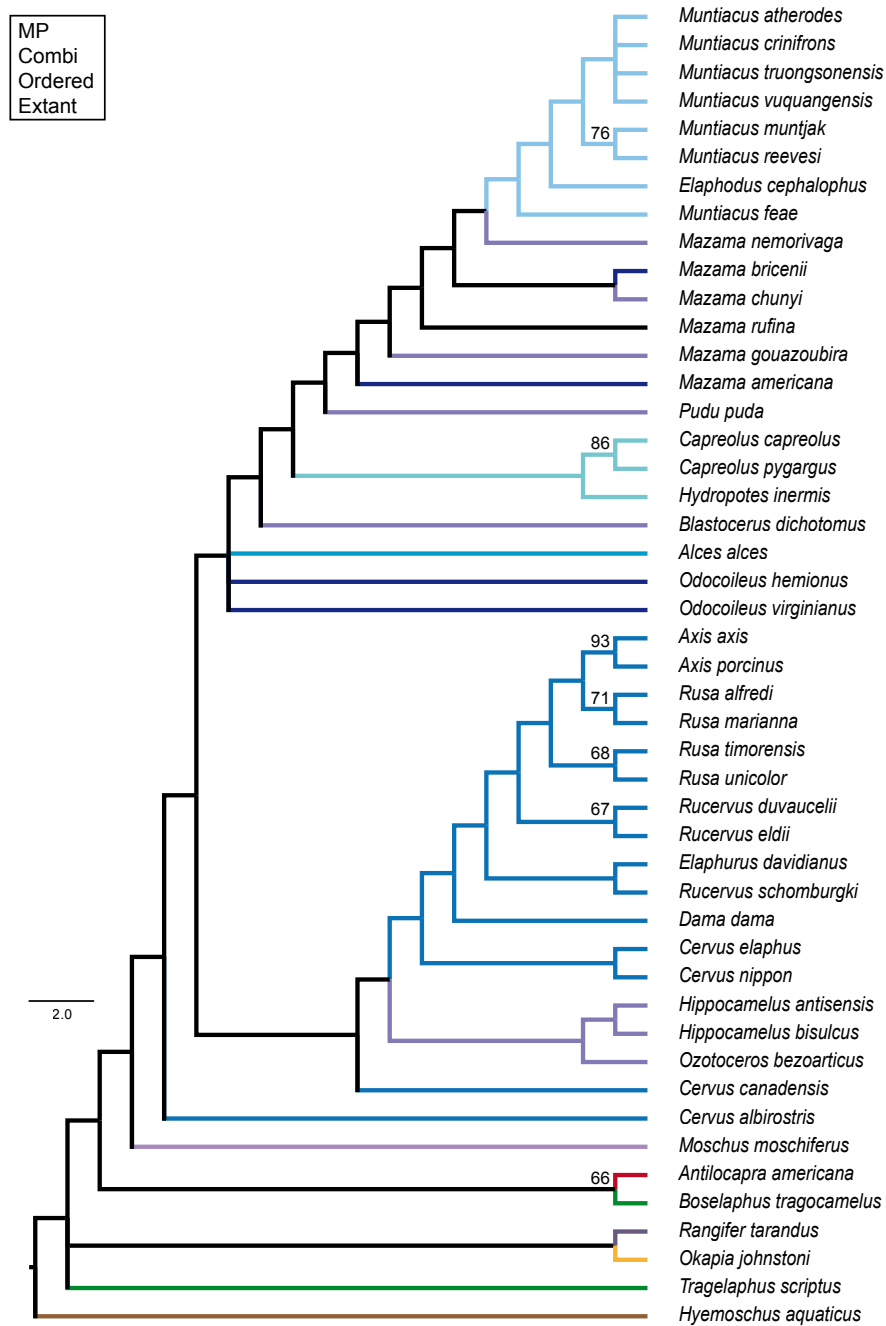


Figure 3.23: Consensus topology of the MP analysis based on the ordered combined character set for extant taxa.

monophyletic. All muntiacine taxa including *Eostyloceros hezhengensis* are sister taxa to the remaining taxa, i.e., placed between the Miocene taxa and the rest, but were also

non-monophyletic. All *Mazama* species, *Pudu puda*, and *Hydropotes inermis* were placed between the muntiacine taxa and the remaining taxa. The remaining taxa split into one clade and several polytomous taxa, which were sister taxa to the clade. The polytomy consisted of several capreoline taxa excluding some fossil taxa; *Procapreolus cusanus* was the sister taxon to both *Capreolus* species. The remaining clade consisted of the *Elaphurus-Rucervus-Rusa*-clade, a bovid-giraffid-antilocaprid-clade, an *Axis*-clade, a *Rangifer tarandus* *Megaloceros giganteus*-clade, and many polytomous taxa. The polytomy consisted of the remaining cervine taxa, most Pliocene and Pleistocene fossil cervids and the two non-cervid fossil taxa.

In the ML topology of the combined data set most nodes had very low bootstrap values (Fig. 3.25). The sister taxon relationships between both *Capreolus* species, between *Muntiacus muntjak* and *Muntiacus reevesi*, both *Axis* species, between *Rusa alfredi* and *Rusa marianna*, and *Rusa timorensis* and *Rusa unicolor* were supported. There was not much that can be inferred from this topology with certainty. Eight Miocene taxa were between the outgroup and the remaining taxa. All small-sized extant deer species formed a clade including Muntiacini. *Eostyloceros hezhengensis* and the fossil *Muntiacus muntjak* are included in Muntiacini. The *Elaphurus-Rucervus-Rusa*-clade is recovered. All cervine taxa except for *Megaloceros giganteus* formed a clade. The remaining taxa formed mixed capreoline, cervine, and non-cervid taxa clades.

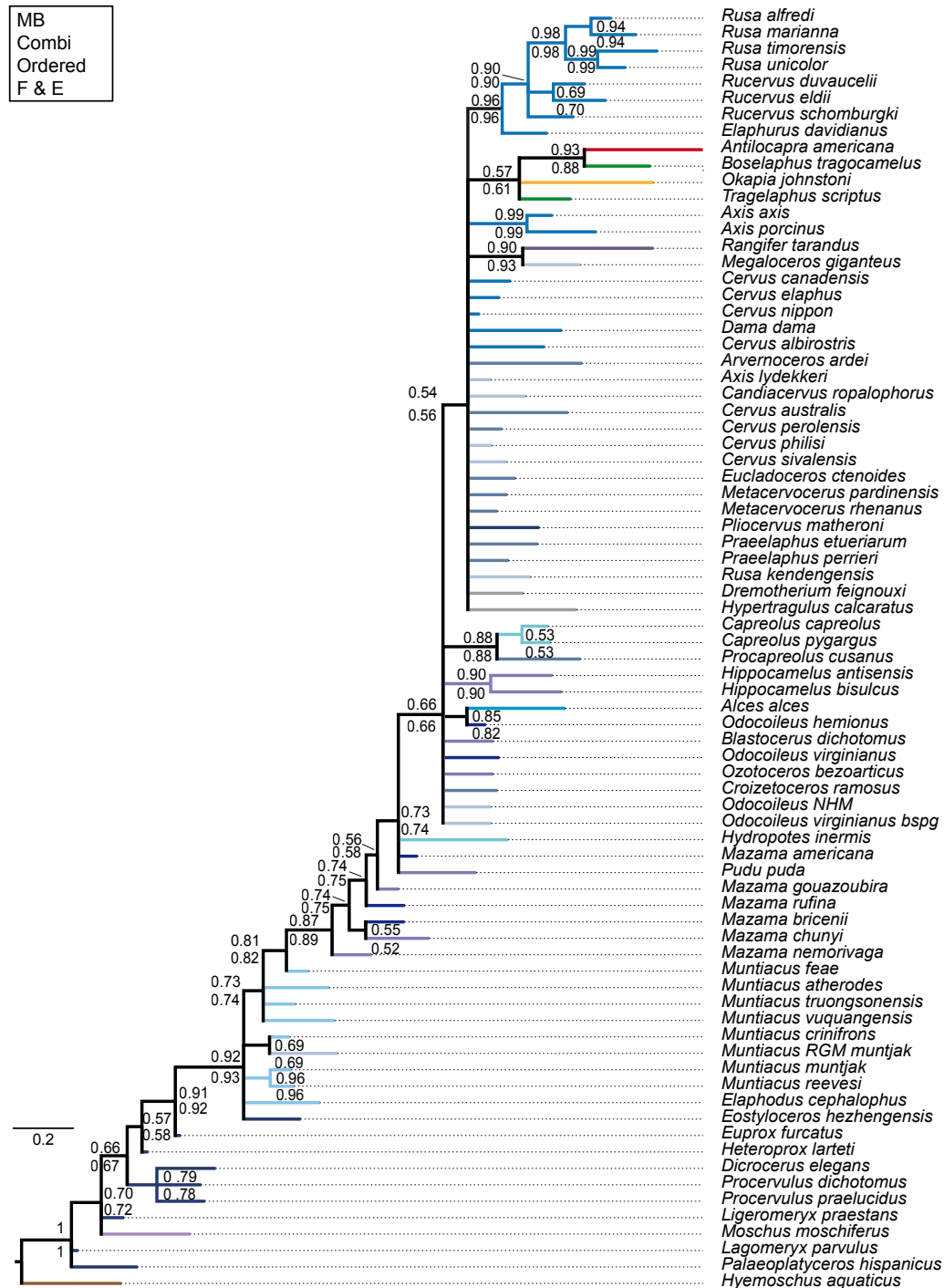


Figure 3.24: Consensus topology of the BI analysis based on the ordered combined character set for fossil and extant taxa. Posterior probabilities of this analysis are above the respective branch, posterior probabilities of the unordered analysis are below the branch.

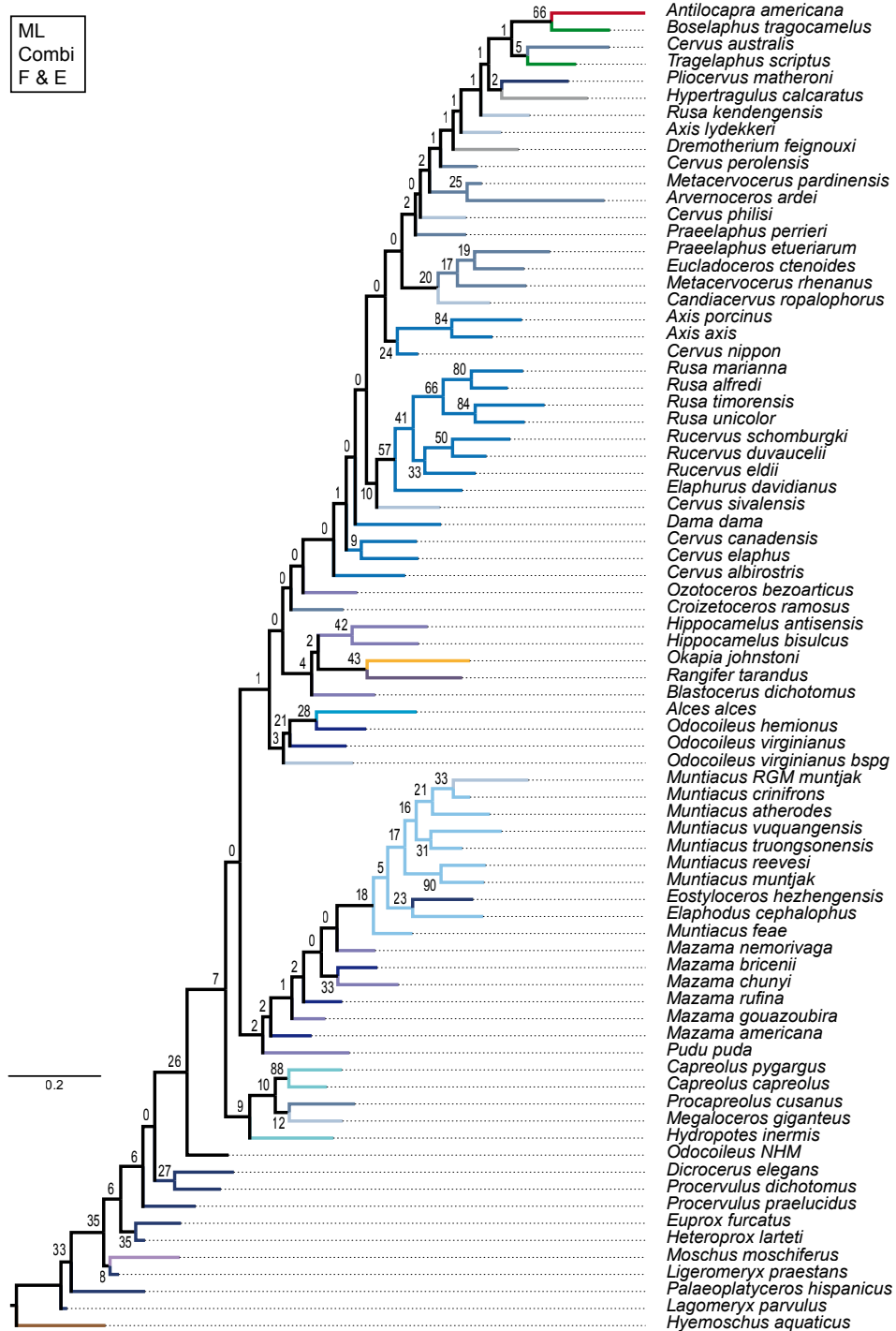


Figure 3.25: Best tree of the ML analysis based on the combined character set for fossil and extant taxa. Bootstrap support values are shown.

Experiments on Consistency Indices The consistency index (CI) is defined as the minimum number of character state changes divided by the number of character state changes required on the current tree (Farris, 1983). If the $CI = 1$, there is no homoplasy in the data set, while if the $CI = 0$ all characters in the data set would be homoplastic. The CI is negatively correlated to the number of species sampled (Farris, 1983). The retention index (RI) is defined as the difference of the maximum number of steps and the observed steps divided by the difference of the maximum number of steps and the minimum number of steps. The RI is 0 for parsimony uninformative characters, i.e., if the fit of characters on the tree is poor, and the RI is 1, if the topology fits the characters perfectly (Swofford, 2002). The homoplasy index (HI) is generally defined as the difference of the CI to 1, i.e., $HI = 1 - CI$. In data sets including polymorphic multistate characters, the ancestral character state is defined from which all other states in the multistate taxon must be derived. The rescaled consistency index (RC) is defined as the product of the CI and RI (Swofford, 2002).

In total, the CIs, RIs, HIs, and RCs of ten data sets with varying partitions, varying taxon sampling, and/or ordered vs. unordered character states were compared. The results from these MP analyses are in Table 3.3 and showed that ordering characters mostly resulted in lower CIs compared to an unordered character set. Generally, Adam's consensus trees showed higher CIs than strict consensus trees and adding fossils to the data set resulted in lower CIs for most characters. Comparing the CIs of the dental characters in the combined morphology analyses with the CIs of the dental characters in the dental only analyses showed that most CIs ($n = 35$) were lower in the combined analyses than in the dental only analyses. However, the CIs did not change in 20 characters and were higher in 24 characters, which is overall a relatively balanced distribution. In the analysis, where the characters with CIs of less than 0.25 were excluded the CIs were lower in 47 characters, equal in 35 characters, and higher in 25 characters.

Ordering characters, where applicable in the combined data set, resulted in higher CIs for 59 characters and remained the same in 61 characters. 46 characters had lower CI values. The overall tree length was slightly shorter compared to the unordered data set. This indicates that ordering is beneficial for finding the optimal tree. Most CIs are higher in the data set without fossils, which is probably due to the fewer number of taxa or due to fewer missing data. The CIs, which were equal in the original analysis and the analysis excluding characters with low CIs, probably indicate characters that are homoplastic regardless of the number of taxa and/or characters.

Additionally, I tested the combined morphology (unordered, including only extant taxa) data set excluding all strongly homoplastic characters ($CI < 0.25$). Compared to the analyses including all characters, exclusion of homoplastic characters did not improve the topology. Therefore, no modifications on the current data sets have been made according to the CI.

Single Fossil Analyses (SFA)

Three different approaches to the single fossil analyses have been undertaken on data sets including 31 fossil taxa. This adds up to 93 analyses in total. Thirty-one analyses used combined matrix of the complete mitochondrial genome and the combined morphological

data set including outgroup taxa. Thirty-one analyses were undertaken using exactly the same data set, but excluding five outgroup taxa. *Hyemoschus aquaticus* remained in the analysis to root the topologies. Thirty-one analyses were undertaken with a constraint topology as a backbone; Capreolinae, Muntiacini and Cervini were constraint as monophyletic polytomous to each other. In each of the 93 analyses only one fossil taxon at the time was included. Figures G.1 –G.10 show all 87 topologies, where fossil cervids were included and Figure 3.26 summarises the placements of all fossil cervid taxa in one topology.

Most topologies were well resolved and have Capreolinae and Cervini as sister taxa with Muntiacini as the sister taxon to both clades. Muntiacini, are not always monophyletic. In total, 44 topologies were fully resolved, 24 topologies contained one trichotomy, but were otherwise resolved, and 25 topologies contain several polytomies. The set of analyses using the concatenated molecular and morphological matrices including 6 non-cervid ruminants resulted in 17 polytomous topologies, 7 fully resolved topologies, and 7 topologies with one trichotomy. The set of analyses using a constraint topology resulted in 17 fully resolved topologies, 7 topologies with one trichotomy and 7 polytomous topologies. The most resolved topologies (20) were found with the set of analyses using the concatenated matrix excluding the 5 non-cervid ruminant taxa; only 1 topology contained several polytomies and 10 topologies contained one trichotomy.

Comparison of the three SFA

Congruent systematic positions in all three analyses. Three fossil cervids were consistently placed in the same position across all three SFA approaches. *Candiacervus ropalophorus* was consistently placed as the sister taxon to both species of *Hippocamelus*. *Lagomeryx parvulus* was consistently placed between *Hyemoschus aquaticus* and the remaining taxa. *Rusa kendengensis* was consistently placed as the sister taxon to the *Cervus*-clade.

Similar systematic positions across all three analyses. Twenty-one fossil taxa were placed in relatively similar positions across all three SFA approaches. *Arvernoceros ardei* was placed as the sister taxon to *Dama* in both supermatrix approaches and as the sister taxon to Cervini in the constraint tree approach. *Axis lydekkeri* was placed as the sister taxon to or within Cervini. '*Cervus*' *perolensis* was placed within the *Cervus*-clade or as the sister taxon to *Cervus elaphus*. *Cervus australis* was the sister taxon to *Hippocamelus bisulcus* in two analyses and between the outgroup and the remaining taxa in the supermatrix approach including outgroup taxa. '*Cervus*' *philisi* was either unresolved within Cervinae or in a polytomy with Cervini and Capreolinae. *Croizetoceros ramosus* was placed as the sister taxon to *Alces alces*, or within Odocoileini, or more closely to *Hippocamelus*, *Ozotoceros*, and two *Mazama*-species. '*Cervus*' *sivalensis* was placed within Cervini or as the sister taxon to the *Cervus*-clade. *Dicrocerus elegans* was placed between *Elaphodus cephalophus* and living muntjacs in both supermatrix approaches and between *Hyemoschus aquaticus* and the remaining taxa in the constraint tree approach. *Eucladoceros ctenoides* was placed twice as the sister taxon to all Cervini and in a polytomy with Capeolinae and Cervinae in the constraint tree analysis. *Euprox furcatus* was placed twice as the sister taxon to *Muntiacus atherodes* and between *Elaphodus cephalophus* and other living muntjacs in the supermatrix approach including outgroup taxa. *Hypertragulus calcaratus* was placed between *Hyemoschus aquaticus* and the remaining taxa in two analyses and as the sister taxon to *Boselaphus tragocamelus* in the supermatrix approach including outgroup taxa. *Megaloceros giganteus* was placed as the sister taxon to *Dama dama* in the two supermatrix approaches and as the sister taxon to *Rangifer tarandus* in the constraint tree approach. The fossil *Muntiacus muntjak* specimen is placed twice in a polytomy within living muntjacs and as the sister taxon to *Muntiacus atherodes* in the constraint tree analysis. *Metacervoceros pardinensis* was placed either as the sister to all Cervini, in a polytomy within Cervini or as the sister taxon to the *Cervus*-clade. *Metacervoceros rhenanus* was placed as the sister taxon to all Cervini, or in a polytomy with Capreolinae and Cervini. The BSPG *Odocoileus* specimen is placed twice in a trichotomy with *Mazama chunyi* and *Mazama gouazoubira* and in a polytomy within Odocoileini in the constraint tree approach. The NHM *Odocoileus* specimen is placed twice as the sister taxon to both species of *Hippocamelus* and as the sister taxon to *Mazama nemorivaga* in the constraint tree analysis. *Procervulus dichotomus* was placed twice as the sister taxon to *Muntiacus atherodes* and between *Hyemoschus aquaticus* and the remaining taxa in the constraint tree approach. *Praeclaphus etueriarum* was placed twice as the sister taxon to the *Cervus*-clade and as the sister taxon to *Tragelaphus* in the supermatrix approach including outgroup taxa. *Pliocervus matheronis* was placed twice as the sister taxon to

Muntiacus atherodes and as the sister taxon to *Boselaphus* in the supermatrix approach including outgroup taxa. *Praeclaphus perrieri* was placed either as the sister taxon to or in a polytomy within Cervini.

Different systematic positions in all three analyses. Seven fossil taxa were placed in different systematic positions across all three SFA approaches. *Dremotherium feignouxii* was placed unresolved in differing positions in the topology, never closely related to one of the two subfamilies. *Eostyloceros hezhengensis* was placed once between *Elaphodus cephalophus* and other living muntjacs, once as the sister taxon to *Elaphodus cephalophus*, and once in an unresolved position. *Heteroprox larteti* was placed once as the sister taxon to *Moschus*, once between *Elaphodus cephalophus* and all other living muntjacs, and once between *Elaphodus cephalophus* and Cervini plus Capreolini. *Ligeromeryx praestans* was placed once in a polytomy with non-cervid ruminant taxa, once as the sister taxon to Muntiacini, and once as the sister taxon to Cervini plus Capreolinae. *Procapreolus cusanus* was placed once as the sister taxon to *Moschus*, once in a polytomy within Capreolinae, and once as the sister taxon to both species of *Hippocamelus*. *Palaeoplatyceros hispanicus* was placed unresolved within outgroup taxa or Cervidae or between *Hyemoschus aquaticus* and the remaining taxa. *Procervulus praelucidus* was placed once in a polytomy within Capreolinae, once closely related to *Mazama chunyi* and *Mazama gouazoubira*, and once between *Hyemoschus aquaticus* and the remaining taxa.

Evolutionary Placement Algorithm (EPA)

The EPA analysis resulted in a resolved topology (Fig. 3.27). Five Miocene taxa were placed in a stem position, *Procervulus praelucidus*, *Pliocervus matheronis*, *Palaeoplatyceros hispanicus*, *Ligeromeryx praestans*, and *Lagomeryx parvulus*. Both fossil *Odocoileus* were placed closely related to blastocerine species, *Croizetoceros ramosus* was the sister taxon to *Ozotoceros bezoarticus*. *Hypertragulus calcaratus* and *Cervus australis* were in a polytomy with *Hippocamelus bisulcus*. *Procapreolus cusanus* was placed as the sister taxon to *Capreolus capreolus*. *Megaloceros giganteus* and *Dremotherium feignouxii* were polytomous sister taxa to Capreolini including *Procapreolus*. *Procervulus dichotomus* was the sister taxon to Muntiacini (including several other fossils); *Dicrocerus elegans* was the sister taxon to all muntjacs and other fossils. *Eostyloceros hezhengensis*, *Euprox furcatus*, *Heteroprox larteti*, and *Praeclaphus etueriarum* were in a polytomy with *Muntiacus reevesi* within Muntiacini. The fossil *Muntiacus muntjak* was the sister taxon to *Muntiacus crinifrons*. *Candiacervus ropalophorus* was the sister taxon to Cervini; *Arvernoceros ardei* was the sister taxon to *Dama dama*. *Eucladoceros ctenoides* and *Rusa kendengensis* were polytomous sister taxa to the *Cervus*-clade (including several fossils). *Axis lydekkeri*, ‘*Cervus*’ *perolensis*, and *Metacervoceros rhenanus* were in a polytomy with *Cervus elaphus*. ‘*Cervus*’ *sivalensis* and *Metacervoceros pardinensis* were in a polytomy with *Cervus canadensis*. ‘*Cervus*’ *philisi* and *Praeclaphus perrieri* were in a polytomy with *Cervus nippon*.

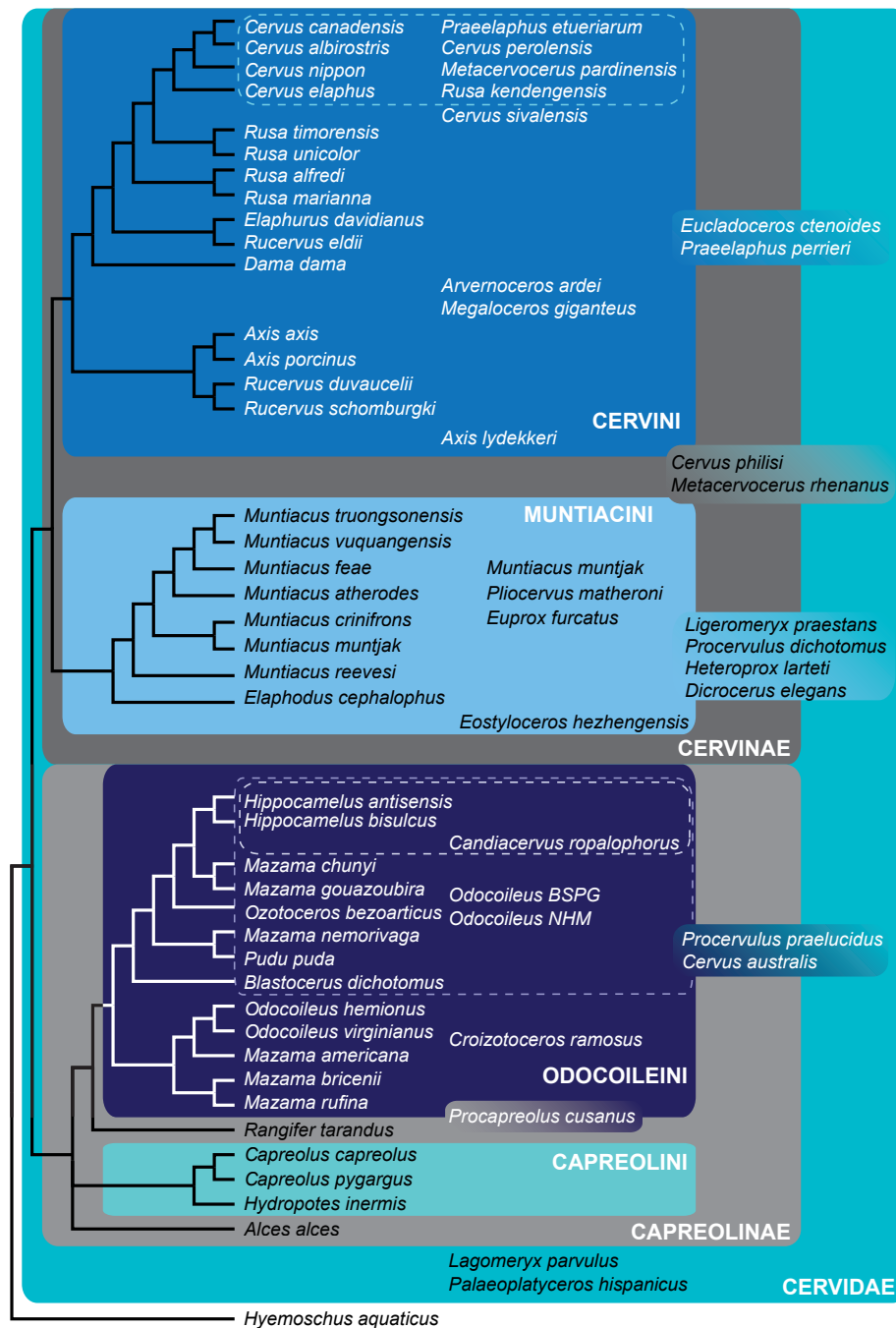


Figure 3.26: Topology summarising the placement of all 29 fossil cervids of the three SFA. The individual trees are shown in Figures G.1 –G.10. The differently shaded boxes on the right indicate different positions of the taxa within the boxes.

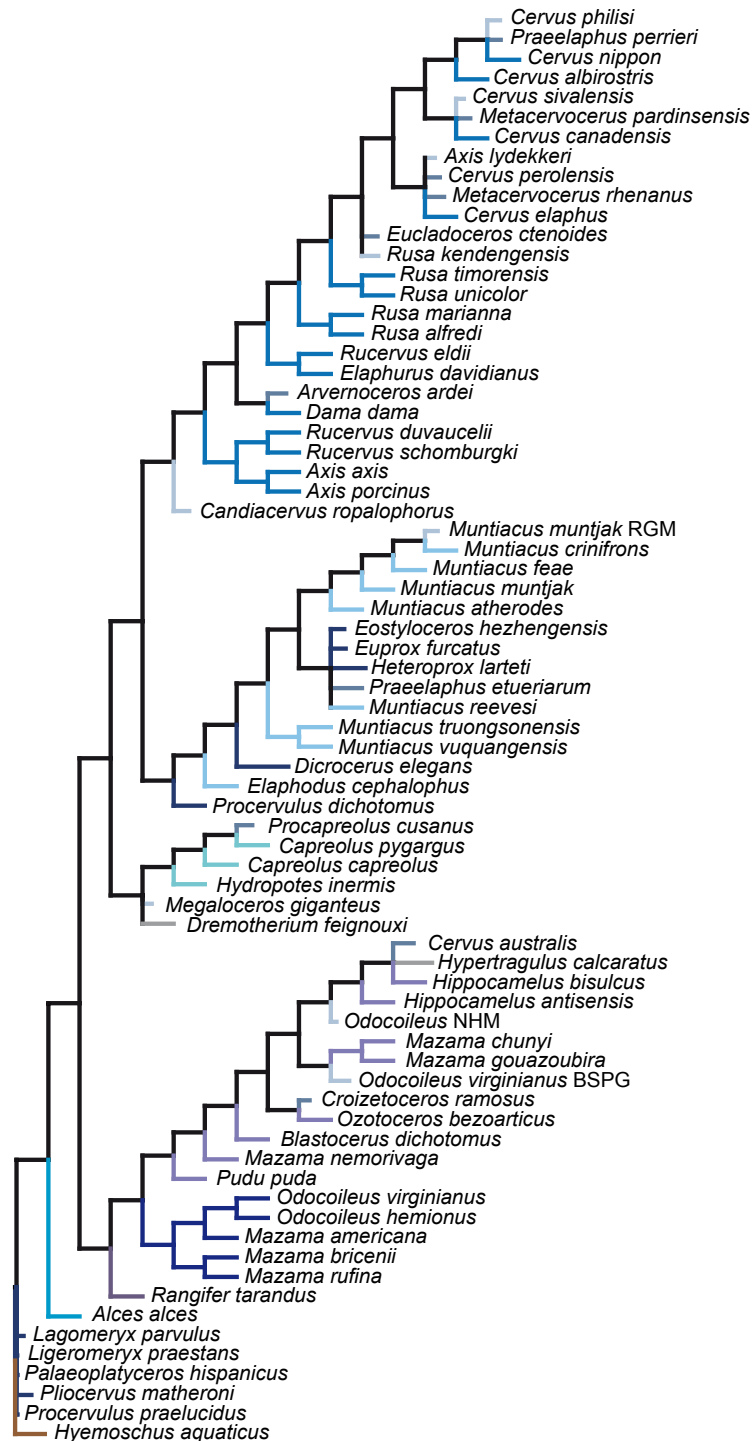


Figure 3.27: Topology resulting from the EPA analysis, which was based on the molecular and morphological data.

3.4 Discussion

The work of this Chapter represents the most comprehensive approach to investigate the systematic relationships of fossil and extant cervids based on morphological data to date. A total of 168 craniodental characters across 70 cervid taxa were scored. The morphology of the scrutinised cervids was described in detail (Appendix E). Several phylogenetic analyses were undertaken on the dental, cranial and combined data set under three different optimality criteria. The taxon sampling included sometimes only fossil cervids, only extant cervids, or both. Most analyses were run with character state ordering as suggested by the SS analyses. In addition, all three data sets were analysed unordered under MP and BI for comparison. The MP topologies were better resolved based on the unordered data set, while there were no topological differences between the ordered and unordered BI analyses. However, more dichotomous topologies do not necessarily represent the better results. As tested by SS analyses the data are better represented if ordered, therefore, the topologies resulting from the ordered analyses may be closer to the ‘truth’ or closer to the amount of information that can actually be gained from the current data set(s), respectively. Apart from these standard phylogenetic analyses, two alternative approaches, SFA and EPA, were undertaken to investigate the systematic positions of fossils in more detail. These alternative analyses provide interesting insights into potential relationships of fossil cervids to extant cervids. None of the morphological topologies can be considered as robust, only a few clades were statistically supported. Despite the homoplasy, some clades were well defined and re-occurring across different data sets. The topologies inferred from the morphological data sets, implications about the systematic positions retain a speculative component.

The taxonomy of fossil cervids in particular needs a thorough revision. A few fossil cervids, e.g., ‘*Cervus*’ *philisi* or ‘*Cervus*’ *perolensis*, are assumed to be synonyms of another species. To test these hypotheses those taxa were analysed and treated as separate species. Fossil taxa, which were repeatedly placed within the same clade or as the sister taxon to certain taxa across different data partitions and approaches, are more likely to be closely related to those taxa than fossils, which were placed differently in each analysis. However, systematic errors resulting from analysing the same data partitions can not be excluded at this state. It is for example likely that the dental partition carrying a slightly stronger phylogenetic signal influenced the combined morphological analyses.

A detailed discussion of the systematic position of fossil cervids based on the literature and on my analyses represents the first part of the discussion. For the most supported clades a short comment about the characters diagnosing those clades is provided; more details are in the apomorphy lists on Open Data LMU. The second part discusses (in less detail, but see Chapter 5) the placement of extant taxa. This systematic section is followed by a discussion about the character state evolution of the dentition and the cranium including antlers.

3.4.1 Miocene Cervids

The earliest cervids are known from the mid early Miocene (MN3) represented by *Procervulus*, *Ligeromeryx*, and *Acteocemas* and became more numerous and widely distributed

during the Miocene. Contemporaneously, in the late early and early middle Miocene *Stephanocemas*, *Heteroprox*, *Lagomeryx*, and *Dicrocerus* appear (Ginsburg & Azanza, 1991; Dong, 1993). Eleven cervid species are reported from China with an increase to 18 until the late Miocene. Middle Miocene forms persisted and new forms such as *Paracervulus* and *Eostylloceros* appeared (Dong, 1993).

During the late early Miocene (late Burdigalian) of Central Europe four cervid species, *Procervulus praelucidus*, *Procervulus dichotomus*, and *Heteroprox larteti*, and *Heteroprox eggeri* are dominant (Böhme et al., 2012). *Dicrocerus elegans* and *Paradicrocerus elegantulus* appeared in the middle Miocene (Langhian), which both coexisted with *Heteroprox larteti*. A little later *Euprox minimus* appeared, while at the same time *Paradicrocerus* and possibly the last representative of *Procervulus* disappeared and the first *Euprox furcatus* appeared coexisting with *Heteroprox larteti* and *Dicrocerus elegans* (Böhme et al., 2012). The diversity of dicrocerines declines at the end of the Middle Miocene Climatic Transition (MMCT 14.2–13.8 Ma, with minimum temperatures around 13.9 Ma) (Shevenell et al., 2004; Holbourn et al., 2005; Azanza et al., 2011). At the same time, *Procapreolus*, *Metacervulus*, *Cervavitus*, and *Axis* appeared (Dong, 1993). *Euprox furcatus* is the only cervid present during the middle Serravallian to the late Miocene (Tortonian) in Central Europe and is then replaced by *Euprox dicranocerus*, *Amphiprox anacerus*, *Cervavitus variabilis*, *Procapreolus loczyi*, and *Lucentia* aff. *pierensis* (Böhme et al., 2012). In general, a low cervid diversity is assumed during the late Miocene and all typical Miocene cervids became extinct before the late Miocene (Ginsburg & Azanza, 1991; Böhme et al., 2012).

Stehlin (1937) classified Miocene cervids into eight genera, *Lagomeryx*, *Procervulus*, *Dicrocerus*, *Stephanocemas*, *Heteroprox*, *Euprox*, *Amphiprox*, and *Palaeoplatyceros*. Further, it has been suggested to classify these eight European Miocene cervids into three groups. The first group consisting of *Euprox*, *Amphiprox*, and *Palaeoplatyceros*, representatives of cervids that further evolved. The second group including *Dicrocerus*, *Heteroprox*, and *Stephanocemas*, with deciduous antlers and the third group consisting of *Lagomeryx* and *Procervulus*, which were assumed to have non-deciduous antlers (Thenius, 1948). While the classification of genera still holds (except for *Stephanocemas*, which is now *Paradicrocerus*; see comment in Chapter 3), the grouping of these genera looks different today. Since all Miocene cervids shed their antlers (Chapter 3), a distinction between cervids with deciduous and permanent antlers is obsolete.

All early cervids have cranial appendages originating from the frontals, mostly perpendicular to the horizontal plane, positioned on the lateral orbit rim and directly above the orbita; further shared characters are a brachyodont dentition, a bifurcating postprotocrista on upper molars, central folds on upper premolars, variably present metaconule folds, enlarged canines, and two lacrimal foramina (Rössner, 1995). It was suggested to put *Lagomeryx*, *Procervulus*, *Heteroprox*, *Euprox*, *Dicrocerus*, *Stephanocemas* into a subfamily as a ‘primitive’ clade within Cervidae (Azanza, 1993b; Ginsburg, 1985; Rössner, 1995).

Azanza Asensio (2000) classified *Lagomeryx*, *Ligeromeryx*, and *Stephanocemas* as Lagomerycidae, *Procervulus* and *Heteroprox* as Procervulinae, *Acteocemas*, *Stehlinoceros*, and *Dicrocerus* as Dicrocerinae, *Euprox*, *Amphiprox*, *Eostylloceros*, *Metacervulus*, and extant *Muntiacus* and *Elaphodus* as Muntiacinae, and *Lucentia* and all living cervids bearing antlers with two or more tines as Cervinae (presumably also including Capreolinae). In Azanza Asensio’s (2000) phylogenetic tree, Muntiacinae and Cervinae are sister taxa with

Palaeoplatyceros as the sister taxon to both of them; Dicrocerinae is the sister taxon to all of the former, Procervulinae is the sister taxon to all of them and Lagomerycidae is the sister taxon to all of these clades. With the exception of lagomerycids all clades belong to Cervidae (Azanza Asensio, 2000).

In the phylogenetic analyses presented here, Miocene cervids are usually placed either between the outgroup and all other cervids, sometimes a few taxa form a clade; they are often in unresolved positions, or in polytomies somewhere else in the topology. The placement between the outgroup and other cervids is expected from their temporal distribution and their shared higher proportion of plesiomorphic characters. This also makes the suggested classification as Procervulinae in a stem position plausible. It is unlikely that any of these stem cervids has a closer relationship to the crown cervids of today (see below). The systematic relationships within early Miocene cervids have been and still are controversial (Rössner, 1995; Azanza et al., 2013).

Procervulus dichotomus and *Procervulus praelucidus*

The genus *Procervulus* was established by Gaudry (1877) based on the type species *Antilope dichotoma* Gervais 1849. Four species of *Procervulus* occur in the early Miocene of Europe, *Procervulus praelucidus* Obergfell 1957, *Procervulus savignensis* Ginsburg 1985 (both MN3, previously regarded as subspecies of *Procervulus dichotomus*), *Procervulus ginsburgi* Azanza 1993 (MN4), and *Procervulus dichotomus* Gervais 1859 (= *P. aurelianensis*) (MN4 & 5, Azanza, 1993b; Rössner, 1995). *P. ginsburgi* is smaller than *Procervulus dichotomus*, the size of the dentition is intermediate between *Procervulus praelucidus* and *Procervulus dichotomus*; the latter is the largest species and with some more apomorphic characters, such as more curved appendages (Rössner, 1995). *Procervulus praelucidus* is assumed to be the direct ancestor of *Procervulus dichotomus* and *Heteroprox larteti* its descendant (MN6) (Azanza, 1993a). *Dremotherium* and *Amphitragulus* have some shared apomorphic characters with *Procervulus* and other early cervids (Rössner, 1995). Therefore, *Procervulus* is assumed to be the Miocene descendant of *Amphitragulus* and *Dremotherium*; the latter two were assigned to Moschidae by Gentry (1994). Presumably, transitional forms existed, which were not documented in the fossil record (Rössner, 1995). *Procervulus* has been erroneously included in lagomerycids for a long time (Azanza & Ginsburg, 1997).

There is a continuous record of 4 million years for *Procervulus* throughout the Miocene Climatic Optimum. *Procervulus* is restricted to Europe and became extinct with the mid-Miocene cooling (Azanza, 1993a; DeMiguel et al., 2010). Ecological and vegetational changes during the middle Miocene affected *Procervulus* increasing the intake of grass and abrasives. Due to its small body size, brachyodont dentition, and low trophic flexibility *Procervulus* disappeared as consequence (DeMiguel et al., 2010). Even though, as shown by mesowear analyses, *Procervulus* changed from the browse-dominated end of the mixed feeding range to the grass-dominated end and the last representatives of this species were better adapted to grass processing than their ancestors, *Procervulus* was unable to compensate for low nutritional content and diet abrasiveness long time (DeMiguel et al., 2010). Also, appearance of the first bovids (e.g., *Tethytragus*) coincides with *Procervulus*; similar wear patterns in *Procervulus* and those first bovids show that competition for food was present and since bovids were better adapted to the higher abrasive diet, this was probably

another reason for the decline of *Procervulus* (DeMiguel et al., 2010).

In the phylogenetic analyses here, *Procervulus dichotomus* and *Procervulus praelucidus* were often placed in a stem position or unresolved in a polytomy, particularly in the analyses based on the dental matrix. Dental characters also put *Procervulus dichotomus* as the sister taxon to *Dicrocerus elegans* in four topologies. In the analyses based on the cranial data set both *Procervulus* were put as the sister taxa in two cases. In the combined analyses a close relationship to each other and to *Dicrocerus elegans* is confirmed. In the SFA *Procervulus dichotomus* is placed twice as the sister taxon to *Muntiacus atherodes* and once in an unresolved stem position. *Procervulus praelucidus* is placed twice in an unresolved position within Cervidae and once as the sister taxon to two *Mazama* species. The EPA analysis placed *Procervulus praelucidus* in a stem position, while *Procervulus dichotomus* was placed as the sister taxon to all Muntiacini. Azanza Asensio's (2000) analyses always placed *Procervulus* as the sister taxon to *Heteroprox* based on the character state 'parallel pedicles'. In Mennecart et al. (2016) *Procervulus dichotomus* was the sister taxon to *Heteroprox larteti*, and both were the sister taxon to the clade containing *Dicrocerus elegans* as the sister taxon to *Euprox furcatus* plus *Cervus elaphus*. In my analyses, a close sister taxon relationship of *Procervulus* and *Heteroprox* was not observed.

Lagomeryx parvulus and *Ligeromeryx praestans*

Three forms of large lagomerycids are described from MN3 localities of France, *Ligeromeryx*, *Heterocemas*, and a Lagomerycidae gen. et sp. indet.; the genus *Lagomeryx* only applies to the small European species (Azanza & Ginsburg, 1997). It was suggested that lagomerycids, which are contemporaneous with *Procervulus* and *Acteocemas*, represent an independent clade within cervoids (Azanza & Ginsburg, 1997). The fossil record of *Lagomeryx parvulus* ranges from MN4 to MN6 (Rössner, 1998). *Lagomeryx* Roger 1904 includes the European representatives *L. parvulus* (Roger 1898), *L. pumilio* (Roger 1896), and *L. ruetimeyeri* Thenius 1948, which range from MN3 to MN6 (Rössner, 2010).

Lagomerycid appendages have been interpreted in various different ways in the past and from this several hypothesis about their systematic affiliation have been put forward; in earliest studies lagomerycids were defined as new family acting as connection between Giraffidae and Cervidae, to which lagomerycids were considered to be equally likely closely related (Teilhard de Chardin, 1939). It was defined comprising *Lagomeryx* (including *Ligeromeryx*), *Procervulus*, and similar cervids with non-deciduous antlers (Teilhard de Chardin, 1939). The name Lagomerycidae was first defined by Pilgrim (1941) under the superfamily Giraffoidea and Simpson (1945) adapted this classification with caveats. Later Lagomerycidae were considered as part of the superfamily Cervoidea (Romer, 1966; Viret, 1961; Young, 1964). It has also been regarded as separate subfamily within Cervidae (Vislobokova et al., 1989), as a family of aberrant giraffoids, junior synonym of Palaeomerycidae (Pilgrim, 1941; Simpson, 1945; Young, 1964), and as junior synonym of Muntiacini/-ae (Chow & Shih, 1978). Lagomerycids have also been considered as more closely related to Antilocapridae (Ginsburg, 1985; Solounias, 1988), or representing an entirely independent clade (Bubenik & Bubenik, 1986; Azanza, 1993b; Azanza & Ginsburg, 1997).

Previously, *Lagomeryx*, including *Ligeromeryx*, and *Stephanocemas* have been considered either as members of the family Lagomerycidae (Pilgrim, 1941; Azanza, 1993b) or as

members of Muntiacini (Janis & Scott, 1987; Gentry, 1994; Gentry et al., 1999; Groves, 2007; Wang et al., 2009). Based on a skull fragment of *Lagomeryx colberti* it was inferred that *Lagomeryx* is most closely related to *Elaphodus* and *Muntiacus*, and thus is considered to belong to the Muntiacini or possibly as a side branch of Muntiacini due to specialised antlers (Chow & Shih, 1978).

It was noted that *Lagomeryx* (including *Ligeromeryx*) shares several morphological similarities with dremotheriids (for details see Vislobokova et al., 1989). A short facial part of the skull with short praemaxillaries and brachyodont molars were pointed out as plesiomorphic characters derived from more distant ancestors, all other characters are derived in dremotheriines (Vislobokova et al., 1989).

Ligeromeryx, *Lagomeryx*, *Heterocemas*, and *Stephanocemas* show four slightly different antler morphologies (Azanza, 1993b). It has been often proposed that *Lagomeryx* did not shed antlers because of the absence of a burr (Dehm, 1944; Thenius, 1948; Azanza, 1993b; Azanza & Ginsburg, 1997). *Ligeromeryx* is a large representative of lagomerycids with relatively large antlers and representatives with these characteristics were affiliated to the newly established genus *Ligeromeryx* Azanza & Ginsburg 1997; refer to this publication for detailed information on the genus and particularly on *Ligeromeryx praestans*.

Lagomerycidae underwent evolutionary trends towards more complex antlers and dental modifications in response to more abrasive diet. It is hypothesised that lagomerycids used overgrowth of bushes and shrubs and woodland with low thickets as habitat. Modifications in limb bones indicates adaptation for swampy ground and living close to water bodies (Vislobokova et al., 1989). Results from mesowear analyses classify *Lagomeryx parvulus* as browser inhabiting a relatively narrow dietary niche avoiding too much grit in their diet (Kaiser & Rössner, 2007). *Lagomeryx parvulus* probably inhabited closed habitats, was crepuscular or partial nocturnal, and lived solitary or in small family groups (Rössner, 2010).

In my analyses, both lagomerycids were placed in an unresolved position either as stem cervids or within crown Cervidae in most topologies. Only in one analysis based on the cranial data set *Lagomeryx parvulus* and *Ligeromeryx praestans* were considered as sister taxa to each other. In the dental analyses including only fossils *Lagomeryx parvulus* was placed as the sister taxon to *Palaeoplatyceros hispanicus*. In the SFA *Lagomeryx parvulus* was placed between the outgroup and all other taxa, which supports its probable stem position. *Ligeromeryx praestans* was placed in an unresolved position, as the sister taxon to all extant Muntiacini, and as the sister taxon to Cervinae and Capreolinae. The EPA analysis placed both lagomerycids unresolved in a stem position. Therefore, interpretations about its systematic position are speculative. Based on qualitative morphological comparisons, especially on antler morphology *Lagomeryx parvulus* and *Ligeromeryx praestans* should be closely related to each other and both be placed in a stem position to crown cervids. Unfortunately, only one analysis supports the sister taxon relationship of these two taxa. Therefore a subfamily Lagomerycinae would be justified based on morphological qualitative comparisons, but is not supported in the topologies. There even is more evidence for a Procervulinae clade than for Lagomerycinae. The reasons for this may lay within the data, i.e., completeness, specific characters preserved in one taxon, but not the other. Also, whether lagomerycids form a family as the sister taxon to Cervidae could not be entirely ruled out, but the tendency of *Ligeromeryx* to be placed within Cervidae indicate

that lagomerycids form a subfamily of Cervidae with a stem position. In Azanza Asensio (2000) *Lagomeryx* is always placed as the sister taxon to *Stephanocemas* (= *Paradicroceros*), which has not been included in the analyses of this chapter. However, the topology in Chapter 3 based on antler characters shows this relationship, too.

The discussions on the taxon in the literature and the new insights resulting from my analyses clearly shows that the systematic position of Lagomerycidae is still controversial. It represents one of the most controversial ruminant families, so far without unambiguous consensus; however, cranial and postcranial morphology support the affiliation as stem Cervidae (Chow & Shih, 1978; Leinders & Heintz, 1980; Vislobokova et al., 1989; Azanza & Ginsburg, 1997). Some ingroup placements of lagomerycids in my analyses suggest that they are more likely a subfamily, Lagomerycinae, within Cervidae. Either as sister group to Procervulinae, which form a clade of stem cervids, or as the sister group to all other cervids.

Eostyloceros hezhengensis

Muntiacine-like cervids are common during the mid-late Miocene in European faunal assemblages (Azanza Asensio, 2000), but decline considerably from the early Pliocene onwards; their geographic range becomes restricted to Eastern Europe and Asia, with only one remaining Western European genus *Paracervulus*, which is common in the late Messinian-early Zanclean faunas (Vislobokova, 1992; Dong, 1996; Abbazzi & Azanza, 2000; Abbazzi, 2001; Abbazzi & Croitor, 2003).

The genus *Eostyloceros* was established by Zdansky (1925) based on the type species *Eostyloceros blainvillei* Zdansky 1925. Members of *Eostyloceros* have been considered as large-sized representatives of the subfamily Muntiacini with relatively short pedicles and a prominent ridge on the frontal bone. Antlers have a well-developed burr, are bifurcating with ridges and furrows (Teilhard de Chardin & Trassaert, 1937; Wang & Wu, 1979; Deng et al., 2014). Contemporaneous muntiacine cervids are *Eostyloceros pidoplitschkoi* Korotkevich 1964 (lower Pliocene south-eastern Moldova, Korotkevich, 1970), *Eostyloceros blainvillei* (latest Miocene of China and Mongolia, Korotkevich, 1970; Vislobokova, 1983; Vislobokova, 1990), and *Muntiacus pliocaenicus* Korotkevich 1965 (early Pliocene of Ukraine, Korotkevich, 1970; Abbazzi & Croitor, 2003).

All other species of *Eostyloceros*, *E. blainvillei*, *E. triangularis* Zdansky 1925, *E. propria* Abdrakhmanova 1974, *E. maci* Vislobokova 1985, *Eostyloceros pierensis* Thomas 1951 (this species is now ascribed to genus *Lucentia*), *E. longchuanensis* Lin et al. 1978, and *E. actauensis* Abdrakhmanova et al. 1989 are known from the latest Miocene to the early Pliocene of China, Mongolia and Kazakhstan, and from the early Pliocene of the Baikal region of Russia, and Europe (Zdansky, 1925; Abdrakhmanova, 1974; Vislobokova, 1985, 1990; Abbazzi & Croitor, 2003; Deng et al., 2014).

Recently, a new species has been described, *Eostyloceros hezhengensis* Deng et al. 2014, from the late Miocene of China, which was used here for scoring characters. The extensive phylogenetic analysis of the genus in their study showed that several species of *Eostyloceros* are paraphyletic (Deng et al., 2014). This might be due to insufficient resolution or because of missing data and/or possible parallel evolution. Based on these analyses *Eostyloceros hezhengensis* was found to be more ‘primitive’ than other species of the genus (Deng et al.,

2014).

The Ukraine *Eostyloceros* is highly similar to *Euprox furcatus* except for the difference in pedicle length (Croitor & Stefaniak, 2009; Croitor, 2014). Therefore, a synonymisation of *Eostyloceros* with *Euprox* has been suggested (Croitor, 2014), but requires further scrutiny. *Euprox* is considered as the direct ancestor of *Eostyloceros*, *Metacervulus*, and *Paracervulus*, and eventually of the extant *Muntiacus* (Vislobokova, 1990; Croitor, 2014).

In my analyses, *Eostyloceros hezhengensis* has been most often placed in an unresolved position; in five cases, particularly in analyses based on the combined data set, it was placed as the sister taxon to *Elaphodus cephalophus*, once it was placed as the sister taxon to Muntiacini, and in two cases it was considered as the sister taxon to *Praeclaphus etueriarum*, and twice as the sister taxon to *Praeclaphus etueriarum* and *Cervus australis* (all dental and combined matrix). In the SFA it was placed as the sister taxon to all *Muntiacus* species, as the sister taxon to *Elaphodus cephalophus*, and in an unresolved position. The EPA analysis placed *Eostyloceros hezhengensis* in an unresolved position within Muntiacini. All this suggests that it is probably more closely related to muntjacs than to other cervids, which would support results from comparative morphology, and thus *Eostyloceros hezhengensis* can be considered as a direct ancestor of muntjacs. In Azanza Asensio (2000) *Eostyloceros* is always closely related to *Muntiacus* and *Metacervulus*, either as polytomy or forming sister taxon relationships in all possible combinations.

Euprox furcatus

Euprox has been considered as the most modern of Miocene cervids, because of the presence of a burr and was assumed to have given rise to later Pliocene cervids (Thenius, 1948). It was hypothesised that *Dicrocerus* and *Euprox* are closely related based on antler evolution and that *Euprox* is possibly the ancestor of *Metacervulus* (Dong et al., 2003). *Euprox* is intermediate in size between *Heteroprox* (smaller) and *Dicrocerus* (Gentry, 1990). The first records of *Euprox* in China are described in Dong et al. (2003) with the large species *Euprox robustus*.

The dentition of *Euprox* and *Heteroprox* has been considered as indistinguishable; however, the following characters from my data set may be useful in distinguishing both species (pers. obs.): Character 19 in the current dental matrix concerns the posterolingual crista and the posterior style of the upper premolars, which are already connected in relatively early wear in *Heteroprox*, but still separate in medium wear in *Euprox* (note that this is based on only one specimen). Obviously, these character state differences need to be confirmed on more specimens, but may represent a potential distinction between the two species. In addition, I observed subtle differences in the orientation of the anterior and posterior elements of p4, which are more diagonally oriented in *Euprox* and more transverse in *Heteroprox*.

Azanza (1993b) classified *Euprox* already as belonging to the Muntiacini/(-ae) and has since often been considered as a member of the Muntiacini/(-ae) and as the ancestor for Capreolinae and Pliocervinae + Cervinae, which are sister taxa to each other (Czyżewska, 1968; Croitor, 2014). Similarly, it was suggested that modern *Muntiacus* and fossil muntiacines such as *Eostyloceros*, *Metacervulus*, and *Paracervulus* diverged from *Euprox* (Vislobokova, 1990; Croitor, 2014).

In my analyses, *Euprox furcatus* most often was placed in an unresolved position or as the sister taxon of *Heteroprox larteti* (mostly dental matrix), sometimes within a clade with other Miocene species. *Euprox* and *Heteroprox* were united in a clade based on shared character states of the P2, P3, upper molars, p2, p4, lower molars, upper canines. It was also placed between the outgroup and cervids four times (combined matrix) and once as the sister taxon to *Muntiacus reevesi* (cranial matrix). In the SFA *Euprox* was placed twice within Muntiacini and once as the sister taxon to *Muntiacus atherodes*. The EPA analysis placed *Euprox furcatus* in an unresolved position within Muntiacini.

In Azanza Asensio (2000) analyses *Euprox* is either placed as the sister taxon to *Amphiprox*; this clade is the sister taxon to a clade containing extant *Muntiacus* and *Elaphodus*, *Eostyloceros*, and *Metacervulus*, or as the sister taxon to a clade containing all five of the above species or a subset thereof.

Although the results indicate that *Euprox furcatus* shares characters with other Miocene cervids, it also appears that *Euprox furcatus* already acquired some apomorphic characters which indicate a closer relationship to extant Muntiacini than to other crown cervids. A great drawback in early putative fossil muntjac-like cervids is that there is a large temporal gap between the first representatives, *Euprox*, and the presumed direct ancestors of muntiacines, e.g., *Eostyloceros*, and additionally an even larger gap between those early fossils and the first members of *Muntiacus*, which appear in the Pleistocene. For more certainty of the systematic relationships it would be crucial to find more fossil cervids that would link the early presumed muntiacines with the crown muntiacines.

Heteroprox larteti

The dentition of *Heteroprox* is similar to that of *Dicrocerus* (but not as indistinguishable compared to that of *Euprox*, see above). Ginsburg & Crouzel (1976) list the following characters, which are diagnostic for *Heteroprox larteti*: the absence of p1, a weak lingual cone on P3, a weak mesolingual conid on p2, a deep labial incision on p3 and p4; other characters are identical with *Dicrocerus*.

The mesowear of *Heteroprox larteti* is similar to that of *Euprox furcatus*, although *Heteroprox larteti* has been classified as mixed feeder with some preference for grazing; hence includes somewhat more abrasives in its diet than *Euprox furcatus* (DeMiguel et al., 2011). The microwear analyses suggest that *Heteroprox larteti* possibly took in more grass in its diet than *Euprox furcatus*; however, both have similar mesowear pattern to extant mixed feeders and *Heteroprox larteti* clusters close to extant browsers, closest to the giraffes (Kaiser & Rössner, 2007; DeMiguel et al., 2011).

In some Spanish localities *Heteroprox larteti* and *Euprox furcatus* with similar body size and tooth crown height coexisted with three bovid species, which were more hypsodont. This resulted in a heavy competition about food (DeMiguel et al., 2011). Several suggestions for habitat use and social structure for *Heteroprox eggeri* were made in Rössner (2010); the presence of dense vegetation could be inferred with high probability for its palaeohabitat. It remains speculative, whether the social structure of *Heteroprox larteti* was solitary, living in pairs or gregarious.

European *Heteroprox* species comprise *Heteroprox anatoliensis* Geraads 2003, *Heteroprox eggeri* Rössner 2010, and *Heteroprox moralesi* Azanza Asensio 2000. Cranial ap-

pendages and dentition of *Heteroprox larteti* are highly similar to those of *Procervulus*, indicating a close relationship (Rössner, 1995, 2010). It has even been considered as the descendant of *Procervulus dichotomus* based on the evidence of successive stratigraphical occurrence of the *Procervulus-Heteroprox*-lineage (Ginsburg & Azanza, 1991; Rössner, 2010). This lineage hypothesis, however, must be rejected based on the recent findings of a new *Heteroprox* species from Sandelzhausen, *Heteroprox eggeri*, from the early Langhian (early middle MN5) (Rössner, 2010). This appearance is contemporaneous with *Procervulus dichotomus* in other localities; therefore the genus *Heteroprox* is likely a divergent branch from the *Procervulus*-line that split in the early Langhian (early middle MN5) (Rössner, 1995, 2010). *Heteroprox eggeri* most likely is the ancestor of *H. larteti* (MN5–MN7) and *H. anatoliensis* (MN6) (Rössner, 1995).

In my analyses, *Heteroprox larteti* was most often placed in an unresolved position or as the sister taxon to *Euprox furcatus* (mainly dental matrix) sometimes within the clade consisting of Miocene cervids. It was placed between the outgroup and cervids four times. In one analysis it was considered as the sister taxon to *Dicrocerus elegans* (cranial matrix). In the SFA it was the sister taxon to *Moschus* in one analysis, within Muntiacini in the other and between muntiacine taxa and the clade consisting of Capreolinae and Cervini in the third analysis. The EPA analysis placed *Heteroprox larteti* in an unresolved position within Muntiacini.

In Azanza Asensio (2000) *Heteroprox* is most often placed as the sister taxon to *Procervulus* or between *Lagomeryx*, *Stephanocemas*, *Procervulus*, *Dicrocerus*, *Acteocemas*, *Stehlinoceros* and all other cervids analysed therein.

Based on the morphological topologies here, *Heteroprox* is sometimes placed close to other Miocene cervids based on its plesiomorphic characters, and some topologies indicate a potential closer relationship to Muntiacini based on apomorphic characters. Similar to *Euprox furcatus*.

Dicrocerus elegans

Dicrocerus elegans is a medium-sized deer widely distributed across Western Europe during the early middle Miocene and particularly well known from Sansan (France) (Stehlin, 1939; Azanza et al., 2011). The high number of *Dicrocerus elegans* specimens from Sansan suggests a gregarious social structure (DeMiguel et al., 2008; Azanza et al., 2011). *Dicrocerus elegans* had a proportion of grass in its diet despite having brachyodont dentition and has been classified as a mixed feeder (Solounias & Moelleken, 1994; Kaiser & Rössner, 2007; DeMiguel et al., 2013). *Dicrocerus* is considered as the more swamp-forest adapted form, while *Euprox* presumably preferred drier habitats, and *Heteroprox* was more generalistic in habitat use (Thenius, 1948). The similarity of *Dicrocerus* antlers to those of modern cervids, dicrocerines were hypothesised to be between procervulines and crown cervids (Azanza et al., 2011). The late Miocene *Cervavitus* is considered as a transitional link between *Dicrocerus* and modern *Cervus* (Croitor, 2014; Flerov, 1952).

In the analyses here, *Dicrocerus elegans* was placed as the sister taxon to *Procervulus dichotomus* (dental matrix), to *Procervulus praelucidus* (combined), or to both (combined). *Dicrocerus* and *Procervulus* shared character states of the upper premolars and molars, lower premolars and molars, upper canines. Also, characters states of the mandible, several

proportions of the of the skull, morphology of the nasals, of the occipital region, presence of a prominent linea temporalis, and several character states referring to the antlers and pedicles. It was also placed as the sister taxon to *Heteroprox larteti* (cranial matrix), *Muntiacus atherodes* (dental matrix), between the outgroup and cervids or in an unresolved position. In the SFA *Dicrocerus elegans* was placed twice within Muntiacini and once between the outgroup and cervids. The EPA analysis placed *Dicrocerus elegans* as the sister taxon to all *Muntiacus* and some fossil taxa.

In Azanza Asensio (2000) *Dicrocerus elegans* is placed as the sister taxon to *Acteocemas* and *Stehlinoceros* (= *Paradicrocerus*) and this clade is the sister taxon to all burr-bearing antlered cervids.

Based on my results and discussions in the literature, *Dicrocerus* is most certainly a stem cervid with affinities to primarily *Procervulus* and secondarily to other Miocene cervids. In a few analyses a potentially closer relationship to Muntiacini was suggested.

Palaeoplatyceros hispanicus

Palaeoplatyceros hispanicus from the Serravallian/Tortonian (Aragonian) can be distinguished from all other contemporaneous cervid species based on the palmation of antlers (Azanza Asensio, 2000). The species is only known from the Serravalian (upper Aragonian) of Spain. Its systematic position is problematic, as its antler morphology differs from all other living and fossil cervids. The most detailed information about *Palaeoplatyceros* can be found in Azanza Asensio (2000). In her analyses *Palaeoplatyceros* was mostly placed as the sister taxon to all other cervids with burr-bearing antlers.

In most analyses here *Palaeoplatyceros hispanicus* was placed between the outgroup and cervids or in an unresolved position; in two analyses it was the sister taxon to *Lagomeryx parvulus* (dental matrix) and in another two analyses it was placed as the sister taxon to most other Miocene taxa (cranial matrix). Similarly, in the SFA it was placed in an unresolved position in two analyses and between the outgroup and cervids in one analysis. The EPA analysis placed *Palaeoplatyceros hispanicus* in a stem position. *Palaeoplatyceros* is highly incomplete and has a combination of several plesiomorphic characters, which would place it more closely to the other Miocene cervids, it also has the apomorphic trait 'presence of a burr' which would place it more closely to crown cervids.

Unless more material can be obtained of this species, its systematic position remains controversial. Based on the analyses here, *Palaeoplatyceros* is likely a stem cervid with burr-bearing antlers, which is an apomorphic trait compared to other Miocene cervids. Alternatively, it could be a primitive representative of burr-bearing cervids.

Pliocervus matheronis

Pliocervus matheronis (Gervais 1859) is known from the Messinian (upper Turolian, MN13). Since its antler remains are fragmentary, the overall antler morphology can only partially be reconstructed (Azanza Asensio, 2000). They are at least three tined with a high first bifurcation, and a weak beam curvature and sit on short slender pedicles; *Pliocervus* is the least distinctive three-tined cervid of that time (Azanza Asensio, 2000; Gentry, 2005). *Pliocervus matheronis* is similar in body size to modern roe deer with relatively larger antlers; pedicles are parallel and close together similar as in *Capreolus*. Revision on *Pliocervus*

material came to the conclusion that fully developed antlers of *Pliocervus matheronis* must have been four-tined (Croitor, 2014). The well-developed, enlarged upper canines resemble those of other contemporaneous Miocene representatives of Cervinae and Capreolinae (Vislobokova, 1990; Gentry et al., 1999; Croitor, 2014).

Although Simpson (1945) included Pliocervinae, comprising *Cervocerus*, *Cervavitus*, *Procervus*, and *Pliocervus*, in Cervinae, others could not find any phylogenetic relationship of *Pliocervus* with Cervini/Cervinae (Petronio et al., 2007). Gentry et al. (1999) placed the valid genera *Cervavitus* and *Pliocervus* among Cervoidea, whereas Azanza & Montoya (1995) and Azanza Asensio (2000) classified *Pliocervus* as Cervinae, including its four species *P. matheroni*, *P. graecus* and *P. kutchurganicus*, and *P. turolensis* (Petronio et al., 2007). A definite morphological characterisation of *Pliocervus* from the late Miocene (MN12–13) of Europe is still missing and its systematic position controversial (Godina et al., 1962; Czyżewska, 1968; Korotkevich, 1970; Croitor, 2014). It has been suggested to be together with holometacarpal *Cervavitus* within Pliocervini, which is included in Cervinae (Czyżewska, 1968; Vislobokova, 1990; Azanza Asensio, 2000).

Cranial, dental, and antler features of *Pliocervus matheronis* are highly similar to those of the late Miocene *Pavlodaria orlovi*, which implies that these two genera must be closely related or possibly even synonymous. Considering this, *Pliocervus* should be included within Capreolinae rather than Cervinae. It was suggested that the subfamily Pliocervinae Symeonidis 1974, containing *Pliocervus* and *Pavlodaria* in that study, is a synonym to Capreolinae (Croitor, 2014).

Previously, remains of *Procapreolus* sometimes have been classified as *Pliocervus*, which led to more confusion concerning the distinction between those two genera (Gentry, 2005; Croitor & Stefaniak, 2009). The systematic position of *Pliocervus* and *Cervavitus* remains enigmatic, while the two taxa clearly differ from each other in antler morphology and *Pliocervus* is considered as primitive (Petronio et al., 2007). In most recent studies *Pliocervus* is regarded as incertae sedis (Croitor, 2014).

In my analyses, *Pliocervus matheronis* was most often placed in an unresolved position; it was also placed between the outgroup and cervids in two analyses (combined) and once each as the sister taxon to six other Miocene taxa (combined), *Axis lydekkeri* (dental), *Heteroprox* and *Euprox* (dental), *Capreolus capreolus* (cranial), and *Hypertragulus calcaratus* (combined). In the SFA it was placed within bovids in one analysis and as the sister taxon to *Muntiacus atherodes* in the other two analyses. The EPA analysis placed *Pliocervus matheronis* in a stem position.

In Azanza Asensio (2000) *Pliocervus matheronis* is variably placed closely related to *Croizetoceros*, *Cervus*, *Rusa*, *Turiacemas*, *Capreolus*, *Odocoileus*. Thus, affiliation of *Pliocervus* to Cervini or Capreolinae remains controversial and cannot be solved to date. Based on my analyses *Pliocervus* is a stem cervid with neglectable affiliations to Muntiacini and was placed only in one analysis close to *Capreolus capreolus*. Based on her results, *Pliocervus matheronis* seems to have the highest proportion of apomorphic characters compared to other Miocene cervids.

3.4.2 Pliocene and Plio-Pleistocene Cervids

During the early Pliocene *Lagomeryx*, *Stephanocemas*, and *Dicrocerus* disappear, while the late Miocene genera persist (14 cervid species in total). During the late Pliocene, only ten early Pliocene taxa remain; they are characterised by larger antlers (Dong, 1993). General evolutionary trends include an increase of the overall body size, a decrease of the pedicle length relative to the antler length, reduction of the premolar row length, reduction of the relative width of the teeth, reduction and loss of the anterior conid in p2, reduction of the anterior conid in p3 and p4, molarisation of the p4, reduction of the protocone and metaconule fold, and reduction of cingula (Heintz, 1970).

There is no generally accepted classification of Plio- and Plio-Pleistocene cervids Pfeiffer (1999); however, for Villafranchian (MN16) cervids the following classifications were suggested: *Croizetoceros ramosus*, *Metacervoceros pardinensis*, '*Cervus*' *philisi*, '*Cervus*' *perolensis*, *Eucladoceros ctenoides* were considered as Cervini, *Arvernoceros ardei* as Megacerini, and *Libralces gallicus* (not included in my work) and *Procapreolus cusanus* were considered as Capreolinae. The Villafranchian lasted 2.5 million years according to Heintz (1970) (but see Figure B.1).

At the end of the Villafranchian only '*Cervus*' *perolensis* and *Eucladoceros ctenoides* persisted, while all other forms became extinct according to Stefaniak & Stefaniak (1995); however, the specimens studied here, *Croizetoceros ramosus*, '*Cervus*' *perolensis*, *Praeclaphus perrieri*, *Praeclaphus etueriarum*, *Eucladoceros ctenoides*, and *Metacervoceros rhenanus* reach the end of the middle Villafranchian and only '*Cervus*' *philisi* persists until the end of the late Villafranchian. During the middle Pleistocene the typical Pleistocene taxa appear (Stefaniak & Stefaniak, 1995).

The new definition of the Pliocene-Pleistocene-boundary from 1.8 mya to 2.5 mya, which newly defined the Gelasian as Pleistocene instead of Pliocene (Fig. 3.2), many taxa, which previously occurred in the Pliocene only, range now across the Pliocene-Pleistocene-boundary and continue throughout the Gelasian. This subsection is about taxa exclusively from the Pliocene, i.e., *Cervus australis*, *Arvernoceros ardei*, *Procapreolus cusanus*, and *Metacervoceros pardinensis* and taxa ranging over the Pliocene-Pleistocene-boundary, i.e., *Croizetoceros ramosus*, '*Cervus*' *perolensis*, *Praeclaphus perrieri*, *Praeclaphus etueriarum*, *Eucladoceros ctenoides*, and *Metacervoceros rhenanus*. All these cervids become extinct at the end of the Gelasian. The taxa in this subsection are ordered according to their first appearance in the fossil record (Fig. 3.2).

Cervus australis

This species was originally described by De Serres (1832), all specimens are from Montpellier, France (Czyżewska, 1959). Gervais (1848–1852) described lyre-shaped antlers approximately 23 cm long. Apart from that, not much can be drawn from the literature concerning this species. Many entries point to muntiacines, e.g., *Paracervulus australis* (Gentry, 2005); however, there are no obvious similarities to muntiacines in the investigated specimens.

In the phylogenetic analyses here, *Cervus australis* was most often placed in an unresolved position, sometimes closer to Muntiacini than to other cervids; it was also placed between the outgroup and cervids, as the sister taxon to *Eostyloceros hezhengensis* and *Praeclaphus etueriarum* (dental matrix), to *Hippocamelus bisulcus* (cranial matrix), and

Muntiacus muntjak (combined matrix). In the SFA it was placed once between the out-group and all other taxa and twice as the sister taxon to *Hippocamelus bisulcus*. The EPA analysis placed *Cervus australis* in a polytomy with *Hippocamelus bisulcus* and *Hypertragulus calcaratus*. This leaves the systematic position of *Cervus australis* highly speculative; even though it apparently shares some (cranial) characters with *Hippocamelus bisulcus* the more likely position may be at the stem of Cervidae, potentially closer to Muntiacini.

Arvernoceros ardei

Arvernoceros ardei is a large sized cervid recorded from the late Ruscinian of Eastern Europe and early Villafranchian of Western Europe (MN15–16) (Croitor & Stefaniak, 2009). It was originally assigned to *Cervus sensu lato* like most of the other Villafranchian cervids as *Cervus ardei* Croizet & Jobert 1828 from the early Villafranchian site Perrier-Etouaires (France) (Croitor, 2009). The holotype is figured in Depéret (1884; Pl. V, Fig 1), and Heintz (1970; text figure 295), however, no specimen in collections corresponds to the figures. Therefore, a neotype has been established (Heintz, 1970: text figure 296, Pl. XVIII Fig. 1a, b) to define the new genus. Unfortunately, there is no complete cranium available. *Arvernoceros ardei* is characterised by a simple unmolarised p4, cingula on upper dentition, relatively long, parallel, inclined pedicles, the first tine of the antler can be flattened, and antlers have a small distal fork, or sometimes a terminal palmation (Croitor, 2009, 2014). The suite of character states of *Arvernoceros ardei* consists of plesiomorphic and apomorphic character states; the large body size and the serrated premetaconule- and postprotocristae on the upper molars are more apomorphic characters.

The lower jaw, dentition, and postcranial material of *Arvernoceros ardei* is almost identical with that of *Praedelaphus perrieri*; they can only be distinguished based on their antler morphology (Heintz, 1970; Croitor, 2014).

The systematic position of *Arvernoceros ardei* has been subject to speculation for decades, its definition is still incomplete and affinities to other cervids unclear. Depéret (1884) found similarity to *Axis*, but no affiliation to *Dama*; however, the palmated antlers indicate a relationship to *Dama*, *Alces* or *Megaloceros*, but are too different from those in *Dama*, and *Alces*. Therefore, it was suggested that it is most similar to Megacerini (Heintz, 1970). This was supported by (Vislobokova, 1990, 2012). Based on the flattened shape of first tine, the presence of a small distal antler palmation, and presence of cingula on the upper molars Heintz (1970) hypothesised that *Arvernoceros ardei* might be the direct ancestor of *Megaloceros giganteus* in Western Europe. In different sources it was suggested that *Arvernoceros ardei* is closely related to modern *Elaphurus* (Teilhard de Chardin & Piveteau, 1930), later it was declared as incertae sedis genus by (Lister, 1987). Di Stefano & Petronio (2002) suggested that *Arvernoceros ardei* is closely related to *Axis* based on the long assumed three-tined antler morphology. More recently it has been hypothesised that it could be closely related to *Rucervus* based on similarity of antler characters to *Rucervus duvaucelii* and a similar basioccipital morphology (Croitor, 2009). Croitor (2014) questioned a close relationship to *Rucervus*, because upper canines are present in an *Arvernoceros* specimen from Valea Graunceanului, but were wrongly assumed to be absent in *Rucervus duvaucelii*. He conceded that they may still be distantly related, despite this difference. As upper canines are regularly present in *Rucervus duvaucelii*, a

close relationship between those two taxa is not yet ruled out. A further feature, which supports this hypothesis, is the presence of serrated premetaconule- and postprotocristae on the upper molars in *Arvernoceros ardei* (pers. obs.). Nevertheless, *Arvernoceros* is considered to be part of the first radiation of Cervinae/-i together with *Metacervocerus*, *Praeclaphus*, *Axis*, and *Rucervus* (Croitor, 2014).

In most of my analyses *Arvernoceros ardei* was placed in an unresolved position; it was considered as the sister taxon to *Metacervocerus pardinensis*, *Dama dama*, *Praeclaphus perrieri*, and *Metacervocerus rhenanus*. *Dama dama* and *Arvernoceros ardei* were united based on characters on the upper premolars, the upper molars, p4, and m3, proportions of the orbita, the processus lacrimalis, several characters on the palate, and the palmation of antlers. In the SFA it was placed as the sister taxon to *Dama dama* twice and as the sister taxon to all Cervini in the third analysis. The EPA analysis placed *Arvernoceros ardei* as the sister taxon to *Dama dama*.

Despite some uncertainties in the morphological analyses, results from the analyses here and previous comparative morphology strongly suggest a closer relationship to *Dama dama* than to other cervids.

Croizetoceros ramosus

Croizetoceros ramosus is a small- to medium-sized cervid and is abundant in the fossil record of the Pliocene and Pleistocene (MN16–MQ1) of France and Spain (Heintz, 1970), in the Pliocene of Ukraine and Moldavia (Korotkevich, 1988; Vislobokova, 1990), in Poland in Weże 2 (MN16) and Rebielice Królewskie 1A (MN16) (Stefaniak & Stefaniak, 1995). The type species is from the Pliocene and Early Pleistocene (MN16–18) of Western Europe and the Mediterranean (Croitor, 2014). The holotype figured in Croizet & Jobert (1828; Fig. 2, Pl. V second sou-genre), but there is no corresponding specimen in the collections; therefore a neotype was erected by Heintz (1970; Pl. V, Fig. 5a, b), which also has been figured in Depéret (1884; Pl. V Fig 7). *Croizetoceros ramosus* is characterised by long lyre-shaped antlers bearing 5–8 tines relatively high above the burr, all on the anterior side of the beam, molarised p4, absence of anterior cingulid on lower molars, presence of protocone fold, and a general more derived tooth morphology (Heintz, 1970; Croitor, 2014).

Croizetoceros ramosus has the smallest pedicle to antler ratio among Plio- and Plio-/Pleistocene cervids. The antler morphology of *Croizetoceros ramosus* is unique without similarities with any extant cervid species or with other cervid species from the Villafranchian, which justifies its own genus (Heintz, 1970). Unfortunately, there is not much known about its skull morphology (Croitor, 2014). The earliest representative of the genus is *Croizetoceros pyrenaicus* from the late Miocene (MN13) of Spain (Morales, 1984; Azanza Asensio, 2000). Since there are no remains of *Croizetoceros* known from Asia, it can be assumed that *Croizetoceros* is endemic to Europe (Croitor, 2014).

In most of my analyses *Croizetoceros ramosus* was placed in an unresolved position; it was the sister taxon to *Procapreolus cusanus* in two topologies and between *Procapreolus cusanus* and other cervines in one analysis (all dental matrix). Analyses based on the cranial and combined matrix result in a close relationship to *Odocoileus*. In the SFA *Croizetoceros ramosus* was placed once as the sister taxon to *Alces alces* and in unresolved position within Capreolinae in the other two analyses. The EPA analysis placed *Croize-*

toceros ramosus as the sister taxon to *Ozotoceros bezoarticus*. These results suggest a placement within Capreolinae and possibly a closer relationship to *Procapreolus cusanus*.

‘*Cervus*’ *perolensis*

‘*Cervus*’ *perolensis* is a medium-sized deer from the upper Villafranchian. The holotype is stored in the British Museum of Natural History (BMNH 34528) and figured in Bout & A. (1952; Fig. 8b p. 51) and in Heintz (1970; Fig. 191). The overall morphology is very similar to ‘*Cervus*’ *philisi* (Heintz, 1970; Spaan, 1992). Unfortunately, antlers are largely unknown; the first tine is often present and differs from ‘*Cervus*’ *philisi* in the angle of bifurcation, but is similar to *Metacervocerus rhenanus*; antlers, dentition and postcranial material are slightly smaller than in ‘*Cervus*’ *philisi*, while the tooth morphology of ‘*Cervus*’ *perolensis* is similar to ‘*Cervus*’ *philisi* (Heintz, 1970; Spaan, 1992). The lower dentition of ‘*Cervus*’ *perolensis* contains more apomorphic features than that of ‘*Cervus*’ *philisi* (Heintz, 1970). While Spaan (1992) states that there are no morphological differences in the dentition of *Metacervocerus rhenanus*, ‘*Cervus*’ *philisi*, and ‘*Cervus*’ *perolensis*, but there are some size differences.

Azzaroli (1953) found that ‘*Cervus*’ *perolensis*, *Metacervocerus rhenanus*, and ‘*Cervus*’ *philisi* cannot be assigned to any known genus, but are most similar to *Dama nestii*. ‘*Cervus*’ *perolensis*, as *Metacervocerus pardinensis*, was classified as *Pseudodama* by Azzaroli & Mazza (1992a), it was considered as descendant of ‘*Cervus*’ *philisi* by Stefaniak & Stefaniak (1995). Spaan (1992) however, concluded that ‘*Cervus*’ *philisi* and ‘*Cervus*’ *perolensis* are junior synonyms of *Metacervocerus rhenanus* and should be renamed as such, which is supported by Pfeiffer (1999). If this is true, ‘*Cervus*’ *philisi* and ‘*Cervus*’ *perolensis* should come out in a similar systematic position as *Metacervocerus rhenanus*.

In my analyses ‘*Cervus*’ *perolensis* was most often placed in an unresolved position; it was once placed between the outgroup and cervids, and twice as the sister taxon to *Metacervocerus pardinensis* (dental matrix), as the sister taxon to seven Miocene taxa (cranial matrix), and as the sister taxon to *Metacervocerus rhenanus* or other cervine taxa (combined matrix). In the SFA it was placed twice as the sister taxon to *Cervus elaphus* and within the *Cervus*-clade in the third analysis. The EPA analysis placed ‘*Cervus*’ *perolensis* in a polytomy with *Axis lydekkeri*, *Metacervocerus rhenanus*, and *Cervus elaphus* within the *Cervus*-clade. This suggests that ‘*Cervus*’ *perolensis* almost certainly belongs to Cervini and is likely closely related to and/or ancestor of *Cervus*.

Procapreolus cusanus

The genus *Procapreolus* was established by Schlosser (1924) including ten Eurasian species ranging from the late Miocene to the early Pleistocene (Valli, 2010). *Procapreolus cusanus* represents the smallest deer from the Villafranchian; the holotype is figured in Croizet & Jobert (1828), but cannot be identified in the collections, therefore, a neotype has been erected, whose detailed description can be found in Heintz (1970; p. 74). It is characterised by moderately long pedicles, antlers with usually three tines, a highly molarised p4, and absence of anterior cingula in lower molars (Croitor, 2014).

Despite the widely accepted assumption that *Procapreolus cusanus* is closely related or even direct ancestor to *Capreolus*, the origin of *Capreolus* within *Procapreolus* is still under

debate (Lechner-Doll et al., 2001). *Procapreolus cusanus* was assigned to telemetacarpal cervids by Valli (2010), because of the state of the ‘post-glenoid foramen’, which is not completely surrounded by the squamosal. According to Korotkevich (1963, 1964, 1965) ‘*Cervus*’ *cusanus* is included in the genus *Procapreolus*. Dong (1996) suggests that *Procapreolus cusanus* is the sister taxon to ‘*Cervus*’ *pyrenaicus* and these two are the sister taxon to *Croizetoceros*. Even though *Procapreolus cusanus* and *Procapreolus ukrainicus* have similar antlers, the dentition of the younger (MN16) *P. cusanus* has a higher proportion of apomorphic characters. Therefore, some authors hypothesise that it may be assigned to *Capreolus* rather than *Procapreolus* (Valli, 2010). Others place it in an intermediate position between lower Pliocene and Pleistocene *Procapreolus* species and extant *Capreolus* based on more upright antlers, loss of upper canine and some other dental and skeletal features (Czyżewska, 1968; Heintz, 1970; Lechner-Doll et al., 2001). *Capreolus capreolus* shares the number of tines, position of tines and overall antler size with *Procapreolus cusanus*, but Heintz (1970; pp. 77, 81, 85) points also to some differences, e.g., the more nodose ornamentation in *Capreolus capreolus* antlers, shorter pedicles, and a more medial insertion of the pedicles. Most authors in the last century suggested to assign ‘*Cervus*’ *cusanus* to *Capreolus*, whereas the studies of the last one or two decades regard it as *Procapreolus*.

In the analyses here, *Procapreolus cusanus* was most often placed in an unresolved position; in topologies based on the dental matrix it was placed as the sister taxon of *Croizetoceros ramosus*, *Moschus*, or both. It was also placed between the outgroup and cervids, as the sister taxon to both fossil *Odocoileus* and *Croizetoceros ramosus*, as the sister taxon to both *Capreolus*, and to *Megaloceros giganteus* (all combined matrix). In the SFA it was the sister taxon to *Moschus* in one analysis, unresolved within Capreolinae in another, and the sister taxon to *Hippocamelus* in the third analysis. The EPA analysis placed *Procapreolus cusanus* as the sister taxon to *Capreolus capreolus* within Capreolini. Thus, *Procapreolus cusanus* most likely belongs to Capreolinae and the previously suggested close relationship to *Capreolus* is confirmed in some analyses.

Metacervocerus pardinensis

The medium-sized *Metacervocerus pardinensis* was distributed from the late Pliocene until the early Pleistocene (Villafranchian; MN 15–16) in Europe (Heintz, 1970; Croitor, 2006a; Croitor & Stefaniak, 2009; Croitor, 2014). Its fossil remains are highly fragmentary; therefore its skull morphology is unknown (Croitor, 2014). The holotype was figured in Croizet & Jobert (1828; Pl. XI Fig. 4 premier sous-genre), however, no specimen exactly corresponds to the figure. Therefore, a neotype was established by Heintz (1970; Pl. VIII Fig. 6a, b, text figure 146).

The genus *Metacervoceros* was established by Dietrich (1938) based on the type species ‘*Cervus*’ *pardinensis*; further he proposed that *Metacervoceros pardinensis* is synonymous with *etueriarum*, *perrieri*, *issiodorensis*, *rhenanus* (Dietrich, 1938). Other species referred to *Metacervoceros pardinensis* include *Metacervoceros rhenanus*, *Metacervoceros warthae* Czyżewska 1968 (Croitor, 2006a). *Metacervoceros pardinensis* is characterised by three-tined antlers on relatively long pedicles, cingula on upper molars, tendency to molarised p4, and presence of a protocone fold. It is very similar to ‘*Cervus*’ *philisi* particularly the

dentition (Heintz, 1970; Croitor, 2006a).

In contrast to Depéret (1884), Heintz (1970) states that the antlers of *Metacervocerus pardinensis* differ considerably from those of *Procapreolus cusanus*, *Croizetoceros ramosus*, *Eucladoceros ctenoides*, and *Arvernoceros ardei*, but are similar to those of *Praeclaphus perrieri* and most similar to ‘*Cervus*’ *philisi* and ‘*Cervus*’ *perolensis*. The temporal distribution suggests that *Metacervocerus pardinensis* could be an ancestor of ‘*Cervus*’ *philisi*. *Metacervocerus pardinensis* and *Metacervocerus rhenanus* have enough morphological differences to justify two different species (Spaan, 1992).

Based on similarities to *Rusa* or smaller *Axis* deer, the genus *Metacervoceros* was erected to represent European rusine deer (Croitor, 2006a, 2014). However, its systematic position remains controversial. *Metacervocerus pardinensis* was classified as *Pseudodama* by Azzaroli & Mazza (1992a), while De Vos & Reumer (1995) assigned *Metacervocerus pardinensis* and *Metacervocerus rhenanus* to *Cervus*, Pfeiffer (1999) assigned them to *Dama*. The more primitive skull shape of *Metacervocerus rhenanus* and differing skull proportions excluded the genus from *Cervus* and *Dama* (Croitor, 2014). Di Stefano & Petronio (2002) assigned *Metacervocerus* to *Rusa*; differences in the skull morphology make this a doubtful affiliation and it is likely that *Metacervocerus* does not belong to the *Cervus*-*Rusa* evolutionary lineage, which needs stronger evidence from the fossil record. It is more likely that *Metacervocerus pardinensis* represents an ancestor of *Dama* (Croitor, 2014).

In most analyses here, *Metacervocerus pardinensis* was placed in an unresolved position, it was the sister taxon to *Arvernoceros ardei* or close to the latter, *Dama*, and *Metacervocerus rhenanus* (dental and combined matrix). In one analysis it was the sister taxon to *Rusa kendengensis* and *Axis lydekkeri* (cranial) and in three analyses it was the sister taxon to ‘*Cervus*’ *sivalensis* (combined matrix). In the SFA *Metacervocerus pardinensis* was the sister taxon to all Cervini, unresolved within Cervini, and the sister taxon to the *Cervus*-clade. The EPA analysis placed *Metacervocerus pardinensis* in a polytomy with ‘*Cervus*’ *sivalensis* and *Cervus canadensis* within the *Cervus*-clade. Thus, *Metacervocerus pardinensis* almost certainly is a member of Cervini and probably a close relative and/or ancestor of *Cervus*.

Praeclaphus perrieri

Praeclaphus perrieri was a large-sized deer with abundant material in the fossil record. The holotype was figured in Croizet & Jobert (1828; Pl. IV Fig. 1), but none of the collection specimens corresponded to the one in the figure. Therefore, a neotype has been established based on an MNHN specimen text Heintz (1970; text figure 261, Pl. XV Fig. 1a, b), which was already figured in Depéret (1884; Pl. VI Fig. 7). Antlers regularly have four tines similar to those of *Cervus nippon* and similar to *Metacervocerus pardinensis*, ‘*Cervus*’ *philisi*, and ‘*Cervus*’ *perolensis*. Antlers and dentition of *Praeclaphus perrieri* have never been found articulated, which is problematic, because in some localities, e.g., Etouaires, the similar sized deer *Arvernoceros ardei* coexists with *Praeclaphus perrieri*, which has a different antler morphology, but almost identical teeth (Heintz, 1970) (note that based on the accompanying data for the specimens studied here these two species represent successors rather than coexisting species!). The upper dentition has no specific morphological features, the size is slightly smaller than that of *Eucladoceros*; there is only

little difference between upper dentition of *Arvernoceros ardei* and *Praeclaphus perrieri*. The lower dentition is different from that of *Arvernoceros ardei* and contains more plesiomorphic traits in *Praeclaphus perrieri*. Size is the only criterion to separate *ardei* and *perrieri* specimens from all other contemporary cervids, as they cannot be distinguished based on morphology alone (Heintz, 1970; Croitor, 2014).

Antlers assigned to *Praeclaphus etueriarum* represent juvenile *Praeclaphus perrieri* specimens, also *Cervus issiodorensis* antlers are variants of *P. perrieri*. They are most similar to antlers of *Cervus nippon* or *Rusa*, but relationships remain uncertain. Neither morphology nor biometric data can distinguish teeth and postcranial material from *Eucladoceros*. However, *Praeclaphus perrieri* and *Eucladoceros ctenoides* do not coexist in any of the known localities, although they occupy the same niches (Croitor, 2014).

Already Portis (1920) has proposed a new subgenus *Praeclaphus* for ‘*Cervus*’ *perrieri*, as well as for *C. avernensis*, *C. etueriarum* from the early Villafranchian (Croitor, 2014). The closest relative of *Praeclaphus perrieri* is *P. lyra* from Val d’Arno (Italy); it is also related to *P. warthae*. The high similarity among them indicates that they may represent synonyms (Croitor, 2014). *Praeclaphus perrieri* was considered as the earliest representative of *Cervus* in Europe by Di Stefano & Petronio (2002), however, even though it is an early cervine, there is no clear evidence that it is directly related to *Cervus* and it more likely represents an extinct lineage within the early cervine evolution (Croitor, 2014).

In most of my analyses *Praeclaphus perrieri* was placed in an unresolved position, sometimes close to or within Cervini. In five topologies it was placed as the sister taxon to ‘*Cervus*’ *philisi* (dental and combined matrix), once it was the sister taxon to *Cervus nippon* (cranial), and once to *Arvernoceros ardei* (combined). In the SFA it was the sister taxon to Cervini in one analysis and unresolved within Cervini in the other two analyses. The EPA analysis placed *Praeclaphus perrieri* in a polytomy with ‘*Cervus*’ *philisi* and *Cervus nippon*. Thus, *Praeclaphus perrieri* is most certainly a member of Cervini and probably closely related to and/or the ancestor of *Cervus*.

Praeclaphus etueriarum

The earliest *Praeclaphus* remains are recorded from the early Pliocene of Eastern Europe (Croitor, 2014). Portis (1920) suggested to assign all early Villafranchian ‘*Cervus*’ species to the subgenus *Praeclaphus*, among them ‘*Cervus*’ *perrieri*, ‘*Cervus*’ *etueriarum*, and ‘*Cervus*’ *arvernensis*; all were first established by Croizet & Jobert (1828). Heintz (1970) noted that *Praeclaphus etueriarum* may have originally been established based on a juvenile *Praeclaphus perrieri*. Croitor (2012) defined *Praeclaphus* as a separate genus based on ‘*Cervus*’ *perrieri*. The medium sized *Praeclaphus* is characterised by moderately long pedicles, large four-tined antlers, a simple p4, primitive dentition and a comparatively short premolar series (but longer than in *Cervus* and *Dama*). The main beam can have flattened extensions and antero-posterior compression; the cranial morphology resembles *Rusa* (Croitor, 2012, 2014).

Specimens from the Lower Val d’Arno (Italy) were assigned to *Praeclaphus lyra* (Azaroli & Mazza, 1992a). The species names *perrieri*, *warthae*, and *lyra* may be synonyms as they represent similar and contemporaneous cervids (see above) (Croitor, 2014). There is consensus that *Praeclaphus* is a member of the early radiation of Cervini (Croitor, 2014)

In most of my analyses *Praeclaphus etueriarum* was placed in an unresolved position, in one topology it was between *Eostyloceros hezhengensis* and *Eucladoceros ctenoides*, in another as the sister taxon to *Metacervocerus rhenanus* (both dental matrix); it formed twice sister taxon to *Eostyloceros hezhengensis* (dental and combined) and was the sister taxon to *Eucladoceros ctenoides* in three analyses (combined matrix). In the SFA it was placed once within bovids and as the sister taxon to the *Cervus*-clade in the other two analyses. The EPA analysis placed *Praeclaphus etueriarum* in a polytomy within Muntiacini. These differing positions make it difficult to certainly assign *Praeclaphus etueriarum* to a cervid subclade; most likely it belongs to Cervini. However, the taxon apparently shares some morphological similarities with muntiacines.

Eucladoceros ctenoides

Eucladoceros ctenoides is a large-sized Villafranchian deer; the holotype is stored in Lyon and was described by Roman (1934; Fig. 17, p. 251), Viret (1954; Fig. 18a, p. 117), and Heintz (1970; Fig. 202, Pl. X Fig. 1). *Eucladoceros ctenoides* is characterised by very large antlers with three to six tines, regression of protocone fold, absence of the anterior cingulid, highly variable p4, absence of protocone fold, cingula on upper molars. The tooth morphology is not distinctive enough to distinguish *Eucladoceros ctenoides* from other contemporaneous cervids, but the large size of the teeth is. Further, it has well developed lacrimal pits and long and narrow praeorbital vacuities (Heintz, 1970; Spaan, 1992; Croitor, 2014). Its dental and cranial morphology suggested a browsing feeding strategy rather than a mixed feeding strategy (Valli & Palombo, 2005).

Most of the described species from Western Europe had an Eurasian distribution (Croitor, 2014). Originally, 12 different species were described based on the intraspecifically highly variable antler morphology; age, environmental factors, nutrition, seasonality, pathology, also geography, and chronology may influence antler shape (De Vos & Reumer, 1995). Later, three true antler morphotypes were described: The first one has four tines, which are bi- or trifurcating, the second one has four to five tines perpendicular to the main beam, with equal distances to each other, and the third one similar to the second, but with a larger distance between the first and the second tine and slightly different orientation of the tines; sometimes there is even an accessory tine between first and second tine (De Vos & Reumer, 1995). Based on this De Vos & Reumer (1995) determined three species of *Eucladoceros*, *E. dicranios* (morphotype 1), *E. tetraceros* (morphotype 2), and *E. ctenoides* (morphotype 3). *Euctenoceros* is a junior synonym of *Eucladoceros* (De Vos & Reumer, 1995). Most of the previously defined species were synonymised with *Eucladoceros ctenoides* (De Vos & Reumer, 1995; Pfeiffer, 1999; Croitor & Bonifay, 2001; Valli & Palombo, 2005). For a detailed synonymy and species list, refer to De Vos & Reumer (1995).

Azzaroli & Mazza (1992a) provide a great overview of *Eucladoceros*. A detailed revision on the material of *E. tegulensis* revealed that its morphology is undistinguishable from *E. senegensis* and *E. tetraceros* (Spaan, 1992). This great similarity has already been found by Viret (1954). Only because *E. tegulensis* is slightly larger than *E. tetraceros* it was suggested to represent a separate species, whereas *E. senegensis* (Depéret & Mayet 1910) is considered as junior synonym of *E. tegulensis* (Dubois 1904) (Spaan, 1992). Already

Germonpré (1983) considered '*E. senezensis*' to be a junior synonym for '*E. tegulensis*'. This opinion was supported by Azzaroli et al. (1988), Spaan (1992) and Azzaroli & Mazza (1992a). Therefore, these two species are now regarded as one species (De Vos & Reumer, 1995).

So far there were only few discussions about the systematic relationship of *Eucladoceros ctenoides*. '*E. senezensis*' has been suggested to be an ancestor of *Megaceroides* or *Megaloceros giganteus* in particular (Azzaroli & Mazza, 1992a,b; Kuehn et al., 2005). Pfeiffer (2002) proposed that *Eucladoceros*, *Megaloceros*, and *Cervus* form one group. Flerov (1952) suggested that *Eucladoceros* is an ancestor of *Alces*, which is not supported (Heintz, 1970; Croitor, 2014). The comb-shaped antler morphology is unique and more similar to *Cervus elaphus* or *Cervus albirostris* than to any other living deer (pers. obs.). Because upper canines in *Eucladoceros ctenoides* are absent it was interpreted that the genus most likely does not belong to the *Cervus-Rusa*-lineage (Croitor, 2014). Based on the literature, the phylogenetic position of *Eucladoceros* remains uncertain; its cranial morphology excludes it from *Cervus*, *Rusa*, *Rucervus* and small *Axis* species. Potentially, it may be the descendant of an early three-tined ancestor of *Axis* or *Metacervocerus* (Croitor, 2014).

Here, *Eucladoceros ctenoides* was placed in an unresolved position in most analyses; it was the sister taxon to *Candiacervus ropalophorus* and *Metacervocerus rhenanus*, to *Praeclaphus etueriarum* and *Metacervocerus rhenanus*, and placed between the former and *Candiacervus ropalophorus* (all dental matrix). In one analyses it was the sister taxon to the fossil NHM *Odocoileus* (cranial), in three analyses it was the sister to *Praeclaphus etueriarum*, and in one analysis it was the sister taxon to *Megaloceros giganteus* (both combined). In the SFA *Eucladoceros ctenoides* was placed twice as the sister taxon to Cervini and unresolved within the Cervini-Capreolinae-clade. The EPA analysis placed *Eucladoceros ctenoides* unresolved with *Rusa kendagensis* as the sister taxon to the *Cervus*-clade. These results indicate that *Eucladoceros ctenoides* most certainly belongs to Cervini, potentially it is closely related to contemporaneous *Metacervocerus rhenanus* and *Praeclaphus etueriarum*.

Metacervocerus rhenanus

Metacervocerus rhenanus is a medium-sized deer known from the latest Pliocene to the Pleistocene (MN17-18) and is characterised by a primitive skull with a short orbitofrontal region, elongated braincase, relatively small bullae, a deep lacrimal pit, and long nasals. Upper canines are absent as is the anterior cingulid and cingula are reduced or lost. The skull proportions resemble *Axis axis* (Croitor, 2006a, 2014). It has relatively long inclined pedicles, three-tined slender antlers with the first bifurcation high above the burr (Kaiser & Croitor, 2004).

The small- to medium-sized deer of the early Pleistocene in Europe belong to three different genera *Cervus*, *Dama*, and *Metacervoceros* (Croitor, 2006a). The genus *Metacervocerus* originated in the late Pliocene - early Pleistocene (Villafranchian) and was established by Dubois (1904) as *Cervus* (*Axis*) *rhenanus* for the small sized deer from Tegelen. Spaan (1992) synonymised '*Cervus*' *philisi* from Senèze with '*C.* *rhenanus*' based on dentition and antler morphology. Croitor & Bonifay (2001) assigned it to the genus *Metacervocerus*.

Several three-tined cervids are described from the early Pleistocene of Europe: '*C.* *par-*

dinensis, *C. suttonensis*, ‘*C.* *rhenanus*’, ‘*C.* *philisi*’, and ‘*C.* *perolensis*’ (De Vos & Reumer, 1995). *Metacervocerus rhenanus* is considered to include ‘*C.* *philisi*’, ‘*C.* *perolensis*’, *C. ischnoceros*, and *Pseudodama lyra*. Antlers of *Metacervocerus rhenanus* are identical to the ones of ‘*Cervus*’ *philisi* and possibly ‘*Cervus*’ *perolensis*, whereas *Metacervocerus pardinensis* shows some differences. The tooth morphology of ‘*Cervus*’ *perolensis*, ‘*Cervus*’ *philisi*, and *Metacervocerus rhenanus* is indistinguishable, but a little different in *Metacervocerus pardinensis*; therefore, the latter is regarded as a distinct species (Spaan, 1992; De Vos & Reumer, 1995). ‘*Cervus*’ *perolensis*, *Metacervocerus rhenanus*, and ‘*Cervus*’ *philisi* resemble *Dama nestii*, whereas they could not be assigned to any known genus (Azzaroli, 1953). Viret (1954) states that the distinction of *Metacervocerus rhenanus* from ‘*Cervus*’ *philisi* is difficult. *Metacervocerus rhenanus* was suggested to be closely related to *Croizetoceros ramosus* by Germonpré (1983). ‘*Cervus*’ *philisi* was considered a junior synonym of *Metacervocerus rhenanus* (Azzaroli et al., 1988; Spaan, 1992). Azzaroli & Mazza (1992a) attributed ‘*Cervus*’ *rhenanus* (= ‘*Cervus*’ *philisi*), to *Pseudodama*. It was hypothesised that *Dama clactoniana* evolved from European forms of rusine deer (‘*Rusa rhenana*’ = *Metacervocerus rhenanus*) (Di Stefano & Petronio, 2002). However, the cranial morphology of *Dama* has more derived features. *Metacervocerus rhenanus* was hypothesised to be an ancestor of *Dama dama*, distinct from *Cervus*, based on the position as the sister taxon to all other *Dama* s. l. (Pfeiffer, 1999). This hypothesis is ruled out by the coexistence of both genera in the early Pleistocene (Croitor, 2014).

Rusine deer are known from Europe since the upper Pliocene (Di Stefano & Petronio, 2002; Lydekker, 1898; Van Bemmelen, 1974); three-tined cervids from the early lower Pleistocene such as ‘*Cervus*’ *philisi* (= *etuerarium* or *rhenanus*), were suggested to be closely related to extant *Rusa* (Kurtén, 1968; Lister, 1987; Leslie, 2011), while *Metacervocerus rhenanus*, was suggested to be close to modern *Axis* (Croitor, 2006a). However, *Metacervocerus rhenanus* has more apomorphic characters (Croitor, 2006a).

Metacervocerus rhenanus and *Eucladoceros ctenoides* are contemporaneous during the latest Villafranchian, where *Eucladoceros ctenoides* is more abundant. Habitat choice between those two species differs with *Metacervocerus rhenanus* having a preference for dense, tall grass or woods close to the water. It possibly lived in small groups. While *Eucladoceros ctenoides* was much larger and probably more gregarious inhabiting more open habitats (Croitor & Bonifay, 2001; Kaiser & Croitor, 2004).

In most analyses here, *Metacervocerus rhenanus* was placed in an unresolved position. Based on the dental matrix it was found to be the sister taxon to *Metacervocerus pardinensis*, *Dama dama*, and *Arvernoceros ardei*, to *Eucladoceros ctenoides* and *Candiacervus ropalophorus*, to the latter two and ‘*Cervus*’ *sivalensis* and *Megaloceros giganteus*, and to *Praeclaphus etueriarum*. With the combined matrix it was the sister taxon to ‘*Cervus*’ *perolensis*, to *Candiacervus ropalophorus*, to *Arvernoceros ardei*, and to *Praeclaphus etueriarum* plus *Eucladoceros ctenoides*. In the SFA it was placed once as the sister taxon to Cervini and unresolved within Cervidae or within the Cervini-Capreolinae-clade. The EPA analysis placed *Metacervocerus rhenanus* in a polytomy with *Axis lydekkeri*, ‘*Cervus*’ *perolensis*, and *Cervus elaphus* within the *Cervus*-clade. Thus, *Metacervocerus rhenanus* most certainly represents a member of Cervini and potentially is either a close relative to and/or ancestor of *Cervus* or *Axis*.

From the analyses based on my data sets, the synonymy of ‘*Cervus*’ *philisi* and ‘*Cervus*’

perolensis with *Metacervocerus rhenanus* could not be confirmed. All analyses place the three taxa differently and not closely related to each other. This is most likely due to different individual characters preserved in each species/specimen. To test the synonymy properly, one would have to include the same suite of characters for each species.

3.4.3 Pleistocene Cervids

In the early Pleistocene, Pliocene forms were successively replaced by more modern cervids, such as *Elaphurus*, *Eucladoceros*, *Rusa*, and *Megaloceros*. By the middle Pleistocene, most Pliocene and some early Pleistocene cervids became extinct, while extant representatives of *Elaphurus*, *Hydropotes*, *Elaphodus*, *Muntiacus*, *Rusa*, and *Alces* appear (Dong, 1993). In the late Pleistocene more extant forms, *Cervus*, *Capreolus*, and *Rangifer* are present; *Megaloceros* became extinct after the last glacial maximum after a short diversification (Dong, 1993).

‘Cervus’ philisi

‘Cervus’ philisi was a medium-sized deer with abundant remains in the fossil record, particularly in Senèze. The holotype NMB Se 549 is stored in Basel and was first described and figured in Schaub (1941; pp. 264-271, Pl. XVII). It is characterised by three tined antlers, molarised p4, a long lower premolar row, the absence of the anterior cingulid on lower molars, and by the presence of a cingulum on upper molars. In the *Metacervocerus pardinensis*-*‘Cervus’ philisi*-*‘Cervus’ perolensis*-lineage the p4 underwent several transformations, and is the most modified in *‘Cervus’ philisi* (Heintz, 1970).

Schaub (1941) stated that *‘Cervus’ philisi* is similar to *‘Cervus (Pseudaxis) mantchuricus’*, which resembles the extant *Rusa*, but *‘Cervus’ philisi* is much more slender and has a more brachyodont dentition. Based on morphological differences and age, Schaub (1941) established the new species *‘Cervus’ philisi* for the small-sized deer from Senèze. Early attempts to assign *‘Cervus’ philisi* to extant (sub)genera are controversial; *‘Cervus’ philisi* despite resembling *Rusa* in terms of antler morphology, cannot be assigned to any extant genus and thus is a representative of an extinct group of cervids (Schaub, 1943). Depéret & Mayet (1911) put it close to *Axis*, Stehlin (1923) assigned it to *Rusa*, while Schlosser (1924) stated that there are no Pliocene cervid teeth, which could be assigned to *Axis* or *Rusa*. Schaub (1941) stated that *Axis* is not closely related to *‘Cervus’ philisi* and suggested a closer relationship with *Cervus nippon*. According to Viret (1954) the cranium *‘Cervus’ philisi* is similar to *Rusa*, but difficult to distinguish from *Metacervocerus rhenanus* (Spaan, 1992).

Members of the *Metacervocerus pardinensis*-*‘Cervus’ philisi*-*‘Cervus’ perolensis*-lineage are all of medium size and occupy the same ecological niche. The dentition of *‘Cervus’ philisi* is most similar to *‘Cervus’ perolensis* and *Metacervocerus pardinensis*, but the antler morphology of *‘Cervus’ philisi* differs from *Metacervocerus pardinensis*; therefore, *‘Cervus’ philisi* was suggested to be more closely related to *‘Cervus’ perolensis* (Schaub, 1941; Heintz, 1970). Based on these comparisons, Heintz (1970) suggested the evolutionary *Metacervocerus pardinensis*-*‘Cervus’ philisi*-*‘Cervus’ perolensis*-lineage. However, the temporal occurrence of these species in the fossil record contradict this hypothesis. Azaroli & Mazza (1992a) assigned *‘Cervus’ philisi* to *Pseudodama*. It was suggested to

have originated from *Metacervocerus pardinensis* in MN17 and that ‘*Cervus*’ *perolensis* is the descendant of ‘*Cervus*’ *philisi* (Stefaniak & Stefaniak, 1995; Croitor, 2006a, 2014). Detailed revision of the original antler and dental morphology led to the conclusion that *Metacervocerus rhenanus* from Tegelen and ‘*Cervus*’ *philisi* from Senèze are synonymous and that ‘*Cervus*’ *philisi* and ‘*Cervus*’ *perolensis* are junior synonyms of *Metacervocerus rhenanus* (see above) (Spaan, 1992). Later, ‘*Cervus*’ *philisi* was included in the genus *Metacervoceros* (Croitor & Bonifay, 2001; Croitor, 2006a)

In most analyses here, ‘*Cervus*’ *philisi* was placed in an unresolved position or as the sister taxon to *Praeclaphus perrieri*. ‘*Cervus*’ *philisi* and *Praeclaphus perrieri* were united by shared character states of the upper premolars and molars, the lower molars, the mandibula, position of foramina, the morphology of the praemaxilla, the basioccipital tuberosities, and bullae, and antler-pedicle proportions. ‘*Cervus*’ *philisi* was placed as the sister taxon to *Hippocamelus antisensis* in one analysis (cranial matrix), to ‘*Cervus*’ *sivalensis* and *Metacervocerus pardinensis*, and to a clade consisting mainly of fossil cervine taxa (both combined matrix). In the SFA it was placed unresolved within Cervinae in two analyses and unresolved within the Cervini-Capreolinae-clade in the third analysis. The EPA analysis placed ‘*Cervus*’ *philisi* in a polytomy with *Praeclaphus perrieri* and *Cervus nippon* within the *Cervus*-clade. These outcomes support previous findings that ‘*Cervus*’ *philisi* cannot be assigned to any extant cervid species except for possibly *Cervus nippon* (see above). A close relationship to *Hippocamelus antisensis* is ruled out, as ‘*Cervus*’ *philisi* belongs to Cervini based on morphological evidence. ‘*Cervus*’ *philisi* together with *Praeclaphus perrieri* potentially represents an extinct clade leading to *Cervus*. The suggested synonymy of *Metacervocerus rhenanus*, ‘*Cervus*’ *philisi*, and ‘*Cervus*’ *perolensis* could not be supported in the morphological analyses. This could be caused by the differing availability of characters for each taxon and should be tested based on exclusively overlapping characters.

‘*Cervus*’ *sivalensis*

‘*Cervus*’ *sivalensis* is one of the first cervids from India (Chinji Formation; 2.9–2.0 mya) (Colbert, 1935; Heintz et al., 1990; Ghaffar et al., 2006). The material is poorly preserved and fragmentary. The holotype NHM 48440 is stored in London. This large-sized deer is characterised by high-crowned molars, folded or indented enamel, cingula on upper molars and resembles *Rucervus duvaucelii* (Colbert, 1935; Azzaroli, 1954; Ghaffar et al., 2010).

Lydekker (1876) described three species of cervids from the Siwalik Hills based on upper molars, *Cervus latidens*, *C. triplidens*, and *C. simplicidens* (similar to *Rucervus duvaucelii*). Later, he established ‘*Cervus*’ *sivalensis* and few remains attributed to the species above were assigned to it (Lydekker, 1884). Revisions on the material a century later state that the Siwalik cervid species all belong to the genus *Cervus* and comprise five species *C. simplicidens*, *C. triplidens*, *C. rewati*, *C. punjabensis* and *C. sivalensis* (Arif et al., 1991; Samiullah & Akhtar, 2007). *Cervus punjabensis* looks exactly like the extant *Axis axis* (pers. obs.). The skull fragment (NHM 39570, NHM 17468) and antler fragments (NHM 41834 & 41834a) resemble *Rucervus duvaucelii* in morphology and size, while the antler fragments NHM 41834b, c and d show a closer affinity to *Rucervus eldii* (Azzaroli, 1954). There is still a lot of confusion concerning the taxonomy and revision of these taxa is

needed (Azzaroli, 1954).

'*Cervus*' *sivalensis* was placed in an unresolved position in most of my analyses; it was placed as the sister taxon to *Megaloceros giganteus* in five analyses (dental matrix), to a clade formed by *Axis lydekkeri*, *Rusa kendengensis*, and *Metacervocerus pardinensis* (cranial matrix), to *Metacervocerus pardinensis* in three analyses, and to the *Elaphurus-Rucervus-Rusa*-clade (both combined matrix). In the SFA it was placed unresolved within Cervini in two analyses and as the sister taxon to the *Cervus*-clade in the third analysis. The EPA analysis placed '*Cervus*' *sivalensis* in a polytomy with *Metacervocerus pardinensis* and *Cervus canadensis* within the *Cervus*-clade. These results show that '*Cervus*' *sivalensis* is most certainly a Cervini and most likely closely related to *Cervus*, *Rusa*, and/or *Rucervus*. Together with *Axis lydekkeri* it could belong to the ancestral group of cervids that leads to *Axis*, *Cervus*, *Rusa*, and *Rucervus*.

Axis lydekkeri

The first diagnosis of *Axis lydekkeri* is based on an antler described and figured in Martin (1886) representing a young individual stored in Leiden (RGM St 18501). Around 60 antlers of the species have been collected from Trinil, Java by Dubois between 1890-1900 and represent a decent documentation of the intraspecific variation, but their uniform morphology (De Vos, 1984). The lyre-shaped antlers are normally three tined, the angle between the brow tine and main beam is about 90°; there is a frequently occurring accessory tine between the brow tine and main beam (Von Koenigswald, 1939; Zaim et al., 2003). Fossil remains of *Axis lydekkeri* are so abundant that it is used as index fossil for the Trinil layers (Von Koenigswald, 1939). New findings showed that *C. zwaani* is a junior synonym of *Axis lydekkeri*, as measurements showed that they fall within size range of the latter (Zaim et al., 2003). Further synonyms of *Axis lydekkeri* are *Cervus lydekkeri* Martin 1886 (p. 63; but see Martin 1888), *Cervus liriocerus* Dubois 1907 (p. 454), and *Cervus (Axis) lydekkeri* Stremme 1911.

The evolutionary history of *Axis*-like cervids started with the Pliocene to mid Pleistocene dispersal of an '*Hyelaphus*'-like ancestor into the Southeast Asian tropics. The vegetation was probably more open with deciduous forests and open grassland. The first appearance of *Axis* on Java was in the early-mid Pleistocene (Meijaard & Groves, 2004). During that time most likely a landbridge existed connecting Java with the Malay Peninsula, which also had a connection to Borneo and possibly to Sumatra. Meijaard & Groves (2004) found in their study that *Axis calamianensis* diverged before *Axis kuhli* and *Axis porcinus* diverged from each other; this probably happened when the Javan population became separated from Southeast Asia in the late middle Pleistocene. The dispersal history of *Axis calamianensis* is unknown, but presumably happened via the landbridge from Borneo to Palawan during the Middle Pleistocene (Heaney, 1985; Meijaard & Groves, 2004). *Axis lydekkeri* and *Axis kuhli* evolved on Java; the former became extinct on the island after the last glaciation, probably caused by increased competition from *Rusa timorensis* and *Muntiacus muntjak* after the climate changed to wetter conditions, but process of extinction involved likely more complex factors. *Axis kuhli* remained on the Bawean Island until today (Meijaard, 2003; Meijaard & Groves, 2004).

Axis lydekkeri is smaller than *Axis axis* and most *Axis lydekkeri* specimens fall within

Axis porcinus very close to *Axis kuhli* (Zaim et al., 2003; Meijaard & Groves, 2004). It is presumably more closely related to the smaller *Axis* species of today (*Hyelaphus*) than to *Axis axis*, but a clear systematic relationship to any of them could not yet be determined (Meijaard & Groves, 2004).

Here, *Axis lydekkeri* most often was in an unresolved position; it was the sister taxon to *Pliocervus matheronis* (dental matrix), to *Rusa kendengensis* (cranial matrix), to *Eucladoceros ctenoides*, *Praeclaphus etueriarum*, and *Candiacervus ropalophorus*, and twice to *Dremotherium feignouxi* (combined matrix). In the SFA it was the sister taxon to Cervini in two analyses and placed unresolved within Cervini in the third analysis. The EPA analysis placed *Axis lydekkeri* in a polytomy with *Cervus perolensis*, *Metacervocerus rhenanus*, and *Cervus elaphus* within the *Cervus*-clade. Even though *Axis lydekkeri* is a fairly complete fossil and from comparative anatomy doubtless closely related to extant *Axis*, it is problematic to place it as such. Based on my analyses, *Axis lydekkeri* belongs certainly to Cervini.

Rusa kendengensis

There are not many studies about *Rusa kendengensis*; the only work on this species reported that it belongs to *Rusa* and not to *Cervus* as previously assumed for most Pleistocene cervids from Java (Zaim et al., 2003).

In my analyses, *Rusa kendengensis* was most often placed in an unresolved position and once between the outgroup and cervids; it was the sister taxon to *Axis lydekkeri* (cranial matrix), to *Dremotherium feignouxi*, to *Axis lydekkeri* and *Dremotherium feignouxi*, and to *Cervus australis* and the fossil muntjac (combined matrix). In the SFA *Rusa kendengensis* was placed consistently as the sister taxon to the *Cervus*-clade. The EPA analysis placed *Rusa kendengensis* unresolved with *Eucladoceros ctenoides* as the sister taxon to the *Cervus*-clade. Thus, *Rusa kendengensis* belongs to Cervini; based on the analyses here it is more closely related to *Cervus*, even though based on comparative anatomy it is more similar to *Rusa*. Potentially *Rusa kendengensis* belongs to an extinct group of ancestors including also *Axis lydekkeri* and *Cervus sivalensis*, which gave rise to modern *Axis*, *Cervus*, and *Rusa*.

Candiacervus ropalophorus

Candiacervus is a sturdy, small- to medium-sized cervid with shortened limb bones and the plesiometacarpal condition. The typical morphological features described based on *Candiacervus cretensis* are a short and tapering snout, small praeorbital vacuities, a weakly developed lacrimal fossa, frontals that are concave between the orbitae, and strongly developed orbit rims (Kuss, 1975; Van der Geer et al., 2006). The supraorbital foramina are far apart and very large (up to 8 mm in diameter) and are often embedded in a deep sulcus supraorbitalis. The antlers are two to four tined and sit on strong pedicles. Upper canines seem to be absent (Kuss, 1975). The holotype of *Candiacervus ropalophorus* has been described in detail by De Vos (1984).

The fossil cervid material from Crete was originally described as *Anoglochis cretensis* by Simonelli (1907) and has been placed in several genera and subgenera since, until Kuss (1975) established the genus *Candiacervus* (Van der Geer et al., 2006). Many authors

have assigned the Cretan cervid material to one single species with a high variability in size and morphology: *Anaglochis cretensis* Simonelli 1907, *Cervus (Eucladoceros) cretensis* Vaufreij 1929, *Megaceros cretensis* Azzaroli 1952 (Azzaroli, 1961; Kuss, 1965, 1966, 1967; Kuss & Misonne, 1968; Accordi, 1972; Melentis, 1974; Caloi & Malatesta, 1974), *Cervus cretensis* Sigogneau 1960 (Kuss, 1969, 1970, 1973), *Megaloceros cretensis* Sondaar 1971, *Nesoleipoceros cretensis* Radulesco & Samson 1967, *Praemegaceros cretensis* Kurtén 1968, Malatesta 1980, *Megaceros (Megaceroides) cretensis* Azzaroli 1971 (De Vos, 1984). Kuss (1975) suggested to assign the small cervid on Crete to *Candiacervus cretensis* and the medium-sized one to *Candiacervus rethymnensis*; while the small cervid on Kasos and Karpathos was defined as *Candiacervus cerigensis* and the medium-sized one *Candiacervus pigadiensis* (Kuss, 1975). Six different size groups have been suggested representing six taxonomic units, where *Candiacervus cretensis* by Simonelli (1907, 1908) corresponds to size groups I, II, and III, *Candiacervus cretensis* by Kuss (1975) corresponds to size groups I and II, postcranial elements of *C. rethymnensis* correspond to size group IV, the large bones described by Kotsakis & Palombo (1979) to size groups V and VI (De Vos, 1984). Based on some morphological differences these six taxonomic units have been extended to eight morphotypes. De Vos (1979), De Vos (1984), and De Vos (2000) classified them as *Candiacervus ropalophorus* (size I), *Candiacervus* spp. (size II), which is subdivided into a, b, c, *Candiacervus cretensis* (size III), *Candiacervus rethymnensis* (size IV), *Candiacervus* sp. V, and *Candiacervus* sp. VI; other taxonomists regard size I and II as one species (Van der Geer et al., 2006). *Candiacervus ropalophorus* is the smallest species of the eight morphotypes, *Candiacervus cretensis* and *Candiacervus rethymnensis* could be assigned to two morphotypes, and the rest is named *Candiacervus* IIa, IIb, IIc, V, VI (De Vos, 1984). Since no cranial material can be unambiguously assigned to *Candiacervus cretensis* or *Candiacervus rethymnensis*, only *Candiacervus ropalophorus* can be considered as clearly recognisable species based on cranial and postcranial elements (De Vos, 1984).

There have been controversies about whether *Candiacervus* is a cervid of the ancient type or a cervid derived from megacerine deer (Kuss, 1975). *Candiacervus cretensis* was regarded as a Neogene relict form, whose original characters were transformed by adaptations to the special island environment (dwarfism); these transformations are specialisations rather than degenerations. The ancestors of the Greek island deer are uncertain, but possibly already originated in the Miocene, as there are indications that the evolutionary process lasted six million years (Kuss, 1975). The Cretan fauna is strongly endemic and it is uncertain which cervid may be the mainland ancestor; however, it is suggested that *C. rethymnensis* is morphologically the most primitive and evolved later to smaller deer with a more stocky build (i.e., *Candiacervus cretensis*, *Candiacervus* sp. II, *Candiacervus ropalophorus*) and to larger forms with more slender limbs (De Vos, 1984). Many of these species were contemporaneous and lived in sympatry. The mosaic evolution of *Candiacervus* led to a distinct radiation into a number of cervid species; the more hypsodont teeth of I and II indicate occupation of a new niche with adaptation to more grazing. The climate change caused sea levels to rise decreasing the size of Crete, which caused reduction in habitat availability and subsequent extinction of deer species except for *Candiacervus ropalophorus* (Kuss, 1975; De Vos, 1984). The latter persisted the longest and presumably became extinct in competition with domestic animals and/or due to overhunting by humans (Kuss, 1975; De Vos, 1984).

The systematic position of *Candiacervus* is controversial. Cretan cervids are best documented by metapodials; the ones of *C. rethymnensis* are comparable to *Cervus elaphus*. Similarities of the position of the brow tine on antlers of *Candiacervus ropalophorus*, *Candiacervus* spp. IIa, IIb, IIc indicate a close relationship to *Megaceros*, *Praemegaceros*, *Eucladoceros*, *Cervus*, or *Croizetoceros*, as has been suggested before (De Vos, 1984) and references therein. Some antler fragments show partly a tendency to palmation resembling *Dama* (Kuss, 1975). While some antlers figured in Kuss (1975) look very similar to antlers of *Croizetoceros* (pers. obs.). All this shows that it remains difficult to determine the ancestor of the Greek island deer, and that data are still insufficient to establish phylogenetic relationship of Cretan deer (Van der Geer et al., 2006).

In my analyses, *Candiacervus ropalophorus* was most often placed unresolved, sometimes close to several fossil cervine taxa; it was the sister taxon to *Eucladoceros ctenoides* and *Metacervocerus rhenanus*, to *Eucladoceros ctenoides*, to *Dama dama* and *Arvernoceros ardei* (dental matrix). *Candiacervus ropalophorus* was the sister taxon to *Cervus elaphus* (cranial matrix), to *Metacervocerus rhenanus*, to *Praeclaphus etueriarum* and *Eucladoceros ctenoides*, to a clade containing all three, and to a clade containing both fossil *Odocoileus*, *Croizetoceros*, and *Procapreolus* (all combined matrix). In the SFA *Candiacervus ropalophorus* was consistently placed as the sister taxon to *Hippocamelus*. The EPA analysis placed *Candiacervus ropalophorus* as the sister taxon to Cervini. The placement of *Candiacervus ropalophorus* proves to be difficult; most often it was placed within Cervini. The consisting placement as the sister taxon to *Hippocamelus* in the SFA indicates that it shares similarities with capreoline taxa; however, the plesiometacarpal condition in *Candiacervus ropalophorus* clearly diagnoses it as a member of Cervini. The often hypothesised close relationship to megacerine/damine deer could only be found in one topology.

Megaloceros giganteus

Megaloceros giganteus is a large-sized deer (up to 2 m shoulder height) common in the mid-late Pleistocene faunas of Europe; it represents one of the largest deer ever and appeared 400 000 years ago in the middle latitudes of Eurasia, spreading to the East of Lake Baikal and became extinct 7700 years ago (Azzaroli & Mazza, 1992b; Hughes et al., 2006). *Megaloceros giganteus* is characterised by concave frontal bones anterior to the pedicles, very small or closed praeorbital vacuities, which may be caused by cranial pachyostosis, lacrimal fossae that vary from very shallow to deep, posteriorly elongated nasals, and a relatively short orbitofrontal part of the skull. The upper molars and sometimes even premolars have cingula, the lower premolar series is short, and the mandible is thickened (pachyostosis). The antler span was huge with up to 4 m and weighing up to 45 kg; the brow tine is palmated, the bifurcation of brow tine and main beam is unique, a second tine is variably present on the main beam, the main beam is characterised by a distal palmation (Lister, 1994; Van der Made et al., 2008; Croitor, 2014).

Originally, two genera have been established for megacerine deer *Megaloceros* by Brookes (1828) and *Megaceros* by Owen (1844), however, only *Megaloceros* has been validated by the ICZN (Lister, 1987). There are several differences between all species (Azzaroli & Mazza 1992b and references therein). The tribe Megacerini was established by Viret (1961), but is a junior synonym of Megalocerotinae Brookes 1828 (Grubb, 2000; Croitor, 2014).

Megaloceros comprises two groups, the ‘*Megaloceros verticornis* group’ with a flattened forehead and more rounded, cylindrical brow tines and the ‘*Megaloceros giganteus* group’ with a concave forehead and flattened or palmated brow tines (Azzaroli, 1953; Abbazzi, 2004; Croitor, 2006b; Lister et al., 2010) and references therein. For the ‘*verticornis*-group’, three genera have recently been suggested *Megaloceros* (Lister, 1996; Pfeiffer, 2002), *Megace-roides* (Azzaroli & Mazza, 1992b; Abbazzi & Masini, 1997), and *Praemegaceros* (Abbazzi, 2004; Croitor, 2006b). For the *giganteus*-group, the name *Megaloceros* applies (Lister et al., 2010). *Praemegaceros* is the most widely used name for the *verticornis*-group and should be further used for this group. Dietrich (1933) introduced the subgenus *Sinomegaceros* based on descriptions by Young (1932), which has been variably used as genus or subgenus (Van der Made et al., 2008, and references therein), but is now mostly considered as a separate genus (e.g., McKenna & Bell, 1997). Previously, megacerine deer have been put into either one genus (*Megaloceros*) or two genera (*Megaloceros*, *Sinomegaceros*), the latter is now widely accepted based on biogeography and morphology (Van der Made et al., 2008). The study of Van der Made et al. (2008) demonstrated the presence of two separate genera based on a phylogenetic model; however, they found no evidence for dispersals between East and West Eurasia, but convergent evolution (Van der Made et al., 2008). Since the relationship of the Eastern genus *Sinomegaceros* to the European forms is uncertain *Megaloceros* should only be applied to the ‘*giganteus*-group’ to avoid confusion and the risk of polyphyly of *Megaloceros* (Lister et al., 2010). *Megaloceros* and *Megaceroides* are considered as sister lineages (Croitor, 2014). Even though other large deer, such as *Eucladoceros*, are included in the term ‘giant deer’, they do not necessarily have a close phylogenetic relationship, although some hypothesise a link between *Eucladoceros* and *Megaceroides* (Azzaroli & Mazza, 1992b).

Central Asia is considered as the origin of megacerine cervids; the record of the most ancient megacerine *Praesinomegaceros* confirms the existence of an Asiatic *Cervavitus-Praesinomegaceros-Sinomegaceros* lineage, which is also considered to be the origin of *Megaloceros* (Vislobokova, 2009). The appearance of these early Asian megacerine deer is contemporaneous with the Miocene adaptive radiation of the most ancient Pliocervini. Thus, *Cervavitus* is suggested to be the ancestor of megacerine deer and also of *Eucladoceros*, *Axis*, *Dama*, *Cervus*, and *Elaphurus* (Vislobokova, 2009).

Megaloceros includes all giant Cervinae from Western Eurasia including smaller ancestors and dwarfed insular forms, but these group members could also represent several distinct lineages, which may have shared similar ecological niches resulting in similar morphological adaptations (Croitor, 2014). Although two Western Eurasian species have been suggested, *Megaloceros giganteus* and *M. savini* (the latter sometimes placed in *Praedama* or *Dolichodoryceros* (Kahlke, 1969; Azanza & Morales, 1989; Van der Made et al., 2008)), there is a broad consensus today that *Megaloceros* consists of only one species *Megaloceros giganteus* (Vislobokova, 1990, 2012, 2013; Azzaroli & Mazza, 1993; Croitor et al., 2006; Croitor & Bonifay, 2001; Croitor, 2014). Controversies about the subspecies of *Megaloceros giganteus* remain. These subspecies were mostly established based on antler morphology (Croitor, 2014).

The systematic position of *Megaloceros* is still uncertain; all phylogenetic analyses consistently place *Megaloceros giganteus* within Cervinae and within Megalocerini comprising at least 14 species (Hughes et al., 2006; Vislobokova, 2009). So far two putative relatives,

Dama and *Cervus elaphus* have been suggested as its closest descendants (Lister et al., 2005).

It was placed more closely related to (Western) *Cervus elaphus* by Kuehn et al. (2005) based on molecular data and by several others based on morphological data (Geist, 1998; Pfeiffer, 1999, 2002; Vislobokova, 2009). Lönnberg (1906) put it close to *Rangifer* because of a completely ossified vomer and palmated brow tines; however, it was found that the division of the nasal cavity is only ossified in the anterodorsal part of the vomerine septum, which is different from the condition in Capreolinae. This was interpreted as a side effect of cranial pachyostosis (Lister, 1994; Croitor, 2006b, 2014).

Already Lydekker (1898) suggested an affiliation of *Megaloceros giganteus* to the damine group; this was supported by several authors later, who placed it close to *Dama dama* (Gould, 1974; Kitchener, 1987; Lister, 1994; Vislobokova, 2009) based on morphological data or morphological and molecular data (separately and combined) (Lister et al., 2005). However, Hughes et al. (2006) stated that despite the placement within the *Dama*-clade, it could not be entirely excluded from the group including *Rucervus* and *Axis*. The different results based on morphology of Pfeiffer (1999) and Lister et al. (2005) are most likely caused by the choice of characters. *Megaloceros* and *Dama* clearly represent two separate lineages (Kuehn et al., 2005). Repeated analysis of cytochrome b sequences of *Megaloceros giganteus* support its close phylogenetic relationship with *Dama dama* and *Dama mesopotamica* (Lister et al., 2005; Hughes et al., 2006). Therefore, *Dama* should probably be included in the Megacerini once this has been tested sufficiently by cladistics (Lister et al., 2010). The cranial morphology *Megaloceros* has a higher proportion of plesiomorphic characters than *Dama* (Croitor, 2014).

Fossil evidence indicates a parallel evolution of Megacerini and Cervini (Vislobokova, 2009). Most cervine lineages including e.g., *Eucladoceros*, *Praemegaceros*, *Arvernoceros*, *Praeclaphus*, and *Megaloceros*, which became extinct at the Plio-Pleistocene boundary had a temperate to boreal distribution. Therefore, the tribe Megalocerotini Brookes 1828 (=Megacerini Viret (1961)) is controversial as it represents a paraphyletic taxon comprising cervines from various phylogenetic lineages that evolved giant ecomorphological forms (Croitor, 2014).

Megaloceros giganteus was placed in an unresolved position in five topologies (dental and combined matrix), as the sister taxon to *Rangifer tarandus* in five topologies (cranial and combined matrix), and to '*Cervus*' *sivalensis* in five topologies (dental). It was placed close to *Rangifer tarandus* and non-cervid ruminants, as the sister taxon to *Rangifer tarandus* and *Okapia*, to *Eucladoceros ctenoides*, and to *Procapreolus cusanus* (all combined matrix). In the SFA *Megaloceros giganteus* is the sister taxon to *Dama dama* in two analyses and the sister taxon to *Rangifer tarandus* in the third analysis. The EPA analysis placed *Megaloceros giganteus* unresolved with *Dremotherium feignouxii* as the sister taxon to Capreolini. Despite all the morphological evidence for a close relationship to *Dama*, *Megaloceros giganteus* was placed only twice as such. More often it was considered to be more closely related to *Rangifer tarandus* presumably because of similar antler morphology. The frequent sister taxon position to '*Cervus*' *sivalensis* is surprising and indicates that these two species share dental traits.

Odocoileus

For a detailed discussion about the evolutionary history of *Odocoileus*, see Chapter 5.

In my analyses, the fossil *Odocoileus* NHM specimen was most often placed in an unresolved position; it was the sister taxon to *Mazama chunyi*, *Alces alces*, and *Odocoileus hemionus*, to *Croizetoceros ramosus* and *Procapreolus cusanus* (both dental matrix), to *Eucladoceros ctenoides* (cranial matrix), and to the other fossil *Odocoileus* (BSPG). In the SFA this specimen was placed twice as the sister taxon to *Hippocamelus* and as the sister taxon to *Mazama nemorivaga* in the third analysis. The EPA analysis placed the NHM *Odocoileus* as the sister taxon to a clade containing both *Hippocamelus*, *Cervus australis*, and *Hypertragulus calcaratus* within Blastocerina.

The fossil *Odocoileus* BSPG specimen was most often placed in an unresolved position in my analyses; it was the sister taxon to *Moschus* in two analyses (dental matrix), to *Pudu puda* (cranial matrix), to *Alces alces*, *Odocoileus hemionus*, and *Odocoileus virginianus*, and to the other fossil *Odocoileus* (NHM) in two analyses (both combined matrix). In the SFA this *Odocoileus* specimen was placed unresolved as the sister taxon to *Mazama chunyi* and *Mazama gouazoubira* in two analyses and unresolved within Capreolinae in the third analysis. The EPA analysis placed the BSPG *Odocoileus* as the sister taxon to *Mazama chunyi* and *Mazama gouazoubira* within Blastocerina.

The analyses here place both fossil *Odocoileus* within Capreolinae and mostly within Odocoileini. However, only a few analyses placed them as sister taxa or closely related to their presumed living descendants *Odocoileus virginianus* and *Odocoileus hemionus*. Particularly the BSPG specimen is more often found to be closely related to *Mazama* species. The only case where both fossil *Odocoileus* were considered as a clade, they were united by character states of the upper and lower premolars, and the morphology of the crista facialis maxillary and the orbit.

Muntiacus

For a detailed discussion about the evolutionary history of *Muntiacus*, see Chapter 5.

The fossil *Muntiacus muntjak* was most often placed either in an unresolved position or within Muntiacini, mostly as the sister taxon to *Muntiacus atherodes*; it was the sister taxon to '*Cervus*' *philisi* and *Hippocamelus antisensis* (cranial matrix), to *Cervus australis* in two analyses, and to *Muntiacus crinifrons* in three analyses (both combined matrix). In the SFA it is placed unresolved within Muntiacini in two analyses and as the sister taxon to *Muntiacus atherodes* in the third analysis. The EPA analysis placed the fossil *Muntiacus* as the sister taxon to *Muntiacus crinifrons* within Muntiacini. The fossil *Muntiacus* is certainly a member of Muntiacini.

3.4.4 Extant Cervids

Because the systematic relationships of extant cervids can be thoroughly investigated using molecular data, here, the discussion of their systematics is kept closely to the inferences that can be drawn solely from morphological data. A much more detailed account of extant cervid systematics is in Chapter 5 using molecular and combined morphological

and molecular data sets. Due to the highly conservative character of cervid craniodental features implications from the topologies based on morphology alone are limited.

Cervini

Cervini were never monophyletic in my analyses based on morphological data sets. The *Elaphurus-Rucervus-Rusa*-clade was always recovered in the analyses based on the dental and combined data set, in most topologies fully resolved. The *Elaphurus-Rucervus-Rusa*-clade was diagnosed based on characters of the upper premolars and molars, the lower premolars and molars, the mandibula, the nasal morphology, the position of the lacrimal foramina, the position of the infraorbital foramen, the tuber maxillae, the morphology of the palatine, the mastoid process, the fissura palatina, the antler morphology. It consists of the *Rusa*-clade, which often has *Rusa alfredi* as the sister taxon to the other three *Rusa*-species, of *Rucervus duvaucelii* and *Rucervus eldii* as the sister taxa to each other and to the *Rusa*-clade, and *Elaphurus davidianus* and *Rucervus schomburgki* as the sister taxa to each other and to the latter taxa. The monophyly of *Rusa* was diagnosed by characters of the upper premolars, the M1, the lower premolars, the m3, morphology of the nasal, the fissura palatina, and the antlers morphology as well as position and opening angle of the antlers. *Rusa alfredi* and *Rusa marianna* were united based on characters of the mandible, the nasal, the morphology of the praeorbital vacuity, the processus lacrimals, the processus mastoideus, and the opening of the meatus acusticus, also the position of the pedicles and the antler-skull proportions. *Rusa timorensis* and *Rusa unicolor* were diagnosed by character states of the P3, M1, p2, the lower molars, the mandible, the proportions of the praeorbital vacuity, the palatine processes, position of the lacrimal foramina, the alisphenoid process, the fissura palatina, the postcornual fossa, and several features of the antlers and pedicles. The sister taxon relationships of *Rusa alfredi* and *Rusa marianna* and *Rusa timorensis* and *Rusa unicolor* are the only consistently recovered cervine clades in all topologies based on the cranial matrix. *Rucervus duvaucelii* and *Rucervus eldii* were diagnosed by characters of the M3, the p4, and the lower molars, the mandibular, proportions of the palate, the position of the lacrimal foramina, and the basioccipital. *Rusa* and *Rucervus* were united by conditions of the P4, the p3, the p4, the upper canines, the processus condylaris, the processus coronoideus, the orbita, and the palatine foramina. *Elaphurus davidianus* and *Rucervus schomburgki* were united based on characters of the P2, P4, p3, p4, and the lower molars, the cranium proportions in lateral view, the proportions of the skull width, the postcornual fossae, the proportions of the praeorbital vacuity, the position of the lacrimal foramina and palatine foramina, and antler-skull proportions.

In many topologies the two *Axis* species were the sister taxon to the *Elaphurus-Rucervus-Rusa*-clade resolved or unresolved. In the Bayesian inference analyses, the *Elaphurus-Rucervus-Rusa*-clade is one of the very few clades present. *Axis* formed a clade based on characters of the upper and lower premolars, upper and lower molars, the lower incisor and canines, the upper canines, some features of the mandible, especially of the angulus, nasal sutures and contact with other bones, the orbita, lacrimal foramina, the processus lacrimalis, the position of palatine foramina and other features of the palate, the direction of the meatus acusticus externus, and the extension of the os zygomaticum.

In some combined analyses the relationships of *Axis* and the subclades of the *Elaphurus-Rucervus-Rusa*-clade is different. Characters uniting *Axis* and *Rusa* include the P2, P3, P4, m3, skull proportions, the morphology of the nasals, the palatine processes, the antler morphology and angle, and the position of the pedicle. Members of the *Elaphurus-Rucervus-Rusa*-clade and *Axis* were united based on character states of the upper molars, the p2, the p3, the lower molars, the mandibula, the position of the lacrimal foramina, the praemaxilla, and the basioccipital. Other cervines like *Dama dama*, *Cervus elaphus*, *Cervus nippon*, *Cervus albirostris*, and *Cervus canadensis* are placed in varying positions. In some analyses *Dama dama* is the sister taxon to the *Elaphurus-Rucervus-Rusa*-clade, *Cervus elaphus* and *Cervus nippon* are sister taxa to each other, and *Cervus canadensis* is the sister taxon to *Cervus elaphus*. *Cervus elaphus* and *Cervus nippon* were united based on characters of the P3, P4, the upper molars, upper canines, the distal end of the nasals, and the morphology of the palate. The other cervine taxa are either unresolved or distributed across the topology.

Muntiacini

Most muntiacines are recovered as a clade in the MP and ML analyses based on the dental data sets. This clade includes *Muntiacus truongsongensis*, *Muntiacus vuquangensis*, *Muntiacus crinifrons*, *Muntiacus muntjak*, *Muntiacus reevesi*, and sometimes *Muntiacus atherodes*. *Muntiacus feae* and *Elaphodus cephalophus* are never included within Muntiacini in those analyses. *Muntiacus feae* is often placed closely related to *Mazama* species, while *Elaphodus cephalophus* takes up different positions. In the dental analysis including only extant species only *Muntiacus muntjak* and *Muntiacus reevesi* form sister taxon relationships. The clade of these two *Muntiacus* was diagnosed by character states of the upper premolars and molars, the lower premolars and molar, the upper canines and the position of the lower incisors and canines in lateral view. In the two BI topologies only *Muntiacus truongsongensis* and *Muntiacus vuquangensis* form a sister taxon relationship, while all other muntiacines are unresolved. All muntiacines form a clade In the MP and the ML analyses based on the cranial character set, while in the BI analyses only *Muntiacus crinifrons* plus *Muntiacus truongsongensis* and *Muntiacus feae*, *Muntiacus vuquangensis* plus *Muntiacus feae* form clades. Some *Muntiacus* and *Elaphodus cephalophus* formed a clade based on the character states of the mandibula, proportions of the praeorbital vacuity, of the occipital region, the morphology of the praemaxilla and nasal, the contact between viscerocranial bones, the lacrimal fossa, the orbita, and the process of the mandibular fossa. *Elaphodus cephalophus* and *Eostyloceros hezhengensis* (sometimes including *Muntiacus feae*) were united based on characters of the upper premolars and molars, the lower premolars and molars, the upper canines, proportions of the lower incisors and canines, the angulus mandibulae, proportions of the palatine, of the lacrimal, of the praeorbital vacuity, the morphology of the praemaxilla, maxilla and nasal, the palatine processes, the linea temporalis, the basioccipital, the mastoid process, the bullae, and several features of the pedicles and antlers. *Muntiacus atherodes*, *Muntiacus feae*, and *Muntiacus vuquangensis* were united based on characters of the mandible, proportions of the skull, of the lacrimal, of the pedicles, the lacrimal fossa, the palatine processes, the extension of the vomer, and facial crests as extension from the pedicles. Muntiacini is recovered in all but one MP

analyses and the ML analysis based on the combined data set; in the strict consensus tree of the ordered analysis including fossil and extant cervids and the BI analyses only *Muntiacus muntjak* and *Muntiacus reevesi* form a sister taxon relationship. The anterior extension of the pedicles as facial crests in *Muntiacus* is unique among cervids. Together with the higher proportion of plesiomorphic dental characters, these are most likely the reasons for forming a clade.

Odocoileini

In most analyses, both *Hippocamelus* are sister taxa. Both *Hippocamelus* species form a clade based on characters of the upper premolars and molars, the lower premolars and molars, the morphology of the lower incisors and canines, the upper canines, proportions of the skull and the palate, the morphology of the praemaxilla, nasals, palate, basioccipital and maxilla, the position of the infraorbital foramen, the tuber maxillae, the exposure of the mastoid process, linea temporalis, and antler morphology, insertion and proportions and origination. Sometimes *Ozotoceros bezoarticus* was the sister taxon to *Hippocamelus*. The sister taxon relationship of *Ozotoceros bezoarticus* and *Hippocamelus* was supported by characters of the upper premolars and molars, the lower premolars and molars, il, the mandible, proportions of the skull, the morphology of the praemaxilla, the nasal, the maxilla and the basioccipital, the mastoid process, the extension of the os zygomaticum, the linea temporalis, the mandibular fossa, and antler morphology, antler angle

In several analyses most *Mazama* species and *Pudu* are in a clade as sister taxa to the Muntiacini. In all analyses based on the combined data set *Mazama bricenii* and *Mazama chunyi* are sister taxa to each other. *Odocoileus hemionus* is the sister taxon to *Alces alces* in most analyses based on the combined data set, and in several topologies *Odocoileus virginianus* is the sister taxon to them. In all other topologies odocoileine taxa are placed in unresolved or varying positions.

Alceini

Alces alces was placed most often in an unresolved position, or as the sister taxon to *Odocoileus hemionus*. In few cases it was placed as the sister taxon to *Mazama chunyi*, *Ozotoceros bezoarticus* or *Cervus canadensis*. Similar to *Rangifer*, *Alces* has a highly derived skull morphology with an elongated viscerocranial proportion and antlers that protrude horizontally. The dentition shows similar modifications as in *Rangifer*, but is a little bit less specialised.

Capreolini

In the dental analyses both *Capreolus* species were sister taxa to each other in an uncertain position, mostly more closely related to Odocoileini than to Cervinae. *Hydropotes* was mostly placed in an unresolved position. In the cranial analyses, all three taxa were usually placed in an unresolved position or as the sister taxon to all cervids as individual lineages (not as a clade).

In most analyses based on the combined data set all three taxa were placed in a clade once including also *Procapreolus* and *Megaloceros*. Both *Capreolus* species were united

by character states of the p3, the p4, the lower molars, the upper premolars and molars, presence of small upper canines during certain life stages, proportions of lower incisors and canines, the mandibula, proportions of the palate, the morphology of the nasal, praemaxilla, and the lacrimal fossa, the extension of the os zygomaticum, and the orbita. Based on morphological evidence both *Capreolus* species are strongly supported to be sister taxa and several analyses support the sister taxon relationship of *Hydropotes* to the *Capreolus*-clade. *Capreolus* and *Hydropotes* from a clade based on characters of the upper premolars and molars, the lower premolars and molars, the mandibula, proportions of the skull and the lacrimal, the morphology of the praemaxilla, maxilla, auditory bulla and palate, the linea temporalis, the lacrimal process, the processus condylaris, the opening of the meatus acusticus, the postcornual fossa, and the vomer.

Rangiferini

In most analyses based on the dental and combined data set *Rangifer tarandus* was not placed closely related to any other cervid; instead it was the sister taxon to *Okapia*. The unusual placement of *Rangifer* as the sister taxon to *Okapia* was based on characters of the upper premolars and molars, lower premolars and molars, and the i1. This supports the evidence from observations of the dental morphology, which is so specialised and derived in *Rangifer tarandus* compared to that of all other cervids. In the analyses based on the cranial data set *Rangifer tarandus* was placed several times as the sister taxon to *Megaloceros giganteus*, once to *Odocoileus virginianus*, and once in an unresolved position. *Rangifer* has laterad protruding orbit rims, which were not observed to that extent in any other cervids. They could represent an adaptation to boreal regions.

3.4.5 Skull Character Evolution

Cranium

Due to the conservative overall morphology of the cervid skull, there are only few evolutionary trends. The most striking differences from early fossil cervids to extant cervids can be observed on the pedicle, which has three aspects of modification; the insertion point, the inclination and the length of the pedicle. In the first Miocene cervids, the pedicle originates directly dorsal to the orbit, is upright and long. In contrast, in the typical modern cervid the pedicle originates more posterior to the orbit, is inclined at 45–60° and short. In Muntiacini, *Euprox* and *Eostyloceros* the pedicles are long, strongly inclined (often less than 45°) and originate posterior to the orbit. *Mazama* and *Pudu* have strongly inclined and short pedicles. It is likely that the degree of inclination is a result of an adaptation to rich vegetation. With the stronger inclination the insertion point naturally moved towards posterior to the orbit. The shortening of the pedicles could be related to the increasing size of antlers, because a longer and heavier set of antlers would put a biomechanically unfavourable leverage on the pedicles. The short pedicles in the cervids with short antlers, *Mazama* and *Pudu*, were presumably maintained, since both genera are most likely secondarily dwarfed cervids with secondarily decreased antler size. In contrast to more advanced cervids, the pedicle in early Miocene cervids is entirely above the supraorbital process and not in contact with the braincase; the pedicles are vertical in lateral view, parallel or

converging in frontal view.

There are several differences in the cervid skull. Some are likely to be interspecific, some are intraspecific variation. Differences in the size of the Praeorbital vacuity are primarily species specific, but have also an ontogenetic component, since they are often smaller in aged individuals. Similarly, the lacrimal fossa varies in size and depth in different species, presumably depending on the presence, size, and usage of the lacrimal gland. Also, there is a difference between males and females. The position of the lacrimal foramina to each other and on the orbit rim can potentially be used to distinguish groups of cervids. The consistent presence of two lacrimal foramina is typical for cervids, but is also present in some bovid species. In *Dremotherium feignouxii* sometimes only one lacrimal foramen is present (Costeur, 2011). The contact of the lacrimal and the frontal at the orbit rim without interlocking sutures was first observed in Rössner (1995). This trait is most likely an intraspecific variability and could be an effect of ageing.

A sagittal crest is present in some early Miocene cervids, e.g., *Dicrocerus*, *Procervulus*, but absent in extant species. The number and size of supraorbital foramina and presence and absence of the supraorbital sulcus could potentially be features to distinguish groups of cervids; however, more specimens per species need to be investigated to confirm this. The vomerine septum and the division between the temporal foramina are long-known features to distinguish Capreolinae and Cervinae. The auditory bullae have a variable morphology. Large inflated bullae are diagnostic for some species, e.g., *Axis*.

Antlers

Evolution of Antlers Cervidae is diagnosed by the presence of antlers (Janis & Scott, 1987; Pitra et al., 2004). This takes into consideration that the lack of antlers in *Hydropotes inermis* must represent a secondary loss. The reason for the absence of antlers in this species is controversial and both, a primitive condition and secondary loss, have been suggested. To solve this issue, thorough research on the process(es), which trigger the growth of the first set of antlers in antler-bearing species and when how and why these processes/prerequisites are absent in *Hydropotes inermis* needs to be undertaken. However, this is far beyond the scope of this project. Therefore, the more widely accepted hypothesis that *Hydropotes inermis* secondarily lost its antlers is applied here and the presence of antlers is the synapomorphy of Cervidae.

There is broad consensus that antlers originated only once (Loomis, 1928; Azanza & Morales, 1989; Azanza, 1993a,b; Azanza et al., 2011). Chapter 3 contains a detailed discussion on the origin of antlerogenesis, thus the topic is only briefly addressed here. It was originally hypothesised that antlers evolved from non-deciduous to deciduous appendages (Dong et al., 2003). This hypothesis cannot be held any longer based on fossil evidence (see Chapter 3).

Early antlers do not have a shaft and the bifurcation originates directly from a broad antler base. Early antlers are majorily bifurcating, sometimes with one additional tine, or coronate (Azanza et al., 2011). Antlers developed a shaft before the first bifurcation and often a more complex branching pattern; they also increased in size. As briefly mentioned in the dentition section, evolution of size and complexity of antlers is associated with reduction or loss of upper canines (Scott, 1937; Beninde, 1937; Geist, 1966; Brokx, 1972).

The absence of antlers in female *Procervulus dichotomus* skulls rules out the presence of antlers in both sexes as the ancestral condition and indicates that the role of testosterone could have been already important in Miocene cervids (Ginsburg & Azanza, 1991). The exceptional antler condition in *Rangifer*, where antler growth seems to be independent of the gonads must be a relatively recent specialisation in cervids (Bubenik, 1966; Brokx, 1972).

Antler Characters

In contrast to Loomis (1928), Gentry et al. (1999) state that cranial appendage morphology proved to be more suitable than tooth morphology to distinguish species. This applies in general to Pecora, but also to Cervidae. It is true that different cervid species can be easily identified based on their antler morphology (branching pattern, orientation, size). Antler characters are often used to solve intra-subfamily relationships, but they are problematic because of convergent development and subsequent homoplasy in antler characters (Pitra et al., 2004).

Even though antlers are species-specific, they have a high variability, intraspecifically and ontogenetically. No antler looks exactly the same, not even the left and the right antler of the same individual are identical. Also, antlers change from one year to the next; the antlers of a yearling usually differs largely from the antlers of an adult. In addition pathologies, abnormal growth, and other phenomena can occur. While cervid genera and most species can be qualitatively distinguished based on antler morphology, translation of these distinctions into discrete characters for quantitative or phylogenetic analyses is much more difficult. Convergences, which can be distinguished by eye, but are sometimes too subtle to be scored differently in the character matrix are the reasons for this. The high variability of antlers is a problem particularly in fossil taxa, where the entire intraspecific variation cannot always be observed due to the lack of a sufficient number of specimens or the complete range of ontogenetic stages. The taxonomy of fossil cervids is often based on antler morphology, because antlers are easy to identify and numerous in the fossil record (Lister et al., 2010). To base classifications just on antler morphology, however, is problematic for the given reasons.

Among extant cervids, three general morphotypes can be distinguished; morphotype one has fewer than three tines, morphotype two has exactly three tines, and morphotype three has more than three tines and a more complex branching pattern. These three morphotypes have previously been associated with ecological habitats: simple antlers for the tropics, a three-tined antler plan for woodland areas typical in East Eurasia or India, and the large and complex display organs in temperate regions (Pitra et al., 2004).

Morphotype 1

This morphotype includes all *Mazama* and *Pudu* species, which have single-tined antlers. *Pudu* rarely has a bifurcation. *Elaphodus cephalophus* has minute, single-tined antlers. From the fossil record no cervid is known with a single-tined antler morphology. The condition in *Mazama* and *Pudu* is considered a secondary adaptation to dense vegetation, while the reduced morphology in *Elaphodus cephalophus* is still controversial and matter of debate.

All *Muntiacus* species have bifurcating antlers on elongated inclined pedicles. *Hippocamelus* has a basic bifurcating antler morphology with an open angle between the brow tine and main tine; the main tine may bear additional small tines. Fossil cervids with a bifurcating antler morphology include *Procervulus*, *Dicrocerus*, *Heteroprox*, *Euprox*, and presumably *Cervus australis*.

Morphotype 2

This morphotype includes all *Rusa*, *Axis*, *Capreolus*, and *Ozotoceros* species. Their antler bauplan consists of three tines, which are organised either in a way, where the brow tine forms a more acute angle to the main beam with the tip of the brow tine pointing backwards (*Axis*, *Rusa*), or where it forms an open angle with the tip of the brow tine pointing more upwards or forwards (*Capreolus*, *Ozotoceros*).

Fossil cervids of the morphotype 2 include *Axis lydekkeri*, *Rusa kendengensis*, *Metacervocerus pardinensis*, ‘*Cervus*’ *philisi*, and *Metacervocerus rhenanus* with the brow tines pointing backwards, *Procapreolus cusanus* with the brow tines pointing upwards. *Pliocervus matheronis* antler remains are too fragmentary to infer the direction of the brow tine unambiguously. It was also suggested that this species had presumably four tines (Croitor, 2014); however, as this could not be observed on the studied specimens and literature, it was scored as possessing three tines.

Morphotype 3

This morphotype is present in *Alces*, *Blastocerus*, *Cervus*, *Dama*, *Elaphurus*, *Odocoileus*, *Rangifer*, *Rucervus*. *Blastocerus dichotomus*, *Cervus albirostris*, and *Cervus nippon* have an antler bauplan, which generally produces not more than four tines in adults (additional smaller tines not included). Possibly, these species should be put in their own morphotype or included in morphotype 2. In *Elaphurus* it is difficult to distinguish between main tines and accessory tines. Characteristic for *Cervus elaphus* are paired lower tines, called brow tine and bez tine, and an additional trez tine (Lister et al., 2010). Characteristic for *Dama* are palmated antlers, however, the first representatives, e.g., *Pseudodama*, had unpalmated antlers with four tines (Lister et al., 2010). *Dama dama* and *Rangifer tarandus* have a ramified palmated morphology, while *Alces alces* has a palmated morphology without much tendency towards ramification, and thus form a subgroup within morphotype 3. Only eight cervid species (excluding the three species with palmated antlers) have the tendency to produce more complex antlers with more tines from year to year, which is widely assumed to happen in all cervids.

Fossil cervids of the morphotype 3 include *Croizetoceros ramosus*, *Eucladoceros ctenoides*, *Lagomeryx parvulus*, *Ligeromeryx praestans*, *Arvernoceros ardei*, *Praeclaphus perrieri*, *Megaloceros giganteus*, and *Palaeoplatyceros hispanicus*. The two lagomerycids, *Croizetoceros ramosus* and *Palaeoplatyceros hispanicus* represent special cases, as their antler morphology and branching pattern is unique among living and fossil cervids. Lagomerycids possess coronate antlers without a shaft, while *Palaeoplatyceros* has palmated antlers without any other tines, and *Croizetoceros ramosus* shows a serial organisation of small tines on the main beam. *Praeclaphus perrieri* has a distally trifurcating main beam with a basal brow tine, which is similar to the condition in *Arvernoceros ardei*, where the branching part of the main beam sometimes forms a palmation. The antler morphology of *Eucladoceros*

ctenoides resembles that of *Cervus elaphus* with several lower tines, similar to the bez and trez tine. *Megaloceros giganteus* has enormous ramified palmated antlers similar to those of *Dama*. Also characteristic for Megacerini are flattened basal brow tines similar to *Rangifer* (Lister et al., 2010).

3.4.6 Tooth Character Evolution

Teeth represent fundamental characters for distinguishing cervids, while antlers are less suitable (Loomis, 1928). Dong et al. (2004) also showed that the main components of cervid teeth lack evident morphological variations, but accessory components show variation. These variations in combination with the degree of molarisation of premolars can be used to identify genera or species. Widely accepted evolutionary trends in cervids concerning the dentition are increasing hypsodonty and the reduction or loss of upper canines (Dong et al., 2004). However, the hypsodonty index, although widely used in ruminant phylogeny, has been considered to be a misleading character due to its ambiguous definition and convergent evolution among all large herbivorous mammals (Janis & Scott, 1987; Hassanin & Douzery, 2003). Therefore, the hypsodonty index is not considered in my analyses.

The first deer traditionally were considered as leaf-eating; recent dental analyses generally support these findings, but also showed that brachyodont *Procervulus ginsburgi* should be considered as a seasonal mixed feeder. Based on this a facultative leaf-grass mixed feeding strategy with preference for leaf-eating is likely the primitive dietary state in cervids and ruminants (DeMiguel et al., 2008). Care should be taken with interpreting results from mesowear, because relying on the wear process, it is least reliable for very brachyodont species (DeMiguel et al., 2008). However, together with other parameters, such as microwear, palaeoclimate information, the implications on the palaeodiet of early deer species become more and more precise.

Some dental characters are highly variable and thus difficult to score unambiguously. Despite convergent modifications depending on dietary requirements, a species-specific pattern underlies these adaptations in most species (pers. obs.), particularly in the lower premolars and upper molars. The difficulty is to score these species-specific patterns without scoring the convergent adaptations and the intraspecific variability. Observations on these adaptations and evolutionary development of tooth morphology is discussed in the following.

Lower tooth row

p1 is usually absent in cervids, although it was present in individual *Lagomeryx parvulus* specimens. In the premolar row, p2 is the tooth with the least changes in occlusal morphology throughout cervid evolution; only a shortening in length is observed in most extant taxa and sometimes this tooth is lost entirely in few individuals. The basic premolar bauplan is maintained. p3 and p4 underwent molarisation to different degrees. While p3 is molarised only in a few species and not to the same extent as p4, p4 is molarised in many species, at least initially, and is completely molarised in three species. This pattern can be explained by different rates of development/evolution of certain structures dependent on the tooth position. Since p3 is in an intermediate position between the primitive p2 and

the often molarised p4, the extent of changes is also intermediate (Nikolskiy & Boeskorov, 2011).

The way how p4 is formed differs in different groups of ruminants (Loomis, 1928). The degree of molarisation of p4 can be defined by the closure of the anterior valley, the connection between the protoconid and paraconid, and the connection between the protoconid and the hypoconid (Nikolskiy & Boeskorov, 2011).

The molarisation of the p4 (and p3) starts with the development and elongation of the mesolingual cristids, especially the anterolingual cristid. Where the anterolingual cristid is in contact, but not yet fused, with the anterior conid, the anterior valley has a lingual wall. The anterior valley becomes entirely closed, when the anterior conid and the anterolingual cristid fuse. Sometimes the transverse cristid is separated from the mesolingual conid, which results either in an isolated lingual wall or in a partially closed anterior valley if fused to the anterior conid. The posterolingual conid may become detached from the posterolabial conid.

In *Rangifer* and *Alces*, which show the most advanced molarisation of p4, the mesolabial conid, transverse cristid, posterolingual conid, and posterior cristid, all of which can be fused, have a diagonal orientation.

The labial incision on premolars is rarely and if so weakly developed in p2; it is more often developed on p3, and most often occurs on p4, where it is also normally the deepest. In the majority of p4, where the labial incision is deep, the anterior part of the tooth is much more prominent than the posterior.

In cases, where p4 is slightly shortened, the compression is caused by a re-orientation of the posterior cristid and stylid towards anterior projecting into the posterior valley (Loomis, 1928).

Some species show a spike like extension of the posterolabial conid of the p4 towards labiad; these species are *Capreolus capreolus*, *Capreolus pygargus*, *Blastocerus dichotomus*, *Hippocamelus* spp., *Hydropotes inermis*, *Ozotoceros bezoarticus*, *Croizetoceros ramosus*, *Procapreolus cusanus*, and '*Cervus*' *philisi*. Whether this feature can be used as a phylogenetic character and is indicative of affiliation to a certain subclade has to be investigated in the future.

p4 represents the most variable tooth of upper and lower teeth in cervids. It can vary extremely from one individual to the other within the same species. Therefore, care should be taken when classifying cervids based on this tooth position alone.

It is remarkable that in both *Axis* species the p4 predominantly seems to lack mesolingual cristids. Even extant muntiacines show mesolingual cristids in most individuals. Among fossil cervids only in early Miocene species mesolingual cristids are often, but not always, absent.

Due to a more posteriorly positioned transverse cristid and mesolingual conid, the p4 and especially the p3 in *Rucervus* and *Rusa* have a widely open anterior valley; however, on the p4 the anterior valley can be closed by a lingual wall, particularly in later wear. This is more often observed in *Rusa* than in *Rucervus*.

There is a trend that the premolar tooth row becomes slightly shorter compared to the molar tooth row through evolution. However, this trend is not significant and there are several exceptions among extant taxa

Lower molars are rather conservative concerning their morphology; the orientation of

the lingual conids and cristids may be more diagonal in some species. Anterior cingulids are variably present throughout the evolutionary history of cervids. In most species they are most prominent on m1 and weaker in m2, and often absent in m3. In *Rucervus* the anterior cingulids are particularly prominent, also partly in *Rusa*. The third lobe on m3 is probably the most variable structure on the lower molars. It is normally crescent-shaped consisting of the entoconulid and the hypoconulid; sometimes the third is reduced to one of these elements or has an additional fold on the posthypoconulidcristid. In a few individuals the third lobe is missing entirely. Ectostylids are variably present and never high, nevertheless they become involved in wear in aged individuals. In *Rucervus* and also to a lesser extent in *Rusa* and *Axis* the anterior and posterior labial walls of the lobes of the lower molars are indented. In almost all Miocene cervids and in *Cervus australis* an external postprotocristid is present on all lower molars. This structure is not present in any more recent fossil cervids nor in extant cervids.

The internal postprotocristid often fuses with the metastylid and the preentocristid; this is mainly due to wear rather than a feature that distinguishes different species from each other. Already Loomis (1928) observed on the lower molars of *Alces* and *Rangifer* that the hypoconid and metaconid are isolated. This is caused by the fusion of the above mentioned elements. He further stated that this fusion is already present in *Dicrocerus* and concluded that this must be a primitive character (Loomis, 1928). However, the fusion of the postprotocristid and the preentocristid appears quite often in later wear throughout living and fossil Cervidae. The *Dicrocerus* specimen figured in the study has a heavily worn occlusal surface. Loomis (1928) further concluded that cervid species, which show the 'crossover' also have an internal and external postprotocrista in the upper molars; this is true for most *Alces* and *Dicrocerus* specimens, but not for *Rangifer*. It is doubtful that these two features are linked with each other and that the 'crossover' is a distinctive character.

Upper tooth row

The upper incisors and the P1 are absent in cervids. The upper premolar row is characterised by robust, compact, predominantly horseshoe-shaped teeth. P3 and P4 are little variable, while P2 may take up more rectangular or triangular outlines, particularly in early fossil cervids. All premolars have at least one prominent central fold, except for *Rangifer*, in which central folds are consistently missing. Sometimes there are tiny additional folds, or the main central fold is serrated. A separation of the lingual cone into an antero- and posterolingual cone is relatively common; this separation can be partial when the separation appears only at the tooth crown while both cones remain connected at the base of the tooth, or there is a complete separation of both cones from the base to the apex of the tooth. The tendency for this separation seems to be variable and persists throughout the fossil record and diversity of today. In all Miocene cervids the P2 is longer than the P4, while in extant taxa the P4 is most often longer than the P2.

The upper molars are all two-lobed with only little tendency to vary in morphology. The posterior lobe of the M3 is distinctively smaller than the anterior one in most species. The entostyles are variably present, absent in some species. In *Axis*, *Rusa*, *Rucervus* and *Elaphurus* they are often λ -shaped. Metaconule folds are variably present within

Cervinae and Capreolinae and are mostly small. Protocone folds are usually absent in Cervinae, while they are regularly present Capreolinae, often well developed on all molars. The same applies to fossil cervids, where tiny metaconule folds are much more common than protocone folds. Only in Miocene cervids protocone folds are common. However, in these species it often looks more like a bifurcation of the postprotocrista than a fold originating from the crista, particularly when the internal part of this bifurcation is longer than the external as on M2 in *Dicrocerus*. It is not entirely evident, whether these are two independent structures or the same structure with variable characteristics. The bifurcation of the postprotocrista into an internal and external one has been debated for decades; Ginsburg & Heintz (1966) for example regarded it as a derived cervid character based on its presence in *Dicrocerus* and *Euprox*. The only other non-cervid pecoran species that has this trait is *Amphimoschus* (Janis & Scott, 1987). The bifurcated postprotocrista has been regarded as an advanced cervoid character in Janis & Scott (1987), while later this character is referred to as ‘primitive presence of bifurcated protocone’. In extant cervids this feature is present in *Odocoileus*, *Blastocerus*, *Alces*, *Mazama*, *Pudu*, and *Capreolus* (Janis & Scott, 1987). One specimen of *Palaeoplatyceros hispanicus* (MNCN 39181) shows both a bifurcating postprotocrista and a tiny protocone fold on the preprotocrista. This indicates that both structures may in fact be developmentally independent, however, as this could only be observed in one specimen, it remains speculation.

Throughout the evolutionary history of cervids the lingual cingulum, regularly present on molars and sometimes even on premolars of fossil cervids, becomes reduced and eventually lost in extant cervids. In *Rucervus*, *Rusa*, and *Axis* the anterior and posterior lingual walls of the molars tend to be indented; this is also observed in *Axis lydekkeri*, *Rusa kendengensis*, and ‘*Cervus*’ *sivalensis*.

Upper canines

Upper canines can occur in any cervid species, but are specific for some species, particularly within Cervinae with the exception of *Axis* and *Dama* (Brooke, 1878; Lydekker, 1898; Flerov, 1952; Pocock, 1943; Brox, 1972). American cervids lack upper canines more often than not except for *Rangifer* (Brox, 1972).

There is an evident trend in cervid evolution from enlarged curved upper canines towards a loss of these teeth. All Miocene cervids have enlarged upper canines; a reduction in length of these enlarged upper canines was observed in late Miocene cervids compared to early Miocene cervids. In Pliocene and younger cervids the canine size was more reduced comparable to the upper canines (if) present in extant cervids. For some Pliocene and younger species their presence could not yet be proven. In extant cervids, muntiacines enlarged upper canines, similar to those of Miocene cervids. *Hydropotes* has strongly elongated sabretooth-like upper canines, which differ in morphology from those in muntiacines and early fossil cervids. They are actively used in intraspecific fights. In all other extant species upper canines are reduced in size or missing entirely. Most cervines possess small upper canines. Among capreolines, *Rangifer* appears to be the only species with upper canines in adults. Sometimes, especially in capreolines, the deciduous upper canines are still present, but do not have a permanent successor.

It is likely that the presence and/or size of upper canines is somehow genetically linked

with the antlers. However, much more research is needed to find this link and associated interactions and effects on behaviour. However, this brings up the question, why female deer have upper canines, too (Brokx, 1972). Even though they are often much smaller, especially in species, where males have enlarged upper canines, they are present without any obvious function. In other ungulates, where males use their canines in intraspecific fights, for example in equids, upper and lower canines are lost in almost all females.

3.5 Conclusions

The combined morphological data set analysed here, represents the most extensive matrix in terms of taxon sampling. It has been phylogenetically analysed with different approaches, most of them were never applied to cervid data sets before. My results showed that the conservative morphology in Cervidae makes it difficult, but not impossible, to infer systematic relationships based on morphological characters alone. Poor resolution impeded robust conclusions on the systematic position of the majority of taxa. However, re-occurring placings of taxa derived from analyses of different data sets or compositions are more likely to represent phylogenetic signal of the data.

For extant cervids the *Elaphurus-Rucervus-Rusa*-clade was consistently recovered, in some cases the *Axis*-clade was included within or sister taxon to the former. This is a new finding that has never been observed before on morphological topological evidence. In the combined analyses Capreolini is often recovered, while in the separate analyses *Capreolus*-species form a clade. Although none of the characters contained direct information on the size of scored taxa, a size bias is present in many topologies, where smaller deer species such as *Mazama*, *Pudu*, and *Muntiacus* are clustered together in a clade. Because of their small size some of their morphological traits are presumably similar.

The incompleteness of fossils makes scoring and analysing those taxa difficult. However, unlike for extant taxa, morphology is the only possibility to quantitatively explore their systematic relationships to each other and to extant cervids. Based on my results and comparisons with the literature, fossil cervids can generally be divided into two groups. Miocene cervids represent one group, because almost all of them have unique phenotypes, which cannot be linked with any extant cervid. Plio- and Pleistocene cervids represent the second group, which share many phenotypic features with living cervids and have proportionally fewer plesiomorphic character states.

The systematic relationship of Miocene fossil cervids remains controversial. In my analyses these taxa were either unresolved or between the outgroup and all other taxa; sometimes they form a clade. The hypothesis that early Miocene cervids form a stem clade, previously proposed to be named Procervulinae, is weakly supported here. *Eostylloceros hezhengensis* and *Euprox furcatus* showed affinities to Muntiacini, presumably because members of extant Muntiacini have a higher proportion of plesiomorphic characters than other extant cervids. The Miocene *Pliocervus matheronis* and *Palaeoplatyceros hispanicus* were unstable. My results are good initial quantitative estimates of the systematic position of Miocene cervids, which have never been accomplished in that much detail and on a comparably extensive data set.

Plio- and Pleistocene cervids were often placed within crown cervids and more closely related to living cervids than the Miocene cervids. However, a more exact placement for

Plio- and Pleistocene taxa remains difficult. *Cervus australis*, *Candiacervus ropalophorus*, and *Megaloceros giganteus* were particularly unstable. *Croizetoceros ramosus*, *Procapreolus cusanus*, and both fossil *Odocoileus* were repeatedly placed within Capreolinae. The fossil *Muntiacus muntjak* was mostly placed within Muntiacini. All other Plio- and Pleistocene cervids were often or repeatedly placed within or closely related to Cervini.

The molarisation of lower premolars, particularly of p4 and to a lesser extent of p3 represent an important evolutionary trend. Lower molars and upper premolars and molars show less obvious trends. The external postprotocristids on the lower molars are present in all Miocene cervids, but disappear in more recent cervids. The upper canines were elongated in early cervids and became reduced or lost in most extant cervids. Exceptions from this are *Hydropotes inermis* and all members of Muntiacini, which still have elongated upper canines. The evolutionary trends in antlers and pedicles is discussed in Chapter 2.

Different morphological character partitions are differently useful to reconstruct phylogenies. Cranial characters had not enough interspecific variation to solve systematic relationships within Cervidae, while they are likely to be useful in solving inter-pecoran relationships. A few cranial characters such as the pedicle morphology and a few antler characters diagnosed some clades. Dental characters were more useful for phylogenetic reconstructions and diagnosing clades. The alternative approaches, SFA and EPA, to reconstruct the phylogenies were more useful for inferring systematic relationships of fossil cervids. The comparisons of the standard and alternative phylogenetic approaches provide comprehensive insights into cervid systematics. Generally, more material of fossil cervids is needed for future analyses to further clarify their systematic relationships. Despite the broad coverage of geological times in my data sets, temporal gaps in the taxon sampling remain (e.g., between *Eostyloceros hezhengensis* and first *Muntiacus* fossils), which will hopefully be narrowed with a denser taxon sampling in the future.

Chapter 4

Systematic Relationships of Five Newly Sequenced Cervid Species

4.1 Introduction

Cervidae forms a subclade of ruminant artiodactyls and is the second most diverse group among terrestrial artiodactyls, with 55 extant species (IUCN, 2016), including one recently extinct species (*Rucervus schomburgki*; (Duckworth et al., 2008). Cervids natively inhabit Eurasia, the Americas, and potentially northernmost Africa (Mattioli, 2011). They are adapted to diverse climatic zones, ranging from the tropics to arctic regions, and to diverse habitats such as tundra, grasslands, swamps, forests, woodlands, and ecotones (Mattioli, 2011). Their unique phenotypic feature is a pair of antlers, which are osseous outgrowths of the frontal bone that are shed and rebuilt regularly. The current conservation status of cervids lists 29 species as ‘threatened’, nine species as ‘data deficient’, and 17 species as ‘least concern’ in the IUCN Red List of Threatened Species (IUCN, 2016). Samples and life history data are much more difficult to obtain from rare and threatened species than from more abundant species. Therefore, there is a discrepancy between the well-studied (e.g., *Cervus elaphus*, red deer; *Odocoileus hemionus*, mule deer; *Rangifer tarandus*, reindeer) and barely known species (e.g., *Mazama* spp., brocket deer; *Pudu* spp., pudu; *Muntiacus* spp., muntjac). Consequently, data for the latter taxa are overdue.

Cervid phylogenetics has improved considerably in recent decades through molecular systematics (e.g., Hassanin & Douzery, 2003; Pitra et al., 2004; Kuznetsova et al., 2005; Hernández Fernández & Vrba, 2005; Hughes et al., 2006; Gilbert et al., 2006; Marcot, 2007; Agnarsson & May-Collado, 2008; Duarte et al., 2008; Hassanin et al., 2012). However, several species are still under-represented in molecular phylogenetic analyses because their current conservation status of threatened or data deficient negatively affects their sample collection.

Consensus has been reached for the monophyly of taxa Cervidae, Muntiacini, Cervini, Capreolini and Odocoileini. Muntiacini and Cervini form the clade Cervinae, which is a sister taxon to Capreolinae comprising Odocoileini, Rangiferini, Capreolini and Alceini (e.g., Hernández Fernández & Vrba, 2005; Gilbert et al., 2006; Hassanin et al., 2012). The Capreolinae-Cervinae-split is commonly supported in previously published topologies and

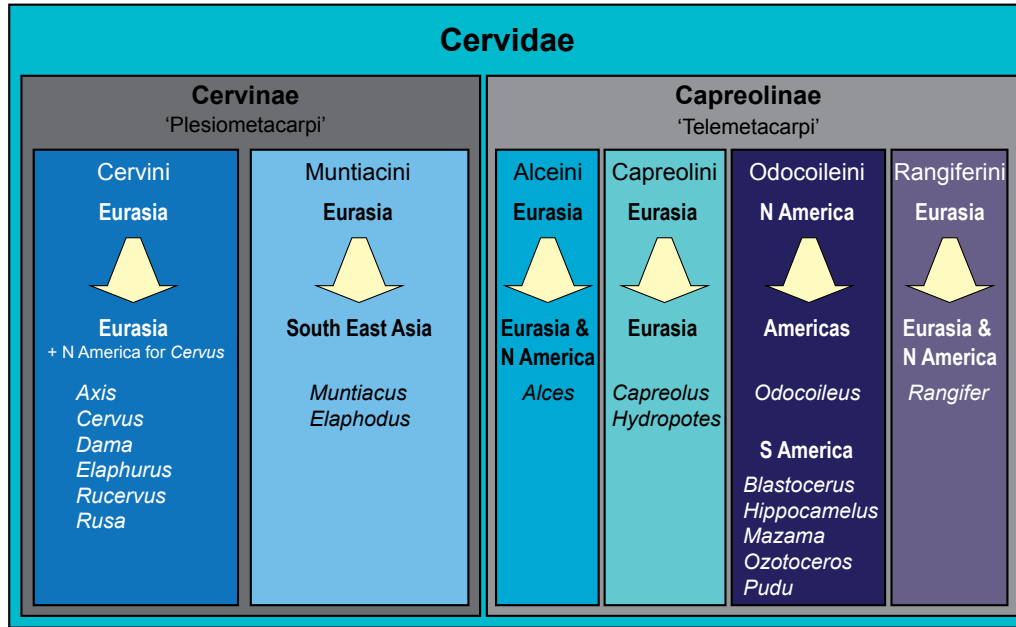


Figure 4.1: Overview of the current state of the art of cervid classification based on literature (e.g., Hassanin & Douzery, 2003; Pitra et al., 2004; Kuznetsova et al., 2005; Hernández Fernández & Vrba, 2005; Hughes et al., 2006; Gilbert et al., 2006; Marcot, 2007; Agnarsson & May-Collado, 2008; Duarte et al., 2008; Hassanin et al., 2012). The diagram shows the different clades, their geographical origination, and their current distribution.

corresponds to the first (though not formally valid) morphological cervid classification by Brooke (1878), who differentiated Plesiometacarpi and Telemetacarpi (Fig. 4.1). Systematic relationships within Cervinae appear to be largely resolved, whereas Capreolinae systematics is more controversial (Pitra et al., 2004; Gilbert et al., 2006; Duarte et al., 2008; Hassanin et al., 2012; Croitor, 2014). For an overview of current cervid classifications, see Figure 4.1.

The mitochondrial cytochrome b (*Cytb*) gene is the best-sampled across cervids. *Cytb* is a marker that is known to be highly variable in mammals, which makes it a suitable marker for resolving genus and species level relationships but less suitable for resolving deeper nodes (family level and above) or for population studies (Hofreiter et al., 2001a). In addition, because mitochondrial genomes are maternally inherited, they may not allow a full reconstruction of a species' evolutionary history if there is no random mating.

However, Hassanin et al. (2012) sequenced and analysed mitochondrial genomes of 33 cervid species as part of a large Artiodactyla phylogenetic reconstruction and provided a robust phylogenetic framework for cervids. To date, sampling of mitochondrial genomes and individual partial *Cytb* sequences cover 46 of the 55 cervid species.

Here, we present the results of phylogenetic analyses that include four species not previously sampled for molecular data: *Mazama chunyi* (Peruvian dwarf brocket), *Muntiacus atherodes* (Bornean yellow muntjac; including holotype), *Pudu mephistophiles* (Northern

pudu; including holotype), and *Rusa marianna* (Philippine brown deer), all of which were taken from museum specimens. We also sequenced three *Mazama bricenii* museum specimens (Mérida brocket; including the holotype), of which *Cytb* sequences have been published recently and were sequenced contemporaneously with our study (Gutiérrez et al., 2015). Except for *M. atherodes* (least concern), all species have been assessed as vulnerable based on the IUCN Red List. Therefore, considering the threat of extinction, our approach of sequencing DNA from museum material is an important contribution to cervid systematics.

The specific aims of our study were (1) to reconstruct the systematic position of *M. bricenii* and *M. chunyi* and further investigate the polyphyly of the genus *Mazama*, (2) to reconstruct the systematic position of *M. atherodes*, (3) to test the monophyly of the Philippine *Rusa* species (*R. alfredi* and *R. marianna*) and their sister taxon position relative to the Indonesian and mainland *Rusa* species (*R. timorensis* and *R. unicolor*), and (4) to test the monophyly of *Pudu*.

To achieve these aims, we experimented with different matrix sizes and parameters to examine the reliability of the phylogenetic signal throughout different data sets.

4.2 Material and Methods

4.2.1 Material

We sampled and sequenced five species from which no molecular data were available previous to our study (but see Gutiérrez et al., 2015; Tabs 4.1 and 4.2). Samples were taken from thirteen museum specimens, nine from the Natural History Museum in London (BMNH) and four from the Museum für Naturkunde Berlin (ZMB). Three specimens represent holotypes (BMNH 1908.6.24.5 *Mazama bricenii*, BMNH 1971.3088 *Muntiacus atherodes*, BMNH 1896.1.28.6 *Pudu mephistophiles*). One sample was derived from a wet specimen, one from a skin, and the remaining samples consisted of bone fragments or dried soft tissue remains of skulls (details in Table 4.2). Figure 4.2 shows where the specimens originated and their currently known species distributions. The collection dates of each specimen are given in Table 4.2.

We obtained complete *Cytb* and/or mitochondrial genome sequences from NCBI GenBank (<http://www.ncbi.nlm.nih.gov/genbank>) for 48 cervid species. These included the 45 extant cervids (full set of available extant cervid data excluding recently published *M. bricenii* sequences; Gutiérrez et al., 2015), one subspecies (*Cervus elaphus canadensis*), a questionable *P. mephistophiles* sequence from Hassanin et al. (2012), and one fossil cervid species (*Megaloceros giganteus*). We also added six non-cervid ruminant taxa (Tab. 4.1). The resulting *Cytb* data set is the most taxonomically extensive for Cervidae to date.

4.2.2 Extraction

The challenges of sequencing ancient DNA are related to the degradation of DNA after an organism's death triggered by exogenous processes such as oxidation and background radiation. These processes affect the sugar-phosphate backbone and nitrous bases of the DNA strand, whereas hydrolytic processes such as depurination and deamination cause

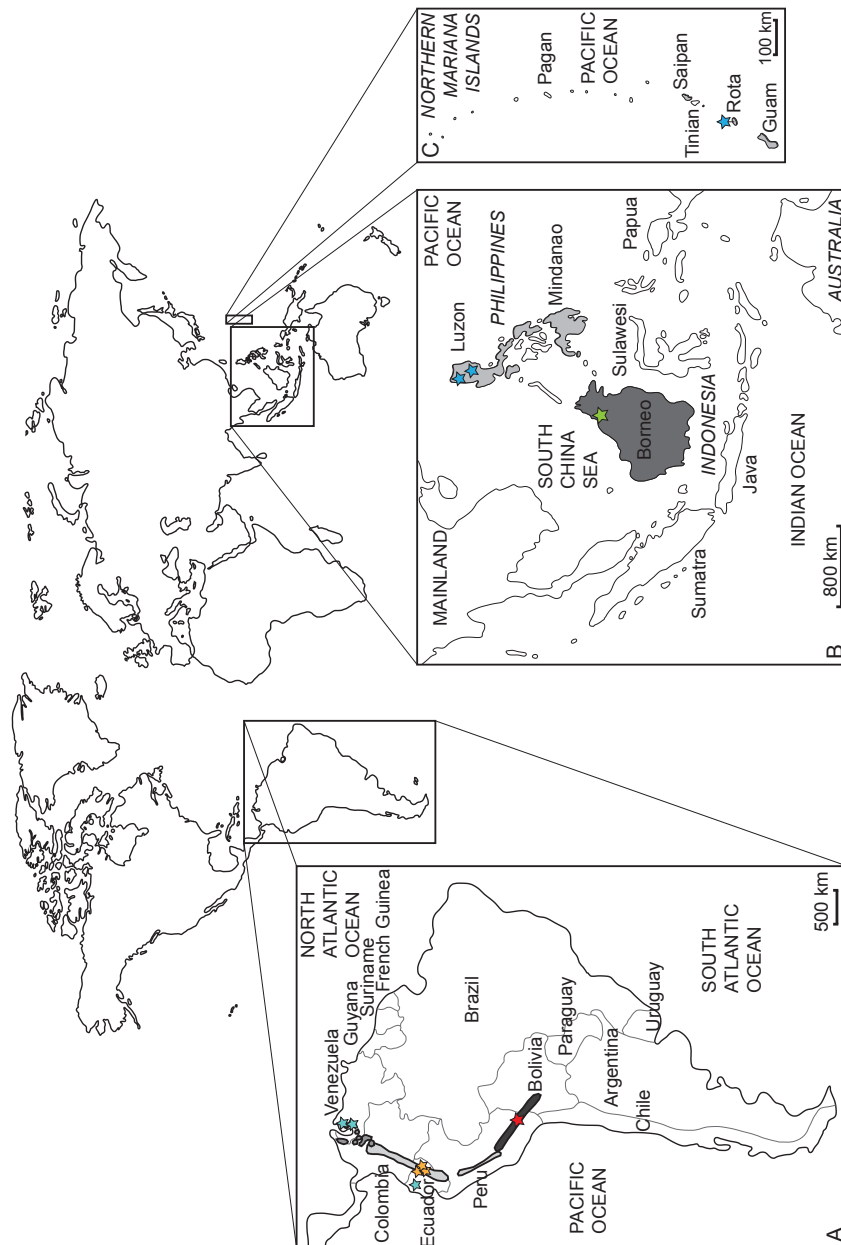


Figure 4.2: Current distribution of the sampled species and the approximate sampling locations of the specimens. (A) Enlarged map of South America; dark grey/red star: *Mazama chunyi*, light grey/yellow stars: *Pudu mephistophiles*, medium grey/turquoise stars: *Mazama bricenii*. (B) Enlarged map of Indonesian and Philippine Islands and (C) enlarged map of the Northern Mariana Islands; dark grey/green star: *Muntiacus atherodes*, light grey/blue stars: *Rusa marianna*.

breakage in the DNA molecules (Hofreiter et al., 2001b). Due to the large number of

mitochondria per cell, mitochondrial gene sequences are more likely to be retrieved from ancient material than is nuclear DNA (Hofreiter et al., 2001a).

DNA was extracted using the Qiagen QIAamp DNA Micro Kit, including an overnight lysis step, following the manufacturer's protocol. After lysis, 1 μ g dissolved carrier RNA was added, as recommended in the protocol, 80 μ l elution buffer was used for the last elution step, and the last incubation step was set for five minutes instead of one minute. After the extraction, the DNA concentration was measured using a spectrometer (NanoDrop 1000; Peqlab Biotechnologie GmbH, software version ND 1000 v3.7.1) (Tab. 4.2).

4.2.3 PCR

Eight cervid-specific *Cytb* primers (Lister et al., 2005) were used to amplify a 747 base pair region from the 1140-base-pair-long mitochondrial *Cytb*, from nucleotide position 64 to 810. Each primer pair amplified a 100–140-base-pair-long sequence with overlap to adjacent sequences (Lister et al., 2005; Tab. 4.2).

Polymerase chain reactions (PCR) were carried out using a TProfessional thermocycler (Biometra). Sequences amplified from each primer pair were validated against contamination with a negative control. The specific PCR components are given in Table 4.3. The PCR programme was as follows: initial denaturation at 95 °C for three minutes, then 35 cycles of denaturation at 95 °C for 30 s, annealing at 55 °C for 30 s, and extension at 72 °C for 30 s, and a final extension at 72 °C for five minutes. Amplification of target sequences was initially attempted using the components in Table 4.3, column (a) and an annealing temperature of 55 °C. Some primer-sample combinations did not result in amplification products. Therefore, we experimented with the components, e.g., not adding Bovine Serum Albumin (BSA), changing the overall reaction volume, and/or increasing the concentration of magnesium chloride (Tab. 4.3). We also experimented with annealing temperatures ranging from 48 °C to 52 °C. These optimisations were successful in most cases; however, a few sections of the individual sequences for certain specimens could not be successfully amplified, which left gaps in the *Cytb* sequence (Tab. 4.2).

Successfully amplified PCR products were sequenced in both directions using the amplification primers and the ABI BigDyeTerminator 3.1 chemistry following the manufacturer's protocol on a capillary sequencer (ABI 3730; AppliedBiosystems) in the Genomic Sequencing Unit, Faculty of Biology, LMU. After quality control, the approximately 100–140-base-pair-long forward and reverse sequencing reads were assembled into contigs.

These individual contigs were then assembled into a contig with a maximum length of 747 base pairs using CodonCodeAligner v.3.7.1.1.

To ensure that a genuine cervid *Cytb* fragment has been amplified, the forward and reverse pre-assembly sequences from each primer, the individual contigs of forward and reverse strands and the final 747-base-pair-long contigs were each BLASTed against NCBI GenBank entries. Only fragments returning a cervid in the first 50 BLAST search results were used. In almost all cases, where the BLAST result was different from the cervid result, the sequences were found to be most similar to *Bos taurus*. This contamination is possibly caused by the BSA added to enhance PCR outcomes. Sequences were submitted to the European Nucleotide Archive under accession numbers LT546647–LT546659 (Tabs 4.1 and 4.2).

Table 4.1: GenBank and ENA accession numbers. Newly sequenced species are in bold.

Species	Cytochrome b	mtGenome
<i>Alces alces</i>	AJ000026	JN632595
<i>Alces americanus</i>	M98484	—
<i>Axis axis</i>	AY607040	JN632599
<i>Axis kuhlii</i>	HQ893538	—
<i>Axis porcinus</i>	DQ379301	JN632600
<i>Blastocerus dichotomus</i>	JN632603	JN632603
	AY607038	
	NC_020682	
<i>Capreolus capreolus</i>	AJ000024	JN632610
<i>Capreolus pygargus</i>	AJ000025	—
<i>Cervus albirostris</i>	AY044863	JN632690
	AF423202	
<i>Cervus elaphus canadensis</i>	AF423198	—
	EF139147	
<i>Cervus elaphus</i>	JF489133	NC_007704
<i>Cervus nippon</i>	JF893484	NC_006993
<i>Dama dama</i>	AJ000022	JN632629
<i>Dama mesopotamica</i>	AY607034	JN632630
<i>Elaphodus cephalophus</i>	NC_008749	NC_008749
<i>Elaphurus davidianus</i>	AF423194	JN632632
<i>Hippocamelus antisensis</i> 1	JN632646	JN632646
	NC_020711	
<i>Hippocamelus antisensis</i> 2	DQ379307	
	GU190862	
<i>Hippocamelus bisulcus</i>	DQ789177	—
	DQ789178	
	GU190863	
<i>Hydropotes inermis</i>	AJ000028	JN632649
<i>Mazama americana</i> 1	DQ789209	JN632656
	DQ789217	
<i>Mazama americana</i> 2	JN632657	
<i>Mazama americana</i> 3	DQ789221	
	JN632656	
	NC_020719	
<i>Mazama americana</i> 4	DQ789201	
	DQ789204	
<i>Mazama americana</i> 5	DQ789219	

Table 4.1: Continued

Species	Cytochrome b	mtGenome
<i>Mazama bororo</i>	DQ789187 DQ789231 DQ789228	—
<i>Mazama bricenii</i>	LT546656 LT546657 LT546658	—
<i>Mazama chunyi</i>	LT546655	—
<i>Mazama gouazoubira</i> 1	JN632658 NC_020720	JN632658
<i>Mazama gouazoubira</i> 2	DQ379308	
<i>Mazama nana</i>	DQ789210 DQ789214 DQ789227	—
<i>Mazama nemorivaga</i> 1	JN632660	JN632660
<i>Mazama nemorivaga</i> 2	DQ789205 DQ789206 DQ789226 JN632659 NC_024812	
<i>Mazama pandora</i>	KC146954 KC146955	—
<i>Mazama rufina</i>	JN632661 NC_020721	JN632661
<i>Mazama temama</i>	KC146956 KC146957 KC146958 KC146959	—
† <i>Megaloceros giganteus</i>	AM182644 AM182645	—
<i>Muntiacus atherodes</i>	LT546659	—
<i>Muntiacus crinifrons</i>	NC_004577 AY239042 DQ445734 DQ445732 DQ445735 DQ445733	NC_004577
<i>Muntiacus feae</i>	AF042721	—

Table 4.1: Continued

Species	Cytochrome b	mtGenome
<i>Muntiacus muntjak</i> 1	NC_004563	NC_004563
	AY225986	
<i>Muntiacus muntjak</i> 2	AF042718	
<i>Muntiacus putaoensis</i>	EF523665	—
	EF523666	
	EF523667	
	EF523668	
	EF523669	
<i>Muntiacus reevesi</i>	AF527537	NC_008491
	NC_004069	
<i>Muntiacus rooseveltorum</i>	KJ425278	—
	KJ425279	
	KJ425281	
	KJ425282	
<i>Muntiacus truongsongensis</i> 1	KJ425277	—
<i>Muntiacus truongsongensis</i> 2	KJ425276	
<i>Muntiacus vuquangensis</i>	FJ705435	FJ705435
	AF042720	
	NC_016920	
<i>Odocoileus hemionus</i> 1	HM222707	JN632670
<i>Odocoileus hemionus</i> 2	FJ188783	
	FJ188870	
<i>Odocoileus virginianus</i> 1	DQ379370	JN632671
<i>Odocoileus virginianus</i> 2	M98491	
<i>Ozotoceros bezoarticus</i>	DQ789190	JN632681
	DQ789193	
	DQ789195	
	DQ789199	
<i>Pudu mephistophiles</i>	JN632691	—
	LT546651	
	LT546652	
	LT546653	
	LT546654	
<i>Pudu puda</i>	JN632692	JN632692
	AY607039	
	NC_020740	
<i>Rangifer tarandus</i>	AB245426	NC_007703
	AY726704	
	KM506758	

Table 4.1: Continued

Species	Cytochrome b	mtGenome
<i>Rucervus duvaucelii</i>	AY607041	JN632696
<i>Rucervus eldii</i>	AY157735	JN632697
<i>Rucervus schomburgki</i>	AY607036	—
<i>Rusa alfredi</i>	JN632698	JN632698
	NC_020744	
<i>Rusa marianna</i>	LT546647	—
	LT546648	
	LT546649	
	LT546650	
<i>Rusa timorensis</i>	AF423200	JN632699
<i>Rusa unicolor</i>	FJ556575	NC_008414
<i>Antilocapra americana</i>	JN632597	JN632597
<i>Boselaphus tragocamelus</i>	EF536350	EF536350
<i>Hyemoschus aquaticus</i>	JN632650	JN632650
<i>Moschus moschiferus</i>	FJ469675	JN632662
<i>Okapia johnstoni</i>	JN632674	JN632674
<i>Tragelaphus scriptus</i>	AF022067	JN632706

Table 4.2: Overview of sampled specimens. Specimens in bold are holotypes. The category 'sample DNA' provides the weight of the tissue sample in the tube prior to DNA extraction and DNA concentration after extraction.

Species	Collection ID	Accession no.	Sample [mg]	DNA [ng/μl]	Gaps in alignment	Collection entry	Locality	Material
<i>Rusa marianna</i>	BMNH 1996.2	LT546647	15.5	93.65	-	1996	Philippines	Soft tissue fragments*
<i>Rusa marianna</i>	ZMB-MAM-75158	LT546648	15.1	60.97	-	NA	Philippines, Luzon	Soft tissue fragments*
<i>Rusa marianna</i>	ZMB-MAM-20409	LT546649	12.0	49.64	-	1915	Captive animal	Soft tissue fragments*
<i>Rusa marianna</i>	ZMB-MAM-75146	LT546650	26.2	38.67	403-467	1905	US, Northern Mariana Islands	Soft tissue fragments*
<i>Pudu mephistophiles</i>	BMNH 1899.2.18.20	LT546651	30.5	97.35	64-118, 176-211	1899	Ecuador	Soft tissue fragments*
<i>Pudu mephistophiles</i>	BMNH 1896.1.28.6	LT546652	7.6	56.57	-	1896	Ecuador, Paramo of Papallacta	Snippet of skin, including hair; immature
<i>Pudu mephistophiles</i>	BMNH 1899.2.18.21	LT546653	9.9	27.34	604-674, 784-810	1899	Ecuador	Soft tissue fragments ; juvenile
<i>Pudu mephistophiles</i>	ZMB-MAM-61577	LT546654	165.8	325.57	-	1970	Captive animal	Wet specimen; neonatal
<i>Mazama chunyi</i>	BMNH 1967.1362	LT546655	15.6	56.22	-	1967	Pertu, Chiquis	Soft tissue & bone fragments from**
<i>Mazama bricenii</i>	BMNH 1913.4.24.3	LT546656	36.0	74.17	-	1913	Venezuela, Merida	Soft tissue fragments*
<i>Mazama bricenii</i>	BMNH 1908.6.24.5	LT546657	2.4	7.07	288-394, 604-674	1908	Venezuela	Soft tissue fragments*
<i>Mazama bricenii</i>	BMNH 1934.9.10.228	LT546658	10.2	77.08	-	1934	Ecuador, Pichincha	Soft tissue fragments*
<i>Mantiacus atherodes</i>	BMNH 1971.3088	LT546659	23.3	87.60	-	1971	Borneo, Brunei/Indonesia/Malaysia	Soft tissue fragments*

Notes.

BMNH, British Museum of Natural History London; ZMB, Zoological collections of the Museum für Naturkunde Berlin.

*From skull.

**From skull & mandible.

#From mandible.

Table 4.3: PCR recipes. Initial PCRs were undertaken using recipe (a), for optimisation recipes (b)–(d) were used depending on fragment and sample. Reagents that were varied are in bold. Components of column (a) in combination with an annealing temperature of 50 °C worked better for primer pair 4, (d) worked well for primer pair 8, and (c) worked better for some samples in combination with primer pair 2 (Lister et al., 2005). Except for one case, varying the annealing temperature had no influence on the reaction.

Reagents	Quantity [μ l]			
	a	b	c	d
PCR Flexi-Buffer (5X)	2.5	2.5	2.5	5
MgCl ₂ (25 mM)	1.5	1.5	2	3
dNTPs (10 mM)	0.5	0.5	0.5	1
Primer forward (5 μ M)	0.5	0.5	0.5	1
Primer reverse (5 μ M)	0.5	0.5	0.5	1
BSA	1.3	0	0	0
H ₂ O	4.6	5.9	5.4	12.9
GoTaq polymerase	0.1	0.1	0.1	0.1
DNA	1	1	1	1
Total Reaction Volume	12.5	12.5	12.5	25

4.2.4 Alignment

The concatenated consensus sequences of each specimen were added to the existing *Cytb* data set (NCBI GenBank) and pairwise aligned by eye using Mesquite v.2.75 (Maddison & Maddison, 2011) and Seaview 4.2 (Gouy et al., 2010). The alignment was carefully checked for stop codons within the alignment and/or unusual nucleotide positions by translation into amino acids to ensure the absence of pseudogenes and sequencing errors. The IUPAC ambiguity code was used in few cases where character states could not be assessed unambiguously after a re-investigation of the raw sequence data. These ambiguities most likely represent misreads from the chromatogram due to the somewhat poor condition of the DNA. Because these ambiguous sites are not numerous, their impact on the phylogenetic signal is negligible.

In total, three different alignments were created. First, we aligned the new 747 base pair long sequences with the complete *Cytb* sequences from GenBank to form a data set of 1140 base pairs. The final data set contained 130 taxa (124 cervids, six other ruminants). Second, to test whether the newly sequenced, shorter fragments carried a sufficient phylogenetic signal, two further alignments were created. One alignment was exactly 747 base pairs long, which was the same length as the new sequences, including internal gaps. The other alignment excluded even the internal gaps and was 569 base pairs long. We also re-analysed the cervid subset (33 species) of the complete mitochondrial genome alignment available for Artiodactyla in Hassanin et al. (2012) without the new sequences. The taxon sampling contained 39 cervid taxa and seven non-cervid ruminants.

4.2.5 Phylogenetic Analyses

To test for the impact of alignment length on phylogenetic signal, we developed three alignments with varying base pair lengths. For each alignment, we used PartitionFinder (Lanfear et al., 2012) to identify the optimal partitioning scheme and mutation model (Tab. 4.4).

A summary of all analyses undertaken including the models and partitioning scheme, is shown in Table 4.4. PartitionFinder analysis on the 1140 *Cytb* data set resulted in a scheme with three different partitions for the individual codon positions using SYM for position 1, HKY for position 2, and GTR for position 3 for Bayesian inference analyses with MrBayes v.3.2.4 (Ronquist et al., 2012) (in the following referred to as BI-1140-part). For the maximum likelihood analyses with RAxML (Stamatakis, 2006), PartitionFinder suggested GTR for all codon positions (ML-1140). Alternatively, we undertook a Bayesian inference analysis without partitioning using the GTR model on the 1140-base-pair-long alignment (BI-1140-unpart). We also undertook a Bayesian analysis with the *Cytb* alignment reduced to 747 base pairs (BI-747-part) using the partitioning scheme suggested by PartitionFinder and the models described above as well as one unpartitioned analysis (BI-747-unpart) using GTR. Further, we undertook another Bayesian analysis on the 569 base pair alignment (BI-569-unpart), excluding the internal gaps, representing the shortest sequence length of the newly sequenced taxa (Maz_bri_Q_BMNH_1908.6.24.5). This analysis was run using the GTR model and no partitioning because of the short alignment length. The Bayesian re-analysis of the complete mitochondrial genome sequences (BI-mtG; without the newly sequenced *Cytb* sequences) was undertaken using GTR and divided the data set into seven partitions (Hassanin et al., 2012). The re-analysis was carried out because previous re-analyses of subsets of the complete mitochondrial genome resulted in different results than those found by Hassanin et al. (2012).

Substitution models for all analyses were implemented with a gamma distribution (Γ) without a proportion of invariant sites (I), although PartitionFinder suggested using $\Gamma + I$ for most partitions. It is known that the combination $\Gamma + I$ may create two areas of equal probability in the tree landscape, which can lead to convergence problems (Moyle et al., 2012). All Bayesian Inference analyses were run with MrBayes v.3.2.4 (Ronquist et al., 2012) using Metropolis-Coupled Markov Chain Monte Carlo (MC3); two separate runs sampled the tree landscape at a temperature of 0.35 sampling every 1,000th tree. The mitochondrial genome analysis was run with MrBayes v.3.2.4 (Ronquist et al., 2012) using MC3 with two separate runs sampling every 5,000th tree at a temperature of 0.35. All analyses automatically stopped when the standard deviation of split frequencies of posterior probabilities reached 0.01. From all post burn-in sampled trees, a consensus tree was generated (burn-in = 25%). For the Maximum Likelihood analysis we used RAxML v.7.3.0 (Stamatakis, 2006) including a rapid bootstrap search with 100 replicates on the 1140 base pair long data set.

Hyemoschus aquaticus (Tragulidae, Artiodactyla), which is an extant representative of crown ruminants, was used as the outgroup. The original tree topologies from all seven analyses are provided in Figures H.1–H.7, and an overview is given in Figure 4.3 and Table 4.4.

Table 4.4: Summary of analyses, model choice, partitioning, and support for major clades in the resulting topologies.

Analysis	Reference	Model(s)	Parti- tioned	Cervidae	Cervinae	Cervini	Munt- iacini	Capreo- linae	Capreolini	Odocoi- leini	Blasto- cerina	Odocoi- leina
BI-mtG	Fig. 4.3 A, H.1	GTR	Y	1	1	1	1	1	1	1	1	1
BI-1140-unpart	Fig. 4.3 B, Fig. 4.4, H.2	GTR	N	1	1	1	1	1	.84	.98	.98	.99
BI-1140-part	Fig. 4.3 C, H.3	SYM HKY	Y	1	.99	1	1	1	—	.75	.87	.87
ML-1140	Fig. 4.3 D, H.4	GTR	N	99	89	99	92	—	100	57	55	41
BI-747-unpart	Fig. 4.3 E, H.5	GTR	N	1	1	1	.81	—	1	—	.85	—
BI-747-part	Fig. 4.3 F, H.6	SYM HKY	Y	1	.99	1	.90	—	1	—	—	—
BI-569-unpart	Fig. 4.3 G, H.7	GTR	N	1	—	.99	.92	—	1	—	—	—

Notes.Abbreviations: BI, Bayesian Inference; ML, Maximum Likelihood, the number represents the *Cytb* sequence length in the current alignment; Y, yes; N, no; part, partitioned; unpart, unpartitioned. The values within cells represent the node support for the respective split either as Bayesian posterior probabilities or as bootstrap support from maximum likelihood analyses; “—” indicates that the clade was not recovered in the respective analysis.

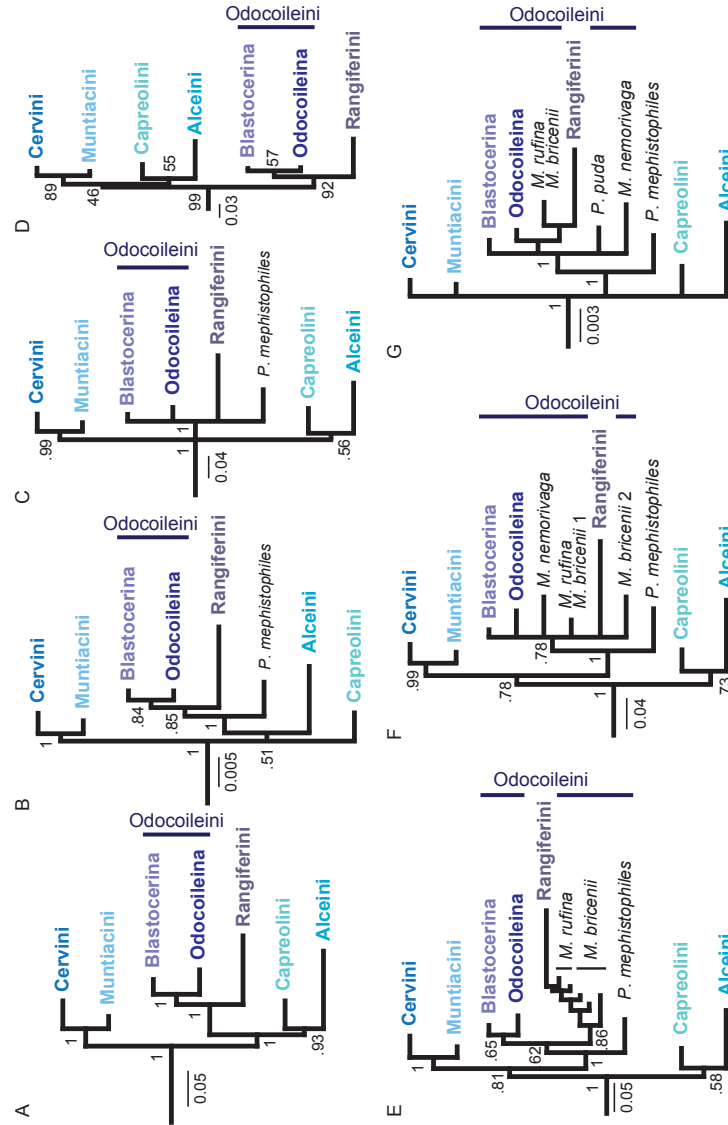


Figure 4.3: Overview of higher level topologies resulting from re-analysis of the complete mitochondrial genome sequences (Hassanin et al., 2012) and six different analyses of our data set. (A) BI-mtG, (B) BI-1140-unpart, (C) BI-1140-part (D) ML-1140, (E) BI-747-unpart, (F) BI-747-part, (G) BI-569-unpart. Support values represent bootstrap values in D, all other support values are posterior probabilities. (A–D) show monophyly for all major cervid lineages, whereas in (E–G) resolution, particularly within Odocoileini is lost. Positioning *P. mephistophiles* proves to be difficult. Scale bars represent substitutions per site.

4.3 Results

4.3.1 Extraction, PCR, Sequencing

The results from the DNA extraction, PCR, and sequencing processes are summarised in Table 4.2. For some of the eight *Cytb* fragments, DNA amplification was not sufficient, which resulted in gaps in the sequence for a few specimens (Tab. 4.2). Upon checking the traces in CodonCodeAligner, we observed in our alignment that Y (C or T; $n = 50$) and R (G or A; $n = 19$) are the most common ambiguities. These nucleotide substitutions are most likely caused by hydrolytic deamination. This is a process by which the deamination of cytosine residues to form uracil residues, 5-methyl-cytosine residues to form thymine residues, or adenine residues to form hypoxanthine residues in the template DNA strand will be misread during the PCR process when a new DNA strand is synthesised. In turn, this leads to evident C \rightarrow T or G \rightarrow A substitutions (Hofreiter et al., 2001a; Pääbo et al., 2004; Briggs et al., 2007, 2010). Across our samples, Y ambiguities occurred up to ten times per specimen, and R ambiguities occurred up to three times per specimen. These numbers represent a very small proportion of approximately 1 % of the overall sequence length of 747 base pairs. We tested the impact of the ambiguities on the reconstruction and found that the ambiguities did not tremendously influence the phylogenetic signal of the samples. However, these ambiguities represent an additional uncertainty in the analyses.

4.3.2 Phylogenetic Analyses

The results from seven analyses are summarised in Table 4.4 and Figure 4.3. Of the full 1140-base-pair-long *Cytb* data set 593 characters are constant, 68 variable characters are parsimony-uninformative, and 479 characters are parsimony-informative. The analyses of the 1140-base-pair-long *Cytb* represent our primary results and are shown in Figure 4.4. In addition to the Bayesian Inference analyses and the Maximum Likelihood analysis of the total *Cytb* data set (including the new sequences), we tested the impact of reduced data sets (569 characters and 747 characters, Bayesian Inference) and different partitioning schemes on the phylogenetic signal (BI-1140-unpart, BI-1140-part, ML-1140, BI-569-unpart, BI-747-unpart, BI-747-part; Tab. 4.4, Figs 4.3, H.2–H.7).

We next re-analysed the complete mitochondrial genome alignment from Hassanin et al. (2012) for the subset of cervids (14904 base pairs, Bayesian Inference; BI-mtG, Fig. H.1), because the authors stated that some of the nodes are not robust, as proven by previous re-analyses (Bibi, 2014). The re-analysis presented here (BI-mtG, Fig. H.1) resulted in the support of a fully resolved topology, which is congruent with the topology in Hassanin et al. (2012).

Data partitioning of the 1140-base-pair-long *Cytb* data set and reduced data sets did not lead to contradictory results compared to unpartitioned analyses or larger data sets. Resolution and node supports generally decreased with decreasing alignment length (Fig. 4.3). Cervid lineages above the genus level were almost always recovered with all matrix sizes and partitioning schemes (Tab. 4.4). None of the topologies supportably contradicted each other; however, all topologies differed from each other to some extent at the tribe, genus, and/or species level. Compared to the *Cytb*-only topologies, the mitochondrial genome topology showed generally higher posterior probabilities (Figs 4.3 and 4.4).

The monophyly of superordinate clades, Cervidae, Cervini, Muntiacini, and Capreolini (including *Hydropotes*), was supported in all topologies (Figs 4.3, 4.4, H.1–H.7, Tab. 4.4). In all but one topology (BI-569-unpart; Fig. 4.3 G, Fig. H.7), the monophyly of Cervinae, was consistently supported (Fig. 4.3, Tab. 4.4). Odocoileini was weakly supported in three topologies (ML-1140, BI-1140-unpart, BI-mtG; Figs 4.3 A, B, D and 4, Figs H.1, H.2, H.4 and Table 4.4). Capreolinae, however, was supported as a monophyly in only one topology (BI-mtG, Fig. 4.3 A, Fig. H.1), and in the other topologies, the taxon splits unresolved into Odocoileini, Rangiferini (*Rangifer*), Alceini (*Alces*), and Capreolini (*Capreolus*, *Hydropotes*) (Fig. 4.3). Alceini and Capreolini sometimes formed a clade (Fig. 4.3 A, C, D, E, F) or were unresolved (Figs 4.3 B and 4.3 G). Systematic relationships of capreoline taxa showed marginal differences in each of our topologies.

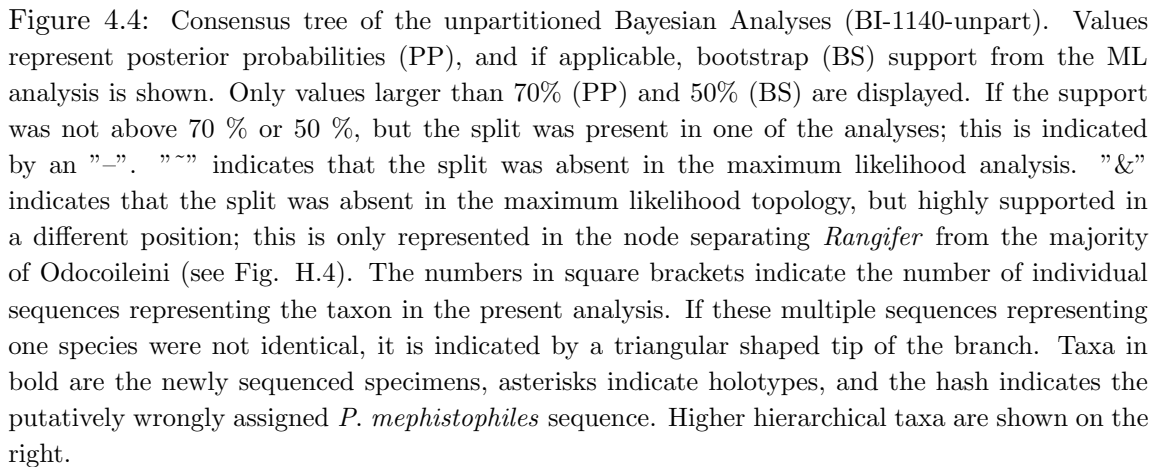
The results at the genus and species levels are shown in Figure 4.4 and Figures H.1–H.7. The newly sequenced *Muntiacus atherodes* nested within Muntiacini, mostly polytomous, with two *Muntiacus*-clades. One clade consisted of *M. muntjak*, *M. feae*, and *M. crinifrons*, and the other consisted of *M. truongsongensis*, *M. putaoensis*, *M. rooseveltorum*, *M. reevesi*, and *M. vuquangensis*. Two topologies (BI-1140-unpart, ML-1140) indicated a poorly supported sister taxon relationship between *M. muntjak* and *M. atherodes* (Fig. 4.4, Figs H.2 and H.4).

We found strong support in Cervini to place all four *Rusa marianna* specimens in a Philippine *Rusa*-clade, with *Rusa alfredi* in all but one topology (BI-569-unpart; Fig. 4.4, Figs H.1–H.7).

The newly sequenced *Mazama chunyi* is consistently placed as a sister taxon to *Mazama gouazoubira*, whereas the three *M. bricenii* specimens are primarily a sister taxon to *M. rufina*.

The four *P. mephistophiles* specimens always form a clade, which is either a sister taxon to or nested within Odocoileini. Interestingly, they are not placed in a sister position to the mitochondrial genome sequence labelled *P. mephistophiles* from Hassanin et al. (2012). In none of our topologies did *P. mephistophiles* and *P. puda* form a sister taxon relationship, which makes the monophyly of the genus questionable. *M. nemorivaga*, *M. rufina*, *M. bricenii*, *P. puda*, and particularly *P. mephistophiles* occasionally take up positions outside the above proposed clades, thus underpinning their yet unsolved systematics.

Regardless of the controversies debated here and elsewhere regarding Odocoileini molecular systematics, topologies (in the literature and here, Figs 4.3 and 4.4, Figs H.2–H.7) show two consistently occurring subclades carrying phylogenetic signal within Odocoileini (e.g., Gilbert et al., 2006; Duarte et al., 2008; Hassanin et al., 2012). One subclade consists of *Hippocamelus*, *Blastocerus*, *Ozotoceros*, *M. gouazoubira*, *M. chunyi*, *M. nemorivaga*, and *Pudu puda*. The other subclade consists of *Odocoileus*, *M. americana*, *M. bororo*, *M. nana*, *M. temama*, *M. pandora*, *M. rufina*, and *M. bricenii*. Based on these results we establish two new subtribes Blastocerina and Odocoileina according to the rules of the ICZN (<http://www.iczn.org/code>). These two subtribes form the tribe Odocoileini and have Rangiferini as sister taxon.



Blastocerina subtribus nova

Type genus: *Blastocerus* Wagner, 1844

Higher taxa: Odocoileini—Capreolinae—Cervidae

The subtribe Blastocerina consists of the following species: *Blastocerus dichotomus*, *Hippocamelus antisensis*, *Hippocamelus bisulcus*, *Mazama chunyi*, *Mazama gouazoubira*, *Mazama nemorivaga*, *Ozotoceros bezoarticus*, and *Pudu puda* (Fig. 4.4). Blastocerina refers to the clade originating from the most recent common ancestor of *Blastocerus dichotomus* (Illiger, 1815) and *Pudu puda* Molina, 1782. *Pudu mephistophiles* potentially falls within that clade, but more data are needed for a definite placement of this taxon.

Odocoileina subtribus nova

Type genus: *Odocoileus* Rafinesque, 1832

Higher taxa: Odocoileini—Capreolinae—Cervidae

The subtribe Odocoileina consists of *Mazama americana*, *Mazama bororo*, *Mazama bricenii*, *Mazama nana*, *Mazama pandora*, *Mazama rufina*, *Mazama temama*, *Odocoileus hemionus*, and *Odocoileus virginianus* (Fig. 4.4). Odocoileina refers to the clade originating from the most recent common ancestor of *Odocoileus virginianus* (Von Zimmermann, 1778–1783) and *Mazama bricenii* Thomas, 1908.

4.4 Discussion

4.4.1 Phylogenetic Analyses

Our results represent the most complete compilation of molecular data in terms of taxon sample for cervids to date. The thorough sampling enabled us to place the de novo sequenced species in topologies representing overall cervid systematics. We were able to solve some relationships but also discovered previously unknown issues. The data set excludes *Muntiacus gongshanensis*, for which only a very short tRNA sequence is available, and *Axis calamianensis*, *M. montanus*, *M. puhoatensis*, and *M. vaginalis*, for which no molecular data are available.

Our experiments with different matrix sizes, partitioning schemes, and models revealed that the resulting topologies do not dramatically differ from each other. However, we could observe that the resolution decreased with decreasing sequence length. All seven analyses recovered major clades within Cervidae (Tab. 4.4 and Fig. 4.3). These experiments were undertaken to single out strong phylogenetic signal and the significance thereof, which is consistent regardless of the data set sizes and parameter changes. We observed that taxa, which are generally unstable across topologies from different studies (e.g., Pitra et al., 2004; Gilbert et al., 2006; Agnarsson & May-Collado, 2008; Hassanin et al., 2012), were the first to lose a supported systematic position with decreasing sequence length (Fig. 4.3 and Tab. 4.4). The partitioning scheme and model choice did not make as much difference as did the matrix size. As expected, partitioning did not necessarily lead to better

resolved topologies or significantly better supported clades. However, some differences were observed comparing maximum likelihood with Bayesian inference methods (Figs 4.3 and 4.4).

The topology resulting from re-analysis of the mitochondrial genome sequences (BI-mtG) representing the largest sequence length is fully resolved and has the highest overall support values. The shortest data set (BI-569-unpart), although less well resolved, recovered all higher-level lineages and is in most points congruent with the other topologies based on larger data sets (Tab. 4.4 and Fig. 4.3). These different analyses enabled us to examine the significance of the individual resulting topologies.

4.4.2 *Muntiacus atherodes*

The species diversity of Muntiacini is the least covered among cervid subclades in molecular phylogenetic analyses. Muntiacini comprises muntjacs (*Muntiacus*) and the tufted deer (*Elaphodus*), includes the smallest members of Cervinae (40 to 70 cm shoulder height), and inhabits Southeast Asia and Eastern China (Mattioli, 2011). The systematic relationships within Muntiacini in our topologies (Fig. 4) are largely congruent with most recent studies and are the least controversial in molecular cervid systematics (e.g., Pitra et al., 2004; Gilbert et al., 2006; Agnarsson & May-Collado, 2008; Hassanin et al., 2012). Here, *M. crinifrons* and *M. feae* are always sister taxa, and when the resolution is sufficiently high, *M. muntjak* is a sister taxon to both of them. In our topologies, *M. putaoensis*, *M. rooseveltorum*, *M. truongsongensis*, and *M. vuquangensis* always form a clade. Most often, with *M. reevesi* is a sister taxon to that clade, but occasionally, *M. reevesi* is sister taxon to all other muntjacs (BI-747-part, BI-569-unpart). Due to the consistent position of *M. muntjak* 2 (AF042718) as sister taxon to *M. truongsongensis*, we suggest re-confirming this sequence.

The monotypic *Elaphodus cephalophus*, which is distributed in southeast China, is always a sister taxon to all muntjacs in both our topologies and previously published trees (Pitra et al., 2004; Gilbert et al., 2006; Agnarsson & May-Collado, 2008; Hassanin et al., 2012).

Because of the presumed primitive antler morphology of *M. atherodes* (Groves & Grubb, 1982), its systematic position was hypothesised to be between *Elaphodus cephalophus* and the *Muntiacus*-clade, which is not supported by our results. The newly sequenced holotype specimen of *M. atherodes* is nested within muntjacs, unresolved in a polytomy in most of our topologies. However, some results indicate a potential closer relationship to *M. muntjak* than to any other muntjac. The predominant separate placement from all other *Muntiacus* spp. is an interesting outcome that strengthens the species status of *M. atherodes*.

Several authors assumed the sympatric existence of a second muntjac species on Borneo that was separate from *M. muntjak* (Kohlbrugge, 1895; Lyon, 1911; Van Bemmelen, 1952; Hill, 1960) before Groves & Grubb (1982) eventually established *M. atherodes* based on a skin and the holotype skull sampled for the present study. The endemic *M. atherodes* differs from *M. muntjak* in colouration and has smaller, simpler antlers, and the latter has a much wider distribution across Southeast Asia and Southern China (Groves & Grubb, 1982).

Though unsupported, the potential close systematic relationship of *M. atherodes* and

M. muntjak would be logical based on the endemic occurrence of *M. atherodes* on Borneo. *M. atherodes* and *M. muntjak* could have diverged from a common ancestor on Borneo via sympatric speciation and with a later invasion of *M. muntjak* to the mainland.

Alternatively, *M. muntjak* could have invaded Borneo during the sea level fluctuations in the Plio-Pleistocene (Voris, 2000; Meijaard, 2003; Woodruff, 2003; Meijaard & Groves, 2004; Bibi & Métais, 2016), resulting in the allopatric speciation of *M. atherodes* and its isolation from the mainland populations during the end-Pleistocene sea level rise.

The high sea levels in the early Pliocene split the Thai-Malayan Peninsula into two landmasses, which separated Indochinese from Sundaic faunas (Woodruff, 2003). This most likely had a large influence on the evolution of Southeast Asian cervids and probably occurred again later during the Pliocene (Meijaard & Groves, 2004). Sea level changes in the Malay Archipelago were important for faunal dispersals. Low sea levels allowed species to spread to landmasses, which would become islands with rising sea levels, resulting in isolation of populations.

Detailed descriptions and maps for sea level changes of Southeast Asia can be viewed in Voris (2000) and Meijaard (2003).

4.4.3 *Rusa marianna*

In the literature, there is a broad consensus about the systematic relationships within Cervini. However, the taxonomy of *Cervus* s. l. is indeed complicated (Randi et al., 2001). The controversy primarily concerns delimitations of genera and/or subgenera. *Rusa*, *Rucervus*, *Przewalskium* (= *Cervus*) *albirostris*, and *Cervus* are occasionally treated as subgenera of the genus *Cervus*, whereas *Axis*, *Elaphurus*, and *Dama* are normally treated as separate genera (Groves & Grubb, 1987; Randi et al., 2001). Here, we refer to *Rucervus* and *Rusa* as individual genera and refer to *Przewalskium albirostris* as *Cervus albirostris*.

The four species of *Rusa*, *R. alfredi*, *R. marianna*, *R. timorensis*, *R. unicolor*, inhabit India, Indochina and the Malay-Archipelago (Grubb & Groves, 1983; Mattioli, 2011). *R. unicolor* is the largest oriental deer and has a highly fragmentary distribution from southern Nepal, India and Sri Lanka along the southern Himalayas through to mainland Southeast Asia and many of the Greater Sunda islands (Timmins et al., 2008; Leslie, 2011). *R. timorensis* is endemic to the Indonesian islands Bali and Java (Hedges et al., 2008). *Rusa alfredi* is one of the rarest deer species according to the IUCN Red List (IUCN, 2016) and is endemic to Panay and Negros (Western Visayan Islands, Central Philippines) (Oliver et al., 2008). In contrast, *Rusa marianna* is more widely distributed across most of the Philippine Islands, with the exceptions of the Negros-Panay, Sulu and Palawan Faunal Region, the Babuyan/Batanes groups, and other isolated islets (MacKinnon et al., 2008).

The four newly sequenced individuals of *Rusa marianna* are positioned to be closely related to each other in a distinct clade. Two of the individuals are in a polytomy with the other Philippine species, *Rusa alfredi*, and two form a clade, which is a sister taxon to the polytomy (Fig. 4.4). Our topology supports the hypothesis that the two Philippine *Rusa* species are closely related and are sister taxon to *R. timorensis* and *R. unicolor*.

Investigations by Grubb & Groves (1983) showed that interpreted relationships within *Rusa* are controversial. *Rusa timorensis* and *R. unicolor* are sister taxa supported in all our topologies (Fig. 4.4, Figs H.1–H.7), and this clade is in a polytomy with the

Cervus-clade (including *C. albirostris*) and the *R. alfredi*-*R. marianna*-clade. A close relationship between *Rusa* and *C. albirostris* was already suggested by Flerov (1952) based on morphological evidence and a supposed divergence of *C. albirostris* from *Rusa* in the Late Pliocene.

The evident phenotypic separation of spotted (*R. alfredi*) and non-spotted (*R. marianna*) *Rusa* deer on the Philippines suggests two invasion events (Grubb & Groves, 1983), but the missing molecular data for *R. marianna* have prohibited further explanations. Grubb & Groves (1983) suggested a Southeast Asian mainland common ancestor from which a peripheral population diverged by evolving into *R. timorensis*. Later, a population of those colonised the Philippines twice at early and later stages in diversification, evolving into *R. alfredi* and *R. marianna*. *R. unicolor* evolved there but failed a third colonisation on additional Philippine Islands and dispersed northwards to the mainland. Meijaard & Groves (2004) pointed to the likely high impact of Plio-Pleistocene sea level fluctuations on Southeast Asian cervid dispersal and speciation.

However, the suggested speciation of *R. marianna* and *R. alfredi* is not clearly evident from our topologies, where *R. alfredi* appears to be a subgroup of *R. marianna* rather than a sister taxon. More data are needed to unambiguously solve their relationships.

4.4.4 Odocoileini

Odocoileini represents the most controversial subclade of extant cervids. They consistently split into two subclades in both our current results and previously published phylogenetic trees. For these two subclades we established the new subtribes Blastocerina and Odocoileina (see above). However, within each of these subclades, systematic relationships are not yet solved. The recent divergence of modern neotropical Odocoileini from extinct Eurasian Capreolinae and related insufficient genomic diversity available to solve systematic relationships could be the reason (Vislobokova, 1980). All genera except for *Odocoileus* are endemic to South America, and their ancestors reached the continent via the Panamanian Isthmus in the Pliocene (5–2.5 million years ago) (Webb, 2000; Gilbert et al., 2006). The first fossil appearances are known from no longer than approximately 2.4 million years ago (Webb, 2000). The consistent split of Blastocerina and Odocoileina potentially represents an asynchronous dispersal history via two invasion events.

Furthermore, our study revealed dubious relationships between available *Hippocamelus* sequences. All of our topologies (Fig. 4.4, Figs H.2–H.7) show that two *H. antisensis* sequences (*H. antisensis* 1; JN632646, NC_020711 (Hassanin et al., 2012)) are a sister taxon to *H. bisulcus*. However, the other two sequences (*H. antisensis* 2; DQ379307 (Gilbert et al., 2006) and GU190862 (Fuentes-Hurtado et al., 2011)), are a sister taxon to *Ozotoceros* in all of our topologies (Figs 4.4, H.2–H.7). This is a critical issue, although its resolution is beyond the scope of this study; however, we found it important to point to this drawback in the base data and suggest re-confirmation of all four sequences.

Systematics of the two dwarfed genera, *Mazama* and *Pudu*, whose small body size and simplified antlers are interpreted as secondary adaptations to dense vegetation (Geist, 1998; Mattioli, 2011), are particularly uncertain. Their habitat use and their decline in individual numbers makes it increasingly difficult to obtain enough data to resolve systematic issues from some of the species (see below).

4.4.5 *Pudu*

Pudus are the smallest living deer (25 to 40 cm shoulder height) and the smallest New World hoofed mammals (Hershkovitz, 1982; Mattioli, 2011). It is difficult to distinguish both pudu species from sympatric small deer species (*Mazama*) based only on the phenotype, without direct comparison (Hershkovitz, 1982; Jiménez, 2010). *Pudu* and *Mazama* likely represent divergent lineages of small odocoileine deer (Hershkovitz, 1982). Although the origin of pudus is unknown, Hershkovitz (1982) stated that *P. mephistophiles* has more primitive phenotypical features than *P. puda*.

Pudu was assumed to be polyphyletic (Hassanin et al., 2012). Whereas *P. puda* has been well-sampled and studied, information for *P. mephistophiles* is scarce. In all of our topologies (Fig. 4.4, Figs H.1–H.7), the four newly sequenced specimens of *Pudu mephistophiles*, including the holotype, form a well-supported clade. However, the position of that clade is variable. In four topologies (BI-1140-unpart, BI-747-part, BI-747-unpart, BI-569-unpart; Fig. 4.4, Figs H.2, H.5, H.6 and H.7), the clade is a sister taxon to all other Odocoileini and Rangiferini; in one topology (ML-1140; Fig. H.4), it is a sister taxon to all Blastocerina with poor support; and in one topology (BI-1140-part; Fig. 4.3 C, Fig. H.3), it is placed in an unresolved position with other Odocoileini clades and Rangiferini. The placement of the individual *Pudu mephistophiles* specimen published prior to our study in Hassanin et al. (2012) (JN632691) is not close to the *P. mephistophiles*-clade in our topologies. Instead, it is placed as a sister taxon to *Mazama rufina* (Fig. 4.4, Figs H.1–H.7) and confirms Hassanin et al.'s (2012) suspicion that it might in fact be a misidentified *Mazama rufina* and is neglected for further interpretation. The holotype specimen included in the four new *P. mephistophiles* samples substantiates that suspicion. In all but one topology (BI-569-unpart), *P. puda* is a sister taxon to all other Blastocerina, which is congruent with Hassanin et al. (2012) and Agnarsson & May-Collado (2008). In Duarte et al. (2008), however, its position was unresolved. The placement of *P. mephistophiles* separate from its congeneric *P. puda* in most topologies suggests polyphyly of the genus.

4.4.6 *Mazama*

The genus *Mazama* comprises several species of small- to medium-sized deer (40 to 80 cm shoulder height) (Hershkovitz, 1959, 1982; Mattioli, 2011). The current distribution of *Mazama* ranges from Southern Mexico to Argentina (IUCN, 2016; Mattioli, 2011; González et al., 2009).

Since the first description of *Mazama pita* Rafinesque, 1817 (= *Moschus americanus* Erxleben, 1777), the genus has been subject to taxonomic controversies. Allen (1915) recognised 18 species of *Mazama*; Cabrera (1960) reduced these to four species, i.e., *M. chunyi*, *M. gouazoubira*, *M. nana*, and *M. rufina*. Czernay (1987) established two more species, *M. americana* and *M. bricenii*, whereas Groves & Grubb (1987) considered *M. temama* a possible separate species based on cytogenetic differences. Medellín et al. (1998) revised *M. pandora* as a separate species based on differences in the skulls and skins. Rossi (2000) established *M. nemorivaga* as a fourth sympatric species in Brazil (together with *M. americana*, *M. nana*, *M. gouazoubira*). Duarte (1992) described *M. bororo* based on karyotype differences, which adds up to ten *Mazama* species being widely accepted today (IUCN, 2016; Mattioli, 2011; González et al., 2009). More recently, Abril & Duarte (2008)

recognised only eight species (*M. americana*, *M. bororo*, *M. chunyi*, *M. gouazoubira*, *M. nana*, *M. nemorivaga*, *M. pandora*, and *M. rufina*), whereas Groves & Grubb (2011) listed 24 different species of *Mazama*. Most of the species share phenotypic similarities, which makes their discrimination almost impossible; however, there are differences in overall body size, coat colour, and/or karyotype (González et al., 2009).

Recently, polyphyly of *Mazama* was observed (Duarte et al., 2008; Hassanin et al., 2012). Within Odocoileina, Duarte et al. (2008) found a separation of the genus into a mixed *Mazama americana*-clade that included *M. bororo* and *M. nana*. *M. americana* appeared polyphyletic because there was an additional clade consisting exclusively of *M. americana* as a sister taxon to *Odocoileus* and the mixed *M. americana*-clade (Duarte et al., 2008). Hassanin et al. (2012) found *M. americana* to be monophyletic and a sister taxon to *Odocoileus*. *M. rufina* is a sister taxon to the *Mazama-Odocoileus*-clade (Hassanin et al., 2012).

Within Blastocerina there were two clades: a *Mazama gouazoubira*-clade and a *M. nemorivaga*-clade. Their position varies from study to study (Agnarsson & May-Collado, 2008; Duarte et al., 2008; Hassanin et al., 2012).

In our topologies, within Odocoileina, the mixed *Mazama americana*-clade that includes the sequences indicated as *M. americana* 1–3 is supported (Fig. 4.4) and has the most stable position, forming the sister taxon to the *Odocoileus*-clade. The pure *M. americana*-clade found by Duarte et al. (2008) is represented in our topology by the sequences indicated as *M. americana* 4 and *M. americana* 5.

M. rufina is nested within Odocoileina and is a sister taxon to the *Mazama-Odocoileus*-clade (BI-1140-unpart, BI-1140-part, ML-1140; Figs 4.3 and 4.4, Figs H.2, H.3 and H.4) or is placed in resolved or unresolved positions outside Odocoileina but within Odocoileini (BI-747-unpart, BI-747-part, BI-569-unpart; Fig. 4.3, Figs H.5, H.6 and H.7).

M. gouazoubira is either a sister taxon to both *Hippocamelus* species (BI-747-unpart, BI-569-unpart; Fig. 4.4, Figs H.5 and H.7), or *Blastocerus* is placed between *Hippocamelus* and *M. gouazoubira*. *M. gouazoubira* itself is polyphyletic in our topologies (Fig. 4.4), and a re-confirmation of the *M. gouazoubira* 2 sequence (DQ379308 (Gilbert et al., 2006)) is suggested.

Finally, the *M. nemorivaga*-clade is mostly nested within Blastocerina or is placed unresolved within Odocoileini (BI-747-part, BI-569-unpart).

In our study, *M. temama* and *M. pandora* were included in a species-rich phylogenetic analysis of cervids with palaeartic and neotropical species for the first time. Similarly to recent results of Escobedo-Morales et al. (2016), our results show that *M. temama* is always within Odocoileina as a sister taxon to the mixed *M. americana*-clade. In Escobedo-Morales et al. (2016) and in our topologies, *M. pandora* is consistently placed within Odocoileina as a sister taxon to *Odocoileus*.

This also indicates a critical issue concerning the dispersal history of South American cervids. The placement of the *M. americana*-splits in Figure 4.4 can be alternatively interpreted as a paraphyletic *M. americana*-clade, within which all other species are nested, i.e., *Odocoileus* sp., *M. pandora*, *M. temama*, *M. nana*, and *M. bororo*. However, the placement of *M. temama* disrupts the continuous genealogy of *M. americana*. Together with the clade consisting of *M. rufina* and *M. bricenii* (see below), Odocoileina is basically a *Mazama*-clade, within which *Odocoileus* diverged and *Mazama* diversified into several

species. This scenario would strongly question the long-held assumption that *Odocoileus* was the first cervid to immigrate to South America and diversify into the extant South American species (Anderson & Wallmo, 1984; Smith, 1991; Geist, 1998) (see also Escobedo-Morales et al., 2016).

Our results from sequencing *M. chunyi* show a sister taxon relationship with *M. gouazoubira* within Blastocerina in all our topologies (Fig. 4.4). The newly sequenced *Mazama bricenii* specimens are always placed in a sister taxon position to *M. rufina* in our topologies but exist as a monophyletic group in only one topology (BI-569-unpart; Fig. 4.3, Fig. H.7).

In two topologies, the specimen BMNH 1908.6.24.5 is placed isolated from the other two specimens (BMNH 1913.4.24.3, BMNH 1934.9.10.228), which remain sister taxa to *M. rufina*. Specifically, in one topology, BMNH 1908.6.24.5 is in an unresolved position within Odocoileina (BI-747-part; Fig. 4.3, Fig. H.6) and is positioned as a sister taxon to *M. chunyi* in the other topology (BI-1140-part; Fig. 4.3, Fig. H.3).

Mattioli (2011) listed *M. bricenii* and *M. chunyi* as subspecies of *M. rufina*. The *Mazama bricenii* specimen BMNH 1934.9.10.228 was originally assigned to *M. rufina*. Additionally, its sampling locality in Ecuador is outside the assumed current distribution of *M. bricenii* (Fig. 4.2 and Tab. 4.2) and thus makes the revised affiliation to *M. bricenii* questionable. *M. bricenii* is scarcely distributed in Northeast Colombia and West Venezuela, whereas *M. rufina* is distributed along the Andes from central Colombia to Ecuador and North Peru (Weber & González, 2003; Lizcano et al., 2010). This distribution is intermediate between the distribution of *M. bricenii* and *M. chunyi*. The latter is certainly known from South Peru and North Bolivia based on isolated museum specimen localities and rare sightings in the wild. Equally scarce is information on the biology and ecology of these species (Rumiz & Pardo, 2010). The results of the most recent study on systematic relationships of *M. bricenii* based on *Cytb* confirm our results and suggest that *M. bricenii* is a junior synonym of *M. rufina* (Gutiérrez et al., 2015).

Despite the extensive taxonomic and phylogenetic interest in the genus *Mazama* due to unsolved questions, the taxon remains enigmatic (e.g., Duarte & Merino, 1997; Medellín et al., 1998; Duarte & Jorge, 2003; Weber & González, 2003; Duarte et al., 2008; González et al., 2009). In particular, the high intraspecific variability in *M. americana* and *M. gouazoubira* stimulated additional taxonomic and genetic research on the genus (see Weber & González). The systematics of *M. americana* is particularly problematic because even the species appears polyphyletic with possible cryptic species (Duarte et al., 2008; Abril et al., 2010). Abril et al. (2010) showed that *M. americana* exhibits an extensive karyotype variation and found two distinct clades within *M. americana* sampled across Brazil. They also found that one clade is more closely related to *M. bororo* and *M. nana*, presumably corresponding to *M. americana* 1–3 in our topology, than to the second (pure) clade of *M. americana* (Fig. 4.4). Additionally, the genetic distance between the *M. americana*-clades was higher than that between *M. nana* and *M. bororo*. This suggests two separation events in the two lineages of *M. americana* (Abril et al., 2010). There is the potential that even more species are hidden in both the *M. americana*-complex and the *M. gouazoubira*-complex (Weber & González, 2003). Cytogenetics seems to be the most reliable technique for distinguishing between sympatric species (Vogliotti & Duarte, 2009). Much more data and thorough research on *Mazama* are needed to shed additional light on their complex

systematic relationships.

4.5 Conclusion

The taxonomically most extensive molecular phylogenetic data set for cervids compiled to date enabled us to undertake phylogenetic analyses to answer and test the initial questions and hypotheses: (1) *Mazama bricenii* is closely related to *M. rufina* and is more closely related to the *M. americana*-clade than to the *M. gouazoubira*-clade. However, from our topology, we infer that *M. rufina* is a subclade of *M. bricenii*. It cannot be excluded that these two taxa may represent the same species with *M. rufina* as the senior synonym. *Mazama chunyi* forms a sister taxon relationship with *M. gouazoubira* and can thus be assigned to the *M. gouazoubira*-clade. The discovery of a fifth clade (*M. pandora*) shows that the polyphyly and systematic relationships within *Mazama* are even more complex than previously thought and remain a challenge to address in future research. (2) *Muntiacus atherodes* is supported to be a valid species distinct from other *Muntiacus* spp. However, its systematic position cannot be resolved with certainty, but the maximum likelihood analysis indicates that it might be more closely related to the sympatric *M. muntjak* than to any other muntjac. (3) The Philippine rusine deer *R. marianna* and *R. alfredi* form a monophyletic clade and are sister taxon to a clade containing the other rusine deer, *R. timorensis* and *R. unicolor* and to the *Cervus*-clade. Our results indicate that *R. alfredi* forms a subclade of *R. marianna* rather than its sister taxon. (4) The genus *Pudu* appears to be polyphyletic, with *P. puda* nested within the *Blastocercina* and *P. mephistophiles*, thereby forming a monophyletic group in a yet-unresolved position.

Based on our topologies and previous work, we established here the new subtribes *Blastocercina* and *Odocoileina*, which form *Odocoileini*. A revision of the current taxonomy based on comparison of phenotypic and genotypic traits is desirable for future research on cervid systematics.

Chapter 5

Combined Phylogenetic Analyses and Evolutionary Aspects

5.1 Introduction

Despite all efforts to resolve cervid (and ruminant) systematics over the past decades no satisfying consensus could be reached from the phylogenetic reconstructions and several problems persist. Controversial species delimitations, unknown taxon affiliation, contradictory information from the data, and/or incomplete phylogenetic reconstruction were specified as possible reasons for these problems. To solve phylogenetic relationships of cervids and ruminants), however, is of considerable interest, because of their important biological and economic role as wild and domestic animals; they are also ideal organisms to investigate evolutionary processes (Cronin, 1991; Randi et al., 2001; Price et al., 2005b).

In contrast to early systematic studies, which were often based only on a few morphological characters, there are now numerous molecular approaches and a few supertree studies to solve cervid systematics. However, combined or total evidence approaches are still scarce (Groves & Grubb, 1987; Groves, 2014). Although the fossil record for cervids is good, systematic relationships of fossil cervids are even more uncertain than those of extant cervids. There are numerous qualitative descriptions and comparative morphological studies for fossil cervids, but there are only very few phylogenetic approaches on early fossil taxa. While these were mainly based on antler characters, Mennecart et al. (2016) presented the first phylogeny for Miocene cervids based on inner ear morphology.

Until the 1960s morphological characters were solely used for the classification of organisms. Molecular and morphological approaches are largely complementary; both have their advantages and disadvantages and neither method is exclusively most informative. Advantages of molecular data are the sufficiently large number of observable characters, the presence of substitution rates, and the objectivity of the selection and definition of characters. The advantages of morphological data are the possibility of a denser taxon sampling, since they are the only possibility to include fossil taxa; fossils represent a large proportion of the Earth's biodiversity and are important to reconstruct the evolutionary history of living taxa (Hillis & Wiens, 2000).

Discrepancies between morphological and molecular studies, make it necessary to con-

tinue attempts to combine fossil and extant species in order to reconstruct accurate phylogenies and to understand macro-evolutionary processes, which should yield better estimates than individual analyses (Hillis & Wiens, 2000; Hernández Fernández & Vrba, 2005). Many previous studies show the benefit of combining molecular and morphological data of fossil and living taxa in supermatrix analyses (e.g., Asher, 2007; Geisler et al., 2011; Bibi et al., 2012). It was hypothesised that long branches, which lead to clades consisting of only a small number of extant species (e.g., Moschidae), produce artefactual relationships. These long branches could be subdivided by including fossil taxa and their intermediate characters (Bibi, 2014).

A common approach to combine morphological and molecular data of fossil and extant taxa is a total evidence (TE) analysis; the challenge of this approach is to collect all the required data. Compiling molecular data is mostly not a problem anymore, but collecting morphological data can be difficult. The completeness and size of the morphological partition depends on the amount of morphological data scored and available for living taxa, the amount of missing data in the fossil taxa, and the total number of morphological characters. Guillerme & Cooper (2016) found that the amount of missing data in fossils plays a minor role compared to the other two factors for inferring the ‘best’ topology. This suggests that increased collection of morphological characters of extant taxa, will increase the accuracy of TE approaches.

In ruminant phylogenetic studies the lack of morphological and fossil data is a big problem. Ideally, there would be a morphological character matrix, with which a reliable species-level topology could be reproduced without the aid of molecular data. To achieve this, at least twice as many parsimony informative characters than taxa have to be scored (Bibi, 2014).

Suitable fossil data are crucial for calibrating rates of morphological and molecular change through time for molecular clock approaches and divergence time estimates; they also act as an independent source of phylogenetic and biogeographic information and control for estimated diversification rates, incorporation of extinct lineages, and for resolving uncertain phylogenetic relationships through combined analyses (Sansom & Wills, 2013; Bibi, 2014).

To achieve a robust reconstruction of the cervid phylogeny, a complete species-level taxon and extensive data sampling are needed. Only with this, the ecological, biological and geographical patterns of cervid and ruminant evolutionary history can be reconstructed (Price et al., 2005b). In my thesis, extensive taxon and data sampling across Cervidae was undertaken. Several nuclear markers and the mitochondrial genome were analysed and combined with the morphological data of Chapter 3. TE approaches incorporated many fossil and living species covering the entire evolutionary history of cervids from the early Miocene until today.

5.2 Material and Methods

5.2.1 Molecular Data

The majority of molecular data was obtained from GenBank (ncbi.nlm.nih.gov/genbank/). The GenBank accession numbers are in Table 4.1 for the mitochondrial markers and in

the alignment files for the nuclear markers. Thirteen cytochrome b (*Cytb*) sequences for five previously unrecorded species presented in Chapter 4 were sequenced in the LMU Molecular Palaeobiology Lab and represent primary data. Five nuclear markers and the mitochondrial genome were chosen based on their availability for cervids. *Cytb* is the marker available for most of the species; therefore, a separate analysis using only this marker was undertaken (see Chapter 4).

Each gene was aligned in SeaView 4.2 (Gouy et al., 2010) and Mesquite v.2.75 (Maddison & Maddison, 2011); alignments were carefully checked by eye for stop codons and/or unusual codon positions by translation into amino acids, where applicable, and were manually corrected if necessary. Some regions have been excluded from the alignment, for example the first and last couple of sites, which were not available for all taxa in the alignment (for specifics see Table I.1).

Distance matrices for each gene analysed show that all nuclear genes have a large proportion of invariant sites, while mitochondrial markers have a higher proportion of variable sites. The similarities were between 88.7 % and 99.9 % across cervid species and nuclear markers and 85.3 % and 96.5 % for mitochondrial markers.

All molecular data sets were run under the two likelihood-based optimality criteria, maximum likelihood (ML) and Bayesian inference (BI).

Model Choice. For each alignment I used PartitionFinder (Lanfear et al., 2012) to identify the appropriate substitution model and the optimal partitioning scheme. The Hasegawa-Kishino-Yano model (HKY; Hasegawa et al., 1985), and the Generalised Time Reversible model (GTR; Tavaré, 1986) are the most commonly used. The HKY model uses five parameters, different mutation rates, the substitution rate, and unequal base frequencies. The GTR model is the most independent and general model with ten possible parameters in total, six substitution rates and four base frequencies, which are often cut down to nine parameters (Spencer & Wilberg, 2013).

All analyses were run with a gamma distribution (Γ) without a proportion of invariant sites (I), where Γ or $\Gamma + I$ was suggested, because combining $\Gamma + I$ is known to cause convergence problems by creating two areas of equal probability in the tree landscape (Moyle et al., 2012). I was used when suggested as the sole analysis parameter.

After completion, the statistics of all Bayesian analyses were checked in Tracer v.1.6 (<http://tree.bio.ed.ac.uk/software/tracer/>) and convergence between runs was checked using the visualisation tool of AWTY (Wilgenbusch et al., 2004).

Nuclear Genes

Five nuclear genes were chosen for phylogenetic reconstructions based on their taxon sampling across cervids ($n > 10$): The non-coding markers, α -lactalbumin (*Lalba*), protein kinase C iota (*Prkci*), and the sex determining region on the Y-chromosome (*Sry*) and the coding markers κ -casein (*Csn*) and prion protein (*Prnp*) (for details see Table I.1). The two coding markers were partitioned according to codon positions 1-3.

First, each gene was analysed separately. Secondly, all five nuclear genes were combined in a supermatrix and were analysed together to investigate, whether there is increased

phylogenetic information in the additive data set. The combined nuclear data set comprised 2805 base pairs for 28 cervid species and nine non-cervid ruminant species.

For the BI analyses, the single nuclear gene analyses were run for five million generations at a temperature for the heated chain of 0.5 and sampled every 1000th generation using MrBayes v.3.2 (Ronquist et al., 2012). The combined nuclear data set was run for eight million generations with the same parameter settings as the single gene analyses. The ML analyses for all single nuclear genes and the combined nuclear data set were analysed with RAxML v.2.7.3 (Stamatakis, 2006). The ML analyses also included a rapid bootstrap analysis.

Mitochondrial Genes

Extensive analyses on *Cytb* including 52 cervid species across 124 taxa and six non-cervid ruminants are in Chapter 4. Additionally, the complete mitochondrial genome (mtG) was re-analysed for 33 cervid species including 39 taxa and seven non-cervid ruminants including 14904 base pairs (Hassanin et al., 2012). For the combined mtG-*Cytb*-analyses, the *Cytb* region in the mitochondrial genome was excluded and the separate, more taxon-rich *Cytb* alignment was included in the mitochondrial genome. The taxon sampling unlike in the *Cytb* only analyses was reduced to one sequence per species, but allowing for the polyphyly found in the *Cytb* analyses of the extended taxon set. The combined matrix included 51 cervid species across 56 cervid taxa and six non-cervid ruminants.

The mtG and the mtG-*Cytb* combined data set contained seven partitions according to Hassanin et al. (2012). For the BI analyses of both data two runs à four chains sampled the tree landscape at a temperature of 0.35 until the standard deviation of split frequencies was below 0.01. Trees were sampled every 5000th generation. The ML analyses for both data sets included rapid bootstrap analyses and used the same partitioning scheme as in the BI analyses.

Combined Molecular Analyses

The molecular combined matrix consisted of 17709 base pairs for 56 cervid taxa including 50 extant and 1 fossil cervid species and 6 non-cervid ruminant species. This data set was analysed using ML and BI with the same settings as above.

5.2.2 Combined Molecular and Morphology Analyses

The total evidence (TE) matrix consisted of 168 morphological and 17709 molecular characters, in total 17877 characters. The 87 taxa included two fossil and six extant non-cervid ruminant species and 29 fossil and 50 extant cervid species. This data set was run using ML, BI, and maximum parsimony (MP).

5.2.3 Node Calibration Dating

Divergence time estimation is based on molecular clocks, which calculate the substitution rates of nucleotides. With this it is possible to date back the time when two or more lineages diverged. The molecular clock node dating (ND) analyses were undertaken with the nuclear

and mitochondrial, and the combined molecular data sets. The nuclear matrix for the node dating analysis consisted of 2805 base pairs for 28 cervid species and one tragulid species. The mitochondrial matrix consisted of 14904 base pair long mitochondrial genome for 40 taxa including 39 cervid taxa (33 species) and one tragulid species. The combined data set consisted of 17709 base pairs for 50 cervid and one tragulid species.

Six fossil calibration points were set a priori. These calibration points were included as age ranges. The root was dated with the putative first fossil tragulid *Archaeotragulus krabiensis* (34 mya); all other fossil calibrations are shown in Table 5.1. *Dicrocerus elegans* was set as the calibration point for Cervini, since it was suggested to be the first member of Cervini recently (Azanza et al., 2011). Several fossil cervids have been suggested as the first Cervini in the past; Di Stefano & Petronio (2002), for example, states *Cervocerus novorossia* is the first cervine deer. It would be useful to test different fossil calibration points in future analysis. However, this was beyond the scope of this project. The clock-constrained branch lengths prior was set to uniform. The independent gamma rates (IGR) model (Lepage et al., 2007) was set as the relaxed clock model with an exponential distribution rate of 10.0 to account for the rate, at which the variance of the effective branch length increases over time (speciality of IGR model). The clock rate prior was set with a normal distribution with a mean of 5.0 and a standard deviation of 0.5.

Table 5.1: More information on the selected fossil calibration points, i.e., locality and stratigraphic information, and diagnoses, are provided in the respective references.

Species	Node	Age [Ma]	Citation
<i>Archaeotragulus krabiensis</i>	root	65-34	Benammi & Jaeger (2001); Métais et al. (2001)
<i>Ligeromeryx praestans</i>	Cervidae	19.5–17.2	Gentry et al. (1999)
<i>Dicrocerus elegans</i>	Cervini	16.4–13.1	Azanza et al. (2011)
<i>Euprox minimus</i>	Muntiacini	14.8–14.2	Böhme et al. (2012)
<i>Procapreolus ukrainicus</i>	Capreolini	10.5–9.5	Korotkevich (1965); Lechner-Doll et al. (2001)
<i>Pavlodaria orlovi</i>	Odocoileini	5.3–3.6	Vislobokova (1980)

5.2.4 Total Evidence Dating

The difference between ND and total evidence dating (TED) is that the placement of fossils, the tree building and the time estimation are calculated simultaneously. The (TED) matrix included the same data partitions as the TE matrix and included 50 extant and 29 fossil cervids and one tragulid species. The absolute ages of all 29 fossils were used to calculate divergence time estimates together with the tree search process. All fossils with their dates are shown in Table 5.2. The clock-constrained branch lengths prior was set to uniform. The independent gamma rates (IGR) model Lepage et al. (2007) was set as the relaxed clock model with an exponential distribution rate of 10.0. The clock rate prior was set with a normal distribution with a mean of 5.0 and a standard deviation of 0.5. The gamma distribution was set for the clockrate prior. The root was dated as in the node dating analyses and the monophyly of Cervidae was set as topology constraint.

Table 5.2: The absolute age of the 29 fossil cervid species included in the TED. The stratigraphic age and locality information are provided in Table B.2. The absolute dates were obtained from Hilgen et al. (2012).

Species	Age [Ma]
<i>Arvernoceros ardei</i>	5.3
<i>Axis lydekkeri</i>	1.0
<i>Candiacervus ropalophorus</i>	0.7
<i>Cervus australis</i>	5.3
<i>Cervus perolensis</i>	3.4
<i>Cervus philisi</i>	2.6
<i>Cervus sivalensis</i>	2.0
<i>Croizetoceros ramosus</i>	4.2
<i>Dicrocerus elegans</i>	15.8
<i>Eostyloceros hezhengensis</i>	8.0
<i>Eucladoceros ctenoides</i>	2.6
<i>Euprox furcatus</i>	14.2
<i>Heteroprox larteti</i>	18.0
<i>Lagomeryx parvulus</i>	17.2
<i>Ligeromeryx praestans</i>	20.0
<i>Megaloceros giganteus</i>	0.126
<i>Metacervocerus pardinensis</i>	3.4
<i>Metacervocerus rhenanus</i>	2.675
<i>Muntiacus muntjak</i> (RGM)	0.781
<i>Odocoileus</i> (NHM)	1.8
<i>Odocoileus virginianus</i> (BSPG)	1.8
<i>Palaeoplatyceros hispanicus</i>	12.5
<i>Pliocervus matheroni</i>	8.2
<i>Praeclaphus etueriarum</i>	3.3
<i>Praeclaphus perrieri</i>	3.4
<i>Procapreolus cusanus</i>	3.4
<i>Procervulus dichotomus</i>	18.3
<i>Procervulus praelucidus</i>	18.5
<i>Rusa kendengensis</i>	1.0

5.3 Results

5.3.1 Nuclear Genes

κ -casein (*Csn*)

The ML and BI topologies were congruent (Fig. 5.1). The monophyly of Cervidae and Cervini was highly supported. The placement of *Muntiacus reevesi* as sister taxon to *Rangifer tarandus*, within Capreolinae with a relatively high support is unexpected.

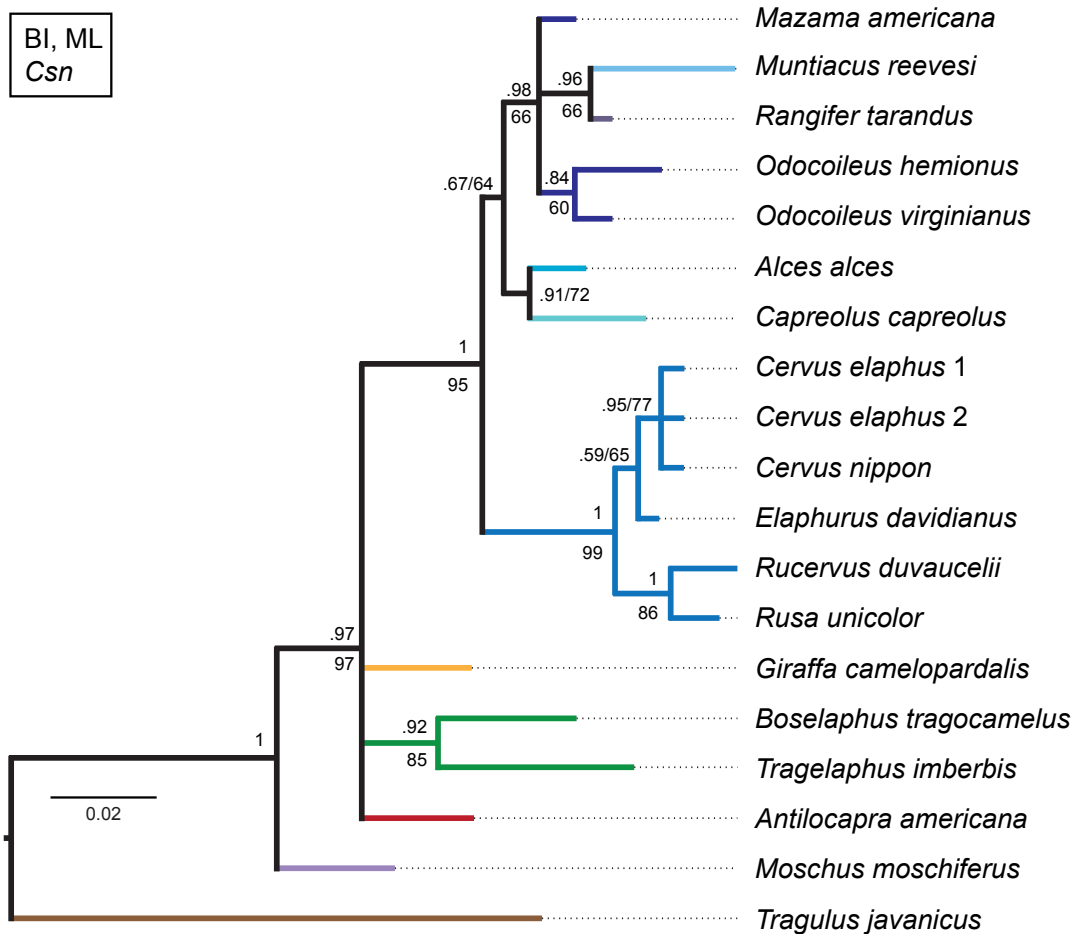


Figure 5.1: Bayesian consensus topology of the analysis of *Csn* including the posterior probabilities (above branches) and the ML bootstrap values (below branches) or as PP/BS.

α -lactalbumin (*Lalba*)

The BI and ML topologies were congruent, both were largely unresolved (Fig. 5.2). The monophyly of Cervidae was supported, as was the monophyly of Odocoileini. Cervinae were monophyletic with the exception of *Axis axis* which was unexpectedly placed as the sister taxon to *Alces alces* with high support. Cervine taxa and *Elaphodus cephalophus* were placed in a polytomy, only the two *Dama* species form a distinct clade.

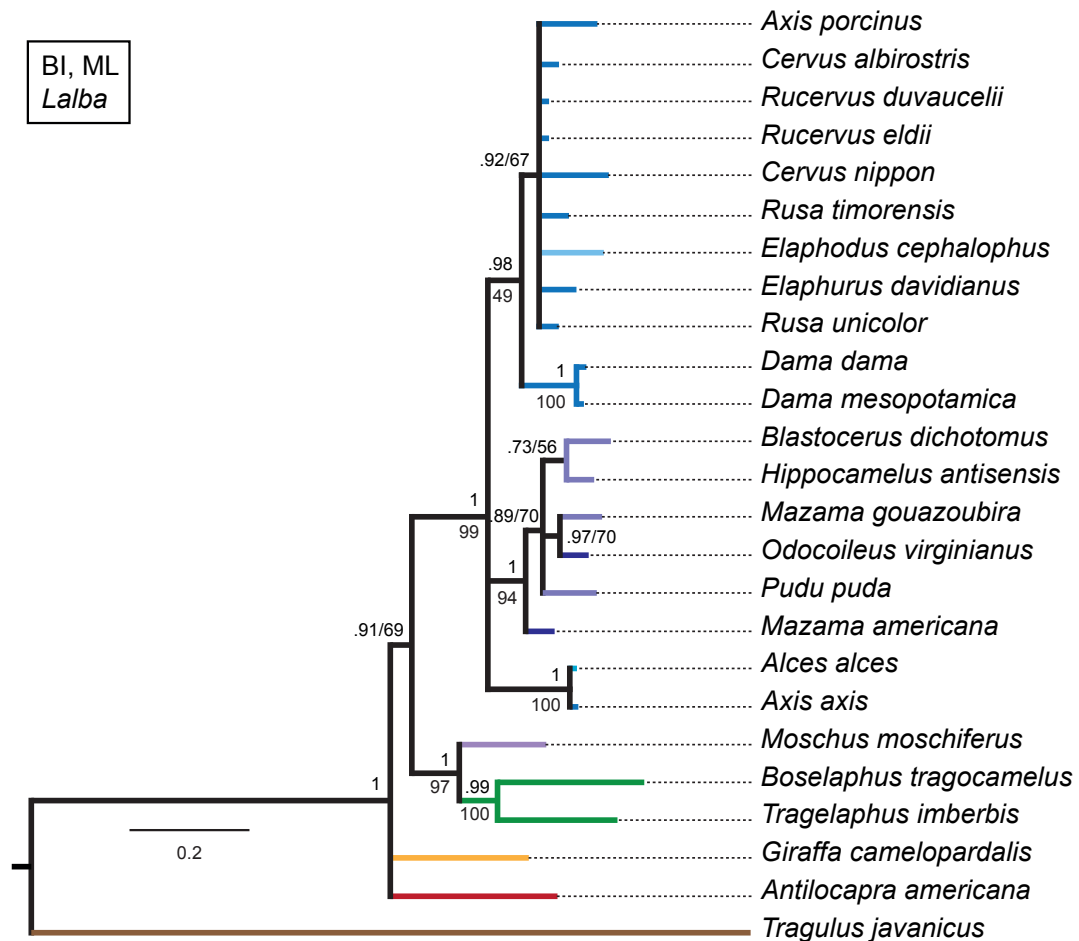


Figure 5.2: Bayesian consensus topology of the analysis of *Lalba* including the posterior probabilities (above branches) and the ML bootstrap values (below branches, or as PP/BS). The colour code is as defined in Figure 1.5.

Protein kinase C iota (*Prkci*)

The BI and ML topologies were largely congruent (Fig. 5.3). Cervidae were monophyletic, the monophyly of Cervinae and of Capreolinae was weakly supported. Odocoileini including *Rangifer* were also monophyletic, but taxa within that clade were unresolved. Some cervine clades were recovered, the two *Dama* species, the two *Axis* species, and the sister taxon relationship of *Rusa timorensis* and *Elaphurus davidianus*.

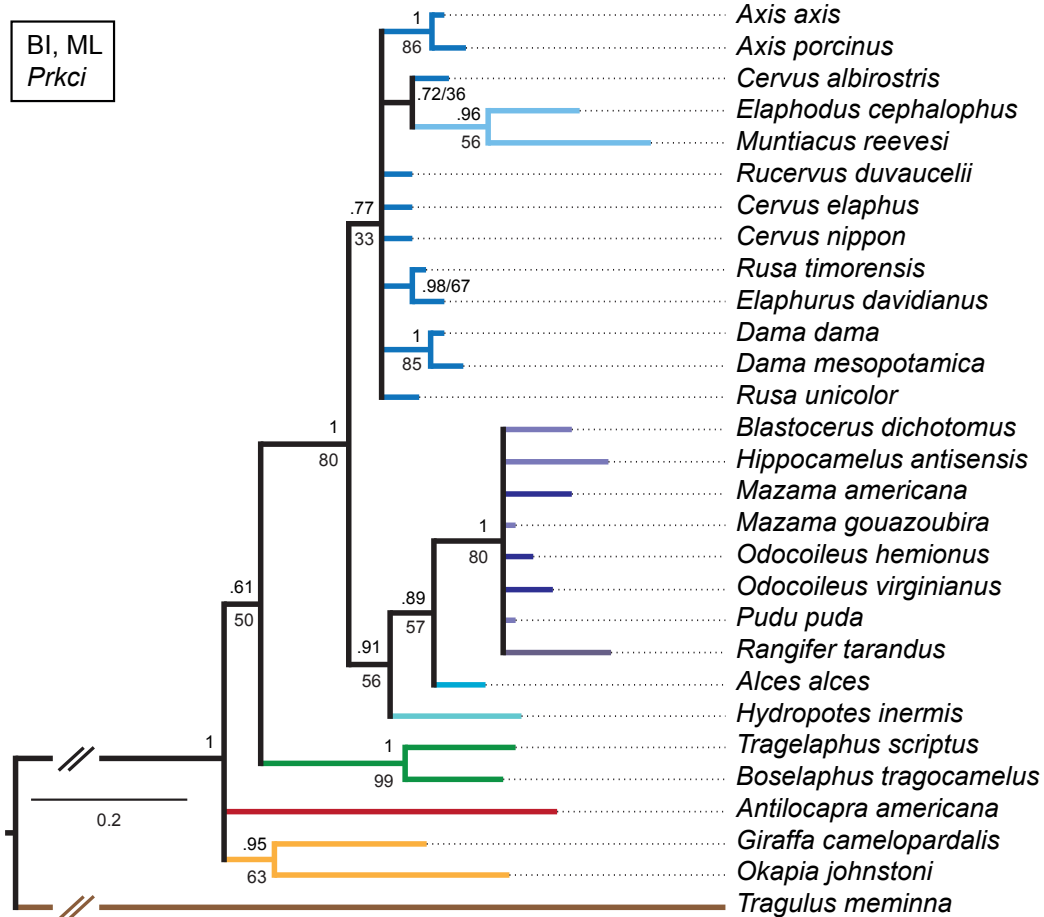


Figure 5.3: Bayesian consensus topology of the analysis of *Prkci* including the posterior probabilities (above branches) and the ML bootstrap values (below branches), or as PP/BS.

Prion protein (*Prnp*)

The BI and ML topologies were largely congruent (Fig. 5.4). Cervidae were monophyletic; the systematic relationships within Cervidae were not fully resolved. In the BI topology there were two cervine clades, in the ML topology there was one *Cervus*-clade.

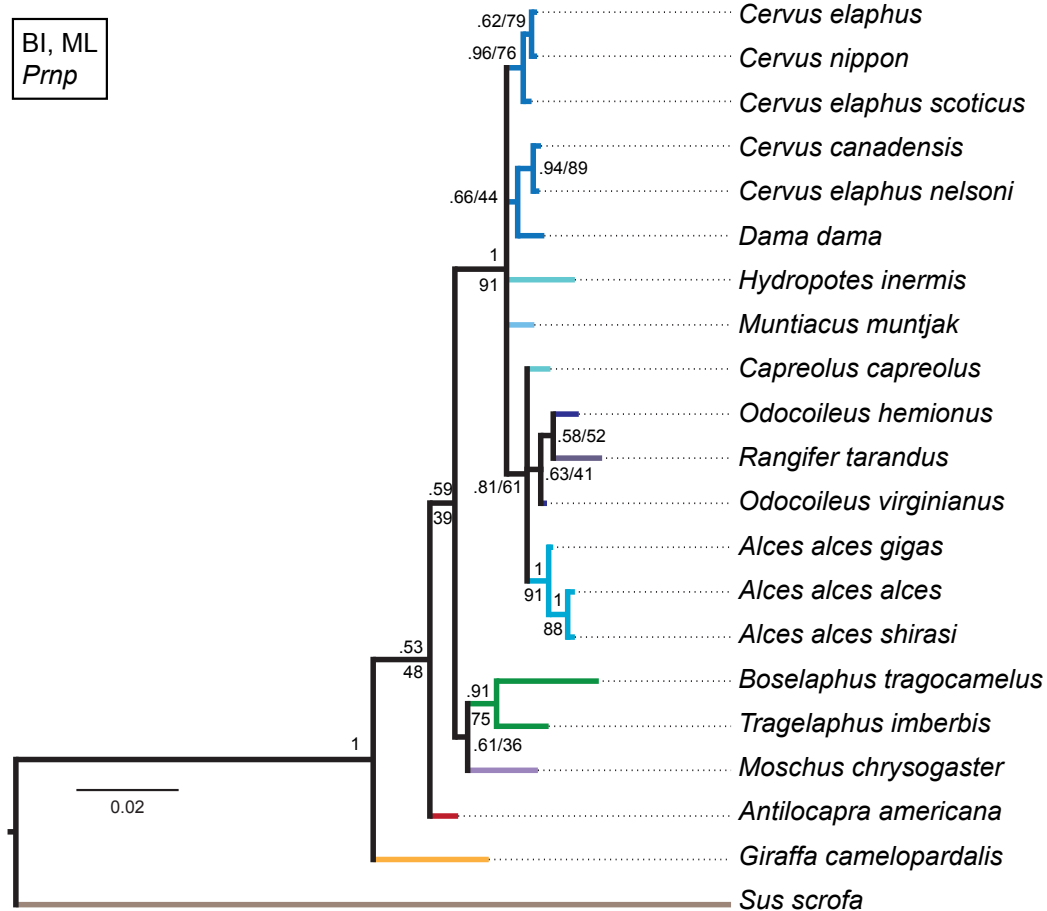


Figure 5.4: Bayesian consensus topology of the analysis of *Prnp* including the posterior probabilities (above branches) and the ML bootstrap values (below branches), or as PP/BS.

Sex determining region on the Y-chromosome (*Sry*)

The BI and ML topology were largely congruent (Fig. 5.5); the main difference was the position of the *Alces*-clade as the sister taxon to all other taxa in the ML topology, while it was in a polytomy with two capreoline clades and the clade containing all other taxa in the BI topology. Cervidae are not monophyletic; there was a bovid-moschid-clade as the sister taxon to monophyletic Cervini and monophyletic Muntiacini (and *Capreolus capreolus*). *Capreolus capreolus* was unexpectedly placed as the sister taxon to Cervini, not as the sister taxon to *Capreolus pygargus*. The sequence for *Capreolus capreolus* (DQ888700) may be misidentified or contaminated.

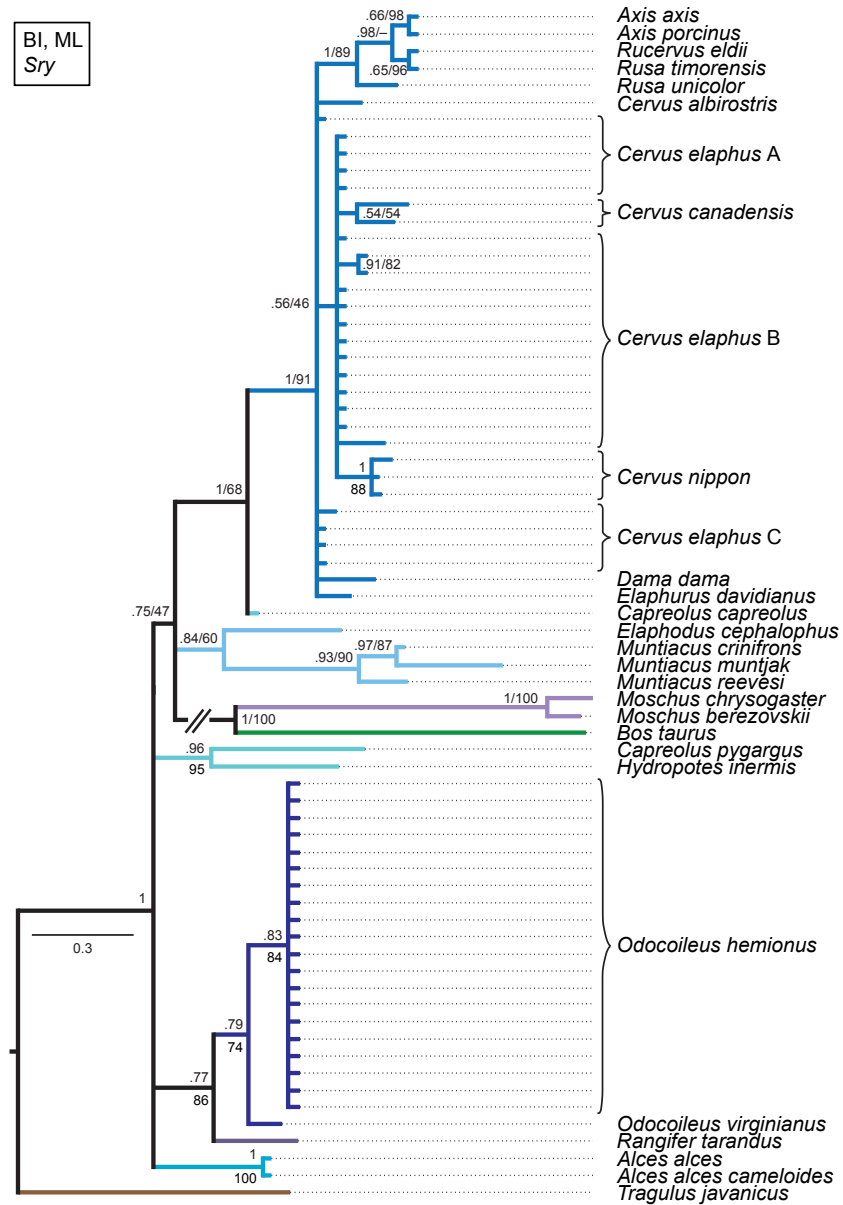


Figure 5.5: Bayesian consensus topology of the analysis of *Sry* including the posterior probabilities (above branches) and the ML bootstrap values (below branches) or as PP/BS.

Combined Nuclear Genes

Although interpretations of the systematic relationships on genus and species level was difficult in the single gene topologies due to low taxon sampling and/or lack of resolution, the combined nuclear topology was comparatively well resolved and supports the higher hierarchical clades. The BI and the ML topology were largely congruent (Fig. 5.6). Cervidae, Cervinae, Cervini, Muntiacini, and Capreolinae were monophyletic. Muntiacini is the sister taxon to Cervini and Cervinae was the sister taxon to Capreolinae. Within Cervini the two *Axis* species and the two *Dama* species each form a clade, *Elaphurus davidianus* was the sister taxon to *Cervus elaphus* and *Cervus nippon*. *Rusa*, *Rucervus*, and *Axis* form a clade. *Cervus albirostris* is in an unresolved position within Cervini in the BI topology, while it was in a poorly supported sister taxon relationship with *Dama* in the ML topology. Odocoileini and *Rangifer* formed a clade; systematic relationships within that clade were largely unresolved and there was no split into Odocoileina and Blastocerina as observed in the topologies based on the mitochondrial markers. *Capreolus pygargus* plus *Hydropotes inermis* and *Capreolus capreolus* plus *Alces alces* formed two clades. The unexpected placement of *Capreolus capreolus* in this topology may be caused by the possibly contaminated *Sry* sequence of this species.

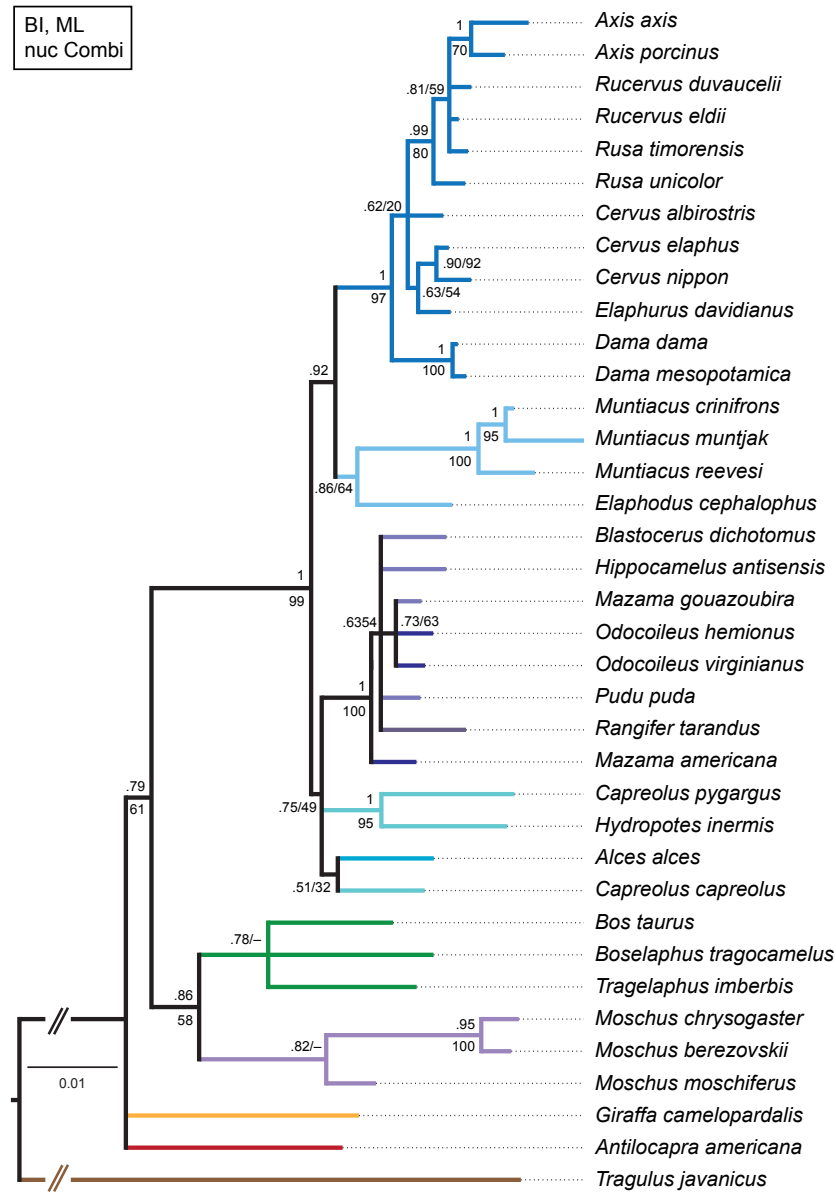


Figure 5.6: Bayesian consensus topology of the analysis combining five nuclear markers including the posterior probabilities (above branches) and the ML bootstrap values (below branches) or as PP/BS.

5.3.2 Mitochondrial Genes

Mitochondrial Genome

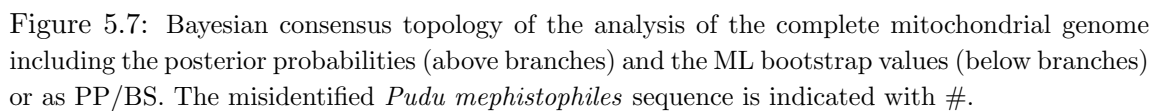
The re-analysis of the complete mitochondrial genomes originally published in Hassanin et al. (2012) resulted in a well resolved topology with high support values throughout. The BI and ML topologies were almost congruent (Fig. 5.7). All non-cervid ruminants were in a sister taxon position to the cervids and were in slightly different positions in both topologies. The position of *Blastocerus dichotomus* varies. Cervidae, Cervinae, Cervini, Muntiacini, Capreolinae, Capreolini, and Odocoileini were monophyletic. Muntiacini were the sister taxon to Cervini. Capreolini and *Alces* formed a clade, which was the sister taxon to Odocoileini. Odocoileini split into the two subclades Blastocerina and Odocoileina. *Pudu*, *Mazama*, *Odocoileus*, and *Rucervus* were polyphyletic. (Note that the mitochondrial genome sequence for *Pudu mephistophiles* was already assumed to be misidentified by Hassanin et al. (2012) and supported by the results of Chapter 4).

Cytochrome b

The detailed description of the phylogenetic analyses of *Cytb* is in Chapter 4.

Combined Mitochondrial Genes

The BI topology of the combined mitochondrial analysis showed higher support values for the majority of nodes than the *Cytb* only topology, but lower support values for some nodes than for the mtG analysis. The ML topology differed in generally lower support values for most nodes, but was otherwise largely congruent (Figs 5.8, 5.9). The placement of non-cervid ruminants differed in both topologies. The main difference concerning cervid taxa is the position of *Pudu mephistophiles* (based on the correct *Cytb* sequence, not the incorrect mtG sequence), which was the sister taxon to Blastocerina in the BI topology and the sister taxon to *Rangifer* and Odocoileini in the ML topology. This combined topology was very similar to the *Cytb* only topology (Chapter 4) and includes the polyphyly for *Rucervus*, *Hippocamelus*, *Odocoileus*, *Mazama*, and *Pudu*. Because of the inclusion of the relatively short *Cytb* fragment into the much larger mtG alignment, a lot of missing data were included, the impact of which has not been thoroughly tested here. Therefore, interpretations based on this topology should be treated with caution.



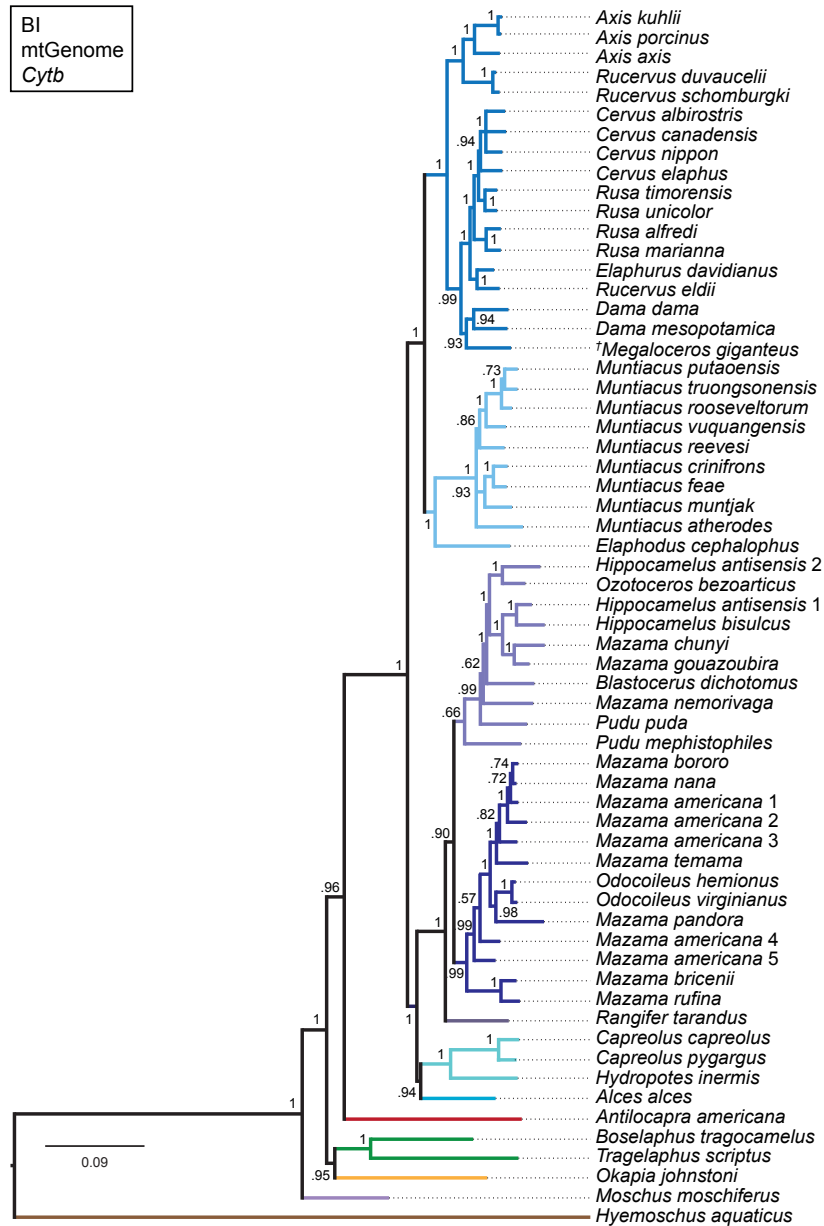


Figure 5.8: Bayesian consensus topology of the analysis of the complete mitochondrial genome including the *Cytb*-region with extended taxon sampling. The values represent Bayesian posterior probabilities.

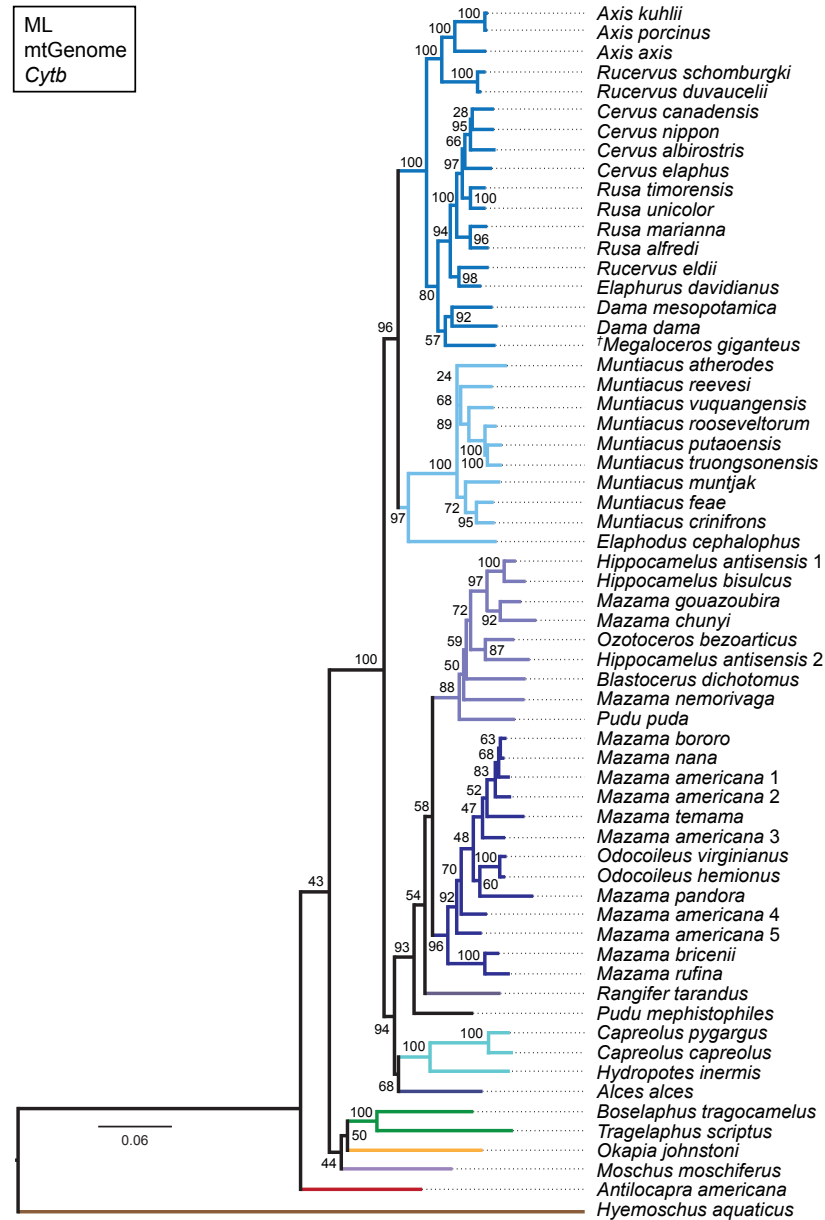


Figure 5.9: Best tree of the ML analysis of the complete mitochondrial genome including the *Cytb*-region with extended taxon sampling. The values represent bootstrap support.

5.3.3 Combined Molecular Analyses

The BI and ML topologies were largely congruent, the support values were partly lower, particularly in the ML topology, in comparison to the topologies based on the mitochondrial markers (Figs 5.10, 5.11). Both topologies differed in the position of non-cervid ruminants, and the positions of *Alces alces* and *Pudu mephistophiles*, which remain uncertain. Cervidae, Cervinae, Cervini, Muntiacini, Capreolinae, Odocoileini (without *Pudu mephistophiles*) and Capreolini were monophyletic. The split of Odocoileini into Blastocercina and Odocoileina was supported. *Rucervus*, *Hippocamelus*, *Mazama*, and *Pudu* were polyphyletic. Because a lot of missing data were included in the combined molecular analyses, interpretations based on these topologies should be treated with caution.

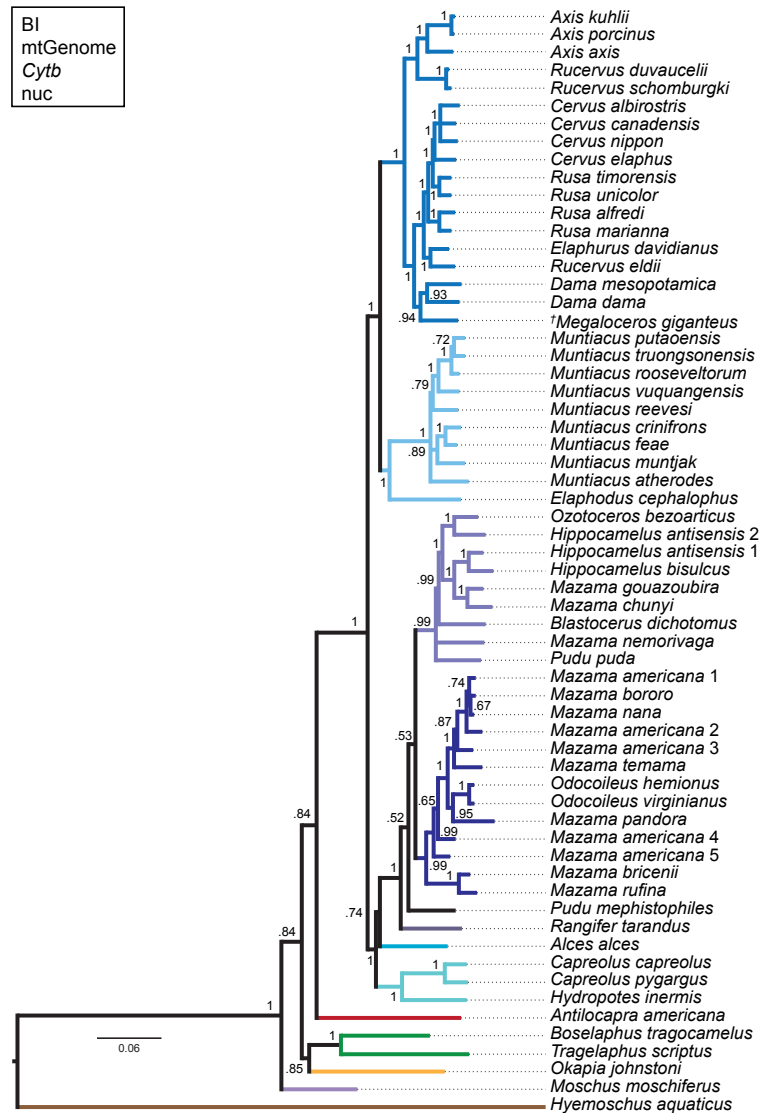


Figure 5.10: Bayesian consensus topology of the analysis of the combined nuclear and mitochondrial data set. The values represent Bayesian posterior probabilities.

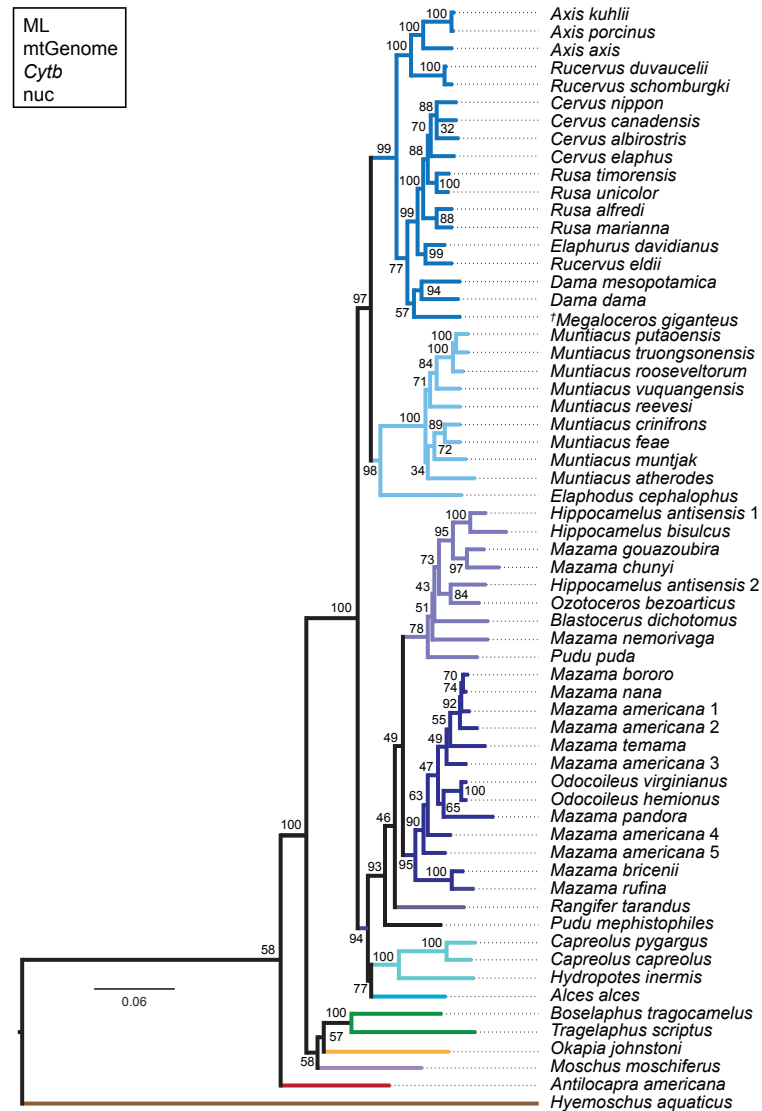


Figure 5.11: Best tree of the ML analysis of the combined nuclear and mitochondrial data set. The values represent bootstrap support.

5.3.4 Combined Molecular and Morphological Analyses

Bayesian Inference

The BI TE analyses were difficult. The first analysis was run with the suggested partitioning scheme and models; the second BI analysis was run with the same the partitioning scheme, but using only the GTR model. The third analysis was run excluding the molecular data for *Megaloceros giganteus* using the suggested partitioning and model scheme. In all of these approaches, *Megaloceros giganteus* was positioned on a disproportionately long branch. Therefore, in the fourth BI analysis this taxon was excluded and only this topology was used for interpretations (Fig. 5.12).

Capreolinae consisted of the *Alces*-Capreolini-clade and the *Rangifer*-Odocoileini-clade. *Procapreolus cusanus* was included in Capreolini as the sister taxon to *Capreolus*. *Rangifer* was the sister taxon to Odocoileini (including *Pudu mephistophiles*). Monophyletic Odocoileina is supported, while most blastocerine taxa were in a polytomy. *Mazama* and *Pudu* were polyphyletic. There was a clade consisting of a polytomy including *Elaphodus cephalophus*, a clade with eight Miocene cervids, and a *Muntiacus*-clade. The fossil *Muntiacus muntjak* was the sister taxon to *Muntiacus crinifrons*. The three *Axis*- and two *Rucervus*-species formed a clade, *Cervus albirostris* and *Cervus canadensis*, the two *Dama*-species, *Rucervus eldii* and *Elaphurus davidianus*, *Rusa marianna* and *Rusa alfredi*, *Rusa timorensis* and *Rusa unicolor*, ‘*Cervus*’ *philisi* and *Praeclaphus perrieri*, and ‘*Cervus*’ *sivalensis* and *Metacervocerus pardinensis* formed clades. All these clades were in a polytomy with the remaining cervid and non-cervid taxa.

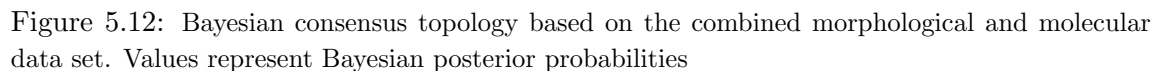
Maximum Likelihood

The majority of nodes were poorly or not at all supported 5.13. All Miocene cervids with the exception of *Eostyloceros hezhengensis* were placed between the two tragulids and all other taxa. *Procervulus* and *Dicrocerus* formed a clade. The extant non-cervid ruminants formed a clade, which was the sister taxon to the clade including the remaining cervids. Unexpectedly, *Praeclaphus etueriarum* was the sister taxon to *Tragelaphus*.

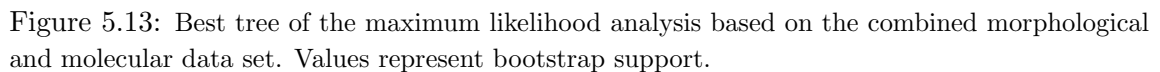
The other cervids split into Capreolinae and Cervinae. Within Capreolinae the *Alces*-Capreolini-clade was the sister taxon to the other capreoline taxa. *Rangifer* was the sister taxon to Odocoileini and *Pudu mephistophiles* was the sister taxon to both of them. Odocoileini split into Odocoileina and Blastocerina. Here *Mazama chunyi* was included in Odocoileina instead of Blastocerina. *Mazama* and *Pudu* were polyphyletic, fossil and extant *Odocoileus* were not monophyletic, *Hippocamelus* was strongly supported to be monophyletic. Cervinae split into Muntiacini and a clade consisting of non-monophyletic extant Cervini and Pliocene and Pleistocene cervids. Within Muntiacini *Elaphodus cephalophus* was the sister taxon to all other muntiacine taxa; *Eostyloceros hezhengensis* was placed between *Elaphodus cephalophus* and all *Muntiacus* species.

Maximum Parsimony

Only few nodes on genus or species level had moderate to high bootstrap support (Fig. 5.14). The non-cervid ruminants were all placed between the outgroup and cervids. *Hypertragulus calcaratus* was in the sister taxon position to *Boselaphus*, *Procapreolus cusanus*



was unexpectedly the sister taxon to *Moschus* and thus not included in the otherwise monophyletic Cervidae. Cervidae split into Capreolinae and Cervinae. Within Capreolinae, Capreolini and *Alces* formed a clade, which was the sister taxon to all other capre-



olines; Odocoileini formed a clade with *Rangifer tarandus* as the sister taxon to that clade and *Pudu mephistophiles* as the sister taxon to both of them. Odocoileini split into Odocoileina, within which all clades have bootstrap support, and Blastocerina. *Mazama* and *Pudu* were polyphyletic, *Hippocamelus* was monophyletic. Cervidae generally into

Muntiacini and Cervini, both including numerous fossil cervids. Muntiacini formed a clade, within which *Elaphodus cephalophus* was the sister taxon to all other taxa. Most Miocene cervids (except for *Eostyloceros hezhengensis* and *Pliocervus matheronis*) formed a clade with *Dremotherium feignouxii* as the sister taxon. This clade was the sister taxon to Muntiacini. Extant Cervini form a clade including three fossil cervids. Most clades within Cervini had a bootstrap support larger than 50. A clade consisting of Plio- and Pleistocene cervids and Miocene *Pliocervus matheronis* was the sister taxon to the Cervini-Plio-/Pleistocene-cervids-clade.

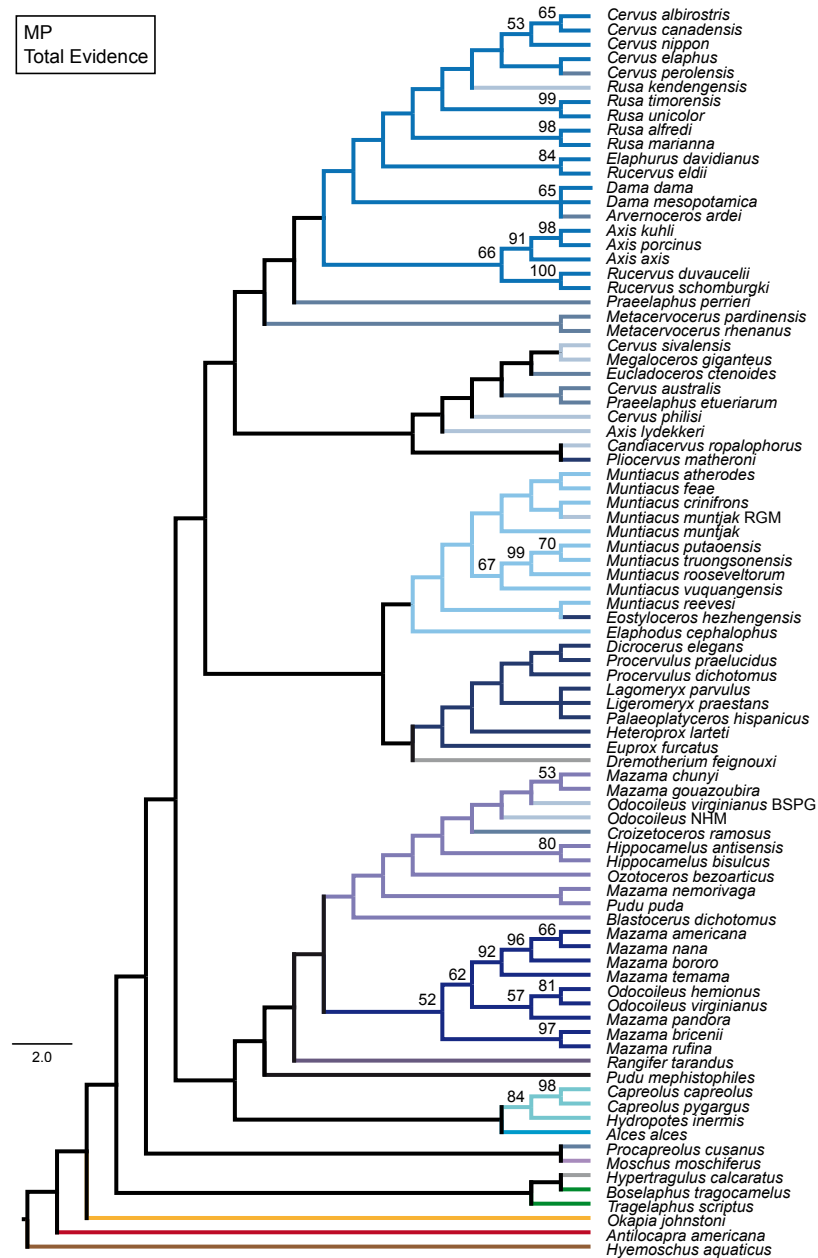


Figure 5.14: Consensus topology of the maximum parsimony analysis based on the combined morphological and molecular data set. Values represent bootstrap support.

5.3.5 Molecular Dating

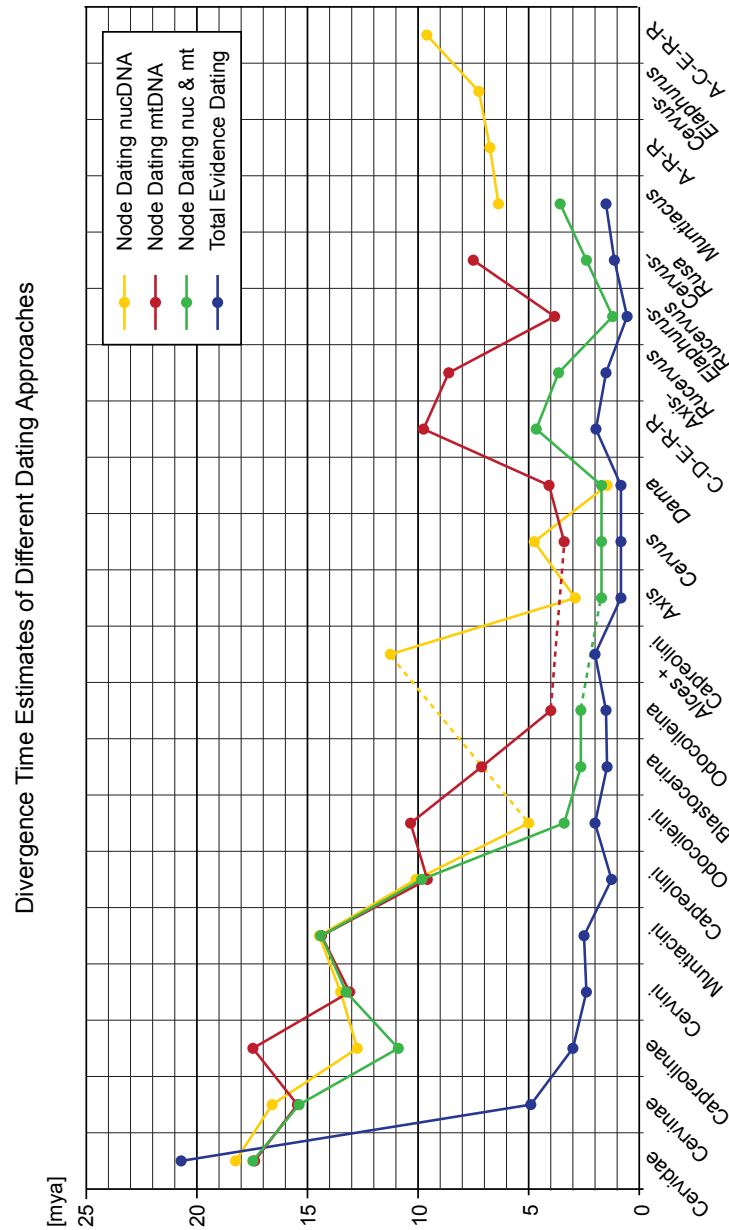


Figure 5.15: Overview of the divergence time estimates of the four different approaches. The age in million years ago before today are on the y-axis, and cervid clades of different hierarchical levels are on the x-axis. The three node dating analyses resulted in older divergence time estimates than the total evidence analysis. C-D-E-R-R = *Cervus-Dama-Elaphurus-Rucervus-Rusa*-clade, A-R-R = *Axis-Rucervus-Rusa*-clade, A-C-E-R-R = *Axis-Cervus-Elaphurus-Rucervus-Rusa*-clade.

Node Calibration

Comparing the nucDNA and mtDNA dated topologies there were differences in the position of several taxa, which was most likely caused by the differing taxon sampling (Figs 5.16, 5.17). The mtDNA topology was less well resolved than the nucDNA topology, but comprised more taxa. There was no tendency of one marker to result in generally younger or older ages than the other marker (Fig. 5.15). Some nodes were younger/older with the nuclear markers, some were older/younger with the mitochondrial markers. The combined mtDNA-nucDNA node dating analyses often resulted in younger divergence time estimates than the separate analyses 5.18. In all three ND approaches, the higher hierarchical splits, i.e., family, subfamily, and tribe level, originated in the Miocene, while subclades of tribes diverged in the Pliocene or later.

Total Evidence Dating

In the TE dating topology divergence time estimates for nearly all crown cervids were young, i.e., Pleistocene (Fig. 5.19). *Megaloceros giganteus* was placed as the sister taxon to all other cervids and its divergence time estimate of 42.1 mya was too old. This taxon also caused difficulties in the BI TE analyses, the reasons for which remain unclear. All Miocene species were placed between the outgroup and all other cervids. The origin of crown cervids including their potential extinct relatives was dated to 6.76 mya (late Miocene) and lower hierarchical nodes all originated around the Pliocene-Pleistocene-boundary. This is in contrast to the ND divergence time estimates, where all higher hierarchical nodes originated already in the Miocene. The TE dating topology should be read as a chronological succession of cervid taxa. Although the systematic relationships within living crown cervids were well resolved, systematic relationships of fossil cervids to extant taxa was only partly resolved. If node ages for crown cervids solely refer to today's species, the divergence time estimates are reasonable. They need to be differently interpreted than those from the ND analyses.

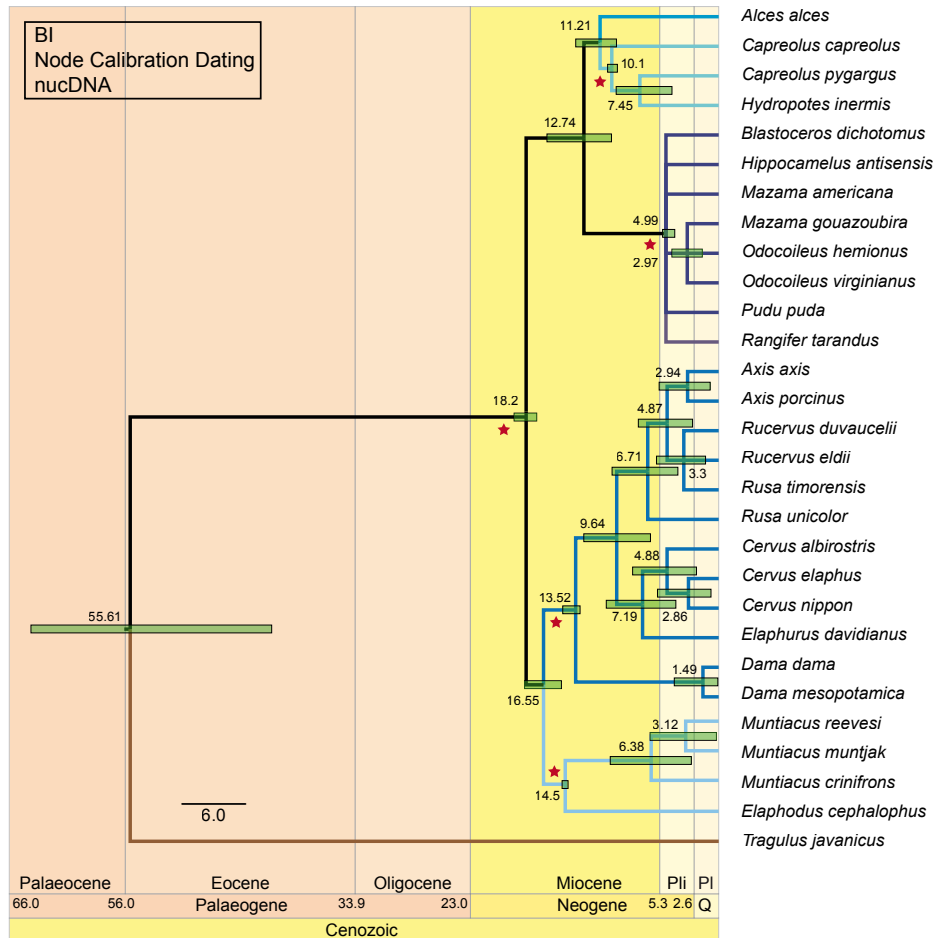


Figure 5.16: Cladogram of the node dating analysis based on the combined nuclear data set. The values represent node ages with their associated error bars (green). The red stars indicate nodes with fossil calibration points. Pli = Pliocene, Pl = Pleistocene, Q = Quaternary.

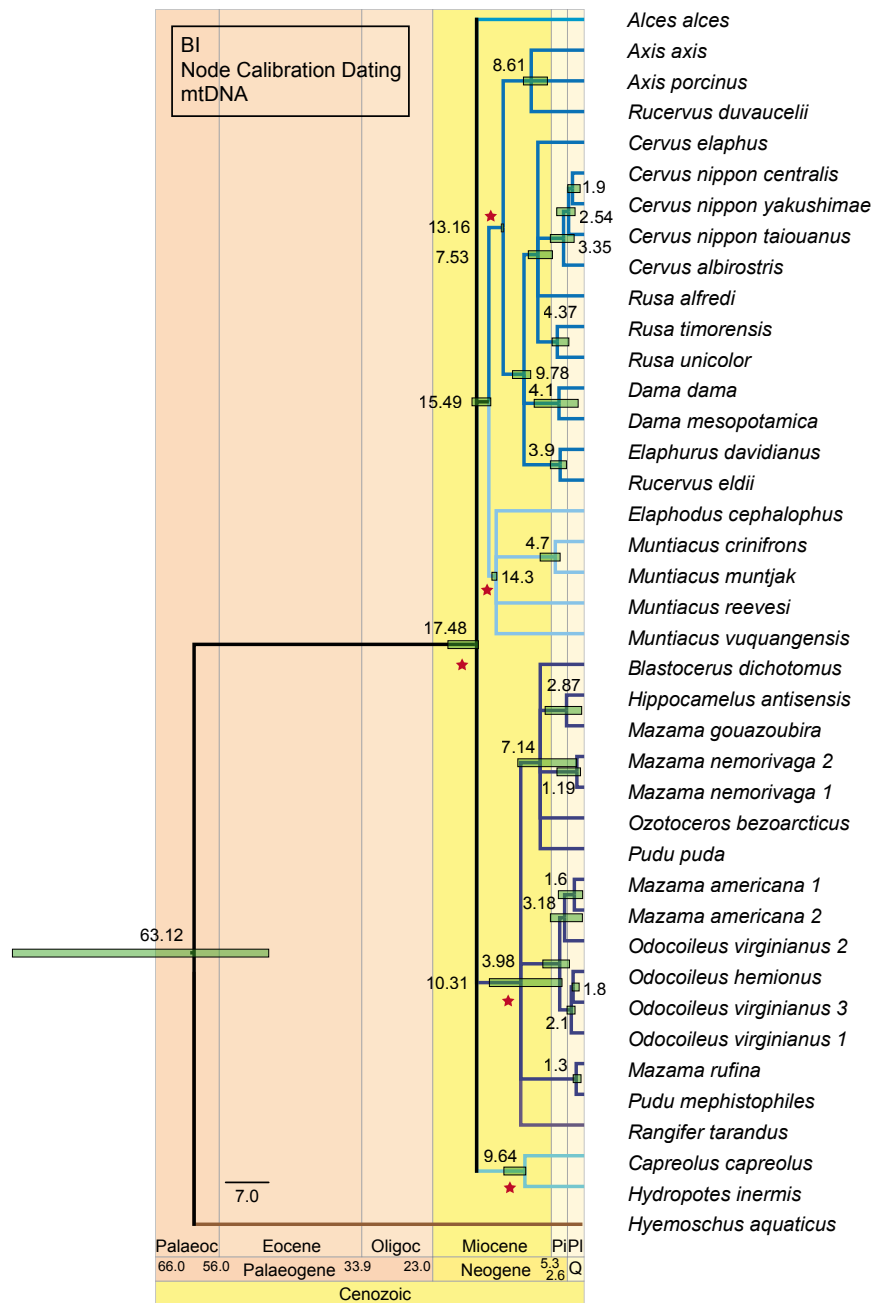


Figure 5.17: Cladogram of the node dating analysis based on the mitochondrial genome. The values represent node ages with their associated error bars (green). The red stars indicate nodes with fossil calibration points. Palaeoc = Palaeocene, Oligoc = Oligocene, Pi = Pliocene, Pl = Pleistocene, Q = Quaternary.

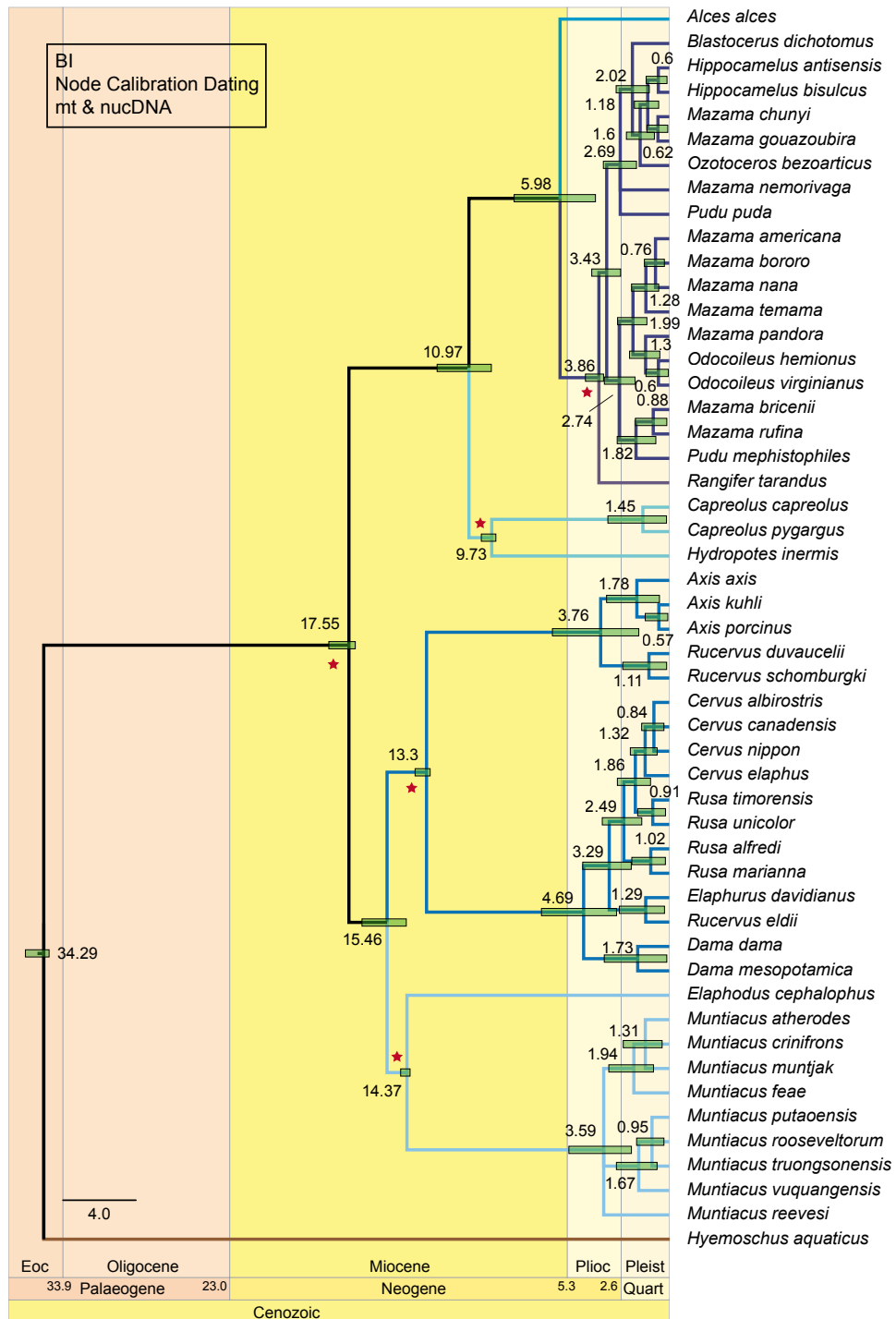


Figure 5.18: Cladogram of the node dating analysis based on the combined molecular data set. The values represent node ages with their associated error bars (green). The red stars indicate nodes with fossil calibration points. Eoc = Eocene, Plioc = Pliocene, Pleist = Pleistocene, Quart = Quaternary.

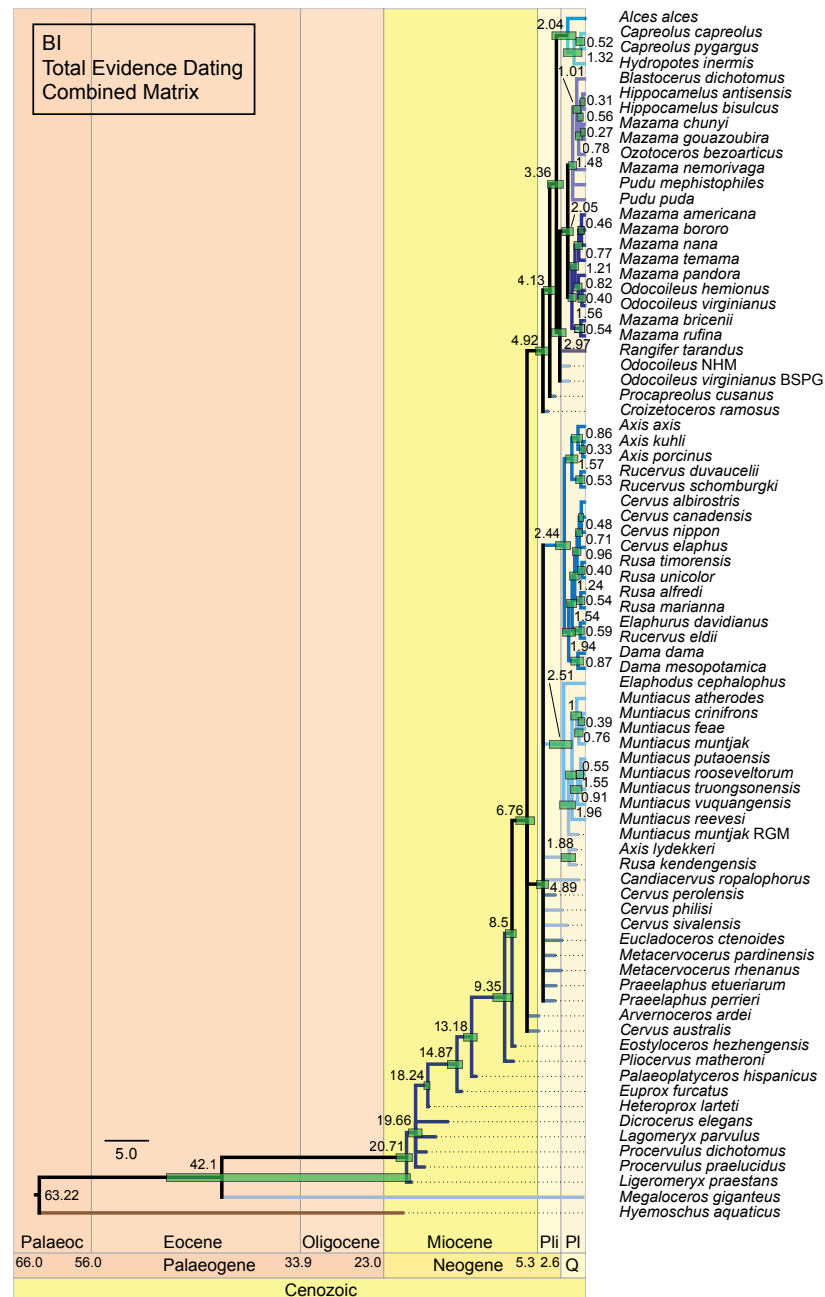


Figure 5.19: Cladogram of the total evidence dating analysis based on the combined morphological and molecular data set. The values represent node ages with their associated error bars (green). The placement and the age estimate of *Megaloceros giganteus* is almost certainly wrong. Palaeoc = Palaeocene, Pli = Pliocene, Pl = Pleistocene, Q = Quaternary.

5.4 Discussion

With the extensive combined molecular and morphological data set and the resulting topologies of my work it was possible to investigate the current state of the art in cervid systematics based on molecular data. More importantly, it was possible to combine fossil and extinct cervid species with their extant relatives and make inferences about their evolutionary history.

Concerning systematic relationships among extant taxa, many hypotheses could be confirmed; however, known controversies persisted, but could be specified in much more detail, which will facilitate to solve them in the future. For most fossil cervids, I was able to find an affiliation to extant relatives, which has so far not been attempted to such an extent as presented here.

For the bigger picture it is important not only to focus on the study group, but also investigate the relationships of closely related groups/taxa. Therefore, relationships within ruminants and particularly the position of Cervidae compared to other ruminant families is briefly discussed here, before a more detailed discussion about the systematics of extant and fossil cervids follows.

The lack of resolution in some parts of the topologies could be explained by high levels of homoplasy in the data (particularly morphology), too few characters, rapid radiations of ruminant tribes and clades around 15 mya and incomplete species sampling. Consensus might be difficult to achieve, because short branch lengths and/or lack of resolution potentially represent a genuine rapid diversification of clades, which may not be further solved just by increasing the sequence length or the taxon sampling. Markers that are less influenced by convergent evolution, such as rare genomic changes or cytogenomics may be useful additions in the future (Rokas & Holland, 2000; Price et al., 2005b; Hernández Fernández & Vrba, 2005).

5.4.1 General Remarks on Phylogenetic Analyses

Missing Data

Missing data represent an unavoidable problem in TE approaches. The influence and impact of missing data on topological accuracy has been extensively tested in past decade(s). While some studies argued that missing data potentially biases phylogenetic inferences (e.g., Lemmon et al., 2009), many studies showed that missing data may not be a problem for a correct placement of incomplete taxa (e.g., Wiens, 2003, 2006; Wiens & Morrill, 2011; Sansom & Wills, 2013; Pattinson et al., 2015; Darriba et al., 2016). Most of these studies investigated the impact of missing data on topologies and the placement of fossils neglecting the effect of missing data on living taxa (Guillerme & Cooper, 2016). As long as enough living and fossil taxa have data for overlapping morphological characters missing data per se is not the problem (Sansom & Wills, 2013).

The phylogenetic signal of morphological characters may be incongruent to that of molecular characters and contain homoplasy, which might affect the ‘best’ tree recovery particularly of smaller data sets (Guillerme & Cooper, 2016). Because of this, it is crucial to focus on coding morphological data for a large number (at least 50 % of the total taxon sampling) of living taxa in the matrix. In my thesis I sampled morphological characters

for almost all included living species.

Species Concepts

Taxonomy is the science of biological classifications and an important aspect in systematics. In other words, classifications are taxonomic schemata, working hypotheses subject to continual testing and potential modification, and do not represent a given rigid framework (Groves, 2003, 2006). The question what exactly defines a species has been a contentious issue in biology and trying to answer this question can become a long philosophical discussion (Amato et al., 1999a)

In order to classify organisms a range of species concepts is available, which define the criteria for an organism to qualify as a distinct species. The biological species concept and the phylogenetic species concept are the two most commonly used. In the biological species concept two species are defined as being reproductively isolated, while the phylogenetic species concept defines two distinct species when each of them can be distinguished by at least one heritable feature, i.e., they are diagnosably different (Groves, 2003, 2006).

The phylogenetic species concept is a poor guide to delimiting species, because basically every population will be diagnosably distinct under this species concept if the resolution power for analysed characters is sufficient. Additionally, a lineage is not enough to reach species status. Delimiting hierarchical levels of lineages in the tree of life (=structured system of lineages) will always have an arbitrary component (Zachos et al., 2013; Heller et al., 2014; Zachos et al., 2014).

A fundamental criterion is that taxa above species level must be monophyletic. However, criteria to define these higher hierarchical monophylyies are subjective (Groves, 2014). De Queiroz & Gauthier (1992) discussed the utility of such rankings and came to the conclusion that all higher taxonomic categories should be discarded and only rankless nodes should be named. In my thesis I applied the biological species concept. Some taxa, e.g., *Cervus canadensis*, *Dama mesopotamica*, are treated as species in some studies and as subspecies in others. The species status was preferably used in my analyses.

Combining Data Sets

There are three approaches to a single phylogenetic hypothesis; one is total evidence, another is a conditional combination of data sets, and the third is taxonomic congruence (Gatesy et al., 1999). For the data set of my thesis, the first and the second approaches were the most suitable. Both have advantages and disadvantages. For example, it is difficult to reach convergence in supermatrix approaches, which was observable in some of my BI analyses. Relatively incomplete fossils that were problematic to place, missing molecular data, and problems with optimisations of branch lengths are possible reasons for these difficulties (Geisler et al., 2011).

Gatesy et al. (1999) found that especially topologies of artiodactyls based on morphological data strongly contradict molecular topologies. Incongruence is very unlikely to occur evenly distributed within and among data partitions. The reason for this is that systematic data sets are finite and evolutionary processes are not stochastic (Gatesy & Baker, 2005). By running data partitions separately, a fortunate case of hidden support could remain unnoticed or interpretations of conflict and support could be distorted by isolating

character partitions depending on whether a parsimony or ML-based framework is applied. Therefore, several data partitions should be run separately and combined. Combination of partitions, markers, or genes can be highly beneficial in giving the ‘right’ answer (Gatesy & O’Leary, 2001; Gatesy & Baker, 2005). I ran all data partitions separately, in varying combinations, and all together, to investigate the phylogenetic signal and support.

Comparison of Morphological Data vs. Molecular Data

Generally, there are no good or bad characters or types of data in terms of utility. It depends strongly on the questions asked, which characters or combinations thereof may be useful for answering these questions (O’Leary, 1999; Bibi et al., 2012).

The advantages of molecular data are the easy retrievability, the potential to detect reticulation, and providing a time control when used for molecular dating. The disadvantages are that the rates of evolution most likely were not constant, which is the assumption in many approaches, a high level of homoplasy, despite the huge quantity of characters in large molecular data sets there are only few phylogenetic informative data (Groves, 2014). Further misleading effects of molecular data include long branch attraction, saturation, paralogy, base composition bias, codon usage bias, autocorrelation, lineage sorting, horizontal gene transfer, convergence, and rate heterogeneity (Lee & Palci, 2015).

Genotypic data partitions usually contain proportionally much more characters than osteological data and this increased number of characters assumedly is crucial for accuracy. On the other hand, osteological data partitions can be sampled for many more taxa, which partly cannot be sampled for molecular data (fossils) (O’Leary, 1999). The majority of life on Earth is now extinct and only represented by morphological traits; not integrating morphology would mean ignoring the majority of organisms. Integrating fossils with their phenotypic data is the only possibility to investigate transitional forms, past diversity of taxa and of phenotypes. However, in order to have robust morphological phylogenies, apart from a meticulous morphologist, better models for morphological evolution (see below) are needed and methods for analysing combined data need improvement (Lee & Palci, 2015).

The homoplasy in morphology may be incongruent with the general molecular signal, but the historical signal in both types of data is congruent; therefore, morphology can increase the support when combined with molecular data (Lee & Camens, 2009). Several studies on combined data sets demonstrated that there often was empirically less homoplasy in the morphological partition than in the molecular partition and the influence on the topology was substantial despite being outnumbered by molecular data (Baker et al., 1998; O’Leary, 1999; Nylander et al., 2004; Asher, 2007). Further homoplasy should not be generalised, because character(s) which may be homoplastic for a particular node may be informative for another (Groves, 2014). Including incomplete but short-branch taxa, such as slowly evolving species or close outgroups can minimise artefacts; the patchy distribution of missing data is less problematic than the limited number of species able to break long branches. Much more critical for the increase of phylogenetic accuracy than reduction of missing data is the selection of an appropriate model of evolution (Roure et al., 2013).

Morphology serves as an independent test for molecular data, because of the relative distance between phenotype and genotype and different evolutionary dynamics between

both types of data. Morphological characters represent the phenotype, where selection targets on. Therefore, the resulting topology could potentially inform us about the selective history of taxa (Groves, 2014). Fossils provide first appearance dates, which are important to time-scale molecular topologies and inferring morphological evolution. Their disadvantage is the incompleteness of the fossil itself and of the total fossil record (Groves, 2014; Lee & Palci, 2015).

As there is not much use for fossils in molecular analyses the fossil record has been largely neglected in these studies (Bibi et al., 2012). Only integrating phenotypic and genotypic data of fossil and living taxa and investigating how phenotypic features are linked with genotype, function, ontogeny and ecology will lead to a comprehensive understanding. New methods investigating (often internal) morphological structure, such as CT scanning and laser microscopy will largely expand the amount of morphological data in the future (Lee & Palci, 2015).

There have been debates particularly in mammalian studies about the phylogenetic utility of morphological data with people arguing against (e.g., Scotland et al., 2003) and arguing for its utility (e.g., Jenner, 2004; Wiens, 2004). Morphological characters still have relevance in times of genomic analyses and provide independent documentation of the molecular mammalian topology (Lee & Camens, 2009).

Within artiodactyl phylogenetic reconstructions there are some examples where morphological and molecular data are incongruent, most likely caused by convergent evolution of phenotypic traits and rapid cladogenesis (Marcot, 2007). Because of these convergences, the utility of morphological characters particularly in reconstructing ruminant phylogenies has been repeatedly questioned (Janis & Scott, 1987; Scott & Janis, 1987; Groves & Grubb, 1987; Gentry, 1994; Hassanin & Douzery, 2003; Gilbert et al., 2006).

Based on the principle of consilience, if the same topology is supported by different data sources, it is more likely that the topology is ‘correct’. The resulting phylogeny should reflect the consilience of biological evidence at all scales (Bibi et al., 2012).

An example for consilience of two (or three) types of data is the systematic position of *Hydropotes inermis* and whether its absence of antlers is a primary or secondary condition. So far morphological character provided little insight into that matter, however, molecular data consistently place it as the sister taxon to *Capreolus*. This position has also been found in a phylogenetic analysis based on male vocal behaviour (Cap et al., 2008). This position is supported by my molecular topologies and by several morphological topologies. Thus, the sister taxon relationship between *Hydropotes* and *Capreolus* was reconstructed based on three different data types.

In my work I intended to incorporate morphological and molecular data with their advantages and disadvantages. Combining different data types helped to investigate the systematic relationships of cervids under different aspects. The separate analyses of the different data sets further provided detailed insights into the potential of the respective data to solve systematic relationships. Some areas of the morphological topologies were congruent with the molecular topologies, some were not. However, the support of the morphological topologies did not contradict the molecular hypotheses.

Models of evolution. Modelling morphological characters is far more complicated than modelling molecular characters. Molecular characters consist of 4 states, A, C, G, T, which all mean the same throughout the matrix. Whereas in morphology each character can have 2–n character states. All these states mean something different for each character, i.e., coding 0 in character X is not equal to coding 0 in character Y. Additionally, the rates of change are different for each character and can be highly variable among characters. So far, there is no appropriate evolutionary model for morphological characters in model-based approaches such as BI and ML (O'Reilly et al., 2016). The only model of morphological evolution, which is widely used in model-based phylogenetic algorithms (BI, ML), is the Markov k (Mk) model by Lewis (2001). By simulating Brownian motion it attempts to approximate morphological evolution; its efficiency, however, has not been empirically tested thoroughly. It is not fully understood how the standard models of molecular evolution (e.g., HKY, GTR) translate variable rate frequencies and substitution rates to morphological data (Spencer & Wilberg, 2013).

Although topologies from model-based approaches, particularly ML, are typically better resolved than strict consensus topologies from parsimony analysis, which was also observed in my analyses, this does not necessarily mean that the better resolution is meaningful. The apparently better resolution may simply be a result of an incorrect model of morphological evolution (Spencer & Wilberg, 2013).

Comparison of mitochondrial vs. nuclear vs. total evidence topologies

Compared to single copy nuclear DNA the nucleotide substitution rate is about 5–10 times higher in maternally inherited mitochondrial DNA. This provides enough variation within and between species to be useful to reconstruct phylogenies on genus, species and subspecies level (Lan et al., 1995). Nuclear DNA markers are considered as slowly evolving genes, while mitochondrial DNA markers are considered as rapidly evolving genes Gilbert et al. (2006). Because of some characteristics of mitochondrial DNA, such as easy isolation, maternal clonal inheritance, relatively small size, existence of single genotypes in individuals and the relatively rapid rate of sequence evolution, it is a popular marker in molecular phylogenetic reconstructions. The estimated rate of evolution for vertebrate mitochondrial DNA is about 1–2 % per 1 my (Cronin, 1991). Particularly, *Cytb* is a remarkably suitable marker for resolving artiodactyl relationships given a dense taxon sampling (see Chapter 3).

Because closely related species are likely to share polymorphic alleles from a common ancestor, it is crucial to take multiple gene trees and intraspecific variation into account when inferring species trees based on molecular data (Cronin et al., 1996). It was demonstrated that combining mitochondrial and nuclear markers increases robustness of higher hierarchical cervid clades (Randi et al., 1998). Comparing molecular topologies with morphological topologies, it was found that topologies resulting from nuclear markers often agree with morphology, but often contradict topologies resulting from mitochondrial markers (Bibi, 2014). This shows that nuclear markers are indeed important and should be sequenced for a broader range of taxa than is available to date. Particularly in ruminant systematics incorporating more nucDNA will help to test relationships based on mtDNA (Bibi, 2014).

There are only few previous cervid phylogenies based on nuclear markers; the *Lalba*

and *Prkci* topologies in Gilbert et al. (2006) do not contradict my topologies of the same markers (Figs 5.2, 5.3). The *Csn* topologies (MP) in Cronin et al. (1996) differs in the position of *Muntiacus reevesi* to my topologies (Fig. 5.1). Analyses of nuclear markers have the potential to characterise the distribution of genetic variation (particularly in the case *Rucervus eldii*) (Balakrishnan et al., 2003). Combining and interpreting nuclear and mitochondrial markers can help to uncover recent hybridisation events, as in *Elaphurus davidianus*, which takes up different positions when analysed with mitochondrial markers compared to nuclear markers (e.g., Figs 5.6, 5.8).

Comparison Node vs. Tip dating

The first molecular divergence time estimate analyses were undertaken by (Zuckerkandl & Pauling, 1962). Molecular node dating is the most widely used method to estimate divergence times. Despite its extensive valuation and usage, node dating has some disadvantages: the initial topology does not contain temporal information, which is vital when the fossil plesiomorphic and apomorphic (i.e., conflicting) characters are excluded, potential relevant morphological information is excluded, highly fragmentary fossils with doubtful affiliations could be used for calibrations of several different nodes, and while the oldest fossil can be used to set an objective minimum age, using the oldest fossil to set the maximum age is rather subjective (Lee & Palci, 2015).

In previously published molecular dating analyses the lack of explicit explanations and justifications of the age and systematic position of the fossils used for calibration is a huge problem, which should be solved by adhering to the guidelines given by Parham et al. (2012) for best practices justifying fossils as temporal calibrations. Following these five key points when selecting a fossil for calibration will lead to more credible calibrations and more reliable divergence time estimates. Here, these key points were addressed where possible (Tabs 5.1, B.2).

Tip or total evidence dating was originally developed to calibrate shallow, i.e., not deep time evolutionary trees, mainly of viruses represented by RNA. TED analyses perform and calculate the phylogenetic tree and the dating simultaneously; during the phylogenetic analysis the stratigraphic age is explicitly incorporated in the analysis using appropriate likelihood-based clock models and substitution models on the molecular and morphological data. The resulting topologies display branch lengths and divergence time estimates. The peculiarity of tip dating is that the divergence ages are maximally consistent with both the ages of the fossils and the rates of morphological evolution, because all variables are co-estimated (Lee & Palci, 2015).

Because tip dating has not been sufficiently empirically tested, it remains a not yet robust method. However, it potentially overcomes the problems of node dating (see above) by considering the fossils (and dates) while inferring the phylogeny, the morphological information and divergence time estimates are integrated, potential systematic uncertainties of fossils are accommodated, no age maxima and distributions, which can be subjective, are required (Lee & Palci, 2015).

The three ND analyses here resulted in comparable divergence time estimates, while the TED analysis estimated younger dates particularly for the origination of the subfamilies

and tribes (Fig. 5.15). An advantage of the TED analysis is that the fossils could be incorporated. They appeared in the temporal sequence as in the fossil record and were assigned to subfamilies and tribes. These affiliations are in congruence with most of the SFA, EPA and TE analyses. The different divergence time estimates of both approaches should be interpreted slightly differently. While the ND estimates presumably refer to the divergence of the two (or more) terminal taxa including all their extinct ancestors until their last common ancestor, TED estimates indicate the ages of the divergence of the actual terminal taxa without including all extinct ancestors. This needs to be further tested in the future. Both estimates provide useful information concerning the timing and origination of taxa.

5.4.2 Systematics of Ruminant Families

Despite decades of research on this subject, there is still no consensus on the systematic relationship of the six ruminant families (see Chapter 1). Also, the relationships among the four pecoran families have been proven to be difficult (Kraus & Miyamoto, 1991; Hassanin et al., 2012). Particularly, the position of Moschidae remains problematic. Hassanin & Douzery (2003) and Price et al. (2005b) presented an overview of the systematic relationships of ruminants dating back to 1934. The position of Antilocapridae was also variable. These two taxa have always been difficult to place. Only relatively recently moschids were recognised as a separate family and not a subfamily within Cervidae (Corbet & Hill, 1980; Leinders & Heintz, 1980). Moschidae now usually are considered to be closely related to Cervidae or Bovidae (Price et al., 2005b).

In the morphological analyses of Hassanin & Douzery (2003), Moschidae, Cervidae and Bovidae form a trichotomy and Giraffidae and Antilocapridae are unresolved sister taxa to that clade. The separate MP analyses of seven molecular markers in the same study revealed systematic relationships as in most other recent analyses with Bovidae and Moschidae as sister taxa, then Cervidae, Giraffidae, Antilocapridae and Tragulidae as the sister taxon to all of them.

In Randi et al. (1998) Cervidae was the sister taxon to Antilocapridae and Giraffidae, which form a clade, two clades of Bovidae were placed between Tragulidae and all other taxa. In both recent supertree analyses by Hernández Fernández & Vrba (2005); Price et al. (2005b) Moschidae was the sister taxon to Cervidae, and Bovidae was the sister taxon to both of them. Antilocapridae and Giraffidae formed a clade, this clade was placed between Tragulidae and the other ruminants. Similarly, Moschidae was the sister taxon to Bovidae in Gilbert et al. (2006); this clade was in an unresolved position with Cervidae and Antilocapridae. In Kuznetsova et al. (2005) Cervidae was the sister taxon to Bovidae with Moschidae as the sister taxon to both of them. Giraffidae was the sister taxon to all of them and Antilocapridae was placed between the tragulids and all other ruminants.

First studies on nuclear DNA (e.g., κ -casein) resulted in similar systematic relationships. Monophyly was supported for the ruminant families. Giraffidae were found to be the sister taxon to either Cervidae or a Bovidae-Cervidae clade and Antilocapridae were the sister taxon to the Bovidae-Cervidae-Giraffidae clade (Cronin et al., 1996). While Moschidae were found to be more closely related to Cervidae based on behavioural characters

(Cap et al., 2002).

Most recent molecular studies relatively consistently showed that the clade consisting of Moschidae plus Bovidae was the sister taxon to Cervidae, which was the sister taxon to Giraffidae, then Antilocapridae; Tragulidae was the sister taxon to all of them (Kuznetsova et al., 2005; Marcot, 2007; Agnarsson & May-Collado, 2008; Hassanin et al., 2012).

Particularly inclusion of fossils has been found to overturn systematic relationships within ruminants, for example placing Moschidae as sister to the remaining Pecora; therefore further work is needed to investigate the impact of inclusion of fossil taxa (Agnarsson & May-Collado, 2008; O’Leary & Gatesy, 2008)

In the molecular topologies presented here the systematic relationships among the six ruminant families varied a lot. Most variation was observed in nuclear markers; Cervidae was sometimes unresolved as the sister taxon to Antilocapridae, Giraffidae and Bovidae, with Moschidae as the sister taxon to all of them. Most often, however, Moschidae and Bovidae were sister taxa to each other and as such the sister taxon to Cervidae with Antilocapridae and Giraffidae as sister taxa to that clade, either unresolved or as clade.

In some of my mitochondrial analyses Antilocapridae and Giraffidae were sister taxa to each other with Bovidae as the sister taxon; that clade was the sister taxon to Cervidae, and Moschidae was the sister taxon to all of them. In other mitochondrial and the combined molecular analyses Antilocapridae was the sister taxon to Cervidae, while Bovidae and Giraffidae formed a clade as the sister taxon to them and Moschidae was the sister taxon to all of them. Alternatively, Giraffidae was the sister taxon to Bovidae with Moschidae as the sister taxon to them; that clade was the sister taxon to Cervidae, and Antilocapridae was the sister taxon to all of them.

In my TE analyses Antilocapridae and Giraffidae formed a clade, which was the sister taxon to Bovidae and Moschidae was the sister taxon to all of them. This clade was placed between most Miocene and all other cervids. The MP TE analysis placed Moschidae as the sister taxon to Cervidae with Bovidae as the sister taxon to them; Giraffidae was placed between Antilocapridae and all other taxa. In the BI TE analysis, relationships among non-cervid ruminants were largely unresolved.

This demonstrates that the supposed consensus about the systematic relationships among ruminant families is an artefact of repeatedly re-analysing identical data sets with similar parameters. More and different types of data are needed to solve this problem in a more sophisticated and consistent way. Especially Cervidae is one of the ruminant families in need of more intensive phylogenetic research as highlighted by Price et al. (2005b), particularly because of the potential implications for conservation in some genera (i.e., *Cervus*, *Mazama*).

Cervidae and particularly Bovidae are the most diverse and successful of the six ruminant families today (Geist, 1998; Mattioli, 2011). Moschidae and especially Giraffidae and Antilocapridae most likely had their peak in diversity and success in the past based on fossil evidence.

Molecular divergence time estimates suggested that the five extant pecoran families each originated in the early Oligocene (32.0–28.1 mya) (Hernández Fernández & Vrba, 2005). Particularly estimates based on transversions suggest similar divergence times and an origination at around the same time, which is consistent with the sudden, contempo-

aneous appearance of pecorans in the fossil record around 21–18 mya (Ginsburg, 1988; Kraus & Miyamoto, 1991). Subsequently, cervid and bovid subfamilies and tribes began to differentiate in the early Miocene and gave rise to the extant subfamilies of cervids and bovids (25.4–13.5 mya) (Hernández Fernández & Vrba, 2005).

5.4.3 Extant Cervidae

The strength of current molecular cervid systematics is that many clades above genus level are consistently recovered by different data sets and show that higher hierarchical systematic relationships are stable and well supported. Many taxa at genus- and/or species-level are also stable and are consistently placed on the same positions in topologies based on various molecular data sets.

However, even though molecular data contributed to delimiting cervid clades and helped understanding the morphological evolution, some nodes remain unresolved or unstable. This makes it difficult to reconstruct the biogeographic history of the family, especially for the American cervids and concerning their colonisation of South America Gilbert et al. (2006).

In the morphological topologies shown in Chapter 3 Cervidae usually form a clade; in almost all cases some or all non-cervid ruminants are included in that clade. Other cervid subclades are usually not recovered as monophyletic. Often the majority of taxa of the subclades form a clade with a few other taxa scattered across the topology.

In my molecular and combined topologies, apart from a very few exceptions, Cervidae, Capreolinae, and Cervinae are monophyletic; Cervini, Muntiacini, Odocoileini including *Rangifer* most often are monophyletic, too. The unstable position of Capreolini and Alceini questions the monophyly of Capreolinae.

Various hypotheses of the intra-cervid systematic relationships have been published in the last decades. While in earlier studies up to six subfamilies of Cervidae have been recognised (Ouithavon et al., 2009 and references therein), the family Cervidae now is usually classified into two subfamilies, Capreolinae and Cervinae, and six tribes, Cervini, Muntiacini, Capreolini, Alceini, Odocoileini, and Rangiferini (which is sometimes included in Odocoileini) (e.g., Gilbert et al., 2006). The latter classification is supported by classical morphological concepts and molecular evidence. In some studies Muntiacini is considered as a subfamily (e.g., Cronin et al., 1996; Randi et al., 1998; Kuznetsova et al., 2005; Marcot, 2007). The evolutionary and taxonomic relationships among Capreolinae are largely enigmatic; there is, however, consensus about the split of ‘Old World’ Capreolinae, i.e., Capreolini, which associate with the holarctic Alceini, and the ‘New World’ Capreolinae, Odocoileini, which associate with the holarctic Rangiferini (Randi et al., 1998; Grubb, 2000; Hernández Fernández & Vrba, 2005; Kuznetsova et al., 2005).

In 2002 Prothero & Schoch hypothesised that *Muntiacus* and *Hydropotes* are primitive relicts of the Miocene, which has now widely been proven to be very unlikely by molecular and morphological evidence. Some studies suggested that three subfamilies of Cervidae (Cervinae, Muntiacinae, Capreolinae) form a clade and that *Hydropotes inermis* is the sister taxon to that clade based on phylogenetic reconstructions using morphological and palaeontological data (Miyamoto et al., 1990). However, more recent studies and my phylo-

genetic reconstructions based on different data types demonstrated that this is not the case. Morphology and physiology of the antlers and the fossil record suggested that Muntiacini is the sister group of the other two subfamilies (Bubenik, 1990; Azanza, 1993a). Similarly, in Marcot (2007) Capreolinae and Cervini were sister taxa with Muntiacini as the sister taxon to both of them. In Agnarsson & May-Collado (2008) one clade of Cervini was the sister taxon to Muntiacini, Capreolini is the sister taxon to both of them. Odocoileini plus *Rangifer* was placed between that clade and the second Cervini-clade. In the more recent literature, most commonly Cervidae split into Capreolinae and Cervinae, with Muntiacini and Cervini as reciprocally monophyletic sister groups based on morphological and molecular data (Groves & Grubb, 1990; Miyamoto et al., 1990; Cronin et al., 1996; Randi et al., 1998, 2001; Hassanin & Douzery, 2003; Kuznetsova et al., 2005; Price et al., 2005b; Gilbert et al., 2006; Hughes et al., 2006; Ouithavon et al., 2009; Hassanin et al., 2012). In the supertree analysis of Hernández Fernández & Vrba (2005) *Hydropotes inermis* was placed as the sister taxon to all other cervids.

The node calibration of 20 ± 2 mya for Cervidae has been used in several previous studies (Douzery & Randi, 1997; Randi et al., 1998, 2001; Hassanin & Douzery, 2003; Ludt et al., 2004; Gilbert et al., 2006) and is based on the first fossil records of antlers in the early Miocene of Europe (see Chapter 2). According to Randi et al. (1998) the split of Cervini, Muntiacini, and Capreolinae occurred in the middle Miocene (16.8–13.6 mya), which is comparatively old. Bubenik (1990) suggested that Muntiacinae appeared in the Late Miocene (11.1–5.3 Ma), and Di Stefano & Petronio (2002) considered the late Miocene *Cervocerus novorosiae* as the most primitive member of the Cervini. In Hassanin & Douzery (2003) the divergence time estimates of Cervidae was 20.1–17.2 mya, of the *Cervus*-*Muntiacus*-split was 13.8–10.1 mya, of Capreolinae was 16.2–13.4 mya, of the *Hydropotes*-*Capreolus*-split was 10.3–6.7, and of the *Rangifer*-*Odocoileini*-split was 11.5–6.6 mya. In my analyses, the Cervinae-Capreolinae-split was estimated to range between 18.2–17.48 mya in the ND approaches, and was 6.76 mya in the TED.

Cervini

In my nuclear topologies, Cervini usually were monophyletic sometimes also including muntiacine species (Figs 5.1–5.6). In the mitochondrial and combined nuclear topologies Cervini were always monophyletic (Figs 5.7–5.11). The systematic relationships in the TE topologies were similar to the molecular topologies, but Cervini were not always monophyletic and sometimes mixed with fossil cervids (Figs 5.12–5.14). In my ND analyses the split of Cervini was between 13.5 and 13.2 mya, while it is 2.4 mya in the TE analysis (Figs 5.16–5.19). Similarly to my ND results, Douzery & Randi (1997) estimated that the Cervini diverged from Odocoileini between 14.4 and 10.6 mya. Genetic calibrations are found to be congruent with the fossil record by some (e.g., Geist, 1998) and incongruent by others (e.g., Gilbert et al., 2006). This is partly due to the different view of which fossils can actually be affiliated to the extant representatives.

Even though systematic relationships within Cervini seemed to be solved since the classic work of Brooke (1878) and have been considered to be much less controversial than for example in Odocoileini, comparison of previous studies with differing taxon sampling and

comparison of topologies based on different types of data, as in my work, shows that there are still many uncertainties. Difficulties of determining phylogenetic relationships within Cervini were presumably caused by studying fossil and extant material independently and using heterogeneous and/or not enough characters (Groves & Grubb, 1987; Meijaard & Groves, 2004; Groves, 2006).

Recent molecular studies including or focusing on Cervini provided similar results, in which Cervini split into two clades, one consisting of *Axis* and *Rucervus*, the other consisting of *Cervus*, *Rusa*, *Rucervus*, *Elaphurus*, and *Dama* (Randi et al., 1998, 2001; Meijaard & Groves, 2004; Pitra et al., 2004; Hernández Fernández & Vrba, 2005; Gilbert et al., 2006; Hughes et al., 2006; Marcot, 2007; Ouithavon et al., 2009; Hassanin et al., 2012). The relationships within the subclades vary slightly depending on the taxon and character sampling. In contrast to almost all other studies, Cervini were not monophyletic in Agnarsson & May-Collado (2008). In the two topologies published by Kuehn et al. (2005) *Cervus* appeared polyphyletic and *Megaloceros giganteus* was nested within one of the *Cervus*-clades. In the topology of Marcot (2007) *Megaloceros giganteus* was the sister taxon to all cervine taxa. While in the topology of Pfeiffer (2002) *Cervus elaphus* and *Cervus nippon* were sister taxa to each other and *Megaloceros* was the sister taxon to them. The controversial systematic position of *Megaloceros giganteus* was supported in some of my analyses, particularly in the TED analysis.

There has been a long ongoing discussion about the genus and subgenus status of cervine taxa. In this study and in most of the recent literature (e.g., IUCN, 2016; Mattioli, 2011) six genera were distinguished: *Axis*, *Cervus*, *Dama*, *Elaphurus*, *Rucervus*, and *Rusa*. Often *Przewalskium* is listed as the seventh separate genus; however, extensive morphological investigation did not find enough difference to retain a separate genus status (pers. obs.; see below). *Elaphurus*, *Rucervus*, and *Rusa* are often considered as subgenera, but have many morphological distinctive features that justify separate genera (pers. obs.).

Randi et al. (2001) concluded from earlier molecular analyses, i.e., restriction fragment length polymorphism (RFLP) analyses of mtDNA (Cronin, 1991), allozyme electrophoresis (Emerson & Tate, 1993), κ -casein sequences (Cronin et al., 1996), and based on their own mtDNA analyses that *Elaphurus* is nested within *Cervus*, and should therefore be affiliated to *Cervus* for the sake of monophyly. *Rusa* was not recovered as monophyletic in Randi et al. (2001), therefore only three genera, *Axis*, *Dama* and *Cervus* were accepted.

Pitra et al. (2004) applied the 5 mya criterion for Cervinae classification and concluded that *Axis* (without *Hyelaphus*), *Dama*, and *Rucervus* (referring to *Rucervus duvaucelii* and *Rucervus schomburgki*) should be retained as genus (not subgenus) and that the remaining cervine taxa should be assigned to the genus *Cervus*. Further it is suggested that the Eld's deer may be separated as the subgenus *Panolia* and the David's Deer may be separated as the subgenus *Elaphurus*. All other species should be retained in the (sub)genus *Cervus* (Pitra et al., 2004). However, Gilbert et al. (2006) and Hassanin et al. (2012) similarly suggested that *Elaphurus davidianus*, *Przewalskium albirostris*, *Rucervus eldii*, and all species of *Rusa* should be classified as *Cervus*. Meijaard & Groves (2004) refer to *Rusa*, *Rucervus*, *Przewalskium*, *Hyelaphus* as subgenera, but later suggest that either *Elaphurus* should be included as subgenus within *Cervus* or that *Cervus* should be partitioned into several genera, as it is the case in most recent studies.

The integration of morphologically clearly distinct genera (pers. obs.) into *Cervus* just to make a clade monophyletic is not a scientific solution to potential problems with polyphylies. Here, it has been shown that all six cervine genera are distinct enough to justify their genus status, based on morphology and in most cases also on molecular data. The apparent polyphyly within *Rucervus* in mitochondrial analyses is an issue that needs further investigation.

***Axis*.** In almost all topologies *Axis* species formed a clade; *Axis axis* and *Axis porcinus* are the most commonly sampled species; molecular data is available for *Axis kuhli* (*Cytb*) but so far, the taxon was only included together with *Axis calamianensis* in the supertree analysis of Hernández Fernández & Vrba (2005) and the study of Meijaard & Groves (2004). *Axis calamianensis* still lacks molecular data. *Axis* was not monophyletic in some studies (Pitra et al., 2004; Marcot, 2007; Agnarsson & May-Collado, 2008). This is most likely caused by re-analysing the same misidentified sequences (see discussion in Gilbert et al. (2006)).

In my analyses *Axis* normally formed a well supported clade. *Axis axis* was always the sister taxon to a clade of the smaller *Axis* species, i.e., *A. porcinus*, *A. kuhli* (and *A. calamianensis*). Based on craniometrics and morphological similarities, *Axis kuhli*, *Axis calamianensis*, *Axis porcinus* were considered to be closely related and distinct from *Axis axis* (Meijaard & Groves, 2004). This constellation was supported by my molecular and combined topologies. Because of the similar morphology, size and habitus of the three smaller *Axis* species, they are often put into the (sub)genus *Hyelaphus* (Grubb, 1990; Meijaard & Groves, 2004; Hernández Fernández & Vrba, 2005; Groves, 2005; Groves & Grubb, 2011). Ouithavon et al. (2009) suggested to maintain *Axis porcinus* for the hog deer and that all other species should remain in the genus *Cervus*. The three smaller *Axis* species inhabit tall grassland except for *Axis kuhli*, which is found in not marshy, low-lying grasslands. *Axis axis* is more adapted to open landscape and ecotone regions; it is also more gregarious than the other three species (Meijaard & Groves, 2004).

All *Axis* species are more similar to each other than to other cervid species, however, depending on the species concept used, differences might be significant enough to justify two different genera. In most of the topologies here *Axis* was most closely related to *Rucervus*; *Rucervus eldii* in the nuclear analyses, *Rucervus duvaucelii* (and *Rucervus schomburgki*) in the mt and combined analyses. However, this is not the case in analyses using the misidentified *Axis porcinus* sequence (Pitra et al., 2004) and the supertree analyses (Hernández Fernández & Vrba, 2005).

In my ND analyses the split of the *Axis*-clade from other cervids was estimated between 8.6 and 3.76 mya, while in the TED analysis this split was 1.57 mya. Gilbert et al. (2006) came to similar results: 8.7–5.5 mya (ND), while others estimated older dates: 12.5–9.5 mya (Randi et al., 2001; Meijaard & Groves, 2004). The split of *Axis axis* from its congeners was estimated to have been between 2.94 and 1.78 mya in my ND analyses and 0.86 mya in my TED analysis. Gilbert et al. (2006) estimated this split to 2.6 mya, which lies in the range of the ND estimates of my analyses. This split was dated to the early Pliocene in Meijaard & Groves (2004), while the split of *Axis* from other cervids was dated to the late Miocene in this study. Because of the non-monophyly of the taxon in Pitra

et al. (2004) interpretations from their divergence time estimates are difficult to interpret. The split of *Axis* and *Rucervus* was dated to around 5 mya. In Di Stefano & Petronio (2002) the intra-*Axis* split is estimated to 1.5 mya based on appearances on Java, where the first *Axis* fossils are known from the early to mid Pleistocene (Meijaard & Groves, 2004). The data in Meijaard & Groves (2004) further suggested that *Axis calamianensis* diverged from *Axis porcinus* and *Axis kuhli* before the latter two separated from each other.

Cervid fossils from the late Pleistocene and early Holocene are common on Palawan island, but are rare afterwards and disappear in the late Holocene. The smaller fossil remains are thought to belong to *Axis calamianensis*. Palawan was presumably colonised during the glacial maxima of the last 500 ky (Piper et al., 2011).

‘Cervocerus’ novorossiae was considered as the ancestor of all *Axis*, with *A. shansius* as the descendant (Di Stefano & Petronio, 2002). *Axis porcinus* was considered as a recent split from *Axis axis* or as an early split in early Pliocene; in their study, *Axis lydekkeri* was on the lineage to *Axis axis*, while *A. punjabensis* was an earlier branch off of this lineage (Di Stefano & Petronio, 2002).

Cervus. *Cervus elaphus* is the most widespread and best studied deer species. Ludt et al. (2004) listed up to 22 known subspecies while Groves & Grubb (2011) listed 20 species of *Cervus* sensu strictu (excluding the five *Rusa* species). However, Groves (2006) critically pointed out to investigate, whether the differences among *Cervus* subspecies are genuine or whether they result from sequencing inadequately sourced and/or mislabelled specimens. Knowledge about the provenance of the sampled taxa is crucial.

Cervus elaphus was the sister taxon to *Cervus nippon* in Lister (1984) and Randi et al. (1998), while *Cervus nippon* was the sister taxon to *Cervus canadensis*, *Rusa* and *Cervus elaphus* were the sister taxa to them or *Rusa* is positioned inbetween in Randi et al. (2001), Pitra et al. (2004), and Hughes et al. (2006). *Cervus albirostris* was the sister taxon to all other *Cervus* in Hernández Fernández & Vrba (2005), while in Marcot (2007) *Cervus albirostris* was the sister taxon to *Cervus nippon*, *Cervus canadensis* was the sister taxon to both and *Cervus elaphus* the sister taxon to all of them; this was also the case in Hassanin et al. (2012), excluding *Cervus canadensis*. In Agnarsson & May-Collado (2008) *Cervus albirostris* was the sister taxon to *Cervus elaphus*, and *Cervus nippon* to both of them. The complexity of *Cervus* subspecies was demonstrated in Kuehn et al. (2005).

In the nuclear analyses here, *Cervus elaphus*, *Cervus canadensis*, and *Cervus nippon* were more closely related to each other than to *Cervus albirostris*. In my mtG analyses *Cervus albirostris* and *Cervus nippon* formed a clade and *Cervus elaphus* was the sister taxon to them; if *Cervus canadensis* was included it was the sister taxon to *Cervus nippon* (and *Cervus albirostris*, if there was a trichotomy) and *Cervus elaphus* was the sister taxon to all of them. This was also the case in my combined molecular and TE analyses. This difference between mt and nuclear genes may imply an ancient hybridisation event.

In my ND analyses the split of *Cervus* from other cervids was estimated between 7.19 mya and 1.86 mya; in the ND analysis based on mitochondrial markers only, the *Cervus-Rusa*-clade split from the other cervids at 7.53 mya. In the TED analysis this split was estimated to be at 0.96 mya. The first split within *Cervus* was between 4.88 and 1.32 mya

in my ND analyses, and 0.71 in my TED analysis.

In the literature the split of *Cervus* from the other cervids was dated to 3.5 mya Pitra et al. (2004), 6.8–4.3, 3.7–2.3 mya and 1.8 mya in different approaches of Gilbert et al. (2006), between 10.2 and 6.8 mya (Meijaard & Groves, 2004), 7.6–6.1 mya (Ludt et al., 2004), between 10.5 and 7.9 mya (Randi et al., 2001), and 8.4 mya (Lorenzini & Garofalo, 2015).

The main evolutionary lineages within *Cervus* diverged in the Pliocene (Randi et al., 2001; Meijaard & Groves, 2004). The intra-*Cervus* split was dated to about 1.5 mya in Gilbert et al. (2006). Douzery & Randi (1997) state that divergences within Cervinae occurred from the Miocene/Pliocene (7.1–3.3 mya within *Cervus*) to the Plio-Pleistocene (2.5–0.4 mya within *Cervus elaphus*). Other sources state that the subspecies within *Cervus elaphus* diverged between 2.5 and 0.4 mya (Meijaard & Groves, 2004). The split into the eastern and western clade was dated to 5.9 mya (Lorenzini & Garofalo, 2015), 7 mya (Randi et al., 2001; Ludt et al., 2004), and to about 0.80 mya (Kuwayama & Ozawa, 2000). Lorenzini & Garofalo (2015) stated that the split of *Cervus elaphus* occurred at 4.0 my and the split of *Cervus nippon* and *Cervus canadensis* occurred 4.3 mya. The latter split was estimated to 0.57 mya in Kuwayama & Ozawa (2000). The first fossil *Cervus nippon* fossils are at least 0.5 million years old (Cook et al., 1999) slightly corrected to around 0.41 mya by Kuwayama & Ozawa (2000). The divergence of *Cervus nippon* was dated to the late Pliocene (3.4–2.9 mya) and the divergence of *Cervus albirostris* from *Cervus elaphus* was dated to about 6.1–5.1 mya (Meijaard & Groves, 2004; Ludt et al., 2004). Other sources stated that the divergence time for *Cervus elaphus*, *Cervus canadensis*, *Cervus nippon*, and *Cervus albirostris* was less than 1 mya (Polziehn & Strobeck, 2002; Kuwayama & Ozawa, 2000).

It is assumed that ancestors of *Cervus* first appeared in Asia during the late Miocene after splitting from their sister lineage *Dama*. The ancestors of *Cervus* presumably occurred at the Miocene-Pliocene-boundary in central and western Asia from where they radiated after climatic and orogenic changes in the Pliocene (Di Stefano & Petronio, 2002; Gilbert et al., 2006; Lorenzini & Garofalo, 2015). *Cervus grayi* (1.3 mya) was considered as the last common ancestor of *Cervus nippon* and *Cervus elaphus* (Di Stefano & Petronio, 2002).

Cervus then further split into a western and eastern clade; both clades migrated almost synchronously, one westward towards the Middle East and then Europe, and the other eastward, respectively. This suggests that *Cervus canadensis* migrated eastwards and diverged from *Cervus elaphus* in the Mindel glacial; however, more recent studies show that there was a common ancestor already separated from the *Cervus elaphus* lineage of *Cervus canadensis* and *Cervus nippon*, which migrated eastward before both lineages split. The mountains surrounding the Himalayan region were assumed to have been the geographical barrier for this split (*Cervus elaphus* and the last common ancestor of *Cervus nippon* and *Cervus canadensis*) (Kuwayama & Ozawa, 2000). The first *Cervus elaphus* appeared in the early Günz glacial in Europe (Kurtén, 1968). The *Cervus nippon* sublineage diverged and migrated southward shortly afterwards, while *Cervus canadensis* dispersed northward. In the late Pleistocene Asian *Cervus canadensis* migrated into North America via Beringia with subsequent gene flow (Vislobokova, 2013; Meiri et al., 2014; Lorenzini & Garofalo, 2015). The Bering land bridge disappeared around 9000 years ago with rising sea levels

and the formation of the Bering Sea. Faunal exchange between American and North Asia (*Cervus canadensis*) ceased after this event (Ludt et al., 2004). The lack of genetic diversity between Asian and American wapiti supports this hypothesis (Kuwayama & Ozawa, 2000; Randi et al., 2001; Polziehn & Strobeck, 2002; Hassanin & Douzery, 2003; Lorenzini & Garofalo, 2015).

Because *Cervus* splits into clades which are partially not congruent with current (taxonomic) species delimitations, the separation of the western, European elaphoid cervid (*Cervus elaphus* s.str.) and the eastern, Eurasian and North American, wapitoid deer (*Cervus canadensis*) into two different species was repeatedly suggested (Randi et al., 2001; Polziehn & Strobeck, 2002; Ludt et al., 2004; Pitra et al., 2004; Lorenzini & Garofalo, 2015). Already Whitehead et al. (1972) and Cockerill (1984) stated that the differences between *Cervus canadensis* and *Cervus elaphus* are sufficient to justify two separate species. Further, a split into an Asian group and a North American group within *Cervus canadensis* was found (Kuwayama & Ozawa, 2000).

Groves (2003) stated that in addition to *Cervus canadensis* more *Cervus elaphus* subspecies, e.g., *wallichii* and *hanglu*, should be raised to species level. In Groves & Grubb (2011), where 20 *Cervus elaphus* subspecies are considered as separated species. Thus, taxonomy at the subspecific level remains uncertain. Discrepancies between morphological and molecular classification may be the cause (Meijaard & Groves, 2004). Although morphological characters in cervids are likely to be homoplastic, and are therefore potentially not the most reliable features in systematics (Lorenzini & Garofalo, 2015).

In most cases *Cervus canadensis* is more closely related to *Cervus nippon* and *Cervus albirostris* and *Cervus elaphus* forms the sister taxon to all of them (Kuwayama & Ozawa, 2000; Groves, 2006; Zachos et al., 2014). This contradicts results from traditional morphology, where *Cervus elaphus* and *Cervus canadensis* are usually sister taxa (Kuwayama & Ozawa, 2000). However, Polziehn & Strobeck (2002) state that the divergence of mtDNA noted for *Cervus nippon*, *Cervus canadensis*, and *Cervus elaphus* is congruent with geographical, morphological, and behavioural distinctions. My morphological analyses resulted in varying positions for the four *Cervus* species. All of them have a very similar cranial and dental morphology (pers. obs.).

Cervus nippon is monophyletic compared to other *Cervus* species (Cook et al., 1999). Several molecular studies found a consistent split within *Cervus nippon* into Japanese island and Japanese mainland/Taiwan sika (Kuwayama & Ozawa, 2000; Randi et al., 2001; Groves, 2006). The dispersal history of this species explains the recurring split; because landbridges formed repeatedly between Japanese islands and the Asian mainland, migration of mammals was facilitated. Presumably more than one invasion event onto Japanese islands led to distinct mtDNA lineages (Nagata et al., 1999).

Cervus albirostris is specialised to montaneous areas, i.e., east Tibetan plateau. It sometimes was the sister taxon to *Cervus canadensis* and *Cervus nippon* and sometimes it was considered to be more closely related to *Cervus nippon* (Polziehn & Strobeck, 2002; Liu et al., 2002; Groves, 2006), which is also confirmed in my analyses. In contrast to this, Flerov (1952) suggested that *Cervus albirostris* diverged from *Rusa* in the late Pliocene and Koizumi et al. (1993) considered it more closely related to *Rucervus*. However, all

recent molecular studies placed it closer to the *Cervus* species (Leslie, 2010). *Cervus albirostris* almost certainly evolved in temperate northern Eurasia; *Epirusa hilzheimeri* or *Eucladoceros* may have been its Pleistocene ancestors (Di Stefano & Petronio, 2002; Flerov, 1952; Zdansky, 1925; Geist, 1998; Grubb, 1990; Leslie, 2010).

The African and Sardinian red deer subspecies may represent relict endemic groups of an ancient African population (Ludt et al., 2004). Particularly, *Cervus elaphus barbarus* was potentially introduced by humans from Europe 8000 years ago (Leslie, 2010).

It is known that hybridisation between *Cervus nippon* and *Cervus elaphus* (mainly *Cervus elaphus* females and *Cervus nippon* males) occurs and that hybrids are fertile. Hybridisation may lead to extensive introgression (Zachos & Hartl, 2011). It was hypothesised that hybridisation may occur between *Cervus canadensis* and *Cervus nippon* where they are geographically in contact and that they may form a mosaic in mitochondrial gene trees, but this was not found in phylogenetic trees. Additionally, the hybridisation between these two species is less likely due to the body size difference (Groves & Grubb, 1987; Kuwayama & Ozawa, 2000).

All these studies on population genetics and subspecies of red deer are to be treated with caution, since they exclusively used mtDNA, which may artificially suggest relationships that are not reproducible when using paternal genes. Hybridisation could have occurred frequently in *Cervus*. My topologies suggested varying sister taxon relationships across the four *Cervus* species.

Dama. In almost all analyses here, both *Dama* species formed a clade, which was sister taxon to other Cervini. In the mitochondrial and combined molecular analyses, the clade was the sister taxon to all Cervini except the *Axis-Rucervus*-clade. My ND analyses estimated the split of *Dama* from other cervines to 13.52–4.69 mya, while my TED analysis estimated it to 1.94 mya. The split of both *Dama* species was estimated to 4.1–1.5 mya (ND) and to 0.87 mya (TED).

The divergence of *Dama* and *Cervus* was estimated to have happened in the late Miocene between 11.9 and 8.2 mya (Randi et al., 1998, 2001; Hassanin & Douzery, 2003; Meijaard & Groves, 2004; Hughes et al., 2006; Croitor, 2006a), 13.5–3.7 mya (Lorenzini & Garofalo, 2015), 12.6–7.6 mya (Ludt et al., 2004). Ludt et al. (2004) stated that these estimates correspond with the fossil record. In contrast to this Pitra et al. (2004) estimated the divergence to 5 mya. However, both date estimates are much older than the fossil record, in which the first certain *Dama* dates to the middle Pleistocene (Lorenzini & Garofalo, 2015). Di Stefano & Petronio (2002) suggested '*Cervus*' *perolensis* as a potential ancestor of *Dama* (1.3 mya); subsequently, the *Dama*-lineage with *Dama clactoniana* split into two lineages leading to *Dama dama* and *Dama mesopotamica* around 0.6 mya. Lister et al. (2005) estimated the split of *Dama dama* and *Dama mesopotamica* to about 700 kya.

Ludt et al. (2004) found that the calibration point of 1.6 mya (Kurtén, 1968) for the last common ancestor of red deer and fallow deer, was incorrect, because it was assumed that *Dama* first appeared in the Pleistocene, which resulted in a much higher (incorrect) substitution rate.

There have been two hypotheses about the split of modern *Dama* and megacerine

cervids. The first suggested that the entire clade originated recently and that the split happened after the divergence of early *Dama*-like forms, which is supported from the fossil record with first megacerines from 1.4 mya. The second suggested that the split of megacerine cervids and all *Dama* is older, which is supported by molecular data where the split of *Dama* and *Megaloceros* is dated between 5–4 mya (Lister et al., 2005).

Other sources speculate that the divergence of *Dama* and *Megaloceros* could have occurred much earlier at around 10.7 mya, which is long before the early *Dama*-like forms dispersed in Western Eurasia (Hughes et al., 2006; Croitor, 2014).

It is still controversial, which fossil is the first *Dama* species; therefore statements about the divergence time estimates of the *Dama* lineage and the *Dama*-*Megaloceros*-split vary a lot. More investigation of fossil specimens and revision of the taxonomy is needed to clarify these controversies.

Both *Dama* species are genetically divergent and distinct and form a clade with the fossil giant deer *Megaloceros giganteus* in almost all topologies, which has been found before (Randi et al., 2001; Lister et al., 2005; Hughes et al., 2006; Hassanin et al., 2012).

Elaphurus. In my nuclear analyses, *Elaphurus davidianus* was often, if only weakly supported, placed close to *Cervus*, while it was consistently placed as the sister taxon to *Rucervus eldii* in all mitochondrial, molecular combined, and TE analyses. In my morphological analyses it was placed closer to *Cervus* based on cranial characters and closer to *Rucervus* and *Rusa*, particularly *Rucervus schomburgki*, based on the dentition and the morphological combined data set. The ND approach estimated the split of *Elaphurus davidianus* from other Cervini between 9.78 and 3.29 mya, while my TED analyses estimated the split to 1.54 mya (Figs 5.16–5.19).

Already Lydekker (1898) found that ‘If antlers count for anything in classification – and it is almost impossible to deny that they do – the genus *Elaphurus* has nothing to do with any of the Old World Deer’. Not only the unique antlers without a brow tine, but also the overall morphology of *Elaphurus davidianus* is distinct from all other cervids (Emerson & Tate, 1993; Meijaard & Groves, 2004; Pitra et al., 2004); although some similarities to *Rucervus eldii* are stated (e.g., Meijaard & Groves, 2004), morphological scrutiny does not necessarily support that (Chapter 3).

The speciation of *Elaphurus* has been discussed as an ancient (late Pliocene or earlier) hybridisation event (Meijaard & Groves, 2004). Divergence time estimates based on mtDNA suggested a separation in the middle Pliocene (Pitra et al., 2004; Groves, 2006) and those of *Elaphurus* to the late Pliocene (3–2 mya) (Taru & Hasegawa, 2002), which is considerably later than 10.5–7.9 Ma (Meijaard & Groves, 2004). According to Taru & Hasegawa (2002) the oldest known fossils of the *Elaphurus davidianus* lineage are known from the late Pliocene or slightly earlier, while Ji (1985) state that the first certain *Elaphurus davidianus* dates from the mid Pleistocene.

Cervus canadensis or a closely related ancestor has been assumed as the male parent and *Rucervus eldii* or a very close ancestral relative as the female parent (Taru & Hasegawa, 2002; Meijaard & Groves, 2004; Pitra et al., 2004; Groves, 2006). The morphology of *Elaphurus* contains apomorphic character states and is not intermediate between its two parent taxa (Groves, 2014) (own observations). This phenomenon is called transgressive segregation and the new phenotypes may be favoured in the new hybridogenetic

population (Rieseberg et al., 1999; Groves, 2014). Both sexes of *Cervus elaphus* and *Elaphurus davidianus* can be hybridised in captivity producing fertile F1 offspring; hybridisation attempts with *Elaphurus davidianus* and *Rusa unicolor* were not successful (Tate et al., 1997; Meijaard & Groves, 2004).

Because of this hybridisation molecular phylogenetic analyses result in conflicting systematic positions as clearly shown in my analyses, but also in earlier studies. When analysing mtDNA, *Elaphurus davidianus* is consistently placed as the sister taxon to *Rucervus eldii* (Figs 5.7–5.9; Randi et al., 2001; Pitra et al., 2004). Electrophoretic patterns of 22 proteins and κ -casein DNA, and the karyotype placed *Elaphurus* closer to *Cervus* (Emerson & Tate, 1993; Cronin et al., 1996; Meijaard & Groves, 2004). Also, in my analyses of the nuclear markers, particularly in the nuclear ND analysis *Elaphurus* was closer to *Cervus* (Fig. 5.6).

The problem of hybrids in phylogenetics is their reticulating or anastomising evolutionary histories. They can show various character patterns, such as the phenotype of only one parent, combine characters of both parents or be intermediate or heterotic (McDade, 2000). This makes it difficult to place hybrids correctly in phylogenetic reconstructions and the special evolutionary history that lead to the hybridisation is rarely known. To get around this problem cautious testing of hypotheses is required either from morphology or different (maternal and paternal) organelles; however, if characters in the hybrid are strongly discordant to those of the parents, this could produce noise and obscure phylogenetic signal (McDade, 2000).

Because of known hybridisation of different deer species in the wild it is likely that there may be more cervine (or even cervid) taxa that originated via an ancient hybridisation event, which potentially complicates solving the systematic relationships (Groves & Grubb, 1987; Pitra et al., 2004). It is to date not clear whether other cervine lineages may also be of hybrid origin Groves (2006). More nuclear markers, particularly studies using Y-chromosome DNA are needed to further investigate the relationship of these cervid species (Groves, 2006).

Rucervus. The antler morphology of *Rucervus* species is unique among cervids; the more flexed skull and the smaller canines led to the assumption that *Rucervus* is more closely related to *Rusa* than to *Cervus*. This was partly supported in the nuclear analyses and the morphological analyses, while in the mitochondrial, molecular combined, and TE analyses *Rucervus* was polyphyletic with *Rucervus eldii* more closely related to *Elaphurus davidianus* and the other two more closely related to *Axis*. Based on this it was hypothesised that *Rucervus eldii* may represent a different evolutionary lineage than the other two *Rucervus* species (Meijaard & Groves, 2004).

Rucervus inhabits open woodland and tall grass of flood plains, swamps and swampy grasslands and is highly adaptive to new environments (Groves, 1982). Their teeth are uniquely folded indicating a specialisation for graminivory (Grubb, 1990; Meijaard & Groves, 2004) and provide useful morphological characters (Chapter 3).

Due to the unstable position of *Rucervus eldii* in dependence of *Elaphurus davidianus* (see above), it was sometimes put into a separate genus *Panolia* (Pocock, 1943; Groves, 2006). Since the first description in 1839 as *Cervus frontalis* it was renamed several times

as *Cervus eldi* McClelland (1841) or *Cervus (Rusa) frontalis* McClelland (1842), and eventually recognised as *Rucervus* by Thomas (1918) aligning it with *Rucervus duvaucelii* and *Rucervus schomburgki* (Angom & Hussain, 2013). It is now widely regarded as *Rucervus eldii* (Wilson & Reeder, 2005; Timmins et al., 2008; Angom & Hussain, 2013). This is also supported by my topologies, particularly the morphological topologies show the close relationship to the other two *Rucervus* species. The placement of *Rucervus eldii* separate from its two congeners in molecular topologies (especially mtDNA) is most likely artificially caused by the hybridisation of *Rucervus eldii* and *Cervus canadensis* in the past.

The last specimen of *Rucervus schomburgki* sadly became extinct in 1938. The first accounts on the species were by Blyth (1863), who noted the distinctive antler pattern. According to Gähler (1936), the geographical distribution of *Rucervus schomburgki* was restricted to Siam. It was assumed to be closely related to *Rucervus duvaucelii* and potentially interbreeding with *Rucervus eldii* in its natural habitat.

The earliest fossils of *Rucervus* date back to 2.9 mya (Azzaroli et al., 1988; Meijaard & Groves, 2004); similarly, Li et al. (1999) estimated the divergence between *Rucervus* and *Cervus* to 2.8–2.4 mya and Meijaard & Groves (2004) to 4.4–3.7 mya.

In my divergence time estimates, the split of *Rucervus eldii*, *Rucervus duvaucelii*, and *Rusa timorensis* was 3.3 mya and this clade split from *Axis* 4.87 mya in the nuclear ND analysis. The split of *Rucervus duvaucelii*, *Axis porcinus*, and *Axis axis* was at 8.61 mya and this clade was dated to have split 13.16 mya from the other Cervini in my mitochondrial ND analysis. In the same analysis, *Rucervus eldii* split 3.9 mya from *Elaphurus davidianus*. *Rucervus duvaucelii* split from *Rucervus schomburgki* 1.11 mya, *Rucervus* from *Axis* 3.76 mya, and this clade from other Cervini 13.3 mya in the combined ND analysis. In the same analysis, *Rucervus eldii* split from *Elaphurus davidianus* 1.29 mya. In my TED analysis *Rucervus duvaucelii* and *Rucervus schomburgki* split 0.53 mya, *Rucervus* and *Axis* 1.57 mya, while *Rucervus eldii* and *Elaphurus davidianus* diverged 0.59 mya.

Rusa. In most of my morphological analyses *Rusa* was more closely related to *Rucervus* (rarely to *Axis*). In the nuclear analyses here, it was close to *Rucervus* or within Cervini, while it was more closely related to *Cervus* in the mitochondrial, combined molecular, and TE analyses. When all four *Rusa* were included in the analyses *Rusa timorensis* and *Rusa unicolor* were sister taxa and *Rusa marianna* and *Rusa alfredi* were sister taxa.

Despite some new insights into the systematic relationships of *Rusa* (Chapter 4), uncertainties remain (Grubb & Groves, 1983). The diploid number of chromosomes, which is $2n=56-62$ in *Rusa timorensis* and *Rusa unicolor*, and $2n=65$ in *Rusa marianna* (Tab. 5.3) suggests that *R. timorensis* and *R. unicolor* form a clade and that this clade forms a sister taxon relationship with a clade consisting of *Cervus albirostris* and *Rucervus* (Leslie, 2011). *Rusa alfredi* and *Rusa marianna* share morphological similarities, and are distinct from the other two *Rusa* because of the overall smaller size of Philippine *Rusa* species. *Rusa unicolor* and *Rusa timorensis* from the mainland and Indonesia were considered to be more derived. *Rusa unicolor* may be the most derived, based on the low diploid no. $2n=60$, which is even lower in some *Rusa unicolor* subspecies (Groves & Grubb, 2011). Based on craniometrics *Rusa unicolor* and *Rusa timorensis* did not appear as similar as anticipated (Meijaard & Groves, 2004).

This hypothesis is in conflict to the fossil record and other hypotheses. The high similarity of *R. unicolor* to pliocervines, an extinct lineage of Pliocene cervids, led to the assumption that it is the most ancestral of the four extant rusine deer (Petronio et al., 2007; Leslie, 2011). ‘*Cervocerus*’ *novorossiae* was suggested to be the ancestor of *Rusa*, *Cervus albirostris* and *Dama* (and *Axis*, see above) diverging 5.9 mya. *R. elegans* was considered the last ancestor of living *Rusa* (Di Stefano & Petronio, 2002). Dong (1993) reports that *Rusa* appeared in China in the late Pliocene and that by the early Pleistocene five fossil species of *Rusa* existed. Several other *Rusa*-like species occurred in the Pleistocene of China (see Meijaard & Groves (2004) for exhaustive list). The first appearance of *R. unicolor* is recorded from the middle Pleistocene (Zong, 1987; Dong, 1993; Meijaard & Groves, 2004).

The oldest *R. timorensis* is reported from the late Pleistocene (Van Mourik & Stelmasiak, 1986; Dong, 1993) and suggested to have then dispersed south-eastwards to Taiwan and Java (Meijaard & Groves, 2004). Although *Rusa*-like deer were described from the upper Pliocene of Europe and west Asia (Schaub, 1941; Czyżewska, 1959), the Pliocene European cervids with similarities to *Rusa* (and *Axis*), ‘*Cervus*’ *philisi* and *Praeclaphus perrieri*, they were considered to be more likely an early/mid Pliocene lineage of *Rusa* or *Axis* that became extinct during the Pleistocene (Schaub, 1941; Heintz, 1970; Meijaard & Groves, 2004). *Rusa timorensis* is gregarious and adapted to open habitats (savannah), while the other three *Rusa* species are solitary and more adapted to thick vegetation (Geist, 1998; Meijaard & Groves, 2004).

In the literature the divergence of the *Cervus*-*Rusa*-clade was dated to 5.2–6.8 mya (Randi et al., 2001) or around 5 mya (Leslie, 2011). The split of *Rusa timorensis* and *Rusa unicolor* was estimated to 0.4 mya (Di Stefano & Petronio, 2002). *Rusa unicolor* split 6.71 mya from a clade including *Axis*, *Rucervus*, and *Rusa timorensis*, while *Rusa timorensis* split with *Rucervus eldii* and *Rucervus duvaucelii* 3.3 mya in my nuclear ND analyses. In the mitochondrial ND analysis here, *Rusa timorensis* and *Rusa unicolor* split 4.37 mya, and this clade and *Rusa alfredi* and other Cervini split 9.78 mya. *Rusa timorensis* *Rusa unicolor* split 0.91 mya from each other and split from *Cervus* 1.86 mya, *Rusa alfredi* and *Rusa marianna* split 1.02 mya and split from *Rusa* and *Cervus* 2.49 mya in my combined ND analysis. The TED estimated the divergence of *Rusa timorensis* and *Rusa unicolor* to 0.40 mya and this clade split from *Cervus* 0.96 mya, while *Rusa alfredi* and *Rusa marianna* diverged 0.54 mya and split from *Cervus* and *Rusa* 1.24 mya.

Leslie (2011) has developed a useful diagnostic key to the four *Rusa* species; all four species are allopatric and differ and vary in mass and size (morphocline). The consistent number of three tines on the antlers was considered as a plesiomorphic condition.

As suggested by Grubb (1990) and Groves (2003), *Rusa* is a distinct genus and not a subgenus of *Cervus*. The monophyly of *Rusa* has been controversial based on morphological and molecular evidence (Meijaard & Groves, 2004; Hernández Fernández & Vrba, 2005; Randi et al., 2001; Leslie, 2011); in my analyses *Rusa* is more often supported to be monophyletic than not.

Muntiacini

***Elaphodus*.** Among all cervids, *Elaphodus cephalophus* carries the smallest antlers, which are normally completely covered by the tufts (Leslie et al., 2013). Groves & Grubb (1990) considered *Elaphodus cephalophus* as the most primitive representative of living muntiacines. However, this is in contrast to the absence of fossils with such diminutive antlers.

Elaphodus cephalophus was always the sister taxon to the other muntiacine species in all my molecular and TE analyses, which is also widely supported in the literature (Wang & Lan, 2000; Hernández Fernández & Vrba, 2005; Agnarsson & May-Collado, 2008; Hassanin et al., 2012). In contrast, in Marcot (2007) *Elaphodus cephalophus* is the sister taxon to all cervids.

The first *Elaphodus* fossils are known from the Pleistocene of China, which were larger than *Elaphodus cephalophus*; therefore, the decrease in size can be considered as evolutionary trend in this species (Leslie et al., 2013). The split of *Elaphodus cephalophus* from muntjacs was dated to 4.8–3.4 mya in the literature (Leslie et al., 2013). The results from my dating analyses differ from this estimate. The split of *Elaphodus cephalophus* from *Muntiacus* was dated to 14.50–14.30 mya in my ND analyses, while this split was dated to 2.51 mya in the TED analysis.

***Muntiacus*.** In the morphological analyses muntiacine taxa were placed as the sister taxa to most other cervids or in an unresolved position. A clade including *Muntiacus truongsensis*, *Muntiacus vuquangensis*, *Muntiacus crinifrons*, *Muntiacus muntjak*, *Muntiacus reevesi*, and sometimes *Muntiacus atherodes* was supported. *Elaphodus cephalophus* and *Muntiacus feae* were more unstable and difficult to place. In the cranial analyses monophyletic Muntiacini were supported in the MP and ML analyses. In most combined analyses the muntiacine-clade is recovered, too, except for the BI analyses. In the MP analyses, Muntiacini were placed more closely related to other small cervids, such as *Mazama* and *Pudu*.

Skull measurements from *Muntiacus putaoensis* resemble *Muntiacus rooseveltorum* and *Muntiacus truongsensis*, but are different (qualitatively) from the sympatric *Muntiacus muntjak* and *Muntiacus crinifrons* (Groves & Grubb, 1990; Amato et al., 1999a). A unique morphological feature in *Muntiacus truongsensis* is that the upper canines in females are almost as long as in males (Giao et al., 1998). Groves & Grubb (1987) found that the general skull shape of *Muntiacus* is more similar to that of *Axis porcinus* than that of *Elaphodus*.

Muntiacini are poorly sampled for nuclear markers, mostly represented by only one species, up to four species in *Sry*. The position of muntiacines was once within Odocoileini, twice in an unresolved position, and twice within Cervini in my nuclear analyses. If there was more than one muntiacine species they formed a clade. In the combined nuclear analysis this clade is the sister taxon to Cervini.

Five to ten muntiacine species were sampled for mitochondrial markers and consistently formed a clade as the sister taxon to Cervini in all my mitochondrial, molecular combined, and TE analyses. A clade consisting of *Muntiacus crinifrons*, *Muntiacus feae*,

and *Muntiacus muntjak*, a clade consisting of *Muntiacus putaoensis*, *Muntiacus truongsensis*, *Muntiacus rooseveltorum*, *Muntiacus vuquangensis*, and *Muntiacus reevesi* were recovered in the mitochondrial and combined molecular analyses. *Muntiacus atherodes* was placed in a polytomy with these clades. In the TE analyses *Muntiacus reevesi* was placed between *Elaphodus cephalophus* and the other taxa, while the other four species of this clade remained monophyletic. The fossil *Muntiacus muntjak* was within the first clade of muntiacines and *Muntiacus atherodes* is the sister taxon to *Muntiacus feae* either within that first clade or as a separate polytomous clade.

In the recent literature, muntiacines have been included in phylogenetic reconstructions to a different extent (Randi et al., 1998; Wang & Lan, 2000; Randi et al., 2001; Pitra et al., 2004; Hernández Fernández & Vrba, 2005; Gilbert et al., 2006; Hughes et al., 2006; Marcot, 2007; Ouithavon et al., 2009; Hassanin et al., 2012). The systematic relationships within Muntiacini vary mostly depending on the taxon sampling, but do not contradict each other. They also did not contradict the results of my phylogenetic reconstructions of the taxon. Generally, the monophyly of Muntiacini (or Muntiacinae) uniting *Muntiacus* and *Elaphodus* has never been questioned (Gilbert et al. (2006)). All muntiacines share synapomorphies, such as long pedicles, facial crests, and bifurcating antlers (pers. obs.; e.g., Ma et al., 1991).

Euprox furcatus is often considered as the first representative of muntiacines (e.g., Bubenik, 1990), see also Chapter 3. The earliest fossil of the *Muntiacus* lineage is *Muntiacus leilaoensis* from Yunnan, China and was dated to the late Miocene 9–7 mya (Dong et al., 2004). It has been suggested that the extant *Muntiacus* species diverged 2–1 mya in the early to middle Pleistocene (Ma et al., 1986a; Leslie et al., 2013). Transverse and longitudinal river systems in times of glaciation caused geographic isolation and ecological disjunction, which resulted in different evolutionary pathways; the speciation of most modern muntjacs was most likely completed by the end of the Pleistocene (Ma et al., 1986a).

Ma et al. (1986b,a) stated that *Muntiacus crinifrons* and *Muntiacus rooseveltorum* derived from *Muntiacus reevesi*, whereas *Muntiacus feae* and *Muntiacus muntjak* were derived from a different lineage. They further state that *Muntiacus rooseveltorum* is not the result of a hybridisation of *Muntiacus muntjak* and *Muntiacus reevesi*. Groves & Grubb (1990) suggested that *Muntiacus rooseveltorum* is the synonym of *Muntiacus feae* and that *Muntiacus feae* is the sister taxon to *Muntiacus muntjak* and *Muntiacus crinifrons*. This is supported by most molecular studies and topologies of this thesis. It has been proposed that *Muntiacus atherodes* should be included in *Muntiacus muntjak* based on morphological evidence, because the holotype of *Muntiacus atherodes* is a subadult male without formed antler branches (Ma et al., 1986b). The two specimens investigated here were indeed subadult individuals with not yet fully developed antlers (pers. obs.). However, molecular topologies indicate a separate species status for *Muntiacus atherodes*; there are also differences in coat colour. Groves & Grubb (1990) stated that *Muntiacus atherodes* and *Muntiacus reevesi* were the most ‘primitive’ muntjac species, while Ma et al. (1986b,a) suggested based on their smaller size that *Muntiacus reevesi* and *Muntiacus feae* were the most ‘primitive’ and were possibly divided into ecological niches before the middle Pleistocene.

Several new muntiacine species have been discovered in the 1990s (Hernández Fernández & Vrba, 2005). In 1995 five to possibly six muntjac species were considered (*Muntiacus gongshanensis*, *Muntiacus crinifrons*, *Muntiacus feae*, *Muntiacus reevesi*, *Muntiacus muntjak*) (Lan et al., 1995) and in 1999 nine species of *Muntiacus* were known, *Muntiacus muntjak* has the most widespread distribution across Asia, while the other species are relatively restricted (Giao et al., 1998). The discovery of several new *Muntiacus* species in the Annamite mountain regions is remarkable; in some regions, there are up to three sympatric species of muntjacs (Giao et al., 1998). This species diversity is possible because in the Annamite mountains there are several geographically distinct habitats resulting from habitat mosaics and dispersal barriers. Less vagile species, particularly those adapted to insular montane forests, have been isolated by steep terrain. Fragmentation of evergreen forests during the Pleistocene created refugia for species adapted to these ecosystems. (Giao et al., 1998).

Reproductive isolation and ecological separation to some extent are prerequisite for stable sympatry within mammals; climatic fluctuations during the Pleistocene coupled with habitat heterogeneity provided ideal conditions for periodic isolation of local populations. In small populations genetic drift and evolutionary specialisations happen faster (Giao et al., 1998). It seems that muntjacs have been successful in a so-called stasipatric speciation with chromosomal tandem fusion as the major genetic mechanism (Wang & Lan, 2000).

Muntiacus muntjak and *Muntiacus vuquangensis* are sympatric species from the forests of the Annamites. *Muntiacus putaoensis* was found to be morphologically distinct from those two and thus represents a third sympatric species, but resembled *Muntiacus crinifrons* in coat colour and shared some morphological characters with *Muntiacus rooseveltorum* (Amato et al., 1999b). *Muntiacus putaoensis* genetically most closely related to *Muntiacus truongsongensis*, *Muntiacus rooseveltorum*, and *Muntiacus vuquangensis* (Amato et al., 1999a). While *Muntiacus putaoensis* occurs in higher altitudes on the mountain tops, the two larger sympatric species inhabit the lower regions of the mountains (Amato et al., 1999a). Colouration in muntjacs seems to be related to habitat; red is typical for more open country species (*Muntiacus muntjak*), brown is typical for lowland forest species (*Muntiacus feae*, *Muntiacus reevesi*, *Muntiacus atherodes*, *Muntiacus vuquangensis*), and a darker blackish colour is typical for montane evergreen forest species (*Muntiacus crinifrons*, *Muntiacus truongsongensis*) (Giao et al., 1998). Amato et al. (1999a) were the first to analyse all muntjac taxa except for *Muntiacus atherodes* based on four mtDNA regions.

The species status of *Muntiacus rooseveltorum* has been controversial for decades (Amato et al., 1999b). Similarly, the species status of *Muntiacus gongshanensis* has been questioned differing from other muntjacs only in one individual karyotype and not being a distinct species based on molecular data; therefore, *Muntiacus crinifrons* and *Muntiacus gongshanensis* are sometimes treated as a single species (Amato et al., 1999b).

Muntiacus vuquangensis is considered relatively closer to *Muntiacus reevesi* than to other muntjacs (Wang & Lan, 2000). *Muntiacus vuquangensis* is the most distinct of the Annamite muntjacs. Genus status of *Megamuntiacus* is not justified demonstrated by the sequence divergence estimated for the mitochondrial variation and by morphological comparisons; therefore, it should be re-affiliated to *Muntiacus* (Schaller, 1996; Giao et al., 1998; Amato et al., 1999a; Rabinowitz et al., 1999; Wang & Lan, 2000). Apart from the larger

size, there are no morphological features that would justify a separate genus (per. obs.).

In their supertree study, Hernández Fernández & Vrba (2005) state that the source topologies were incongruent concerning muntjacs and that the phylogenetic relationships within muntiacines were controversial. The instable position of *Muntiacus atherodes* for which no molecular data had been available until recently (Chapter 4), was put forward as the reason for this incongruence. Since that study several molecular topologies have been published, which consistently place muntiacine species in similar positions depending on the taxon sampling (see above).

The split of Muntiacini from Cervini has been estimated to 16.7–15.0 mya (Randi et al., 1998, 2001); in contrast Li et al. (1998) and Miyamoto et al. (1990) estimated that Muntiacini diverged from Cervini around 8–6 mya. These differing dates are presumably caused by the different fossils used for calibration. The first certain representative of muntiacines is *Muntiacus leilaoensis* from the late Miocene (9–7 mya) of Yunnan (Dong et al., 2004). The divergence of *Elaphodus* and *Muntiacus* was estimated to 3.7–1.9 mya (Lan et al., 1995; Wang & Lan, 2000). The genus *Muntiacus* seems to have evolved in the mid or late Pliocene; Ma et al. (1986b) listed five fossil *Muntiacus* species *M. nanus* and *M. cf. nanus*, *M. fenghoensis*, *M. lacustris*, and *M. bohlini*. The first fossils of *Muntiacus reevesi* are known from the early Pleistocene, while *Muntiacus muntjak* and *Muntiacus feae* are known from the middle Pleistocene (Ma et al., 1986b; Dong, 1993; Wang & Lan, 2000). The divergence ages were estimated to 1.8–0.9 mya for *Muntiacus vuquangensis* and *Muntiacus reevesi*, to 1.5–0.8 mya for *Muntiacus feae* and *Muntiacus muntjak*, and to 0.5–0.3 mya for *Muntiacus crinifrons* and *Muntiacus gongshanensis* (Wang & Lan, 2000).

In my analyses, the split of Muntiacini from Cervini was estimated to 16.55–15.46 mya in the ND analyses and to 4.89 mya in the TED analysis. Further splits within the clade occurred between 6.38 and 0.95 mya in the ND analyses and between 1.91 and 0.39 mya in the TED analysis (Figs 5.16–5.19).

Alceini

Alces. In the morphological analyses *Alces alces* was most often placed in an unresolved position or as the sister taxon to *Odocoileus hemionus* supporting the affiliation to Capreolinae. The systematic position of *Alces alces* was unstable in my nuclear analyses. When several subspecies were sampled, they always formed a clade. *Alces* was observed to be the sister taxon to *Capreolus capreolus* in one marker and the combined nuclear topology, once to *Axis axis*, to Odocoileini plus *Rangifer*, to Odocoileini plus *Rangifer* and *Capreolus capreolus*, in an unresolved position, and as the sister taxon to all other cervids (plus a moschid-bovid-clade). In the mitochondrial, combined molecular and TE analyses *Alces alces* was consistently placed as the sister taxon to Capreolini, except for the BI combined molecular topology, where it was placed between Capreolini and Odocoileini plus *Rangifer*. Unfortunately, due to highly fragmentary taxa and difficult taxonomy no fossil precursors of *Alces* could be included in my data set.

In most recent analyses, *Alces* was placed as the sister to Capreolini (Randi et al., 1998; Pitra et al., 2004; Hughes et al., 2006; Agnarsson & May-Collado, 2008; Hassanin et al., 2012) or as the sister taxon to *Capreolus* (Hernández Fernández & Vrba, 2005). In

Marcot (2007) *Alces* was the sister taxon to Capreolini and Odocoileini and Rangiferini, while it was in a polytomy with Odocoileini plus *Rangifer* and Capreolini or the sister taxon to Odocoileini plus *Rangifer* in Gilbert et al. (2006). More controversial positions include *Alces* as the sister taxon to Cervini or *Dama dama* in Kuehn et al. (2005) (no capreoline taxa included except for *Rangifer*) and the sister taxon position to *Rangifer* in Pfeiffer (2002). *Alces* was in a polytomy with Odocoileini and Rangiferini in Lister (1984) and various positions based on previous literature are summarised in Lister (1998). As all these phylogenetic studies show, the systematic position of *Alces* remains unresolved.

Alces alces is the largest living cervid and is distributed in the circumpolar boreal forests of North America and Eurasia (Franzmann, 1981). The first fossil representatives included *Libralces*, which is certainly known from the late Villafranchian, in Europe as *Libralces gallicus* and in Eurasia as *Libralces latifrons*; they most likely inhabited savannah habitats (Franzmann, 1981; Azzaroli, 1982). These forms were similar in size to extant *Alces*, but differed in antler morphology; in contrast to extant *Alces*, its fossil precursor *Libralces gallicus* was characterised by a long antler beam and a small palmated part. The largest known alceine cervid, *L. latifrons*, from the late Pleistocene has a shorter beam with more palmation (Franzmann, 1981). This shows that there was an evolutionary trend towards a gradual shortening of the antler beam. The type species *Libralces gallicus* Azzaroli 1952 has a broad cranium, palmated antlers with a long lateral main beam, long nasals, which are in contact with the praemaxillaries. The upper C is probably present and a weak anterior cingulid is variably present. The p4 has the same morphology as in *Alces*. Azzaroli (1982) suggested only two species of *Libralces* *L. gallicus* and *L. latifrons*. (Azzaroli, 1982) determined *Libralces* as subgenus of *Cervalces* due to similarities in skull and dentition. In North America the first alceine cervids are known from the late Pleistocene as *Libralces latifrons postremus*, and from the postglacial period as *Libralces scotti*. It probably represents a transitional form between *L. gallicus* and *L. latifrons* (Franzmann, 1981; Azzaroli, 1982). The first *Alces alces* is known from the Riss glaciation 200-100 kya; those late Pleistocene moose were larger than their extant representatives (Franzmann, 1981).

Divergence times for the last common ancestor of *Alces* plus Capreolini was estimated to around 7.4 mya and for the alternative possibility *Alces* and *Rangifer* plus Odocoileini it was estimated to 7.5 mya. Since those dates are very close together, the lineages probably diverged within a very short time Gilbert et al. (2006). The divergence of *Alces alces* from Capreolini or Odocoileini was estimated to 17.48–11.21 mya in my ND analyses; only in the combined molecular ND analysis the split is dated to 5.98 mya, while Capreolini diverged here earlier. In my TED analysis *Alces alces* split from Capreolini at 2.04 mya and from Odocoileini 3.36 mya.

Capreolini

***Capreolus*, *Hydropotes*.** In the morphological analyses, both *Capreolus* species were placed as sister taxa in almost all analysis; *Hydropotes* was often placed in an unresolved position. Most analyses based on the combined morphological data set support monophyletic Capreolini. However, the systematic position of Capreolini varied and could not

be determined with certainty using morphological data only.

Capreolini were always placed close to Odocoileini in my nuclear analyses, but their definite systematic position remains uncertain. *Capreolus* was placed as the sister taxon to *Alces*, to two capreoline clades, or to Odocoileini plus *Rangifer*. *Hydropotes inermis* was placed as the sister taxon to all Capreolinae, all cervids, or in an unresolved position. In the *Sry* topology, *Capreolus pygargus* and *Hydropotes inermis* were sister taxa in an unresolved position, while *Capreolus capreolus* was the sister taxon to Cervini. Similarly, in the nuclear combined topology, *Capreolus pygargus* and *Hydropotes inermis* were sister taxa and *Capreolus capreolus* and *Alces* were sister taxa. In the mitochondrial, molecular combined and TE topologies, *Capreolus* was always highly supported the sister taxon to *Hydropotes*. Capreolini was always monophyletic closely related to or in most cases the sister taxon to Odocoileini plus *Rangifer*.

Hydropotes and all members of Moschidae share similarities such as absence of antlers, enlarged upper canines that are used in intraspecific fights and defence against predators. This led to the assumption that this set of characters must be the plesiomorphic condition for all cervids (Harrington, 1985; Groves & Grubb, 1987; Janis & Scott, 1987); similarly, the karyotype of *Hydropotes* was interpreted as primitive ($2n = 70$) (Flerov, 1952; Harrington, 1985; Vislobokova, 1990; Miyamoto et al., 1990) and Dubost et al. (2011) also stated that *Hydropotes inermis* should be considered as a cervid with ancestral characters. Therefore, *Hydropotes* has been put into a separate subfamily Hydropotinae and was considered as the sister taxon of all other cervids (e.g., Groves & Grubb, 1987; Janis & Scott, 1987; Hernández Fernández & Vrba, 2005; Kuznetsova et al., 2005). However, if Muntiacini are hypothesised as the most ancestral deer, which is the case in a few studies, but not supported by the majority of topologies here and in the literature, this would be in conflict with the diploid number, which is 46–48 or less in muntiacines.

Already Bouvrain et al. (1989) favoured the hypothesis that *Hydropotes* and Capreolinae are sister taxa with Cervinae as the sister taxon over the hypotheses that Capreolinae is the sister taxon to *Hydropotes* plus Cervinae or that *Hydropotes* is the sister taxon to Caprolinae and Cervinae. They conclude that Cervinae and Capreolinae, including Rangiferini, Capreolini, and Alceini, are monophyletic and that *Hydropotes* is closely related to Capreolinae (Bouvrain et al., 1989).

The first molecular studies indicated that *Hydropotes* is included in monophyletic Cervidae (Kraus & Miyamoto, 1991). From this follows that *Hydropotes* lost the antlers secondarily and developed enlarged upper canines as compensation (Douzery & Randi, 1997; Randi et al., 1998; Hassanin & Douzery, 2003). Molecular studies of the past decades further supported the consistent placement of *Hydropotes* as the sister taxon to *Capreolus* forming monophyletic Capreolini (Douzery & Randi, 1997; Randi et al., 1998; Hassanin & Douzery, 2003; Pitra et al., 2004; Hughes et al., 2006; Gilbert et al., 2006; Marcot, 2007; Agnarsson & May-Collado, 2008; Hassanin et al., 2012). Since then the subfamily status of Hydropotinae was doubtful and under debate. It is now widely agreed on that these two genera are united in the tribe Capreolini as suggested by Kuznetsova et al. (2005).

Randi et al. (1998) demonstrated that the two *Capreolus* species and *Hydropotes* share a G at position 525 of *Cytb*, which occurs only rarely in other mammal species and stated that ‘this replacement represents a nearly exclusive synapomorphy for the *Hydropotes*-

Capreolus-clade'. Hu et al. (2006) noted that *Hydropotes inermis* has a high genetic diversity and Buntjer et al. (1998) and Lee et al. (2002) pointed out that the satellite DNA family III occurs only in *Capreolus* and *Hydropotes*, but not in other cervids. Further, the telemetacarpal condition and a large medial opening of the temporal canal are morphological features that *Hydropotes* shares with other Capreolinae (Bouvrain et al., 1989; Douzery & Randi, 1997; Randi et al., 1998). Behavioural characters also suggested that *Hydropotes inermis* secondarily lost its antlers (Cap et al., 2002). In Pfeiffer (2002) *Capreolus capreolus* was the sister taxon to *Capreolus pygargus* with a fossil *Capreolus* as the sister taxon; this clade was the sister taxon to *Alces* plus *Rangifer* based on morphological data.

Douzery & Randi (1997) stated that the divergence of Capreolini may have occurred 10.4–8.7 mya. In contrast to this, Randi et al. (1998) suggested a slightly older separation of *Hydropotes* from *Capreolus* in the late Miocene between 11.3–10.9 and 11.9–8.2 mya, which is closer to my divergence time estimates. Capreolini diverged from *Alces* between 11.21 and 10.97 mya in the ND analyses and 2.04 mya in the TED analysis. The split of *Hydropotes* and *Capreolus* was between 10.1–9.64 mya in the ND analyses and 1.32 mya in the TED analysis, the split of both *Capreolus* species was estimated at 1.45 mya (ND) and 0.52 mya (TED). Di Stefano & Petronio (2002) estimated the split of *Capreolus capreolus* and *Capreolus pygargus* to 0.4 mya.

Miyamoto et al. (1990) suggested that Capreolinae probably originated in the late Miocene in the Old World. This was inferred from their topology showing a split of Capreolinae and Cervinae and from investigating 'other information', which indicated that the early fossil cervids were not closely related to any living subfamily. The assumption of a late Miocene Old World origin of Capreolinae is in congruence with my findings considering the placement of *Procapreolus*. Cronin (1991) hypothesised that the *Alces* and *Rangifer* lineage split earlier than the *Capreolus* lineage, but after the separation of Cervinae and Capreolinae.

Rangiferini

***Rangifer*.** In the morphological analyses *Rangifer tarandus* was often placed as the sister taxon to *Okapia* due to similarities in the dental morphology. The systematic position relative to other cervids was variable. *Rangifer* has some apomorphic characters, which are not shared by other cervids. This probably causes the difficulties to place the taxon based on morphology only.

In the nuclear analyses *Rangifer* was unexpectedly placed once as the sister taxon to *Muntiacus reevesi*, but was otherwise included in or the sister taxon to Odocoileini. In the mitochondrial, molecular combined and TE topologies *Rangifer tarandus* was consistently placed as the sister taxon to Odocoileini. In my ND analyses *Rangifer* split from Odocoileini between 4.99 and 3.86 mya, while the polytomy of *Rangifer*, *Odocoileus* and Odocoileini diverged 2.97 mya in my TED analyses.

In the literature, *Rangifer* is consistently placed as the sister taxon to Odocoileini, where the taxon sampling has been sufficient (Randi et al., 1998; Hassanin & Douzery, 2003; Pitra et al., 2004; Hernández Fernández & Vrba, 2005; Gilbert et al., 2006; Hughes et al., 2006; Agnarsson & May-Collado, 2008; Duarte et al., 2008; Hassanin et al., 2012). In Kuehn

et al. (2005) *Rangifer* was the sister taxon to all cervids, but *Alces* and *Rangifer* were the only capreoline taxa included in this study. *Rangifer* was in a polytomy with Odocoileini and Alceini in Lister (1984) and a detailed overview of various possible relationships of capreoline taxa is given in Lister (1998). Pfeiffer (2002) found that *Rangifer* is the sister taxon to *Alces*.

Rangifer tarandus is the only cervid species in which females regularly grow antlers. There have been several hypotheses for this. Geist (1968) suggested that the antlers may be used as defence against predators (this was assumed for antlers in general), which seems plausible considering the high mortality of reindeer caused by wolves and bears (Crête et al., 2001). However, a comparable predation pressure is present in other deer species, e.g., *Alces*, *Odocoileus*, where females do not develop antlers. Alternatively, Gilbert et al. (2006) suggested that the highly gregarious social structure of reindeer favoured antler growth in females to be able to compete with males for food, because intraspecific competition for food is assumed to be crucial in large herds, especially during the winter when food is scarce.

Odocoileini

In the morphological topologies most odocoileine taxa were in unresolved and/or variable positions. In several topologies the small odocoileine cervids were in a clade with muntiacine taxa.

In the nuclear topologies here, both *Odocoileus* species usually were in a sister taxon position, *Blastocerus* and *Hippocamelus* formed sister taxa and *Mazama gouazoubira* and *Odocoileus virginianus* (where included individually) formed sister taxa. *Mazama americana* was mostly placed as the sister taxon to Odocoileini. Often, systematic relationships within Odocoileini were partly or entirely unresolved. Interestingly, in the nuclear topologies, *Mazama gouazoubira* is more closely related to *Odocoileus* than *Mazama americana*, which was the sister taxon to all other odocoileine species and *Rangifer*. *Mazama* appeared polyphyletic, however, more sampling for nuclear markers is required for the taxon.

In the mitochondrial, combined molecular, and TE topologies, Odocoileini split into the two subclades Blastocerina and Odocoileina (see Chapter 4). *Mazama gouazoubira* was more closely related to *Hippocamelus* or other blastocerine species, while *Mazama americana* was more closely related to *Odocoileus*. Polyphyly occurred in *Mazama*, *Hippocamelus*, *Pudu*, and *Odocoileus*. The most unstable taxon is *Pudu mephistophiles* which was sometimes included within Odocoileini and more often the sister taxon to Odocoileini and *Rangifer*. It never was placed as the direct sister taxon to its congener *Pudu puda*, only in the BI mitochondrial topology it was placed as the sister taxon to Blastocerina.

In previous studies, the taxon sampling for Odocoileini varied greatly, therefore, it is difficult to compare these topologies (Douzery & Randi, 1997; Randi et al., 1998; Pitra et al., 2004; Hernández Fernández & Vrba, 2005; Hughes et al., 2006; Gilbert et al., 2006; Marcot, 2007; Agnarsson & May-Collado, 2008; Duarte et al., 2008; Hassanin et al., 2012). Odocoileini usually formed a monophyletic group with Rangiferini as the sister taxon to them. *Blastocerus dichotomus*, *Ozotoceros bezoarticus*, and *Pudu puda* were particularly unstable across studies with comparable taxon sampling and in my topologies and were

sensitive to changes in the analysis parameters. Odocoileina and Blastocerina were sister taxa in several recent studies (Pitra et al., 2004; Hughes et al., 2006; Gilbert et al., 2006; Marcot, 2007; Agnarsson & May-Collado, 2008; Hassanin et al., 2012). This is also the case in Duarte et al. (2008), but *Pudu puda* was in a polytomy to those clades. In addition, results of this work and that of previous studies showed polyphyly for three odocoileine genera *Hippocamelus*, *Mazama*, and *Pudu* and for both species of *Odocoileus* (Pitra et al., 2004; Gilbert et al., 2006; Agnarsson & May-Collado, 2008; Duarte et al., 2008; Hassanin et al., 2012). It remains uncertain whether *Pudu* is monophyletic, polyphyletic within Blastocerina or polyphyletic with one species in Blastocerina and one species in Odocoileina.

The split between Odocoileini and *Rangifer* was suggested to have occurred in the middle Miocene between 15.4 and 13.6 mya, although their origins and relationships are unknown; the presence of close relatives of *Rangifer* among South American odocoileine fossils from the Pleistocene has been suggested (Groves & Grubb, 1987; Douzery & Randi, 1997). The split of Odocoileini into Blastocerina and Odocoileina was dated to around 3.4 mya, after the formation of the Panamanian Isthmus and subsequent rapid radiation. It was hypothesised that there was a diversification within Odocoileini in North America 5.1 mya, which is also supported by the fossil record (Vrba & Schaller, 2000; Gilbert et al., 2006; Hassanin et al., 2012). The radiations of some odocoileine species, particularly within the *Odocoileus*, appeared to be Pliocene/Pleistocene events, 4.3–1.4 mya (Douzery & Randi, 1997). In Gilbert et al. (2006) the dates of divergence of Odocoileini (15.5–11.5 mya), of Odocoileina (12.8–9.1 mya), and of Blastocerina (10.8–7.3 mya) are inconsistent with the fossil record, where the oldest cervid fossils in the New World were from the Miocene-Pliocene-boundary (5 mya), with *Bretzia* and *Eocoileus* (Fry & Gustafson, 1974; Webb, 2000; Gilbert et al., 2006). In my ND analyses Odocoileini split from other cervids between 4.99–3.48 mya, and 2.05 mya in the TED analysis.

The fossil record of Plio- and Pleistocene deer is scarce (Fry & Gustafson, 1974). There is broad consensus that ancestral odocoileine cervids entered America from Siberia via the Bering Strait in the late Miocene/early Pliocene (Gustafson, 1985; Webb, 2000; Merino et al., 2005).

Bretzia pseudalces was a medium sized deer of the Plio-/Pleistocene boundary with broadly palmated antlers, which resemble those of *Alces*, but are otherwise not similar to any other living deer. The dentition of *Bretzia* is similar to *Odocoileus*. It is assumed that its ancestors were Eurasian Pliocene deer with three-tined antlers, such as *Cervavitus*; an independent development of palmation is also possible (Fry & Gustafson, 1974; Gustafson, 1985). In Gustafson (1985) *Bretzia* was placed as the sister taxon to *Odocoileus* plus *Blastocerus*, and *Rangifer* was placed as the sister taxon to Odocoileini plus *Capreolus*, and *Alces* was the sister to all of them. He concluded that *Bretzia* is probably closely related to *Odocoileus* and that the latter replaced *Bretzia* around 3.5 mya. The first unambiguous adult antler fragment of *Odocoileus* is from 3.8–3.4 mya (Gustafson, 1985).

Cervids migrated from North to South America via the Panamanian bridge 2.5 mya (Plio-Pleistocene boundary) (Webb, 2000; Merino et al., 2005). Hershkovitz (1982) assumed a small odocoileine ancestor living in North, Central, or South America during the Miocene-Pliocene-boundary from which *Mazama* and *Pudu* diverged. This hypothesis

suggested an increase in body size over time in other odocoileines, which is in contrast to the traditional view of secondarily dwarfed *Mazama* and *Pudu*. As a logical consequence, the existence of medium sized forms during the late Miocene and Pliocene of Asia and North America was assumed, which would be the ancestors of the small odocoileines. This is also supported by the fossil record (Webb, 2000). Slightly differently, Merino & Rossi (2010) hypothesised that the first deer entering South America were medium sized with branched antlers; these presumably diverged into *Mazama* and *Pudu* with simpler antlers, most likely independently from each other. Because of some apomorphic characters, such as absence of upper canines, they were considered secondarily dwarfed.

Neotropical cervids underwent a rapid radiation after migration into South America, where they filled niches, which are occupied by bovids on other continents, making them the most diverse group of ungulates in South America (Merino & Rossi, 2010). The radiation most likely was influenced by the absence of other ruminant artiodactyls and appears to be the opposite scenario as in Africa, where bovids dominated (see below). Morphology, physiology, adaptation of the digestive system, temporal and spatial distribution of vegetation, and physicochemical properties of plants triggered the diversification, thus making the evolutionary patterns very complex.

Six fossil cervid genera are known from South America; they include *Agalmaceros* (1.8–0.8 mya), *Charitoceros* (1.8–subrecent), *Antifer* (1.2–subrecent), *Epieuryceros* 1.2–subrecent, *Morenelaphus* 0.5–subrecent, and *Paraceros* (0.5–0.2 mya) (Hoffstetter, 1952; Tomiati & Abbazzi, 2002; Merino et al., 2005; Merino & Rossi, 2010; Gonzalez et al., 2014). *Agalmaceros* is assumed to have been similar to *Hippocamelus* (Merino & Rossi, 2010). *Antifer* was a large sized deer, similar to *Blastocerus dichotomus* with irregularly dichotomous and large antlers and presumably inhabiting arid to semi-arid environments. Three species, distinguished by size, are known mostly from Argentina, Brasil, and Uruguay: *A. ensenadensis*, *A. ultra*, and *A. niemeyeri*. Their fossil record is scarce and thus, the validity of the species is doubtful (Alcaraz & Zurita, 2004; Menegaz, 2000; Merino & Rossi, 2010). *Charitoceros* is only known from the Pleistocene of Bolivia (Hoffstetter, 1963). Two species of *Epieuryceros* are known, distinguished by differences of the antlers, *E. truncus* and *E. proximus*. They were very large cervids with palmate antlers bearing 4–6 times and presumably inhabited shrub environments (Alcaraz & Zurita, 2004; Merino & Rossi, 2010). Sometimes the genus is included within *Blastocerus* (McKenna & Bell, 1997). *Morenelaphus* was a small to medium sized deer with large S-shaped antlers, which probably inhabited open/partly open habitats of Uruguay, Paraguay, Brasil, Argentina. Two species are known from the middle to late Pleistocene, distinguished by antler morphology, *M. brachyceros*, *M. lujanensis* (Merino & Rossi (2010) and references therein). *Paraceros* was a medium sized cervid with moderately sized antlers, show some similarities to *Ozotoceros*, *Blastocerus*, and *Hippocamelus*. *Paraceros fragilis* is known from the early Pleistocene of Argentina (Merino & Rossi, 2010). So far, there are only few studies on extinct neotropical cervids and even fewer attempting to reconstruct the phylogeny of fossil and extant neotropical deer.

The origination of living cervids of South America was estimated to 200 kya for *Hippocamelus*, *Blastocerus*, *Ozotoceros*, 65 kya for *Mazama*, 48 kya for *Odocoileus*, and 16 kya for *Pudu* (Merino et al., 2005). These recent dates show the rapid radiation of South American cervids, which is probably the reason for the difficulties in resolving their rela-

tionships.

After decades of research, the taxonomy and evolutionary history of South American cervids remains enigmatic, partly because of the scarce fossil record (Webb, 2000). Phylogenetic reconstructions are conflicting or unresolved. More morphological and molecular, particularly nuclear markers, and cytogenetic data are needed to reconstruct the complex evolutionary history of Odocoileini (Duarte et al., 2008; Hassanin et al., 2012).

***Blastocerus*.** *Blastocerus* is an unstable taxon, which was the sister taxon to *Hippocamelus bisulcus* plus *Mazama gouazoubira* (Duarte et al., 2008), the sister taxon to *Mazama gouazoubira* (Agnarsson & May-Collado, 2008), in a polytomy with *Mazama gouazoubira*, *Pudu puda*, *Hippocamelus antisensis* (Gilbert et al., 2006), the sister taxon to *Pudu puda* (Hughes et al., 2006), and sister taxon to *Mazama nemorivaga* (Hassanin et al., 2012). Studies with a more extensive taxon sampling and my analyses indicated a systematic position of *Blastocerus* as the sister taxon to most blastocerine species, with *Mazama nemorivaga* as the sister taxon to them and *Pudu puda* as the sister taxon to all other Blastocerina. A few analyses placed *Blastocerus* as the sister taxon to all other Blastocerina. These differing placements of *Blastocerus* most likely resulted from a differing taxon sampling. In my analyses *Blastocerus dichotomus* was positioned in an unresolved position based on morphological data and consistently placed within Blastocerina based on the molecular and TE analyses. Most often it was positioned between *Pudu puda* (sometimes also *Mazama nemorivaga*) and the other Odocoileini.

Blastocerus dichotomus is restricted to wetlands and depends on aquatic vegetation; due to these requirements and habitat fragmentation along the Paraná river prevents free movement of (Marquez et al., 2006; Mauro et al., 1998). The first *Blastocerus* fossils are known from the Pleistocene of Brazil and Paraguay. The populations in central Brazil most likely expanded between 28–25 kya and it was assumed that there were no geographical barriers until about 300 years ago (Merino & Rossi, 2010). The split of *Blastocerus* from other cervids was dated to 7.14–2.02 mya in my ND analyses and 1.01 mya in the TED analysis. The younger dates correspond with the literature.

***Hippocamelus*.** *Hippocamelus antisensis* is a medium sized and robustly built cervid ranging from northern Peru to north-western Argentina. Since there is no evidence for a more widespread distribution, it is likely that the historical distribution was similar as today. Populations are fragmented and can live in high altitude up to 5000 m, usually on rocky, cliff-like outcrops, grassland, short-shrub vegetation (Barrio, 2010).

Hippocamelus bisulcus is endemic to the South Andes. The first *Hippocamelus bisulcus* is known from the late Pleistocene of Chile, Argentina, and Bolivia (Canto et al., 2010; Merino & Rossi, 2010). *Navahoceros fricki* was historically assumed to be most closely related to *Hippocamelus bisulcus*. After revision of material assigned to *Odocoileus* and *Navahoceros* it has been found that all material assigned to *Navahoceros* should be synonymised with *Odocoileus*. Thus, *O. lucasi* is considered as the ancestor of *Hippocamelus bisulcus*, although there was no direct lineage from *Odocoileus* to *Hippocamelus* in my topologies.

In several of my morphological topologies, both *Hippocamelus* species form a clade, sometimes with *Ozotoceros* as the sister taxon. This clade was sometimes unexpectedly

placed more closely related to cervine than to capreoline taxa. In the molecular combined and TE analyses here, I included those *Hippocamelus antisensis* mt-sequence(s), with which the genus is monophyletic (see Chapter 4). In all analyses both *Hippocamelus* species were therefore the sister taxa to each other and to *Mazama gouazoubira* (plus *Mazama chunyi*, if included). In my ND analyses *Hippocamelus* diverged from other cervids between 7.14–1.18, and 0.56 mya in my TED analysis. The split within *Hippocamelus* was dated to 0.6 and 0.31 mya.

Duarte et al. (2008) stated that it is surprising that members of morphologically cohesive genera such as *Hippocamelus*, *Mazama*, or *Pudu* were not monophyletic based on molecular data. In the case of *Hippocamelus*, there is a problem with the four sequences for *Hippocamelus antisensis*, two of which formed a clade with *Hippocamelus bisulcus*, while the other two formed a clade with *Ozotoceros bezoarticus* (Chapter 4). This makes it almost certain that two of the four sequences are misidentified or mislabelled; a less likely possibility is that this polyphyly represents a valid split potentially indicating cryptic species within the genus. Without knowing the exact provenance of the samples it cannot be determined which sequences are truly *Hippocamelus antisensis*.

Hippocamelus antisensis and *Hippocamelus bisulcus* are considered to be osteologically nearly indistinguishable (pers. obs.) (Flueck & Smith-Flueck, 2011). Based on this (see also Chapter 3), monophyletic *Hippocamelus* is more likely than a polyphyly as suggested by some of the molecular data. Based on shared morphological traits (Chapter 3), monophyletic *Hippocamelus* is more likely than a polyphyly as suggested by some of the molecular data.

Thus, the potential polyphyly within *Hippocamelus* cannot be confirmed or ruled out yet; new sequences and more investigations are needed to clarify which of the available sequences genuinely belong to *H. antisensis*.

Mazama. The taxonomy of *Mazama* is complex and no comprehensive study has been published on systematic relationships (Medellín et al., 1998; Eisenberg, 2000; Gilbert et al., 2006, ; but see Chapter 4). While the monophyly of *Mazama* has never been questioned based on morphological characters, molecular studies repeatedly suggest polyphyletic relationships Gilbert et al. (2006); Duarte et al. (2008). Duarte et al. (2008) suggested that *Mazama gouazoubira* and *Mazama nemorivaga* should be assigned to a different genus. The low morphological diversity among *Mazama* is not correlated with the karyotypic diversification (Tab. 5.3), which leads to the problematic taxonomy; thus, a varying number of species has been created based on different types of data (see Chapter 4) (Groves & Grubb, 1987, 1990; Duarte & Merino, 1997; Duarte et al., 2008). In the morphological analyses most *Mazama* species were placed as closely related to each other most likely based on their small size and because they are morphologically almost indistinguishable (González et al., 2009). The systematic placement of *Mazama* was discussed in detail in Chapter 4 and polyphylies persist throughout different molecular data. This polyphyly of *Mazama* questions the current taxonomy.

Cervids underwent a rapid adaptive radiation in South America after their Pliocene dispersal across the Isthmus of Panama (Gilbert et al., 2006). The low resolution among *Odocoileina* haplotypes suggests a rapid radiation event dating to about 2.5 mya, which

coincides with the land mammal invasion from North to South America (Webb, 2000; Gilbert et al., 2006). This event potentially included eight different ancestral cervids. The ecological plasticity in *Mazama* of the Odocoileina-clade is low (Duarte et al., 2008).

Fossil *Mazama* are known from the Pleistocene of Argentina, Ecuador, Peru, and Brasil (Merino & Rossi, 2010). *Mazama americana* began to separate in the late Pliocene, 2 mya. The other representatives of Odocoileina quickly diverged within South America in glacial refugia during the Pleistocene, where *Mazama bororo* and *Mazama nana* separated from the ancestral *Mazama americana*-group at around 1 mya, the divergence time of *Mazama bororo* and *Mazama nana* was estimated to about 0.7 mya, supporting the hypothesis that these two species despite being cytogenetically distinct are closely related species (Duarte & Jorge, 2003; Duarte et al., 2008). In the ND analyses different *Mazama* species split between 7.14 and 0.62 mya; these dates contradict the fossil record.

Detailed descriptions of the more common *Mazama* species are in the literature, while only very little is known about rarer *Mazama* (and neotropical cervid) species, particularly of the Northern Andes, which represent the least studied organisms and many aspects of their life history are poorly understood (Duarte et al., 2012e,d,b,a,f; Lizcano et al., 2010; Gutiérrez et al., 2015). Only little is known about the Brazilian *Mazama nana*, which has a high karyotypic diversity (Tab. 5.3) (Abril & Duarte, 2008; De Abreu et al., 2009). *Mazama americana* is the largest brocket deer, dense forest habitat. There are very likely several cryptic species hidden within the morphotype *Mazama americana* (Abril et al., 2010). High karyotypic diversity and the trend of decreasing chromosome numbers may be a synapomorphy for *Mazama americana* independent of morphology and molecular differentiation, but with a regional pattern. Previous molecular studies and my topologies showed polymorphisms of *Mazama americana*, which suggested presence of more than just one species, or several evolutionary units. The genetic distance between the two *Mazama americana*-clade was higher than the genetic difference of *Mazama bororo* and *Mazama nana*. Therefore, at least two species were assumed to be within the *Mazama americana*-complex, with a separate evolution of the two clades starting 1 mya and 2 mya, respectively (Duarte et al., 2008; Abril et al., 2010).

The karyotype of *Mazama bororo* is different to that of *Mazama americana* and *Mazama nana*; speciation mechanisms have involved chromosome rearrangements and chromosome instability, which cannot be detected in morphology (Duarte & Jorge, 2003). More karyotypic data will certainly help to investigate systematic relationships within *Mazama*, but they are difficult to obtain, because it involves capturing and sampling living animals; however, DNA sampling from faeces has been demonstrated to be a successful and potentially powerful non-invasive method (González et al., 2009).

The species delimitations of *Mazama rufina* and *Mazama bricenii* are based on geographical occurrence; there are no morphological differences between the two species. *Mazama rufina* is slightly larger than *Mazama bricenii* and *Mazama chunyi* and is restricted to the Andes (Lizcano et al., 2010). In Gutiérrez et al. (2015), the suggested potential morphological difference of *Mazama bricenii* and *Mazama rufina* referring to the degree of concavity of the dorsal outline in lateral view is controversial, as both individuals seem to differ greatly in age based on the tooth crown height. The second character, the

lacrimal fossa can generally be highly variable among species. In the specimens I scrutinised, all *Mazama bricenii* skulls show a weak concavity in the dorsal outline, not as deep as in the figure of Gutiérrez et al. (2015). One of the two *Mazama rufina* specimens (NHMW 528) has a more clearly concave outline, the other one (ZSM 1927/41) has a straight outline. In my molecular analyses *Mazama bricenii* consistently was the sister taxon to *Mazama rufina* (see also Chapter 4), which was also found by Gutiérrez et al. (2015). There it was concluded that *Mazama bricenii* is not a valid taxon, but a junior synonym of *Mazama rufina*.

***Odocoileus*.** In my morphological analyses both *Odocoileus* species were only rarely placed as closely related to each other. In the analyses including mitochondrial markers and a broad taxon sampling, both species were polyphyletic. In the analyses based on the nuclear markers, polyphylies of the species were not observed.

Odocoileus virginianus is a highly plastic species occupying a great variety of geographically and ecologically extensive habitats between Canada and Peru. Although this cervid species represents one of the most studied deer, most of the research was conducted in North America (Moscarella et al., 2003; Merino & Rossi, 2010; Duarte et al., 2012c).

Despite all the research undertaken on this genus, the taxonomy remains difficult. There are numerous subspecies (8–10 for *O. hemionus*, 37–38 for *O. virginianus*; Wilson & Reeder (2005); Mattioli (2011)), which possibly, at least partly, represent separate species (Groves & Grubb, 2011).

Smith et al. (1986) investigated the genetic divergence in *Mazama americana*, *Mazama gouazoubira*, and *Odocoileus virginianus* from the USA and *Odocoileus virginianus* from Suriname and found that they shared a large number of alleles and had a high genetic similarity. The few morphological differences between those species may be caused by a comparatively small number of regulator loci (Wilson et al., 1977; Smith et al., 1986). Further, it seems that particularly in cervids extreme habitat differences do not necessarily lead to large morphological divergence (Smith et al., 1986).

Latch et al. (2009) demonstrated that there are two different morphotypes of *O. hemionus*, the mule deer and black-tailed deer, which is supported by a strong genetic discontinuity across the spatial distribution. Early investigations of mtDNA data demonstrated that *O. hemionus* is polyphyletic because the sequences of the mule deer (*O. hemionus*) and *O. virginianus* are more similar than the DNA of the black-tailed deer (*O. hemionus columbianus*) is to both of them (5–7 % different) (Carr et al., 1986; Cronin et al., 1988, 1996; Latch et al., 2009). This divergence between black-tailed deer and mule deer, exceeds species-level divergence.

Similarly, the genetic divergence within *O. virginianus* is remarkably high, even higher than the genetic distance between other subspecies and between *O. virginianus* and mule deer. This led to the classification of white tailed deer into two distinct groups, the *cariacou*-division and the *virginianus*-division (Smith et al., 1986; Groves & Grubb, 1987; Grubb, 1990). Some topologies here (Figs 4.4, 5.7–5.9) most likely show the two distinct genetic groups in each of the *Odocoileus* species. Discordant genetic divergence between mt and nucDNA sequences in *Odocoileus* is relatively common among related species and can be explained by several phenomena, such as by introgressive hybridisation, lineage sorting of ancestral alleles, or interspecific transfer of mtDNA (Cronin, 1991). Particularly

introgression seems to be the likely explanation because natural hybridisation and interbreeding between both species of *Odocoileus* have been documented (Groves & Grubb, 2011; Hassanin et al., 2012). More investigations and a reassessment of this genus, its species and subspecies is overdue and final taxonomic decisions are needed to untangle the (sub)species relationship within *Odocoileus*.

The first *Odocoileus* is known from the early Pliocene (3.5 mya) of North America, where they were the most common cervids until the Pleistocene. *Odocoileus virginianus* appeared 2 mya presumably as the descendant of *O. brachyodontus*, which originated in Central America and dispersed to higher latitudes only recently (Hershkovitz, 1972; Smith, 1991; Merino & Rossi, 2010). It has been assumed that *Odocoileus virginianus* evolved in North America; it was further suggested that all South American cervid fossils belong to *Odocoileus* and that *Mazama* later diverged as a consequence of isolation within South America (Smith et al., 1986; Moscarella et al., 2003). This is in contrast with the most recent molecular topologies in this work (Figs 4.4, 5.7–5.9) and the literature (e.g., Escobedo-Morales et al., 2016), from which it looks more like *Odocoileus* originated from the odocoileine *Mazama*-clade.

In my divergence time analyses, the split of *Odocoileus* from other cervids was dated to 3.98–1.3 mya in the ND analyses and 0.82 mya in the TED analysis. *Odocoileus hemionus* and *Odocoileus virginianus* diverged between 2.10 and 0.60 mya (ND) and 0.40 mya (TED).

Ozotoceros Similar to the systematic position of *Blastoceros*, the position of *Ozotoceros* varied with the taxon sampling. With an extensive taxon sampling *Ozotoceros bezoarticus* was relatively consistently placed as the sister taxon to a clade consisting of the two *Hippocamelus* species, *Mazama gouazoubira* and *Mazama chunyi* (if included) in my analyses.

Ozotoceros bezoarticus is a medium sized deer with a considerable variation in body size and varying coat colour depending on habitat, which includes grassland, pampas, and savannahs. The historic population sizes have assumedly been larger than today reflected by one of the most polymorphic control region among mammals. Habitat fragmentation most likely caused a decline in population sizes and *Ozotoceros bezoarticus* is now among the most endangered neotropical cervids (Duarte et al., 2012g; González et al., 2010).

The origin of *Ozotoceros bezoarticus* possibly dates back to 2.5 mya coinciding with a substantial cooling event; fossils are known from the late Pleistocene and Holocene of Brasil, the late Pleistocene of Uruguay, and the Holocene of Argentina (Gonzalez et al., 1998; Merino & Rossi, 2010).

In my divergence time estimates, *Ozotoceros* diverged in a polytomy with blastocerine taxa from other cervids 7.14 mya (mtND) and 1.6 mya from *Mazama* and *Hippocamelus* (combinedND), which is congruent with the literature. In the TED analysis this split was estimated to 0.78 mya.

Pudu *Pudu* is another example of a genus, whose species are almost indistinguishable based on morphology, but do not evidently form a monophyletic group based on molecular data (Chapter 4). *Pudu puda* was placed as the sister taxon to all Blastocerina in almost all of my analyses and in previous studies with a sufficient taxon sampling. The systematic

position for its congener, unfortunately, is much less certain. *Pudu mephistophiles* is most often placed as the sister taxon to all Odocoileini plus *Rangifer* or to Odocoileini. Only in one topology there is an indication that *Pudu mephistophiles* potentially is included within Blastocerina.

The spatial and chronological origin of *Pudu* is unknown. *Pudu* and *Mazama* most likely diverged from an odocoileine lineage, which existed in America since the Miocene-Pliocene-boundary (Merino & Rossi, 2010; Gonzalez et al., 2014). *Pudu* was probably restricted to South America since the Pliocene. The current distribution is fragmented; pudus inhabit high altitude mountain forests (4500 m) and humid grasslands (Escamilo et al., 2010).

The split of *Pudu* was estimated to be between 7.14 and 1.82 mya, depending on the resolution and the taxon sampling, for the ND analyses, which generally is congruent with statements in the literature. In the TED analysis *Pudu* diverged 1.48 mya in a polytomy with Blastocerina.

5.4.4 Fossil Cervidae

After analysing various data sets and partitions under different optimality criteria, the TE analyses provided interesting results concerning the systematic positions of fossils. The alternative approaches to the systematics of fossils undertaken in Chapter 3, however, proved partly to be more useful. Therefore, the section below focuses on implications for the systematic position of fossil cervids from the topologies in this chapter. The TED approach provided some genuinely interesting and useful insights into the phylogeny of cervids. Also the section Evolutionary History will discuss the larger context of the findings of Chapter 2, 3, and 5 for fossil taxa and how they can be related to extant taxa.

Miocene

In the morphological topologies Miocene cervids were usually placed either between the outgroup and all other cervids, sometimes with a few taxa forming a clade, or in unresolved positions across the topology. In several analyses *Euprox furcatus* and *Heteroprox larteti* formed a clade, sometimes *Dicrocerus elegans* and *Procervulus dichotomus* were sister taxa, but more often *Procervulus dichotomus* and *Procervulus praelucidus* were sister taxa with *Dicrocerus* as the sister taxon.

The placement of most Miocene taxa proved to be difficult in the TE analyses. *Eostylloceros hezhengensis* was placed either within Muntiacini (MP, ML) or unresolved between the outgroup and cervids (BI, TED). All other Miocene taxa formed either a clade, which was the sister taxon to Muntiacini (MP, BI), or were placed closely related to each other between the outgroup and all other taxa (ML, TED). Within the Miocene taxa there was evidence that *Dicrocerus* plus *Procervulus* and *Ligeromeryx*, *Lagomeryx* plus *Palaeoplatyceros* were more closely related, since they often form clades. Because of the calibrated time constraints all Miocene taxa were placed between the outgroup and all other taxa in the TED topology.

Miocene cervids were usually considered to be distant from crown cervids and represent a distinct group of stem cervids. They were subdivided into Lagomerycinae(/-dae), Procervulinae(/-dae) and Dicrocerinae(/-ini). All of them were regarded as sister clades

to Cervidae (Mennecart et al., 2016). It was suggested that *Lagomeryx*, *Ligeromeryx*, and *Paradicrocerus* form the lagomerycids, *Heteroprox* and *Procervulus* form the procervulines, and *Acteocemas*, *Stehlinoceros*, and *Dicrocerus* form the dicrocerines (Gentry et al., 1999). In none of my analyses this split into three groups was distinctive; however, some tendencies of closer relationships of some taxa to each other than to other Miocene taxa could be observed (Chapter 3). So far, not many attempts to reconstruct the phylogeny of Miocene cervids have been made (Azanza Asensio, 2000). Most recently, Mennecart et al. (2016) presented the first phylogenetic analysis based on petrosal bone characters for *Procervulus dichotomus*, *Heteroprox larteti*, *Dicrocerus elegans*, *Euprox furcatus*.

Ligeromeryx praestans and *Procervulus praelucidus* from the MN3 are the oldest cervids included in my analyses. *Procervulus* has often been hypothesised to be the sister taxon to all other cervids (Janis & Scott, 1987; Groves, 2007). In most analyses *Procervulus* was placed in a stem position and *Procervulus*, *Dicrocerus*, and *Heteroprox* were more closely related to each other than to other cervids in some analyses. *Heteroprox* was assumed to be the descendant of *Procervulus*. Azanza et al. (2011) suggested that the *Dicrocerus* is transitional between the Procervulinae and crown Cervidae, which had also been hypothesised by Vislobokova (1990). There is an indication in very few topologies that *Ligeromeryx*, *Lagomeryx*, and *Palaeoplatyceros* may be more closely related to each other than to other cervids.

Euprox is the first cervid, which has burr-bearing antlers and a pedicle inclination similar to that of muntjacs. Therefore, it has been suggested in several studies that *Euprox* may be the earliest representative of crown cervids from around 13.8 mya (Azanza, 1993b; Gentry et al., 1999; Dong, 2007; Azanza et al., 2013; Mennecart et al., 2016). It is often considered as a member of Muntiacini (but see section on *Euprox* in Chapter 3), which would imply that Muntiacini is the sister taxon to all other cervids. Unlike *Eostyloceros hezhengensis*, *Euprox furcatus* is not placed within Muntiacini in the four topologies of this chapter, but it is in some topologies in Chapter 3. In the topology of Mennecart et al. (2016), *Euprox furcatus* was placed as the sister taxon to *Cervus elaphus*. Based on the phylogenetic evidence in my topologies, *Euprox furcatus* shared more characters with other Miocene cervids than with crown Muntiacini.

Mennecart et al. (2016) stated that *Dicrocerus elegans*, *Euprox furcatus*, and *Cervus elaphus* differ from the other Miocene cervids, i.e., Procervulinae, in certain inner ear characters; *Euprox furcatus* had the most derived characters among them. It remains uncertain, whether *Euprox* belongs to crown cervids or represents a stem cervid with apomorphic characters. More detailed morphological characters such as those of the petrosal bone and the bony labyrinth seem to carry important phylogenetic signal and data sets should be expanded to investigate and include those characters in the future (Mennecart et al., 2016). Basicranial and ear region characters are not yet widely used when inferring morphological phylogenies, but have strong potential to provide characters, which are less prone to convergent evolution caused by climatic change (Janis & Theodor, 2014). There was a change from subtropical to more temperate climate and *Euprox*-like cervids were replaced by representatives *Eostyloceros* (Azanza Asensio & Menendez, 1989; Azanza, 1993b; Pitra et al., 2004).

Pliocervinae is a controversial taxon because it was originally not based on a generic

name and hence invalid (Dong, 2011; Croitor, 2014), but since Symeonidis (1974) established the taxon based on *Pliocervus*, it is available for taxonomy. It was later suggested that Pliocervinae are synonymous with Capreolinae. Pliocervinae existed in the late Miocene and the Pliocene and are characterised by the presence of upper canines, antlers with three or more tines, a *Palaeomeryx*-fold, and short pedicles (Dong, 1993). The taxon included *Cervavitus*, *Pliocervus*, *Cervocerus*, which were regarded as the immediate crown Cervini precursors (Gentry, 1994; Groves, 2007). However, their systematic relationships are difficult to reconstruct, because they have heterogeneous features, which was also demonstrated by the unstable placement of *Pliocervus matheronis* in my analyses. More and new morphological and biometric data are needed to solve the systematic relationships among those cervids (Di Stefano & Petronio, 2002).

Pliocene and Plio-/Pleistocene

In most morphological analyses, Plio- and Pleistocene cervids were distributed across the topologies, sometimes forming subclades. There was some evidence that particularly *Arvernoceros ardei* and *Dama* are more closely related and also the two *Metacervocerus* species. The two *Praeclaphus* species never formed a clade.

Croizetoceros ramosus, was placed within Blastocerina in all three TE analyses and as the sister taxon to Odocoileini in the TED analysis. *Procapreolus cusanus* was included within Capreolini in the BI analysis, as stem capreoline in the TED analysis, and placed within Cervini in the MP and ML TE analyses. The other Plio- and Pleistocene cervids were considered to be more closely related to extant Cervini. Most of them are nested in a clade together with Pleistocene cervids. In a few topologies the majority of Pliocene cervids are in an unresolved sister taxon position to all other Cervinae taxa/-subclades.

During the Pliocene and Pleistocene, cervids were the most common macromammals in Europe (Di Stefano & Petronio, 2002). The taxonomy of the fossil tribes is still largely unclear. In the early and middle Pliocene the first cervids occur, which were more similar to modern cervids, e.g., *Axis*, *Rusa*, *Cervus*, *Elaphurus*, *Pseudaxis*. Di Stefano & Petronio (2002) state that *Rusa* has the most primitive features among cervines concerning antler morphology and teeth and was found to be similar to '*Pseudodama*'. Based on my detailed investigations on the tooth morphology, the dentition of *Rusa* contains several derived features, which are not primitive.

There were two main migration pathways from central Asia to Europe during the Plio- and Pleistocene; along the main pathway, which was north of the Alpine-Himalayan range and active since the Oligocene, *Rusa*, *Cervus*, and *Capreolus* migrated. The second pathway was active during the Plio- and Pleistocene between Caucasus Carpathian and Taurus-Zagros-Belouchi, where *Axis*, bovids, and elephants immigrated (Di Stefano & Petronio, 2002).

Pleistocene

Pleistocene cervids are more similar to extant forms. However, it was difficult to place most of them close to their presumed living descendants in my analyses. In the morphological analyses, similarly to the Plio- and Plio-/Pleistocene cervids, the Pleistocene cervids were distributed across each topology, sometimes forming subclades. *Megaloceros giganteus* was

sometimes the sister taxon to '*Cervus*' *sivalensis* and sometimes to *Rangifer tarandus*. The fossil *Muntiacus* was always placed within Muntiacini in the TE and TED analyses.

The majority of Pleistocene cervids were placed within Cervini often unresolved in the TE and TED analyses. In only a few topologies both fossil *Odocoileus* species were sister taxa based on morphological characters. The two Pleistocene *Odocoileus* were consistently placed within Odocoileini or as the sister taxon to Odocoileini. They were never considered as sister taxa to the extant *Odocoileus*.

Despite these morphological similarities, *Axis lydekkeri* was not placed as closely related to extant *Axis* in my analyses. *Axis lydekkeri* originated approximately 1.5 mya on Java (Di Stefano & Petronio, 2002). Pitra et al. (2004) state that the '*Hyelaphus*' morphology is plesiomorphic for the entire *Rusa-Axis*-clade in their study (which is based on a most likely misidentified *Rusa*-sequence). Based on this *Axis lydekkeri* could be positioned to any point along the stem of the *Axis-Rusa*-clade. Meijaard & Groves (2004) recommended to affiliate *Axis lydekkeri* as *A. (Hyelaphus) lydekkeri*, which is a senior synonym for *Cervus zwaani* according to (Zaim et al., 2003).

'*Cervus*' *sivalensis* was within the Plio-Pleistocene cervine clade, sometimes close to *Megaloceros giganteus*, or unresolved in a more stemward position. Not much is known about this '*Cervus*' *sivalensis*. Its tooth morphology resembles *Rucervus* (pers. obs.), but a placement closely related to *Rucervus* could not be found.

Rusa kendengensis was not placed closely related to *Rusa*. However, a cervine affiliation could be confirmed and in some topologies (SFA, EPA, MP TE), it was placed as the sister taxon to extant *Cervus*. More material of this species is needed to further investigate its systematic relationships.

'*Cervus*' *philisi*, proposed as a synonym of *Metacervocerus rhenanus*, was not placed closely related to this taxon in the topologies of this chapter. Its position within early cervines was confirmed and a close relationship to *Praeclaphus perrieri* was indicated in two analyses (ML, BI).

Candiacervus ropalophorus has been considered as a megacerine cervid. It was never positioned close to *Megaloceros giganteus* or *Dama*, but within the Plio-/Pleistocene cervine clade. The specimens scrutinised were fairly complete, so it is unexpected that this taxon is so difficult to place. In the morphological analyses it was highly unstable.

Megaloceros giganteus was difficult to place in the TE and TED analyses under BI. The reasons for this are unknown. Eventually it had to be excluded from the BI TE analysis. In the TED *Megaloceros* was placed as the sister taxon to all other cervids and the corresponding node was dated to 42.1 mya, although it was entered in the matrix with a late Pleistocene calibration point at 126 kya. This phenomenon is extremely peculiar. In the literature, the earliest remains of *Megaloceros giganteus* were dated to around 400 kya (Lister, 1994; Lister et al., 2005; Croitor, 2014). A close relationship to *Dama*, as strongly suggested by molecular analyses (Figs 5.8, 5.9, 5.10, 5.11; Lister et al. 2005), could not be found in the TE analyses. It was included in the Plio-Pleistocene cervine clade in the MP and ML analyses.

5.4.5 Aspects of Origin, Dispersal and Evolution of Cervidae

Evolutionary History

Already Brooke (1878) suggested that *Dremotherium* from the early Miocene of Europe is the earliest member of cervids. Similarly, dremotheriids were assumed to be ancestors of Cervidae and Giraffidae or of Cervidae in later studies (Ginsburg & Heintz, 1966; Vislobokova, 1983). *Dremotherium* was consistently found to be most similar to cervids and together with *Amphitragulus* is now widely considered to be an early cervoid (Heintz et al., 1990; Gentry et al., 1999).

In Pomel (1853) there is a detailed description of *Dremotherium*, and Costeur (2011) gave a nice overview of the genus and reviewed several morphological features in comparison with *Moschus*, *Hydropotes*, and fossil *Amphitragulus* and *Micromeryx*, which all lack cranial appendages. The affinities of *Dremotherium feignouxii* remain problematic as it shares morphological traits with cervids and moschids. In my analyses *Dremotherium feignouxii* is most often placed in an unresolved position, confirming its controversial affinities.

Gilbert et al.'s (2006) reconstruction of the ancestral cervine heavily violates evidences from the fossil record in most cases. It was assumed to have lived in woodland or open habitats instead of dense forests, in tropical climate in eastern Eurasia instead western Eurasia nor Southeast Asia. It was reconstructed to have had antlers with three tines, sexual dimorphism, moderately sized upper canines (smaller than in muntjacs), and a deep lacrimal fossa. Apart from the latter the reconstructions cannot be confirmed by the fossil record.

During the Eocene selenodont artiodactyls diversified; from this radiation ruminants are the only successful descendants. Subsequent rapid radiations of ruminants resulted in the most diverse group of large mammals today, a remarkable event in mammalian evolution (Hernández Fernández & Vrba, 2005).

Collision of the African and Indian continents with Eurasia forming the Himalayas and the Alps around 40 mya caused drastic changes triggering artiodactyl evolution. The expansion and diversification of grasslands at the Eocene-Oligocene-boundary (34 mya) coincided with climate changes from warm and humid conditions to colder and drier conditions (Prothero & Heaton, 1996; Meng & McKenna, 1998; Hassanin & Douzery, 2003). Stadler (2011) showed that there were no major shifts of the diversification rates of mammals before 33 mya coinciding with global cooling. The divergence of major ruminant lineages has occurred within a very short period of time since their origination. From the Oligocene to the mid Pliocene global climatic and vegetational changes led to several successive rapid radiations within Pecora with additional short termed diversification events within Bovidae and Cervidae (Hernández Fernández & Vrba, 2005). This rapidity of cladogenesis and parallel evolution may explain lack of resolution or taxon instability in ruminant topologies and the plethora of convergent morphological characters (Hernández Fernández & Vrba, 2005; Janis & Theodor, 2014). Ruminant evolution was not constant through time (DeMiguel et al., 2013).

Between the Oligocene and the Miocene cooler and more arid climate led to the replacement of forest habitats with open grasslands in Asia favouring the diversification

and dispersal of many pecoran groups (Meijaard & Groves, 2004; Lorenzini & Garofalo, 2015). At the Oligocene-Miocene boundary the first cervoids appeared diverging from Oligocene taxa like *Dremotherium* or *Bedenomeryx* (Ludt et al., 2004). Although Central Asia/Eastern Eurasia has been long regarded as the centre of origin and evolution of Cervidae (Vislobokova, 1990; Groves, 2006), evidence from the fossil record now shows that the origin of cervids may be in Europe (see Chapter 3). Their past diversity is known from around 26 fossil genera (Dong, 1993).

Based on mammalian body-weight structures of early-middle Miocene taxa, the climate of south-central Spain was reconstructed to have been arid with open habitats, and that of northern areas (Aquitaine basin, central eastern France, Switzerland, and northern Germany) with densely forested and closed habitats with more humid conditions. There was a strong latitudinal environmental gradient during this period, but almost no temperature gradient (evidence by ectothermic vertebrates and plants, with mean annual temperatures of about 20°C. From this follows that there was a southwest-northeast aridity-humidity gradient during the Miocene Climatic Optimum in western Europe (Costeur & Legendre, 2008a).

Palaeogeographical reorganisations and warming and cooling events can be regarded as the driving force behind faunal interchange. In the early Miocene particularly geography played an important role by opening migration routes in Europe, Asia, and Africa. This had an rapid increase of ungulate diversity as a consequence, which remained like that during the warm climate of the Miocene Climatic Optimum throughout the middle Miocene. Stadler (2011) showed that there was a slight but not significant increase in diversification rate of mammals 15.85 mya. From the late Miocene onwards the climate changed (cooling, increasing seasonality), which may have played a crucial role in the decline of large mammal diversity and causing endemism to occur in the climate belts. The low diversity and the endemism of today may have originated already in the late Miocene (12 mya) and may be more complex than assumed (to lay in the Quaternary Climatic Cycles) (Costeur & Legendre, 2008b).

Even though the Miocene was in the late phase of the Cenozoic cooling, the climate was relatively warm and humid. In the late Miocene the temperature gradient from equator to pole was weak and higher latitudes were warmer than today, the reasons and processes of which are still not yet fully understood (Micheels et al., 2011).

During the Miocene forest habitats were replaced by grasslands, which favoured the greatest radiation of ruminants. Also, important dispersal events between Africa, Eurasia, and North America happened during this time (Hassanin & Douzery, 2003). Around 15 mya sea-levels fell due to cooling climate in the high latitudes and forming ice sheets in the Eastern Antarctic; the fallen dry areas became grasslands (Haq et al., 1987; Flower & Kennett, 1994; Miller et al., 1991; Ludt et al., 2004). The climate further cooled causing colder winters and drier summers when the circulation of warm deep water between the Mediterranean and the Indo-Pacific was interrupted. Subsequently grasslands spread over Europe and Asia between 8 and 7 mya providing perfect conditions for ruminants to further diversify (Ludt et al., 2004).

During the Late Miocene of Asia environmental changes and uplift of the Tibetan plateau (11–7.5 mya; Amano & Taira (1992)) coincided with a global increase in aridity,

seasonality and subsequent spread of grassland in Asia (Flower & Kennett, 1994; Gilbert et al., 2006). C3 grass dominated habitats occurred around 22 mya, C4 grass expanded around 17.5 mya (DeMiguel et al., 2013). These conditions were perfect for the origin and diversification of Cervidae and also other ruminant groups, i.e., Caprini, Boselaphini, Bubalina. The resulting competition of overlapping habitats of grazers and browsers must have played a crucial role in the evolution of Cervidae (Gilbert et al., 2006). Another glaciation period at the Miocene/Pliocene boundary caused a drop in sea levels triggering further diversification particularly within cervids (Ludt et al., 2004).

A crucial factor for South East Asian cervid evolution was the split of the Indochinese and Sundaic faunistic subregions caused by high sea levels, which cut through the Thai/Malay Peninsula during the Early Pliocene separating faunas for the duration of around 1 my (Woodruff, 2003; Meijaard & Groves, 2004). After the warm Middle Pliocene, the Pliocene-Pleistocene boundary was characterised by drastic cooling (2.4–1.8 Ma) (Meijaard & Groves, 2004).

The first (presumed) odocoileine taxa are *Eocoileus* from Florida and *Bretzia* from Nebraska from around 5 mya. Based on similarities with *Pavlodaria* from Northeastern Kazakhstan Vislobokova (1980) and Webb (2000) suggested that they migrated to America via Beringia from the latest Miocene onwards.

Today's South American cervids have a diverse variation and are adapted to a wide range of ecological habitats. This indicates an adaptive radiation. Stadler (2011) reported a significant rate shift of speciation to a decreasing diversification rate at 3.35 mya, which coincides with high tectonic activity and the peak of the Great American Biota Interchange. The polyphyletic split of the *Mazama* species into the two subclades, Blastocerina and Odocoileina, led to the interpretation that South America was colonised at least twice. First, by the ancestor of Blastocerina in the Early Pliocene (4.9–3.4 mya), although this cannot yet be confirmed by the fossil record nor by a certain presence of a connection between North and South America. However, a much earlier closure of the Panama Isthmus between 15 and 13 mya was recently suggested (Montes et al., 2015). The second colonisation was by the ancestor of *Mazama americana* and *Odocoileus virginianus* around the Plio-/Pleistocene boundary Gilbert et al. (2006).

Apart from the recent dispersal and radiation into South America, cervids are mainly restricted to the Northern Hemisphere (Geist, 1998; Gentry, 2000; Scott & Janis, 1987; Webb, 2000). *Rangifer* appears in the fossil record in the Pleistocene; based on its arctic specialisations it is hypothesised that it dispersed to America during the Pleistocene contemporaneously with *Alces* and three bovid genera, which were also adapted to the tundra (Gilbert et al., 2006).

Bovid - Cervid Co-evolution

Today, there are about 2.5 times as many bovid species than there are cervid species. While the geographical distribution of cervids and bovids in the early middle Miocene was still balanced, today this is only the case on the northern hemisphere, where bovids and cervids are almost equally diversely represented (Costeur & Legendre, 2008b). Conversely, on the southern hemisphere cervids dominate South America, where native bovids are ab-

sent, while bovids dominate Africa, where only a single cervid species is present in the northernmost realms of the continent (whether these occurrences are native or not is still a matter of debate). The bovid diversity in Africa greatly outnumbers that of South American cervids. The difference in diversity of the two (sub)continents could be explained that neotropical cervids immigrated to South America only relatively recently at around 2.5 mya (Webb, 1991), while bovids in sub-Saharan Africa had a much longer time span available to radiate and diversify. The certainly first African bovid is *Eotragus* from the middle Miocene (15–14 my), but possibly there are even earlier members, like *Namibiomeryx* from around 20–18 mya (Gentry, 1970; Morales et al., 1995; Heywood, 2010). Additionally, the highly diverse sub-Saharan Africa savannah biome has been assumed to be the primary influence of the high bovid diversity. Due to the geographical position of South America the open habitat is restricted to a only one single area south of the equator. This limited the options for endemic cervid speciation (Heywood, 2010).

Explanations for the absence of cervids from certain dietary niches/habitats and the impact of this on the reduced diversity of the family (which had potential to a higher diversity) are based on certain contingencies and constraints. Sometimes the large faunal extinction events at the end of the Pleistocene were suggested as one possible explanation. However, the fossil record demonstrates that both groups suffered equally from these extinction events (Heywood, 2010).

If savannah biomes, as stated above, were/are centres of mammalian and particularly ungulate diversification, it remains still unclear, why cervids were/are absent from these habitats. One simple, but plausible explanation is that cervids were not in the right place at the time Africa was colonised by (other) ungulates; the absence of bovids in the Great American Biotic Interchange was similarly explained (Webb, 1991; Heywood, 2010). Another explanation put forward for the absence of cervids in Africa was the competition with antelopes (Prothero & Schoch, 2002).

Cervids are absent from open arid grasslands, even on continents they already inhabit (e.g., Asia). Grazing in cervids is only common in habitats close to the water or grazing on fresh grass, but they never have diets consisting exclusively of grass. There are only two extant cervids that qualify as open habitat taxa, *Cervus albirostris* and *Rangifer tarandus*. However, the latter is highly specialised on lichens and other tundra vegetation, which makes it rather different from other typical open habitat ungulates. To the contrary, there are well over 50 bovid species, which are classified as open habitat ungulates and/or grazers (Heywood, 2010).

The development of antlers during cervid evolution required the intake of high quality food, which was at least seasonally available. This is a constraint that possibly prevented cervids from entering and adapting to grasslands (Geist, 1998; Heywood, 2010).

Another constraint is represented by the adaptation of teeth to the much tougher grass diet. The distinction between C3 and C4 grazers may have been important in the colonisation of Africa by ungulates (Heywood, 2010). In brachyodont teeth, the four main cusps may remain unfused or only fuse in later wear, in most cases cusp fusion occurs to varying degrees, while in modern bovids these four cusps already fuse in very early wear, isolating two central cavities. The speciality here is the fusion of the postpara- and

postprotocrista with the premeta- and premetaconulecrista. This phenomenon is called the cusp fusion hypothesis, and is considered the necessary prerequisite in order to cope with the highly abrasive diet in open habitats (Heywood, 2010). It is likely that a combination of several or all of these contingencies and constraints (appendages, dental, zoogeographic, phylogenetic) influenced cervid and bovid evolution and dispersal.

The Ecological Role of Antlers

There is broad consensus that the four types of pecoran cranial appendages, horns, ossicones, antlers, pronghorns, evolved independently; because of the absence of a last common ancestor of Pecora with cranial appendages and the differing ontogeny of the four appendages, the hypothesis of an independent origin is plausible and most likely (e.g., Janis & Scott, 1987; Gentry & Hooker, 1988; Scott & Janis, 1993; Hassanin & Douzery, 2003; Davis et al., 2011). Ruminant cranial appendages are intraspecifically used to recognise species, age, size, sexual maturity, and the social status (Prothero & Schoch, 2002). The assumption that antlers appeared independently in at least 5 groups of cervids (Vislobokova, 1990), can be rejected based on numerous topological evidences, which clearly show monophyly of Cervidae and thus unique development of antlers. Similar climatic conditions caused convergent adaptations of cervid features (homoplasy); cervids of the temperate regions will develop large and more complex antlers with additional tines (e.g., bez tines), which is possibly related to seasonality (Pitra et al., 2004).

In cervids the relative antler mass significantly correlates with sexual dimorphism (weight). It was observed that increased grass intake causes decrease in antler mass, because the protein and especially mineral content in grasses is lower than in browse; therefore, temperate cervid species of forest habitats, e.g., *Capreolus*, *Alces*, *Odocoileus*, are less dimorphic (Geist & Bayer, 1988). It is assumed that cervids adapting to more open landscapes, like *Rangifer tarandus*, also develop a male-like sexual monomorphism; a phenomenon that has been observed in other gregarious ungulates of open habitats. The presence of antlers in female reindeer may therefore be explained by this (Jarman, 1983; Geist & Bayer, 1988). Adaptations to closed habitats such as dense forests, are reduction and simplification of antlers (less than three tines) and a small body size and sexual monomorphism (size/weight). The reductions in the antlers are because of inhibited mobility with large complexly ramified antlers and minimised effect of the display function of antlers when not in open habitats (restricted visibility). This resulted in positive selection for these traits. While these traits are most likely secondary adaptations in the small neotropical cervids, *Mazama* and *Pudu*, contrary to Gilbert et al. (2006)'s statement, they are most likely the primary condition in Muntiacini and Capreolini.

It has been hypothesised that the positive allometry between body size and relative antler length resulted from possibly better access to better food resources of larger cervid species, which live in more open habitats. This would mean that these large cervids could assimilate more nutrients. In addition females may use the antler length as indication of physiological strength (Plard et al., 2011). Mating tactics do not have a direct influence on antler length; instead, the amount of inter male competition and assessment is assumed to be the main evolutionary driver of relative antler size in cervids. Antlers are presumably

primarily used to assess the opponents' physical strength in order to keep costly fights to a minimum (Clutton-Brock, 1982; Plard et al., 2011).

There are different mating systems, e.g., monogyny, polygyny, polyandry, and promiscuity, as opposed to different mating tactics, e.g., harem, territoriality, and tending. While matings systems are much less variable on intraspecific level, mating tactics can vary among populations or even male individuals of the same species. It is expected that at the interspecific level, the average antler length should vary more in correlation to the mating system than to the mating tactic (Plard et al., 2011). The effect of the mating system is relatively greater than that of the mating tactic (Plard et al., 2011). There is no obvious correlation between differences in sexual dimorphism and differences in mating behaviour among species of *Cervus* (Geist & Bayer, 1988). Polygyny played an important role during antler evolution; it was observed that highly polygynous species had larger antlers, while the breeding group size had little effect on the antler size (Plard et al., 2011).

Karyotypic Diversity

A speciality of cervids is the great diversity of the karyotype; the diploid number ranges from $2n = 6$ to $2n = 70$. The ancestral karyotype for cervids has been assumed to be $2n = 70$ (Neitzel, 1987; Hall, 2009). The extreme chromosomal fragility in cervids led to the highest karyotypic evolutionary rate in mammals (Vargas-Munar, 2003). Robertsonian translocations in Cervini and Capreolinae, and tandem chromosome fusions in Muntiacini led to the high karyotype diversity (Fontana & Rubini, 1990; Hall, 2009).

Particularly within Muntiacini, the high karyotypic diversity and the radical and rapid chromosomal reorganisation within *Muntiacus* together with the recent discovery of several new species has attracted the attention of mammalogists and increased evolutionary research interest (Lan et al., 1995; Wang & Lan, 2000). *Muntiacus muntjak* has the lowest diploid chromosomal number in mammals ($2n = 6$ in females and 7 in males), while *Muntiacus reevesi* has a $2n$ number of 46 in both sexes. The diploid numbers of other muntjacs, if known, are intermediate, i.e., 8/9 in *Muntiacus crinifrons* and *Muntiacus gongshanensis*, and 13/14 in *Muntiacus feae*. The diploid number in *Elaphodus cephalophus* varies between 46, 47, and 48 (Wang & Lan, 2000). It was hypothesised based on cytogenetic studies that the *Muntiacus muntjak* karyotype evolved from a *Muntiacus reevesi*-like ancestral species by tandem and centromeric fusion (Yang et al., 1995; Lan et al., 1995). Alternatively, Neitzel (1987); Fontana & Rubini (1990) suggested that the ancestor of extant muntjacs might have had more than 46 chromosomes; similarly, studies on chromosome painting disagree with a *Muntiacus reevesi*-like ancestor (Yang et al., 1995; Lan et al., 1995). Initial reductions resulted in the karyotypes of $2n = 46$ in *Muntiacus reevesi* and $2n = 46-48$ in *Elaphodus cephalophus*, respectively. Further reductions and parallel events led to the low diploid numbers known from the other muntjacs (Wang & Lan, 2000). The reduction in diploid number during karyotypic evolution is remarkable and not linear. The rate of change in chromosome number in *Muntiacus* is one of the fastest in vertebrates (Wang & Lan, 2000).

Chromosome polymorphism found in *Mazama* is also remarkable and similar to that found in *Muntiacus* (Groves & Grubb, 1990). The diploid number in the genus varies from 32 chromosomes in *Mazama bororo* to 70 chromosomes in *Mazama gouazoubira*. Therefore,

Mazama species can be divided according to chromosomal numbers into gray brackets (those belonging to Blastocercina) with a diploid number of $2n = 66$ – 70 chromosomes with low intraspecific polymorphism, which is similar to the karyotypes of *Blastocercus dichotomus* and *Ozotoceros bezoarticus* ($2n = 66$ and $2n = 68$) and into red brackets (those belonging to Odocoileina) with a diploid number ranging from $2n = 32$ (*Mazama bororo*) to $2n = 54$ (*Mazama americana*), which show high levels of intra- and interspecific chromosomal variation (Duarte & Jorge, 2003; Abril & Duarte, 2008). The chromosome polymorphism in *Mazama americana* correlates with the geographic distribution. Based on this cytotypes from different localities could be identified. These cytotypes could not be correlated with external morphological features.

Compared to the high variability of the diploid number in the two taxa above, the diploid number of chromosomes is much more conservative in Cervini. It is also closer to the assumed ancestral karyotype of $2n = 70$. The karyotype diversity and cytogenetics in general have great potential to provide reliable taxonomic characters and useful insights into the evolutionary history of cervids in the future (Huang et al., 2006; Spotorno et al., 1987).

Table 5.3: Variation of karyotypic diversity in cervids shown by the diploid number of chromosomes 2n.

Species	2n
<i>Muntiacus muntjak</i>	6–7
<i>Muntiacus crinifrons</i>	8–9
<i>Muntiacus gongshanensis</i>	8–9
<i>Muntiacus feae</i>	12–14
<i>Muntiacus reevesi</i>	46
<i>Elaphodus cephalophus</i>	46–48
<i>Alces alces</i>	68
<i>Hydropotes inermis</i>	70
<i>Capreolus capreolus</i>	70
<i>Capreolus pygargus</i>	70–?80
<i>Mazama gouazoubira</i>	63–64
<i>Mazama bororo</i>	32–34
<i>Mazama nana</i>	36–39
<i>Mazama americana</i>	42–56; 68–70
<i>Mazama temama</i>	49–50
<i>Blastocerus dichotomus</i>	66
<i>Ozotoceros bezoarticus</i>	68
<i>Hippocamelus bisulcus</i>	70
<i>Pudu puda</i>	70
<i>Axis axis</i>	66
<i>Axis porcinus</i>	68
<i>Cervus albirostris</i>	66
<i>Cervus elaphus</i>	62
<i>Cervus nippon</i>	66
<i>Rucervus eldii</i>	58
<i>Rucervus duvaucelii</i>	56
<i>Rusa timorensis</i>	56–62
<i>Rusa unicolor</i>	56–62
<i>Rusa marianna</i>	65

5.5 Conclusion

The separate nuclear and mitochondrial and combined molecular analyses gave insights into the systematic relationships and demonstrated robust areas and problematic areas of the phylogeny in much more detail than in previous analyses. Topologies based on individual nuclear markers were less well resolved than the combined nuclear, mitochondrial and combined molecular topologies. The higher hierarchical clades were usually recovered; only the monophyly of Capreolinae could not always be confirmed. Systematic relationships within Cervinae are less controversial than within Capreolinae. In Muntiacini only *Muntiacus atherodes* could not robustly be placed. Within Cervini a few uncertainties remain within *Cervus* and the position of *Rucervus eldii* could not be determined with certainty, because this taxon is in conflicting positions in nuclear vs. mitochondrial markers.

Within Capreolinae, Alceini and Capreolini were particularly difficult to place, sometimes forming a clade within Capreolinae or were unresolved within Cervidae, and sometimes they did not form a clade. The sister taxon relationship of *Capreolus* and *Hydropotes* is confirmed and supported in my analyses. The position of *Rangifer* was relatively stable as the sister taxon to Odocoileini. The systematic relationships within Odocoileini are the most controversial within Cervidae. Their rapid radiation makes it difficult to track the exact cladogenesis. There are several polyphylies concerning (probably) *Pudu*, *Odocoileus*, and *Mazama*; the previously presumed polyphyly in *Hippocamelus*, is probably caused by misidentified sequences. This issue needs further scrutiny, as does the complex systematics of *Mazama*.

The TE analyses combined molecular and morphological data, including fossil and extant species. This approach provided further interesting results. In combination with the SFA and EPA approaches introduced in Chapter 3, as much insight into fossil systematics as currently possible, was gained. Most Miocene taxa formed a clade, which was either placed between the outgroup and all other cervids or as the sister taxon to Muntiacini. *Eostylaceros hezhengensis* was placed within Muntiacini. Most Plio- and Pleistocene cervids were close to or within Cervini or unresolved within Cervidae. The two fossil *Odocoileus* were placed within or closely related to Odocoileini. *Croizetoceros ramosus* was placed within Capreolinae, and *Procapreolus cusanus* was often placed within Capreolini or Capreolinae. For none of the other fossil cervids a robust placement could be observed in the TE analyses. For three taxa, *Pliocervus matheronis*, *Candiacervus ropalophorus*, and *Cervus australis*, no coherent placement could be found.

The ND analyses provided interesting results, which were comparable to those in the literature. The ND analyses here are based on more complete data sets concerning partly the taxon and the character sampling since they have been applied to nuclear and mitochondrial characters, which has not been done before. The TED analyses resulted in younger divergence time estimates than the ND analyses. The positions of the fossils correspond with their occurrence in the fossil record and subfamilial and tribal affiliations were indicated. ND and TED provided different divergence time estimates, which were both highly informative for interpreting the evolutionary history of cervids.

Based on the systematic positions of fossil cervids the evolutionary history could be reviewed (literature) and complemented with the new findings of my work. Since there are not many phylogenetic reconstructions including a large set of fossil cervids, several

hypotheses on systematic positions inferred from comparative morphology could be confirmed and are now supported by quantitative methods (phylogenetic analyses). Some hypotheses could not be confirmed or were contradicted.

The distribution of bovids and cervids today results from a Miocene invasion and subsequent radiation of bovids into Africa. Due to certain biogeographic and/or anatomical (dentition) conditions, cervids did not enter and diversify in Africa, but remained restricted to the Northern hemisphere until their late Pliocene dispersal to South America. This is a very interesting aspect within ruminant evolution. The diversity and ecological role of antlers and the high level of karyotypic variability are specialities of cervid evolution, which will provide further exciting insights into cervids in the future.

Chapter 6

Conclusion and Perspectives

6.1 Conclusions

My comprehensive data collection and analyses provided new insights into the systematic relationships of fossil and extant cervids. These relationships were investigated using molecular and morphological characters separately and combined in several approaches. New insights were gained into the evolutionary history of cervids and problematic areas concretised in more detail.

Data

Morphology Due to the conservative morphology in cervids, phylogenetic analyses based on the morphological data sets were only partly informative for extant taxa, but gave new insights into the systematic relationships of several fossil taxa. The single fossil analyses and evolutionary placement analyses were particularly useful. Despite partial incongruence for extant taxa in the topologies (molecular vs. morphological), some consistent splits within the morphological trees were observed. These splits included the *Elaphurus-Rucervus-Rusa*-clade, *Axis*, which sometimes was closely related to the *Elaphurus-Rucervus-Rusa*-clade, *Capreolus*, and some muntjacs. There is phylogenetic signal for Muntiacini and Capreolini within the morphological data sets. A size bias was observed for small cervids in some analyses.

Some morphological characters or character partitions are more useful for solving intrafamilial relationships (dental), while some are more informative for solving higher hierarchical relationships (cranial). Antler characters are useful to distinguish cervid genera and species qualitatively, but could so far not equally well be used for phylogenetic reconstructions.

Several evolutionary trends of the dentition were observed; the most remarkable is the molarisation of the lower premolars, particularly of the p4 and partly of the p3. Also, with the exception of *Hydropotes inermis* and muntiacines, upper canines become reduced in size or entirely lost throughout cervid evolution.

The morphological features of the abscission area, were described for the first time (Chapter 2). Extensive comparative morphological scrutiny provided evidence that antlerogenesis was already present in the first early Miocene cervids. It was shown that the burr

is not required for shedding to occur. Further, lack of ornamentation does not indicate permanent skin coverage and therefore permanently attached antlers as demonstrated by the partly rich and diverse, or wanting ornamentation in antlers of extant cervids. Therefore, *Procervulus praelucidus* (Germany), *Acteocemas* (France), and *Ligeromeryx* (France) all from the early Miocene (MN3) are so far the oldest known members of Cervidae. This strongly supports that the systematic position of all these Miocene taxa is within the total group of Cervidae. These findings were important for the node calibrations in the molecular clock analyses presented here and will be important for future divergence time estimates.

There are several evolutionary trends in antler development from the late Miocene until today. These concern the concavity of the abscission area, the development of a longer shaft, the development of a burr, and the development of a long main antler beam, where the branching patterns become more complex, and pedicles become shorter.

Molecular Data A substantial amount of molecular data was already available for most cervid species at the start of the project; they consisted of the complete mitochondrial genome and five nuclear markers. Ten species did not have any molecular record on public data bases.

I was able to sequence five cervid species, for which no molecular data were available previous to the start of my project (see Chapter 4), the number of cervid species without molecular data could thus be reduced from ten to five. *Axis calamianensis*, three *Muntiacus* species without data and one *Muntiacus* species with only a short mtDNA fragment are left to be sequenced.

Systematics

It was shown that the phylogenetic position of the non-cervid ruminants included here are unstable. This concerns particularly Antilocapridae, Giraffidae, and partly Moschidae. These taxa were sensitive to changes in the character or taxon sampling. In more robust analyses Moschidae formed the sister taxon to Bovidae, both are the sister clade to Cervidae. This issue is far from solved and requires thorough investigation and compilation of different data types in the future.

The monophyly of Cervidae could be repeatedly confirmed. Figures 6.1–6.3 summarise the systematic positions of the higher hierarchical extant cervid clades and the position of fossil cervids. The topology in Figure 6.1 provides an overview of the Total group Cervidae, while Figures 6.2 and 6.3 show detailed parts of the topology for Miocene cervids and fossil Cervini. These three topologies represent a qualitative summary of the results of Chapter 3, Chapter 4, and Chapter 5.

Cervinae was monophyletic in the majority of analyses consisting of Muntiacini and Cervini as sister taxa. The monophyly of the latter was also often recovered. Relationships within Muntiacini are not entirely resolved, but *Elaphodus cephalophus* usually is the sister taxon to muntjacs.

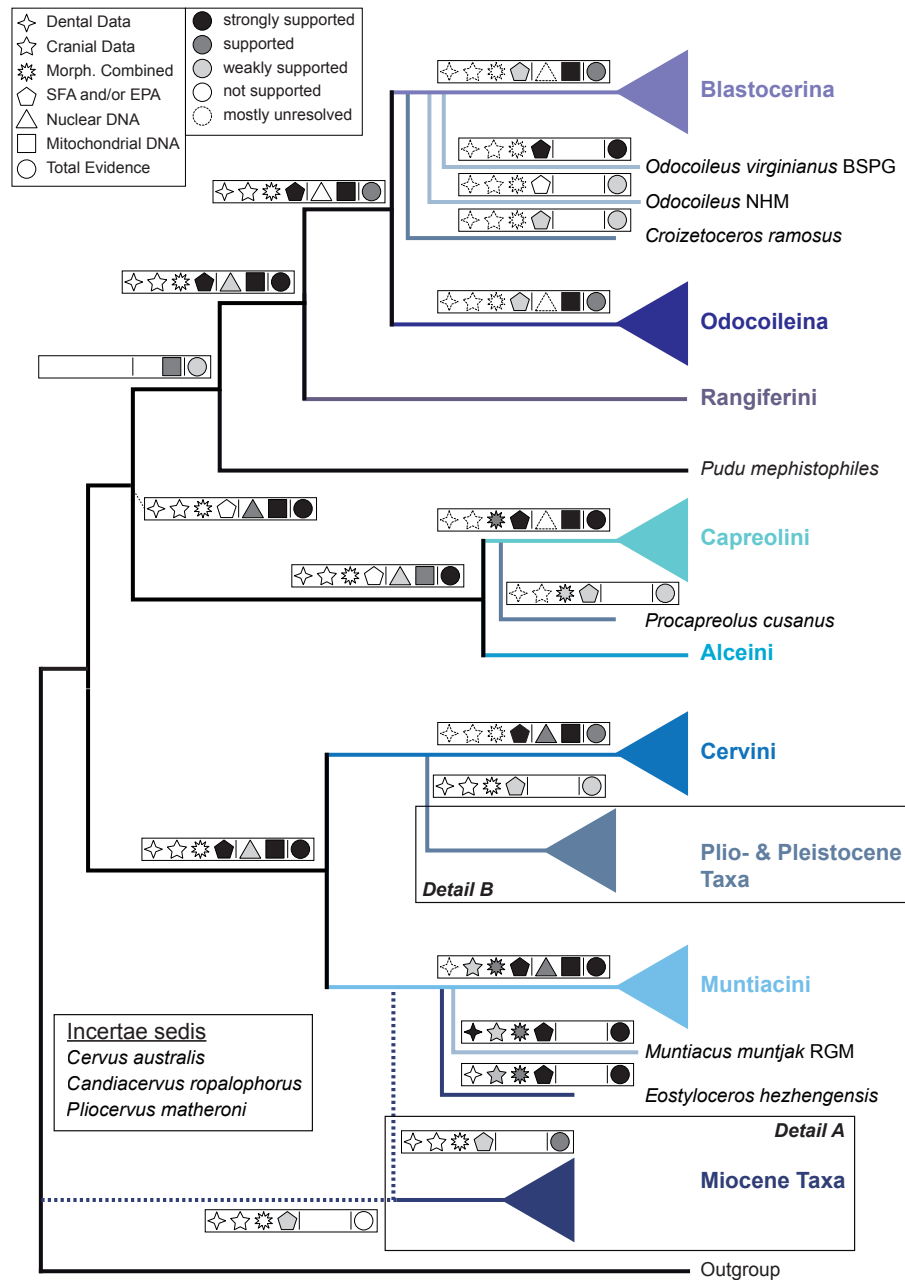


Figure 6.1: This topology represents a summary of all topologies retrieved from the numerous analyses of my thesis. The phylogenetic relationships on higher hierarchical level for extant species and on species-level for fossil cervids is qualitatively summarised based on observations from the topologies. The support for each node is given by a series of symbols (see Figure legend). Two more detailed sections of the topology are in Figure 6.2 and 6.3. The systematic position of three fossil cervids were unstable (incertae sedis).

Systematic relationships within Cervini are relatively stable, with many consistently recovered subclades. *Rucervus eldii* is often placed in a polyphyletic position to the other two *Rucervus* species. There is a high probability that this polyphyly is caused by the hybridisation of *Cervus canadensis* and *Rucervus eldii*, which resulted in the divergence of *Elaphurus davidianus*; *Rucervus eldii* presumably inherited maternal genes and is therefore artificially placed as the sister taxon to *Elaphurus davidianus*. The nuclear topology, based on at least partially solely paternally inherited genes shows a close relationship between *Elaphurus davidianus* and *Cervus* and *Rucervus* is monophyletic. More nuclear markers need to be sampled to further investigate this issue.

Cervus always forms a clade, with only little variation in the internal relationship. It was demonstrated based on molecular and morphological evidence that the genus *Przewalskium* should be synonymised with *Cervus*. Adding new sequence data for *Rusa marianna* showed that both Philippine *Rusa* species are more closely related to each other and that Indonesian and mainland *Rusa* species are sister taxa to each other. *Rusa* most often form a clade, which is closely related to *Cervus*.

Systematic relationships within Capreolinae are much more variable. Even the monophyly of this subfamily could not be confirmed in all topologies, but was supported in the more robust analyses (Fig. 6.1). In most analyses Alceini was the sister taxon to Capreolini; however, there were a few topologies, where this was not the case and those two tribes are not even included in Capreolinae but take up unresolved positions somewhere else in the topology. *Capreolus* almost always forms a clade, and mostly with *Hydropotes* as the sister taxon. Therefore, Capreolini most likely is monophyletic including *Capreolus* and *Hydropotes*; the latter presumably lost its antlers due to genetic mutations.

Rangifer was almost consistently placed as the sister taxon to Odocoileini. Odocoileini usually splits into two subclades, Odocoileina and Blastocerina (Fig. 6.1). According to my topologies *Odocoileus* seems to have originated from *Mazama* rather than the other way around, which had been assumed so far. Both *Mazama* species are polyphyletic and possibly contain more separate species, which are now only considered as subspecies. *Mazama* is also represented in Blastocerina, which otherwise consists of *Ozotoceros*, *Hippocamelus*, *Blastocerus*, and *Pudu puda*. *Ozotoceros* and *Blastocerus* are unstable taxa taking up varying positions depending on the taxon sampling. *Hippocamelus* has been assumed to be polyphyletic, but morphological and molecular evidence suggest that it most likely is monophyletic, and that two sequences of putative *Hippocamelus antisensis* are possibly misidentified. Adding new sequence data for *Pudu mephistophiles* did not solve whether the genus is mono- or polyphyletic. A few topologies suggest that both species belong to Blastocerina, but most topologies put *Pudu mephistophiles* in a position as the sister taxon to Odocoileini or to Odocoileini plus *Rangifer*. Polyphyletic *Mazama* is the most complex cervid taxon; sampling of two new *Mazama* species supported this.

Placing fossil cervids was difficult. No link between particularly incomplete taxa and phylogenetic instability could be found, however, the incompleteness of fossils can be problematic in the tree search process. For the placement of fossils it is most likely more important which characters are preserved and can be linked with other taxa, than overall character completeness. Morphology is the only possibility to analytically test phylogenetic hypotheses and even incomplete and problematic fossils should be included.

For Miocene cervids a placement in a stem position between the outgroup and all other

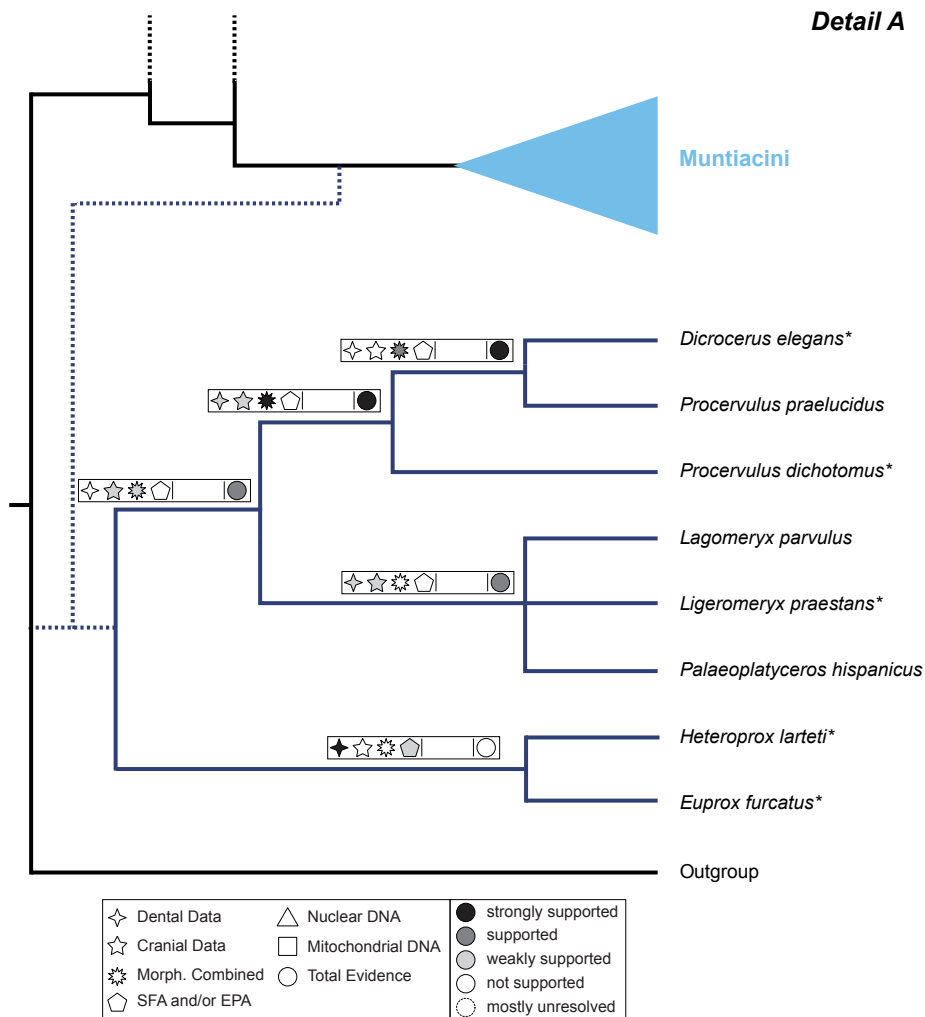


Figure 6.2: This topology summarises the phylogenetic positions of Miocene taxa. The asterisk (*) indicates taxa, which were placed closely related to extant muntiacines in some analyses.

cervids, or in a sister position to Muntiacini is supported in my analyses. Most of them were considered as closely related; thus, there seems to be a distinct group of Miocene cervids, which potentially is a stem lineage (Figs 6.1, 6.2).

Lagomeryx, *Ligeromeryx*, and *Palaeoplatyceros* are sometimes more closely related to each other than to the other cervids, although *Palaeoplatyceros hispanicus* is a highly unstable taxon. Similarly and more often *Procervulus*, *Dicrocerus* and sometimes *Heteroprox* are closely related. No clear phylogenetic signal could be gained for *Pliocervus matheronis*. *Eostyloceros hezhengensis* showed affinities to extant Muntiacini; in very few analyses this was observed for *Euprox furcatus* as well.

In Plio- and Pleistocene cervids many apomorphic characters are already present. This mixture of plesiomorphic and apomorphic characters makes it sometimes difficult to place

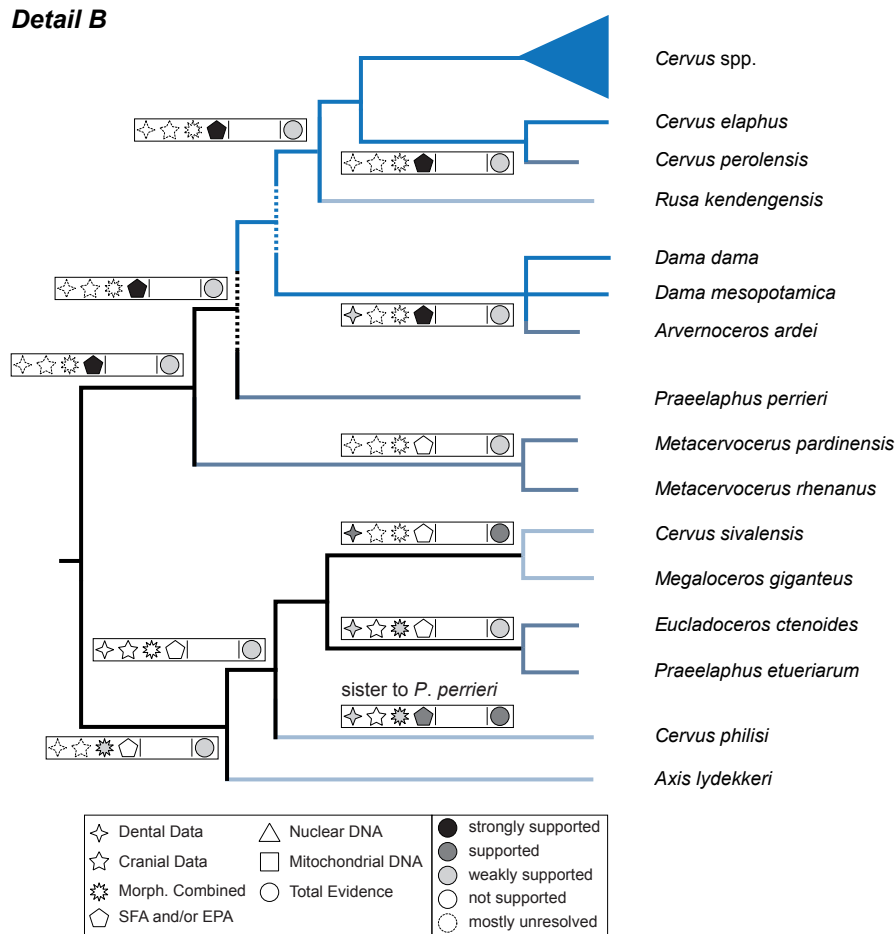


Figure 6.3: This topology summarises the phylogenetic positions of Plio- and Pleistocene cervids. All these taxa were closely related to living cervines in most analyses.

them in the topology. However they were most often placed within or close to crown Cervidae (Fig. 6.1). Some taxa were particularly unstable, *Cervus australis*, *Candiacervus ropalophorus*; also, placing *Megaloceros giganteus* was unexpectedly difficult even though this taxon had molecular and morphological data available. Based on solely molecular data it is most likely closely related to *Dama*. *Praelaphus etueriarum*, *Eucladoceros ctenoides*, and ‘*Cervus*’ *philisi* were also unstable but showed closer affinities to Cervini in some analyses. *Arvernoceros ardei*, ‘*Cervus*’ *perolensis*, *Metacervocerus pardinensis*, *Praelaphus perrieri*, *Metacervocerus rhenanus*, ‘*Cervus*’ *sivalensis*, *Axis lydekkeri*, and *Rusa kendengensis* were repeatedly placed within Cervini (Fig. 6.3). *Croizetoceros ramosus*, *Procapreolus cusanus*, and both fossil *Odocoileus* were often placed within Capreolinae. The fossil *Muntiacus muntjak* was almost always placed within Muntiacini.

Croizetoceros ramosus and *Procapreolus cusanus* are most likely ancestors of Capreolinae, the latter probably of Capreolini. The fossil *Odocoileus* species could not be identified

as the ancestors of the extant representatives, while the fossil *Muntiacus muntjak* is an ancestor of the extant species (Fig. 6.1).

The resulting systematic positions for fossil cervids represent a good initial quantitative estimate of relationships among fossil cervids and between fossil and extant cervids, which has never been accomplished in such detail before. Some confirmed previous hypotheses, some were observed for the first time and some others contradict previous positions. This extensive data basis can be used in the future to expand the data set. More material of fossil cervids is needed for future analyses to further clarify their systematic relationships.

Evolution

The origin of cervids was presumably in Eurasia, in the early Miocene (MN3). The current evidence of the fossil record suggests that cervids appeared first in Europe. They certainly diversified and dispersed rapidly in Eurasia and reached a high diversity. It was assumed that *Euprox furcatus* represents the first ancestor of crown Muntiacini (Azanza et al., 2013), a hypothesis still under debate. *Eostyloceros* is most likely a precursor of muntiacines based on its repeated position within this clade. Most Miocene cervids, however, represent extinct lineages without descendants. Members of the Pliocervinae were considered as potential ancestors of crown Cervini.

Cervids thrived and successfully populated Eurasia until the latest Miocene, when the first cervids entered North America via the Bering Strait. These immigrating taxa were most likely the ancestors of the endemic American cervids, which gave later rise to *Odocoileus* and *Mazama*. Descendants of these early odocoileine cervids entered South America around 2.5 mya and diversified rapidly occupying a variety of ecological niches.

In Eurasia Capreolini and Alceini diverged from Cervinae in the late Miocene and diversified. The split of Capreolini from Alceini is uncertain, but was most likely prior to the cervid invasion of America. While Capreolini remained in Eurasia, Alceini also migrated to America. Similarly, *Rangifer* whose origins are also uncertain, entered North America. Its systematic relationship is less controversial, consistently as the sister taxon to Odocoileini and the divergence between those taxa was presumably before odocoileine taxa diversified. *Alces* and *Rangifer* are successful in the boreal regions of the northern continents. Odocoileini are endemic to the Americas, while Capreolini, Muntiacini and all but one member of the Cervini (*Cervus canadensis*) remained in Eurasia.

Arvernoceros ardei, '*Cervus*' *perolensis*, *Metacervocerus pardinensis*, *Praeclaphus perrieri*, *Metacervocerus rhenanus*, '*Cervus*' *sivalensis*, *Praeclaphus etueriarum*, *Eucladoceros ctenoides*, and '*Cervus*' *philisi* probably are ancestors of crown Cervini or even extant *Cervus*. *Axis lydekkeri* and *Rusa kendengensis* were also placed as ancestors of living Cervini and possibly (based on qualitative morphological evidence) represent ancestors of extant *Axis* or *Rusa*, respectively. *Megaloceros giganteus* is most likely an early member of the *Dama*-lineage, even though this is hardly supported in my analyses. *Procapreolus cusanus* was considered as the ancestor of *Capreolus* and *Croizetoceros ramosus* as the the ancestor of other Capreolinae or potentially Odocoileini.

Several constraints and contingencies, such as dental, biogeographic, and phylogenetic conditions, prevented cervids from entering and establishing themselves in Africa, while bovids migrated to Africa, quickly diversified and still thrive there today. South American

cervids will potentially reach a similar diversity, since their dispersal happened far more recently and they probably are only at the beginning of a radiation.

6.2 Perspectives

More comprehensive sampling of species and characters will improve phylogenetic analyses and will potentially minimise or eliminate phylogenetic conflicts. As shown by Pfeiffer (1999) combining postcranial and craniodental characters will most likely improve the ability to distinguish different lineages of cervids.

Other anatomical characters, such as soft anatomy data, inner ear and brain case characters would be phylogenetically useful additions to morphological data sets. Also, behavioural characters can effectively be used as phylogenetic markers in cervids and should be sampled and incorporated in future analyses (Cap et al., 2002, 2008). Palaeontological and/or osteological information should be incorporated more often in combined approaches (Gatesy & O’Leary, 2001).

Many stages of the antler cycle are not yet fully understood; some aspects of antler regeneration have the potential to be useful in medical research (Kierdorf & Kierdorf, 2010). Therefore, more extensive research on the antlerogenetic process will provide exciting new insights into the development of such organs.

Due to the high level of karyotypic diversity, cytogenetics has been suggested as possibility to solve systematic relationships of cervids and *Mazama* in particular. Rare Genomic changes, e.g., gene duplication and genetic code changes, intron indels, and mitochondrial (or chloroplast) gene order changes, and SNP chips have become more popular as complementary markers and should be included as addition to the molecular partition in cervids Rokas & Holland (2000); Bixley et al. (2009); Lee & Palci (2015).

Phylogenetic trees represent hypotheses about the systematic relationships and branching patterns, because it is impossible to know the historical accuracy. As with all hypotheses, phylogenetic topologies will and should be further tested and revised with additional data, which makes reconstructing phylogenetic hypotheses an active and debatable area of research (Gregory, 2008).

I would like to conclude my work with a quote, which summarises the current cervid and ruminant systematics quite accurately: ‘There is as yet no resolution to this mess, but certainly we live in interesting times’ (Groves, 2014). Surely, I was able to solve some of the ‘mess’ at least in cervid systematics, but often answering one problem led to more questions, which makes this field indeed interesting with many more exciting results to be expected in the future. The outcomes and data of this project will be a valuable contribution to further resolve ruminant systematics.

Bibliography

- Abbazzi L (2001). Cervidae and Moschidae (Mammalia, Artiodactyla) from the Baccinello V-3 assemblage (Late Miocene, Late Turolian, Grosseto, Italy). *Rivista Italiana di Paleontologia e Stratigrafia*, **107**(1): 107–123.
- Abbazzi L (2004). Remarks on the validity of the generic name *Praemegaceros* Portis 1920, and an overview on *Praemegaceros* species in Italy. *Rendiconti Fisici dell'Accademia dei Lincei*, **9**(15): 115–132.
- Abbazzi L & Azanza B (2000). Deer fauna from Late Miocene (Messinian) Italian localities. *Les Ongulés holarctiques du Pliocène et du Pléistocène. 19-22 Septembre 2000*.
- Abbazzi L & Croitor R (2003). *Eostyloceros* cf. *pidoplitschkoi* Korotkevitsch 1964 (Cervidae, Muntiacinae): new element in the Neogene mammal assemblage of lower Valdarno (Tuscany, Central Italy). *Rivista Italiana di Paleontologia e Stratigrafia*, **109**(3): 575–580.
- Abbazzi L & Masini F (1997). *Megacerooides solilhacus* and other deer from the middle Pleistocene site of Isernia La Pineta (Molise, Italy). *Bollettino-Società Paleontologica Italiana*, **35**: 213–227.
- Abdrakhmanova L (1974). Fossil ruminants from Lake Karabastuz. *Materialy po Istorii Fauny i Flory Kazakhstana*, **6**: 83–92.
- Abdrakhmanova L, Bayshashov B, & Kostenko N (1989). Novyye dannyye po paleontologii Dzhungarskovo Aktau (Vostochnyi Kazakhstan)[New data on the paleontology of Dzhungarian Aktau (eastern Kazakhstan)]. *Vestnik Akademii Nauk Kazakhskoi SSR*, **3**: 76–78.
- Abril VV, Carnelossi EaG, González S, & Duarte JMB (2010). Elucidating the evolution of the red brocket deer *Mazama americana* complex (Artiodactyla; Cervidae). *Cytogenetic and Genome Research*, **128**: 177–187.
- Abril VV & Duarte JMB (2008). Chromosome polymorphism in the Brazilian dwarf brocket deer, *Mazama nana* (Mammalia, Cervidae). *Genetics and Molecular Biology*, **31**(1): 53–57.
- Accordi B (1972). *Lo scavo della 'Grotta Simonelli', con cervi mani del quaternario, effettuato a Creta nel 1971 dall'ist. di geologia e paleontologia dell'Univ. di Roma*. Accademia Nazionale del Lincei.

- Addicott FT (1982). *Abscission*. University of California Press, Berkeley, Los Angeles, London.
- Agnarsson I & May-Collado LJ (2008). The phylogeny of Cetartiodactyla: The importance of dense taxon sampling, missing data, and the remarkable promise of cytochrome b to provide reliable species-level phylogenies. *Molecular Phylogenetics and Evolution*, **48**: 964–985.
- Aguilar JP, Antoine PO, Crochet JY, López-Martínez N, Métais G, Michaux J, & Welcomme JL (2003). Les mammifères du Miocène inférieur de Beaulieu (Bouches-du-Rhône, France), comparaison avec Wintershof-West et le problème de la limite MN3/MN4. *Coloquios de Paleontología*, **1**: 1–24.
- Alcaraz MA & Zurita AE (2004). Nuevos registros de cérvidos poco conocidos: *Epieuryceros* cf. *proximus* Castellanos y *Antifer* sp. (Mammalia, Artiodactyla, Cervidae). *Revista del Museo Argentino de Ciencias Naturales, n. s.*, **6**(1): 41–48.
- Amano K & Taira A (1992). Two-phase uplift of Higher Himalayas since 17 Ma. *Geology*, **20**(5): 391–394.
- Amato G, Egan MG, & Rabinowitz A (1999a). A new species of muntjac, *Muntiacus putaoensis* (Artiodactyla: Cervidae) from northern Myanmar. *Animal Conservation*, **2**(1): 1–7.
- Amato G, Egan MG, Schaller GB, Baker RH, Rosenbaum HC, Robichaud WG, & DeSalle R (1999b). Rediscovery of Roosevelt's barking deer (*Muntiacus rooseveltorum*). *Journal of Mammalogy*, **80**(2): 639–643.
- Anderson AE & Wallmo OC (1984). *Odocoileus hemionus*. *Mammalian species*, **219**: 1–9.
- Angom S & Hussain SA (2013). A Review on Genetic Status of Eld's Deer *Rucervus eldii*: With Notes On Distribution, Population Status and Future Perspectives. *Octa Journal of Environmental Research*, **1**(2).
- Arif M, Shah S, & Vos J (1991). *Cervus rewati* sp. nov (Mammalia, Cervidae) from the Upper Siwaliks of Pakistan. *Geological Survey of Pakistan, Memoirs*, **17**.
- Asher RJ (2007). A web-database of mammalian morphology and a reanalysis of placental phylogeny. *BMC evolutionary biology*, **7**: 108.
- Azanza B (1993a). Sur la nature des appendices frontaux des cervidés (Artiodactyla, Mammalia) du Miocène inférieur et moyen. Remarques sur leur systématique et leur phylogeny. *Comptes Rendus de l'Académie des Sciences de Paris, Série II*, **316**: 1163–1169.
- Azanza B (1993b). Systématique et évolution du genre *Procervulus*, cervidé (Artiodactyla, Mammalia) du Miocène inférieur d'Europe. *Comptes Rendus de l'Académie des Sciences de Paris, Série II*, **316**: 717–723.

- Azanza B, DeMiguel D, DeMiguel D, Andrés M, & Andrés M (2011). The antler-like appendages of the primitive deer *Dicrocerus elegans*: morphology, growth cycle, ontogeny, and sexual dimorphism. *Estudios Geológicos*, **67**(2): 579–602.
- Azanza B & Ginsburg L (1997). A revision of the large lagomerycid artiodactyls of Europe. *Palaeontology*, **40**: 461–485.
- Azanza B & Montoya P (1995). A new deer from the Lower Turolian of Spain. *Journal of Paleontology*, **69**(6): 1163–1175.
- Azanza B & Morales J (1989). Los artiodáctilos de Huélago, Huéscar-1 y Cúllar de Baza-1 (Cuenca de Guadix-Baza, Granada). *Trabajos sobre el Neógeno-Cuaternario*, **11**: 289–316.
- Azanza B, Rössner GE, & Ortiz-Jaureguizar E (2013). The early Turolian (late Miocene) Cervidae (Artiodactyla, Mammalia) from the fossil site of Dorn-Dürkheim 1 (Germany) and implications on the origin of crown cervids. *Palaeobiodiversity and Palaeoenvironments*, **93**: 217–258.
- Azanza Asensio B (2000). Los Cervidae (Artiodactyla, Mammalia) del Mioceno de las cuencas del Duero, Tajo, Calatayud-Teruel y Levante. *Memorias del Museo Paleontológico de la Universidad de Zaragoza*, **8**: 376.
- Azanza Asensio B & Menendez E (1989). Los ciervos fósiles del neógeno español. *Paleontología i evolució*, **23**: 75–82.
- Azzaroli A (1952). La sistematica dei cervi giganti e i cervi nani delle isole. *Atti della Società Toscana di Scienze Naturali, Mem. A*, **59**: 119–127.
- Azzaroli A (1953). The deer of the Weybourn Crag and Forest Bed of Norfolk. *Bulletin of the British Museum (Natural History)*, **2**(i): 1–96.
- Azzaroli A (1954). Critical observations upon Siwalik deer. *Proceedings of the Linnean Society of London*, **165**(1): 75–83.
- Azzaroli A (1961). Il nanismo nei cervi insulari. *Palaeontographica Italia*, **56**: 1–32.
- Azzaroli A (1971). Il significato delle faune insulari quaternarie. *Le Scienze*, **30**: 84–93.
- Azzaroli A (1982). On the Quaternary and recent cervid genera *Alces*, *Cervalces*, *Libralces*. *Bollettino della Società Paleontologica Italiana*, **20**(2): 147–154.
- Azzaroli A, De Giuli C, Ficarelli G, & Torre D (1988). Late Pliocene to early mid-Pleistocene mammals in Eurasia: faunal succession and dispersal events. *Palaeogeography, Palaeoclimatology, Palaeoecology*, **66**(1-2): 77–100.
- Azzaroli A & Mazza P (1992a). The cervid genus *Eucladoceros* in the early Pleistocene of Tuscany. *Palaeontographia Italica*, **79**: 43–100.
- Azzaroli A & Mazza P (1992b). On the possible origin of the Giant Deer genus *Megaceroides*. *Rendiconti Lincei*, **3**(1): 23–32.

- Azzaroli A & Mazza P (1993). Large Early Pleistocene deer from Pietrafitta lignite mine, Central Italy. *Palaeontographia Italica*, **80**: 1–24.
- Baker RH, Yu X, & DeSalle R (1998). Assessing the relative contribution of molecular and morphological characters in simultaneous analysis trees. *Molecular phylogenetics and evolution*, **9**(3): 427–436.
- Balakrishnan CN, Monfort SL, Gaur A, Singh L, & Sorenson MD (2003). Phylogeography and conservation genetics of Eld's deer (*Cervus eldi*). *Molecular Ecology*, **12**(1): 1–10.
- Bärmann EV (2012). *Towards a Comprehensive Phylogeny of Bovidae*. PhD thesis, University of Cambridge.
- Bärmann EV & Rössner GE (2011). Dental nomenclature in Ruminantia: Towards a standard terminological framework. *Mammalian Biology-Zeitschrift für Säugetierkunde*, **76**(6): 762–768.
- Barrio J (2010). Chapter 9 - Taruka *Hippocamelus antisensis* (d'Orbigny 1834). In Duarte JMB & Gonzalez S (Eds.), *Neotropical Cervidology: Biology and Medicine of Neotropical Deer*, FUNEP and IUCN, Jaboticabal, Brazil, pp. 77–88.
- Benammi M & Jaeger JJ (2001). Magnetostratigraphy and palaeontology of the continental Middle Miocene of the Aït Kandoula Basin, Morocco. *Journal of African Earth Sciences*, **33**(2): 335–348.
- Beninde J (1937). Der Merkmalswert des Hirschgeweihs für die paläontologische Systematik der Genus *Cervus*. *Paläontologische Zeitschrift*, **19**(1-2): 52–56.
- Berger SA, Krompass D, & Stamatakis A (2011). Performance, accuracy, and web server for evolutionary placement of short sequence reads under maximum likelihood. *Systematic biology*, **60**(3): 291–302.
- Bibi F (2014). Assembling the ruminant tree: combining morphology, molecules, extant taxa, and fossils. *Zitteliana B*, **32**(September 2013): 197–212.
- Bibi F & Métais G (2016). Evolutionary history of the large herbivorous of south and southeast Asia (Indomalayan Realm). In Areshtani F & Sankaran M (Eds.), *The ecology of large herbivores in south and southeast Asia*, Springer, Dordrecht, Heidelberg, Berlin, p. 15–88.
- Bibi F, Vrba E, & Fack F (2012). A new African fossil caprin and a combined molecular and morphological Bayesian phylogenetic analysis of Caprini (Mammalia: Bovidae). *Journal of Evolutionary Biology*, **25**: 1843–1854.
- Bixley M, Ward J, Brauning R, Archer J, & Fisher P (2009). Building A Deer SNP Chip. *Biotechnology tools and challenges*, pp. 300–303.
- Blumenbach JF (1803). *Specimen archaeologiae telluris terrarumque imprimis Hannever-anarum*. Goettingae.

- Blyth E (1863). On some horns of ruminants. *Proceedings of the Zoological Society London*, p. 155.
- Böhme M, Aiglstorfer M, Uhl D, & Kullmer O (2012). The antiquity of the Rhine River: Stratigraphic coverage of the Dinotheriensande (Eppelsheim Formation) of the mainz basin (Germany). *PLoS ONE*, **7**(5).
- Bout P & A A (1952). Stratigraphie et Faune du creux de Peirolles près Perrier (Puy-de-Dôme). *Annales de Paléontologie*, **38**: 3–22.
- Bouvrain G, Geraads D, & Jehenne Y (1989). Nouvelles données relatives à la classification des Cervidae (Artiodactyla, Mammalia). *Zoologischer Anzeiger*, **223**: 82–90.
- Briggs AW, Stenzel U, Johnson PL, Green RE, Kelso J, Prüfer K, Meyer M, Krause J, Ronan MT, Lachmann M et al. (2007). Patterns of damage in genomic DNA sequences from a Neandertal. *Proceedings of the National Academy of Sciences*, **104**(37): 14616–14621.
- Briggs AW, Stenzel U, Meyer M, Krause J, Kircher M, & Pääbo S (2010). Removal of deaminated cytosines and detection of in vivo methylation in ancient DNA. *Nucleic acids research*, **38**(6): e87–e87.
- Brokx PA (1972). The superior canines of *Odocoileus* and other deer. *Journal of Mammalogy*, **53**(2): 359–366.
- Brooke V (1878). On the classification of Cervidae with a synopsis of the existing species. *Proc. Zool. Soc. London*, **1878**(1878): 883–928.
- Brookes J (1828). *A Catalogue of the Anatomical & Zoological Museum of Joshua Brookes, esq. F.R.S., F.L.S. etc.* George Robins, London, United Kingdom.
- Brown C (1980). *An evaluation of selection factors for antler growth in red deer (Cervus elaphus)*. Diploma thesis, Lincoln College, University of Canterbury, NZ.
- Bubenik AB (1966). *Das Geweih: Entwicklung, Aufbau und Ausformung der Geweihe und Gehörne und ihre Bedeutung für das Wild und für die Jagd*. P. Parey Verlag, Hamburg, Berlin, 214 pp.
- Bubenik AB (1990). Epigenetical, morphological, physiological, and behavioral aspects of evolution of horns, pronghorns, and antlers. In Bubenik G & Bubenik A (Eds.), *Horns, pronghorns, and antlers: Evolution, morphology, physiology, and social significance*, Springer-Verlag, New York, pp. 3–113.
- Bubenik G & Bubenik AB (1986). Phylogeny and ontogeny of antlers and neuro-endocrine regulation of the antler cycle - a review. *Säugetierkundliche Mitteilungen*, **33**: 97–123.
- Buntjer J, Nijman I, Zijlstra C, & Lenstra J (1998). A Satellite DNA Element Specific for Roe Deer (*Capreolus capreolus*). *Chromosoma*, **107**(1): 1–5.
- Caloi L & Malatesta A (1974). Il cervo pleistocenico di Sardegna. *Memorie dell'Istituto Italiana di Paleontologia*, **2**: 163–247.

- Canto J, Yáñez J, & Rovira J (2010). Estado actual del conocimiento de los mamíferos fósiles de Chile. *Estudios Geológicos*, **66**(2): 255–284.
- Cap H, Aulagnier S, & Deleporte P (2002). The phylogeny and behaviour of Cervidae (Ruminantia Pecora). *Ethology Ecology & Evolution*, **14**: 199–216.
- Cap H, Deleporte P, Joachim J, & Reby D (2008). Male vocal behavior and phylogeny in deer. *Cladistics*, **24**: 917–931.
- Caro TM, Graham CM, Stoner CJ, & Flores MM (2003). Correlates of horn and antler shape in bovids and cervids. *Behavioral Ecology and Sociobiology*, **55**(1): 32–41.
- Carr SM, Ballinger SW, Derr JN, Blankenship LH, & Bickham JW (1986). Mitochondrial DNA analysis of hybridization between sympatric white-tailed deer and mule deer in west Texas. *Proceedings of the National Academy of Sciences*, **83**(24): 9576–9580.
- Chow Bs & Shih Mc (1978). A skull of *Lagomeryx* from the middle Miocene of Linchu, Shantung. *Vertebrata Palasiatica*, **16**(2): 111–122.
- Clutton-Brock T (1982). The functions of antlers. *Behaviour*, **79**(2): 108–124.
- Clutton-Brock TH (1989). Review lecture: mammalian mating systems. *Proceedings of the Royal Society of London B: Biological Sciences*, **236**(1285): 339–372.
- Cockerill R (1984). Deer. *The Encyclopedia of Mammals. Facts on File Publishing, NY*, pp. 520–529.
- Cohen K, Finney S, Gibbard P, & Fan JX (2013). The ICS international chronostratigraphic chart. *Episodes*, **36**(3): 199–204.
- Colbert EH (1935). Siwalik mammals in the American Museum of Natural History. *Transactions of the American Philosophical Society, New Series*, **26**: 1–401.
- Cook CE, Wang Y, & Sensabaugh G (1999). A Mitochondrial Control Region and Cytochrome b Phylogeny of Sika Deer (*Cervus nippon*) and Report of Tandem Repeats in the Control Region. *Molecular phylogenetics and evolution*, **12**(1): 47–56.
- Corbet G & Hill J (1980). *A World List of Mammalian Species*. British Museum (Natural History) London and Cornell University Press Ithaca (New York).
- Costeur L (2011). A partial skull of *Dremotherium feignouxii* from the Aquitanian of France (MN2, Saint-Gérard-le-Puy, Allier). *Acta Geologica Slovaca*, **3**(2): 105–112.
- Costeur L & Legendre S (2008a). Mammalian Communities Document a Latitudinal Environmental Gradient during the Miocene Climatic Optimum in Western Europe. *Palaios*, **23**(1997): 280–288.
- Costeur L & Legendre S (2008b). Spatial and temporal variation in European Neogene large mammals diversity. *Palaeogeography, Palaeoclimatology, Palaeoecology*, **261**: 127–144.

- Crête M, Ouellet JP, & Lesage L (2001). Comparative effects on plants of caribou/reindeer, moose and white-tailed deer herbivory. *Arctic*, pp. 407–417.
- Croitor R (2006a). Early Pleistocene small-sized deer of Europe. *Hellenic Journal of Geosciences*, **41**: 89–117.
- Croitor R (2006b). Taxonomy and systematics of large-sized deer of the genus *Praemegaceros* Portis, 1920 (Cervidae, Mammalia). *CFS Courier Forschungsinstitut Senckenberg*, pp. 91–116.
- Croitor R (2009). Systematical Position and Evolution of the genus *Arvernoceros* (Cervidae, Mammalia) from Plio-Pleistocene of Eurasia. *Muzeul Olteniei Craiova. Oltenia. Studii si comunicari. S tiintele Naturii*, **25**: 375–382.
- Croitor R (2012). Lower Pleistocene ruminants from Monte Riccio (Tarquinia, Italy). *Oltenia, Studii și comunicări, Științele naturii*, **28**(1): 221–226.
- Croitor R (2014). Deer from Late Miocene to Pleistocene of Western Palearctic: matching fossil record and molecular phylogeny data. *Zitteliana B*, **32**: 115–154.
- Croitor R & Bonifay MF (2001). Étude préliminaire des cerfs du gisement Pléistocène inférieur de Ceysse (Haute-Loire). *PALEO*, **13**: 129–144.
- Croitor R, Bonifay MF, & Bonifay E (2006). Origin and evolution of the Late Pleistocene island deer *Praemegaceros (Nesoleipoceros) cazioti* (Depéret) from Corsica and Sardinia. *Bulletin du Musée d'Anthropologie préhistorique de Monaco*, **46**: 35–68.
- Croitor R & Stefaniak K (2009). Early Pliocene deer of Central and Eastern European regions and inferred phylogenetic relationships.
- Croizet JB & Jobert ACG (1828). *Recherches sur les ossements fossiles du département du Puy-de-Dôme*. Delahays, Paris, 224 pp.
- Cronin MA (1991). Mitochondrial-DNA Phylogeny of Deer (Cervidae). *Journal of Mammalogy*, **72**: 553–566.
- Cronin MA, Stuart R, Pierson BJ, & Patton JC (1996). K-casein gene phylogeny of higher ruminants (Pecora, Artiodactyla). *Molecular Phylogenetics and Evolution*, **6**(2): 295–311.
- Cronin MA, Vyse ER, & Cameron DG (1988). Genetic relationships between mule deer and white-tailed deer in Montana. *The Journal of Wildlife Management*, pp. 320–328.
- Czyżewska T (1959). *Cervus (Rusa)* sp. z pliocenkiej brekcji kostnej z Weżów. *Acta Palaeontologica Polonica*, **4**(4): 389–429.
- Czyżewska T (1968). Deer from Weże and their relationship with the Pliocene and Recent Eurasiatic Cervidae. *Acta Palaeontologica Polonica*, **8**(4): 537–593.
- Darriba D, Weiß M, & Stamatakis A (2016). Prediction of missing sequences and branch lengths in phylogenomic data. *Bioinformatics*, **32**(9): 1331–1337.

- Davis EB, Brakora Ka, & Lee AH (2011). Evolution of ruminant headgear: a review. *Proceedings. Biological sciences / The Royal Society*, **278**(July): 2857–2865.
- De Abreu C, Martinez AC, de Moraes W, Juvenales J, & Moreira N (2009). Características reprodutivas de veado-bororó-do-sul ou veado-mão-curta (*Mazama nana*). *Pesq. Vet. Bras*, **29**(12): 993–998.
- de Queiroz K (2000). Logical problems associated with including and excluding characters during tree reconstruction and their implications for the study of morphological character evolution. In Wiens JJ (Ed.), *Phylogenetic analysis of Morphological data*, Smithsonian Institution Press, Washington and London, pp. 192–212.
- De Queiroz K & Gauthier J (1992). Phylogenetic taxonomy. *Annual review of ecology and systematics*, **23**: 449–480.
- De Serres MM (1832). *Recherches sur les ossements humatiles de la caverne de Lunel-Viel*. Boehm, Montpellier, 275 pp.
- De Vos J (1979). The endemic Pleistocene deer of Crete. *Proceedings of the Koninklijke Nederlandse Akademie van Wetenschappen Amsterdam, Series B*, **82**(1): 59–90.
- De Vos J (1984). The endemic Pleistocene deer of Crete. *Verhandelingen der Koninklijke Nederlandse Akademie van Wetenschappen, afd. Natuurkunde, eerste reeks*, **31**: 1–110.
- De Vos J (2000). Pleistocene Deer Fauna in Crete: Its adaptive Radiation and Extinction. *Tropics*, **10**(1): 125–134.
- De Vos J & Reumer JWF (1995). Early Pleistocene Cervidae (Mammalia, Artiodactyla) from the Oosterschelde (the Netherlands), with a revision of the cervid genus *Eucladoceros* Falconer, 1868. *Deinsea*, pp. 95–121.
- Dehm R (1944). Frühe Hirschgeweihe aus dem Miocän Süddeutschlands. *Neues Jahrbuch für Mineralogie, Geologie und Palaontologie, Monatshefte*, pp. 81–98.
- DeMiguel D, Azanza B, & Morales J (2010). Trophic flexibility within the oldest Cervidae lineage to persist through the Miocene Climatic Optimum. *Palaeogeography, Palaeoclimatology, Palaeoecology*, **289**: 81–92.
- DeMiguel D, Azanza B, & Morales J (2011). Paleoenvironments and paleoclimate of the Middle Miocene of central Spain: A reconstruction from dental wear of ruminants. *Palaeogeography, Palaeoclimatology, Palaeoecology*, **302**(3–4): 452–463.
- DeMiguel D, Azanza B, & Morales J (2013). Key innovations in ruminant evolution: a paleontological perspective. *Integrative zoology*, pp. 1–52.
- DeMiguel D, Fortelius M, Azanza B, & Morales J (2008). Ancestral feeding state of ruminants reconsidered: earliest grazing adaptation claims a mixed condition for Cervidae. *BMC evolutionary biology*, **8**: 13.

- Deng T, Lu XK, Shi QQ, Sun BY, & Wang SQ (2014). A new species of crown-antlered deer *Stephanocemas* (Cervidae, Artiodactyla) from the Middle Miocene of the Linxia Basin in Gansu, China. *Vertebrata Palasiatica*, **52**(2): 171–182.
- Depéret C (1884). Nouvelles études sur les Ruminants pliocènes et quaternaires d'Auvergne. *Bulletin de la Société Géologique de France, Série 3*, **T12**: 247–284.
- Depéret C (1910). *Etudes sur la famille des Lophiodontidés*. Société Géologique de France.
- Depéret C & Mayet L (1911). Le gisement de Senèze et sa faune paléomammalogique. *Association Française pour l'Avancement des Sciences, Comptes rendus 39e session, Toulouse, 1910, Notes et Mémoires*, **2**: 261–263.
- Di Stefano G & Petronio C (2002). Systematics and Evolution of the Eurasian Plio-Pleistocene tribe Cervini (Artiodactyla, Mammalia). *Geologica Romana*, **36**: 311–334.
- Dietrich WO (1933). [Review of] C.C. Young: On the Artiodactyla from the *Sinanthropus* Site at Choukoutien. *Neues Jahrbuch für Mineralogie, Geologie und Paläontologie. Referate III*, **2**: 475–477.
- Dietrich WO (1938). Zur Kenntnis der o-pliozänen echten Hirsche. *Zeitschrift der Deutschen Geologischen Gesellschaft*, **90**.
- Dong W (1993). The Fossil Records of Deer in China. In Ohtaishi N & Sheng HL (Eds.), *Deer of China*, Elsevier Science Publishers, pp. 95–102.
- Dong W (1996). Les Cervidae (Artiodactyla) rusciniens (Pliocene) du Languedoc et du Roussillon (France). *Bulletin du Muséum National d'Histoire Naturelle*, **18**(1985): 133–163.
- Dong W (2007). New material of Muntiacinae (Artiodactyla, Mammalia) from the Late Miocene of the northeastern Qinghai-Tibetan Plateau, China. *Comptes Rendus - Palevol*, **6**: 335–343.
- Dong W (2011). Reconsideration of the systematics of the Early Pleistocene *Cervavitus* (Cervidae, Artiodactyla, Mammalia). *Estudios Geológicos*, **67**(2): 603–611.
- Dong W, Liu J, & Pan Y (2003). A new *Euprox* from the Late Miocene of Yuanmou, Yunnan Province, China, with interpretation of its paleoenvironment. *Chinese Science Bulletin*, **48**(5): 485–491.
- Dong W, Pan Y, & Liu J (2004). The earliest *Muntiacus* (Artiodactyla, Mammalia) from the Late Miocene of Yuanmou, southwestern China. *Comptes Rendus Palevol*, **3**: 379–386.
- d'Orbigny A (1834). *Voyage dans l'Amérique Méridionale... exécuté pendant les années 1826-1833*, vol. 2.
- Douzery E & Randi E (1997). The mitochondrial control region of Cervidae: evolutionary patterns and phylogenetic content. *Molecular Biology and Evolution*, **14**(11): 1154–1166.

- Duarte JMB (1992). *Aspectos taxonômicos e citogenéticos de algumas espécies de cervídeos brasileiros*. MSc Thesis, Faculdade de Ciências Agrárias e Veterinárias, Universidade Estadual Paulista, Jaboticabal, Brazil.
- Duarte JMB, Abril VV, Vogliotti A, dos Santos Zanetti E, de Oliveira ML, Tiepolo LM, Rodrigues LF, & de Almeida LB (2012a). Avaliação do risco de extinção do veado-cambuta *Mazama nana* Hensel, 1872, no Brasil. *Biodiversidade Brasileira*, **2**(3): 59–67.
- Duarte JMB, González S, & Maldonado JE (2008). The surprising evolutionary history of South American deer. *Molecular phylogenetics and evolution*, **49**: 17–22.
- Duarte JMB & Jorge W (2003). Morphologic and cytogenetic description of the small red brocket (*Mazama bororo* Duarte, 1996) in Brazil. *Mammalia*, **67**(3): 403–410.
- Duarte JMB & Merino M (1997). Taxonomia e evolução. In Duarte JMB (Ed.), *Biologia e conservacao de Cérvidos Sul-americanos: Blastocerus, Ozotoceros e Mazama*, FUNEP, Jaboticabal, Brasil, pp. 2–21.
- Duarte JMB, Vogliotti A, dos Santos Zanetti E, de Oliveira ML, Tiepolo LM, Rodrigues LF, & de Almeida LB (2012b). Avaliação do risco de extinção do veado-catingueiro *Mazama gouazoubira* G. Fischer [von Waldhein], 1814, no Brasil. *Biodiversidade Brasileira*, **2**(3): 50–58.
- Duarte JMB, Vogliotti A, dos Santos Zanetti E, de Oliveira ML, Tiepolo LM, Rodrigues LF, & de Almeida LB (2012c). Avaliação do risco de extinção do veado-galheiro *Odocoileus virginianus* Zimmermann, 1780, no Brasil. *Biodiversidade Brasileira*, **2**(3): 15–19.
- Duarte JMB, Vogliotti A, dos Santos Zanetti E, de Oliveira ML, Tiepolo LM, Rodrigues LF, & de Almeida LB (2012d). Avaliação do risco de extinção do veado-mateiro-pequeno *Mazama bororo* Duarte, 1996, no Brasil. *Biodiversidade Brasileira*, **2**(3): 42–49.
- Duarte JMB, Vogliotti A, dos Santos Zanetti E, de Oliveira ML, Tiepolo LM, Rodrigues LF, & de Almeida LB (2012e). Avaliação do risco de extinção do veado-mateiro *Mazama americana* Erxleben, 1777, no Brasil. *Biodiversidade Brasileira*, **2**(3): 33–41.
- Duarte JMB, Vogliotti A, dos Santos Zanetti E, de Oliveira ML, Tiepolo LM, Rodrigues LF, & de Almeida LB (2012f). Avaliação do risco de extinção do veado-roxo *Mazama nemorivaga* Cuvier, 1817, no Brasil. *Biodiversidade Brasileira*, **2**(3): 68–73.
- Duarte JMB, Vogliotti A, dos Santos Zanetti E, de Oliveira ML, Tiepolo LM, Rodrigues LF, de Almeida LB, & Braga FG (2012g). Avaliação do risco de extinção do veado-campeiro *Ozotoceros bezoarticus* Linnaeus, 1758, no Brasil. *Biodiversidade Brasileira*, **2**(3): 20–32.
- Dubois E (1904). Over een equivalent van het Cromer Forest-Bed in Nederland. *Verslag van de Gewone Vergadering der Wis- en Natuurkunde Afdeeling van de Koninklijke Akademie van Wetenschappen te Amsterdam*, **13**: 243–251.

- Dubois E (1907). Eenige van Nederlandschen kant verkregen uitkomsten met betrekking tot de kennis der Kendeng-fauna (fauna van Trinil). *Tijdschrift Koninklijk Nederlandsch Aardrijkskundig Genootschap, Series 2*, **24**: 449–458.
- Dubois E (1908). *Das geologische Alter der Kendeng-oder Trinil-fauna*. EJ Brill.
- Dubost G, Charron F, Courcoul A, & Rodier A (2011). The Chinese water deer, *Hydropotes inermis* – A fast-growing and productive ruminant. *Mammalian Biology - Zeitschrift für Säugetierkunde*, **76**: 190–195.
- Duckworth J, Robichaud W, & Timmins R (2008). *Rucervus schomburgki*. *The IUCN red list of threatened species. Version 2014.3*. Available at www.iucnredlist.org (accessed on 17 April 2015).
- Eisenberg J (2000). The contemporary Cervidae of South America. In Vrba E & Schaller G (Eds.), *Antelopes, Deer, and Relatives. Fossil record, Behavioral Ecology, Systematics, and Conservation*, Yale University Press, New Haven and London, pp. 189–202.
- Emerson B & Tate M (1993). Genetic analysis of evolutionary relationships among deer (subfamily Cervinae). *Journal of Heredity*, **84**(4): 266–273.
- Erxleben J (1777). *Systema regni animalis per classes, ordines, genera, species, varietates, cum synonymia et historia animalium. Classis I. Mammalia*. Weygandianis, Lipsiae, 636 pp.
- Escamilo L, Barrio J, Benavides J, & Tirira D (2010). Northern pudu *Pudu mephistophiles* (De Winton 1896). *Neotropical cervidology. Biology and medicine of Latin American deer.*, (1975): 133–139.
- Escobedo-Morales LA, Mandujano S, Eguiarte LE, Rodríguez-Rodríguez MA, & Maldonado JE (2016). First phylogenetic analysis of Mesoamerican brocket deer *Mazama pandora* and *Mazama temama* (Cetartiodactyla: Cervidae) based on mitochondrial sequences: Implications on Neotropical deer evolution. *Mammalian Biology-Zeitschrift für Säugetierkunde*, **81**(3): 303–313.
- Farris JS (1983). The logical basis of phylogenetic analysis. In Platnick NI & Funk VA (Eds.), *Advances in Cladistics. Proceedings of the second meeting of the Willi Hennig Society*, Columbia University Press, New York, pp. 1–36.
- Fischer G (1814). *Zoognosia tabulis synopticis illustrata: in usum praelectionum Academiae imperialis medico-chirurgicae mosquensis edita*. Typis Nicolai Sergeidis Vsevolozsky, Mosquae, 1–732 pp.
- Flerov KK (1952). *Fauna of the USSR., Mammals 1(2). Musk deer and deer*. The Academy of Sciences of the USSR, Moscow.
- Flower BP & Kennett JP (1994). The middle Miocene climatic transition: East Antarctic ice sheet development, deep ocean circulation and global carbon cycling. *Palaeogeography, palaeoclimatology, palaeoecology*, **108**(3-4): 537–555.

- Flueck WT & Smith-Flueck JM (2011). Osteological comparisons of appendicular skeletons: A case study on Patagonian huemul deer and its implications for conservation. *Animal Production Science*, **51**: 327–339.
- Fontana F & Rubini M (1990). Chromosomal evolution in Cervidae. *Biosystems*, **24**(2): 157–174.
- Fortelius M, Eronen JT, Kaya F, Tang H, Raia P, & Puolamäki K (2014). Evolution of Neogene Mammals in Eurasia: Environmental Forcing and Biotic Interactions. *Annual Review of Earth and Planetary Sciences*, **42**(1): 579–604.
- Franzmann AW (1981). *Alces alces*. *Mammalian Species*, **154**: 1–7.
- Fry W & Gustafson E (1974). Cervids from the Pliocene and Pleistocene of central Washington. *Journal of Paleontology*, **48**(2): 375–386.
- Fuentes-Hurtado M, Marín JC, Gonzalez-Acuna D, Verdugo C, Vidal F, & Vianna JA (2011). Molecular divergence between insular and continental Pudu deer (*Pudu puda*) populations in the Chilean Patagonia. *Studies on Neotropical Fauna and Environment*, **46**(1): 23–33.
- Gatesy J & Baker RH (2005). Hidden likelihood support in genomic data: can forty-five wrongs make a right? *Systematic biology*, **54**(3): 483–492.
- Gatesy J, O'Grady P, & Baker RH (1999). Corroboration among Data Sets in Simultaneous Analysis: Hidden Support for Phylogenetic Relationships among Higher Level Artiodactyl Taxa. *Cladistics*, **15**: 271–313.
- Gatesy J & O'Leary MA (2001). Deciphering whale origins with molecules and fossils. *Trends in Ecology and Evolution*, **16**(10): 562–570.
- Gaudry MA (1877). *Les enchaînements du monde animal dans les temps géologiques mammifères tertiaires*, vol. 1. F. Savy, Paris, 295 pp.
- Geisler JH, McGowen MR, Yang G, & Gatesy J (2011). A supermatrix analysis of genomic, morphological, and paleontological data from crown Cetacea. *BMC evolutionary biology*, **11**(1): 112.
- Geist V (1966). The evolution of horn-like organs. *Behaviour*, **27**: 175–214.
- Geist V (1968). Horn-like structures as rank symbols, guards and weapons. *Nature*, **220**: 813–814.
- Geist V (1998). *Deer of the world: their evolution, behaviour, and ecology*. Stackpole books, Mechanicsburg, 421 pp.
- Geist V & Bayer M (1988). Sexual dimorphism in the Cervidae and its relation to habitat. *Journal of Zoology*, **214**: 45–53.

- Gentry A, Rössner G, & Heizmann EPJ (1999). Suborder Ruminantia. In Rössner G & Heissig K (Eds.), *The Miocene Land Mammals of Europe*, Verlag Dr. Friedrich Pfeil, München, pp. 225–258.
- Gentry AW (1970). The Bovidae (Mammalia) of the Fort Ternan fossil fauna. *Fossil vertebrates of Africa*, **2**: 243–323.
- Gentry AW (1990). Ruminant artiodactyls of Paşalar, Turkey. *Journal of Human Evolution*, **19**: 529–550.
- Gentry AW (1994). The Miocene differentiation of old world Pecora (Mammalia). *Historical Biology*, **7**: 115–158.
- Gentry AW (2000). The ruminant radiation. In Vrba ES & Schaller GB (Eds.), *Antelopes, deer, and relatives*, Yale University Press, New Haven, pp. 11–25.
- Gentry AW (2005). Ruminants of Ruabánya. *Palaeontographica Italica*, **90**: 283–303.
- Gentry AW & Hooker JJ (1988). The phylogeny of the Artiodactyla. In Benton M (Ed.), *The phylogeny and classification of the tetrapods. Volume 2. Mammals. Systematics Association Special Volume 35B*, Clarendon Press, Oxford, pp. 235–272.
- Geraads D (2003). Ruminants, other than Giraffidae from the middle Miocene hominoid locality of Çandir (Turkey). *Courier Forschungs-Institut Senckenberg*, **240**: 181–199.
- Germonpré M (1983). Les mammifères de la Formation de la Campine. *Bulletin de la Société géologique Belge*, **92**(2): 111–123.
- Gervais FLP (1859). *Zoologie et paléontologie françaises (animaux vertébrés): ou Nouvelles recherches sur les animaux vivants et fossiles de la France*. Arthus Bertrand, Paris, 544 pp.
- Gervais MP (1848–1852). *Zoologie et paléontologie françaises (animaux vertébrés) ou nouvelles recherches sur les animaux et fossiles de la France*, vol. t.1. Arthus Bertrand, Paris, 271 pp.
- Gervais MP (1849). Sur la répartition des mammifères fossiles entre les différents âges tertiaires qui composent le sol de la France. *Comptes Rendu hebdomadaire de l'Académie de Sciences*, **28**: 546–552.
- Ghaffar A, Khan M, & Akhtar M (2010). Early Pliocene Cervids (Artiodactyla-Mammalia) from the Siwaliks of Pakistan. *Yerbilimleri (Earth Sciences)*, **31**(3): 217–231.
- Ghaffar A, Khan MA, Akhtar M, Qureshi MA, Farooq U, & Nazir M (2006). The Oldest Cervid from the Siwalik Hills of Pakistan. *Journal of Applied Sciences*, **6**(1): 127–130.
- Giao PM, Tuoc D, Dung V, Wikramanayake E, Amato G, Arctander P, & MacKinnon J (1998). Description of *Muntiacus truongsongensis*, a new species of muntjac (Artiodactyla: Muntiacidae) from central Vietnam, and implications for conservation. *Animal Conservation*, **1**(01): 61–68.

- Gilbert C, Ropiquet A, & Hassanin A (2006). Mitochondrial and nuclear phylogenies of Cervidae (Mammalia, Ruminantia): Systematics, morphology, and biogeography. *Molecular Phylogenetics and Evolution*, **40**: 101–117.
- Gilbert MTP, Bandelt HJ, Hofreiter M, & Barnes I (2005). Assessing ancient DNA studies. *Trends in Ecology and Evolution*, **20**(10): 541–544.
- Ginsburg L (1985). Essai de phylogénie des Eupecora (Ruminantia, Artiodactyla, Mammalia). *Comptes Rendus de l'Académie des Sciences de Paris, Série II*, **301**(17): 319–322.
- Ginsburg L (1988). La faune des mammifères des sables Miocènes du synclinal d'Esvres (Val de Loire). *Comptes rendus de l'Académie des Sciences. Série 2, Mécanique, Physique, Chimie, Sciences de l'univers, Sciences de la Terre*, **307**(3): 319–322.
- Ginsburg L (1989). The faunas and stratigraphical subdivisions of the Orleanian in the Loire Basin (France). In Lindsay E, Fahlbusch V, & Mein P (Eds.), *European Neogene Mammal Chronology*, Springer, vol. 180 of *NATO ASI Series A*, pp. 157–176.
- Ginsburg L & Azanza B (1991). Présence de bois chez les femelles du cervidé miocène *Dicrocerus elegans* et remarques sur le problème de l'origine du dimorphisme sexuel sur les appendices frontaux des Cervidae. *Comptes Rendus de l'Académie des Sciences de Paris, Série II*, **313**: 121–126.
- Ginsburg L, Cheneval J, Janvier P, Pouit D, & Sen S (2000). Les Vertébrés des sables continentaux d'âge Orléanien inférieur (MN 3) de Mauvières à Marcilly-sur-Maulne (Indre-et-Loire), La Brosse à Meigné-le-Vicomte (Maine-et-Loire) et Chitenay (Loir-et-Cher). *Geodiversitas*, **22**(4): 597–631.
- Ginsburg L & Crouzel F (1976). Contribution à la connaissance d'*Heteroprox larteti* (Filhol): Cervidé du Miocène européen. *Bulletin du Muséum National d'Histoire Naturelle, 3e Série, Sciences de la Terre*, **58**(399): 345–357.
- Ginsburg L & Heintz E (1966). Sur les affinités du genre *Palaeomeryx* (Ruminant du Miocène européen). *Comptes rendus de l'Académie des sciences, Série D*, **262**: 979–982.
- Godina AY, Gromova VI, Sokolov II, Trofimov BA, Flerov KK, & Haveson YI (1962). Order Artiodactyla, even-toed ungulates. In Gromova V (Ed.), *Basics of Palaeontology: Mammals*, Moscow, pp. 337–341.
- Gonzalez E, Labarca R, Chavez-Hoffmeister M, & Pino M (2014). First Fossil Record of the Smallest Deer cf. *Pudu* Molina, 1782 (Artiodactyla, Cervidae), in the Late Pleistocene of South America. *Journal of Vertebrate Paleontology*, **1782**(March): 483–488.
- González S, Cosse M, Braga FG, Vila AR, Merino ML, Dellafiore C, Cartes JL, Maffei L, & Dixon MG (2010). Pampas deer *Ozotoceros bezoarticus* (Linnaeus 1758). In Duarte JMB & Gonzalez S (Eds.), *Neotropical Cervidology: Biology and Medicine of Neotropical Deer*, FUNEP and IUCN, Jaboticabal, Brazil, pp. 119–132.

- Gonzalez S, Maldonado JE, Leonard JA, Vilà C, Barbanti Duarte JMB, Merino M, Brum-Zorrilla N, & Wayne R (1998). Conservation genetics of the endangered Pampas deer (*Ozotoceros bezoarticus*). *Molecular Ecology*, **7**(1): 47–56.
- González S, Maldonado JE, Ortega J, Talarico AC, Bidegaray-Batista L, Garcia JE, & Duarte JMB (2009). Identification of the endangered small red brocket deer (*Mazama bororo*) using noninvasive genetic techniques (Mammalia; Cervidae). *Molecular ecology resources*, **9**(3): 754–758.
- Goss RJ (1983). *Deer antlers: regeneration, function and evolution*. Academic Press, Inc., New York.
- Goss RJ (1990). Of antlers and embryos. In Bubenik G & Bubenik A (Eds.), *Horns, pronghorns, and antlers: Evolution, morphology, physiology, and social significance*, Springer-Verlag, New York, pp. 298–312.
- Goss RJ, Van Praagh A, & Brewer P (1992). The mechanism of antler casting in the fallow deer. *The Journal of experimental zoology*, **264**: 429–436.
- Gould SJ (1974). The origin and function of 'bizarre' structures: antler size and skull size in the 'Irish Elk', *Megaloceros giganteus*. *Evolution*, **28**(2): 191–220.
- Gouy M, Guindon S, & Gascuel O (2010). SeaView version 4: a multiplatform graphical user interface for sequence alignment and phylogenetic tree building. *Molecular biology and evolution*, **27**(2): 221–224.
- Gregory TR (2008). Understanding Evolutionary Trees. *Evolution: Education and Outreach*, **1**: 121–137.
- Groves C (1982). Geographic variation in the Barasingha or swamp deer (*Cervus duvauceli*). *Journal of Bombay Natural History*, **79**.
- Groves C (2003). Taxonomy of ungulates of the Indian subcontinent.
- Groves C (2006). The genus *Cervus* in eastern Eurasia. *European Journal of Wildlife Research*, **52**: 14–22.
- Groves C (2014). Current taxonomy and diversity of crown ruminants above the species level. *Zitteliana B*, **32**: 5–14.
- Groves C & Grubb P (1987). Relationships of living deer. In CM W (Ed.), *Biology and management of the Cervidae*, Smithsonian Institution Press, Washington, DC, pp. 21–59.
- Groves CP (2005). Domestic and wild mammals: naming and identity. In Minelli A, Ortalli G, & Sangha G (Eds.), *Animal Names*, Istituto Veneto di Scienze, Lettere ed Arti, Venice, pp. 151–157.
- Groves CP (2007). Family Cervidae. In Prothero DR & Foss SE (Eds.), *The Evolution of Artiodactyls*, Johns Hopkins University Press, Baltimore and London, pp. 249–256.

- Groves CP & Grubb P (1982). The species of muntjac (genus *Muntiacus*) in Borneo: unrecognised sympatry in tropical deer. *Zoologische Mededelingen*, **56**(17): 203–216.
- Groves CP & Grubb P (1990). Muntiacidae. In Bubenik G & Bubenik A (Eds.), *Horns, pronghorns, and antlers: Evolution, morphology, physiology, and social significance*, Springer, pp. 134–168.
- Groves CP & Grubb P (2011). *Ungulate taxonomy*. Johns Hopkins University Press, Baltimore, 309 pp.
- Grubb P (1990). Cervidae of Southeast Asia. In Bubenik G & Bubenik A (Eds.), *Horns, pronghorns, and antlers: Evolution, morphology, physiology, and social significance*, Springer, pp. 169–179.
- Grubb P (2000). Valid and invalid nomenclature of living and fossil deer, Cervidae. *Acta Theriologica*, **45**(3): 289–307.
- Grubb P & Groves C (1983). Notes on the taxonomy of the deer (Mammalia, Cervidae) of the Philippines. *Zoologischer Anzeiger*, **210**: 119–144.
- Gühler U (1936). Beitrag zur Geschichte von *Cervus* (*Rucervus*) *schomburgki* Blyth. *Zeitschrift für Säugetierkunde*, **11**: 155.
- Guillerme T & Cooper N (2016). Effects of missing data on topological inference using a Total Evidence approach. *Molecular Phylogenetics and Evolution*, **94**: 146–158.
- Gustafson EP (1985). Antlers of *Bretzia* and *Odocoileus* (Mammalia, Cervidae) and the evolution of New World deer. *Transactions of the Nebraska Academy of Sciences*, **13**: 83–92.
- Gutiérrez EE, Maldonado JE, Radosavljevic A, Molinari J, Patterson BD, Martínez-C JM, Rutter AR, Hawkins MT, Garcia FJ, & Helgen KM (2015). The Taxonomic Status of *Mazama bricenii* and the Significance of the Táchira Depression for Mammalian Endemism in the Cordillera de Mérida, Venezuela. *PloS ONE*, **10**(6): e0129113.
- Hall BK (2005). *Bones and Cartilage: Developmental and Evolutionary Skeletal Biology*. Academic Press, London, 792 pp.
- Hall RJ (2009). Deer. *Genome Mapping Genomics in Domestic Animals*, **3**: 47–74.
- Haq BU, Hardenbol J, & Vail PR (1987). Chronology of fluctuating sea levels since the Triassic. *Science*, **235**(4793): 1156–1167.
- Harrington R (1985). Evolution and distribution of the Cervidae. In Fennessy P & Drew K (Eds.), *Biology of deer reproduction*, Bulletin 22 of the Royal Society of New Zealand, Wellington, New Zealand, pp. 3–11.
- Hasegawa M, Kishino H, & Yano T (1985). Dating of human-ape splitting by a molecular clock of mitochondrial DNA. *Journal of Molecular Evolution*, **22**(2): 160–174.

- Hassanin A, Bonillo C, Nguyen BX, & Cruaud C (2010). Comparisons between mitochondrial genomes of domestic goat (*Capra hircus*) reveal the presence of numts and multiple sequencing errors. *Mitochondrial DNA*, **21**(3-4): 68–76.
- Hassanin A, Delsuc F, Ropiquet A, Hammer C, Jansen Van Vuuren B, Matthee C, Ruiz-Garcia M, Catzeflis F, Areskoug V, Nguyen TT, & Couloux A (2012). Pattern and timing of diversification of Cetartiodactyla (Mammalia, Laurasiatheria), as revealed by a comprehensive analysis of mitochondrial genomes. *Comptes Rendus - Biologies*, **335**: 32–50.
- Hassanin A & Douzery EJP (2003). Molecular and morphological phylogenies of Ruminantia and the alternative position of the Moschidae. *Systematic biology*, **52**(2): 206–228.
- Heaney LR (1985). Zoogeographic evidence for middle and late Pleistocene land bridges to the Philippine Islands. *Modern Quaternary Research in Southeast Asia*, **9**: 127–144.
- Hedges S, Duckworth J, Timmins R, Semiadi G, & Priyono A (2008). *Rusa timorensis*. *The IUCN red list of threatened species. Version 2014.3*. Available at www.iucnredlist.org (accessed on 17 April 2015).
- Heintz E (1970). Les cervidés villafranchiens de France et d’Espagne. *Mémoires du Muséum national d’histoire naturelle. Série C, Sciences de la terre*, **22**(1–2): 1–303, 1–206.
- Heintz E, Brunet M, Battail B, & Jehenne Y (1990). The main features of the Cervid palaeobiogeography. *Quartärpaläontologie*, **8**: 79–82.
- Heller R, Frandsen P, Lorenzen ED, & Siegmund HR (2014). Is diagnosability an indicator of speciation? response to ‘Why one century of phenetics is enough’. *Systematic biology*, **63**(5): 833–837.
- Hensel R (1859). Über einen fossilen Muntjac aus Schlesien. *Zeitschrift der Deutschen Geologischen Gesellschaft*, **11**: 251–279.
- Hernández Fernández M & Vrba ES (2005). A complete estimate of the phylogenetic relationships in Ruminantia: a dated species-level supertree of the extant ruminants. *Biological reviews of the Cambridge Philosophical Society*, **80**: 269–302.
- Hernández-Pacheco E (1930). *Un suido y un nuevo cévido del yacimiento paleontológico de Concud (Teruel)*, vol. 30. 331–344 pp.
- Hershkovitz P (1959). A New Species of South American Brocket, Genus *Mazama*, Cervidae. *Proceedings of the Biological Society Washington*, **72**: 45–54.
- Hershkovitz P (1972). The recent mammals of the Neotropical region: a zoogeographic and ecological review. In Keast A, Erk F, & Glass B (Eds.), *Evolution, mammals and southern continents*, University of New York Press, Albany, pp. 311–431.
- Hershkovitz P (1982). Neotropical Deer (Cervidae) Part I. Pudus, Genus *Pudu* Gray. *Fieldiana. Zoology, New Series*, **11**: 1–86.

- Heywood JJN (2010). Explaining patterns in modern ruminant diversity: Contingency or constraint? *Biological Journal of the Linnean Society*, **99**: 657–672.
- Hilgen F, Lourens L, Van Dam J, Beu A, Foyes A, Cooper R, Krijgsman W, Ogg J, Piller W, & Wilson D (2012). The Neogene Period. In Gradstein F, Ogg J, Schmitz M, & Ogg G (Eds.), *The Geologic Time Scale 2012*, Elsevier, Amsterdam, vol. 2, pp. 923–978.
- Hill J (1960). The Robinson collection of Malaysian mammals. *Bulletin of the Raffles Museum*, **29**: 1–112.
- Hillis DM & Wiens JJ (2000). Molecules versus morphology in systematics: conflicts, artifacts, and misconceptions. In Wiens JJ (Ed.), *Phylogenetic analysis of Morphological data*, Smithsonian Institution Press, Washington and London, pp. 1–19.
- Hoffstetter R (1952). Les mammifères pléistocènes de la République de l'Equateur. *Mémoires de la Société Géologique de France Nouvelle Serie*, **11**(1-4): 1–391.
- Hoffstetter R (1963). La faune pléistocène de Tarija (Bolivie). Note préliminaire. *Bulletin Muséum National d'Histoire Naturelle*, **35**(2): 194–203.
- Hofreiter M, Jaenicke V, Serre D, von Haeseler A, & Pääbo S (2001a). DNA sequences from multiple amplifications reveal artifacts induced by cytosine deamination in ancient DNA. *Nucleic acids research*, **29**(23): 4793–4799.
- Hofreiter M, Serre D, Poinar HN, Kuch M, & Pääbo S (2001b). Ancient DNA. *Nature Reviews, Genetics*, **2**: 353–359.
- Holbourn A, Kuhnt W, Schulz M, & Erlenkeuser H (2005). Impacts of orbital forcing and atmospheric CO₂ on Miocene ice-sheet expansion. *Nature*, **438**: 483–487.
- Hu J, Fang SG, & Wan QH (2006). Genetic diversity of Chinese water deer (*Hydropotes inermis inermis*): Implications for conservation. *Biochemical Genetics*, **44**(April): 161–172.
- Huang L, Chi J, Nie W, Wang J, & Yang F (2006). Phylogenomics of several deer species revealed by comparative chromosome painting with Chinese muntjac paints. *Genetica*, **127**: 25–33.
- Huelsenbeck JP (1991). When are Fossils Better than Extant Taxa in Phylogenetic Analysis? *Systematic Biology*, **40**(4): 458–469.
- Huelsenbeck JP & Rannala B (2000). Using stratigraphic information in phylogenetics. In Wiens JJ (Ed.), *Phylogenetic analysis of Morphological data*, Smithsonian Institution Press, Washington and London, pp. 165–191.
- Hughes S, Hayden TJ, Douady CJ, Tougaard C, Germonpré M, Stuart A, Lbova L, Carden RF, Hänni C, & Say L (2006). Molecular phylogeny of the extinct giant deer, *Megaloceros giganteus*. *Molecular Phylogenetics and Evolution*, **40**: 285–291.

- Illiger JKW (1815). *Überblick der Säugethiere nach ihrer Vertheilung über die Welttheile: gelesen in der Akademie der Wissenschaften in Berlin am 28. Febr. 1811*. Realschul-Buchhandlung.
- IUCN (2016). The IUCN red list of threatened species. Version 2016.2. Available at <http://www.iucnredlist.org>. (accessed on 09 September 2016).
- Janis CM (1990). Correlation of reproductive and digestive strategies in the evolution of cranial appendages. In Bubenik G & Bubenik A (Eds.), *Horns, Pronghorns, and Antlers*, Springer Verlag, New York, pp. 114–133.
- Janis CM & Scott KM (1987). The origin of the higher ruminant families with special reference to the origin of Cervoidea and relationships within the Cervoidea. *American Museum Novitates*, **2893**: 1–85.
- Janis CM & Scott KM (1988). The phylogeny of the Ruminantia (Artiodactyla, Mammalia). In Benton MJ (Ed.), *The Phylogeny and Classification of the Tetrapods. Vol. 2. Mammals*, Clarendon Press, Oxford, pp. 273–282.
- Janis CM & Theodor JM (2014). Cranial and postcranial morphological data in ruminant phylogenetics. *Zitteliana B*, **32**: 1–17.
- Jarman P (1983). Mating System and Sexual Dimorphism in Large Terrestrial, Mammalian Herbivores. *Biological Reviews*, **58**(4): 485–520.
- Jenner RA (2004). Accepting Partnership by Submission? Morphological Phylogenetics in a Molecular Millennium. *Systematic Biology*, **53**(2): 333–342.
- Ji H (1985). Geographical history of genus *Elaphurus*. *Vertebrata Palasiatica*, **23**(3): 215–222.
- Jiménez JE (2010). Southern pudu *Pudu puda* (Molina 1782). In Duarte JMB & González S (Eds.), *Neotropical Cervidology: Biology and Medicine of Latin American Deer*, FUNEP in collaboration with IUCN, Jaboticabal, Brasil & Gland, Switzerland, pp. 140–150.
- Kahlke HD (1969). Die Cervidenreste aus den Kiesen von Süssenborn bei Weimar. In Kahlke HD (Ed.), *Das Pleistozän von Süssenborn.*, Paläontologische Abhandlungen, A III (3–4), pp. 547–611.
- Kaiser TM & Croitor R (2004). Ecological interpretations of early Pleistocene deer (Mammalia, Cervidae) from Ceysaguet (Haute-Loire, France). *Geodiversitas*, **26**(4): 661–674.
- Kaiser TM & Rössner GE (2007). Dietary resource partitioning in ruminant communities of Miocene wetland and karst palaeoenvironments in Southern Germany. *Palaeogeography, Palaeoclimatology, Palaeoecology*, **252**: 424–439.
- Kierdorf U & Kierdorf H (2010). Deer antlers - A model of mammalian appendage regeneration: An extensive review. *Gerontology*, **57**: 53–65.
- Kitchener A (1987). Fighting behaviour of the extinct Irish elk. *Modern Geology*, **11**(1.28).

- Kohlbrugge J (1895). Zoogdieren van Zuid-oost Borneo. *Natuurkundig tijdschrift voor Nederlandsch Indië*, **55**: 176–200.
- Koizumi T, Ohtaishi N, Kaji K, Yu Y, & Tokida K (1993). Conservation of white-lipped deer in China. In Ohtaishi N & Sheng HI (Eds.), *Deer in China: Biology and Management*, Elsevier Science Publishers, Amsterdam, The Netherlands, pp. 309–318.
- König HE & Liebich HG (2015). *Anatomie der Haussäugetiere: Lehrbuch und Farbatlas für Studium und Praxis*. Schattauer Verlag, Stuttgart, 812 pp.
- Korotkevich E (1963). New data on the taxonomy and phylogeny of fossil roe deer of the genus *Procapreolus*. *Proceedings of the Ukrainian Academy of Sciences*, **10**: 1390–1393.
- Korotkevich E (1964). A new species of fossil *Muntiacus* from the Pliocene deposits of the south of the USSR. *Dopovidi Akademii Nauk URSR*, **6**: 807–810.
- Korotkevich E (1965). A new roe deer species from the Maeotis of the Ukraine. *Paleontological Journal*, **4**: 60–67.
- Korotkevich EL (1970). *Late Neogene Deer of the North Black Sea Area*. Naukova Dumka, Kiev, 175 p pp.
- Korotkevich EL (1988). *The history of development of the Hipparion fauna from Eastern Europe*. Naukova Dumka, Kiev, 160 p pp.
- Kotsakis T & Palombo M (1979). Vertebrati continentali e paleogeografia della Sardegna durante il Neogene. *Annales Géologiques des Pays Héliéniques, tome hors serie*, **2**: 621–630.
- Kraus F & Miyamoto MM (1991). Rapid cladogenesis among the pecoran ruminants: evidence from mitochondrial DNA sequences. *Systematic Biology*, **40**(2): 117–130.
- Kuehn R, Ludt CJ, Schroeder W, & Rottmann O (2005). Molecular phylogeny of *Megaloceros giganteus*—the giant deer or just a giant red deer? *Zoological science*, **22**: 1031–1044.
- Kurtén B (1968). *Pleistocene mammals of Europe*. Weidenfeld and Nicolson, London, UK.
- Kuss S (1965). Eine pleistozäne Säugetierfauna der Insel Kreta. *Berichte der Naturforschenden Gesellschaft zu Freiburg im Breisgau*, **55**(2): 271–348.
- Kuss S (1966). Beiträge zur pleistozänen-Fauna der Insel Kreta. I. Die von Bate 1904 gesammelten Elefanten- und Cerviden-Reste. *Berichte der Naturforschenden Gesellschaft zu Freiburg im Breisgau*, **56**(2): 169–181.
- Kuss S (1967). Pleistozäne Säugetierfunde auf dem ostmediterranen Inseln Kythera und Karpathos. *Berichte der Naturforschenden Gesellschaft zu Freiburg im Breisgau*, **57**(2): 207–216.
- Kuss S (1969). Die erste pleistozäne Säugetierfauna der Insel Kassos, Griechenland. *Berichte der Naturforschenden Gesellschaft zu Freiburg im Breisgau*, **59**: 169–177.

- Kuss S (1970). Abfolge und Alter der pleistozänen Säugetierfauna der Insel Kreta. *Berichte der Naturforschenden Gesellschaft zu Freiburg im Breisgau*, **60**: 35–83.
- Kuss S & Misonne X (1968). Pleistozäne Muriden der Insel Kreta. *Neues Jahrbuch für Mineralogie, Geologie und Paläontologie*, **132**(1): 55–69.
- Kuss SE (1973). Die pleistozänen Säugetierfaunen der ostmediterranen Inseln. *Berichte der Naturforschenden Gesellschaft zu Freiburg im Breisgau*, **93**(1-2): 49–71.
- Kuss SE (1975). Die pleistozänen Hirsche der ostmediterranen Inseln Kreta, Kasos, Karpathos und Rhodos (Griechenland). *Berichte der naturforschenden Gesellschaft zu Freiburg im Breisgau*, **65**(1-2): 25–79.
- Kuwayama R & Ozawa T (2000). Phylogenetic relationships among European red deer, wapiti, and sika deer inferred from mitochondrial DNA sequences. *Molecular phylogenetics and evolution*, **15**(1): 115–123.
- Kuznetsova MV, Kholodova MV, & Danilkin aa (2005). Molecular phylogeny of deer (Cervidae: Artiodactyla). *Russian Journal of Genetics*, **41**(7): 742–749.
- Lan H, Wang W, & Shi L (1995). Phylogeny of *Muntiacus* (Cervidae) based on mitochondrial DNA restriction maps. *Biochemical genetics*, **33**(11-12): 377–388.
- Lanfear R, Calcott B, Ho SY, & Guindon S (2012). PartitionFinder: combined selection of partitioning schemes and substitution models for phylogenetic analyses. *Molecular biology and evolution*, **29**(6): 1695–1701.
- Lartet E (1837). Sur les débris fossiles trouvés à Sansan, et sur les animaux antédiluviens en général. *Comptes Rendus de l'Académie des Sciences*, **5**: 158–159.
- Lason K, Lechner-Doll M, Lüpke M, & Clauss M (2001). Adaptations to seasonality—a comparative view of energy expenditure during lactation in two ruminant species: European roe deer (*Capreolus capreolus*) and mouflon (*Ovis orientalis musimon*). *Zoosystematics and Evolution*, **77**(2): 217–221.
- Latch EK, Heffelfinger JR, Fike Ja, & Rhodes OE (2009). Species-wide phylogeography of North American mule deer (*Odocoileus hemionus*): Cryptic glacial refugia and post-glacial recolonization. *Molecular Ecology*, **18**: 1730–1745.
- Lechner-Doll M, Lason K, Lang D, & Behrend A (2001). Evolutionary aspects of dietary selection and digestion in the European roe deer. *Mitteilungen des Museum für Naturkunde Berlin, Zoologische Reihe*, **77**(February): 223–227.
- Lee M & Palci A (2015). Morphological Phylogenetics in the Genomic Age. *Current Biology*, **25**(19): R922–R929.
- Lee MSY & Camens AB (2009). Strong morphological support for the molecular evolutionary tree of placental mammals. *Journal of Evolutionary Biology*, **22**: 2243–2257.
- Lee Y, Chang W, & Li S (2002). Isolation and Identification of a Novel Satellite DNA Family Highly Conserved in Several Cervidae Species. *Chromosoma*, **111**(3): 176–183.

- Leinders JJM & Heintz E (1980). The configuration of the lacrimal orifice in pecorans and tragulids (Artiodactyla; Mammalia) and its significance for the distinction between Bovidae and Cervidae. *Beaufortia*, **30**: 155–160.
- Lemaître JF, Vanpé C, Plard F, & Gaillard JM (2014). The allometry between secondary sexual traits and body size is nonlinear among cervids. *Biology letters*, **10**(March).
- Lemmon AR, Brown JM, Stanger-Hall K, & Lemmon EM (2009). The effect of ambiguous data on phylogenetic estimates obtained by maximum likelihood and Bayesian inference. *Systematic Biology*, **58**(1): 130–145.
- Lepage T, Bryant D, Philippe H, & Lartillot N (2007). A general comparison of relaxed molecular clock models. *Molecular Biological Evolution*, **24**: 2669–2680.
- Leslie DM (2010). *Przewalskium albirostre* (Artiodactyla: Cervidae). *Mammalian Species*, **42**(849): 7–18.
- Leslie DM (2011). *Rusa unicolor* (Artiodactyla: Cervidae). *Mammalian Species*, **43**(1): 1–30.
- Leslie DM, Lee DN, & Dolman RW (2013). *Elaphodus cephalophus* (Artiodactyla: Cervidae). *Mammalian Species*, **904**(904): 80–91.
- Lewis PO (2001). A likelihood approach to estimating phylogeny from discrete morphological character data. *Systematic biology*, **50**(6): 913–925.
- Li M, Sheng H, Tamate H, Masuda R, Nagata J, & Ohtaishi N (1998). MtDNA difference and molecular phylogeny among musk deer, Chinese water deer, and muntjak deer. *Acta Theriologica*, **18**: 184–191.
- Li M, Wang XM, Sheng HL, Tamate H, Masuda R, Nagata J, & Otaishi N (1999). Mitochondrial DNA divergence and phylogeny of four species of deer of the genus *Cervus*. *Acta Zoologica Sinica*, **45**: 99–105.
- Lin Y, Pan Y, & Lu Q (1978). The Early Pleistocene mammalian fauna from Yuanmou, Yunnan. In of Vertebrate Paleontology I & Paleoanthropology (Eds.), *Proceedings of Paleoanthropology*, Science Press, Beijing, pp. 101–125.
- Linnaeus C (1758). *Systema Naturae*. Holmiae, Stockholm.
- Lister A (1987). Diversity and evolution of antler form in Quaternary deer. In Wemmer C (Ed.), *Biology and Management of the Cervidae*, Smithsonian Institution, Washington, pp. 81–98.
- Lister A (1996). The morphological distinction between bones and teeth of fallow deer (*Dama dama*) and red deer (*Cervus elaphus*). *International Journal of Osteoarchaeology*, **6**(August 1995): 119–143.
- Lister A (1998). The age of early Pleistocene mammal faunas from the ‘Weybourne Crag’ and Cromer Forest-bed Formation (Norfolk, England). *Mededelingen Nederlands Instituut voor Toegepaste Geowetenschappen*, **60**: 271–280.

- Lister AM (1984). Evolutionary and ecological origins of British deer.
- Lister AM (1994). The evolution of the giant deer, *Megaloceros giganteus* (Blumenbach).
- Lister AM, Edwards CJ, Nock DAW, Bunce M, van Pijlen IA, Bradley DG, Thomas MG, & Barnes I (2005). The phylogenetic position of the 'giant deer' *Megaloceros giganteus*. *Nature*, **438**(December): 850–853.
- Lister AM, Parfitt SA, Owen FJ, Collinge SE, & Breda M (2010). Metric analysis of ungulate mammals in the early Middle Pleistocene of Britain, in relation to taxonomy and biostratigraphy. II: Cervidae, Equidae and Suidae. *Quaternary International*, **228**: 157–179.
- Liu XH, Wang YQ, Liu ZQ, & Zhou KY (2002). Phylogenetic relationships of Cervinae based on sequence of mitochondrial cytochrome b gene. *Zoological Research*, **24**(1): 27–33.
- Lizcano DJ, Álvarez SJ, Delgado-V CA, Duarte JMB, & Gonzales S (2010). Dwarf red brocket *Mazama rufina* (Pucheran 1951). In Duarte JMB & Gonzalez S (Eds.), *Neotropical Cervidology: Biology and Medicine of Neotropical Deer*, FUNEP and IUCN, Jaboticabal, Brazil, pp. 177–180.
- Lönnberg E (1906). Which is the Taxonomic Position of the Irish Giant Deer and Allied Races? *Arkiv för Zoologi*, **3**(14): 1–8.
- Loomis FB (1928). Phylogeny of the deer. *American Journal of Sciences*, **16**: 531–542.
- Lorenzini R & Garofalo L (2015). Insights into the evolutionary history of *Cervus* (Cervidae, tribe Cervini) based on Bayesian analysis of mitochondrial marker sequences, with first indications for a new species. *Journal of Zoological Systematics and Evolutionary Research*, **53**(4): 340–349.
- Ludt CJ, Schroeder W, Rottmann O, & Kuehn R (2004). Mitochondrial DNA phylogeography of red deer (*Cervus elaphus*). *Molecular Phylogenetics and Evolution*, **31**: 1064–1083.
- Lydekker R (1876). Molar teeth and other remains of Mammalia. *Memoirs of the Geological Survey of India, Palaeontologia Indica Series 10*, **1**: 19–87.
- Lydekker R (1880). *A sketch of the history of the fossil vertebrata of India*. JW Thomas, Baptist Mission Press.
- Lydekker R (1884). Rodents and new ruminants from the Siwaliks, and synopsis of Mammalia. *Paleontologia Indica*, **10**(3): 1–5.
- Lydekker R (1898). *Deer of all lands: A history of the family Cervidae living and extinct*. Rowland Ward, Ltd., London, 329 pp.
- Lyon MWJ (1911). Mammals collected by Dr. WL Abbott on Borneo and some of the small adjacent islands. *Proceedings of the United States National Museum*, **40**: 53–156.

- Ma S, Wang Y, & Xu L (1986a). Taxonomic and phylogenetic studies on the genus *Muntiacus*. *Acta Theriologica Sinica*, **6**(3): 006.
- Ma S, Wang Y, & Xu L (1986b). Taxonomic and Phylogenetic Studies on the Genus *Muntiacus*. *Acta Theriologica Sinica*, **VI**: 190–209.
- MacKinnon J, Ong P, & Gonzales J (2008). *Rusa marianna*. *The IUCN red list of threatened species. Version 2014.3*. Available at www.iucnredlist.org (accessed on 17 April 2015).
- Maddison W & Maddison D (2011). Mesquite: a modular system for evolutionary analysis. Version 2.75. URL <http://mesquiteproject.org>.
- Malatesta A (1980). Dwarf Deer and Other Late Pleistocene Fauna of the 'Simonelli' Cave in Crete. *Quaderno Accademia Nazionale dei Lincei, Roma*, **249**: 1–128.
- Marcot JD (2007). Molecular phylogeny of terrestrial artiodactyls. Conflicts and resolution. In DR P & SE F (Eds.), *The evolution of artiodactyls*, Johns Hopkins University Press, Baltimore, pp. 4–18.
- Marquez A, Maldonado J, González S, Beccaceci M, Garcia J, & Duarte JMB (2006). Phylogeography and Pleistocene demographic history of the endangered marsh deer (*Blastocerus dichotomus*) from the Río de la Plata Basin. *Conservation genetics*, **7**: 563.
- Martin K (1886). Bericht über eine Reise ins Gebiet des oberen Surinam, Bijdr. *TLV Ned. Indië*, **35**.
- Martin K (1888). Neue Wirbelthierreste vom Pati-Ajam auf Java-Leiden. *Sammlungen des geologischen Reichs-Museums*, **4**: 87–116.
- Mattioli S (2011). Family Cervidae (Deer). In Wilson DE & Mittermeier RA (Eds.), *Handbook of the mammals of the world Volume 2*, Lynx Edicion, Barcelona, p. 886.
- Mauro RdA, Mourão GdM, Coutinho M, Silva M, & Magnusson W (1998). Abundance and distribution of marsh deer *Blastocerus dichotomus* (Artiodactyla: Cervidae) in the Pantanal, Brazil. *Reviews in Ecology of Latin America*, **5**(1-2): 13–20.
- McClelland J (1841). *The Calcutta Journal of Natural History, Vol II*. International Book Distributers, Dehra Dun, India, 415–417 pp.
- McClelland J (1842). *The Calcutta Journal of Natural History, Vol III*. International Book Distributers, Dehra Dun, India, 401–409 pp.
- McDade LA (2000). Hybridisation and phylogenetics: special insights from morphology. In Wiens JJ (Ed.), *Phylogenetic analysis of Morphological data*, Smithsonian Institution Press, Washington and London, pp. 146–164.
- McKenna M & Bell S (1997). *Classification of Mammals Above the Species Level*. Columbia University press, New York.

- Medellín RA, Gardner AL, & Aranda JM (1998). The taxonomic status of the Yucatán brown brocket, *Mazama pandora* (Mammalia: Cervidae). *Proceedings of the Biological Society of Washington*, **111**: 1–14.
- Meijaard E (2003). Mammals of south-east Asian islands and their late Pleistocene environments. *Journal of Biogeography*, **30**(8): 1245–1257.
- Meijaard E & Groves C (2004). Morphometrical relationships between Southeast Asian deer (Cervidae, tribe Cervini): Evolutionary and biogeographic implications. *Journal of Zoology*, **263**: 179–196.
- Meiri M, Lister AM, Collins MJ, Tuross N, Goebel T, Blockley S, Zazula GD, van Doorn N, Guthrie RD, Boeskorov GG et al. (2014). Faunal record identifies Bering isthmus conditions as constraint to end-Pleistocene migration to the New World. *Proceedings of the Royal Society, Series B*, **281**(1776): 20132167.
- Melentis J (1974). Paläontologische Ausgrabungen in den Höhlen des Gebietes von Rhethymnon. *Kreta-Scientific Annals, Faculty of Physics & Mathematics, University of Thessaloniki*, **14**: 17–24.
- Menegaz AN (2000). *Los camélidos y cérvidos del cuaternario del sector bonaerense de la Región Pampeana*. Ph.D. thesis, Universidad Nacional de La Plata, Argentina.
- Meng J & McKenna MC (1998). Faunal turnovers of Palaeogene mammals from the Mongolian Plateau. *Nature*, **394**(6691): 364–367.
- Mennecart B, Rössner GE, Métais G, DeMiguel D, Schulz G, Müller B, & Costeur L (2016). The petrosal bone and bony labyrinth of early to middle Miocene European deer (Mammalia, Cervidae) reveal their phylogeny. *Journal of Morphology*, **277**(10): 1329–1338.
- Merino M & Rossi RV (2010). Origin, systematics and morphological radiation. In Duarte JMB & Gonzalez S (Eds.), *Neotropical Cervidology: Biology and Medicine of Neotropical Deer*, FUNEP and IUCN, Jaboticabal, Brazil, pp. 2–11.
- Merino ML, Milne N, & Vizcaíno SF (2005). A cranial morphometric study of deer (Mammalia, Cervidae) from Argentina using three-dimensional landmarks. *Acta Theriologica*, **50**(1): 91–108.
- Métais G, Chaimanee Y, Jaeger JJ, & Ducrocq S (2001). New remains of primitive ruminants from Thailand: evidence of the early evolution of the Ruminantia in Asia. *Zoologica Scripta*, **30**(4): 231–248.
- Micheels A, Bruch AA, Eronen J, Fortelius M, Harzhauser M, Utescher T, & Mosbrugger V (2011). Analysis of heat transport mechanisms from a Late Miocene model experiment with a fully-coupled atmosphere-ocean general circulation model. *Palaeogeography, Palaeoclimatology, Palaeoecology*, **304**(3–4): 337–350.
- Mickoleit G (2004). *Phylogenetische Systematik der Wirbeltiere*. Pfeil Verlag, München, 671 pp.

- Miller KG, Wright JD, & Fairbanks RG (1991). Unlocking the ice house: Oligocene-Miocene oxygen isotopes, eustasy, and margin erosion. *Journal of Geophysical Research: Solid Earth*, **96**(B4): 6829–6848.
- Milne-Edwards A (1866). On the Mi-lou or Sseu-pou-siang, a mammal from the north of China, which forms a new section in the family Cervidæ. *Journal of Natural History*, **18**(103): 71–72.
- Milne Edwards A (1872). Mémoire sur la faune mammalogique du Tibet oriental et principalement de la Principauté de Moupin. *Milne Edwards H, Recherches pour servir à l'histoire naturelle des mammifères. Librairie de l'Académie de Médecine, Paris*, pp. 231–304.
- Miyamoto MM, Kraus F, & Ryder OA (1990). Phylogeny and evolution of antlered deer determined from mitochondrial DNA sequences. *Proceedings of the National Academy of Sciences*, **87**(16): 6127–6131.
- Molina GI (1782). *Saggio sulla storia naturale del Chili*. Stamperia di S. Tommaso d'Aquino, Bologna.
- Montes C, Cardona a, Jaramillo C, Pardo a, Silva JC, Valencia V, Ayala C, Pérez-Angel LC, Rodriguez-Parra La, Ramirez V, & Niño H (2015). Middle Miocene closure of the Central American Seaway. *Science*, **348**(6231): 226–229.
- Morales J (1984). *Venta del Moro: su macrofauna de mamiferos y biostratigrafia continental del Mioceno mediterraneo*. Editorial Universidad Complutense, Madrid, 340 pp.
- Morales J, Pickford M, & Soria D (1993). Pachyostosis in a Lower Miocene Giraffoid from Spain, *Lorancameryx pachyostoticus* nov. gen. nov. sp. and its bearing on the evolution of bony appendages in artiodactyls. *Geobios*, **26**(2): 207–230.
- Morales J, Soria D, & Pickford M (1995). Sur les origines de la famille des Bovidae (Artiodactyla, Mammalia). *Comptes rendus de l'Académie des sciences. Série 2. Sciences de la terre et des planètes*, **321**(12): 1211–1217.
- Moscarella Ra, Aguilera M, & Escalante Aa (2003). Phylogeography, Population Structure, and Implications for Conservation of White-Tailed Deer (*Odocoileus virginianus*) in Venezuela. *Journal of Mammalogy*, **84**(4): 1300–1315.
- Moyle RG, Andersen MJ, Oliveros CH, Steinheimer FD, & Reddy S (2012). Phylogeny and biogeography of the core babblers (aves: Timaliidae). *Systematic Biology*, **61**(785): 631–651.
- Nagata J, Masuda R, Tamate HB, Hamasaki Si, Ochiai K, Asada M, Tatsuzawa S, Suda K, Tado H, & Yoshida MC (1999). Two genetically distinct lineages of the sika deer, *Cervus nippon*, in Japanese islands: Comparison of mitochondrial D-loop region sequences. *Molecular phylogenetics and evolution*, **13**(3): 511–519.

- Neitzel H (1987). Chromosome evolution of Cervidae: karyotypic and molecular aspects. In Obe G & Basler A (Eds.), *Cytogenetics - Basic and Applied Aspects*, Springer Verlag, Berlin, pp. 91–112.
- Nickel R, Schummer A, & Seiferle E (2004). *Lehrbuch der Anatomie der Haustiere, Band 1*. Verlag Paul Parey, Stuttgart, 644 pp.
- Nikolskiy Pa & Boeskorov GG (2011). Primitive and derived features in the teeth of modern moose (*Alces*, Cervidae, Mammalia) from Eastern Siberia. *Russian Journal of Theriology*, **10**(1): 27–30.
- Nylander JAA, Ronquist F, Huelsenbeck JP, & Nieves-Aldrey JL (2004). Bayesian phylogenetic analysis of combined data. *Systematic biology*, **53**(1): 47–67.
- Obergfell FA (1957). Vergleichende Untersuchungen an Dentitionen und Dentale Altburdigaler Cerviden von Wintershof West in Bayern und rezenter Cerviden (eine phylogenetische Studie).
- O’Leary Ma (1999). Parsimony Analysis of Total Evidence from Extinct and Extant Taxa and the Cetacean – Artiodactyl Question (Mammalia, Ungulata). *Cladistics*, **15**: 315–330.
- O’Leary MA & Gatesy J (2008). Impact of increased character sampling on the phylogeny of Certiodactyla (Mammalia): combined analysis including fossils. *Cladistics*, **24**(4): 397–442.
- Oliver W, MacKinnon J, Heaney L, & Lastica E (2008). *Rusa alfredi*. *The IUCN red list of threatened species. Version 2014.3*. Available at www.iucnredlist.org (accessed on 17 April 2015).
- Olson LE & Hassanin A (2003). Contamination and chimerism are perpetuating the legend of the snake-eating cow with twisted horns (*Pseudonovibos spiralis*). A case study of the pitfalls of ancient DNA. *Molecular phylogenetics and evolution*, **27**: 545–548.
- O’Reilly JE, Puttick MN, Parry L, Tanner AR, Tarver JE, Fleming J, Pisani D, & Donoghue PC (2016). Bayesian methods outperform parsimony but at the expense of precision in the estimation of phylogeny from discrete morphological data. *Biology letters*, **12**(4): 20160081.
- Ouithavon K, Bhumpakphan N, Denduangboripant J, Siriaronrat B, & Trakulnaleamsai S (2009). An analysis of the phylogenetic relationship of thai cervids inferred from nucleotide sequences of protein kinase C iota (PRKCI) intron. *Kasetsart Journal - Natural Science*, **43**: 709–719.
- Owen R (1844). Report on the British fossil Mammalia. *Reports of the British Association meeting, Cork*, p. 237.
- Pääbo S, Poinar H, Serre D, Jaenicke-Després V, Hebler J, Rohland N, Kuch M, Krause J, Vigilant L, & Hofreiter M (2004). Genetic analyses from ancient DNA. *Annu. Rev. Genet.*, **38**: 645–679.

- Pallas PS (1771). *Reise durch verschiedene Provinzen des russischen Reichs*, vol. 3. gedruckt bey der Kayserlichen Academie der Wissenschaften.
- Parham JF, Donoghue PCJ, Bell CJ, Calway TD, Head JJ, Holroyd Pa, Inoue JG, Irmis RB, Joyce WG, Ksepka DT, Patané JSL, Smith ND, Tarver JE, Van Tuinen M, Yang Z, Angielczyk KD, Greenwood JM, Hipsley Ca, Jacobs L, Makovicky PJ, Müller J, Smith KT, Theodor JM, Warnock RCM, & Benton MJ (2012). Best practices for justifying fossil calibrations. *Systematic Biology*, **61**(2): 346–359.
- Pattinson DJ, Thompson RS, Piotrowski AK, & Asher RJ (2015). Phylogeny, paleontology, and primates: do incomplete fossils bias the tree of life? *Systematic Biology*, **64**(2): 169–186.
- Petronio C, Krakhmalnaya T, Bellucci L, & Di Stefano G (2007). Remarks on some Eurasian pliocervines: Characteristics, evolution, and relationships with the tribe Cervini. *Geobios*, **40**: 113–130.
- Pfeiffer T (1999). Die Stellung von *Dama* (Cervidae, Mammalia) im System pleistometacarpaler Hirsche des Pleistozäns. Phylogenetische Rekonstruktion, metrische Analyse. *Senckenbergische Naturforschende Gesellschaft*, **211**: 1–218.
- Pfeiffer T (2002). The first complete skeleton of *Megaloceros verticornis* (Dawkins, 1868), Cervidae, Mammalia, from Bilshausen (Lower Saxony, Germany): description and phylogenetic implications. *Mitteilungen aus dem Museum für Naturkunde in Berlin, Geowissenschaftliche Reihe*, **5**(July): 289–308.
- Pilgrim GE (1941). The relationship of certain variant fossil types of ‘horn’ to those of the living Pecora. *The Annals and Magazine of Natural History*, **7**(38): 172–184.
- Piper PJ, Ochoa J, Robles EC, Lewis H, & Paz V (2011). Palaeozoology of Palawan Island, Philippines. *Quaternary International*, **233**(2): 142–158.
- Pitra C, Fickel J, Meijaard E, & Groves CP (2004). Evolution and phylogeny of old world deer. *Molecular Phylogenetics and Evolution*, **33**: 880–895.
- Plard F, Bonenfant C, & Gaillard JM (2011). Revisiting the allometry of antlers among deer species: Male-male sexual competition as a driver. *Oikos*, **120**(August 2010): 601–606.
- Pocock RI (1943). The larger deer of British India. Part II. *Journal of the Bombay Natural History Society*, **43**: 553–572.
- Poe S & Wiens JJ (2000). Character selection and the methodology of morphological phylogenetics. In Wiens JJ (Ed.), *Phylogenetic analysis of Morphological data*, Smithsonian Institution Press, Washington and London, pp. 20–36.
- Pohle C (1989). Geburt eines Schopfhirsches im Tierpark Berlin sowie Angaben zu Gewicht und Geweihwechsel von *Elaphodus cephalophus*. *Der Zoologische Garten*, **59**: 188–194.

- Polziehn RO & Strobeck C (2002). A phylogenetic comparison of red deer and wapiti using mitochondrial DNA. *Molecular phylogenetics and evolution*, **22**(3): 342–356.
- Pomel A (1853). *Catalogue méthodique et descriptif des Vertébrés fossiles du bassin de la Loire*. Baillière, Paris, 193 pp.
- Portis A (1920). Elenco delle specie di Cervicorni fossili in Roma e attorno a Roma. *Bollettino della Societa Geologica Italiana*, **39**: 132–139.
- Price JS, Allen S, Fauchaux C, Althnaian T, & Mount JG (2005a). Deer antlers: a zoological curiosity or the key to understanding organ regeneration in mammals? *Journal of Anatomy*, **207**(5): 603–618.
- Price SA, Bininda-Emonds ORP, & Gittleman JL (2005b). A complete phylogeny of the whales, dolphins and even-toed hoofed mammals (Cetartiodactyla). *Biological reviews of the Cambridge Philosophical Society*, **80**(April 2005): 445–473.
- Prothero DR & Heaton TH (1996). Faunal stability during the early Oligocene climatic crash. *Palaeogeography, Palaeoclimatology, Palaeoecology*, **127**(1): 257–283.
- Prothero DR & Schoch RM (2002). *Horns, Tusks, and Flippers: The Evolution of Hoofed Mammals*. The Johns Hopkins University Press, Baltimore and London, 307 pp.
- Przewalski N (1883). Iz Zaisana cherez Khami v Tibet i na verkhov'ia Zheltoi rieki [From Zaisan through Khami to Tibet and to the headwaters of the Yellow River]. *VS Balasheva, St. Petersburg, Russia (in Russian)*.
- Pucheran J (1851). Note sur une espèce nouvelle de Cerf (*Cervus rufinus* Bourc. et Puch). *Rev et Mag Zool*, **2**: 561–565.
- Rabinowitz A, Myint T, Khaing ST, & Rabinowitz S (1999). Description of the leaf deer (*Muntiacus putaoensis*), a new species of muntjac from northern Myanmar. *Journal of Zoology*, **249**(4): 427–435.
- Radulesco C & Samson P (1967). Sur un nouveau cerf mégacérin du Pleistocène moyen de la depression de Brasov (Roumanie). *Geologia Romana*, **6**: 317–344.
- Randi E, Mucci N, Claro-Hergueta F, Bonnet A, & Douzery EJP (2001). A mitochondrial DNA control region phylogeny of the Cervinae: speciation in *Cervus* and implications for conservation. *Animal Conservation*, **4**: 1–11.
- Randi E, Mucci N, Pierpaoli M, & Douzery E (1998). New phylogenetic perspectives on the Cervidae (Artiodactyla) are provided by the mitochondrial cytochrome b gene. *Proceedings. Biological sciences / The Royal Society*, **265**: 793–801.
- Rieseberg LH, Archer MA, & Wayne RK (1999). Transgressive segregation, adaptation and speciation. *Heredity*, **83**(4): 363–372.
- Roger O (1896). Vorläufige Mitteilungen über Säugethierreste aus dem Dinotheriensand von Stätzling bei Augsburg. *Bericht des Naturwissenschaftlichen Vereins für Schwaben und Neuburg*, **32**: 547–552.

- Roger O (1898). Wirbelthierreste aus dem Dinotheriensande der bayerisch-schwäbischen Hochebene. *Bericht des Naturwissenschaftlichen Vereins für Schwaben und Neuburg*, **33**: 1–64.
- Roger O (1904). Wirbelthierreste aus dem Obermiocän der bayerisch-schwäbischen Hochebene. *Bericht des Naturwissenschaftlichen Vereins für Schwaben und Neuburg*, **36**: 3–22.
- Rokas A & Holland PWH (2000). Rare genomic changes as a tool for phylogenetics. *Trends in Ecology and Evolution*, **15**(11): 454–459.
- Roman F (1934). Les collections de géologie et de paléontologie de la Faculté des Sciences de Lyon. *Annales de la Société Linnéenne de Lyon*, **78**: 197–264.
- Romer AS (1966). *Vertebrate Paleontology*. University of Chicago Press, Chicago, Illinois, third edition edn., 468 pp pp.
- Ronquist F, Klopstein S, Vilhelmsen L, Schulmeister S, Murray DL, & Rasnitsyn AP (2012). A total-evidence approach to dating with fossils, applied to the early radiation of the hymenoptera. *Systematic Biology*, **61**(June): 973–999.
- Rose KD (1996). On the origin of the order Artiodactyla. *Proceedings of the National Academy of Sciences of the United States of America*, **93**(February): 1705–1709.
- Rossi R (2000). Taxonomia de *Mazama* Rafinesque, 1817 do Brasil (Artiodactyla, Cervidae).
- Rössner GE (1995). Odontologische und schädelanatomische Untersuchungen an *Procervulus* (Cervidae, Mammalia). *Münchner Geowissenschaftliche Abhandlungen (A)*, **29**: 127.
- Rössner GE (1997). Biochronology of Ruminant Assemblages in the Lower Miocene of Southern Germany. In Aguilar JP, Legendre S, & Michaux J (Eds.), *Actes du Congrès BiochroM'97. Mémoires et Travaux de l'E.P.H.E*, Institut de Montpellier, vol. 21, pp. 609–618.
- Rössner GE (1998). Wirbeltiere aus dem Unter-Miozän des Lignit-Tagebaues Oberdorf (Weststeirisches Becken, Österreich): 9. Ruminantia (Mammalia). *Annalen des Naturhistorischen Museums in Wien (A)*, **99**: 169–193.
- Rössner GE (2007). Family Tragulidae. *The Evolution of Artiodactyls*, pp. 213–220.
- Rössner GE (2010). Systematics and palaeoecology of Ruminantia (Artiodactyla, Mammalia) from the Miocene of Sandelzhausen (southern Germany, Northern Alpine Foreland Basin). *Palaontologische Zeitschrift*, **84**: 123–162.
- Roure B, Baurain D, & Philippe H (2013). Impact of missing data on phylogenies inferred from empirical phylogenomic data sets. *Molecular Biology and Evolution*, **30**(1): 197–214.

- Rumiz D & Pardo E (2010). Chapter 21 Peruvian dwarf brocket deer *Mazama chunyi* (Herskovitz 1959). In Duarte JMB & Gonz  lez S (Eds.), *Neotropical cervidology: biology and medicine of Latin American deer*, FUNEP in collaboration with IUCN, Jaboticabal, Brasil and Gland, Switzerland, pp. 185–189.
- Samiullah K & Akhtar M (2007). An evidence of *Cervus punjabensis* from the lower Siwaliks of the Punjab, Pakistan. *Punjab University Journal of Zoology*, **22**(1-2): 63–68.
- Sansom RS & Wills Ma (2013). Fossilization causes organisms to appear erroneously primitive by distorting evolutionary trees. *Scientific reports*, **3**: 2545.
- Schaller GB (1996). Description of the giant muntjac (*Megamuntiacus vuquangensis*) in Laos. *Journal of Mammalogy*, **77**(3): 675–683.
- Schaub S (1941). Die kleine Hirschart aus dem Oberpliocaen von Sen  ze (Haute-Loire). *Eclogae geologicae Helvetiae*, **34**(2): 264–272.
- Schaub S (1943). Die oberpliocaene S  ugetierfauna von Sen  ze (Haute-Loire) und ihre verbreitungsgeschichtliche Stellung. *Eclogae Geologicae Helvetiae*, **36**(2): 270–289.
- Schlosser M (1924). Tertiary vertebrates from Mongolia. *Palaeontologia Sinica, Series C*, **1**(1): 1–119.
- Sclater PL (1870). Remarks on the Arrangement and Distribution of the Cervidae. *Proceedings of the Zoological Society of London*, pp. 114–117.
- Scotland RW, Olmstead RG, & Bennett JR (2003). Phylogeny reconstruction: the role of morphology. *Systematic Biology*, **52**(4): 539–548.
- Scott K & Janis C (1987). Phylogenetic relationships of the Cervidae, and the case for a superfamily ‘Cervoidea’. In Wemmer C (Ed.), *Biology and management of the Cervidae*, Smithsonian Institution, Washington, London, pp. 3–20.
- Scott KM & Janis CM (1993). Relationships of the Ruminantia (Artiodactyla) and an analysis of the characters used in ruminant taxonomy. *Mammal phylogeny*, **2**: 282–302.
- Scott WB (1937). *A History of Land Mammals in the Western Hemisphere*. Macmillan Co., New York, 786 pp.
- Shapiro B & Hofreiter M (2014). A paleogenomic perspective on evolution and gene function: new insights from ancient DNA. *Science (New York, N.Y.)*, **343**: 1236573.
- Shevenell AE, Kennett JP, & Lea DW (2004). Middle Miocene southern ocean cooling and Antarctic cryosphere expansion. *Science*, **305**(5691): 1766–1770.
- Sigogneau D (1960).   tude d’un cervid   Pleistoc  ne de Corse. *Annales de Pal  ontologie*, **46**: 49–77.
- Simonelli V (1907). Mammiferi Quaternari dell’Isola di Candia. *Memoirie, Accademia delle Scienze dell Istituto di Bologna, Classe di Scienze Fisiche, Serie VI*, **4**: 251–267.

- Simonelli V (1908). Mammiferi quaternari dell' isola di Candia II. *Memorie, Accademia delle Scienze. Istituto di Bologna Classe di Scienze Fisiche, Ser. VI*, **5**: 103–111.
- Simpson GG (1945). Principles of classification and a classification of mammals. *Bulletin of the American Museum of Natural History*, **85**: 1–350.
- Smith MH, Branen WV, Marchinton RL, Johns PE, & Wooten MC (1986). Genetic and morphologic comparisons of red brocket, brown brocket, and white-tailed deer. *Journal of Mammalogy*, **67**(1): 103–111.
- Smith WP (1991). *Odocoileus virginianus*. *Mammalian species*, **388**: 1–13.
- Solounias N (1988). Evidence from horn morphology on the phylogenetic relationships of the pronghorn (*Antilocapra americana*). *Journal of mammalogy*, **69**(1): 140–143.
- Solounias N & Moelleken SMC (1994). Differences in diet between two archaic ruminant species from Sansan, France. *Historical Biology*, **4**: 203–220.
- Sondaar P (1971). Palaeozoogeography of the Pleistocene Mammals from the Aegean. In Strid A (Ed.), *Evolution in the Aegean*, Carl Blom, Lund, vol. 30, pp. 60–70.
- Spaan A (1992). A revision of the deer from Tegelen (Province of Limburg, The Netherlands). *Scripta Geologica*, **98**: 1–85.
- Spencer MR & Wilberg EW (2013). Efficacy or convenience? Model-based approaches to phylogeny estimation using morphological data. *Cladistics*, **29**: 663–671.
- Spotorno AE, Brum N, & Di Tomaso M (1987). Comparative cytogenetics of South American deer. *Fieldiana Zoology*, **39**: 473–483.
- Stadler T (2011). Mammalian phylogeny reveals recent diversification rate shifts. *Proceedings of the National Academy of Sciences of the United States of America*, **108**: 6187–6192.
- Stamatakis A (2006). RAxML-VI-HPC: maximum likelihood-based phylogenetic analyses with thousands of taxa and mixed models. *Bioinformatics*, **22**(21): 2688–2690.
- Stamatakis A (2014). RAxML version 8: a tool for phylogenetic analysis and post-analysis of large phylogenies. *Bioinformatics*, **30**(9): 1312–1313.
- Stefaniak K & Stefaniak K (1995). Late Pliocene cervids from Weze 2 in southern Poland. *Acta Palaeontologica Polonica*, **40**: 327–340.
- Stehlin HG (1923). Die oberpliocäne Fauna von Senèze (Haute-Loire). *Eclogae Geologicae Helvetiae*, **18**(2): 268–281.
- Stehlin HG (1928). Bemerkungen über die Hirsche von Steinheim am Aalbuch. *Eclogae Geologicae Helvetiae*, **21**(1): 245–256.
- Stehlin HG (1937). Bemerkungen über die miocänen Hirschgenera *Stephanocemas* und *Lagomeryx*. *Verhandlungen der Naturforschenden Gesellschaft in Basel*, **48**: 193–214.

- Stehlin HG (1939). *Dicroceros elegans* Lartet und sein Geweihwechsel. *Eclogae Geologicae Helvetiae*, **32**(2): 162–179.
- Steininger FF (1999). Chronostratigraphy, geochronology and biochronology of the Miocene “European land mammal mega-zones” (ELMMZ) and the Miocene “Mammal-zones (MN-zones)”. In Rössner GE & Heissig K (Eds.), *The Miocene land mammals of Europe*, Verlag Dr. Friedrich Pfeil, München, pp. 9–24.
- Stremme H (1911). Die Säugetiere mit Ausnahme der Proboscider. In Selenka M & Blanckenhorn M (Eds.), *Die Pithecanthropus-Schichten auf Java: Geologische und paläontologische Ergebnisse der Trinil-Expedition (1907 und 1908)*., Engelmann, Leipzig, pp. 82–160.
- Swinhoe R (1870). *Zoological notes of a journey from Canton to Peking and Kalgan*.
- Swofford DL (2002). PAUP*. Phylogenetic Analysis Using Parsimony (*and other methods). Version 4. Sinauer Associates, Sunderland, Massachusetts.
- Symeonidis NK (1974). Ein vollständiges Geweih von *Pliocervus pentelici* (Gaudry) aus Pikermi (Griechenland). *Annales Géologiques des Pays Helléniques*, **23**: 308–316.
- Taru H & Hasegawa Y (2002). The Plio-Pleistocene fossil mammals from the Kasumi and Tama Hills. *Memoirs of the National Science Museum, Tokyo*, **38**: 43–56.
- Tate ML, Goosen GJ, Patene H, Pearse aJ, McEwan KM, & Fennessy PF (1997). Genetic analysis of Pere David’s x red deer interspecies hybrids. *J Hered*, **88**(5): 361–365.
- Tavaré S (1986). Some Probabilistic and Statistical Problems in the Analysis of DNA Sequences. *Lectures on Mathematics in the Life Sciences. American Mathematical Society*, **17**: 57–86.
- Teilhard de Chardin P (1939). The Miocene cervids from Shantung. *Bulletin of the Geological Society of China*, **19**: 269–278.
- Teilhard de Chardin P & Piveteau J (1930). *Les mammifères fossiles de Nihowan (Chine)*. Masson et Cie, Paris, 136 pp.
- Teilhard de Chardin P & Trassaert M (1937). The Pliocene Camelidae, Giraffidae, and Cervidae of South Eastern Shansi. *Palaeontologia Sinica, New Series C*, **1**: 1–56.
- Temminck CJ (1838). *Over de Kennis en de Verbreiding der Zoogdieren van Japan*.
- Thenius E (1948). Zur Kenntnis der fossilen Hirsche des Wiener Beckens, unter besonderer Berücksichtigung ihrer stratigraphischen Bedeutung. *Annalen des Naturhistorischen Museums in Wien*, **56**: 262–308.
- Thenius E (1950). Die tertiären Lagomeryciden und Cerviden der Steiermark. *Sitzungsberichte Österreichische Akademie der Wissenschaften Mathematisch-Naturwissenschaftliche Klasse*, **159**(6-9): 219–254.

- Thomas J (1951). *Eostyloceros pierensis* nov. sp., nouveau cervuline du Pontien européen. *Comptes Rendus sommaires des séances de la Société géologique de France*, **6**: 255–257.
- Thomas O (1908). LVI. A new deer of the Brocket group from Venezuela. *Journal of Natural History*, **1**(4): 349–350.
- Timmins R, Steinmetz R, Sagar Baral H, Samba Kumar N, Duckworth J, Anwarul Islam M, Gimán B, Hedges S, Lynam A, Fellowes J, Chan B, & Evans T (2008). *Rusa unicolor*. *The IUCN red list of threatened species. Version 2014.3*. Available at www.iucnredlist.org (accessed on 17 April 2015).
- Tomíati C & Abbazzi L (2002). Deer fauna from Pleistocene and Holocene localities of Ecuador (South America) Cervidés du Pléistocène et Holocène d'Équateur (Amérique du Sud). *Geobios*, **35**: 631–645.
- Tuoc D, Dung V, Dawson S, Arctander P, & MacKinnon J (1994). Introduction of a new large mammal species in Vietnam. *Science and Technology News*, **3**: 4–12.
- Valli A (2010). Dispersion of the genus *Procapreolus* and the relationships between *Procapreolus cusanus* and the roe deer (*Capreolus*). *Quaternary International*, **212**(2): 80–85.
- Valli aMF & Palombo MR (2005). Le régime alimentaire du Cervidae (Mammalia) *Euccladoceros ctenoides* (Nesti 1841) reconstitué par la morphologie du crâne et par l'usure dentaire. *Eclogae Geologicae Helvetiae*, **98**: 133–143.
- Van Bemmél ACV (1952). Contribution to the knowledge of the genera *Muntiacus* and *Arctogalidia* in the Indo-Australian Archipelago (Mammalia, Cervidae & Viverridae). *Beaufortia*, **16**: 1–50.
- Van Bemmél ACV (1974). The concept of superspecies applied to Eurasiatic Cervidae. *Zeitschrift für Säugetierkunde*, **38**(5): 295–302.
- Van der Geer A, De Vos J, Lyras G, & Dermitzakis M (2006). New data on the Pleistocene Cretan deer *Candiacervus* sp. II (Cervinae, Mammalia). *CFS Courier Forschungsinstitut Senckenberg*, pp. 131–137.
- Van der Made J (2003). Suoidea (pigs) from the Miocene hominoid locality Çandır in Turkey. In Güleç E, Begun D, & Geraads D (Eds.), *Geology and Vertebrate Paleontology of the Middle Miocene Hominoid Locality Ç (Central Anatolia, Turkey)*, Courier Forschungsinstitut Senckenberg, vol. 240, pp. 149–180.
- Van der Made J, Carlos Calero JA, & Mancheño MA (2008). New material of the goat *Capra alba* from the Lower Pleistocene of Quibas (Spain); notes on sexual dimorphism, stratigraphic distribution and systematics. *Bollettino della Società Paleontologica Italiana*, **47**: 13–23.
- Van Mourik S & Stelmasiak T (1986). *Rusa* deer - from past to present. *Zoologischer Anzeiger*, **217**: 309–320.

- Vargas-Munar DSF (2003). *Relação entre fragilidade cromossômica e trocas entre cromátides irmãs com a variabilidade cariotípica de Cervídeos brasileiros*. Master Thesis, Faculdade de Ciências Agrárias e Veterinárias, UNESP, Jaboticabal.
- Vaufrey R (1929). Les éléphants nains des îles méditerranéennes et la question des isthmes Pleistocènes. *Archives de l'Institut de Paleontologie Humaine*, **6**.
- Viret J (1954). Le loess à bancs durcis de Saint-Vallier (Drôme) et sa faune de mammifères Villafranchiens. *Nouvelles Archives du Muséum d'Histoire Naturelle de Lyon*, **4**: 1–200.
- Viret J (1961). Artiodactyla. In Piveteau J (Ed.), *Traité de Paléontologie*, Masson et Cie, Paris, vol. VI(1), pp. 887–1084.
- Vislobokova I (2013). Morphology, taxonomy, and phylogeny of megacerines (Megacerini, Cervidae, Artiodactyla). *Paleontological Journal*, **47**(8): 833–950.
- Vislobokova IA (1980). On systematical position of the deer from Pavlodar and the origin of neocervines. *Paleontological Journal*, **3**: 91–106.
- Vislobokova IA (1983). The fossil deer of Mongolia. *Transaction of the Joint Soviet-Mongolian Paleontological Expedition*, **23**: 1–78.
- Vislobokova IA (1985). Concerning a new *Eostyloceros* from the Pliocene of Olkhon Island (Lake Baykal). *Paleontological Journal*, **4**: 123–125.
- Vislobokova IA (1990). The fossil deer of Eurasia. *Transactions of the Palaeontological Institute*, **240**: 1–206.
- Vislobokova IA (1992). Neogene deer in Eurasia. *Paleontologia i evolució*, **24–25**: 149–154.
- Vislobokova IA (1997). Eocene-Early Miocene ruminants in Asia. *Mémoires et Travaux de l'E.P.H.E, Institut de Montpellier*, **21**: 215–223.
- Vislobokova Ia (2009). The most ancient megacerine deer from the Late Miocene of Siberia and its implications to the evolution of the group. *Palaeoworld*, **18**(2008): 278–281.
- Vislobokova IA (2012). The history of giant deer (Meracerini, Cervidae, Artiodactyla). *Transactions of Paleontological Institute*, **293**: 1–102.
- Vislobokova IA, Changkang H, & Sun B (1989). On the systematic position of the Lagomerycinae. *Vertebrata Palasiatica*, **27**: 130–132.
- Vogliotti A & Duarte JMP (2009). Discovery of the first wild population of the small red brocket deer *Mazama bororo* (Artiodactyla: Cervidae). *Mastozoología Neotropical*, **16**(2): 499–503.
- Von Koenigswald G (1939). Das Pleistocän Javas. *Quartär*, **2**: 28–53.
- Voris HK (2000). Maps of Pleistocene sea levels in Southeast Asia: Shorelines, river systems and time durations. *Journal of Biogeography*, **27**: 1153–1167.

- Vrba E & Schaller G (2000). *Antelopes, Deer, and Relatives: Fossil Record, Behavioral Ecology, Systematics, and Conservation*. Yale University Press, Yale.
- Wada K, Nishibori M, & Yokohama M (2007). The complete nucleotide sequence of mitochondrial genome in the Japanese Sika deer (*Cervus nippon*), and a phylogenetic analysis between Cervidae and Bovidae. *Small Ruminant Research*, **69**: 46–54.
- Wang B & Wu W (1979). Artiodactyla. *Vertebrate Fossils of China*, p. 501–620.
- Wang W & Lan H (2000). Rapid and parallel chromosomal number reductions in muntjac deer inferred from mitochondrial DNA phylogeny. *Molecular biology and evolution*, **17**: 1326–1333.
- Wang X, Xie G, & Dong W (2009). A new species of crown-antlered deer *Stephanocemas* (Artiodactyla, Cervidae) from the middle Miocene of Qaidam Basin, northern Tibetan Plateau, China, and a preliminary evaluation of its phylogeny. *Zoological Journal of the Linnean Society*, **156**: 680–695.
- Webb S (2000). Evolutionary history of new world Cervidae. In Vrba E & Schaller G (Eds.), *Antelopes, deer, and relatives: fossil record, behavioral ecology, systematics, and conservation*, Yale University Press, New Haven, pp. 38–64.
- Webb SD (1991). Ecogeography and the great American interchange. *Paleobiology*, **17**(03): 266–280.
- Webb SD & Taylor BE (1980). The phylogeny of hornless ruminants and a description of the cranium of *Archaeomeryx*. *Bulletin of the American Museum of Natural History*, **167**: 3–57.
- Weber M & González S (2003). Latin American deer diversity and conservation: a review of status and distribution. *Ecoscience*, **10**(4): 443–454.
- Whitehead GK et al. (1972). *Deer of the World*. Constable, London, 194 pp.
- Wiens JJ (2000). Coding morphological variation within species and higher taxa for phylogenetic analysis. In Wiens JJ (Ed.), *Phylogenetic analysis of Morphological data*, Smithsonian Institution Press, Washington and London, pp. 115–145.
- Wiens JJ (2003). Missing data, incomplete taxa, and phylogenetic accuracy. *Systematic Biology*, **52**(4): 528–538.
- Wiens JJ (2004). The Role of Morphological Data in Phylogeny Reconstruction. *Systematic Biology*, **53**(4): 653–661.
- Wiens JJ (2006). Missing data and the design of phylogenetic analyses. *Journal of biomedical informatics*, **39**(1): 34–42.
- Wiens JJ & Morrill MC (2011). Missing data in phylogenetic analysis: reconciling results from simulations and empirical data. *Systematic Biology*, p. syr025.

- Wilgenbusch J, Warren D, & DL S (2004). *AWTY: A system for graphical exploration of MCMC convergence in Bayesian phylogenetic inference*.
- Wilson AC, Carlson SS, & White TJ (1977). Biochemical evolution. *Annual review of biochemistry*, **46**(1): 573–639.
- Wilson DE & Reeder DM (2005). *Mammal species of the world: a taxonomic and geographic reference*, vol. 1. JHU Press.
- Woodruff DS (2003). Neogene marine transgressions, palaeogeography and biogeographic transitions on the Thai–Malay Peninsula. *Journal of Biogeography*, **30**(4): 551–567.
- Xie W, Lewis PO, Fan Y, Kuo L, & Chen MH (2011). Improving marginal likelihood estimation for bayesian phylogenetic model selection. *Systematic Biology*, **60**: 150–160.
- Yang F, Carter N, Shi L, & Ferguson-Smith M (1995). A comparative study of karyotypes of muntjacs by chromosome painting. *Chromosoma*, **103**(9): 642–652.
- Yang Z (1994). Maximum likelihood phylogenetic estimation from DNA sequences with variable rates over sites: approximate methods. *Journal of Molecular Evolution*, **39**(3): 306–314.
- Young C (1932). On the Artiodactyla from the *Sinanthropus* site at Choukoutien. *Palaeontologia Sinica, Series C*, **8**(2): 159.
- Young C (1937). On a Miocene mammalian fauna from Shantung. *Bulletin of the Geological Society of China*, **17**(2): 209–244.
- Young C (1964). On a new *Lagomeryx* from Lantian, Shensi. *Vertebrata Asiatica*, **4**: 336–340.
- Zachos F, Mattioli S, Ferretti F, & Lorenzini R (2014). The unique Mesola red deer of Italy: taxonomic recognition (*Cervus elaphus italicus* nova ssp., Cervidae) would endorse conservation. *Italian Journal of Zoology*, **81**(1): 136–143.
- Zachos FE, Apollonio M, Bärmann EV, Festa-Bianchet M, Göhlich U, Habel JC, Haring E, Kruckenhauser L, Lovari S, McDevitt AD et al. (2013). Species inflation and taxonomic artefacts—A critical comment on recent trends in mammalian classification. *Mammalian Biology-Zeitschrift für Säugetierkunde*, **78**(1): 1–6.
- Zachos FE & Hartl GB (2011). Phylogeography, population genetics and conservation of the European red deer *Cervus elaphus*. *Mammal Review*, **41**: 138–150.
- Zaim Y, De Vos J, Huffman OF, Aziz F, & Rizal Y (2003). A new antler specimen from the 1936 Peking hominid site, East Jawa, Indonesia, attributable to *Axis lydekkeri*. *Journal of Mineral Technology*, **X**(1): 1–9.
- Zdansky O (1925). Fossile Hirsche Chinas. *Palaeontologia Sinica, Series C*, **2**(3): 1–90.

- Zimmermann E (1780). Geographische Geschichte des Menschen, und der vierfüßigen Thiere: nebst einer hieher gehörigen zoologischen Weltcharte. *Weygandschen Buchhandlung, Leipzig, Germany*.
- Zong GF (1987). Note on some mammalian fossils from the Early Pleistocene of Di-Qing County, Yunnan. *Vertebrata Palasiatica*, **25**: 69–76.
- Zuckerlandl E & Pauling L (1962). Molecular disease, evolution, and genic heterogeneity. In Kasha M & Pullman B (Eds.), *Horizons in Biochemistry*, Academic Press, New York, pp. 189–225.

Declaration

I hereby confirm that my thesis entitled ‘**A Comprehensive Approach towards the Phylogeny and Evolution of Cervidae**’, is the result of my own original work. Furthermore, I certify that this work contains no material which has been accepted for the award of any other degree or diploma in my name, in any university and, to the best of my knowledge and belief, contains no material previously published or written by another person, except where due reference has been made in the text. In addition, I certify that no part of this work will, in the future, be used in a submission in my name, for any other degree or diploma in any university or other tertiary institution without the prior approval of the Ludwig-Maximilians-Universität Munich.

Place, Date, Signature

A Extant Cervid Species

Table A.1: Overview of extant cervid species, their vernacular names in English and German, the number of species according to different references (third set of columns), their IUCN status, size categories and ecology. *only as subspecies; °as separate genus *Panolia*; †plus additional 39 spp.; †m = minute (≤ 50 cm), S = small (50–75 cm), M = medium (75–110 cm), L = large (110–160 cm), G = gigantic >160 cm.

Acronym	Species	Vernacular names (English)	Vernacular (German)	names	IUCN	Mattioli et al. (2011)	Groves & Grubb (2011)	Wilson & Reeder (2005)	IUCN status	Size†	Ecology
Alc.alc	<i>Alces alces</i>	Eurasian elk	Elch		x	x	x	x	least concern	G	temperate, taiga, tundra, boreal
Alc.ame	<i>Alces americanus</i>	moose	Nordamerikanischer Elch		x	–	x	x	least concern	G	temperate, taiga, tundra, boreal
Axi.axi	<i>Axis axis</i>	chital	Axishirsch		x	x	x	x	least concern	M	tropical, subtropical
Axi.cal	<i>Axis calamianensis</i>	Calamian deer	Calamian-Hirsch		x	x	x	x	endangered	S	tropical, subtropical
Axi.kuh	<i>Axis kuhli</i>	Bawean deer	Bawean-Hirsch		x	x	x	x	critically endangered	S	tropical, subtropical
Axi.por	<i>Axis porcinus</i>	hog deer	Schweinhirsch		x	x	x	x	endangered	S	temperate - subtropical
Blad.c	<i>Blastocercus dichotomus</i>	marsh deer	Sumpfhirsch		x	x	x	x	vulnerable	M,L	tropical, subtropical
Cap.cap	<i>Capreolus capreolus</i>	European roe deer	Europäisches Reh		x	x	x	x	least concern	S,M	temperate, mediterranean, taiga, tundra
Cap.pyg	<i>Capreolus pygargus</i>	Siberian roe deer	Sibirisches Reh		x	x	x	x	least concern	M	temperate, mediterranean, taiga, tundra
Cer.alb	<i>Cervus albirostris</i>	white-lipped deer	Weißlippenhirsch		x	x	x	x	vulnerable	L	temperate, montane
Cer.can	<i>Cervus canadensis</i>	wapiti	Wapiti		–	x	x	–	not assessed	L	temperate
Cer.ela	<i>Cervus elaphus</i>	red deer	Rothirsch		x	x	x	x	least concern	M,L	temperate, mediterranean, tundra
Cer.nip	<i>Cervus nippon</i>	sika deer	Sikahirsch		x	x	x	x	least concern	S,M	temperate
Cer.wal	<i>Cervus wallichi</i>	Central Asian red deer	China-Rothirsch		–	x	x	–	not assessed	–	temperate, montane
Dam.-dam	<i>Dama dama</i>	fallow deer	Damhirsch		x	x	x	x	least concern	M	temperate, mediterranean
Dam.-mes	<i>Dama mesopotamica</i>	Persian fallow deer	Mesopotamischer Damhirsch		x	x	x	x*	endangered	M	mediterranean
Ela.cep	<i>Elaphodus cephalophus</i>	tufted deer	Schopfhirsch		x	x	x	x	near threatened	S	tropical, subtropical
Ela.dav	<i>Elaphurus davidianus</i>	Pere David's deer	Davidshirsch		x	x	x	x	extinct in the wild	L	temperate
Hip.ant	<i>Hippocamelus antisensis</i>	North Andean Deer	Nordandenhirsch		x	x	x	x	vulnerable	M	tropical, subtropical, montane
Hip.bis	<i>Hippocamelus bisulcus</i>	South Andean Huemul	Südandenhirsch		x	x	x	x	endangered	M	temperate, montane
Hvd.ine	<i>Hydropotes inermis</i>	Chinese water deer	Chinesisches Wasserreh		x	x	x	x	vulnerable	S	temperate
Maz.-ame	<i>Mazama americana</i>	red brocket	Großmazama		x	x	x	x	data deficient	S,M	tropical, subtropical
Maz.bor	<i>Mazama bororo</i>	small red brocket	Kleiner Rotmazama		x	x	x	x	vulnerable	S	tropical, subtropical

Table A.1: Continued

Maz.bri	Mazama bricenii	Merida brocket	Nördlicher Zwergmazama	x	x	x	x	vulnerable	m	tropical, subtropical
Maz.chu	Mazama chunyi	common dwarf brocket	Südlicher Zwergmazama	x	x	x	x	vulnerable	m	tropical, subtropical
Maz.gou	Mazama gouazoubira	gray brocket	Graumazama	x	x	x	x	least concern	S	tropical, subtropical
Maz.nana	Mazama nana	lesser brocket	Kleinmazama	x	x	x	x	vulnerable	m	tropical, subtropical
Maz.-nem	Mazama nemorivaga	Amazonian gray brocket	Amazonien-Mazama	x	x	x	-	least concern	-	tropical, subtropical
Maz.pan	Mazama pandora	Yucatan brown brocket	Yucatan-Mazama	x	x	x	x	vulnerable	S	tropical, subtropical
Maz.ruf	Mazama rufina	little red brocket	Roter Kleinmazama	x	x	x	x	vulnerable	m	tropical, subtropical
Maz.tem	Mazama temama	Mexican red brocket	Mexikanischer mazama	x	x	x	x	data deficient	S	tropical, subtropical
Mun.ath	Muntiacus atherodes	Bornean yellow muntjac	Borneo-Muntjak	x	x	x	x	least concern	S	tropical, subtropical
Mun.cri	Muntiacus crinifrons	black muntjac	Schwarzer Muntjak	x	x	x	x	vulnerable	S	tropical, subtropical
Mun.fea	Muntiacus feae	Pea's muntjac	Tenasserin-Muntjak	x	x	x	x	data deficient	S	tropical, subtropical
Mun.-gon	Muntiacus gongshanensis	Gongshan muntjac	Gongshan-Muntjak	x	x	x	x	data deficient	S	tropical, subtropical
Mun.-mon	Muntiacus montanus	Sumatran muntjac	Sumatra-Muntjak	x	-	x	-	data deficient	-	?tropical, subtropical, montane
Mun.-mun	Muntiacus muntjak	red muntjac	Indischer Muntjak	x	x	x	-	least concern	S	tropical, subtropical
Mun.-puh	Muntiacus puhoatensis	Pu Hoat muntjac	Vietnam-Muntjak	x	x	x	x	data deficient	m	tropical, subtropical
Mun.put	Muntiacus putaoensis	leaf muntjac	Burma-Muntjak	x	x	x	x	data deficient	m,S	tropical, subtropical
Mun.ree	Muntiacus reevesi	Reeves's muntjac	Chinesischer Muntjak	x	x	x	x	least concern	m	temperate, tropical, subtropical
Mun.roo	Muntiacus rooseveltorum	Roosevelt's muntjac	Roosevelt-Muntjak	x	x	x	x	data deficient	m	tropical, subtropical
Mun.tru	Muntiacus truongsongensis	Annamite muntjac	Annan-Muntjak	x	x	x	x	data deficient	m	tropical, subtropical
Mun.vag	Muntiacus vaginalis	Northern red muntjac	Nordindischer Muntjak	x	-	x	x	least concern	-	tropical, subtropical
Mun.-vuq	Muntiacus vuquangensis	giant muntjac	Riesenmuntjak	x	x	x	-	endangered	S	tropical, subtropical
Odo.-hem	Odocoileus hemionus	mule deer	Maultierhirsch	x	x	x	x	least concern	M	temperate, mediterranean, boreal
Odo.-vir	Odocoileus virginianus	white-tailed deer	Weißwedelhirsch	x	x	x	x	least concern	S,M	temperate, tropical, subtropical
Ozo.bez	Ozotoceros bezoarticus	pampas deer	Pampashirsch	x	x	x	x	near threatened	S	tropical, subtropical
Pud.-mep	Pudu mephistophiles	Northern pudu	Nordpudu	x	x	x	x	vulnerable	m	tropical, subtropical
Pud.-pud	Pudu pudu	Southern pudu	Südpudu	x	x	x	x	vulnerable	m	temperate
Ran.tar	Rangifer tarandus	caribou, reindeer	Rentier	x	x	x	x	least concern	M,L	temperate, taiga, tundra, boreal

Table A.1: Continued

Ruc_duv	<i>Rucervus duvaucelii</i>	barasingha	Barasingha	x	x	x	x	x	L	tropical, subtropical
Ruc_eld	<i>Rucervus eldii</i>	Eld's deer	Leierhirsch	x	x	x ^a	x	x	M,L	tropical, subtropical
Ruc_sch	<i>Rucervus schomburgki</i>	Schomburgk's deer	Schomburgk-Hirsch	x	–	x	x	x	–	no data
Rus_alf	<i>Rusa alfredi</i>	Philippine spotted deer	Prinz-Alfred-Hirsch	x	x	x	x	x	S	tropical, subtropical
Rus_mar	<i>Rusa marianna</i>	Philippine brown deer	Philippinenhirsch	x	x	x	x	x	S	tropical, subtropical
Rus_tim	<i>Rusa timorensis</i>	Javan rusa	Mähnenhirsch	x	x	x	x	x	M	tropical, subtropical
Rus_uni	<i>Rusa unicorn</i>	sambar	Sambar	x	x	x	x	x	L	tropical, subtropical
57				55	53	57 [†]	51			

B Lists of Extant and Fossil Specimens

Table B.1: List of all investigated specimens of extant cervids and outgroup taxa.

Collection ID	Species	Sex	Comment
UMZC H.17691	<i>Alces alces</i>	male	
ZSM 1952/142	<i>Alces alces</i>	female	
ZSM 1962/310	<i>Alces alces</i>	female	
ZSM 1970/8	<i>Alces alces</i>	male	
ZSM 1972/1	<i>Alces alces</i>	female	
ZSM 1962/298	<i>Alces alces</i>	male	photos only
NHM 46.199	<i>Axis axis</i>	male	
NHM 697 t	<i>Axis axis</i>	male	
NHM 67.4.12.240	<i>Axis axis</i>	male	
ZSM 1951/70	<i>Axis axis</i>	female	
ZSM 1958/88	<i>Axis axis</i>	female	
ZSM 1963/27	<i>Axis axis</i>	female	
ZMH 4764	<i>Axis axis</i>	female	photos only; tooth pathology
ZSM 1969/63	<i>Axis porcinus</i>	female	
NHM 2004.956	<i>Axis porcinus</i>	female	
NHM 27.2.14.106	<i>Axis porcinus</i>	male	skull
MNHN 1933 212	<i>Axis porcinus</i>	male	
MNHN 1902 13	<i>Axis porcinus</i>	female	
MNHN 1962 4188	<i>Axis porcinus</i>	female	photos only; skull
MNHN 1904 60	<i>Axis porcinus</i>	male	photos only; partial skull
MNHN AE 742	<i>Axis porcinus</i>	male	photos only; antler pathology
UMZC H.16052	<i>Axis porcinus</i>	male	subadult
NHM 98.10.11.1	<i>Blastocerus dichotomus</i>	male	
ZSM 1926/283	<i>Blastocerus dichotomus</i>	male	incomplete skull
ZSM 1931/397	<i>Blastocerus dichotomus</i>	male	skull
MNHN 1933 207	<i>Blastocerus dichotomus</i>	female	
MNHN 190	<i>Blastocerus dichotomus</i>	female	
ZSM 1940/138	<i>Capreolus capreolus</i>	male	
ZSM 1955/130	<i>Capreolus capreolus</i>	male	
ZSM 1979/161	<i>Capreolus capreolus</i>	female	
ZSM 1979/165	<i>Capreolus capreolus</i>	female	
ZSM 1971/558	<i>Capreolus capreolus</i>	female	
UMZC H.18004	<i>Capreolus capreolus</i>	male	
ZSM 1980/40	<i>Capreolus pygargus</i>	female	
ZSM 1978/286	<i>Capreolus pygargus</i>	female	
NHM 1938.5.18.1	<i>Capreolus pygargus</i>	male	
NHM 42.3.13.1	<i>Capreolus pygargus</i>	male	
NHM 31.6.1.75	<i>Capreolus pygargus</i>	male	skull
MNHN 1902 815	<i>Capreolus pygargus</i>	female	
MNHN AE 734	<i>Capreolus pygargus</i>	male	

Table B.1: Continued

NHM 92.10.11.1	<i>Cervus albirostris</i>	male	
ZSM 1968/703	<i>Cervus canadensis</i>	female	
ZSM 1966/221	<i>Cervus canadensis</i>	female	
ZSM 1959/260	<i>Cervus canadensis</i>	female	
UMZC H.16971	<i>Cervus canadensis</i>	male	measurements only
ZMH 7590	<i>Cervus canadensis</i>	male	
ZMH 3506	<i>Cervus canadensis</i>	male	photos only; antler pathology
ZSM 1956/224	<i>Cervus elaphus</i>	male	
ZSM 1971/695	<i>Cervus elaphus</i>	male	
ZSM 1952/213	<i>Cervus elaphus</i>	female	
ZSM 1954/237	<i>Cervus elaphus</i>	female	
ZSM 1915/127	<i>Cervus elaphus</i>	female	
UMZC H.16620	<i>Cervus elaphus</i>	male	
ZSM 1961/285	<i>Cervus nippon</i>	male	
ZSM 1904/1576	<i>Cervus nippon</i>	female	
ZSM 1905/1042	<i>Cervus nippon</i>	female	
NHM 85.2.23.1	<i>Cervus nippon</i>	male	
NHM 72.1066	<i>Cervus nippon</i>	male	
MNHN 1974 95	<i>Cervus nippon</i>	female	
NHM 1980.374	<i>C. elaphus</i> x <i>C. nippon</i>	male	
NHM 1980.375	<i>C. nippon</i> x <i>C. elaphus</i>	male	
ZSM 2010/302	<i>Dama dama</i>	male	skull
ZSM 1964/142	<i>Dama dama</i>	male	mandible
ZSM no ID	<i>Dama dama</i>	male	
NHM 1958.4.24.1	<i>Dama dama</i>	female	
UMZC H.17179	<i>Dama dama</i>	female	
UMZC H.17174	<i>Dama dama</i>	male	
UMZC H.17175	<i>Dama dama</i>	male	
MNHN A 1480	<i>Elaphodus cephalophus</i>	male	
NHM 92.7.13.1	<i>Elaphodus cephalophus</i>	female	
NHM 26.9.1.1	<i>Elaphodus cephalophus</i>	male	
NHM 55.605	<i>Elaphodus cephalophus</i>	female	
NHM 1.3.2.17	<i>Elaphodus cephalophus</i>	male	
NHM 98.3.7.18	<i>Elaphodus cephalophus</i>	female	
ZSM 1974/50	<i>Elaphurus davidianus</i>	female	
MNHN 1966 02	<i>Elaphurus davidianus</i>	male	
MNHN 1972 67	<i>Elaphurus davidianus</i>	female	
UMZC H.16231	<i>Elaphurus davidianus</i>	male	
UMZC H.16235	<i>Elaphurus davidianus</i>	male	photos only; subadult
NHM 97.11.11.4	<i>Hippocamelus antisensis</i>	male	
NHM 97.11.11.5	<i>Hippocamelus antisensis</i>	female	

Table B.1: Continued

MNHN 1957 1303	<i>Hippocamelus antisensis</i>	female	
MNHN 1933 201	<i>Hippocamelus antisensis</i>	female	
ZMB 2000	<i>Hippocamelus antisensis</i>	male	
ZSM 1949/1355	<i>Hippocamelus bisulcus</i>	male	incomplete skull
NHM 72.11.11.1	<i>Hippocamelus bisulcus</i>	male	
UMZC H.18902	<i>Hippocamelus bisulcus</i>	female	
MNHN 1874 733	<i>Hippocamelus bisulcus</i>	male	skull
ZSM 1977/4438	<i>Hydropotes inermis</i>	male	
NHM 8.11.14.9	<i>Hydropotes inermis</i>	female	
NHM 8.11.14.11	<i>Hydropotes inermis</i>	male	
NHM 2003.294	<i>Hydropotes inermis</i>	male	
UMZC H.15351	<i>Hydropotes inermis</i>	male	
ZSM 1982/159	<i>Mazama americana</i>	male	
ZSM 1925/919	<i>Mazama americana</i>	female	
ZMH 9462	<i>Mazama americana</i>	male	
ZMH 9460	<i>Mazama americana</i>	female	
NHM 8.6.24.5	<i>Mazama bricenii</i>	female	
NHM 1913.4.24.3	<i>Mazama bricenii</i>	male	
NHM 34.9.10.228	<i>Mazama cf. bricenii</i>	female	
NHM 67.1362	<i>Mazama chunyi</i>	male	
ZSM 1930/67	<i>Mazama gouazoubira</i>	male	
ZSM 1930/53	<i>Mazama gouazoubira</i>	female	
NMB 6672	<i>Mazama nemorivaga</i>	male	
ZSM 1927/41	<i>Mazama rufina</i>	male	
NHMW 528	<i>Mazama rufina</i>	male	photos only
NHM 71.3088	<i>Muntiacus atherodes</i>	male	
NHM 91.3.4.1	<i>Muntiacus crinifrons</i>	male	
NHM 32.11.1.171	<i>Muntiacus feae</i>	male	
NHM 24.1.6.2	<i>Muntiacus feae</i>	female	
ZSM 1966/206	<i>Muntiacus muntjak</i>	male	
ZSM 1969/100	<i>Muntiacus muntjak</i>	female	
ZSM 1966/237	<i>Muntiacus muntjak</i>	male	photos only; shed antlers
NHM 65.555	<i>Muntiacus muntjak</i>	female	
NHM 85.754	<i>Muntiacus muntjak</i>	male	
NHMW 3026	<i>Muntiacus muntjak</i>	female	photos only
ZMH 4919	<i>Muntiacus muntjak</i>	male	
NHMW 42296	<i>Muntiacus reevesi</i>	female	photos only
UMZC H.15531	<i>Muntiacus cf. reevesi</i>	male	photos only

Table B.1: Continued

UMZC H.15535	<i>Muntiacus reevesi</i>	male	
UMZC H.15536	<i>Muntiacus reevesi</i>	female	
UMZC H.15537	<i>Muntiacus reevesi</i>	male	measurements only
ZMH 8062	<i>Muntiacus reevesi</i>	male	
ZMH 6399	<i>Muntiacus reevesi</i>	female	
NHM 2010.462	<i>Muntiacus truongsongensis</i>	male	mandible
NHM 2010.459	<i>Muntiacus truongsongensis</i>	male	skull
NHM 2010.484	<i>Muntiacus vuquangensis</i>	male	
UMZC H.18641	<i>Odocoileus</i> cf. <i>hemionus</i>	male	
ZSM 1971/720	<i>Odocoileus hemionus</i>	male	
NHM 48.71.4.4	<i>Odocoileus hemionus</i>	female	
MNHN AE 722	<i>Odocoileus hemionus</i>	male	
MNHN AE 717	<i>Odocoileus hemionus</i>	female	
MNHN AE 714	<i>Odocoileus hemionus</i>	male	
MNHN AE 724	<i>Odocoileus hemionus</i>	male	photos only
UMZC H.18623	<i>Odocoileus hemionus</i>	female	photos only; subadult
UMZC H.18621	<i>Odocoileus hemionus</i>	male	
ZSM 1971/531	<i>Odocoileus virginianus</i>	male	
ZSM 1963/130	<i>Odocoileus virginianus</i>	female	
NHM 8.3.7.53	<i>Odocoileus virginianus</i>	female	
NHM 2.3.5.25	<i>Odocoileus virginianus</i>	male	
UMZC H.18448	<i>Odocoileus virginianus</i>	male	
UMZC H.18441	<i>Odocoileus virginianus</i>	male	
UMZC H.18483	<i>Odocoileus virginianus</i>	female	
ZSM 1980/244	<i>Ozotoceros bezoarticus</i>	female	
NHM 9.12.1.63	<i>Ozotoceros bezoarticus</i>	female	
NHM 14.11.9.1	<i>Ozotoceros bezoarticus</i>	male	
UMZC H.18781	<i>Ozotoceros bezoarticus</i>	male	
ZSM 1954/448	<i>Pudu puda</i>	male	
ZSM 1967/12	<i>Pudu puda</i>	female	
ZSM 1954/446	<i>Pudu puda</i>	female	
ZSM AM/1067	<i>Pudu puda</i>	male	
MNHN 2006 501	<i>Pudu puda</i>	male	
MNHN 2000 144	<i>Pudu puda</i>	female	incomplete skull
ZSM 1959/211	<i>Rangifer tarandus</i>	male	
ZSM 1951/296	<i>Rangifer tarandus</i>	male	
ZSM 1962/309	<i>Rangifer tarandus</i>	female	
UMZC no ID	<i>Rangifer tarandus</i>	male	

Table B.1: Continued

NHM 1884.4.14.2	<i>Rucervus duvaucelii</i>	female	
ZSM 1956/239	<i>Rucervus duvaucelii</i>	male	
ZSM 1954/269	<i>Rucervus duvaucelii</i>	male	
ZSM 1957/60	<i>Rucervus duvaucelii</i>	female	
ZMH 7492	<i>Rucervus eldii</i>	female	
ZSM 1905/3018	<i>Rucervus eldii</i>	male	
UMZC H.16191	<i>Rucervus eldii</i>	male	
UMZC H.16194	<i>Rucervus eldii</i>	female	
ZSM 1918/28	<i>Rucervus schomburgki</i>	male	skull, mounted
NHM 8.3.17.5	<i>Rucervus schomburgki</i>	male	mandible
NHM 59.4847	<i>Rucervus schomburgki</i>	male	skull
NHM 48.325	<i>Rucervus schomburgki</i>	male	skull
NHM 51.543	<i>Rucervus schomburgki</i>	male	skull
NHM 75.1393	<i>Rucervus schomburgki</i>	male	skull
NHMW 28793	<i>Rucervus schomburgki</i>	male	photos only; skull, mounted
NHM 79.3.20.1	<i>Rusa alfredi</i>	female	
NHM 86.183	<i>Rusa alfredi</i>	female	
ZMB 73526	<i>Rusa alfredi</i>	female	
ZMB 20395	<i>Rusa alfredi</i>	female	
NHM 940	<i>Rusa marianna</i>	?	mandible
NHM 655c	<i>Rusa marianna</i>	male	skull
ZMB 46575	<i>Rusa marianna</i>	female	
ZMB 75158	<i>Rusa marianna</i>	female	
ZSM 1972/439	<i>Rusa timorensis</i>	female	
NHM 97.4.3.2	<i>Rusa timorensis</i>	male	
NHM 2003.298	<i>Rusa timorensis</i>	female	
NHM 61.12.11.27	<i>Rusa timorensis</i>	male	photos only; subadult
NHM 2003.297	<i>Rusa timorensis</i>	female	
MNHN 1927 44	<i>Rusa timorensis</i>	male	
ZSM 1952/145	<i>Rusa unicolor</i>	female	
NHM 24.10.5.49	<i>Rusa unicolor</i>	male	skull
NHM 16.5.16.4	<i>Rusa unicolor</i>	female	
NHM 43.1.26.16	<i>Rusa unicolor</i>	male	
MNHN 1884 543	<i>Rusa unicolor</i>	male	
MNHN 1919 46	<i>Rusa unicolor</i>	female	
UMZC H.15911	<i>Rusa unicolor</i>	male	skull
UMZC H.20541	<i>Antilocapra americana</i>	?	
UMZC H.24741	<i>Boselaphus tragocamelus</i>	?	
NMB 2692	<i>Hyemoschus aquaticus</i>	female	
UMZC H.15315	<i>Moschus moschiferus</i>	male	
NMB 10917	<i>Okapia johnstoni</i>	male	
NMB 10817	<i>Okapia johnstoni</i>	female	
UMZC H.24922	<i>Tragelaphus scriptus</i>	?	

Table B.2: List of all investigated specimens of fossil cervids

Specimen ID	Species	Description	Epoch	Locality	Comments	Sources of figures in the literature
BMNH 34590	<i>Arvernoceros ardei</i>	antler fragment	Pliocene	Ardé, France		Heintz (1970), Pl. XIX, 4
MNHN PET 1020	<i>Arvernoceros ardei</i>	antler-pedicle fragment	Pliocene	Perrier, France	photos only	Heintz (1970), Pl. XX, 4a, b
MNHN PET 1024	<i>Arvernoceros ardei</i>	antler-pedicle fragment	Pliocene	Perrier, France	photos only	Heintz (1970), Pl. XVIII, 2
MNHN PET 1051	<i>Arvernoceros ardei</i>	antler-pedicle fragment	Pliocene	Perrier, France	photos only	Heintz (1970), Pl. XIX, 3a, b
MNHN PET 1054	<i>Arvernoceros ardei</i>	antler-pedicle fragment	Pliocene	Perrier, France	photos only	Heintz (1970), Pl. XX, 3a, b
MNHN PET 407	<i>Arvernoceros ardei</i>	P3-M3 dex	Pliocene	Perrier, France		Heintz (1970), Pl. XXIV, 3
MNHN PET 409	<i>Arvernoceros ardei</i>	2 Ms	Pliocene	Perrier, France		Heintz (1970), Pl. XXXIV, 4
MNHN PET 408	<i>Arvernoceros ardei</i>	M	Pliocene	Perrier, France		Heintz (1970), Pl. XXXIV, 5
MNHN PET 310	<i>Arvernoceros ardei</i>	P3-M3 sin & P3-M2 dex	Pliocene	Perrier, France		Heintz (1970), Pl. XVII, 4a, b
MNHN PET 1053	<i>Arvernoceros ardei</i>	skull fragment & pedicle & antlerbase	Pliocene	Perrier, France		Heintz (1970) Pl. XXXIII, 1 (as C. perrieri)
MNHN B5	<i>Arvernoceros ardei</i>	mandible fragment dex p2-m3	Pliocene	Perrier, France	in showcase	
NMB TL 65	<i>Axis lydekkeri</i>	antlers/skull fragment	Pleistocene	Trinil, Java, Indonesia	photos only	
RGM 1551	<i>Axis lydekkeri</i>	skull fragment & pedicle	Pleistocene	Trinil, Java, Indonesia		
RGM 1559	<i>Axis lydekkeri</i>	snout fragment, dentition	Pleistocene	Trinil, Java, Indonesia		
RGM 1961	<i>Axis lydekkeri</i>	skull fragment & pedicle & antler fragment	Pleistocene	Trinil, Java, Indonesia	photos only	
RGM 1642 & 1644	<i>Axis lydekkeri</i>	skull fragment	Pleistocene	Trinil, Java, Indonesia		
RGM 1957	<i>Axis lydekkeri</i>	mandible fragment dex p3-m3	Pleistocene	Trinil, Java, Indonesia	photos only	
RGM 667	<i>Axis lydekkeri</i>	mandible fragment dex p3-m1	Pleistocene	Trinil, Java, Indonesia	photos only	
RGM 13796	<i>Axis lydekkeri</i>	mandible fragment sin p3-m3	Pleistocene	Trinil, Java, Indonesia	photos only	
RGM 13795	<i>Axis lydekkeri</i>	mandible fragment sin p4-m3	Pleistocene	Trinil, Java, Indonesia	photos only	
RGM 2558	<i>Axis lydekkeri</i>	antler shed dex	Pleistocene	Trinil, Java, Indonesia		
RGM 2571	<i>Axis lydekkeri</i>	antler shed dex	Pleistocene	Trinil, Java, Indonesia		
RGM 2570	<i>Axis lydekkeri</i>	antler shed dex	Pleistocene	Trinil, Java, Indonesia		
RGM 11187	<i>Axis lydekkeri</i>	antler shed dex	Pleistocene	Trinil, Java, Indonesia		
RGM 2550	<i>Axis lydekkeri</i>	antler fragment sin	Pleistocene	Trinil, Java, Indonesia		
RGM 2551	<i>Axis lydekkeri</i>	antler fragment sin	Pleistocene	Trinil, Java, Indonesia		
RGM 11188	<i>Axis lydekkeri</i>	antler fragment sin	Pleistocene	Trinil, Java, Indonesia		
RGM 2538	<i>Axis lydekkeri</i>	antler fragment sin	Pleistocene	Trinil, Java, Indonesia		
RGM 1909 IV 3	<i>Axis lydekkeri</i>	skull	Pleistocene	Trinil, Java, Indonesia		
SNSB-BSPG 1909 IV 3b	<i>Axis lydekkeri</i>	skull & mandible	Pleistocene	Trinil, Java, Indonesia		
RGM 437811	<i>Candiacervus ropalophorus</i>	skull fragment, dentition	Pleistocene	Gerani 4, Crete, Greece		
RGM 437827	<i>Candiacervus ropalophorus</i>	skull fragment	Pleistocene	Gerani 4, Crete, Greece		
RGM 437854	<i>Candiacervus ropalophorus</i>	skull	Pleistocene	Gerani 4, Crete, Greece	holotype	deVos (1984) Pl. X
RGM 437825	<i>Candiacervus ropalophorus</i>	skull	Pleistocene	Gerani 4, Crete, Greece	juvenile; photos only	
RGM 437844	<i>Candiacervus ropalophorus</i>	skull fragment	Pleistocene	Gerani 4, Crete, Greece		
RGM 437848	<i>Candiacervus ropalophorus</i>	skull fragment	Pleistocene	Gerani 4, Crete, Greece		

Table B.2: Continued

RGM 437847	<i>Candiacervus ropalophorus</i>	skull	Pleistocene	Gerani 4, Crete, Geece	juvenile; photos only
RGM 437937	<i>Candiacervus ropalophorus</i>	mandible fragment sin p2-m3	Pleistocene	Gerani 4, Crete, Geece	photos only
RGM 437935	<i>Candiacervus ropalophorus</i>	mandible fragment	Pleistocene	Gerani 4, Crete, Geece	photos only
RGM 437938	<i>Candiacervus ropalophorus</i>	mandible fragment	Pleistocene	Gerani 4, Crete, Geece	photos only
RGM 437948	<i>Candiacervus ropalophorus</i>	mandible fragment sin p2-m3	Pleistocene	Gerani 4, Crete, Geece	photos only
RGM 438460	<i>Candiacervus ropalophorus</i>	antler fragment dex	Pleistocene	Gerani 4, Crete, Geece	photos only
RGM 437856	<i>Candiacervus ropalophorus</i>	skull	Pleistocene	Gerani 4, Crete, Geece	juvenile; photos only
RGM 437968	<i>Candiacervus ropalophorus</i>	mandible fragment sin p2-m3	Pleistocene	Gerani 4, Crete, Geece	
NMB Rss. 30	<i>Cervus australis</i>	mandible fragment sin p3-m3	Pliocene	Roussillon, France	
NMB M.P. 740	<i>Cervus australis</i>	skull fragment, pedicle, antler	Pliocene	Montpellier, France	
NMB M.P. 465	<i>Cervus australis</i>	mandible fragment dex p2-m3	Pliocene	Montpellier, France	
NMB M.P. 511	<i>Cervus australis</i>	mandible fragment dex p2-m3	Pliocene	Montpellier, France	
BMNH 34528	<i>'Cervus' perolensis</i>	antler fragment	Plio-/Pleistocene	Peyrolles, France	holotype
BMNH 34523	<i>'Cervus' perolensis</i>	antler fragment	Plio-/Pleistocene	Peyrolles, France	
BMNH 34484	<i>'Cervus' perolensis</i>	mandible fragment p2-m3	Plio-/Pleistocene	Peyrolles, France	
BMNH 34485	<i>'Cervus' perolensis</i>	mandible fragment p2-m3	Plio-/Pleistocene	Peyrolles, France	
BMNH 34486	<i>'Cervus' perolensis</i>	mandible fragment p2-m3	Plio-/Pleistocene	Peyrolles, France	
BMNH 34459	<i>'Cervus' perolensis</i>	P2-M3 sin	Plio-/Pleistocene	Peyrolles, France	
BMNH 34460	<i>'Cervus' perolensis</i>	P2-M3 dex	Plio-/Pleistocene	Peyrolles, France	
MNHN 1	<i>'Cervus' phillisi</i>	P4-M3 dex	Pleistocene	Senèze, France	
MNHN 26	<i>'Cervus' phillisi</i>	P4-M3 dex	Pleistocene	Senèze, France	
MNHN 1922-5	<i>'Cervus' phillisi</i>	skull on rock, full dentition, pedicle, antler base	Pleistocene	Senèze, France	
NMB St. V. 599	<i>'Cervus' phillisi</i>	mandible fragment sin p2-m3	Pleistocene	St. Vallier, France	
NMB St. V. 605	<i>'Cervus' phillisi</i>	mandible fragment sin p2-m3	Pleistocene	St. Vallier, France	
NMB St. V. 891	<i>'Cervus' phillisi</i>	mandible fragment dex p2-m3	Pleistocene	St. Vallier, France	
NMB St. V. 98	<i>'Cervus' phillisi</i>	P2-M3 dex	Pleistocene	St. Vallier, France	
NMB St. V. 576	<i>'Cervus' phillisi</i>	P3-M3 dex	Pleistocene	St. Vallier, France	
NMB St. V. 887	<i>'Cervus' phillisi</i>	skull fragment, occiput, pedicle, antlers	Pleistocene	St. Vallier, France	
NMB St. V. 900	<i>'Cervus' phillisi</i>	skull fragment	Pleistocene	St. Vallier, France	
NMB Se. 628	<i>'Cervus' phillisi</i>	skull fragment	Pleistocene	Senèze, France	juvenile; photos only
NMB Se. 435	<i>'Cervus' phillisi</i>	skull	Pleistocene	Senèze, France	
NMB Se. 437	<i>'Cervus' phillisi</i>	mandible fragment p2-m3	Pleistocene	Senèze, France	
NMB Se. 1043	<i>'Cervus' phillisi</i>	mandible fragment p2-m3	Pleistocene	Senèze, France	
NMB Se. 614	<i>'Cervus' phillisi</i>	mandible fragment dex p2-m3	Pleistocene	Senèze, France	
NMB Se. 1036	<i>'Cervus' phillisi</i>	dentition	Pleistocene	Senèze, France	
NMB Se. 1043	<i>'Cervus' phillisi</i>	mandible fragment p2-m2	Pleistocene	Senèze, France	
NMB Se. 445	<i>'Cervus' phillisi</i>	dentition	Pleistocene	Senèze, France	
NMB Se. 1848	<i>'Cervus' phillisi</i>	i, c	Pleistocene	Senèze, France	
NMB Se. 1022	<i>'Cervus' phillisi</i>	mandible fragment p2-m3, i, c	Pleistocene	Senèze, France	
NMB Se. 1845	<i>'Cervus' phillisi</i>	maxilla P2-M3, mandibles	Pleistocene	Senèze, France	
NMB Se. 213	<i>'Cervus' phillisi</i>	skull fragments	Pleistocene	Senèze, France	photos only
BMNH 41834d	<i>'Cervus' sivalensis</i>	antler fragment	Pleistocene	Siwalik Hills, India	
BMNH 41834a	<i>'Cervus' sivalensis</i>	antler fragment	Pleistocene	Siwalik Hills, India	
BMNH M 2307	<i>'Cervus' sivalensis</i>	antler fragment	Pleistocene	Siwalik Hills, India	
BMNH 41834	<i>'Cervus' sivalensis</i>	skull fragment	Pleistocene	Siwalik Hills, India	
BMNH M 2310	<i>'Cervus' sivalensis</i>	maxilla fragment, Ms	Pleistocene	Siwalik Hills, India	
BMNH 48440	<i>'Cervus' sivalensis</i>	antler fragment	Pleistocene	Siwalik Hills, India	holotype
BMNH 41834	<i>'Cervus' sivalensis</i>	antler fragment	Pleistocene	Siwalik Hills, India	

Table B.2: Continued

BMNH M 2308	' <i>Cervus</i> ' <i>stivalensis</i>	antler fragment	Pleistocene	Siwalik Hills, India	Heintz (1970), Pl. III, 5
BMNH 41834b	' <i>Cervus</i> ' <i>stivalensis</i>	antler base	Pleistocene	Siwalik Hills, India	
BMNH 27680	' <i>Cervus</i> ' <i>stivalensis</i>	occiput	Pleistocene	Siwalik Hills, India	
BMNH M 2309	' <i>Cervus</i> ' <i>stivalensis</i>	antler base	Pleistocene	Siwalik Hills, India	
BMNH 17468	' <i>Cervus</i> ' <i>stivalensis</i>	skull fragment (snout)	Pleistocene	Siwalik Hills, India	
BMNH 39570	' <i>Cervus</i> ' <i>stivalensis</i>	skull fragment & dentition	Pleistocene	Siwalik Hills, India	
BMNH M 16667	' <i>Cervus</i> ' <i>stivalensis</i>	mandible fragment m2-m3	Pleistocene	Siwalik Hills, India	
BMNH 34607	<i>Croizetoceros ramosus</i>	antler fragment	Pleistocene	Ardé, France	
BMNH 34608	<i>Croizetoceros ramosus</i>	left mandible fragment wt p2-m3	Pleistocene	Ardé, France	
MNCN 47192	<i>Croizetoceros ramosus</i>	antler fragment	Plio-/Pleistocene	Villaroya, Spain	photos only
MNCN 47193	<i>Croizetoceros ramosus</i>	antler fragment	Plio-/Pleistocene	Villaroya, Spain	photos only
MNCN 50430	<i>Croizetoceros ramosus</i>	dentition	Plio-/Pleistocene	La Puebla De Valverde, Spain	no photos
MNCN 50431	<i>Croizetoceros ramosus</i>	dentition	Plio-/Pleistocene	La Puebla De Valverde, Spain	photos only
MNCN 50432	<i>Croizetoceros ramosus</i>	mandible fragment sin m2-m3	Plio-/Pleistocene	La Puebla De Valverde, Spain	no photos
MNCN 50433	<i>Croizetoceros ramosus</i>	mandible fragment dex p2-m3	Plio-/Pleistocene	La Puebla De Valverde, Spain	no photos
MNCN 50434	<i>Croizetoceros ramosus</i>	dentition	Plio-/Pleistocene	La Puebla De Valverde, Spain	photos only
MNCN 50435	<i>Croizetoceros ramosus</i>	dentition	Plio-/Pleistocene	La Puebla De Valverde, Spain	photos only
MNCN 54685	<i>Croizetoceros ramosus</i>	i1 sin	Plio-/Pleistocene	La Puebla De Valverde, Spain	photos only
MNCN 54686	<i>Croizetoceros ramosus</i>	i2/3	Plio-/Pleistocene	La Puebla De Valverde, Spain	photos only
MNCN 54882	<i>Croizetoceros ramosus</i>	antler fragment	Plio-/Pleistocene	La Puebla De Valverde, Spain	photos only
MNCN 66515	<i>Croizetoceros ramosus</i>	antler fragment	Plio-/Pleistocene	Villaroya, Spain	photos only
MNCN 66516	<i>Croizetoceros ramosus</i>	antler fragment	Plio-/Pleistocene	Villaroya, Spain	photos only
MNCN 55004	<i>Croizetoceros ramosus</i>	frontal, pedicle, antler fragment	Plio-/Pleistocene	La Puebla De Valverde, Spain	photos only
MNHN no nr	<i>Croizetoceros ramosus</i>	mandible fragment sin p2-m3	Plio-/Pleistocene	Perrier, France	photos only
MNHN PET 328	<i>Croizetoceros ramosus</i>	mandible fragment dex p2-p3	Plio-/Pleistocene	Perrier, France	photos only
MNHN PET 1002	<i>Croizetoceros ramosus</i>	antler fragment	Plio-/Pleistocene	Perrier, France	photos only
MNHN PET 982	<i>Croizetoceros ramosus</i>	antler fragment	Plio-/Pleistocene	Perrier, France	photos only
MNHN PET 977	<i>Croizetoceros ramosus</i>	antler fragment	Plio-/Pleistocene	Perrier, France	photos only
MNHN PET 986	<i>Croizetoceros ramosus</i>	front pedicle antler fragment	Plio-/Pleistocene	Perrier, France	photos only
MNHN PET 987	<i>Croizetoceros ramosus</i>	front pedicle antler fragment	Plio-/Pleistocene	Perrier, France	photos only
MNHN PET 988	<i>Croizetoceros ramosus</i>	front pedicle antler fragment	Plio-/Pleistocene	Perrier, France	photos only
MNHN PET 985	<i>Croizetoceros ramosus</i>	front pedicle antler fragment	Plio-/Pleistocene	Perrier, France	photos only
MNHN 1923 4	<i>Croizetoceros ramosus</i>	fragment skull roof, pedicle, antlers	Plio-/Pleistocene	Senèze, France	photos only
MNHN no nr [5]	<i>Croizetoceros ramosus</i>	antlers	Plio-/Pleistocene	Perrier, France	in showcase no. 95; neotype
NMB St. V. 496	<i>Croizetoceros ramosus</i>	mandible fragment sin p2-m3	Plio-/Pleistocene	St. Vallier, France	

Table B.2: Continued

NMB St. V. 494	<i>Croizetoceros ramosus</i>	mandible fragment dex p2-m3	Plio-/Pleistocene	St. Vallier, France	
NMB St. V. 164	<i>Croizetoceros ramosus</i>	maxilla dex P2-M2	Plio-/Pleistocene	St. Vallier, France	
NMB St. V. 480	<i>Croizetoceros ramosus</i>	maxilla dex P4-M3	Plio-/Pleistocene	St. Vallier, France	photos only
NMB Pr. 341	<i>Croizetoceros ramosus</i>	skull fragment, pedicle, antler	Plio-/Pleistocene	Perrier, France	photos only
NMB St. V. 496	<i>Croizetoceros ramosus</i>	skull fragment, pedicle, antler	Plio-/Pleistocene	St. Vallier, France	photos only
BMNH M 4477	<i>Dicrocerus elegans</i>	antler & pedicle fragments	Miocene	Sausan, France	photos only
MNHN Sa 140	<i>Dicrocerus elegans</i>	compressed skull fragments	Miocene	Sausan, France	photos only
MNHN Sa 3379	<i>Dicrocerus elegans</i>	skull roof, occiput, pedicle bases	Miocene	Sausan, France	
MNHN Sa 1098	<i>Dicrocerus elegans</i>	mandible fragment dex, complete dentition	Miocene	Sausan, France	
MNHN Sa 9929	<i>Dicrocerus elegans</i>	mandible fragment dex, complete dentition	Miocene	Sausan, France	
MNHN Sa 2990	<i>Dicrocerus elegans</i>	upper dentition	Miocene	Sausan, France	
MNHN Sa 2999	<i>Dicrocerus elegans</i>	upper dentition	Miocene	Sausan, France	
MNHN Sa 3040	<i>Dicrocerus elegans</i>	upper dentition	Miocene	Sausan, France	
MNHN Sa 3092	<i>Dicrocerus elegans</i>	upper dentition	Miocene	Sausan, France	
MNHN Sa 3047	<i>Dicrocerus elegans</i>	upper dentition	Miocene	Sausan, France	
MNHN Sa 2987	<i>Dicrocerus elegans</i>	upper dentition	Miocene	Sausan, France	
MNHN Sa 10343	<i>Dicrocerus elegans</i>	upper dentition	Miocene	Sausan, France	
MNHN Sa 3003	<i>Dicrocerus elegans</i>	upper dentition	Miocene	Sausan, France	
MNHN Sa 3008	<i>Dicrocerus elegans</i>	upper dentition	Miocene	Sausan, France	
MNHN Sa 3009	<i>Dicrocerus elegans</i>	skull fragment	Miocene	Sausan, France	
MNHN Sa 3010	<i>Dicrocerus elegans</i>	C	Miocene	Sausan, France	
MNHN Sa 3015	<i>Dicrocerus elegans</i>	C	Miocene	Sausan, France	
MNHN Sa 3050	<i>Dicrocerus elegans</i>	P2-M3 dex	Miocene	Sausan, France	
MNHN Sa 3049	<i>Dicrocerus elegans</i>	upper dentition	Miocene	Sausan, France	
MNHN Sa 10138	<i>Dicrocerus elegans</i>	mandible fragment dex p2-m3	Miocene	Sausan, France	
MNHN Sa 3125	<i>Dicrocerus elegans</i>	mandible fragment sin p2-m3	Miocene	Sausan, France	
MNHN Sa 3161	<i>Dicrocerus elegans</i>	skull fragment, M3 dex, pedicle base	Miocene	Sausan, France	
MNHN Sa 3163	<i>Dicrocerus elegans</i>	skull fragment, P2-M3 dex, M2-M3 sin	Miocene	Sausan, France	damaged
MNHN Sa 3329	<i>Dicrocerus elegans</i>	antler fragment	Miocene	Sausan, France	Azanza et al. (2011) Fig. 2
MNHN Sa 3323	<i>Dicrocerus elegans</i>	antler fragment	Miocene	Sausan, France	
MNHN Sa 3486	<i>Dicrocerus elegans</i>	antler fragment	Miocene	Sausan, France	Azanza et al. (2011) Fig. 2
MNHN Sa 3456	<i>Dicrocerus elegans</i>	antler fragment	Miocene	Sausan, France	Azanza et al. (2011) Fig. 2
MNHN Sa 3552	<i>Dicrocerus elegans</i>	antler fragment	Miocene	Sausan, France	Azanza et al. (2011) Fig. 2
MNHN Sa 9995	<i>Dicrocerus elegans</i>	antler fragment	Miocene	Sausan, France	Azanza et al. (2011) Fig. 2
MNHN Sa 3326	<i>Dicrocerus elegans</i>	antler fragment	Miocene	Sausan, France	Azanza et al. (2011) Fig. 2
MNHN Sa 3327	<i>Dicrocerus elegans</i>	shed antler fragment	Miocene	Sausan, France	
MNHN Sa 10563	<i>Dicrocerus elegans</i>	shed antler fragment	Miocene	Sausan, France	
MNHN Sa 10353	<i>Dicrocerus elegans</i>	shed antler fragment	Miocene	Sausan, France	
MNHN Sa 3345	<i>Dicrocerus elegans</i>	antler fragment	Miocene	Sausan, France	
MNHN Sa 3364	<i>Dicrocerus elegans</i>	antler fragment	Miocene	Sausan, France	
MNHN Sa 3322	<i>Dicrocerus elegans</i>	antler fragment	Miocene	Sausan, France	
MNHN Sa 10338	<i>Dicrocerus elegans</i>	antler fragment	Miocene	Sausan, France	
MNHN Sa 3320	<i>Dicrocerus elegans</i>	antler fragment	Miocene	Sausan, France	Azanza et al. (2011) Fig. 2
MNHN Sa 3363	<i>Dicrocerus elegans</i>	shed antler fragment	Miocene	Sausan, France	Azanza et al. (2011) Fig. 2

Table B.2: Continued

MNHN Sa 3346	<i>Dicrocerus elegans</i>	antler fragment	Miocene	Sausan, France	photos only	Azanza et al. (2011) Fig. 2
MNHN Sa 3392	<i>Dicrocerus elegans</i>	antler fragment	Miocene	Sausan, France	photos only	
MNHN Sa 3395	<i>Dicrocerus elegans</i>	antler fragment	Miocene	Sausan, France	photos only	Azanza et al. (2011) Fig. 2
MNHN Sa 3382	<i>Dicrocerus elegans</i>	antler fragment	Miocene	Sausan, France	photos only	
MNHN Sa 3494	<i>Dicrocerus elegans</i>	antler fragment	Miocene	Sausan, France	photos only	Azanza et al. (2011) Fig. 2
MNHN Sa 3481	<i>Dicrocerus elegans</i>	antler fragment	Miocene	Sausan, France	photos only	
MNHN Sa 3513	<i>Dicrocerus elegans</i>	antler fragment	Miocene	Sausan, France	photos only	Azanza et al. (2011) Fig. 2
MNHN Sa 11433	<i>Dicrocerus elegans</i>	antler fragment	Miocene	Sausan, France	photos only	
MNHN Sa 3476	<i>Dicrocerus elegans</i>	antler fragment	Miocene	Sausan, France	photos only	Azanza et al. (2011) Fig. 2
MNHN Sa 3374	<i>Dicrocerus elegans</i>	skull fragment	Miocene	Sausan, France	photos only	
MNHN Sa 3425	<i>Dicrocerus elegans</i>	antler fragment	Miocene	Sausan, France	photos only	Azanza et al. (2011) Fig. 2
MNHN Sa 3560	<i>Dicrocerus elegans</i>	antler fragment	Miocene	Sausan, France	photos only	
MNHN Sa 3505	<i>Dicrocerus elegans</i>	antler fragment	Miocene	Sausan, France	photos only	Azanza et al. (2011) Fig. 2
MNHN Sa 3483	<i>Dicrocerus elegans</i>	antler fragment	Miocene	Sausan, France	photos only	
MNHN Sa 3507	<i>Dicrocerus elegans</i>	antler fragment	Miocene	Sausan, France	photos only	Azanza et al. (2011) Fig. 2
MNHN Sa 9996	<i>Dicrocerus elegans</i>	antler fragment	Miocene	Sausan, France	photos only	
MNHN Sa 3366	<i>Dicrocerus elegans</i>	antler fragment	Miocene	Sausan, France	photos only	Azanza et al. (2011) Fig. 2
MNHN Sa 3396	<i>Dicrocerus elegans</i>	antler fragment	Miocene	Sausan, France	photos only	
MNHN Sa 3393	<i>Dicrocerus elegans</i>	antler fragment	Miocene	Sausan, France	photos only	Azanza et al. (2011) Fig. 2
MNHN Sa 9990d	<i>Dicrocerus elegans</i>	antler fragment	Miocene	Sausan, France	photos only	
MNHN Sa 3499	<i>Dicrocerus elegans</i>	antler fragment	Miocene	Sausan, France	photos only	Azanza et al. (2011) Fig. 2
MNHN Sa 3398	<i>Dicrocerus elegans</i>	antler fragment	Miocene	Sausan, France	photos only	
MNHN Sa 2003	<i>Dicrocerus elegans</i>	antler fragment	Miocene	Sausan, France	photos only	Azanza et al. (2011) Fig. 2
MNHN Sa 3531	<i>Dicrocerus elegans</i>	antler fragment	Miocene	Sausan, France	photos only	
MNHN Sa 11461	<i>Dicrocerus elegans</i>	skull fragment, pedicle, antler	Miocene	Sausan, France	photos only	Azanza et al. (2011) Fig. 2
MNHN Sa 11434	<i>Dicrocerus elegans</i>	skull fragment, pedicle, antler	Miocene	Sausan, France	photos only	
MNHN Sa 3567	<i>Dicrocerus elegans</i>	dentition	Miocene	Sausan, France	photos only	Azanza et al. (2011) Fig. 2
MNHN Sa 9956	<i>Dicrocerus elegans</i>	petrosium	Miocene	Sausan, France	photos only	
MNHN Sa 9957	<i>Dicrocerus elegans</i>	petrosium	Miocene	Sausan, France	photos only	Azanza et al. (2011) Fig. 2
MNHN Sa 10193	<i>Dicrocerus elegans</i>	petrosium	Miocene	Sausan, France	photos only	
MNHN Sa 9801	<i>Dicrocerus elegans</i>	petrosium	Miocene	Sausan, France	photos only	Azanza et al. (2011) Fig. 2
MNHN Sa 10191	<i>Dicrocerus elegans</i>	petrosium	Miocene	Sausan, France	photos only	
MNHN Sa 9952	<i>Dicrocerus elegans</i>	petrosium	Miocene	Sausan, France	photos only	Azanza et al. (2011) Fig. 2
MNHN Sa 9954	<i>Dicrocerus elegans</i>	petrosium	Miocene	Sausan, France	photos only	
MNHN Sa 9911	<i>Dicrocerus elegans</i>	petrosium	Miocene	Sausan, France	photos only	Azanza et al. (2011) Fig. 2
MNHN Sa 9953	<i>Dicrocerus elegans</i>	petrosium	Miocene	Sausan, France	photos only	
MNHN Sa 10679	<i>Dicrocerus elegans</i>	occiput & basioccipital	Miocene	Sausan, France	photos only	Azanza et al. (2011) Fig. 2
MNHN Sa 10308	<i>Dicrocerus elegans</i>	skull roof	Miocene	Sausan, France	photos only	
MNHN Sa 9990a	<i>Dicrocerus elegans</i>	upper dentition dex	Miocene	Sausan, France	photos only	Azanza et al. (2011) Fig. 2
MNHN Sa 10307 i-1 [4]	<i>Dicrocerus elegans</i>	incisors & ?canines	Miocene	Sausan, France	photos only	
MNHN Sa 15643	<i>Dicrocerus elegans</i>	mandible fragment dex deciduous dentition	Miocene	Sausan, France	photos only	Azanza et al. (2011) Fig. 2
SNSB-BSPG 1987 V 333	<i>Dicrocerus elegans</i>	antler fragment shed	Miocene	Sausan, France	photos only	
MNHN 1922-3	<i>Eucladoceros ctenoides</i>	P3-M3 dex	Plio-/Pleistocene	Senèze, France	photos only	Heintz (1970), Pl XI, 1, Pl XII
MNHN no nr.	<i>Eucladoceros ctenoides</i>	P2-M3 sin	Plio-/Pleistocene	Senèze, France	photos only	
MNHN no nr.	<i>Eucladoceros ctenoides</i>	P2-M3 dex	Plio-/Pleistocene	Senèze, France	photos only	Heintz (1970), Pl XI, 1, Pl XII
MNHN 17	<i>Eucladoceros ctenoides</i>	skull & mandible & antlers	Plio-/Pleistocene	Senèze, France	photos only	
MNHN 1922-3	<i>Eucladoceros ctenoides</i>	skull fragment & dentition	Plio-/Pleistocene	Senèze, France	photos only	Heintz (1970), Pl XI, 1, Pl XII
MNHN 1922-5	<i>Eucladoceros ctenoides</i>	compressed skull fragment & deciduous dentition	Plio-/Pleistocene	Senèze, France	photos only	
NMB Se. 566	<i>Eucladoceros ctenoides</i>	antlers/skull fragment	Plio-/Pleistocene	Senèze, France	photos only	Heintz (1970), Pl XI, 1, Pl XII
					photos only	

Table B.2: Continued

NMB Se. 1016	<i>Eucladoceros ctenoides</i>	skull fragment, pedicle, antler	Plio-/Pleistocene	Senèze, France	
NMB Se. 569	<i>Eucladoceros ctenoides</i>	skull fragment, dentition	Plio-/Pleistocene	Senèze, France	
NMB Se. 1803	<i>Eucladoceros ctenoides</i>	skull fragment	Plio-/Pleistocene	Senèze, France	
NMB Se. 1798	<i>Eucladoceros ctenoides</i>	mandible fragment, skull fragment & dentition	Plio-/Pleistocene	Senèze, France	
NMB Se. 1797	<i>Eucladoceros ctenoides</i>	mandible fragment sin p2-m3	Plio-/Pleistocene	Senèze, France	
NMB V.A. 829	<i>Eucladoceros ctenoides</i>	skull fragment, dentition	Plio-/Pleistocene	Val d'Arno, Italy	
NMB V.A. 557	<i>Eucladoceros ctenoides</i>	skull fragment, dentition	Plio-/Pleistocene	Val d'Arno, Italy	
NMB V.A. 1865	<i>Eucladoceros ctenoides</i>	mandible fragment sin p2-m3	Plio-/Pleistocene	Val d'Arno, Italy	
NMB V.A. 555	<i>Eucladoceros ctenoides</i>	antler fragment	Plio-/Pleistocene	Tegelen, Netherlands	
RGM 53230	<i>Eucladoceros ctenoides</i>	mandible dp2, dp4-m1 sin	Plio-/Pleistocene	Tegelen, Netherlands	photos only
RGM 86834	<i>Eucladoceros tegulensis</i>	antler fragment sin	Pleistocene	Tegelen, Netherlands	<i>tegulensis</i> is synonymised with <i>ctenoides</i>
RGM 79043	<i>Eucladoceros tegulensis</i>	mandible fragment sin p2-p4	Pleistocene	Tegelen, Netherlands	<i>tegulensis</i> is synonymised with <i>ctenoides</i>
RGM 53108	<i>Eucladoceros tegulensis</i>	il sin	Pleistocene	Tegelen, Netherlands	<i>ctenoides</i>
RGM 65963	<i>Eucladoceros tegulensis</i>	antler fragment	Pleistocene	Tegelen, Netherlands	<i>tegulensis</i> is synonymised with <i>ctenoides</i>
BMNH 34408	<i>Eucladoceros tetraceros</i>	antler fragment	Plio-/Pleistocene	Peyrolles, France	<i>ctenoides</i>
BMNH 34406	<i>Eucladoceros tetraceros</i>	antler fragment	Plio-/Pleistocene	Peyrolles, France	<i>tetraceros</i> is synonymised with <i>ctenoides</i>
BMNH 34407	<i>Eucladoceros tetraceros</i>	antler fragment	Plio-/Pleistocene	Peyrolles, France	<i>ctenoides</i>
BMNH 34407a	<i>Eucladoceros tetraceros</i>	antler fragment	Plio-/Pleistocene	Peyrolles, France	<i>tetraceros</i> is synonymised with <i>ctenoides</i>
BMNH 34409	<i>Eucladoceros tetraceros</i>	antler fragment	Plio-/Pleistocene	Peyrolles, France	<i>ctenoides</i>
BMNH 34408	<i>Eucladoceros tetraceros</i>	antler fragment	Plio-/Pleistocene	Peyrolles, France	<i>tetraceros</i> is synonymised with <i>ctenoides</i>
BMNH 34405	<i>Eucladoceros tetraceros</i>	antler fragment	Plio-/Pleistocene	Peyrolles, France	<i>ctenoides</i>
BMNH 34408a	<i>Eucladoceros tetraceros</i>	antler fragment	Plio-/Pleistocene	Peyrolles, France	<i>tetraceros</i> is synonymised with <i>ctenoides</i>
BMNH no nr.	<i>Eucladoceros tetraceros</i>	antler fragment	Plio-/Pleistocene	Peyrolles, France	<i>ctenoides</i>
BMNH 34425	<i>Eucladoceros tetraceros</i>	mandible fragment p2-m3	Plio-/Pleistocene	Peyrolles, France	<i>tetraceros</i> is synonymised with <i>ctenoides</i>

Table B.2: Continued

BMNH 34426	<i>Eucladoceros tetraceros</i>	mandible fragment p3-m3	Plio-/Pleistocene	Peyrolles, France	<i>tetraceros</i> is syn-onymised with <i>clenoides</i>
BMNH 34427	<i>Eucladoceros tetraceros</i>	mandible fragment p3-m3	Plio-/Pleistocene	Peyrolles, France	<i>tetraceros</i> is syn-onymised with <i>clenoides</i>
BMNH M6369	<i>Eucladoceros tetraceros</i>	antler fragment	Plio-/Pleistocene	East Runton, UK	<i>tetraceros</i> is syn-onymised with <i>clenoides</i>
BMNH M6370	<i>Eucladoceros tetraceros</i>	antler fragment	Plio-/Pleistocene	East Runton, UK	<i>tetraceros</i> is syn-onymised with <i>clenoides</i>
BMNH no nr.	<i>Eucladoceros tetraceros</i>	antler fragment	Plio-/Pleistocene	Peyrolles, France	<i>tetraceros</i> is syn-onymised with <i>clenoides</i>
BMNH 37358	<i>Euproz furcatus</i>	antler & pedicle fragments	Miocene	Steinheim, Germany	cast
NMB Sth. 223	<i>Euproz furcatus</i>	mandible fragment p2-m3	Miocene	Steinheim, Germany	
NMB Sth. 1345	<i>Euproz furcatus</i>	pedicle antler fragment	Miocene	Steinheim, Germany	
NMB Sth. 1346	<i>Euproz furcatus</i>	pedicle antler fragment	Miocene	Steinheim, Germany	
NMB Sth. 658	<i>Euproz furcatus</i>	antler fragment	Miocene	Steinheim, Germany	
NMB Sth. 260	<i>Euproz furcatus</i>	antler fragment	Miocene	Steinheim, Germany	
SMNS 4768	<i>Euproz furcatus</i>	antler & pedicle fragment	Miocene	Steinheim, Germany	
SMNS 44208	<i>Euproz furcatus</i>	antler & pedicle fragment	Miocene	Steinheim, Germany	
SNBS-BSPG 1962 XII 12	<i>Euproz furcatus</i>	mandible fragment dex p2-m3	Miocene	Friedberg, Germany	
SNBS-BSPG 1964 XXIV 234	<i>Euproz furcatus</i>	mandible fragment dex P3-M3	Miocene	Steinheim, Germany	
SNBS-BSPG 1966 XIV 34	<i>Euproz furcatus</i>	antler fragment shed	Miocene	Breitenbrunn, Germany	
MNHN Sa 3317	<i>Heteroproz larteti</i>	antler-pedicle fragment	Miocene	Pontlevoy, France	photos only; holotype
MNHN Sa 3399	<i>Heteroproz larteti</i>	antler, pedicle, skull fragment, dentition	Miocene	Sansan, France	Filhol (1891) Pl. XXXVII, Fig. 5; Ginsburg & Crouzel (1976) Fig. 9
NMB Sth. 1343	<i>Heteroproz larteti</i>	antler fragment	Miocene	Steinheim, Germany	<i>?Euproz furcatus</i>
NMB Sth. 695	<i>Heteroproz larteti</i>	antler fragment	Miocene	Steinheim, Germany	<i>?Euproz furcatus</i>
NMB Sth. 696	<i>Heteroproz larteti</i>	antler fragment	Miocene	Steinheim, Germany	<i>?Euproz furcatus</i>
SMNS 47709	<i>Heteroproz larteti</i>	skull fragment, antlers, M	Miocene	Steinheim, Germany	
SMNS 47708	<i>Heteroproz larteti</i>	skull fragment, antlers	Miocene	Steinheim, Germany	
SMNS 47707	<i>Heteroproz larteti</i>	skull dentition dex	Miocene	Steinheim, Germany	
SMNS 47706	<i>Heteroproz larteti</i>	skull fragment, pedicles, dentition	Miocene	Steinheim, Germany	
SMNS 47705	<i>Heteroproz larteti</i>	antler & pedicle fragment	Miocene	Steinheim, Germany	photos only
SMNS 44207	<i>Heteroproz larteti</i>	antler fragment	Miocene	Steinheim, Germany	photos only
SMNS 40178	<i>Heteroproz larteti</i>	antler & pedicle fragment	Miocene	Steinheim, Germany	photos only
SMNS 42853	<i>Heteroproz larteti</i>	occiput fragment, petrosal, antlers	Miocene	Steinheim, Germany	
SMNS 43320	<i>Heteroproz larteti</i>	skull, dentition	Miocene	Steinheim, Germany	
SNBS-BSPG AS I 933	<i>Heteroproz larteti</i>	antler fragment shed	Miocene	Häder, Germany	
SNBS-BSPG 1881 IX 654	<i>Heteroproz larteti</i>	antler fragment shed	Miocene	Reisenburg, Germany	
SNBS-BSPG AS I 934	<i>Heteroproz larteti</i>	antler fragment shed	Miocene	Häder, Germany	
SNBS-BSPG 1972 XVI 321	<i>Heteroproz larteti</i>	mandible fragment sin p4-m3	Miocene	Kleisenbach, Germany	
SNBS-BSPG 1959 II 5258	<i>Heteroproz larteti</i>	antler fragment shed	Miocene	Sandelzhausen, Germany	

Table B.2: Continued

SNSB-BSPG 1959 II 5268	<i>Heteroproz larteti</i>	antler fragment shed	Miocene	Sandelzhausen, Germany	Rössner (2010)
SNSB-BSPG 1987 V 262	<i>Heteroproz larteti</i>	antler fragment shed	Miocene	Elkekirchen, Germany	Rössner (2010)
SNSB-BSPG 1881 IX 55	<i>Heteroproz larteti</i>	antler fragment shed	Miocene	Reisensburg, Germany	Rössner (2010)
SNSB-BSPG 1959 II 7814	<i>Lagomeryx parvulus</i>	p2 sin	Miocene	Sandelzhausen, Germany	Rössner (2010)
SNSB-BSPG 1959 II 3952	<i>Lagomeryx parvulus</i>	p2 sin	Miocene	Sandelzhausen, Germany	Rössner (2010)
SNSB-BSPG 1959 II 4323	<i>Lagomeryx parvulus</i>	p1 dex	Miocene	Sandelzhausen, Germany	Rössner (2010)
SNSB-BSPG 1959 II 5152	<i>Lagomeryx parvulus</i>	p1 dex	Miocene	Sandelzhausen, Germany	Rössner (2010)
SNSB-BSPG 1959 II 4305	<i>Lagomeryx parvulus</i>	p3 sin	Miocene	Sandelzhausen, Germany	Rössner (2010)
SNSB-BSPG 1959 II 4006	<i>Lagomeryx parvulus</i>	p3 sin	Miocene	Sandelzhausen, Germany	Rössner (2010)
SNSB-BSPG 1959 II 4611	<i>Lagomeryx parvulus</i>	p4 sin	Miocene	Sandelzhausen, Germany	Rössner (2010)
SNSB-BSPG 1959 II 10782	<i>Lagomeryx parvulus</i>	m1 dex	Miocene	Sandelzhausen, Germany	Rössner (2010)
SNSB-BSPG 1959 II 6614	<i>Lagomeryx parvulus</i>	m1-m2 sin	Miocene	Sandelzhausen, Germany	Rössner (2010)
SNSB-BSPG 1959 II 4312	<i>Lagomeryx parvulus</i>	m2-m3 sin	Miocene	Sandelzhausen, Germany	Rössner (2010)
SNSB-BSPG 1959 II 6610	<i>Lagomeryx parvulus</i>	m3 dex	Miocene	Sandelzhausen, Germany	Rössner (2010)
SNSB-BSPG 1959 II 4302	<i>Lagomeryx parvulus</i>	m3 sin	Miocene	Sandelzhausen, Germany	Rössner (2010)
SNSB-BSPG 1959 II 6603	<i>Lagomeryx parvulus</i>	C	Miocene	Sandelzhausen, Germany	Rössner (2010)
SNSB-BSPG 1959 II 3954	<i>Lagomeryx parvulus</i>	P2 dex	Miocene	Sandelzhausen, Germany	Rössner (2010)
SNSB-BSPG 1959 II 4604	<i>Lagomeryx parvulus</i>	P2 sin	Miocene	Sandelzhausen, Germany	Rössner (2010)
SNSB-BSPG 1959 II 4012	<i>Lagomeryx parvulus</i>	P3 dex	Miocene	Sandelzhausen, Germany	Rössner (2010)
SNSB-BSPG 1959 II 3973	<i>Lagomeryx parvulus</i>	P3 dex	Miocene	Sandelzhausen, Germany	Rössner (2010)
SNSB-BSPG 1959 II 5370	<i>Lagomeryx parvulus</i>	P4 dex	Miocene	Sandelzhausen, Germany	Rössner (2010)
SNSB-BSPG 1959 II 3953	<i>Lagomeryx parvulus</i>	P4 sin	Miocene	Sandelzhausen, Germany	Rössner (2010)
SNSB-BSPG 1959 II 4073	<i>Lagomeryx parvulus</i>	P4 dex	Miocene	Sandelzhausen, Germany	Rössner (2010)
SNSB-BSPG 1959 II 8991	<i>Lagomeryx parvulus</i>	M1 sin	Miocene	Sandelzhausen, Germany	Rössner (2010)
SNSB-BSPG 1959 II 3974	<i>Lagomeryx parvulus</i>	M1 dex	Miocene	Sandelzhausen, Germany	Rössner (2010)
SNSB-BSPG 1959 II 12308	<i>Lagomeryx parvulus</i>	M2 sin	Miocene	Sandelzhausen, Germany	Rössner (2010)
SNSB-BSPG 1959 II 3851	<i>Lagomeryx parvulus</i>	M2 sin	Miocene	Sandelzhausen, Germany	Rössner (2010)
SNSB-BSPG 1959 II 10783	<i>Lagomeryx parvulus</i>	M3 dex	Miocene	Sandelzhausen, Germany	Rössner (2010)
SNSB-BSPG 1959 II 4089	<i>Lagomeryx parvulus</i>	M3 sin	Miocene	Sandelzhausen, Germany	Rössner (2010)
SNSB-BSPG 1959 II 4313	<i>Lagomeryx parvulus</i>	M1-M3 dex	Miocene	Sandelzhausen, Germany	Rössner (2010)
SNSB-BSPG 1959 II 7803	<i>Lagomeryx parvulus</i>	antler fragment shed	Miocene	Sandelzhausen, Germany	Rössner (2010)
MNHN FS 223	<i>Ligeromeryx praestans</i>	mandible fragment m1-m2	Miocene	Pontigné, France	Azanza & Ginsburg (1997) Pl. 1, 9
MNHN FS 754	<i>Ligeromeryx praestans</i>	p3-p4 sin	Miocene	Pontigné, France	Azanza & Ginsburg (1997) Textfig. 4 C-E
MNHN FS 3609	<i>Ligeromeryx praestans</i>	m1-m2	Miocene	Pontigné, France	
MNHN FS 3163	<i>Ligeromeryx praestans</i>	p3-m1 dex	Miocene	Pontigné, France	
MNHN FS 3639	<i>Ligeromeryx praestans</i>	m2-m3 sin	Miocene	Pontigné, France	
MNHN FS 2176	<i>Ligeromeryx praestans</i>	antler fragment	Miocene	Pontigné, France	
MNHN FS 2263	<i>Ligeromeryx praestans</i>	C	Miocene	Pontigné, France	
MNHN FS 2397	<i>Ligeromeryx praestans</i>	mandible fragment sin p4-m3	Miocene	La Brasse, France	

Table B.2: Continued

MNHN 827a & b MNHN 1938 8	<i>Ligeromeryx praestans</i> <i>Ligeromeryx praestans</i>	antler fragment antler fragment	Miocene Miocene	Fay-aux-Loges, France Chitenay, France	cast cast	Stehlin Fig. 10 (1937)
MNHN 1938 9 MNHN 1938 10 MNHN FS 1393	<i>Ligeromeryx praestans</i> <i>Ligeromeryx praestans</i> <i>Ligeromeryx praestans</i>	antler fragment antler fragment antler-pedicle fragment	Miocene Miocene Miocene	Chitenay, France Chitenay, France Faluns d'Anjou/Touraine, France	cast cast cast	
MNHN FS 1626	<i>Ligeromeryx praestans</i>	antler-pedicle fragment	Miocene	Faluns d'Anjou/Touraine, France		Azanza & Gins- burg (1997) Pl. 1, 7-8
MNHN no ID MNHN FS 6297	<i>Ligeromeryx praestans</i> <i>Ligeromeryx praestans</i>	antler-pedicle fragment antler-pedicle fragment	Miocene Miocene	Faluns d'Anjou/Touraine, France Faluns d'Anjou/Touraine, France	cast cast	
MNHN FS 5936	<i>Ligeromeryx praestans</i>	antler-pedicle fragment	Miocene	Faluns d'Anjou/Touraine, France		
MNHN no ID	<i>Ligeromeryx praestans</i>	antler-pedicle fragment	Miocene	Faluns d'Anjou/Touraine, France	cast	Azanza & Gins- burg (1997) Textfig. 2B
MNHN M4802 MNHN M31622	<i>Ligeromeryx praestans</i> <i>Ligeromeryx praestans</i>	antler-pedicle fragment antler-pedicle fragment	Miocene Miocene	Faluns d'Anjou/Touraine, France Faluns d'Anjou/Touraine, France	cast cast	
MNHN FS 283	<i>Ligeromeryx praestans</i>	antler-pedicle fragment	Miocene	Faluns d'Anjou/Touraine, France		Azanza & Gins- burg (1997) Pl. 1, 5-6
MNHN FS 3169	<i>Ligeromeryx praestans</i>	antler-pedicle fragment	Miocene	Faluns d'Anjou/Touraine, France		Azanza & Gins- burg (1997) Pl. 1, 1-2
MNHN FS 301 MNHN FS 296 MNHN FS 300	<i>Ligeromeryx praestans</i> <i>Ligeromeryx praestans</i> <i>Ligeromeryx praestans</i>	antler-pedicle fragment antler-pedicle fragment antler-pedicle fragment	Miocene Miocene Miocene	Faluns d'Anjou/Touraine, France Faluns d'Anjou/Touraine, France Faluns d'Anjou/Touraine, France		
MNHN FS 6845 MNHN FS 6844	<i>Ligeromeryx praestans</i> <i>Ligeromeryx praestans</i>	antler-pedicle fragment antler-pedicle fragment	Miocene Miocene	Faluns d'Anjou/Touraine, France Faluns d'Anjou/Touraine, France		
NMB S.O. 2060 NMB S.O. 3027 NMB S.O. 2078	<i>Ligeromeryx praestans</i> <i>Ligeromeryx praestans</i> <i>Ligeromeryx praestans</i>	mandible fragment p4-m3 mandible fragment p2-m3 antler fragment shed?	Miocene Miocene Miocene	Chitenay, France Chitenay, France Chitenay, France		Stehlin Fig. 12 (1937)
NMB S.O. 5728 BMNH M2328 BMNH M2326 BMNH 28968 RGM 369792 RGM 139565	<i>Ligeromeryx praestans</i> <i>Megaloceros giganteus</i> <i>Megaloceros giganteus</i> <i>Megaloceros giganteus</i> <i>Megaloceros giganteus</i>	antler fragment shed? mandible skull & mandible mandible fragment dex p2-m3 mandible fragment dex p2-m4	Miocene Pleistocene Pleistocene Pleistocene Pleistocene	Chitenay, France Ireland Ireland Bruine Bank, North Sea voor Cadzand, Nether- lands		
RGM 40620	<i>Megaloceros giganteus</i>	snout fragment, dentition	Pleistocene	Zwarte Meer, Overijssel, Netherlands		
RGM 40617	<i>Megaloceros giganteus</i>	skull	Pleistocene	Zwolsche Diep, Gauverdie, Netherlands		
RGM 117787	<i>Megaloceros giganteus</i>	skull	Pleistocene	Rossum, Gelderland, Netherlands		

Table B.2: Continued

RGM no nr. RGM no nr. SNSB-BSPG 1956 I 494	<i>Megaloceros giganteus</i> <i>Megaloceros giganteus</i> <i>Megaloceros giganteus</i>	skull skull complete skull, antlers, mandible	Pleistocene Pleistocene Pleistocene	Ireland	
MNHN AC 5045 MNHN PET 825	<i>Metacervoceros pardinensis</i> <i>Metacervoceros pardinensis</i>	maxilla fragment P2-M3 dex shed antler fragment	Pliocene Pliocene	Perrier, France Perrier, France	Heintz (1970), Pl. VIII, 4 Heintz (1970), Pl. VIII, 3 Heintz (1970), Pl. XXVI, 1
MNHN PET 769	<i>Metacervoceros pardinensis</i>	antler fragment	Pliocene	Perrier, France	photos only
MNHN no nr	<i>Metacervoceros pardinensis</i>	mandible fragment sin p2-m3	Pliocene	Perrier, France	photos only
RGM 86968 RGM 86968	<i>Metacervoceros rhenanus</i> <i>Metacervoceros rhenanus</i>	mx fragment dex P2-M3 2 mandible fragments sin & dex p2-m3	Plio-/Pleistocene Plio-/Pleistocene	Tegelen, Netherlands Tegelen, Netherlands	
RGM 86968 RGM 28145 RGM 36979 RGM 28148 RGM 28290 RGM 93195A RGM 85554 RGM 96655	<i>Metacervoceros rhenanus</i> <i>Metacervoceros rhenanus</i> <i>Metacervoceros rhenanus</i> <i>Metacervoceros rhenanus</i> <i>Metacervoceros rhenanus</i> <i>Metacervoceros rhenanus</i> <i>Metacervoceros rhenanus</i>	antler-pedicle fragment mandible fragment sin p2-m3 mandible fragment sin p2-m3 antler fragment sin antler fragment dex frontlet & antler fragment occiput	Plio-/Pleistocene Plio-/Pleistocene Plio-/Pleistocene Plio-/Pleistocene Plio-/Pleistocene Plio-/Pleistocene Plio-/Pleistocene	Tegelen, Netherlands Tegelen, Netherlands Tegelen, Netherlands Tegelen, Netherlands Tegelen, Netherlands Tegelen, Netherlands Tegelen, Netherlands	photos only photos only photos only
RGM 1879b RGM 15999 RGM 16000 RGM 16001 RGM 10044-2 RGM 10045 RGM 1457-54	<i>Muntiacus muntjak</i> <i>Muntiacus muntjak</i> <i>Muntiacus muntjak</i> <i>Muntiacus muntjak</i> <i>Muntiacus muntjak</i> <i>Muntiacus muntjak</i> <i>Muntiacus muntjak</i>	antler fragment shed m3 m3 mandible fragment sin p2-m3 C sin maxilla fragment P2-M2	Pleistocene Pleistocene Pleistocene Pleistocene Pleistocene Pleistocene	Bangle, Java, Indonesia Bangle, Java, Indonesia Bangle, Java, Indonesia Kates, Java, Indonesia Kates, Java, Indonesia Kediri, Java, Indonesia	photos only photos only photos only photos only photos only looks unusual for <i>Muntiacus</i> denti- tion
BMNH 18703 BMNH 18704 BMNH 18605 BMNH 18700 BMNH 18706d BMNH 18699 BMNH 18706a BMNH 18705 BMNH 18699 BMNH 18702 BMNH 18701 BMNH M 80348 SNSB-BSPG 2012 I 77	<i>Odocoileus</i> <i>Odocoileus</i> <i>Odocoileus</i> <i>Odocoileus</i> <i>Odocoileus</i> <i>Odocoileus</i> <i>Odocoileus</i> <i>Odocoileus</i> <i>Odocoileus</i> <i>Odocoileus</i> <i>Odocoileus</i> <i>Odocoileus</i> <i>Odocoileus</i>	mandible fragment dex p2-m3 mandible fragment dex p2-m3 maxilla fragment maxilla fragment maxilla fragment maxilla fragment skull fragment skull fragment mandible fragment sin p2-m3 skull fragment mandible fragment dex p2-m3 skull fragment	Pleistocene Pleistocene Pleistocene Pleistocene Pleistocene Pleistocene Pleistocene Pleistocene Pleistocene Pleistocene Pleistocene Pleistocene	Minas Geraes, Brasil Minas Geraes, Brasil Minas Geraes, Brasil Minas Geraes, Brasil Minas Geraes, Brasil Minas Geraes, Brasil Minas Geraes, Brasil Minas Geraes, Brasil Santa Fe River, FL, USA Saginaw County, MI, USA	photos only photos only photos only photos only photos only
MNCN 4416	<i>Palaeoplatyceros hispanicus</i>	antler-pedicle fragment	Miocene	Cerro del Otero, Spain	Azanza Asensio (2000) Fig. 51, Pl. 12, Fig. 1a-c Azanza Asensio (2000) Pl. 13, Fig. 2a-c
MNCN 39138	<i>Palaeoplatyceros hispanicus</i>	antler-pedicle fragment	Miocene	Cerro del Otero, Spain	photos only
MNCN 39139 MNCN 39140	<i>Palaeoplatyceros hispanicus</i> <i>Palaeoplatyceros hispanicus</i>	antler-pedicle fragment antler fragment	Miocene Miocene	Cerro del Otero, Spain Cerro del Otero, Spain	photos only
MNCN 39141	<i>Palaeoplatyceros hispanicus</i>	antler-pedicle fragment	Miocene	Cerro del Otero, Spain	photos only

Table B.2: Continued

MNCN 39142 MNCN 39143	<i>Palaeoplatyceros hispanicus</i> <i>Palaeoplatyceros hispanicus</i>	antler-pedicle fragment antler-pedicle fragment	Miocene Miocene	Cerro del Otero, Spain Cerro del Otero, Spain	Azanza (2000) Pl. 11, Fig. 2a-c Asensio (2000) Fig. 52 Azanza (2000) Fig. 52 Asensio (2000) Fig. 52
MNCN 39167	<i>Palaeoplatyceros hispanicus</i>	P4	Miocene	Cerro del Otero, Spain	photos only
MNCN 39168	<i>Palaeoplatyceros hispanicus</i>	P3	Miocene	Cerro del Otero, Spain	photos only
MNCN 39169	<i>Palaeoplatyceros hispanicus</i>	M1	Miocene	Cerro del Otero, Spain	photos only
MNCN 39170	<i>Palaeoplatyceros hispanicus</i>	dentition	Miocene	Cerro del Otero, Spain	photos only
MNCN 39171	<i>Palaeoplatyceros hispanicus</i>	dentition	Miocene	Cerro del Otero, Spain	photos only
MNCN 39172	<i>Palaeoplatyceros hispanicus</i>	m3 dex	Miocene	Cerro del Otero, Spain	photos only
MNCN 39173	<i>Palaeoplatyceros hispanicus</i>				
MNCN 39174	<i>Palaeoplatyceros hispanicus</i>	dentition	Miocene	Cerro del Otero, Spain	photos only
MNCN 39175	<i>Palaeoplatyceros hispanicus</i>	dentition	Miocene	Cerro del Otero, Spain	photos only
MNCN 39176	<i>Palaeoplatyceros hispanicus</i>	dentition	Miocene	Cerro del Otero, Spain	photos only
MNCN 39177	<i>Palaeoplatyceros hispanicus</i>	dentition	Miocene	Cerro del Otero, Spain	photos only
MNCN 39178	<i>Palaeoplatyceros hispanicus</i>	dentition	Miocene	Cerro del Otero, Spain	photos only
MNCN 39179	<i>Palaeoplatyceros hispanicus</i>	dentition	Miocene	Cerro del Otero, Spain	photos only
MNCN 39180	<i>Palaeoplatyceros hispanicus</i>	dentition	Miocene	Cerro del Otero, Spain	photos only
MNCN 39181	<i>Palaeoplatyceros hispanicus</i>	maxilla fragment mandible fragment	M2-M3, p4-m3	Cerro del Otero, Spain	Azanza (2000) Fig. 52; Pl. 14, Fig. 9a-c; Pl. 15, Fig. 1a-c
MNCN 39182	<i>Palaeoplatyceros hispanicus</i>	mandible fragment dex	Miocene	Cerro del Otero, Spain	photos only
MNCN 39195	<i>Palaeoplatyceros hispanicus</i>	M2 sin	Miocene	Cerro del Otero, Spain	photos only
MNCN 39196	<i>Palaeoplatyceros hispanicus</i>	M2 dex	Miocene	Cerro del Otero, Spain	photos only
MNCN 39197	<i>Palaeoplatyceros hispanicus</i>	dentition	Miocene	Cerro del Otero, Spain	photos only
MNCN 39198	<i>Palaeoplatyceros hispanicus</i>	M3 dex	Miocene	Cerro del Otero, Spain	photos only
MNCN 39199	<i>Palaeoplatyceros hispanicus</i>	M1 sin	Miocene	Cerro del Otero, Spain	photos only
MNCN 39200	<i>Palaeoplatyceros hispanicus</i>	M3 dex	Miocene	Cerro del Otero, Spain	photos only
MNCN 39201	<i>Palaeoplatyceros hispanicus</i>	dentition	Miocene	Cerro del Otero, Spain	photos only
MNCN 39202	<i>Palaeoplatyceros hispanicus</i>	dentition	Miocene	Cerro del Otero, Spain	photos only
MNCN 39203	<i>Palaeoplatyceros hispanicus</i>	dentition	Miocene	Cerro del Otero, Spain	photos only
MNCN 39204	<i>Palaeoplatyceros hispanicus</i>	dentition	Miocene	Cerro del Otero, Spain	photos only
MNCN 39205	<i>Palaeoplatyceros hispanicus</i>	mandible fragment dex	p4-m3	Cerro del Otero, Spain	photos only
MNCN 39207	<i>Palaeoplatyceros hispanicus</i>	antler-pedicle fragment		Cerro del Otero, Spain	photos only
MNCN 66513	<i>Palaeoplatyceros hispanicus</i>				
MNCN 66514	<i>Palaeoplatyceros hispanicus</i>	antler-pedicle fragment	Miocene	Cerro del Otero, Spain	Azanza (2000) Pl. 13, Fig. 1a-b Asensio (2000) Pl. 12, Fig. 2a-c

Table B.2: Continued

MNCN 62134	<i>Pliocervus matheronis</i>	mandible fragment sin p2-m2	Miocene	El Arquillo, Spain	Azanza (2000) Pl. 26, Fig. 4a-c
MNCN 62135	<i>Pliocervus matheronis</i>	m2-m3 sin	Miocene	El Arquillo, Spain	Azanza Asensio (2000) Fig. 85; Pl. 28, Fig. 6a-c
MNCN 62139 MNCN 62140	<i>Pliocervus matheronis</i> <i>Pliocervus matheronis</i>	dentition p3 dex	Miocene Miocene	El Arquillo, Spain El Arquillo, Spain	Azanza Asensio (2000) Fig. 85; Pl. 28, Fig. 2a-c
MNCN 62141	<i>Pliocervus matheronis</i>	P3 dex	Miocene	El Arquillo, Spain	Azanza Asensio (2000) Pl. 28, Fig. 1a-c
MNCN 62142	<i>Pliocervus matheronis</i>	p4 dex	Miocene	El Arquillo, Spain	Azanza Asensio (2000) Fig. 85; Pl. 28, Fig. 4a-c
MNCN 62143	<i>Pliocervus matheronis</i>	dentition	Miocene	El Arquillo, Spain	Azanza Asensio (2000) Pl. 27, Fig. 3a-c
MNCN 62144 MNCN 62145	<i>Pliocervus matheronis</i> <i>Pliocervus matheronis</i>	dentition M3 dex	Miocene Miocene	El Arquillo, Spain El Arquillo, Spain	Azanza Asensio (2000) Fig. 84; Pl. 27, Fig. 4a-c
MNCN 62146 MNCN 62147 MNCN 62148 MNCN 62149 MNCN 62150	<i>Pliocervus matheronis</i> <i>Pliocervus matheronis</i> <i>Pliocervus matheronis</i> <i>Pliocervus matheronis</i> <i>Pliocervus matheronis</i>	dentition dentition dentition dentition m2 sin	Miocene Miocene Miocene Miocene Miocene	El Arquillo, Spain El Arquillo, Spain El Arquillo, Spain El Arquillo, Spain El Arquillo, Spain	Azanza Asensio (2000) Pl. 28, Fig. 5a-c
MNCN 62151	<i>Pliocervus matheronis</i>	p4 sin	Miocene	El Arquillo, Spain	Azanza Asensio (2000) Fig. 85; Pl. 28 Fig. 3a-c
MNCN 62152 MNCN 62153	<i>Pliocervus matheronis</i> <i>Pliocervus matheronis</i>	dentition P4 dex	Miocene Miocene	El Arquillo, Spain El Arquillo, Spain	Azanza Asensio (2000) Fig. 84; Pl. 27, Fig. 2a-c
MNCN 62154	<i>Pliocervus matheronis</i>	m3 sin	Miocene	El Arquillo, Spain	Azanza Asensio (2000) Pl. 27, Fig. 7a-c
MNCN 62155 MNCN 62156 MNCN 62157 MNCN 62158	<i>Pliocervus matheronis</i> <i>Pliocervus matheronis</i> <i>Pliocervus matheronis</i> <i>Pliocervus matheronis</i>	dentition dentition dentition M2 dex	Miocene Miocene Miocene Miocene	El Arquillo, Spain El Arquillo, Spain El Arquillo, Spain El Arquillo, Spain	Azanza Asensio (2000) Fig. 84; Pl. 27, Fig. 2a-c
MNCN 62159 MNCN 62160 MNCN 62161	<i>Pliocervus matheronis</i> <i>Pliocervus matheronis</i> <i>Pliocervus matheronis</i>	dentition dentition m2 sin	Miocene Miocene Miocene	El Arquillo, Spain El Arquillo, Spain El Arquillo, Spain	Azanza Asensio (2000) Fig. 84
BMNH 28834 BMNH 28833 BMNH M 4479 BMNH M 4480	<i>Praelaphus etueriarum</i> <i>Praelaphus etueriarum</i> <i>Praelaphus etueriarum</i> <i>Praelaphus etueriarum</i>	antler fragment antler fragment maxillary fragments/palate mandible fragment p3-m3	Plio-/Pleistocene Plio-/Pleistocene Plio-/Pleistocene Plio-/Pleistocene	Val d'Arno, Italy Val d'Arno, Italy Val d'Arno, Italy Castelfranco, Italy	Azanza Asensio (2000) Fig. 84
BMNH 34589 MNHN 138 (74974)	<i>Praelaphus perrieri</i> <i>Praelaphus perrieri</i>	shed antler fragment maxilla fragment dex P2-M3	Plio-/Pleistocene Plio-/Pleistocene	Arde, France Perrier, France	Azanza Asensio (2000) Pl. 28, Fig. 7a-c

Table B.2: Continued

MNHN PET 265	<i>Praelaphus perrieri</i>	P2-M3 sin	Plio-/Pleistocene	Perrier, France	Heintz (1970) Pl. XXXII, 1
MNHN PET 266	<i>Praelaphus perrieri</i>	P2-M3 sin	Plio-/Pleistocene	Perrier, France	Heintz (1970) Pl. XXXII, 2
MNHN 680	<i>Praelaphus perrieri</i>	antler fragment	Plio-/Pleistocene	Perrier, France	
MNHN PET 321	<i>Praelaphus perrieri</i>	mandible fragment, i2	Plio-/Pleistocene	Perrier, France	
MNHN PET 406	<i>Praelaphus perrieri</i>	mounted upper dentition	Plio-/Pleistocene	Perrier, France	
MNHN PET 410	<i>Praelaphus perrieri</i>	P2-M3 dex	Plio-/Pleistocene	Perrier, France	
MNHN PET 303	<i>Praelaphus perrieri</i>	P3-M3 sin	Plio-/Pleistocene	Perrier, France	
MNHN PET 299	<i>Praelaphus perrieri</i>	P3-M3 sin	Plio-/Pleistocene	Perrier, France	
MNHN PET 301	<i>Praelaphus perrieri</i>	P3-M3 sin	Plio-/Pleistocene	Perrier, France	
MNHN PET 305	<i>Praelaphus perrieri</i>	P3-P4, M2-M3 dex	Plio-/Pleistocene	Perrier, France	
MNHN PET 302	<i>Praelaphus perrieri</i>	P3-M3 dex	Plio-/Pleistocene	Perrier, France	
MNHN PET 300	<i>Praelaphus perrieri</i>	P3-M3 dex	Plio-/Pleistocene	Perrier, France	
MNHN PET 298	<i>Praelaphus perrieri</i>	P4-M3 dex	Plio-/Pleistocene	Perrier, France	
MNHN Pet. 273	<i>Praelaphus perrieri</i>	P3-M3 sin	Plio-/Pleistocene	Perrier, France	
MNHN PET 304	<i>Praelaphus perrieri</i>	P3-M3 sin	Plio-/Pleistocene	Perrier, France	
NMB Prr. 357	<i>Praelaphus perrieri</i>	maxilla fragment P2-M3	Plio-/Pleistocene	Etouaires, France	
NMB Prr. 355	<i>Praelaphus perrieri</i>	mandible fragment dex p2-m3	Plio-/Pleistocene	Etouaires, France	
BMNH 34610	<i>Procacpreolus cusanus</i>	antler fragment	Pliocene	Ardé, France	
MNHN no nr	<i>Procacpreolus cusanus</i>	skull fragment, pedicle, antler base	Pliocene	Perrier, France	Heintz (1970), Pl. I, 1a, b
MNHN PET 828	<i>Procacpreolus cusanus</i>	antler fragment	Pliocene	Perrier, France	photos only
MNHN PET 831	<i>Procacpreolus cusanus</i>	antler fragment	Pliocene	Perrier, France	photos only; neo-type
MNHN no nr	<i>Procacpreolus cusanus</i>	mandible fragment sin p2-m3	Pliocene	Perrier, France	in exhibition cabinet
MNHN no nr	<i>Procacpreolus cusanus</i>	mandible fragment sin p2-m3	Pliocene	Perrier, France	in exhibition cabinet
MNHN PET 799	<i>Procacpreolus cusanus</i>	mandible fragment dex p2-m3	Pliocene	Perrier, France	
MNHN PET 793	<i>Procacpreolus cusanus</i>	mandible fragment sin p3-m3	Pliocene	Perrier, France	
MNHN PET 791	<i>Procacpreolus cusanus</i>	mandible fragment dex p2-m3	Pliocene	Perrier, France	
MNHN PET 795	<i>Procacpreolus cusanus</i>	mandible fragment dex p3-m2	Pliocene	Perrier, France	
MNHN PET 797	<i>Procacpreolus cusanus</i>	m2-m3 dex	Pliocene	Perrier, France	
MNHN PET 792	<i>Procacpreolus cusanus</i>	p4-m3 sin	Pliocene	Perrier, France	
MNHN PET 800	<i>Procacpreolus cusanus</i>	mandible fragment sin p3-m3	Pliocene	Perrier, France	
SNSB-BSPG 1937 II 16794	<i>Procervulus praelucidus</i>	antler-pedicle-frontal fragment	Miocene	Wintershof West, many	Ger-
SNSB-BSPG 1937 II 16842	<i>Procervulus praelucidus</i>	antler fragment shed	Miocene	Wintershof West, many	Ger-
SNSB-BSPG 1937 II 16845	<i>Procervulus praelucidus</i>	antler fragment shed	Miocene	Wintershof West, many	Ger-
SNSB-BSPG 1937 II 16810	<i>Procervulus praelucidus</i>	antler fragment shed	Miocene	Wintershof West, many	Ger-
SNSB-BSPG 1937 II 15153	<i>Procervulus praelucidus</i>	mx fragment dex P4-M2	Miocene	Wintershof West, many	Ger-
SNSB-BSPG 1937 II 12232	<i>Procervulus praelucidus</i>	mx dex P2-M1	Miocene	Wintershof West, many	Ger-
SNSB-BSPG 1937 II 12236	<i>Procervulus praelucidus</i>	mx fragment sin P4-M3	Miocene	Wintershof West, many	Ger-
SNSB-BSPG 1937 II 12234	<i>Procervulus praelucidus</i>	mx fragment dex P4-M3	Miocene	Wintershof West, many	Ger-
SNSB-BSPG 1937 II 12022	<i>Procervulus praelucidus</i>	mandible fragment sin p4-m3	Miocene	Wintershof West, many	Ger-
SNSB-BSPG 1937 II 12001	<i>Procervulus praelucidus</i>	mandible fragment dex p4-m3	Miocene	Wintershof West, many	Ger-

Table B.2: Continued

SNSB-BSPG 1937 II 12008	<i>Procervulus praelucidus</i>	mandible fragment dex p3-m3	Miocene	Wintershof West, Ger-many
SNSB-BSPG 1937 II 12073	<i>Procervulus praelucidus</i>	mandible fragment dex p2-m2	Miocene	Wintershof West, Ger-many
SNSB-BSPG 1937 II 12074	<i>Procervulus praelucidus</i>	mandible fragment dex p2-m2	Miocene	Wintershof West, Ger-many
SNSB-BSPG 1937 II 12018	<i>Procervulus praelucidus</i>	mandible fragment sin p3-m3	Miocene	Wintershof West, Ger-many
MNHN Ar 3425	<i>Procervulus dichotomus</i>	mandible fragment	Miocene	Artenay, France
MNHN Ar 3433	<i>Procervulus dichotomus</i>	mandible fragment	Miocene	Artenay, France
MNHN Ar 3434	<i>Procervulus dichotomus</i>	mandible fragment	Miocene	Artenay, France
MNHN Ba 835	<i>Procervulus dichotomus</i>	antler fragment	Miocene	Baigneaux, France
MNHN Ba 836	<i>Procervulus dichotomus</i>	antler fragment	Miocene	Baigneaux, France
MNHN Ba 837	<i>Procervulus dichotomus</i>	antler fragment	Miocene	Baigneaux, France
MNHN Ba 833	<i>Procervulus dichotomus</i>	antler fragment	Miocene	Baigneaux, France
MNHN FP 262	<i>Procervulus dichotomus</i>	mandible frag dex	Miocene	Pontlevoy, France
MNHN FP 830	<i>Procervulus dichotomus</i>	mandible frag sin	Miocene	Pontlevoy, France
MNHN FP 943	<i>Procervulus dichotomus</i>	M1-M3	Miocene	Pontlevoy, France
MNHN FP 944	<i>Procervulus dichotomus</i>	M	Miocene	Pontlevoy, France
MNHN FP 946	<i>Procervulus dichotomus</i>	M	Miocene	Pontlevoy, France
MNHN Or 98	<i>Procervulus dichotomus</i>	mandible fragment dex p2-m3	Miocene	Orléanais, France
SNSB-BSPG 1979 XV 555	<i>Procervulus dichotomus</i>	skull, mandible, skeleton	Miocene	Rauscheröd, Germany
SNSB-BSPG no nr	<i>Procervulus dichotomus</i>	antler fragment	Miocene	Langenau, Germany
RGM 16926	<i>Rusa kendengensis</i>	maxilla dex P2-M3	Pleistocene	Kali Gedeh, Java, Indone-sia
RGM 16927	<i>Rusa kendengensis</i>	maxilla fragment P2-M2	Pleistocene	Kali Gedeh, Java, Indone-sia
RGM 16928	<i>Rusa kendengensis</i>	maxilla fragment M1-M3	Pleistocene	Kali Gedeh, Java, Indone-sia
RGM 16934	<i>Rusa kendengensis</i>	mandible fragment dP,P	Pleistocene	Kali Gedeh, Java, Indone-sia
RGM 13775	<i>Rusa kendengensis</i>	m3 dex	Pleistocene	Kali Gedeh, Java, Indone-sia
RGM 13773	<i>Rusa kendengensis</i>	m3 dex	Pleistocene	Kali Gedeh, Java, Indone-sia
RGM 13778	<i>Rusa kendengensis</i>	m3 dex	Pleistocene	Kali Gedeh, Java, Indone-sia
RGM 13781	<i>Rusa kendengensis</i>	m3 dex	Pleistocene	Kali Gedeh, Java, Indone-sia
RGM 13768	<i>Rusa kendengensis</i>	m3 dex	Pleistocene	Kali Gedeh, Java, Indone-sia
RGM 655A	<i>Rusa kendengensis</i>	mandible fragment dex p4-m2	Pleistocene	Kali Gedeh, Java, Indone-sia
RGM 13802	<i>Rusa kendengensis</i>	mandible fragment m2-m3	Pleistocene	Kali Gedeh, Java, Indone-sia
RGM 13804	<i>Rusa kendengensis</i>	mandible fragment m1-m3	Pleistocene	Kali Gedeh, Java, Indone-sia
RGM 1971	<i>Rusa kendengensis</i>	antler fragment sin	Pleistocene	Bangle, Java, Indonesia
RGM 1969	<i>Rusa kendengensis</i>	antler & frontal fragment	Pleistocene	Kebon Doeren, Java, In-donesia
				holotype

Table B.2: Continued

SNSB-BSPG 1985 I 63	<i>Hypertrogulus calcaratus</i>	skull, mandible	Oligocene	Shannon County, South Dakota	partly reconstructed neotype; only	reconstructed photos
MNHN SG 4304	<i>Dremotherium feignouzi</i>	skull fragment	Miocene	Saint-Gérard-le-Puy, France		Viret (1929) Pl. XX, 2; Costeur (2011) Fig. 3
MNHN SG 4470	<i>Dremotherium feignouzi</i>	p3-m3	Miocene	Saint-Gérard-le-Puy, France		
MNHN SG 13634	<i>Dremotherium feignouzi</i>	deciduous dentition	Miocene	Saint-Gérard-le-Puy, France	photos only	
NMB St.G. 548	<i>Dremotherium feignouzi</i>	skull fragment	Miocene	Saint-Gérard-le-Puy, France		Costeur (2011) Fig. 1
NMB St.G. 3052	<i>Dremotherium feignouzi</i>	skull fragment	Miocene	Saint-Gérard-le-Puy, France		
NMB St.G. 600	<i>Dremotherium feignouzi</i>	skull, dentition	Miocene	Saint-Gérard-le-Puy, France		
NMB M.A. 7954	<i>Dremotherium feignouzi</i>	md fragment, p2-m3	Miocene	Montaigu-le-Blin, France		

Erathem/ Era	System/ Period	Series/ Epoch	Stage/Age	European Land Mammal Megazones	Regional Stages (Europe)	Paratethys	age [Ma]
Cenozoic	Quaternary	Pleistocene	Middle Upper 0.13	MQ2 = MN19	Toringian		0
			0.78	0.6 MQ1 = MN18	Biharian	Upper Villafranchian	1.0
			1.80	MN17 2.0–1.8		Middle	2.0
		Pliocene	Piacenzian 2.58	2.5 MN16	Villanyian	Lower Villafranchian after Heintz (1970)	3.0
			3.60	3.6–3.5 MN15	Ruscinian		4.0
				5.0 MN14			5.0
	Neogene	Messinian	5.33	5.3 MN13		Pannonian	6.0
			7.25	7.4–6.8 MN12	Turolian		7.0
				7.6 MN11			8.0
		Tortonian		8.9 MN10			9.0
				9.9 MN9	Vallesian		10.0
				11.2			11.0
		Serravallian	11.63	MN7–8	Astaracian	Upper Aragonian	12.0
				13.1–12.6 MN6			13.0
		Langhian	13.82	14.2 MN5	Orleanian	Middle Aragonian	14.0
				16.4 MN4		Lower Aragonian	15.0
			15.97	17.2 MN3			16.0
	Miocene	Burdigalian		~19.5	Ramblian		17.0
						Ottnangian	18.0
						Eggenburgian	19.0
		Aquitanian	20.44	MN2	Agenian		20.0
				max 21.7 MN1		Egerian	21.0
	Palaeogene	Oligocene	23.03				22.0
							23.0

Figure B.1: Correlation of Stage Names. Geological Stage/Age names are on the left, followed by the European Land Mammal Mega Zones (MN), regional stages defined based on these zones (two columns), and the Paratethys Zones on the right (Steininger, 1999; Hilgen et al., 2012; Böhme et al., 2012; Cohen et al., 2013)

C Supplementary Information of Chapter 2

C.1 A review on antlerogenesis

C.1.1 Antler cycle and histological aspects

The antler shedding mechanism is driven by the necrosis of the antler bone, caused by the cut off of the arterial supply. This mechanism resembles ‘abacterial sequestration’ (= ‘self-amputation’), which induces growth of a new set of antlers (Goss, 1983). Nowhere else in the Animal Kingdom is a necrotic body part tolerated on an organism for days or weeks; necrosis of the antler triggers eventual shedding. Shedding and onset of growth are associated with each other, but the timing is different across groups; it happens simultaneously in Old World deer or Cervinae, whilst there can be an offset of several months in New World deer or Capreolinae (Goss et al., 1992).

Goss et al. (1992) showed that osteoclasts, specialised cells for bone resorption appearing with declining testosterone levels, are involved in this process. Typically, they emerge directly below the burr on top of the skin-covered pedicle with a centripetal spread. After the osteoclasts leave this zone, large cavities remain, which are filled with blood vessels and surrounded by connective tissue (Goss et al., 1992). At the moment of antler detachment, the residual central bone trabeculae break from the weight of the antler. Due to the preceding severance of the blood supply, the abscission area is white and clean, but the pedicle is left with a bleeding wound (Goss, 1983; Goss et al., 1992). The surface of the abscission area is covered in impressions of osteoclasts and copious bony spicules from the previous erosion (Goss, 1983; Goss et al., 1992).

During shedding most of the osteoclasts remain on the pedicle, where the connective tissue, which previously surrounded the enlarged cavities in the resorption zone, provides the potential source of cells for the antler bud formation (Goss et al., 1992). This tissue bed is protected from desiccation by a scab, which forms after the rupture of blood vessels on the pedicle (Price et al., 2005b).

The centripetal bone erosion provides a head start for antler regeneration. Following resorption, the mesodermal tissue grows inward from the periphery and forms a thickening mass, which pushes up beneath the scab. Eventually, the highly vascularised epidermis migrates between the dead scab and the living tissue (Goss et al., 1992). Within a few days after shedding osteoclasts are no longer visible on the distal pedicle surface (Goss et al., 1992); instead a layer of osteoblasts, cells specialised for bone formation, develops.

In absence of an orderly configuration of collagen fibers the healing pedicle skin does not form a normal scar. Instead, a blastema or regeneration bud develops. Thus, antlerogenesis can be regarded as a subset of an abnormal, exaggerated scar formation. The antlerogenic transformation within the blastema (i.e., the pedicle to antler bud transformation) is a gradual process and not analogous to embryonic limb or tail bud formation (Goss, 1983).

During antlerogenesis the inductive periosteum is important (Bubenik, 1990). Bud formation involves development of slightly mineralised osteons, which grow by apposition of bone matrix on the apex of the pedicle. Therefore, the circumference of the antler does not increase subsequently resulting in the similar or equal diameter of the antler shaft and the pedicle (Bubenik, 1990).

The internal cancellous bone develops during chondrification when a non-ordinary cartilage with a honeycombed structure forms, allowing for rich vascularisation (in contrast to ordinary cartilage, which is not vascularised) (Goss, 1983). The rich vascularisation with its extensive blood supply is required for the high metabolic rate of the local antler tissue during antler growth. As antlers are formed from connective tissue as cartilaginous trabeculae, the conversion to bony tissue results in a rigid structure of spongy tissue, which is surrounded by a wall of compact cortical bone (Brown, 1980). During growth, antlers are covered in specialised skin (velvet), which is highly vascularised and innervated (Bubenik, 1990) and possesses *de novo* hairs, which are permanently erected with a velvet-like appearance (Goss, 1983). Palmated antlers often show impressions of these nerves and blood vessels.

Even though antler and pedicle are built of similar tissues (skin, bone, blood vessels, nerves), they differ greatly developmentally (Goss, 1990); this difference can be seen in the deciduous condition of the antler versus the permanent condition of the pedicle, by the velvet cover of antlers versus normal skin cover of pedicles, and by the more cancellous bone in antlers compared to the pedicles.

C.1.2 Physiology and extrinsic control of the antler cycle

The whole antler cycle is strongly dependent on intrinsic and extrinsic factors with levels of several interacting hormones as the main agents. These belong to three different categories: Hormones acting directly on the target tissue, hormones which have either a general metabolic effect on or stimulating other hormones and thus have an indirect effect on antlerogenesis, and hormones, which respond to photoperiod cyclicity in higher latitudinal regions (Bubenik, 1990). The androgen testosterone presumably plays the most important role by influencing antler mineralisation. High testosterone levels maintained during the rutting season prevent shedding, whereas a drop of testosterone levels induces antler shedding. Low testosterone levels inhibit mineralisation and trigger continuous antler growth (Bubenik, 1990).

In regions with distinct seasonality, testosterone levels are controlled by photoperiodicity; in regions without seasons such as the tropics, the controlling mechanism for the hormones is not known. The correlation between antler cycle and seasons is important concerning the timing of reproduction, lactation, and antler growth to seasons with optimal food abundance and quality; this optimal timing is particularly essential in temperate and boreal climates (Lason et al., 2001). Therefore, birth times in such regions are syn-

chronised and timed to late spring and early summer, when abundance of high quality food is ensured, and the rutting season is timed to late summer and early autumn, when males are the strongest. In contrast, in tropical species antler casting is not synchronised between individuals, and sometimes the antler cycle lasts longer than a year. Antler casting in *Elaphodus cephalophus* is assumed to be irregular or absent in the wild (Groves & Grubb, 1990; Geist, 1998; Hall, 2005; Mattioli, 2011), but has certainly been observed in captivity (Pohle, 1989; Leslie et al., 2013).

Only the first antlers in yearlings, generally bare knobs, small, unbranched spikes or forklettes without burrs, do not yet respond to photoperiodicity (Bubenik, 1990). They are unaffected by the photoperiodic cycle and, although their growth is under endocrine control, hormone secretion in response to photoperiodic cycles (in photoperiodically dependent species) only starts in the second year with sexual maturity (Goss, 1983). The first antlers of yearlings in modern cervids do not develop a burr and are scarcely ornamented; nevertheless they are shed. In sequences of cast antlers collected throughout the life span of an individual (e.g., *Cervus elaphus*) it can be seen how the size and complexity of the antlers develop over time until they reach their prime at around 11–12 years. After that time the development of the antlers becomes simplified and degenerated, until only a highly reduced set of antlers is grown in the last year.

The evolutionary advantage of antler development in intraspecific display and reproductive success (Geist, 1998) has a critical aspect in the substantial physiological effort of annual shedding and regeneration; however, repeated growth of antlers brings some advantages. Firstly, they are in synchrony with the animal's ontogeny, which means that antlers reach their maximal dimensions and complexity when the animal is at its prime. That means that mature males are most likely to outcompete less mature or fit males in intraspecific conflicts, when their reproduction ability is at its peak (Goss, 1983; Geist, 1998). With increasing senescence, due to less available energy resources, cervids exhibit degenerated, less well-developed antlers at lower physiological cost (Goss, 1983; Geist, 1998), which probably is advantageous for maintaining a certain social status and for carrying around less heavy headgear. This is in contrast to bovids, whose horns grow lifelong and reach their maximum dimensions and weight in old aged individuals.

C.1.3 Ethological role of antlers

Although it is often assumed that the primary function of antlers is their role for sexual behavior and use in intraspecific combats, antlers are relatively ineffective weapons and are carried for much longer than during the short rutting season (Brown, 1980). The role of antlers for the social ranking of an individual is much more significant. Therefore, many authors consider antlers to have evolved for display purposes rather than head-head-combat (Brown, 1980; Goss, 1983; Gilbert et al., 2006). This visual display of physical superiority keeps strenuous, wasting battles to a minimum and secures the social rank, which, for species in seasonal habitats, is particularly important during the winter, when food is scarce (Brown, 1980). It is known that damage or loss of antlers lowers the social status and reduces reproductive success (Bubenik, 1990; Geist, 1998). Considering this, a trigger in cervid evolution towards annual regrowth of antlers might have been the enhanced potential of achieving a higher social status and rutting success.

Caro et al. (2003) showed that there is almost no support for a correlation of antler morphology with environmental factors; however, the morphology is not arbitrary. Since there are many more possibilities of combining certain morphological features of antlers than exist in nature, the selection for a particular antler morphology is very likely driven by female preference (Caro et al., 2003). Cervid females seem to have inherited anlagen for an assessment of the species-specific range of antler shape and its rank (Bubenik, 1990). The social rank plays a bigger role in more gregarious species, but is also important to defend territories of solitary living males.

The overall antler morphology shows weak patterns of association with fighting, mating, and social structure (Caro et al., 2003). Thus, antler morphology is influenced only by a little extent by the type of intraspecific fighting or the degree of fighting. The antler morphology has most likely an epigenetic component (Bubenik, 1990; Caro et al., 2003).

Table C.1: List of examined fossil specimens with their respective collection numbers, localities and age.

Species	Collection ID	Locality	Stage (Euro-pean)	Stage (IUGS)
<i>Dicrocerus elegans</i>	MNHN Sa 3327	Sansan, France	Aragonian; Orléanien	Langhian
<i>Dicrocerus elegans</i>	MNHN Sa 10563	Sansan, France	Aragonian; Orléanien	Langhian
<i>Dicrocerus elegans</i>	MNHN Sa 10333	Sansan, France	Aragonian; Orléanien	Langhian
<i>Dicrocerus elegans</i>	MNHN Sa 3363	Sansan, France	Aragonian; Orléanien	Langhian
<i>Dicrocerus elegans</i>	MNHN Sa 3329	Sansan, France	Aragonian; Orléanien	Langhian
<i>Dicrocerus elegans</i>	MNHN Sa 3323	Sansan, France	Aragonian; Orléanien	Langhian
<i>Dicrocerus elegans</i>	MNHN Sa 3486	Sansan, France	Aragonian; Orléanien	Langhian
<i>Dicrocerus elegans</i>	MNHN Sa 3456	Sansan, France	Aragonian; Orléanien	Langhian
<i>Dicrocerus elegans</i>	MNHN Sa 3552	Sansan, France	Aragonian; Orléanien	Langhian
<i>Dicrocerus elegans</i>	MNHN Sa 9995	Sansan, France	Aragonian; Orléanien	Langhian
<i>Dicrocerus elegans</i>	MNHN Sa 3326	Sansan, France	Aragonian; Orléanien	Langhian
<i>Dicrocerus elegans</i>	MNHN Sa 3327	Sansan, France	Aragonian; Orléanien	Langhian
<i>Dicrocerus elegans</i>	MNHN Sa 10563	Sansan, France	Aragonian; Orléanien	Langhian
<i>Dicrocerus elegans</i>	MNHN Sa 10333	Sansan, France	Aragonian; Orléanien	Langhian
<i>Dicrocerus elegans</i>	MNHN Sa 3345	Sansan, France	Aragonian; Orléanien	Langhian
<i>Dicrocerus elegans</i>	MNHN Sa 3364	Sansan, France	Aragonian; Orléanien	Langhian
<i>Dicrocerus elegans</i>	MNHN Sa 3322	Sansan, France	Aragonian; Orléanien	Langhian
<i>Dicrocerus elegans</i>	MNHN Sa 10338	Sansan, France	Aragonian; Orléanien	Langhian
<i>Dicrocerus elegans</i>	MNHN Sa 3320	Sansan, France	Aragonian; Orléanien	Langhian
<i>Dicrocerus elegans</i>	MNHN Sa 3363	Sansan, France	Aragonian; Orléanien	Langhian
<i>Dicrocerus elegans</i>	MNHN Sa 3483	Sansan, France	Aragonian; Orléanien	Langhian
<i>Dicrocerus elegans</i>	MNHN Sa 3507	Sansan, France	Aragonian; Orléanien	Langhian
<i>Dicrocerus elegans</i>	MNHN Sa 9996	Sansan, France	Aragonian; Orléanien	Langhian
<i>Dicrocerus elegans</i>	MNHN Sa 3366	Sansan, France	Aragonian; Orléanien	Langhian
<i>Dicrocerus elegans</i>	MNHN Sa 3396	Sansan, France	Aragonian; Orléanien	Langhian
<i>Dicrocerus elegans</i>	MNHN Sa 3393	Sansan, France	Aragonian; Orléanien	Langhian
<i>Dicrocerus elegans</i>	MNHN Sa 9990d	Sansan, France	Aragonian; Orléanien	Langhian
<i>Dicrocerus elegans</i>	MNHN Sa 3499	Sansan, France	Aragonian; Orléanien	Langhian
<i>Dicrocerus elegans</i>	MNHN Sa 3398	Sansan, France	Aragonian; Orléanien	Langhian
<i>Dicrocerus elegans</i>	MNHN 2003	Sansan, France	Aragonian; Orléanien	Langhian
<i>Dicrocerus elegans</i>	MNHN Sa 3531	Sansan, France	Aragonian; Orléanien	Langhian
<i>Dicrocerus elegans</i>	MNHN Sa 3346	Sansan, France	Aragonian; Orléanien	Langhian
<i>Dicrocerus elegans</i>	MNHN Sa 3392	Sansan, France	Aragonian; Orléanien	Langhian
<i>Dicrocerus elegans</i>	MNHN Sa 3395	Sansan, France	Aragonian; Orléanien	Langhian
<i>Dicrocerus elegans</i>	MNHN Sa 3382	Sansan, France	Aragonian; Orléanien	Langhian
<i>Dicrocerus elegans</i>	MNHN Sa 3494	Sansan, France	Aragonian; Orléanien	Langhian
<i>Dicrocerus elegans</i>	MNHN Sa 3481	Sansan, France	Aragonian; Orléanien	Langhian
<i>Dicrocerus elegans</i>	MNHN Sa 3513	Sansan, France	Aragonian; Orléanien	Langhian

Table C.1: Continued

<i>Dicrocerus elegans</i>	MNHN Sa 11433	Sansan, France	Aragonian; Orléanian	Langhian
<i>Dicrocerus elegans</i>	MNHN Sa 3476	Sansan, France	Aragonian; Orléanian	Langhian
<i>Dicrocerus elegans</i>	MNHN Sa 3425	Sansan, France	Aragonian; Orléanian	Langhian
<i>Dicrocerus elegans</i>	MNHN Sa 3560	Sansan, France	Aragonian; Orléanian	Langhian
<i>Dicrocerus elegans</i>	MNHN Sa 3505	Sansan, France	Aragonian; Orléanian	Langhian
<i>Dicrocerus</i> sp.	SNSB-BSPG 1987 V 333	Ehekirchen, Germany	Aragonian; Orléanian	Langhian
<i>Euprox dicranoceras</i>	MNCN 62162	Los Valles De Fuentidueña, Spain	Aragonian	Langhian-Serravallian
<i>Euprox dicranoceras</i>	MNCN 62163	Los Valles De Fuentidueña, Spain	Aragonian	Langhian-Serravallian
<i>Euprox dicranoceras</i>	MNCN 62164	Los Valles De Fuentidueña, Spain	Aragonian	Langhian-Serravallian
<i>Euprox dicranoceras</i>	MNCN 62165	Los Valles De Fuentidueña, Spain	Aragonian	Langhian-Serravallian
<i>Euprox dicranoceras</i>	MNCN 62166	Los Valles De Fuentidueña, Spain	Aragonian	Langhian-Serravallian
<i>Euprox dicranoceras</i>	MNCN 62167	Los Valles De Fuentidueña, Spain	Aragonian	Langhian-Serravallian
<i>Euprox dicranoceras</i>	MNCN 62168	Los Valles De Fuentidueña, Spain	Aragonian	Langhian-Serravallian
<i>Euprox dicranoceras</i>	MNCN 62176	Los Valles De Fuentidueña, Spain	Aragonian	Langhian-Serravallian
<i>Euprox dicranoceras</i>	MNCN 62177	Los Valles De Fuentidueña, Spain	Aragonian	Langhian-Serravallian
<i>Euprox dicranoceras</i>	MNCN 62178	Los Valles De Fuentidueña, Spain	Aragonian	Langhian-Serravallian
<i>Euprox dicranoceras</i>	MNCN 62179	Los Valles De Fuentidueña, Spain	Aragonian	Langhian-Serravallian
<i>Euprox dicranoceras</i>	MNCN 62180	Los Valles De Fuentidueña, Spain	Aragonian	Langhian-Serravallian
<i>Euprox dicranoceras</i>	MNCN 62181	Los Valles De Fuentidueña, Spain	Aragonian	Langhian-Serravallian
<i>Euprox furcatus</i>	NMB Sth. 658	Steinheim, Germany	Aragonian	Langhian-Serravallian
<i>Euprox furcatus</i>	NMB Sth. 260	Steinheim, Germany	Aragonian	Langhian-Serravallian
<i>Euprox furcatus</i>	SMNS 4768	Steinheim, Germany	Aragonian	Langhian-Serravallian
<i>Euprox furcatus</i>	SMNS 44208	Steinheim, Germany	Aragonian	Langhian-Serravallian
<i>Euprox furcatus</i>	SNSB-BSPG 1966 XIV 34	Breitenbrunn, Germany	Aragonian	Langhian-Serravallian
<i>Heteroprox eggeri</i>	SNSB-BSPG 1959 II 5258	Sandelzhausen, Germany	Aragonian	Langhian-Serravallian
<i>Heteroprox eggeri</i>	SNSB-BSPG 1959 II 5268	Sandelzhausen, Germany	Aragonian	Langhian-Serravallian
<i>Heteroprox eggeri</i>	SNSB-BSPG 1987 V 262	Ehekirchen, Germany	Aragonian	Langhian-Serravallian
<i>Heteroprox eggeri</i>	SNSB-BSPG AS I 933	Häder, Germany	Aragonian	Langhian-Serravallian
<i>Heteroprox larteti</i>	SNSB-BSPG 1881 IX 654	Reisensburg, Germany	Aragonian	Langhian-Serravallian
cf. <i>Heteroprox</i> sp.	SNSB-BSPG 1971 XIX 24	Voggersberg, Germany	Aragonian	Langhian-Serravallian
<i>Heteroprox</i> sp.	SNSB-BSPG 1881 IX 55	Reisensburg, Germany	Aragonian	Langhian-Serravallian
<i>Heteroprox larteti</i>	SNSB-BSPG AS I 934	Häder, Germany	Aragonian	Langhian-Serravallian
<i>Heteroprox larteti</i>	MNHN Sa 3399	Sansan, France	Aragonian	Langhian-Serravallian
<i>Heteroprox moralesi</i>	MNCN 7856	Puente De Vallecas, Spain	Aragonian	Langhian-Serravallian
<i>Heteroprox</i>	SMNS 47709	Steinheim, Germany	Aragonian	Langhian-Serravallian
<i>Heteroprox</i>	SMNS 47708	Steinheim, Germany	Aragonian	Langhian-Serravallian
<i>Heteroprox</i>	SMNS 47707	Steinheim, Germany	Aragonian	Langhian-Serravallian
<i>Heteroprox</i>	SMNS 47706	Steinheim, Germany	Aragonian	Langhian-Serravallian
<i>Heteroprox</i>	SMNS 44207	Steinheim, Germany	Aragonian	Langhian-Serravallian
<i>Heteroprox</i>	SMNS 40498	Steinheim, Germany	Aragonian	Langhian-Serravallian
<i>Heteroprox</i>	SMNS 40178	Steinheim, Germany	Aragonian	Langhian-Serravallian
<i>Heteroprox</i>	SMNS no nr	Steinheim, Germany	Aragonian	Langhian-Serravallian

Table C.1: Continued

<i>Lagomeryx</i> sp.	SNSB-BSPG no ID	Niederaichbach, Germany	Ramblian- Aragonian; Orléanien	Burdigalian- Langhian
<i>Lagomeryx</i> sp.	SNSB-BSPG no ID	Puttenhausen, Germany	Ramblian- Aragonian; Orléanien	Burdigalian- Langhian
<i>Lagomeryx parvulus</i>	SNSB-BSPG 1959 II 7803	Sandelzhausen, Germany	Ramblian- Aragonian; Orléanien	Burdigalian- Langhian
<i>Lagomeryx pumilio</i>	SNSB-BSPG no no.	Upfkofen, Germany	Ramblian- Aragonian; Orléanien	Burdigalian- Langhian
<i>Ligeromeryx praestans</i>	MNHN 1938-8	Chitenay, France	Ramblian- Aragonian; Orléanien	Burdigalian- Langhian
<i>Ligeromeryx praestans</i>	MNHN 827a & b	Fay-aux-Loges, France	Ramblian- Aragonian; Orléanien	Burdigalian- Langhian
<i>Ligeromeryx praestans</i>	MNHN FS 2176	Faluns d'Anjou/ Touraine, France	Ramblian- Aragonian; Orléanien	Burdigalian- Langhian
<i>Ligeromeryx praestans</i>	MNHN 1938-9	Chitenay, France	Ramblian- Aragonian; Orléanien	Burdigalian- Langhian
<i>Ligeromeryx praestans</i>	MNHN FS 1393	Faluns d'Anjou/ Touraine, France	Ramblian- Aragonian; Orléanien	Burdigalian- Langhian
<i>Ligeromeryx praestans</i>	MNHN FS 1626	Faluns d'Anjou/ Touraine, France	Ramblian- Aragonian; Orléanien	Burdigalian- Langhian
<i>Ligeromeryx praestans</i>	MNHN MD12	Faluns d'Anjou/ Touraine, France	Ramblian- Aragonian; Orléanien	Burdigalian- Langhian
<i>Ligeromeryx praestans</i>	MNHN FS 6297	Faluns d'Anjou/ Touraine, France	Ramblian- Aragonian; Orléanien	Burdigalian- Langhian
<i>Ligeromeryx praestans</i>	MNHN FS 5936	Faluns d'Anjou/ Touraine, France	Ramblian- Aragonian; Orléanien	Burdigalian- Langhian
<i>Ligeromeryx praestans</i>	MNHN MD2	Faluns d'Anjou/ Touraine, France	Ramblian- Aragonian; Orléanien	Burdigalian- Langhian
<i>Ligeromeryx praestans</i>	MNHN M4802	Faluns d'Anjou/ Touraine, France	Ramblian- Aragonian; Orléanien	Burdigalian- Langhian
<i>Ligeromeryx praestans</i>	MNHN M31622	Faluns d'Anjou/ Touraine, France	Ramblian- Aragonian; Orléanien	Burdigalian- Langhian
<i>Ligeromeryx praestans</i>	MNHN FS 283	Faluns d'Anjou/ Touraine, France	Ramblian- Aragonian; Orléanien	Burdigalian- Langhian
<i>Ligeromeryx praestans</i>	MNHN FS 3169	Faluns d'Anjou/ Touraine, France	Ramblian- Aragonian; Orléanien	Burdigalian- Langhian
<i>Ligeromeryx praestans</i>	MNHN FS 301	Faluns d'Anjou/ Touraine, France	Ramblian- Aragonian; Orléanien	Burdigalian- Langhian
<i>Ligeromeryx praestans</i>	MNHN FS 296	Faluns d'Anjou/ Touraine, France	Ramblian- Aragonian; Orléanien	Burdigalian- Langhian
<i>Ligeromeryx praestans</i>	MNHN FS 300	Faluns d'Anjou/ Touraine, France	Ramblian- Aragonian; Orléanien	Burdigalian- Langhian
<i>Ligeromeryx praestans</i>	MNHN FS 6845	Faluns d'Anjou/ Touraine, France	Ramblian- Aragonian; Orléanien	Burdigalian- Langhian
<i>Ligeromeryx praestans</i>	MNHN FS 6844	Faluns d'Anjou/ Touraine, France	Ramblian- Aragonian; Orléanien	Burdigalian- Langhian
<i>Ligeromeryx praestans</i>	NMB S.O. 2078	Chitenay, France	Ramblian- Aragonian; Orléanien	Burdigalian- Langhian
<i>Ligeromeryx praestans</i>	NMB S.O. 5728	Chitenay, France	Ramblian- Aragonian; Orléanien	Burdigalian- Langhian
<i>Palaeoplatyceros hispanicus</i>	MNCN 4416	Cerro del Otero, Spain	Aragonian	Langhian
<i>Palaeoplatyceros hispanicus</i>	MNCN 39138	Cerro del Otero, Spain	Aragonian	Langhian
<i>Palaeoplatyceros hispanicus</i>	MNCN 39139	Cerro del Otero, Spain	Aragonian	Langhian
<i>Palaeoplatyceros hispanicus</i>	MNCN 39140	Cerro del Otero, Spain	Aragonian	Langhian
<i>Palaeoplatyceros hispanicus</i>	MNCN 39141	Cerro del Otero, Spain	Aragonian	Langhian
<i>Palaeoplatyceros hispanicus</i>	MNCN 39142	Cerro del Otero, Spain	Aragonian	Langhian
<i>Palaeoplatyceros hispanicus</i>	MNCN 39143	Cerro del Otero, Spain	Aragonian	Langhian

Table C.1: Continued

<i>Palaeoplatyceros hispanicus</i>	MNCN 66513		Cerro del Otero, Spain	Aragonian	Langhian
<i>Palaeoplatyceros hispanicus</i>	MNCN 66514		Cerro del Otero, Spain	Aragonian	Langhian
<i>Paradicrocerus elegans</i>	SNSB-BSPG XIV 132	1985	Stätzling, Germany	Aragonian	Langhian
<i>Paradicrocerus elegantulus</i>	SNSB-BSPG XIV 1	1966	Stätzling, Germany	Aragonian	Langhian
<i>Paradicrocerus elegantulus</i>	SNSB-BSPG 1993 I 21		Wollersdorf, Germany	Aragonian	Langhian
<i>Paradicrocerus elegantulus</i>	NMB T.D. 1197		Stätzling, Germany	Aragonian	Langhian
<i>Paradicrocerus elegantulus</i>	NMB T.D. 1192		Germany	Aragonian	Langhian
<i>Paradicrocerus elegantulus</i>	NMB T.D. 1196		Germany	Aragonian	Langhian
<i>Paradicrocerus elegantulus</i>	NMB T.D. 1194		Germany	Aragonian	Langhian
<i>Paradicrocerus elegantulus</i>	NMB T.D. 1195		Germany	Aragonian	Langhian
<i>Procervulus praelucidus</i>	SNSB-BSPG 1937 II 16842		Wintershof West, Ger-many	Ramblian	Burdigalian
<i>Procervulus praelucidus</i>	SNSB-BSPG 1937 II 16845		Wintershof West, Ger-many	Ramblian	Burdigalian
<i>Procervulus praelucidus</i>	SNSB-BSPG 1937 II 16810		Wintershof West, Ger-many	Ramblian	Burdigalian
<i>Procervulus dichotomus</i>	SNSB-BSPG no no.		Langenau, Germany	Ramblian	Burdigalian
<i>Procervulus dichotomus</i>	MNHN FS 286		Faluns d'Anjou/ Touraine, France	Ramblian	Burdigalian
<i>Procervulus dichotomus</i>	MNHN Ba 835		Baigneaux, France	Ramblian	Burdigalian
<i>Procervulus dichotomus</i>	MNHN Ba 836		Baigneaux, France	Ramblian	Burdigalian
<i>Procervulus dichotomus</i>	MNHN Ba 835		Baigneaux, France	Ramblian	Burdigalian
<i>Procervulus dichotomus</i>	MNHN Ba 836		Baigneaux, France	Ramblian	Burdigalian
<i>Procervulus dichotomus</i>	MNHN Ba 833		Baigneaux, France	Ramblian	Burdigalian
<i>Procervulus dichotomus</i>	MNHN Ba 837		Baigneaux, France	Ramblian	Burdigalian
<i>Procervulus dichotomus</i>	MNHN FS 286		Faluns d'Anjou/ Touraine, France	Ramblian	Burdigalian
<i>Procervulus dichotomus</i>	MNHN FS 1401		Faluns d'Anjou/ Touraine, France	Ramblian	Burdigalian
<i>Procervulus dichotomus</i>	MNHN FS 5123		Faluns d'Anjou/ Touraine, France	Ramblian	Burdigalian
<i>Procervulus dichotomus</i>	MNHN FS 1594		Faluns d'Anjou/ Touraine, France	Ramblian	Burdigalian
<i>Procervulus dichotomus</i>	MNHN FS 284		Faluns d'Anjou/ Touraine, France	Ramblian	Burdigalian

Table C.2: List of examined extant male specimens with their respective collection numbers.

Species	Collection ID
<i>Alces alces</i>	ZSM 1970/8
<i>Alces alces</i>	ZSM 1962/298
<i>Alces alces</i>	ZSM 1963/37
<i>Alces alces</i>	ZSM 1962/298
<i>Alces alces</i>	UMZC H.17691
<i>Axis axis</i>	BMNH 46.199
<i>Axis axis</i>	BMNH 697 t
<i>Axis axis</i>	BMNH 67.4.12.240
<i>Axis kuhli</i>	NMS 2015 148
<i>Axis kuhli</i>	NMS 2000 378 001
<i>Axis porcinus</i>	BMNH 27.2.14.106
<i>Axis porcinus</i>	MNHN 1933 212
<i>Axis porcinus</i>	MNHN 1904 60
<i>Axis porcinus</i>	UMZC H.16052
<i>Blastocerus dichotomus</i>	ZSM 1931/419
<i>Blastocerus dichotomus</i>	ZSM 1931/382
<i>Blastocerus dichotomus</i>	BMNH 98.10.11.1
<i>Blastocerus dichotomus</i>	ZSM 1926/283
<i>Blastocerus dichotomus</i>	ZSM 1931/397
<i>Capreolus capreolus</i>	ZSM 1940/138
<i>Capreolus capreolus</i>	ZSM 1955/130
<i>Capreolus capreolus</i>	UMZC H.18004
<i>Capreolus pygargus</i>	BMNH 1938.5.18.1
<i>Capreolus pygargus</i>	BMNH 42.3.13.1
<i>Capreolus pygargus</i>	BMNH 31.6.1.75
<i>Capreolus pygargus</i>	MNHN AE734
<i>Cervus albirostris</i>	BMNH 92.10.11.1
<i>Cervus albirostris</i>	NMS 1999 187 14
<i>Cervus albirostris</i>	NMS 2009 129 3
<i>Cervus canadensis</i>	NMB C 2642
<i>Cervus elaphus</i>	ZSM 1956/224
<i>Cervus elaphus</i>	ZSM 1971/695
<i>Cervus elaphus</i>	ZSM 1956/66
<i>Cervus elaphus</i>	ZSM 1962/205
<i>Cervus elaphus</i>	UMZC H.16620
<i>Cervus elaphus</i>	SNSB-BSPG 1955 I 513
<i>Cervus nippon</i>	ZSM 1961/285
<i>Cervus nippon</i>	BMNH 85.2.23.1
<i>Cervus nippon</i>	BMNH 72.1066

Table C.2: Continued

<i>Dama dama</i>	ZSM 2010/302
<i>Dama dama</i>	ZSM no nr
<i>Dama dama</i>	ZSM 1954/253
<i>Dama dama</i>	ZSM 1964/222
<i>Dama dama</i>	UMZC H.17174
<i>Dama dama</i>	UMZC H.17175
<i>Dama mesopotamica</i>	ZSM 1980/179
<i>Dama mesopotamica</i>	ZSM 1975/25
<i>Dama mesopotamica</i>	ZSM 2007
<i>Elaphodus cephalophus</i>	MNHN A 1480
<i>Elaphodus cephalophus</i>	MNHN 1901 1349
<i>Elaphodus cephalophus</i>	BMNH 26.9.1.1
<i>Elaphodus ichangensis</i>	BMNH 1.3.2.17
<i>Elaphurus davidianus</i>	MNHN 1966-02
<i>Elaphurus davidianus</i>	UMZC H.16231
<i>Elaphurus davidianus</i>	UMZC H.16.235
<i>Hippocamelus</i> sp.	MNHN 1907-283
<i>Hippocamelus antisensis</i>	BMNH 97.11.11.4
<i>Hippocamelus antisensis</i>	ZMB 2000
<i>Hippocamelus bisulcus</i>	ZSM 1949/1355
<i>Hippocamelus bisulcus</i>	BMNH 72.11.11.1
<i>Mazama americana</i>	ZSM 1982/159
<i>Mazama americana</i>	ZMH 9462
<i>Mazama bricenii</i>	BMNH 1913.4.24.3
<i>Mazama chunyi</i>	BMNH 67.1362
<i>Mazama gouazoubira</i>	ZSM 1930/67
<i>Mazama nemorivaga</i>	NMB 6672
<i>Mazama rufina</i>	ZSM 1927/41
<i>Mazama rufina</i>	NHMW 528
<i>Muntiacus atherodes</i>	BMNH 71.3088
<i>Muntiacus atherodes</i>	ZMB 70933
<i>Muntiacus crinifrons</i>	BMNH 91.3.4.1
<i>Muntiacus feae</i>	BMNH 32.11.1.171
<i>Muntiacus muntjak</i>	ZSM 1966/206
<i>Muntiacus muntjak</i>	ZSM 1966/237a & b
<i>Muntiacus muntjak</i>	BMNH 85.754
<i>Muntiacus muntjak</i>	ZMH 4919
<i>Muntiacus</i> cf. <i>reevesi</i>	UMZC H.15531
<i>Muntiacus reevesi</i>	UMZC H.15537
<i>Muntiacus reevesi</i>	UMZC H.15535
<i>Muntiacus reevesi</i>	ZMH 8062
<i>Muntiacus truongsongensis</i>	BMNH 2010.462
<i>Muntiacus truongsongensis</i>	BMNH 2010.459
<i>Muntiacus vuquangensis</i>	BMNH 2010.484

Table C.2: Continued

<i>Odocoileus cf. hemionus</i>	UMZC H.18641
<i>Odocoileus hemionus</i>	ZSM 1971/720
<i>Odocoileus hemionus</i>	MNHN AE722
<i>Odocoileus hemionus</i>	MNHN AE 714 (1539)
<i>Odocoileus hemionus</i>	MNHN AE724
<i>Odocoileus hemionus</i>	UMZC H.18621
<i>Odocoileus virginianus</i>	ZSM 1971/531
<i>Odocoileus virginianus</i>	ZSM 1971/555
<i>Odocoileus virginianus</i>	BMNH 2.3.5.25
<i>Odocoileus virginianus</i>	UMZC H.18448
<i>Odocoileus virginianus</i>	UMZC H.18441
<i>Ozotoceros bezoarticus</i>	BMNH 14.11.9.1
<i>Ozotoceros bezoarticus</i>	UMZC H.18781
<i>Ozotoceros bezoarticus</i>	NMB C 2313
<i>Ozotoceros bezoarticus</i>	NMB C 2312
<i>Pudu puda</i>	ZSM 1954/448
<i>Pudu puda</i>	ZSM AM/1067
<i>Pudu puda</i>	MNHN 2006 501
<i>Rangifer tarandus</i>	ZSM 1959/211
<i>Rangifer tarandus</i>	ZSM 195/296
<i>Rucervus duvaucelii</i>	ZSM1954/235
<i>Rucervus duvaucelii</i>	ZSM 1971/744
<i>Rucervus duvaucelii</i>	ZSM 1956/239
<i>Rucervus duvaucelii</i>	ZSM 1954/269
<i>Rucervus duvaucelii</i>	NMS 1913 178
<i>Rucervus eldii</i>	ZSM 1905/3018
<i>Rucervus eldii</i>	UMZC H.16191
<i>Rucervus eldii</i>	NMS 2004 54
<i>Rucervus eldii</i>	NMS 2003 4
<i>Rucervus schomburgki</i>	ZSM 1918/28
<i>Rucervus schomburgki</i>	BMNH 8.3.17.5
<i>Rucervus schomburgki</i>	BMNH 59.4847
<i>Rucervus schomburgki</i>	BMNH 48.325
<i>Rucervus schomburgki</i>	BMNH 51.543
<i>Rucervus schomburgki</i>	BMNH 751393
<i>Rucervus schomburgki</i>	NHMW 28793
<i>Rusa alfredi</i>	NMS 2009 37 3
<i>Rusa alfredi</i>	NMS 2005 113

Table C.2: Continued

<i>Rusa marianna</i>	BMNH 655c
<i>Rusa marianna</i>	MNHN A11310
<i>Rusa timorensis</i>	BMNH 97.4.3.2
<i>Rusa timorensis</i>	BMNH 61.12.11.27
<i>Rusa timorensis</i>	MNHN 1927-44
<i>Rusa unicolor</i>	ZSM 1949/1190
<i>Rusa unicolor</i>	ZSM 1949/1191
<i>Rusa unicolor</i>	BMNH 24.10.5.49
<i>Rusa unicolor</i>	BMNH 43.1.26.16
<i>Rusa unicolor</i>	MNHN 1884-543
<i>Rusa unicolor</i>	UMZC H.15911
<i>Rusa unicolor</i>	ZMH 9398

D Measurements

Table D.1: List of measurements taken on the mandible including the dentition. Abbreviations correspond to those in Figures D.1. Measurements are on <https://edoc.ub.uni-muenchen.de/view/autoren/index.H.html>.

Abbr.	Measuring distances - Mandibula
pxL	Length of lower premolar
WAB	Total width of lower antepremolar tooth arch at base
WAT	Total width of lower antepremolar tooth arch at tips
TLL	Total length of lower premolars & molars
LLP	Length of lower premolars
LLM	Length of lower molars
LSY	Length of symphysis
TLM	Total length of mandibula
HRM	Height of ramus mandibulae
DCC	Distance: dorsal end of processus coronoideus - processus condylaris
LIM	Length of incisura mandibulae (parallel to tooth row at level of ventral rim of articulation surface of pr. condylaris)
LMD	Length of diastema
LCO	Length of processus coronoideus (at level of articular surface of pr. condylaris)

Table D.2: List of measurements taken on the cranium including the dentition. Abbreviations correspond to those in Figures D.2 and D.3. Measurements are on <https://edoc.ub.uni-muenchen.de/view/autoren/index.H.html>.

Abbr.	Measuring distances - Cranium
PxL	Length of upper premolar
LUP	Length of upper premolars
LUM	Length of upper molars
ICD	Distance between cristae on diastema on maxilla (smallest)
WMX	Width of maxilla at diastema
TLP	Total length of palate
TWP	Total width of palate between tooth rows
IPF	Distance between foramina palatina
TLS	Total length skull (ventral)
LBU	Length of bulla
WBU	Width of bulla
WBC	Width of braincase (widest)
NFM	Distance: crista nuchae - dorsal rim foramen magnum
NBO	Distance: crista nuchae - ventral end of basioccipital
OPX	Distance: anterior rim of orbita - anterior end of praemaxilla
LOR	Length of orbita
HOR	Height of orbita
LPV	Length of praeorbital vacuity
WPV	Width of praeorbital vacuity
LNA	Length of nasal (along midline)
TWS	Total width of skull (usually at zygomatic arch/orbita)
LLA	Length of lacrimal (facial portion)
HLA	Height of lacrimal (facial portion)
LPM	Medial length of pedicle
LPL	Lateral length of pedicle
PAP	Pedicle diameter anterior - posterior
PML	Pedicle diameter medial - lateral
LAN	Length of antler (main beam)

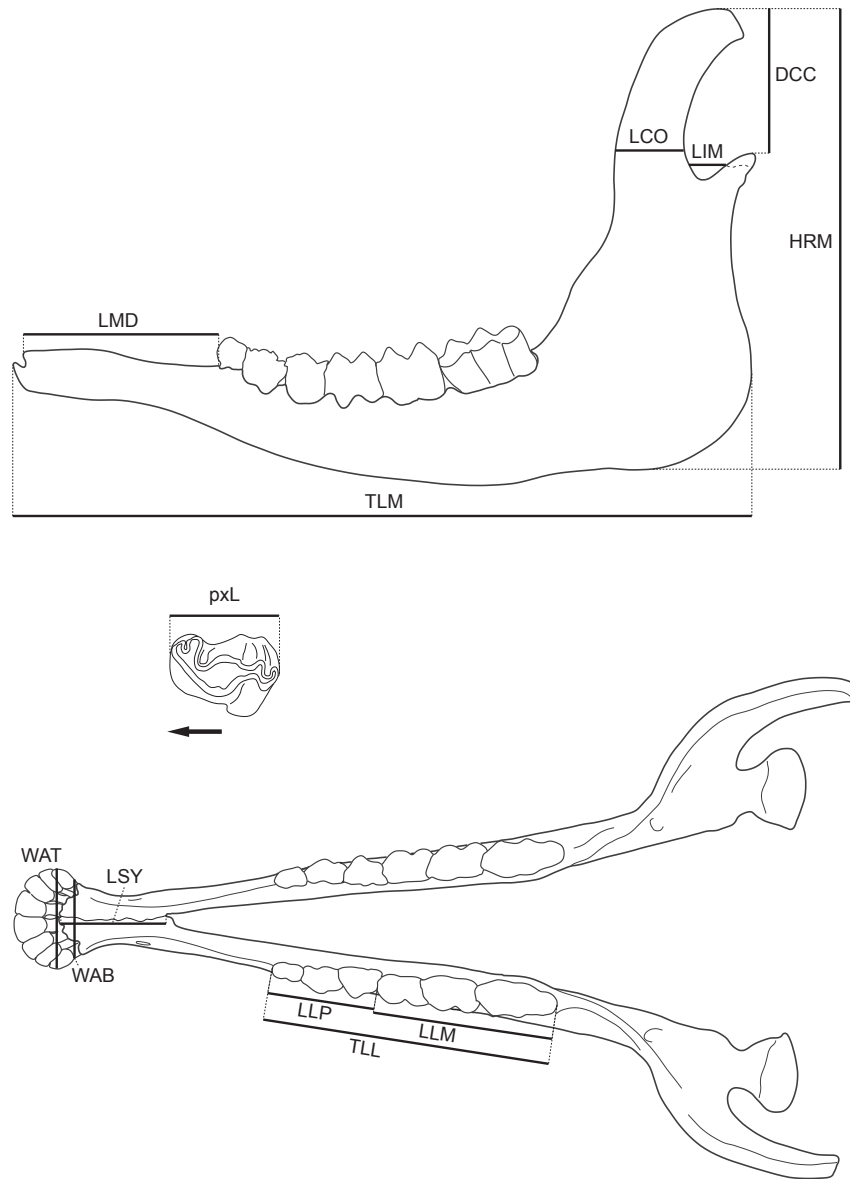


Figure D.1: All measuring distances of the mandible in lateral and dorsal view and of the lower premolar.

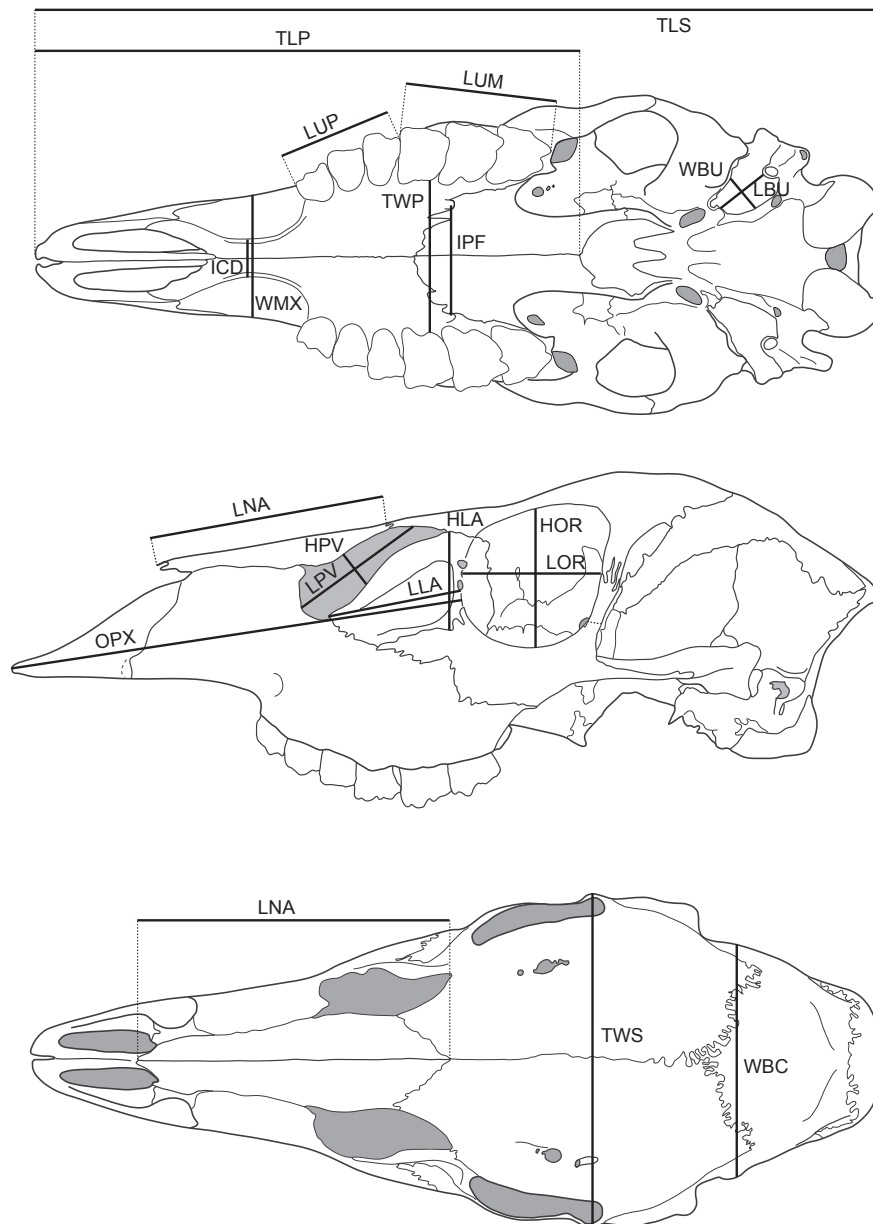


Figure D.2: All measuring distances of the skull in ventral, lateral and dorsal view.

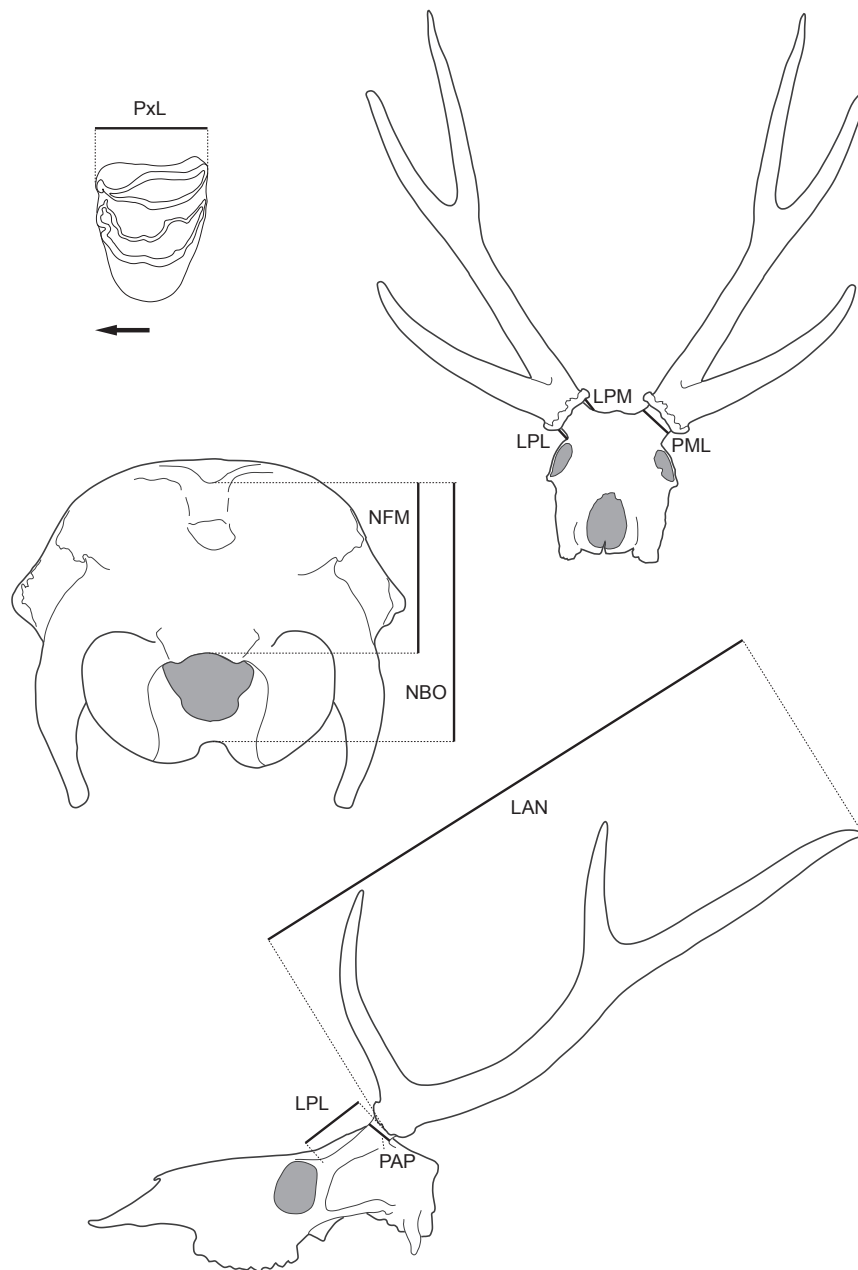


Figure D.3: All measuring distances of the skull in occipital view of the upper premolar, and of antlers and pedicles.

E Morphological Description of Extant and Fossil Cervids

E.1 Morphology Extant Cervidae

E.1.1 Capreolinae

Alces alces Linnaeus 1758

The posterior part of the corpus mandibulae is thickened and the foramen mandibularis large. There are strong crests on and anterior to the angulus mandibulae.

Skulls of *Alces alces* are characterised by very short nasals and elongated slender prae-maxillae; the dorsal skull outline in lateral view is concave. The nasals have much shorter medial than lateral nasal processes. At the praeorbital vacuity, nasals protrude posteroven-trally between the maxilla and the frontal. Sometimes, there is a prominent facial crest on the maxilla. The fossa lacrimalis is shallow even in males and almost absent in females. The zygomatic arch is slender with a dorsally protruding process on its posterior part. The supraorbital foramina are small. The supraoccipital is elongated posteriad, which is unusual in cervids. The basioccipital shows weak ridges, the auditory bullae are small. There is a sulcus on the tuber maxillae.

Generally, the skull is characterised by distinctive features, such as crests or protrusions, especially in males. The frontal-frontal suture may form a strong bulge. Males can have up to four more or less strong protrusions on the parietal, these are weaker, but often still visible in females. In some specimens, there is an incision between the lacrimal and frontal at the orbit. The foramina lacrimalis are on the external side of the orbit rim and are offset to each other. In ZSM 1970/8, there is a triangular-oval bone protrusion between the nasals and frontals.

In contrast to all other cervids, the lateral part of the pedicle is shorter than the medial part. Therefore, the pedicle and antler shafts are orientated horizontally-laterally and perpendicular rather than parallel to the sagittal plane. The antlers are characterised by a shaft and a large palmated main beam with multiple points on each side.

In the p2 anterior elements are weakly developed or absent; there is a very short transverse cristid and the posterolingual conid is oriented posteriad. The p3 shows an initial molarisation, the anterior styloid and conid are weakly present, the mesolingual conid is separated from the transverse cristid. The p4 is molariform showing an isolated anterolabial cristid, which is often fused with the transverse cristid, and separate from the posterolabial conid. The mesolingual conid is separate from the transverse cristid and the posterolingual

conid and posterior cristid are separate until later wear. There is a separate posterolabial conid with a short posterior stylid. In most premolars, the posterolabial conid bulges labiad. There is a prominent labial incision between the mesolabial and posterolabial conid. The postmetacristid and metastylid on the molars are strongly lingually oriented; none of the molar elements are fused. Ectostylids are commonly present on all molars. The m3 often shows a separate hypoconulid and entoconulid. In comparison to other cervids, the i1 is only a little broader than the other incisors.

All upper premolars have a separate posterior style and a central fold. The P2 has a separate anterolingual and posterolingual cone; the anterolingual crista is fused with the anterior style, which is not the case in P3 and P4. The P4 shows a strong labial style with a crest and the anterolabial crista is strongly bent towards labial with an anterior-posterior oriented anterior style. All upper molars have separate lingual and labial complexes, the cristae are separated from the styles; a protocone and metaconule fold is present and an entostyle is present at least on M3 in most specimens. There are no upper canines.

Blastocerus dichotomus Illiger 1815

The anterior side of the ramus mandibulae is inclined, the processus coronoideus is curved posteriad. The foramen mandibularis is large; the ramus mandibulae is strongly indented above the angulus mandibulae.

Skulls of *Blastocerus dichotomus* are generally long and slender in dorsal view, particularly the snout is slender. Lacrimal foramina are situated on the orbit rim and in line, the fossa lacrimalis is deep. The praeorbital vacuity is relatively large. Some specimens show two additional foramina on the palate in asymmetrical position, the foramina palatinae are far apart. There are several supraorbital foramina. The bullae are medium-sized and have several small processes.

The pedicles are strong. The antlers have a relatively long shaft, from which they bifurcate; the anterior and posterior part of the beam bifurcate again further distal. Four tines per antler is the general antler morphology in *Blastocerus dichotomus*.

On the p2 the anterior stylid is commonly absent and shows a very long posterolingual conid; the posterolabial conid bulges labiad, the posterior stylid is present. The p3 has an anterior stylid, the posterolabial conid is elongated labiad, forming a short spike. The anterior stylid is present on the p4, the mesolingual conid and associated cristids can be separate from the transverse cristid, the posterolingual conid is long including a posterior cristid, the posterior stylid is short. Sometimes the posterolabial cristid is separated from the mesolabial conid; the fusion of anterolingual cristid with anterior conid is possible. Initial molarisation of the p4 is present. On the lower molars two or more ectostylids are present, the premetacristid and preprotocristid fuse in later wear. The entoconulid and hypoconulid on the m3 are almost round, sometimes with an additional fold. The i1 and i2 are slightly broadened.

The P2 has a separate anterolingual and posterolingual cone. It shows generally an interesting morphology sometimes with a reduced or barely developed anterolingual crista and sometimes with two central folds. The P3 and P4 have an elongated central fold, which sometimes connects with the posterolabial cone/posterolabial crista. The P4 has a large lingual part. All upper molars have a prominent protocone fold and there is no fusion between the postprotocrista and premetaconulecrista; entostyles are variably

present. Some specimens show small alveoli at the position of C indicating possible presence of deciduous upper canines; however, permanent upper canines could not be observed.

Capreolus

Capreolus capreolus Linnaeus 1758

The mandible has a relatively broad ramus, the angulus mandibulae is moderately indented.

The nasal and praemaxillary are mostly in contact. The dorsal rim of the foramen magnum is two-lobed. Sometimes, the vomer is visible between the maxillary and praemaxillary ventrally. The pedicles are slender and closely together. The antlers are strongly ornamented with ridges and nodes, always with a long shaft and usually three tines. Sometimes the most proximal parts of the shaft and burr from one side are in contact with the ones from the other side.

The p2 has a relatively simple morphology and is short; its stylids and cristids are not elongated. In the p3 the anterior stylid is present, as is the mesolingual conid, the transverse cristid, the posterolingual conid, and the posterior stylid including a cristid, which is oriented transversely to the mandible axis. All of these structures are elongated. The molariform p4 shows a transverse posterolingual conid, a short posterior stylid, which sometimes lacks a cristid, a short transverse cristid, and a mesolingual conid, which is fused with the anterior conid. There are very deep labial incisions on all premolars. There are prominent ectostylids on all lower molars. In the m3 the ento- and hypoconulid may be separated (only in 1 specimen), otherwise they are crescent shaped. The i1 are slightly broadened and there is a v-shaped gap between the left and the right i1.

In the P2 the anterolingual and posterolingual cone are present, sometimes completely separated from each other. All premolars have one to two prominent central folds and sometimes accessory folding. All upper molars have separated postparacrista and premetacrista and separated postprotocrista and premetaconulecrista. The metaconule fold is present on all molars, the protocone fold is variably present. The upper canine is absent.

Capreolus pygargus Pallas 1771

The mandible is robustly built; the angulus mandibulae is indented, particularly on the ventral side of the corpus mandibulae. The processus coronoideus is relatively broad and slightly leaning posteriad.

The skull is short and robust; generally, this species is larger than the *Capreolus capreolus*. The praemaxillaries often have two mediad pointing processes on the most anterior part. The fossa lacrimalis is relatively shallow. The dorsal rim of the foramen magnum is two-lobed. Some females have protuberances on the frontal, where the pedicles would grow in males. There are numerous perforations on the parietal and squamosal. The processi praemaxillaris of the nasal are equally long. The foramina lacrimalis are on the orbit rim and level to each other.

The antlers are characterised by a very long shaft and a distal usually three-tined end. The ornamentation is rich, but not as strong as in *Capreolus capreolus*.

The p2 is short, posterior elements are more developed than anterior elements. The p3 has an anterior stylid and a prominent mesolingual conid, sometimes with initial cristids;

the transverse cristid can be zig-zagging. The medial and posterior elements are oriented in parallel and transverse to the mandible axis, the posterior stylid is short. In the p4, the posterolabial conid is prominent, the mesolingual conid is fused with the anterior conid, but not with the posterior elements. The transverse cristid is short. There are very deep labial incisions on p3 and p4. On the lower molars ectostylids are rarely present, in the m3 the hypoconulid is more prominent than the entoconulid. Weak anterior cingulids are present in a few specimens. The lower incisors and canines are relatively small, the i1 is slightly broadened.

All upper premolars possess one to two prominent central folds. On the P2 and P3 there is a weak incision between the antero- and posterolingual cone. On the P3 and P4 the anterior styles are bent labiad. All upper molars have separate postparacristae and premetacristae; the metaconule folds are present and the protocone folds are sometimes present. Entostyles are rarely present, usually only on one molar. Mesostyles are often bent labiad. The upper canine is absent.

Hippocamelus

Hippocamelus antisensis d'Orbigny 1834

The ramus mandibulae is inclined posteriad, the angulus mandibulae is round and only slightly indented on the ventral side. The processus coronoideus is broad.

The praemaxillaries often have two mediad pointing processes on the most anterior part. The cristae maxillaris are prominent in males. The zygomatic arch is thin and has a dorsally pointing protrusion dorsal to the fossa mandibularis. There are often more than two (usually four) palatine foramina. There is a deep groove posterior to the posterior tuberosities of the basioccipital in males. The lacrimal fossa is deep. There are multiple supraorbital foramina. Most females have small processii posterodorsal to the orbit rim. Both lacrimal foramina are on the orbit rim and level to each other. The auditory bullae are relatively small. The antlers are moderately sized and bifurcating, the shaft is short. The anterior beam is curved, the posterior beam is straight. Both are ridged and nodose.

The p2 is short with a simple morphology, the posterolingual conid is present. On the p3 the anterior stylid is present, the transverse cristid is slightly offset; the orientation of the posterolingual conid and the posterior stylid is transverse. There are deep labial incisions on the p3 and p4. On the p4 the mesolingual conid is often fused with the anterior conid; in these cases the transverse cristid is separate from the mesolingual conid. The posterior part of the p4 is often much smaller than the anterior part. The posterior stylid is reduced and the connection between the posterolingual conid and posterolabial conid is thin. Ectostylids on lower molars are usually absent. The third lobe of m3 often consists only of the hypoconulid. The lower incisors and canines are almost equally broad, relatively straight/parallel, and less arched. The cervid-specific broadening of the i1 is absent.

All upper premolars have at least one central fold. The P2 often has reduced lingual elements, missing the anterolingual crista. All premolars usually have an incision between the antero- and posterolingual cone, the P4 often has two separated cones. The entostyles on the upper molars are absent. M3 has a protocone fold, the other upper molars have no folds. The upper canines (or large alveoli thereof) are regularly present.

Hippocamelus bisulcus Molina 1782

The mandible has a thin corpus mandibulae, a weakly inclined ramus mandibulae, and an indented angulus mandibulae. The lacrimal fossae are deep. The lacrimal foramina are situated on the orbit rim and on top of each other. The tuber maxillae is well developed. There are commonly four palatine foramina. There are a lot of perforations on the squamosal and the parietal. The zygomatic arch is thin with a dorsally oriented protrusion dorsal to the fossa mandibularis. The auditory bullae are relatively small. There is one prominent supraorbital foramen and several small additional foramina. Females often have a posterodorsal pointing protrusion dorsal to the orbit rim. The antlers are normally bifurcating, weakly curved with a short shaft. The posterior beam can have accessory tines.

On the p2 the anterior conid is present, the transverse cristid points posteriad; the posterolingual conid and the posterior stylid are long. The anterior stylid is present on the p3; there is a long anterior conid, and a zig-zagging transverse cristid. The mesolingual conid is barely developed and the posterolingual conid has a thin connection to the posterolabial conid. There are deep labial incisions on the p3 and p4. On the p4 the mesolingual conid is connected with the anterior conid; the posterolingual conid can be isolated, the posterior stylid is reduced. The posterolabial conid protrudes labiad. The lower molars have a simple morphology, they sometimes have a weakly developed anterior cingulid, while ectostylids are absent. The third lobe of m3 is usually crescent-shaped, but can be reduced to two small isolated conulids.

Similarly to *Hippocamelus antisensis*, the crowns of the lower incisors are only weakly broadened and more parallel to each other than arched.

The P2 is relatively long with an interesting morphology; it sometimes has reduced lingual elements and dominant labial elements. There is a weak central fold. P2 and P3 commonly have an incision between the antero- and posterolingual cone. P3 and P4 have at least one prominent central fold, often several central folds. Low weak entostyles are present on the upper molars, the protocone fold is commonly present, the metaconule fold is variably present (here on M2). Alveoli of the upper canines are variably present, but no adult with in situ canines was observed. This indicates that they are potentially only present as deciduous teeth.

Hydropotes inermis Swinhoe 1870

The corpus mandibulae is thin with a strongly indented angulus mandibulae, the processus coronoideus is relatively broad in lateral view and curving backwards. The anterior part of the diastema has a strong dorsal protrusion. The skull is slender with a short snout and a pointy snout tip. In males the maxillary at the alveoli of the enlarged canines is extremely broadened. There is one prominent supraorbital foramen with a deep sulcus surrounding it. In dorsal view the posterior part of the zygomatic arch curves laterad. The auditory bullae are relatively big including a median process. The praeorbital vacuity is oriented more dorsoventrally. The fossa lacrimalis is deep. The temporal lines on the parietal are prominent. The medial processus praemaxillaris on the nasal is longer than the lateral one. The antlers are missing in this cervid species.

The p2 has a simple morphology, the anterior elements are reduced, the posterolabial conid and the posterior stylid are prominent, sometimes connecting with the transverse

cristid (via the mesolingual conid). The anterior stylid is present on the p3; the transverse cristid, posterolingual conid, and posterior stylid are long, almost parallel, and transverse to the mandible axis. The p3 has a moderate, the p4 a deep labial incision. The molariform p4 often has no anterior stylid, the mesolingual conid is connected to the anterior conid, sometimes the mesolingual conid is separate from the transverse cristid; the connection between the posterolingual conid and the posterolabial conid is thin, the posterolabial conid is prominent and pointing labiad. The lower molars sometimes have a weak anterior cingulid. Ectostylids are present on at least two molars; the m3 has a well developed hypoconulid and a weak entoconulid. The lower incisors and canines are fanned, the i1 is broadened and there is a v-shaped gap between the left and right i1.

The anterior elements of the P2 are reduced, the posterolingual cone is prominent, from which the central fold originates sometimes connecting with the mesolabial crista. The P2 and P3 often have an incision between the antero- and posterolingual cone, which are sometimes completely separated. The P3 has a prominent central fold pointing posteriad. The P4 has one or two central folds. Entostyles are variably present on upper molars, and there is no fusion between premetaconulecristae and postprotocristae. Upper canines are strongly enlarged in males and contain an opening on the lingual side; small upper canines are always present in females.

Mazama

Mazama americana Erxleben 1777

The mandible is relatively robust considering the small size; the angulus mandibulae is strongly indented and elongated posteroventrally. The processus coronoideus is relatively broad and curving backwards.

The skulls are robust and have a relatively large viscerocranial portion. The orbitae are large, the lacrimal foramina are on the orbit rim and on top of each other. Both processi praemaxillaris of the nasals are equally long. The lacrimal fossa is shallow. The auditory bullae are round and inflated. There are often four palatine foramina instead of two. Females usually have a well-developed triangular protrusion postero-dorsally to the orbit rim.

There is a strong crest on the ventral side of the pedicle, which continues anteriad as the postorbital bar. The antlers are short single spikes and are richly ornamented on the proximal end.

On the p2 the anterior, mesial, and posterior elements are short, the posterior stylid is variably present. In some specimens the p2 is even reduced to a small cusp or missing. On the p3 the anterior stylid is variably present, the transverse cristid is short, and the mesolingual conid weak. The posterolabial conid sometimes points labiad. On the p4 the mesolingual conid is often fused with the anterior conid, the transverse cristid is separate from the mesolingual conid. The posterolingual conid can be isolated, the posterolabial conid is well developed pointing labiad. The ectostylids are variably present on the lower molars; the metaconid-metastylid-complex is tilted linguad. A fusion of the postprotocristids and preentocristids is common. The third lobe on the m3 is crescent-shaped. Lower incisors and canines have a relatively short crown; the i1 is distinctively broadened, there is a v-shaped gap between the right and left i1.

The P2 is relatively long, the lingual wall is reduced, and its posterior elements are more developed than the anterior elements. All upper premolars have a prominent central fold and show variably an incision between the antero- and posterolingual cone, which is sometimes entirely separated on the P4. The anterior and posterior styles can be strongly bent. Entostyles are mostly present on two or more molars. All upper molars have a protocone fold and metaconule fold. There is no fusion between the postprotocristae and premetaconulecristae. The mesostyles are well developed. The upper canines are absent in adult individuals, but small alveoli in juveniles indicate presence of deciduous upper canines.

Mazama bricenii Thomas 1908

The mandible is slender and curved; the angulus mandibulae is extremely indented and elongated posteroventrally. The processus coronoideus is relatively broad in lateral view and strongly curving posteriad.

Skulls are short; the frontals have a convex transition to the nasals and both processus praemaxillaris of the nasals are equally long. The lacrimal fossa is deep and both lacrimal foramina are on the orbit rim on top of each other. The processus paracondylaris are curved mediad; the foramen lacerum between the bulla and the basioccipital is very large. The supraorbital foramina are moderately sized and surrounded by a sulcus. The foramen ovale is large. Females have a ridge postero-dorsally to the orbit rim. The antlers in males are single-spiked and they are positioned far posterior to the orbit. The pedicles have a prominent crest on the ventral side.

The p2 has developed anterior, mesial and posterior elements, p2 and p3 have a weak labial incision. The p3 has an anterior stylid, the transverse cristid is strong; the posterior elements are partly reduced and the posterolingual conid is isolated. The p4 is molariform with a lingual wall, which closes the anterior valley in later wear. In early wear the transverse cristid can be separate from the mesolingual conid. The p4 has a deep labial incision. The posterior stylid is absent. Lower molars have a weak anterior cingulid. The ectostylids are present on two or more molars. The third lobe on m3 consists mainly of the hypoconulid, the entoconulid is thin; both form a crescent.

The lower incisors and canines are short and the i1 is only weakly broadened with a v-shaped gap between the left and the right i1. All upper premolars have at least one central fold; P3 and P4 commonly with multiple central folds. Sometimes premolars have a fold originating from the labial crista. On the P2 anterolingual elements are reduced; P2 and P3 have an incision between the antero- and the posterolingual cone. Entostyles are present on all molars; there are protocone and metaconule folds on all molars. Parastyles are bent posteriad. Upper canines are absent in adults, but small alveoli indicate potential presence of deciduous upper canines.

Mazama chunyi Hershkovitz 1959

The mandible is short and slender with an extremely posteriorly elongated angulus mandibulae. The ramus mandibulae is perpendicular with a relatively broad processus coronoideus curving posteriad. The snout is very short. The cristae on the ventral side of the maxillary are far apart. The lacrimal fossa is shallow, both lacrimal foramina are situated on the orbit rim and on top of each other. The praeorbital vacuity is small. The lateral palatal indents extend far anterior and the vomer extends far posterior. The foramen lacerum is large. The os incisivum is short in ventral view.

The p2 is very slender, mainly oriented in anteroposterior direction, missing all elements with a transverse component. The p3 has an anterior stylid and conid, a mesolingual conid and a transverse cristid, and the posterior elements are reduced; the posterolingual conid is tiny and connected with the posterolingual cristid. The p4 is moderately molariform, with a lingual wall and a connection between the anterolingual cristid and the anterior conid. The transverse cristid is not connected to the mesolingual conid and the posterolingual conid is isolated. There is no posterior stylid. Ectostylids are present on at least two molars. The third lobe of the m3 is crescent-shaped and open anteriorly.

The i1 is distinctively broadened with a small v-shaped gap between the left and the right incisor; the crowns of lower incisors and canines are relatively long. The P2 has a long central fold connecting to the mesolabial crista/cones, the posterior part of P2 is more prominent and there is a weak incision between the antero- and posterolingual cone. P3 and P4 have at least two central folds; the orientation of all upper premolars is slightly tilted to the jaw axis. All upper molars have entostyles. A protocone fold is present on all molars, a weak metaconule fold is present on M1 and M3. No evidence for the presence of upper canines was observed.

Mazama gouazoubira Fischer 1814

The mandible is slender with a round, strongly indented and elongated angulus mandibulae. The ramus mandibulae is perpendicular with a relatively broad processus coronoideus curving posteriad. The skull is short, with a shallow lacrimal fossa. The praeorbital vacuity is large and dorsoventrally oriented. There are several supraorbital foramina embedded in a sulcus. The nasals have convex protrusions into the frontals in dorsal view. Both lacrimal foramina are situated on the orbit rim on top of each other. The protuberantia on the crista nuchae is prominent. The pedicles are strongly inclined with a ventral ridge. Antlers are single-tined and situated far posterior on the skull. Females have a prominent ridge on the posteroventral corner of the orbit rim.

On the p2, a weak anterior conid is present and the transverse cristid, posterolingual conid, and posterior stylid. The p3 has an anterior stylid, a long transverse cristid, weak mesolingual and -labial conid; posterior elements are long. The p4 is molariform with a lingual wall, which is not connected to the anterior conid; the transverse cristid is sometimes disconnected from the mesolingual conid and the posterolingual conid is sometimes isolated. The p3 and p4 have moderate to strong labial incisions. Lower molars can have a weak anterior cingulid, metastylids are bent linguad. An ectostylid is variably present on the lower molars; the third lobe of the m3 is crescent shaped and open anteriorly. The lower i1 is distinctively broadened, curving strongly towards i2, and there is a small v-shaped gap between both i1. All upper premolars have one prominent and at least one additional

central fold. The premolars are slightly tilted from the jaw axis. The P2 is longer and rounder than the P3 and P4. All upper molars have a protocone fold and a metaconule fold. Entostyles are variably present on one molar. The upper canine is missing in adults, but the deciduous upper canines are regularly present in juvenile specimens.

Mazama nemorivaga Cuvier 1817

The angulus mandibulae varies in shape from broad and round to strongly indented and elongated. The ramus mandibulae is perpendicular with a slightly posteriad curving processus coronoideus. The skull is short with a moderate lacrimal fossa. The praeorbital vacuity is large, both lacrimal foramina are on the orbit rim and on top of each other. The nasals have convex protrusions at the nasal-frontal contact. Both processi praemaxillaris of the nasals are equally long. The protrusion on the crista nuchae is prominent, the dorsal rim of the foramen magnum is two-lobed. The antlers are single-tined; the pedicles have a prominent ventral ridge. Females have strong protrusions above the posterodorsal corner of the orbit.

All lower premolars have a moderate to deep labial incision. the p2 has a transverse cristid, posterolingual conid, posterior stylid and a weak anterior conid. The p3 has an additional weak anterior stylid. The p4 is molariform with a lingual wall, which connects to the anterior conid in later wear. the transverse cristid is not connected to the mesolingual conid, the posterolingual conid is isolated. The lower molars sometimes have a weak anterior cingulid, ectostylids are variably present. The third lobe of the m3 is crescent-shaped. The lower i1 is distinctively broadened. The P2 has reduced lingual elements and is long and slender; the central fold connects with the labial cones. P3 and P4 have at least one prominent central fold, anterior and posterior styles are bent. Upper molars have prominent protocone folds and weak metaconule folds. An entostyle is variably present on one molar. Small alveoli for the upper C indicate presence of deciduous upper canines in juveniles.

Mazama rufina Pucheran 1851

The mandible is slender with a strongly indented angulus mandibulae. The anterior edge of the ramus mandibulae is inclined posteriad, the processus coronoideus is strongly curving posteriad. The skull is short with a moderate lacrimal fossa. Both lacrimal foramina are on the orbit rim and on top of each other, the praeorbital vacuity is large, nasals protrude into the latter. The nasals have a posterior protrusion at the nasal-frontal contact. There are several supraorbital foramina embedded in a weak sulcus. In some specimens four palatine foramina are present. The foramen lacerum is large. The protuberantia cristae nuachae is prominent. Antlers are single-tined and moderately ornamented, the pedicles have a strong ventral ridge.

The p2 varies in morphology from simple and slender, with only few elements present, to broad, with a prominent mesolabial conid and short posterior elements. The p3 and p4 have moderate to deep labial incisions. The p3 has an anterior stylid, the posterolingual conid is isolated. The p4 is molariform with an open lingual wall, the transverse cristid is not connected to the mesolingual conid, the posterolingual conid is isolated, the posterolabial conid can be elongated. Lower molars have a weak to moderate anterior cingulid, ectostylids are variably present. The hypoconulid is crescent-shaped, the entoconulid is an

isolated conid. The i1 is distinctively broadened with a small v-shaped gap between the left and right incisor. The P2 has reduced lingual elements, the posterolingual part of the tooth is more developed than the anterolingual part. All upper premolars have at least one central fold. Upper molars have a protocone fold and a metaconule fold. entostyles are variably present on two or more molars. The C are absent in adults, but small alveoli indicate presence of deciduous upper canines in juveniles.

Odocoileus

Odocoileus hemionus Rafinesque 1817

The mandible is slender, the ramus mandibulae is long, slender and inclined posteriad. The angulus mandibulae is moderately indented and elongated. The skull is long and low with a deep lacrimal fossa including a prominent crest; the praeorbital vacuity is large, both lacrimal foramina are situated on the orbit rim and on top of each other. The praemaxillae taper considerably. The zygomatic arch is thin and protrudes dorsally above the fossa mandibularis. The bulla is flat and spiky with a large median process. The processi praemaxillaris on the nasals are approximately equally long. The vomer extends far posteriad, the pterygoid is visible on the interior of the alisphenoid. There is one prominent supraorbital foramen and often several smaller ones embedded in a sulcus. The pedicles are strongly developed, antlers are richly ornamented proximally and curve slightly anteriad before their first bifurcation. There is a short straight medial tine, the branching pattern of the upper beam is characterised by repetitive bifurcations. Females sometimes have a protrusion on the posterodorsal rim of the orbit.

The p2 is relatively short and has a prominent mesolabial and posterolabial conid. The p3 has an anterior stylid, a prominent mesolabial conid and a weak mesolingual conid, and a short transverse cristid; The posterolingual conid is isolated, but often fuses in later wear. All lower premolars have weak to strong labial incisions. The p4 is molariform with a sometimes closed lingual wall, in which case the anterior stylid is reduced. The posterolingual conid is often isolated, sometimes the posterolabial conid is separate from the mesolabial conid. Ectostylids are rarely present on one molar, a weak anterior cingulid is often present, particularly on m1. On the m3 the hypoconulid is prominent, and the entoconulid is weak or absent. The i1 is slightly broadened. The P2 has a reduced lingual wall. A prominent central fold is present in all upper premolars. Sometimes there is a separate antero- and posterolingual cone, particularly in the P4. Entostyles are variably present on one molar. all molars have a protocone and metaconule fold, sometimes there are two metaconule folds. Upper canines in adults are absent.

Odocoileus virginianus Zimmermann 1780

The mandible is slender with a long, thin and backwards inclined ramus mandibulae. The processus coronoideus is slender and also curving backwards; the angulus mandibulae is moderately indented and elongated.

The skull is long and low, with a long snout proportion. The praemaxillae taper considerably. The praemaxillary and nasal are not in contact. The lacrimal fossa is moderate to deep, the praeorbital vacuity is large. Both lacrimal foramina are situated on the orbit rim and sometimes slightly shifted to the outside. The processus lacrimalis is prominent. The

zygomatic arch is slender and protrudes dorsally above the fossa mandibularis. Sometimes the fossa mandibularis has a small dorsally pointing process on the dorsal rim. The medial indent of the palatine is relatively far posterior. Tuberosities on the basioccipital are strongly developed. There is one prominent and several additional supraorbital foramina embedded in a weak sulcus. The processi praemaxillaris on the nasals are equally long. Sometimes four instead of two palatine foramina are present. Pedicles and antlers are inclined, there is a median, straight tine before the main beam curves anteriorly and several tines branch in a row. Antlers are ornamented on the proximal parts.

The p2 is short and has a prominent posterolabial and mesolabial conid. On the p3 anterior elements and mesial elements are far apart, an anterior stylid is present. The labial incision varies from moderate to deep, the posterolabial conid sometimes extends labially. The p4 is extremely molariform, with an often closed anterior valley, the transverse cristid is sometimes bent. When the anterior valley is open, a reduced anterior stylid is present. The posterior elements are sometimes separated from the anterior and mesial ones; the labial incision is deep and the posterolabial conid strongly extends labially. Ectostylids are variably present on one or two molars; the m1 sometimes has a weak anterior cingulid. On the m3 the hypoconulid is more prominent than the weak or absent entoconulid. The i1 is distinctively broadened and the i2 is slightly broadened. Upper molars have at least one central fold, P3 and P4 regularly with two long central folds, which sometimes connect to the labial crista. The P2 is long and has a reduced anterolingual wall and sometimes a separate antero- and posterolingual cone. The P4 sometimes also has two separate lingual cones. All upper molars have a prominent protocone fold and a weak metaconule folds, entostyles are variably present on one or two molars. Upper canines are absent in adult individuals.

Ozotoceros bezoarticus Linnaeus 1758

The mandible is robust with a slightly inclined ramus and a moderately indented and elongated angulus mandibulae. The processus coronoideus is slender and curving posteriorly. The skull is intermediate in length and height. The lacrimal fossa is moderate to deep, both lacrimal foramina are on top of each other and positioned slightly outside the orbit rim. The praeorbital vacuity is large. The basioccipital tuberosities are strong, the vomer extends far posteriorly. There is a posteriorly protruding process on the posterior edge of the fossa mandibularis. There is one prominent and several additional supraorbital foramina embedded in a sulcus. There is a dorsally extending protrusion on the zygomatic arch. Sometimes there are four palatine foramina. The auditory bullae are small. The pedicles have a strong ventral ridge and curve slightly upwards. Antlers are weakly ornamented on their bases and consistently three-tined, with one brow tine and a more distal bifurcation.

The p2 is often reduced to a single conid; otherwise it has a prominent mesolabial conid and a prominent posterolabial conid, and a deep labial incision. On the p3 the anterior stylid is present; the p3 has a broad and prominent mesolabial conid, a deep labial incision, and the posterolabial conid is often directed lingually. The p4 is strongly molarised with a prominent mesolabial conid and a mesolingual conid, which forms a wall and sometimes (late wear) fuses to the anterior conid. The posterolingual conid is often isolated. the labial incision is very deep and sometimes divides the tooth in an anterior and posterior unit. All lower molars have a weak to prominent (m1) anterior cingulid. Ectostylids are variably

present on one molar. The hypoconulid on the m3 is crescent-shaped and much more prominent than the entoconulid. The i1 is distinctively broadened. All upper premolars have a prominent central fold, the posterolingual crista is often open. Minimal incisions between the antero- and posterolingual cone can be variably observed on all premolars. The P2 often has a more prominent posterolingual cone. Entostyles are variably present on one molar. Weak protocone and metaconule folds were observed in some specimens. Fusion of elements rarely occur before late in wear. Upper canines are variably present in adult individuals.

Pudu puda Molina 1782

The mandible is short and robust with a perpendicular ramus and a broad processus coronoideus, which is curving slightly posteriad on its most dorsal part. The angulus mandibulae is moderately indented, often more prominently on the dorsal side. The skull is compact with a slightly longer neurocranial proportion than the viscerocranial proportion. The lacrimal pit is very deep, the praeorbital vacuity is large, but becomes smaller in aged individuals. The posterior rim of the orbit is relatively straight and strong. The lacrimal foramina are situated on the orbit rim with the inferior foramen often more anterior. The supraorbital foramina are small and above the anterior half of the orbit; there is a small sulcus anterior to the supraorbital foramina. The nasals are short, the medial processus praemaxillaris are longer than the lateral ones. Sometimes there are four palatine foramina and there is often a prominent spina caudalis at the palatal indent. The auditory bullae are relatively small. In one specimen the vomer protrudes between the praemaxillary and the maxillary. There are small processes on the lateral indents of the palatine. The pedicles are strongly inclined and reach far posterior; antlers are single-tined and originate above the posterior half of the braincase. Rarely, a second tine on the antlers can be observed.

The p2 is simple and longitudinally oriented, the posterolabial conid is the most prominent structure. On the p3 an anterior stylid is present, the mesolingual conid is weak without additional cristids, the posterolabial conid extends labiad. Both p3 and p4 have deep labial incisions. The p4 is molariform with a lingual wall, which often closes the valley entirely in later wear; the transverse cristid is connected to the mesolabial conid and the posterior elements (rarely the posterolingual conid is isolated in early wear). The posterolabial conid extends labiad, the posterior stylid is short. Ectostylids are usually absent from the lower molars, the elements fuse only in late wear. The third lobe of the m3 almost always consists of the hypoconulid only, sometimes a tiny entoconulid is present. The lower incisors and canines are arranged more in parallel than arched. The i1 is only slightly broader than the i2. All upper premolars have a prominent central fold. The anterior lingual elements are often reduced on the P2, sometimes there is a separate antero- and posterolingual cone. The P3 and P4 tend to have a bent anterior style; P4 often has a separate antero- and posterolingual cone. All upper molars have a protocone fold and variably a metaconule fold; elements fuse only in very late wear. Entostyles are absent. Upper canines are absent in adults, but deciduous upper canines may be present in juveniles as indicated by small alveoli.

Rangifer tarandus Linnaeus 1758

The mandible is long and slender with a strongly inclined ramus and relatively slender and equally inclined processus coronoideus. The angulus mandibulae is weakly to moderately indented more prominently on the ventral side. The symphysis is long. The skull is long and low with a long viscerocranial proportion and a shorter neurocranial proportion. The praeorbital vacuity is small, the lacrimal fossa is moderate; both lacrimal foramina are situated on the orbit rim and on top of each other. The orbit rim strongly extends laterad, the processus lacrimalis is prominent and elongated. The foramen ovale is relatively small and round. The auditory bullae are in a medial location in the skull with a long meatus accusticus externus. The vomer extends far posteriad. Commonly, there are four palatine foramina present. Frontals are large, nasals protrude into the praeorbital vacuity, both processus praemaxillaris are approximately equally long. The supraorbital foramina are relatively small. The praemaxillary bones have a peculiar angular shape, not seen in any other cervid. The supraoccipital region extends strongly posteriad. The pedicles and antlers are at the same level as the frontoparietal suture. Antlers are present in most females. The antlers are slender and elegant with a complex branching pattern. The brow tines are strongly asymmetrical; there is one main bifurcation on the main beam, one branch points anterior and develops several tines, the other beam grows posteriad and then curves smoothly anterior. The main beam has a back tine and several tines at the crown.

The anterior conid on p2 curves around posterolinguad, the transverse cristid is strongly developed and diagonally oriented, the posterolingual conid is well developed, and the posterolabial conid indented. The p3 has an isolated posterolabial conid and posterior stylid, the posterolingual conid is connected to the mesolabial conid and diagonally oriented; the transverse cristid is perpendicular to the former. An anterior stylid is present, the anterior valley is open on the anterior side. On the p4 the posterolingual conid is connected to the mesolabial conid and diagonally oriented, the mesolingual conid including its cristids are separate; often the connection to a very reduced transverse cristid is lost, the posterolabial conid is isolated. The morphology of lower premolars is unique among cervids. The elements in lower molars fuse already in early wear, the lobes are round. The m3 is very narrow and the third lobe of the m3 sometimes consists of the hypoconulid only. Molars strongly resemble those of bovids. Ectostylids are absent. The metastylids on the lower molars and the posterolingual cristids on the lower premolars sometimes form peculiar, linguad bent structures (ZSM 1959-211). The i1 is only very little broadened compared to the i2. All upper premolars have a round appearance, the labial and lingual elements are often separate until late wear, the posterior style can be bipartite. Central folds are usually absent. The M1 has a well developed entostyle, and often a metaconule fold. The posterior lobe on M3 is very reduced in size. Small upper canines are regularly present in adults.

E.1.2 Cervini

Axis

Axis axis Erxleben 1777

The mandible has a slender corpus and a more robust ramus, which is slightly inclined. The processus coronoideus is curving posteriad. The angulus mandibulae is indented, particularly on the ventral side.

The skull is intermediate in length and height and the neurocranial and viscerocranial proportions are balanced. The lacrimal pit is moderate in females and deep in males, the praeorbital vacuity is large. The inferior lacrimal foramen is situated more external on the orbit rim than the superior one, the lacrimal process is prominent. Auditory bullae are large and inflated; there is a “curtain” as extension of the ventral side of the meatus accusticus externus. The tuberosities on the basioccipital in males are prominent. Well developed crista facialis present. Pedicles have a strong ventral edge. Antlers are consistently three-tined with a relatively upright brow tine and a backwards and upright curving main beam with one distal bifurcation.

The p2 can be very short; posterolingual conid and posterior stylid are present, a transverse cristid is variably present, the mesial elements are the most prominent. On the p3 an anterior stylid is present, the short transverse cristid is parallel to the posterolingual conid and posterior stylid. The weak mesolingual conid is weak. p3 and p4 have weak to moderate labial incisions. On the p4 the separation of anterior stylid and anterior conid are not always clear, the transverse cristid is orientated posteriad, the mesolingual conid is bent in the opposite direction, variably with a posterolingual cristid present. the posterior stylid can be elongated and diagonally/posteriad orientated. Lower molars have prominent ectostylids on two, often all three teeth. A prominent anterior cingulid present on m1 and m2; on m3 this is visible not before late wear. The third lobe on m3 is mostly reduced to the hypoconulid or entirely missing. In one specimen (ZMH 4764) there is an additional unicuspid tooth erupting posterior to the left m3 resulting in strange wear facettes on both M3s, the left p2 is also weirdly shaped in this specimen. The i1 are extremely broadened.

All premolars with prominent central fold, sometimes with small accessory folds; the posterolingual part of the lingual cone is more prominent. On the P2 an incision or separation of the antero- and posterolingual cone is common; it sometimes has a triangular appearance. All molars with prominent entostylids, which appear λ-shaped in later wear. Parastyles are well developed. A tiny metaconule fold is present on most upper molars, the mesostyle is often bipartite. The posterior lobe of M3 is noticeably smaller. Deciduous upper canines are present in juveniles, adults have alveoli, but the presence of a C could not be observed.

Axis porcinus Zimmermann 1780

The mandible is relatively short and slender with a perpendicular ramus. The processus coronoideus is curving backwards. The angulus mandibulae is moderately to strongly indented and elongated. The skull is compact and robust with balanced viscerocranial and neurocranial proportions. The lacrimal pit is deep, the praeorbital vacuity enlarged; the lacrimal foramina are situated slightly external to the orbit rim and the inferior foramen

is often somewhat more anterior. The crista maxillaris is prominent. The foramen ovale is relatively big and the auditory bullae are inflated. Basioccipital tuberosities are well developed in males. The medial processi praemaxillaris of the nasals are longer than the lateral ones, which can be missing entirely. The pedicles are strongly inclined and elongated. Antlers consistently have three tines, one short brow tine and a long main beam with a tine branching off posteriad at two thirds height of the main beam.

The p2 has more prominent posterior elements, the transverse cristid is mostly present and oriented posteriad; the anterior conid is curving around linguad. p3 and p4 have weak labial incisions. On the p3 the anterior stylids are present, the transverse cristid and mesolingual conid can be offset from the mesolabial conid, posterior elements are long and transversely orientated. An anterior stylid is present on p4, the transverse cristid is transversely or posteriad orientated with the mesolingual conid orientated in the opposite direction; the posterolingual conid often has a kink. All lower molars have a strong anterior cingulid and prominent ectostylids are present on two or more molars. The mesostylid is well developed and bent posteriad. The third lobe of m3 often consists of the hypoconulid only. The i1 is extremely broadened, the lateral part of the crown partly overlapping i2.

All upper premolars have the tendency to indent or separate the antero- and posterolingual cone. The anterior and posterior styles are strongly bent. All premolars have a prominent central fold, often a second small accessory fold is present. On P3 and P4 the posterolingual part of lingual cone is more developed. P4 sometimes has a lingual cingulum. M1 and M2 may have a weak anterior cingulum. All molars have a well developed parastyle. Entostyles are present on at least two molars, which become λ -shaped in wear. A metaconule fold is present on all molars. Posterior lobe of M3 noticeably smaller. Upper canines are absent in adult individuals.

Cervus

Cervus albirostris Przewalski 1883

The mandible is long with a slender corpus and a broader and inclined ramus. The processus coronoideus smoothly curves posteriad. Sometimes there is a channel and small process anterior to foramen mandibulae. The angulus mandibulae is wide and round and only weakly indented. The skull is robust and relatively long and low. The lacrimal pit is very deep and has a prominent dorsal edge, the praeorbital vacuity is large. The superior lacrimal foramen is situated slightly more on the internal orbit rim than the inferior foramen, which is slightly more on the external orbit rim. The nasals protrude laterally into the praeorbital vacuity. The medial processi praemaxillaris on the nasals are longer than the lateral ones. The auditory bullae are small, the basioccipital tuberosities are well developed in males. The crista nuchae is well developed and weakly protruding posteriad. Pedicles are short; antlers very long and slender, are usually four-tined with a proximal anteriad pointing brow tine and a more distal trifurcation.

The p2 is short and its elements weakly developed; an anterior conid, mesolabial conid, posterolingual conid, and posterior stylid are present. The p3 has an anterior stylid, mesolingual conid and short transverse cristid, both are slightly offset posteriad from mesolabial conid; the posterior stylid is short or absent. The anterior valley of p4 is entirely closed only in later wear; p4 has a deep, p3 a weak labial incision. The transverse

cristid is slightly offset posteriad, the mesolingual and mesolabial conid are in line with each other. An ectostylid may be present on one molar (usually m1); There is a weakly developed anterior cingulid on all molars. Conids appear rounded and smooth; the third lobe of m3 is crescent-shaped or almost circular, the hypoconulid on m3 is enlarged. The i1 is clearly broadened, i2 intermediately broadened.

The P2 has an incision between antero- and posterolingual cone, the posterolingual cone is more developed than the anterior one. On two short central folds are present on all upper premolars, anterior styles are well developed. Entostyles are present on two or more molars, which often become λ -shaped in late wear. Parastyles are well developed, a protocone fold is variably present as well as a tiny metaconule fold. Upper canines are present in adult individuals.

Cervus canadensis Erxleben 1777

The mandible corpus is slender, the ramus is more robust and little inclined, the processus coronoideus strongly bends posteriad. The angulus mandibulae is broad and wide and sometimes weakly indented on the ventral side. The skull is long and low, with a longer viscerocranial proportion. The lacrimal pit is very deep with a dorsal crest, even in females, the praeorbital vacuity is enlarged. The superior lacrimal foramen is situated on the orbit rim, whereas the inferior foramen is situated external to the orbit rim. The processus lacrimalis is prominent. There is a tendency to initial suture fusion (frontal-frontal, frontoparietal). Well developed crista facialis and crista nuchae. Auditory bullae are small and possess several processes. Tuber maxillae are prominent. There is one large supraorbital foramen and several smaller ones. The medial praemaxillary processes on the nasals are a little longer than the lateral ones. Pedicles are short and robust. Antlers are long and complexly branched; they consist of a long anteriad pointing brow tine, a bez and trez tine and a distal bi- rarely trifurcation.

The p2 is short, its anterior element(s) weak; there is a mesolabial conid, a short posterolingual conid and posterior stylid, which are longitudinally oriented. The p3 has an anterior stylid, a thin transverse cristid originating slightly offset posteriad from the mesolabial conid; the posterior elements are in parallel with the transverse cristid. p2 and p3 have weak, p4 moderately deep labial incisions. On the p4 an anterior stylid is present, if it is not fused with anterolingual cristid; the anterior valley is usually closed in later wear. The posterior stylid is short, the posterolingual conid may have origination on transverse cristid rather than on labial cristid. All lower molars with weak anterior cingulid (at least on m1 and m2), weak ectostylids are present on one or two molars, metastylids are well developed. The third lobe on the m3 is crescent-shaped or circular. The i1 are broadened; all lower canines and incisors are broad and arranged in an arch.

All upper premolars have at least one prominent central fold and often smaller accessory folds. Premolars have a tendency to indent or separate the antero- and posterolingual conid. On the P2 the posterolingual cone is more prominent. On P3 and P4 the anterior styles are bent posterolabial. The P4 may have weak lingual cingulum. Molars have well developed parastyles, which partly bent posteriad, entostyles present on two or more molars, a weak anterior cingulum can be present on M1 and M2. Upper canines are present in adults.

Cervus elaphus Linnaeus 1758

The corpus mandibulae is relatively slender, the ramus more robust with a smoothly posteriad curving processus coronoideus. The angulus mandibulae is wide and round, sometimes weakly indented ventrally, sometimes even slightly receding. The skull is long and low with a longer viscerocranial proportion (long praemaxillary). The lacrimal pit is deep including a dorsal crest, the praeorbital vacuity is enlarged. The superior lacrimal foramen is on the orbit rim, the inferior foramen offset slightly on the external orbit rim. The medial and lateral processi praemaxillaris on the nasal are more or less equally long, sometimes one is slightly longer than the other. Supraorbital foramina are large, additional smaller foramina are usually absent. The basioccipital tuberosities are well developed in males. Pedicles are short and robust. Antlers are long and consist of an antieriad pointing brow tine, a bez tine, a trez tine, and a distal coronate trifurcation. The latter can be multiple-tined in stages of strong breeding programmes.

The p2 is short with a weak anterior conid, a short transverse cristid can be present, and short posterior elements all longitudinally oriented. On p3 an anterior stylid is present, the transverse cristid is a little offset posteriad to the mesolabial conid; the posterior stylid is very short or absent, the mesolingual conid has no cristids and is separate from the anterior conid. An anterior stylid is present on the p4, the transverse cristid and posterior elements are bending posteriad. The anterior valley remains open until late wear. Most lower molars have a weak anterior cingulid, ectostylids are mostly absent. The third lobe on m3 is crescent-shaped or circular. Lower incisors and canines are relatively broad, i1 is distinctively broadened.

All premolars have a central fold and an incision between the antero- and posterolingual cone. Particularly on P3 and P4 the posterolingual part of the tooth is more prominent, also anterior styles are well developed bending posteriad. Small entostyles are usually present on all molars, parastyles are prominent. Tiny metaconule and protocone folds are rarely present on M1. The posterior lobe of M3 is distinctively smaller than the anterior lobe. Upper canines are present in adults.

Cervus nippon Temminck 1838

The mandible has a robust ramus with a posteriad curving processus coronoideus; the angulus mandibulae is wide and round, sometimes weakly indented on the ventral side. The skull is intermediate in length, shorter than those of other *Cervus*-species. The lacrimal pit is moderately deep, the praeorbital vacuity enlarged. Both lacrimal foramina are close together, the inferior foramen a little offset more external on the orbit rim. The basioccipital tuberosities are weakly developed. Auditory bullae are relatively large and round. The tuber maxillae are strongly developed. There is one prominent supraorbital foramen, often accompanied by several smaller ones. The praemaxillary processes on the nasals are approximately equally long, sometimes the medial process is slightly longer. Often two spinae caudalis present. The foramen ovale is large. Pedicles are long and slender; antlers are regularly four-tined with a proximal brow tine, a more distal bifurcation, of which the longer beam bifurcates again distally.

The p2 has a short anterior conid, a transverse cristid, which is strongly oriented posteriad, more prominent posterior elements. p2 and p3 have weak, p4 deep labial incisions. An anterior stylid is present on p3, the transverse cristid and mesolingual conid are ori-

ented posteriad, the posterior elements are long. The p4 sometimes has a weak anterior conid, the anterior valley is regularly closed, at least in later wear. The posteriad oriented posterolingual cristid is elongated and sometimes almost forms a mesial valley. Ectostylids are variably present on one molar (usually m1); m1 and m2 have a weak and short anterior cingulid. The metastylids are bent linguad. The third lobe on m3 is crescent-shaped. The i1 is distinctively broadened.

All upper premolars have a prominent central fold, the anterior and posterior styles are bent. Particularly P2 and P3 have an incision between the antero- and posterolingual cone, the posterolingual cone is more prominent. The central fold can be connected to the labial crista. Entostyles are variably present on one or more molars; a metaconule fold may be weakly present on all molars, prominent parastyles and mesostyles. The posterior lobe of M3 is noticeably smaller than the anterior one. Upper canines are present in adult individuals.

Dama dama Linnaeus 1758

The mandible is slender with a broader ramus, which is also inclined. The angulus mandibulae is weakly indented and elongated. The skull intermediate in length with a slightly longer viscerocranial proportion. The braincase is round and convex (dorsal outline). The lacrimal pit is very deep with a dorsal ridge in males, moderate in females, the praeorbital vacuity is enlarged. Both lacrimal foramina are on top of each other and situated on the orbit rim, sometimes more external. The processus lacrimalis is prominent. The orbit rim extends somewhat laterally. There is usually one large supraorbital foramen, sometimes there are additional smaller ones. The basioccipital tuberosities are well developed in males and visible in females. The number of infraorbital foramina is variable. Prominent protuberantia on the crista nuchae. The foramen ovale is large. The lateral praemaxillary processes of the nasals are clearly longer than the medial ones. Pedicles are moderately long; antlers are large, with an anteriad-upward pointing brow tine. The main beam has another single tine in the middle before its multi-tined palmated distal end.

The p2 has an anterior conid, a short transverse cristid, a posterolingual conid, and a posterior stylid, all with a transverse orientation. The labial proportion of the p2 is more prominent. An anterior stylid is present on the p3; the transverse cristid originates offset posteriad. The posterolingual conid is long, the posterior stylid short; the anterior stylid and conid sometimes connect with each other in later wear forming a circle. p2 and p3 have weak labial incisions. The p4 has a variably closed anterior valley; if it is not closed, the anterior stylid is present, which also sometimes connects to the anterior conid forming a circle. The posterolingual cristid is long and distinct, the posterolingual conid long, and the posterior stylid short. The labial incision on p4 is deep. Ectostylids are absent on molars, weak anterior cingulids are present, and are the strongest on m1. The third lobe of m3 very reduced mostly consisting of a tiny ento- and hypoconulid. Lower incisors and canines are short, the i1 is distinctively broadened.

P2 is often triangular-shaped with a clearly separate antero- and posterolingual cone, both rather small. a short central fold is present. The labial elements are more dominant. P3 and P4 have a prominent central fold; P3 often with indented or separate antero- and posterolingual cone. Molars with small entostyles on at least two molars. Tiny protocone and metaconule folds are variably present, never large, and disappear in wear. Upper

canines are absent in adults.

Elaphurus davidianus Milne-Edwards 1866

The mandible is broad and robust with a wide and round, often receding angulus mandibulae. The processus coronoideus is relatively short and curving posteriad. The skull is long and low with a large viscerocranial proportion. The processus nasalis of the praemaxillary extends far posteriad. The lacrimal pit is deep and the praeorbital vacuity large, longer than wide. The two lacrimal foramina are situated somewhat external on the orbit rim and the inferior foramen is more anterior than the superior. The posterior rim of the orbit is straight; The basioccipital tuberosities are well developed and prominent even in females and have a deep groove between the anterior tuberosities. There is one main and several accessory supraorbital foramina. The lateral processi praemaxillaris of the nasals are longer than the medial ones. The zygomatic arch is straight in lateral view. Pedicles are strong; the antlers have a unique complex branching pattern. There is a proximal bifurcation, from which one beam grows posteriad mostly without further bifurcations, and one anterior beam that grows more or less upright and with one or more more distal bifurcations. All tines and beams may develop accessory tiny spurs around them. Female often have a protrusion dorso-posterior to the orbit.

The p2 often has an anterior conid and stylid, a distinct, but short transverse cristid on the mesolabial conid, and a transverse posterolingual conid and posterior stylid. All elements become more prominent in later wear, whereas p2 looks very slender and longitudinal in early wear. All lower premolars may have weak labial incisions. The p3 has an anterior stylid, sometimes an initial anterolingual cristid; the transverse cristid, posterolingual conid plus cristid and the posterior stylid are in parallel and transversely oriented. On the p4 the anterior stylid is only present, if the anterior conid is not fused with the anterolingual cristid forming a lingual wall. The transverse cristid can have a kink and may be detached from mesolingual conid, if the latter forms lingual wall. The posterior elements are long, the posterolabial conid may be separate from the labial cristid. The m1 sometimes has a weak anterior cingulid; ectostylids are absent on lower molars. The third lobe of m3 is small and crescent-shaped or circular. All lower incisors and canines have a strong medial ridge on the lingual side of the tooth and tiny cuspids on the base of the tooth crowns. i1 are a little broadened.

P2 and P3 have indented or separate antero- and posterolingual cones. P2 variably has a short central fold, P3 and P4 have prominent central folds with accessory tiny folds, or several small central folds (in later wear). The posterior wall is open until late in wear. There are sometimes weak lingual cingula on P3 and P4. The anterior and posterior styles are strongly bent. Entostyles are usually present on all molars; they are λ-shaped and form part of the occlusal surface in late wear. M1 (sometimes also on other Ms) can have a weak anterior and lingual cingulum and a metaconule fold. Parastyles are prominent on all molars. The postprotocrista and premetaconulecrista of all molars show serrations mainly on their mesial sides. The posterior lobe of M3 is heavily reduced (half the size). Upper canines are present in adult individuals.

*Rucervus**Rucervus duvaucelii* Cuvier 1823

The mandible has a smaller corpus and a very wide and round angulus and broad ramus. The processus coronoideus is relatively short, broad and curving posteriad.

Skulls are long and low with a slightly longer viscerocranial proportion. The nasal process on the praemaxillary extend far posteriad. The lacrimal pit is deep, the praeorbital vacuity is large. Both lacrimal foramina are on top of each other and situated on the orbit rim. The processus lacrimalis is prominent. The tooth row extends relatively far posteriad. The postorbital bar is straight. The lateral praemaxillary processes on the nasals are longer than the medial ones, which are sometimes absent. There is one large supraorbital foramen. The basioccipital tuberosities are well developed and prominent with a groove between the two anterior tuberosities. The foramen ovale is large. Auditory bullae are rounded. Prominent crista nuchae and protuberantia. Pedicles are robust. Antlers are long and partly with a complex branching pattern. There is a proximal bifurcation with an antierad-upwards directed brow tine and a long posteriad-upwards curving main beam that carries several smaller tines on its distal, antierad curving end.

The p2 has a longitudinal anterior conid, the transverse cristid can be long, the posterior elements are well developed. The p3 has a widely open anterior valley, an anterior stylid, a transverse cristid, which originates posterior to the mesolabial conid, the posterior stylid is short. The p4 is molariform sometimes with an entirely closed anterior valley. The anterior part of the tooth is more dominant, whereas the posterior part is reduced; sometimes the mesolingual conid is detached from the transverse cristid. The labial incision on p4 is deep. All molars have well developed, strong anterior cingulids, ectostylids are present on at least two molars. The third lobe on m3 is crescent-shaped, sometimes circular. The lingual outline of the molars is strongly folded, labial tooth walls are weakly indented. All lower incisors and canines have weak ridges on the lingual sides. i1 is broadened.

All premolars have a prominent central fold, Which sometimes connects to walls of the tooth forming fossettas, and well-developed, bent anterior and posterior styles. P2 sometimes has a separate antero- and posterolingual cone. On P4 sometimes an anterior cingulum occurs. All upper molars have an anterior cingulum, all four cones develop enlarged dentine areas with lingual-labial extensions. Very well developed parastyles, mesostyles and metastyles. The postproto- and premetaconulecrista can be bi- or trifurcating and a connection to labial elements is possible. Entostyles are present on all molars, and often become λ-shaped in later wear. Upper canines are variably present in adults, certainly present in juveniles.

Rucervus eldii McClelland 1842

The corpus mandibulae is slender, broadening towards the angulus; the ramus mandibulae is broad and short with a posteriad curving processus coronoideus. The angulus mandibulae is wide and round weakly indented ventrally. The skull is long and low with a slightly longer viscerocranial proportion. The lacrimal pit is deep with a dorsal crest, the praeorbital vacuity is large and longer than wide. Both lacrimal foramina are situated external on the orbita rim, often the inferior foramen is slightly more anterior; the processus

lacrimalis is relatively weak. The nasal processes of the praemaxillaries extend far posteriad. The tuber maxillae are well developed, there is commonly a prominent spina caudalis on the palatine. Auditory bullae are rounded with a prominent medial process, the meatus acusticus externus contains a ventral process. The crista facialis is prominent. The basioccipital tuberosities are moderately developed. There is one large supraorbital foramen often accompanied by one or more smaller ones. The medial praemaxillary processes on the nasals are longer than the lateral ones. The crista nuchae and protuberantia are well developed. Pedicles are slender and relatively close together. Antlers are characterised by a complex branching pattern. They have a proximal bifurcation, from which a long anterior beam originates directing anteriorly and upwards, which can have several smaller tines on it. The other main beam curves posteriad, then laterad and anteriorly; its distal end contains multiple smaller tines. Sometimes there is a middle tine on the proximal bifurcation. In females there is sometimes a protrusion dorso-posterior to the orbit.

The anterior conid on p2 is longitudinal, the mesolabial conid is clearly present and has a transverse cristid, the posterolabial and -lingual conid are well developed including a posterior stylid. p2 and p3 have weak labial incisions. The p3 has an anterior stylid and conid, the transverse cristid originates far posterior to the mesolabial conid, the posterior stylid is short. The anterior valley is widely open in p3 and p4. The labial incision on p4 is deep; the p4 has an anterior stylid and anterior conid, a broad mesolingual conid, a transverse cristid originating posterior to the mesolabial conid. The posterolingual conid may be separate from other elements; the anterior part of the tooth is more well prominent. All lower molars have a strong anterior cingulid, an ectostylid is present on one molar. All conids have an enlarged dentine area (labio-lingually). The third lobe of m3 is crescent-shaped. Lower incisors and canines have weak ridges on the lingual sides; the i1 are broadened.

P2 and P3 have indented or separate antero- and posterolingual cones. All premolars have a prominent central fold, which is sometimes serrated, all have well-developed, bent anterior and posterior styles. Entostylids are present on all molars, which are triangular-shaped. A metaconule fold is present on all molars. The premetaconulecrista is serrated. There are linguo-labially enlarged dentine areas on all cones. Parastyles, mesostyles and metastyles are prominent. Upper canines are regularly present in adults.

Rucervus schomburgki Blyth 1863

The mandible corpus is slender, the ramus broad with a long posteriad curving process coronioideus. The angulus mandibulae is wide and round, weakly indented on the ventral side, otherwise shows a receding tendency. The skull is long and low with a slightly longer viscerocranial proportion. The processi nasalis on the praemaxillaries extend posteriad. The lacrimal pit is deep, the praeorbital vacuity large. Both lacrimal foramina are situated on the orbit rim with the inferior foramen slightly more anterior; the processus lacrimalis is prominent. The lateral praemaxillary processes on the nasals are longer than the medial ones, which are sometimes absent. There is one large supraorbital foramen. The basioccipital tuberosities are well developed with a groove between the anterior tuberosities. The pedicles are relatively close together and slender. Antlers have a very complex, unique branching pattern. From the proximal bifurcation a long, anterior-upwards directed brow tine originates; the main beam branches off laterally and has one main bifurcation,

form which tines originate and further bifurcate.

The only mandible available for *Rucervus schomburgki* is unfortunately already very worn and lacks p2 and p3. The heavily worn p4 has a closed anterior valley; the anterior part of tooth is more prominent than the posterior part. p4 has a deep labial incision. All lower molars have a strong anterior cingulid, ectostylids are absent in this specimen. The third lobe of m3 is crescent-shaped and becomes circular in late wear. Mesostylids and Metastylids are strongly developed. Lower incisors have weak ridges on their lingual sides; the i1 presumably is broadened.

P2 and P3 have indented or separate antero- and posterolingual cone; there are several small central folds, on the triangular-shaped P2. P3 and P4 have one prominent and often several accessory central folds. Some P4 have a posterolingual cingulum. Anterior and posterior styles are prominent. At least two molars have entostyles, which become λ-shaped in later wear. All parastyles, mesostyles and metastyles are well developed, the dentine area is enlarged on all four cones, there are weak anterior cingula. Upper canines are present in adult individuals.

Rusa

Rusa alfredi Sclater 1870

The mandible is relatively robust with a wide and round angulus mandibulae, which is weakly indented. The ramus is broad with a strongly posteriad curving processus coronoideus. The skull is long and low with a slightly longer viscerocranial proportion. Lacrimal pits are moderate in females, very deep with a dorsal ridge in males, the praeorbital vacuity is large. The foramen lacrimale inferior is situated much more anterior/external to the orbit rim than the superior one, which is mostly on the orbit rim or minimally external. The nasals sometimes protrude into the praeorbital vacuity. The crista facialis on the maxilla is clearly visible. The processus praemaxillaris on the maxilla extend far anterior. The processus praemaxillaris of the nasals are approximately equally long. There is one large supraorbital foramen embedded in a sulcus, and accessory foramina can occur. Prominent protuberantia on the crista nuchae. The zygomatic arch is slender in dorsal view. There is a medial gap between the praemaxillary bones. Basioccipital tuberosities are weakly developed in females and prominent in males including a medial groove between them. Auditory bullae are rounded with a prominent medial process. The foramen ovale is relatively large. Pedicles are a little elongated and inclined. Antlers are consistently three-tined, richly ornamented with ridges and furrows. All tines are inclined in a posterodorsal direction. Females have protrusions posterodorsally to the orbit.

The p2 is relatively broad, mesolabial conid and posterior elements are more dominant; the tooth is short, has an anterior conid, which sometimes curves linguad. A weak to moderate labial incision is present on p2 and p3, on p4 the labial incision is deep. An anterior stylid is variably present on the p3; it has a prominent mesolabial conid, the transverse cristid originates slightly posterior to the mesolabial conid, the mesolingual conid simple without cristids. On the p4 the anterior stylid is present, if the anterior conid is not fused with the mesolingual elements, the anterolabial cristid bulges labiad. The posterior elements are oriented diagonally. If the anterior valley is closed, tooth appears molariform. Ectostylids are variably present on one molar, a clear anterior cingulid is

present on, a weak anterior cingulid sometimes occurs on m2. The third lobe of m3 often consists of the hypoconulid only. The i1 is distinctively broadened.

P2 and P3 mostly have an indented or separate antero- and posterolingual cone. All premolars have a prominent central fold, which is sometimes serrated. On the P2 anterolingual elements can be reduced, posterolingual elements are dominant. The posterior wall fuses late in wear on all premolars. Entostyles are rarely present on one molar, metaconule and protocone folds are usually absent, rarely a metaconule can be observed. The parastyle can be prominent. Upper canines are present in adults.

Rusa marianna Desmarest 1822

The corpus mandibulae is relatively slender, the ramus a little broader with a slender and posteriad curving processus coronoideus. The angulus mandibulae is round and weakly indented. The skull is long and low with a slightly longer viscerocranial proportion. The lacrimal pit is very deep and sometimes develops a dorsal ridge, the praeorbital vacuity is elongated. The nasals sometimes protrude into the praeorbital vacuity. Both lacrimal foramina are on top of each other and situated on the orbit rim, the inferior foramen can be slightly more anterior. The processi praemaxillaris on the maxilla extend far anterior. The basioccipital tuberosities are weakly developed in females and prominent in males including a median groove. The braincase is round/convex in lateral view. The praemaxillary processes on the nasals are barely detectable in the scrutinised specimens. There is one large supraorbital foramen embedded in a long sulcus, sometimes accompanied by several smaller foramina. Auditory bullae are rounded with a median process. There is a foramen anterior to the foramen ovale. Pedicles are a little elongated and inclined, quite divergent in dorsal view. Antlers are consistently three-tined, richly ornamented with ridges and furrows. Rarely there is an accessory small tine on the brow tine. All tines are inclined in a posterodorsal direction. Females have protrusions posterodorsally to the orbit.

Lower premolars appear curved, convex in the labial direction. The p2 is broad and compact, the anterior conid short, sometimes curving linguad; the mesolabial conid and posterior elements are dominant. The p3 has an anterior stylid, the mesolabial conid is prominent, the transverse cristid originates posterior to the mesolingual conid, forming a trifurcating structure together with the mesolabial conid and the posterolingual cristid with diagonal orientation. p2 and p3 have weak to moderate labial incisions, p4 has a deep labial incision. The anterior valley is widely open on p3 and p4. On the p4 the transverse cristid originates posterior to the mesolingual conid, forming a trifurcating structure similar to the one in p3. An anterior stylid is present on p4, posterior elements may connect forming a ring-like structure in later wear. All molars have a well developed anterior cingulid, ectostylids are present on one molar (usually m3). The third lobe of m3 is crescent-shaped, mesostylids are strongly developed and elongated. The i1 are distinctively broadened.

All premolars can develop indented or entirely separate antero- and posterolingual cones. All premolars have at least one well developed central fold often two, sometimes more, which can be serrated. Lingual cingula are possible on premolars. On P2 lingual elements may be reduced. Anterior and posterior styles are prominent and bent. Entostyles are present on all molars, and tend to become λ -shaped in later wear. All molars have strongly developed parastyles and mesostyles, premetaconule crista sometimes bifurcated often serrated. Metaconule and protocone folds are usually absent. Upper canines are

present in adult individuals.

Rusa timorensis Blainville 1822

The mandible is neither particularly slender nor robust with a wide and round angulus mandibulae, which is weakly indented and sometimes receding. The ramus is upright with a posteriad curving processus coronoideus. The skull is long and low with a slightly longer viscerocranial proportion. The nasal processes of the praemaxillae are long. The lacrimal pit is deep with a dorsal ridge, the praeorbital vacuity is enlarged. The foramen lacrimale inferior is situated more anterior/external to the orbit rim than the superior one, which is mostly on the orbit rim or minimally external. The braincase is rounded and convex in lateral view. Auditory bullae are rounded with a small median process. The foramen ovale is large. The processi praemaxillaris on the maxilla extend far anteriad. The basioccipital tuberosities are weakly developed in females and stronger in males. The crista nuchae is prominent. The postorbital bar is straight. There is one large and multiple smaller supraorbital foramina embedded in a sulcus. Pedicles are relatively long and inclined and divergent in dorsal view. Antlers are consistently three-tined, richly ornamented with ridges and furrows. All tines are inclined in a posterodorsal direction. Females have protrusions posterodorsally to the orbit.

The p2 is compact, has an anterior conid, which sometimes curves linguad. The mesolabial conid is prominent, the mesolingual conid can be isolated; the posterior elements are more prominent and transversely oriented. On the p3 an anterior stylid present, the transverse cristid originates far posterior to the mesolabial conid; the mesolabial conid is prominent, posterior elements are long. p2 and p3 have weak labial incisions, the p4 has a deep labial incision. p3 has a widely open anterior valley. On the p4 a weak anterior stylid is present, the transverse cristid originates far posterior to the mesolabial conid. The mesolabial conid is prominent, posterior elements are long, the mesolingual conid may or may not develop cristids and shows tendency to close the otherwise wide anterior valley. m1 and m2 usually have a strong anterior cingulid, m3 sometimes has a weakly developed anterior cingulid. Ectostylids are present on two or more molars. The third lobe on m3 is crescent-shaped. Mesostylids, metastylids and entostylids are strongly developed. The i1 is distinctively broadened.

P2 and P3 regularly have indented or entirely separated antero- and posterolingual cones. All premolars have at least one central fold, mostly two or more, which can be serrated. Anterior and posterior styles are strong and bent labiad. Entostyles are present on all molars and become λ-shaped in wear, parastyles and mesostyles are strongly developed and bent labiad. The premetaconulecrista is sometimes bifurcated and often serrated. Protocone and metaconule folds are usually absent, rarely a metaconule fold appears. Often molars have anterior cingula. The lingual tooth walls are indented. Upper canines in adults are present.

Rusa unicolor Kerr 1792

The mandible corpus is neither slender nor robust; the ramus is broader with a posteriad curving processus coronoideus. The angulus mandibulae is wide and round and weakly indented, sometimes receding. The skull is long and low with a slightly longer viscerocranial proportion. The nasal processes of the praemaxillae are long. The lacrimal pit is deep with

a dorsal ridge, the praeorbital vacuity is enlarged. Nasals often protrude laterally into the praeorbital vacuity. The foramen lacrimale inferior is situated more anterior/external to the orbit rim than the superior one, which is mostly on the orbit rim or minimally external. The lateral and medial praemaxillary processes of the nasals are equally long. The processi praemaxillaris on the maxilla extend far anteriorly. There is a moderately sized and several smaller supraorbital foramina embedded in a deep sulcus. The basioccipital tuberosities are weakly to moderately developed in females, stronger in males with an occasionally occurring medial groove. Auditory bullae are rounded with a median process, the foramen ovale is large. The crista nuchae is well developed. Pedicles are relatively long and inclined, and divergent in dorsal view. Antlers are consistently three-tined, richly ornamented with ridges and furrows. All tines are inclined in a posterodorsal direction. Females have protrusions posterodorsally to the orbit.

The p2 has an anterior conid, the mesolabial conid becomes prominent in late wear, the posterior elements are well developed. On the p3 the anterior stylid is present, the transverse cristid originates posterior to the mesolingual conid. The posterior elements are variable in length. p2 and p3 have weak labial incisions, p4 has a moderate to deep labial incision. The anterior valley is widely open on p3 and p4, sometimes there is a tendency on the p4 to closing the valley. On the p4 an anterior stylid is present, the mesolingual conid has cristids, the posterior elements are long. All lower molars have a strong anterior cingulid and well-developed mesostylids, metastylids, and entostylids. Ectostylids are present on one or two molars; the third lobe on m3 crescent-shaped. The i1 are distinctively broadened.

P2 and P3 tend to indent or entirely separate the antero- and posterolingual cone. All premolars have at least one most often two central folds, which can be serrated, and have well-developed, bent anterior and posterior styles. Lingual cingula can appear in all premolars and molars. All upper molars have entostyles, which become λ-shaped in wear, a metaconule or protocone fold can rarely be present, the premetaconule crista is serrated, sometimes the postprotocrista is serrated, too. The parastyles and mesostyles are well-developed. M1 often with anterior cingulum. The posterior lobe on M3 is distinctively smaller. Upper canines are present in adult individuals.

E.1.3 Muntiacini

Elaphodus cephalophus Milne Edwards 1872

The corpus mandibulae is relatively slender, the ramus mandibulae is broader and low with a broad and slightly backwards curving processus coronoideus. The angulus mandibulae is rounded, indented on the ventral side and sometimes bears a prominent crest. The cristae on the diastema on the mandible are high; The skull is compact robust and low with distinct structures. The fossa lacrimale is huge and deep, oval or round. The area dorsal to the cheek teeth is broad and laterally extended in dorsal view. The praeorbital vacuity is small, sometimes even closed if the nasal protrudes into it, which can occur already in juveniles. The nasal and lacrimal hence are sometimes partly in contact. The foramen lacrimale superior is situated on the internal orbit rim, the foramen lacrimale inferior on the external orbit rim. The diastema on the maxilla is short due to the enlarged upper canine. The foramen infraorbitale is positioned far anterior to the tooth row. The

crista maxillaris is prominent. there is one large supraorbital foramen and multiple smaller ones, which are embedded in a deep and long sulcus. The medial and lateral processi premaxilaris on the nasals are variably longer or shorter to each other or sometimes even not distinguishable. The palatine foramina can be relatively far anterior. The contact between the pterygoid and alisphenoid is broadened and the hamulus pterygoideus is hook-shaped. Auditory bullae are small. The antlers are minute and only up to 2 cm long and single-tined.

The p2 has an anterior conid and often also an anterior styloid, a mesolabial conid, a posterolingual conid and a posterior styloid. On the p3 an anterior conid and styloid are present, there is a kink in the transverse cristid. The posterolingual cristid is mostly developed; the p3 has a weak labial incision, and relatively long posterior elements. The p4 has a deep labial incision; the posterolingual and posterolabial conid are often separated from other elements (fusion possible in later wear), the transverse cristid is separated from the mesolingual conid, the mesolingual conid is connected with the anterior conid, partly closing the anterior valley. Lower molars have an anterior cingulid, which is most prominent on the m1, ectostyloid may be variably present on one molar. The metaconid and/or entoconid on m2 and m3 have additional folding. The third lobe on m3 is either circular or trifurcated. The i1 is extremely broadened, the other incisors and canines are pencil-shaped.

P2 and P3 mostly with indented or separate antero- and posterolingual cone. The P2 is longer than the other two premolars. All premolars have one large and several smaller central folds. Molars sometimes have an anterior cingulum. Entostyles are variably present on one molar (usually M1). The posterior lobe of M3 is reduced. The premetaconulecrista may be bipartite, M1 often with a metaconule fold, protocone folds may be present. Upper canines in males are enlarged, females have distinctively smaller upper canines.

Muntiacus

Muntiacus atherodes Groves & Grubb 1982

The corpus mandibulae is long and slender, the ramus is short and strongly curving backwards, as is the slender processus coronoideus. The angulus mandibulae is slightly elongated and indented. The cristae on the diastema are relatively high. The skull is relatively long and low, the nasal processes of the praemaxillae extend far posteriad. The lacrimal fossa is very deep and oval, the praeorbital vacuity is moderate in size. There is a prominent crista facialis. Orbits are relatively large and round; both lacrimal foramina are on top of each other and on the orbit rim. The interfrontal suture may form a crest. Prominent tuberosities on the basioccipital are absent. The ventral cristae on the maxillae are well-developed. The lateral sides of the nasals protrude into the praeorbital vacuity. The medial processus praemaxillaris of the nasal is longer than the lateral one. The medial nasal-frontal contact is rectangular. The oval foramina are relatively large. The crista nuchae and the associated protuberantia are prominent. Auditory bullae are small. The pedicles are strongly inclined, almost horizontal, and long. Antlers on the two available specimens are single-tined and presumably represent early ontogenetic stages.

On the p2 the anterior conid, transverse cristid, posterolingual conid and posterolabial conid including a posterior styloid are present. All elements are transversely oriented,

the transverse cristid bends posteriad. On the p3 the anterior conid is present with the potential for developing an anterior stylid; there is a long transverse cristid bent posteriad, but no mesolingua cristids, posterior elements are long and transversely oriented. p3 and p4 have shallow labial incisions. p4 possesses an anterior conid and stylid, which form a circle here, the transverse cristid is bent posteriad without mesolingual cristids. Posterior elements are present, long and transversely oriented. The m1 shows a clear anterior cingulid and an ectostylid, the other lower molars do not have these features in the available specimen(s). The third lobe of m3 consists of a strong hypoconulid, the posthypocristid bends slightly posteriad. Lower incisors and canines were only fragmentary present, but apart from the i1, which is broadened, incisors and canines are peg-like.

All premolars have multiple tiny central folds, the posterior wall is closed, the anterior open. P2 is longer than P3 and P4. P2 and P3 have a strong indent on the posterolabial crista. Entostyles on the upper molars are absent. Parastyles, paracones, and mesostyles are prominent. Protocone and metaconule folds are absent. Upper canines are elongated, slender, and curving posteriad.

Muntiacus crinifrons Sclater 1885

The mandible has a strong and robust angulus, which is indented and elongated, triangular-shaped. The ramus is perpendicular with a strongly posteriad curving processus coronoideus. The cristae on the anterior part of the diastema are high. The skull is relatively low and appears robust due to the strongly developed frontal ridges. The lacrimal fossa is deep and oval. The praeorbital vacuity is relatively small. Both lacrimal foramina are on top of each other and positioned slightly more on the inside of the orbit rim. There is a strong facial crest. The lateral sides of the nasals grow into the praeorbital vacuity, the medial and lateral praemaxillary processes on the nasals are approximately equally long. There is one moderately sized supraorbital foramen and few smaller accessory ones. There are no prominent tuberosities on the basioccipital. Foramina ovale are large, auditory bullae small. The ventral intermaxillary suture forms a deep groove. Pedicles are long, strongly inclined and continue anteriorly with a strongly developed frontal ridge. Antlers were not present on the scrutinised specimen.

The only specimen available was very aged and thus teeth were worn. Anterior element(s) on p2 are longitudinally oriented, posterior elements are present, but heavily worn. Anterior and posterior elements are present on p3 and p4, also a strongly posteriad bent transverse cristid. Unfortunately, no more details can be observed. Apart from a skinny i3 all lower incisors and canines are missing.

P2 is longer than P3 and P4; P2 has several tiny central folds, which cannot be detected in P3 and P4 any more. Entostyles seem to be present on one or two molars. The posterior lobe of M3 is distinctively smaller. Upper canines are elongated, and slightly curve posteriad.

Muntiacus feae Thomas 1889

The mandible is relatively robust, with a round sometimes indented angulus. The ramus mandibulae is perpendicular with a posteriad curving processus coronoideus. The cristae on the diastema are high. The skull is low and relatively long; the nasal processes of the praemaxillae extend far posteriad. The lacrimal fossa is deep, large, and round, the

praeorbital vacuity moderately sized. Both lacrimal foramina are more or less on top of each other situated on the orbit rim. There is a prominent facial crest. The lateral sides of the nasals protrude into the praeorbital vacuity. The medial processi praemaxillaris on the nasals are slightly longer than the lateral ones. There is one large supraorbital foramen, embedded in a sulcus, often several smaller accessory ones. The tuberosities on the basioccipital are weak. Relatively large foramen ovale, small auditory bulla. The crista and protuberantia nuchae are well-developed. In the female specimen the frontal ridges bulge dorsally (in lateral view) and there is a protrusion above the posterodorsal corner of the orbit. Pedicles are very long, strongly inclined, almost horizontal and continue as a ridge on the frontals. Antlers in the examined specimen are short and single-tined.

A diagonally oriented anterior conid is present on the p2; there is a short transverse cristid and transversely oriented posterior elements. p3 has an anterior conid and most likely a small anterior stylid, the mesolabial conid is prominent, the transverse cristid short and bent posteriad, there is a weak mesolingual conid without cristids; the posterior elements are relatively long and transversely oriented. p3 and p4 have weak labial incisions. On the p4 the anterior conid and stylid are present, the latter shows a tendency to fuse with the mesolingual cristids. The mesolingual conid is separated from the short diagonally oriented transverse cristid and positioned more anterior to the mesolabial conid, closing the anterior valley. Posterior elements are diagonally oriented and, the posterior stylid is relatively short. All lower molars have a slightly larger anterior lobe. m1 has an anterior cingulid. The hypoconulid on the m3 can be a small cuspid or crescent-shaped. Lower incisors and canines are peg-shaped except for the i1, which is extremely enlarged.

All upper premolars have one prominent and several small central folds and an indentation between the antero- and posterolingual cone; the anterior styles are bent posteriad. The P2 is longer than the P3 and P4. On the molars the protocone and metaconule folds are mostly present. Parastyles and paracones are well-developed. The posterior lobe of the M3 is distinctively smaller. Weak entostyles are present on one or more molars. Upper canines are present in both sexes; they are enlarged, relatively slender and curving posteriad in males.

Muntiacus muntjak Zimmermann 1780

The corpus mandibulae is slender, the ramus broad and robust with a strongly posteriad bent processus coronoideus. The angulus mandibulae is elongated and indented. The cristae on the anterior part of the diastema are high. The skull is low and relatively long. The nasal processes of the praemaxillaries extend far posteriad. The lacrimal fossa is deep, large and oval, the praeorbital vacuity is relatively small. The lacrimal foramina can be offset, the inferior slightly more anterior than the superior one, both are situated on the orbit rim. There is a lacrimal process. The frontal ridges bulge dorsally and in females there is a protrusion above the posterodorsal corner of the orbit. The crista and protuberantia nuchae are well-developed. there is on moderately sized supraorbital foramen embedded in a sulcus; sometimes there are one or two additional smaller foramina. The basioccipital tuberosities are moderately developed, in some male specimens there is a deep channel between the anterior tuberosities. Auditory bullae are relatively small, oval foramen can be elongated. The medial praemaxillary processes of the nasals are mostly slightly longer than the lateral ones. Pedicles are extremely long and inclined, but not as near horizontal

as in other species. Antlers are short and two-tined with a short brow tine and longer main tine. The bifurcation is very close to the burr.

p2 has a short anterior conid, a mesolabial conid with a short and posteriorly oriented transverse cristid; posterior elements are present and diagonally oriented. On the p3 anterior conid and stylid are present often fused to a circle, there is a mesolabial conid with a strongly posteriad oriented transverse cristid, a weak mesolingual conid may be present, but no mesolingual cristids. There is a posterolabial conid and a posterior stylid, the posterolingual conid may be detached from the posterolabial cristid and fuse with the mesolingual conid/transverse cristid instead. Anterior conid and stylid are present in p4 and show also a tendency to fuse to a circle. There is a mesolingual conid with short mesolingual cristids; it is offset to the mesolabial conid, as the transverse cristid is diagonally oriented. Sometimes the transverse cristid is separated from the mesolabial conid. The posterolabial conid has only a short posterior stylid, the posterolingual conid is separated from the posterolabial cristid. m1 has an anterior cingulid, m2 may have a weak anterior cingulid. The third lobe of m3 is crescent-shape or circular. Ectostylids are present on one or more molars. The i1 are extremely broadened whereas the other lower incisors and canines are peg-like.

All premolars are approximately equally long, sometimes the P2 may be slightly longer. All premolars have one often two, sometimes more central folds. P2 sometimes shows an indentation between the antero- and posterolingual cone, the posterolabial cone is more prominent. P3 and P4 have posteriad bent anterior styles. A metaconule fold is mostly present in all molars, the protocone fold is variably present. The posterior lobe of M3 is smaller than the anterior one. entostyles are variably present one molar. Females have small upper canines with tiny accessory cusps on the posterior edge; males have enlarged upper canines curving posteriad.

Muntiacus reevesi Ogilby 1839

The corpus mandibulae is slender, the ramus more robust. The angulus mandibulae is slightly elongated and indented, the processus coronoideus bent strongly posteriad. The cristae on the anterior half of the diastema extend dorsally. The skull is low and moderately long. The nasal processes of the praemaxillaries extend far posteriad. The lacrimal pit is deep and oval, the praeorbital vacuity is relatively small; both lacrimal foramina are on top of each other and situated on the orbit rim. There is a small processus lacrimalis. The maxillary often protrudes into the praeorbital vacuity. The praemaxillary processes on the nasals are variably equally long, or one slightly longer than the other. There are prominent ridges on the frontals as anterior extension of the pedicles. There is one large supraorbital foramen sometimes embedded in a weak sulcus. Posterior basioccipital tuberosities are more developed than the anterior ones. The auditory bullae are relatively small, the foramen ovale is elongated. The anterior edge of fossa mandibularis is strongly transverse. The pedicles are inclined, but not close to horizontal, very robust, and moderately elongated. Antlers are two-tined with a short brow tine and a longer often inwards curving main beam. The bifurcation is close to the burr.

On the p2 an anterior conid is present, the mesolabial conid is the most dominant feature, posterior elements are short and transversely oriented. On p3 the anterior stylid is usually absent, the transverse cristid short and diagonally oriented, posterior elements

relatively long; there is a labial incision on p3 and p4. p4 has an anterior conid and stylid, the mesolingual conid has both mesolingual cristids; posterior elements are present, long, and diagonally oriented. m1 often with weak anterior cingulid, ectostylids are variably present on one molar. The postparacrista may be bipartite; the third lobe on m3 is crescent-shaped. The metacone sometimes shows an additional folding. The i1 is extremely broadened, the other lower incisors and canines are peg-like

All premolars have either one large, serrated central fold or several tiny folds, the posterior style is sometimes bipartite. The anterior styles on P3 and P4 are bent posteriad. There are up to two metaconule folds on upper molars. The protocone fold is variably present, mostly on M3. The posterior lobe on M3 is smaller than the anterior one. Sometimes upper molars have a serrated or additionally folded postprotocrista and premetaconulecrista. Entostyles are present on one or two molars. tiny C In females upper canines are small, in males they are enlarged and curving backwards.

Muntiacus truongsongensis Giao et al. 1998

The corpus mandibulae is slender, the ramus more robust. the angulus mandibulae is slightly elongated and indented. The cristae on the anterior half of the diastema extend dorsally. The skull is low and long; the nasal processes of the praemaxillaries extend far posteriad. The lacrimal fossa is deep and round, the praeorbital vacuity relatively small. Both lacrimal foramina are on top of each other and situated on the orbit rim, with a small processus lacrimalis between them. The orbitae are large and round. The medial praemaxillary processes on the nasals are a little longer than the lateral ones. There is one large supraorbital foramen embedded in a weak sulcus. The foramina palatina seem to be completely in the palatine. Basioccipital tuberosities are weak, the auditory bullae small and the foramen ovale elongated. There is a relatively deep groove at the ventral intermaxillary contact. The crista nuchae is M-shaped. The pedicles are strongly inclined, almost horizontal; antlers are two-tined

The only lower dentition available was in very poor condition. The p2 has a weak anterior conid and weak posterior elements, the mesolabial conid is the most prominent feature. The same applies to p3; there is a transverse cristid, which is strongly bent posteriad. On p4 most likely an anterior conid and stylid are present, a mesolingual conid, which is slightly offset to the mesolabial conid, due to the diagonally oriented transverse cristid. m1 and m2 have an anterior cingulid. An ectostylid is present on at least one molar. The i1 are extremely broadened, whereas the other lower incisors and canines are peg-like.

The upper dentition available for scrutiny was very worn. All premolars are approximately of the same length and have at least one central fold. Entostyles are present on two or more molars. Protocone and metaconule folds may be variably present. The posterior lobe of M3 is slightly smaller than the anterior one. Upper canines in males are enlarged and curving posteriad.

Muntiacus vuquangensis Tuoc et al. 1994

The mandible is slender, with a posteriad curving processus coronoideus. The angulus mandibulae is little elongated and indented. The cristae on the anterior half of the diastema are dorsally extended. The skull is low and moderately long. The nasal processes of

the praemaxillaries extends far posteriad. The lacrimal pit is large deep and oval. The praeorbital vacuity is relatively large; both lacrimal foramina are on top of each other and situated on the orbit rim with a prominent lacrimal process between them. The orbitae have two straight rims. There is one large supraorbital foramen with a weak sulcus anterior to it. There is a groove at the ventral intermaxillary contact. Basioccipital tuberosities are weak., auditory bullae are small and the foramen ovale elongated. The crista and protuberantia nuchae are well-developed. Pedicles are long and inclined and continue as a ridge on the frontal anteriad. Antlers are two-tined with a short brow tine and a longer main beam.

The anterior and posterior elements on p2 have almost no transverse component, the most prominent feature is the mesolabial conid. On the p3 a weak anterior stylid is present and an anterior conid. The mesolingual conid is offset to the mesolabial conid. There are no mesolingual cristids. p3 and p4 have a weak labial incision. p4 has an anterior conid and stylid, the transverse cristid is straight and there is a short posterolingual cristid; the posterolingual conid and the posterior cristid are long, the posterior stylid short. m1 has a weak anterior cingulid. Ectostylids are absent in this specimen. The third lobe of m3 is crescent-shaped. The i1 are extremely broadened, whereas the other lower incisors and canines are peg-like.

All premolars with at least one central fold. The P2 is slightly longer than P3 and P4 and has a more prominent posterolabial cone. P3 and P4 have a fold on the posterolabial crista. Entostyles are present on at least 2 molars. A metaconule fold is present on all molars, a protocone fold is sometimes present (M3). The posterior lobe of the M3 is little smaller than the anterior one. Upper canines in males are long, enlarged, curving backwards.

E.2 Morphology Fossil Cervidae

E.2.1 Miocene

Dicrocercus elegans Lartet 1837

The corpus mandibulae is relatively slender, the ramus more robust. The angulus mandibulae is rounded dorsally and indented only on the ventral side. The processus coronoideus is weakly curving posteriad. The skull has prominent temporal lines almost like a sagittal crest, the dorsal line of the braincase is straight in lateral view. Prominent tuberosities are absent in the basioccipital, instead there are weak grooves and ridges. The crista nuchae extends posteriad. There is one large supraorbital foramina, sometimes accompanied by one or two smaller ones. In lateral view the orbit, pedicle, and antler are all in one line (approximately perpendicular to the horizontal plane); in frontal view, the pedicles are inclined towards medial, while antlers are inclined towards lateral. The pedicle is strong and robust, originating directly above the orbit. Antlers do not have a shaft and bifurcate directly above the antler base. Often, there is a medial burr-like thickening on the base of the antler. Antlers are almost always bifurcating and strongly furrowed.

Lower premolars are slender/narrow; in the p2 the transverse cristid is sometimes missing, posterior elements are short, the anterior conid sometimes with transverse tendency. The p3 has an elongated anterolabial cristid, anterior conid (and stylid) are mostly longi-

tudinally oriented, the anterior stylid is variably present, the transverse cristid is strongly diagonally oriented pointing posteriad. There is a weak mesolingual conid, the posterior elements are relatively short and diagonally to transversely oriented. The anterior stylid and conid are present on p4; it has a widely open anterior valley, the transverse cristid has a strong kink. The mesolingual conid is prominent, mesolingual cristids are usually absent. The posterior elements are relatively long and are diagonally to transversely oriented. There is a weak labial incision on the p4. Ectostylids are regularly present on all molars and are involved in wear in later stages. A strong anterior cingulid is present on m1, weaker on m2 and variably present on m3. In some specimens an external postprotocristid is present (mostly on m1), sometimes m1 and m2 have a low posterior cingulid. External postprotocristids are regularly present on all molars. The third lobe of m3 is crescent-shaped. Lower incisors are only fragmentary available, no i1 could be scrutinised.

All upper premolars have at least one prominent central fold, often there is an additional fold originating from the posterolabial crista. P2 and P3 are considerably longer than P4 and have a dominant anterolingual cone compared to the posterolingual one. There is a weak indentation between the antero- and posterolingual cone. On P4 and on all upper molars a lingual cingulum is regularly present. Molars also often have an anterior cingulum with low entostyles. In M3 the anterior and posterior cone are approximately equally large. The postprotocrista and premetaconule crista fuse in later wear. The postprotocrista is bipartite (coded as protocone fold), the mesostyles are prominent. Upper canines are enlarged, curving mediolaterally, and have a very sharp posterior edge.

Heteroprox larteti Stehlin 1928

Most skull fragments studied were heavily crushed. Orbits are round. Pedicles originate directly above orbita and may be inclined at about 60 degrees. Antlers mostly with prominent ridges, normally bifurcated, but some show a third tine in the middle of the bifurcation (e.g., SMNS 44207), rarely more accessory tines can occur. There is sometimes a thickening on the proximal part of the antler.

p2 with a longitudinally oriented anterior conid, posterior elements are short and diagonally oriented, the transverse cristid if present is short and diagonally oriented. On the p3 the anterior conid and stylid are present, the transverse cristid and posterior elements are diagonally oriented. There is a weak labial incision on p3 and a deeper labial incision on p4. p4 has an anterior stylid and conid, the transverse cristid is often zigzagging, one or two mesolingual cristids can be weakly present, posterior elements are transverse and relatively long. The labial cones on the lower molars are pointy; ectostylids are present on at least two molars, an external postprotocristid is present on all molars. The third lobe of m3 is crescent-shaped. No lower incisor and canine material was available.

P2 and P3 are considerably longer than P4; P2 is long and narrow, the posterolingual cone is more prominent and has a tiny central fold. P3 is a little bit wider than P2 with a short central fold and a prominent anterior style. P3 and P4 have a lingual cingulum. P4 is shorter than P3 and P2 with a tiny central fold. On upper molars entostyles are present on all molars, parastyles and mesostyles are prominent. All molars with lingual cingula, often also with anterior and posterior cingula. The anterolingual base of the protocone bulges lingually; the postprotocrista and premetaconulecrista fuse in early wear via a complex pattern (see M3 sin in SMNS 43320). Metastyles are well-developed. Protocone folds are

mostly absent, instead a split into an internal and external postprotocrista can be observed, a tiny metaconule fold is present in some specimens. The posterior lobe on M3 is variably smaller than the anterior lobe. Upper canines are enlarged and curving posteriad.

Euprox furcatus (Hensel 1859)

The corpus mandibulae is slender, the ramus mandibulae and processus coronoideus are slightly inclined. The angulus mandibulae is strongly indented and elongated. Pedicles are very long and inclined. Antlers have a clear burr and are always bifurcating close to the burr. There is a weak indication for the presence of frontal ridges. Antler-pedicle complex is similar to *Muntiacus*.

The anterior conid on p2 is either longitudinal or slightly transverse, the transverse cristid is bent posteriad, posterior elements are transverse. There is a weak labial incision on p2 and p3. An anterior stylid and conid are present on p3, with a tendency to transverse orientation. The transverse cristid is with a weak mesolingual conid, mesolingual cristids are absent; the posterior elements are transversely oriented. On the p4 anterior conid and stylid are present, the mesolingual conid is clearly present, the posterolingual cristid is variably present. Posterior elements are elongated and transverse. In NMB Sth. 223 it looks like the posterolingual conid/posterior cristid connected to the posterolingual cristid and became separated from the posterolabial conid. More specimens are needed to check, whether this is a common or a single phenomenon. There is a deep labial incision on p4. There are ectostylids on all lower molars, which become involved in wear in medium to late wear stages; an anterior cingulid is present on all molars. The third lobe of m3 is crescent-shaped.

No P2 was available for scrutiny. The P3 is short and triangular with a weak central fold; the lingual cone is prominent, a weak lingual cingulum is visible. P4 has a lingual cingulum and a very short central fold. Entostyles are present on all molars, which may extend to a lingual cingulum. There is no protocone fold, but an internal and external postprotocrista, a tiny metaconule fold on M1 is variably present. The postprotocrista and premetaconulecrista fuse in later wear via a complex pattern similar to that observed in *Heteroprox*. The posterior lobe of M3 is almost the same size as the anterior one.

Lagomeryx parvulus (Roger 1898)

Antlers are tiny deciduous crowns with up to seven tines on long pedicles.

p2 has a diagonal-longitudinal anterior conid, the transverse cristid is present and strongly bent diagonal, posterior elements are transverse-diagonal; there is a tendency of the transverse cristid and the posterior elements to fuse. On the p3 the diagonally-transversely oriented transverse cristid and posterior elements are parallel. The anterior conid is diagonally-longitudinally oriented, the posterolabial conid is bulging and prominent. The p4 has a diagonally oriented anterior conid, a zigzagged transverse cristid, and a posterolingual cristid. The posterior cristid is fused to the posterior stylid, the posterolabial conid is prominent. All lower molars have ectostylids, an anterior cingulid, and an external postprotocristid; a posterior cingulid is often present. The third lobe on m3 varies in size, but is always crescent-shaped. A p1 is often present. Highly variable in appearance, sometimes similar morphology as p2, sometimes very reduced in elements.

The P2 has three cusps on the labial side (i.e. a prominent anterior and posterior style and labial cone) and one prominent lingual cone. There is a weak central fold oriented posteriad. P3 is slightly longer than P2; there are also three labial cusps and one strong lingual cone. It is triangular-shaped with a weak central fold. The P4 is shorter than P3 and P2, anterior and posterior styles are prominent and bent posteriad; a central fold is present. In upper molars the anterior complex is often more prominent than the posterior one; a protocone fold is variably present on M3. There is a lingual cingulum on all molars, which sometimes forms an entostyle. The upper canine has a sharp posterior edge and is very long considering the size of the other dentition.

Ligeromeryx praestans (Stehlin 1937)

Antlers are relatively large, often with three branches and sometimes with accessory sprouts. The morphology is intermediate between palmated crown-shaped antlers of the smaller *Lagomeryx* and trifurcated antlers. The pedicles are long, divergent, slightly curved, and convex on lateral side.

The posterior part of p2 is more prominent, anterior and posterior elements have a longitudinal orientation, a transverse cristid is present. On p3 the posterior elements are transverse, the transverse cristid is diagonal. There are no mesolingual cristids, the anterior elements are more longitudinal, due to wear detection of a separate anterior stylid is not possible. On the p4 an anterior stylid may be variably present, the transverse cristid is zigzagged, mesolingual cristid are variably present; the posterior elements are diagonally oriented. There is a weak labial incision. All lower molars have an anterior cingulid and an external postprotocristid, ectostylids are regularly present on all three molars; the metastylids are prominent and sometimes bent linguad. The third lobe of m3 is relatively small, both elements are present, but the hypoconulid is more prominent.

Procervulus dichotomus (Gervais 1849)

Most of the observations made on the cranium refer to the specimen BSPG 1979 XV 555. The corpus mandibulae is slender, the ramus a little more robust. The angulus mandibulae is strongly indented and elongated; the processus coronoideus curves posteriad. The skull is intermediately long. The nasals are long, the praemaxillary short with a pointy snout tip. It is not possible to detect the number of lacrimal foramina. Orbits are round. There is one moderately to large sized supraorbital foramen and one or two additional smaller ones. The temporal lines are close together forming a weak sagittal crest. The medial praemaxillary process on the nasals is longer than the lateral one. The foramina ovale are moderately sized, there are no tuberosities on the basioccipital, auditory bullae are relatively small. The fossa mandibularis is transverse (not perpendicular). Pedicles originate directly above the orbit and are near perpendicular in lateral view; they are not entirely straight in frontal view, but curve slightly medially and laterally. Antlers are sometimes smooth, sometimes furrowed, and always bifurcated.

The p2 is slender and has a slightly transversely oriented anterior conid; the transverse cristid is present pointing posteriad. The posterior elements are present, the posterolingual conid is longer than the posterior stylid. On the p3 an anterior conid and stylid are weakly present, the stylid may be absent in some specimens. There is a longitudinal, prominent mesolabial conid, a transverse cristid, and mesolingual conid, but no mesolingual cristids.

The posterolingual conid is longer than the posterior stylid. An anterior stylid and conid are present on p4, the transverse cristid is diagonal to straight; weak mesolingual cristids are variably present, as well as a weak labial incision. Often the posterolingual conid is longer than the posterior stylid. All lower molars have ectostylids, prominent metastylids, and external postprotocristids. The third lobe of m3 is crescent-shaped. Lower incisors and canines are small, the i1 minimally broadened compared to the other incisors.

All upper premolars available unfortunately were very worn; P2 has a primitive morphology, an indentation between the antero- and posterolingual cones, and the posterior part of the tooth is much larger than the anterior part. P2 is less wide than P3. P3 has a lingual cingulum, is triangular-shaped, and the posterior part of the tooth is more prominent. there is at least one small central fold. The P4 has an anterior cingulum, there are two central folds; P4 is the shortest of the three premolars with a simple morphology. Low entostylids are present on all molars, the metacone is inclined compared to the paracone, mesostyles are prominent. It is impossible to make a statement about the presence of protocone and metaconule folds. The anterior and posterior lobe on M3 approximately are of the same size. Upper canines are elongated and weakly curved posteriad.

Procervulus praelucidus (Obergfell 1957)

Holotype: BSPG 1937 II 12018, several paratypes, Wintershof West, MN3.

The mandible is slender with an indented angulus mandibulae.

There is one large and at least one smaller supraorbital foramen. *Procervulus praelucidus* represents the smallest species of *Procervulus*. Pedicles are slightly divergent, originating directly above the orbita; pedicles are longer than antlers. The antlers slightly inclined towards medial in frontal view, they have a smooth surface with occasional ridges.

The p2 is short, the anterior conid, transverse cristid, and posterior elements are present and transversely oriented. On p3 the anterior conid is oriented diagonally (anteriad), an anterior stylid is rarely present. The transverse cristid and the posterior elements are diagonally oriented (posteriad); a mesolingual conid can hardly be identified. On p4 the anterior stylid is variably present, the anterior conid is oriented longitudinally-diagonally. the transverse cristid is zig-zagging, there are no mesolingual cristids. External postprotocristids and ectostylids are present on all lower molars; molars have a broad base and are robustly built. Anterior cingulids are clearly present on m1 and m2, sometimes weakly on m3. The third lobe on m3 consists of a more prominent hypoconulid, and a reduced entoconulid, which is sometimes absent.

P2 and P3 are triangular and have an elongated labial part, central folds are weakly present, and both have a different morphology from P4. The P4 is narrow, has a lingual cingulum, and a central fold. Lingual cingula are present on all upper molars, protocone and metaconule folds are absent or only weakly developed, but a bipartite postprotocrista is variably present. The overall tooth size increases from M1 to M3. Low entostyles are present on all molars.

Eostyloceros hezhengensis Deng et al. 2014

This specimen was entirely scored from the literature. Although this is not the preferred way of scoring taxa, it was found to be necessary, as this genus represents a potential

important member of the muntiacines bridging the gap between *Euprox* and the extant *Muntiacus*. For a detailed morphological description see Deng et al. (2014).

Palaeoplatyceros hispanicus Hernández-Pacheco 1930

Pedicles medium to long and originate directly above the orbits. Antlers are slender, palmated and have a simple burr.

The p4 has an anterior conid and probably a weak stylid, the transverse cristid is extremely inclined and pointing posteriad, the mesolingual conid is perpendicular to the transverse cristid and offset to the mesolabial conid. Posterior elements are long and transversely oriented. A weak labial incision is present. The lower molars have a simple morphology, low anterior cingulids are present on all molars, ectostylids are present on at least two molars. The third lobe of m3 is crescent-shaped

P3 is long with a simple morphology; there are three dominant cusps on the labial wall, one long cusp on lingual wall. The central fold is connected to the labial crista. P4 is short, horseshoe-shaped, a central fold is present tending to fuse with the posterolabial crista. Upper molars with weak lingual cingula, low entostyles are present on all molars. Metaconule folds are absent, the M3 has a bipartite postprotocrista and sometimes an additional protocone fold

Pliocervus matheronis Gervais 1859

The p2 is short with a weak, longitudinal anterior conid, a transverse cristid and posterior elements, which are short and transversely oriented. The p3 has a widely open anterior valley, a tiny anterior stylid is present, a short anterolingual cristid is present. Posterior elements are transversely oriented. On the p4 an anterior conid and stylid are present and short mesolingual cristids. there is a labial incision. The anterior valley is open, the posterior elements are transverse. Lower molars often have a weak anterior cingulid, low ectostylids are present on most molars, The third lobe of m3 is crescent-shaped.

The P4 is horseshoe-shaped with a simple morphology and a central fold. A metaconule fold is variably present, protocone folds are absent, but bipartite postprotocristae occur. Entostyles are variably present.

No cranial material was available for scrutiny.

E.2.2 Pliocene

Arvernoceros ardei Croizet & Jobert 1828

Basioccipital tuberosities are well-developed. Pedicles are slightly elongated. Antlers observed had three tines, a posteriad curving brow tine and a long and curved main beam with a bifurcating tip; the bifurcation has a small angle. There are clear ridges on the antlers especially on the base and a clearly developed burr is present. Specimen NMHN PET 1020 has an accessory ‘middle tine’, three tines, curved antler beam, first tine, then bifurcation on end of beam.

p2 with transversely oriented anterior conid, the transverse cristid is oriented strongly diagonally pointing posteriad, the posterior elements are more transverse. The anterior conid in p3 is longitudinally oriented the transverse cristid/mesolingual conid is separate from the mesolabial conid and diagonally oriented. The anterior valley is widely open. The

posterior elements are long and transversely oriented. p3 has a weak, p4 a strong labial incision. The p4 has an anterior conid and stylid, transversely oriented; the anterior valley is open. The transverse cristid in p4 is zigzagging. There is a prominent mesolingual conid with a posterolingual cristid, the posterolingual conid can be separated from the posterolabial cristid, the posterior stylid is long and transversely orientated. There are low ectostylids on at least two molars; lower molars have a simple morphology and mostly have an anterior cingulid. The third lobe of m3 is crescent-shaped.

No P2 was available for investigation; all upper cheek teeth have lingual cingula. premolars with clear indentation between anterolingual and posterolingual cone, which may end up in completely separated cones in P3, both premolars have a prominent, elongated central fold. The upper molars have serrated premetaconule- and postprotocristae, a protocone fold is present on M2 and M3, metaconule fold may be variably present on M2. The posterior lobe on M3 is distinctively smaller than the anterior lobe.

'Cervus' australis Linnaeus 1758

The mandible is slender and the angulus mandibulae is clearly indented and elongated.

Pedicles are relatively short. Antlers have a burr, are bifurcating after a clear shaft. There are ridges on the antlers.

p2 has a longitudinally orientated anterior conid and no distinct transverse cristid. All premolars have transversely orientated posterior elements. p3 and p4 with have an anterior conid and stylid, a transverse cristid, which originates posterior to the mesolabial conid and is oriented diagonal. The anterior valley is open. On p3 there are no lingual cristids, the mesolingual conid is tiny. On p4 there is a small anterolingual cristid, the posterolabial conid is enlarged. p3 has a weak, p4 a deep labial incision. Ectostylids are present on at least two molars. m2 and m3 have an external postprotocristid, presumably also on m1, which is missing in this specimen (NMB M.P. 511) and too worn in the other specimen (NMB M.P. 465). The lingual walls are slightly indented. The third lobe on m3 is crescent-shaped.

Procapreolus cusanus Croizet & Jobert 1828

The skull is slender and elegant. The temporal lines are further apart than in some Miocene species (e.g. *Dicrocerus*). The basioccipital tuberosities are weakly developed and there is a groove between the anterior tuberosities. Pedicles are slender, slightly elongated, and inclined; pedicles are close together. The slender antlers are always three-tined, branching in a typical pattern, with the first tine originating relatively high above burr, and a bifurcation at the end of the main beam. The antler surface bears weak to moderate ridges.

p2 has a weak, longitudinally orientated anterior conid, the transverse cristid and posterior elements are transversely oriented. On the p3 an anterior stylid and conid are present, the transverse cristid is diagonal with a connection to the mesolingual conid; anterior and posterior elements are transversely orientated. p3 has a weak and p4 a deep labial incision. p4 has a closed anterior valley via a connection between the anterior conid and mesolingual conid; posterior elements are transversely oriented, the posterolabial conid is enlarged [similar as in *Capreolus*]. Ectostylids are present on all molars, there is a very weak anterior

cingulid present on one or more molars. The third lobe on m3 is either crescent-shaped or consisting of a trifurcating hypoconulid.

The mandible labelled 'no nr vitrine' probably is Nr 5237 according to drawing in Croitor (2014).

Praeclaphus etueriarum Croizet & Jobert 1828

Antlers have a very short shaft with immediate bifurcation in an open angle; the 'brow' tine is upright, the main beam available for examination was broken, but indicating a terminal bifurcation. Weak ridges are present.

no p2 was available. p3 has an anterior conid and stylid, the transverse cristid and mesolingual conid are posterior to the mesolabial conid; posterior and anterior elements are transversely oriented. p3 and p4 have labial incisions. p4 has a separate posterolingual conid, mesolingual are cristids present; the anterior stylid and conid are connected with each other forming a small fossetta due to wear. Anterior elements are transversely oriented, posterior elements are diagonal.

All lower molars have prominent ectostylids, which are relatively high compared to other cervids, in m1 it is even worn; there is a weak anterior cingulid present on m2, very weak on m3, not visible on m1 one, because of a breakage. The third lobe of m3 is circular.

P2 and P3 have a tiny central fold. On the P2 the antero- and posterolabial cone are separate, on P3 there is an indentation between the two cones. P4 has a simple morphology and is horseshoe-shaped. The protocone fold is absent, a tiny metaconule fold present on all three molars. Molars are broad and have prominent labial cingula.

Metacervocerus pardinensis Croizet & Jobert 1828

The only two antler fragments available show a clear burr, the first bifurcation is above a short shaft and forms an acute angle; there are ridges on the antler surface.

p2 has relatively long elements; anterior and posterior elements are transversely oriented, the transverse cristid is diagonal. p3 and p4 have an anterior stylid and conid, which are fused forming a fossetta. On p3 the anterior elements are diagonally oriented, the posterior elements are more transverse. The transverse cristid is diagonally oriented with a mesolingual conid; mesolingual cristids are absent. On p4 anterior elements are oriented transversely, as is the transverse cristid. Mesolingual cristids are present on p4, the posterolingual conid is angled. There is a deep labial incision. All lower molars have a weak anterior cingulid, ectostylids are present on at least one molar. The third lobe on m3 is crescent-shaped.

All upper premolars have a deep incision between the antero- and posterolingual cones and a prominent central fold, partly with small accessory fold(s). P3 and P4 have a lingual cingulum. On P4 the anterior and posterior styles are strongly curved. All upper molars have lingual cingula and entostyles. Tiny protocone and metaconule folds are variably present on molars, sometimes the postprotocrista is bipartite.

'Cervus' perolensis Azzaroli 1952

Antlers sit on short pedicles, have ridges and a clear burr.

p2 has an enlarged posterolabial conid, the anterior conid is slightly transversely oriented, there is a short transverse cristid. The anterior valley in p3 is wide, transverse

cristid is short, diagonally oriented without mesolingual cristids. Posterior elements are transversely oriented. On p4 mesolingual cristids are present, the anterior valley is open. The posterolingual conid is angled. A weak anterior cingulid and relatively high ectostylids are present on all molars. The third lobe on m3 is crescent-shaped.

All specimens available are heavily worn. P2 and P3 have an indentation between the antero- and posterolingual cone; P2 bulges linguad at the base. All premolars have a central fold. Entostyles are present on all molars. On M1 and M2 a metaconule fold is present. Parastyles and mesostyles are bent posteriad.

Praeclaphus perrieri Croizet & Jobert 1828

Antler fragments have a clear burr, the bifurcation is close to the burr. Antlers have at least three tines.

On the p2 the anterior conid is longitudinally oriented, posterior elements are transversely oriented, a short transverse cristid present. p3 and p4 probably have an anterior stylid and conid, diagonally oriented, but are very worn; p3 has a mesolingual conid, which is more posterior to the mesolabial conid, posterior elements are transverse. The anterior valley is widely open. p3 has a weak, p4 a deep labial incision. On p4 short mesolingual cristids are present. Posterior elements are very worn, but were transversely oriented. All lower molars have weak anterior cingulids and ectostylids. The third lobe of m3 is crescent-shaped.

P2 and P3 have a deep P4 a weak incision between the antero- and posterolingual cone. All premolars have a prominent central fold. P2 and P3 have more prominent posterolabial cones; posterior styles are bent labiad in all premolars. simple morphology. Upper molars have pronounced mesostyles. A tiny metaconule fold is variably present on one or more molars. Low entostyles are present on one or two molars.

‘Cervus’ philisi Schaub 1941

The mandible is slender with a slightly posteriad inclined ramus mandibulae and processus coronoideus. The angulus mandibulae is weakly indented on the dorsal side and elongated. The skull is slender with the typical cervid outline. The lacrimal fossa is relatively deep and oval, even in females, there is a large praeorbital fossa. There are two lacrimal foramina, whose exact position is difficult to determine due to the condition of the available specimens. A posterodorsal protrusion is present above the orbits in females. The nasals have only little lateral extension. The protuberantia on the crista nuchae is prominent. Basioccipital tuberosities are weakly present. Antlers have a clear burr and ridges on their surface. There is a short shaft before the first bifurcation, which forms an acute angle. The main beam has one distal bifurcation (Schaub, 1941).

The p2 has a short anterior conid, a short diagonally oriented transverse cristid is present, posterior elements are long. The p3 has an anterior stylid and conid, the mesolingual conid is offset from the mesolabial conid; in some specimens there is a small anterolingual cristid. The posterior elements are long and transversely oriented. There is a weak labial incision on p3 and a relatively deep labial incision on p4. The p4 is variably molarised, ranging from the development of only one of the mesolingual cristids to complete closure of the anterior valley. An anterior stylid and conid are present, if not fused with

the mesolingual conid. The posterior elements are relatively long, the posterolabial conid extends labiad. The i1 is distinctively broadened.

P2 and P3 have an incision between the antero- and posterolingual cone, which sometimes also is weakly present on P4. All upper premolars have a central fold, small accessory folds sometimes occur. P2 has a simpler morphology than P3. P4 is comparatively short. There is no protocone fold in the upper molars, but the metaconule fold is variably present on M1 and M2. Mesostyles are pronounced, entostyles are present on all molars; sometimes a weak posterior cingulum is present.

'Cervus' sivalensis Lydekker 1880

The skull is slender. The lacrimal fossa is clearly present and oval, there is a praeorbital vacuity. Both lacrimal foramina are situated on the orbit rim. Cristae on the maxilla are strongly developed. The nasals are narrow in dorsal view. The temporal lines are prominent and the frontals are bulging. The basioccipital tuberosities are well developed and there is a clear groove between them. The pedicles are relatively long and slender. The antlers are strongly curved; the first bifurcation is close to the burr and opens in an open angle. There is another bifurcation more distal on the beam. There are ridges all over the antler surface.

Only one m2 and m3 were available for scrutiny. The m3 has a trifurcated hypoconulid. Very weak anterior cingulids are present on all molars.

P2 has a separate antero- and posterolingual cone and a weak central fold; the overall morphology is less pronounced than in P3. The P3 has an incision between the antero- and posterolingual cones, a well developed central fold, and a posteriad bent posterior style; P4 has one lingual cone, a long central fold, and a weak lingual cingulum. Upper molars have weakly indented anterior and posterior tooth walls and strong labial ribs. An anterior cingulum and lingual cingulum is present on all upper molars. Entostyles are variably present and become λ -shaped in later wear. Overall, the upper dentition resembles that of *Rucervus*.

Croizetoceros ramosus Croizet & Jobert 1828

No sufficiently well preserved mandible was available for scrutiny.

There is one moderately sized supraorbital foramen on each side. The lacrimal fossa is oval.

Pedicles are short, slender, and divergent from sagittal plane. Antlers are slender, flattened, and elegant compared to their length; the angle between the brow tine and the main beam is wide. Antlers have at least three main tines which are organised in a unique pattern. The first bifurcation is relatively high above burr and there are multiple tines on the main beam.

The p2 is relatively long and has a longitudinally oriented anterior conid; a short transverse cristid is present. The posterior elements are long and transversely oriented. p3 and p4 have a deep labial incision. On the p3 a long anterior conid and stylid are present, the transverse cristid is connected to the mesolingual conid and can be zig-zagging. There are no mesolingual cristids. The posterior elements are long and transversely oriented. The p4 has a closed anterior valley, the anterior elements are often fused with the mesolingual cristid. The posterolingual conid has a prominent kink. The posterolabial extends strongly

labiad with. All lower molars have anterior cingulids and ectostylids on two or more molars, The third lobe of m3 is crescent-shaped.

P2 and P3 have a weak incisions between the antero- and posterolingual cone. All upper premolars likely have a central fold, specimens available for scrutiny of P2 and P3 are very worn. The central fold is clearly present in P4. Upper molars have no lingual cingulum; the metaconule fold is variably present, protocone folds are absent. Entostyles are present on at least one molar.

Eucladoceros ctenoides Depéret 1910

The Mandible is slender with a posteriad curving ramus and processus coronoideus. The angulus mandibulae is broad and wide and slightly indented.

The skull is relatively long and robustly built in males. The praemaxillae are broad. The lacrimal fossa is deep and oval the praeorbital vacuity is trapezoid. Both lacrimal foramina are situated on the orbit rim. The nasals are relatively long and narrow. There are prominent anterior tuberosities on a well-developed, near square-shaped basioccipital. The supraorbital foramina are large, the temporal lines are well-developed.

Antlers are extremely long and wide with comb-like pattern. The basic bauplan has four tines, each of them may have accessory tines and/or a bifurcation on distal end. The distance between the first and the second tine is larger than between second to fourth/fifth tine (except in the subspecies *E. tetraceros*).

On the p2 the anterior elements are longitudinal; there is a short transverse cristid as well a transversely oriented posterior elements. p3 has an anterior conid and stylid, a broad mesolabial conid, and a weak mesolingual conid without cristids. The posterior elements are short. p3 and p4 have a moderate to deep labial incision. The p4 has an anterior conid and stylid, a mesolingual conid with weakly to moderately developed cristids, rarely (NHM 34426) closing the anterior valley. The posterior elements are long and transversely oriented. All lower molars have a weak anterior cingulid, ectostylids are present on one or more molars. The third lobe on m3 is crescent-shaped.

The lower canines and incisors show the cervid-typical morphology with a broadened il.

All upper premolars have a central fold. The P2 often has a separate antero- and posterolingual cone. On P3 there is an indentation between the antero- and posterolingual cone. There are entostyles on at least one or two upper molars. A metaconule fold is present on M2 and M3, there are no protocone folds. Parastyles are prominent.

There is an indication of the presence of an upper canine in NMB Se 1798 and MNHN 17.

E.2.3 Pleistocene

Candiacervus ropalophorus (Simonelli 1907)

The mandible is robustly built with an upright ramus and processus coronoideus; the angulus mandibulae is wide and round and indented on the ventral side.

The skull is low with a slightly elongated viscerocranial proportion, the snout is very low/slender in lateral view. The dorsal outline in lateral view is strongly convex at the braincase and strongly concave between the orbitae (similar to *Dama* and straight at the

nasals. The lacrimal fossa is shallow, if at all developed, the praeorbital vacuity is very small. The orbit rims and zygomatic arch are robustly built; the ventral rim of the orbits extends laterally. Both lacrimal foramina are situated on or slightly more anterior to the orbit rim and the inferior foramen is more anterior than the superior one. There is a well-developed processus lacrimalis. The anterior two thirds of the nasals are narrow and straight in dorsal view; on the posterior end they protrude into the praeorbital vacuity. The maxillary and frontals sometimes are in contact. Rarely, there are two infraorbital foramina. There is initial suture fusion of the supraoccipital-parietal, parietal-frontal, frontal-frontal, and frontal-nasal sutures. The supraorbital foramina are extremely large. The basioccipital is quadrangular with weakly developed tuberosities. The foramina ovale are large. There is one foramen on each side of the occipital condyle in ventral view. There are two lateral protuberantiae lateral to the main protuberantia on the crista nuchae, which extends far ventrally.

There are bulges around the pedicles on the frontals and dorsal to the orbits. The pedicles are strong with a deep postcornual fossa. They are situated far apart and are divergent in dorsal view. Antlers are very long compared to the overall size of the species with only few tines (two to three tines).

All the available lower dentition was heavily worn. The p2 is short with a weak labial incision; the anterior conid and posterior elements are transversely oriented. On p3 an anterior stylid and conid are present, posterior elements are transverse; there is a weak labial incision. The transverse cristid is short and diagonally oriented, the mesolabial conid is prominent, mesolingual cristids are absent. The p4 is variably molarised with a weak labial incision. The anterior portion of p4 is more prominent, particularly the labial part. An anterior conid and stylid are present, if the anterior valley is not closed, mesolingual cristids are variably present and sometimes connecting to the anterior conid. The posterolingual conid sometimes has a kink. Ectostylids are present on at least one molar. A weak anterior cingulid is present on all molars. The third lobe of m3 is crescent-shaped.

The P2 is distinctively longer than P3 and P4; there is an indentation between the antero- and posterolingual cones. The morphology is more primitive than in the other premolars. All premolars have one or two short central folds. P3 and P4 are short with one lingual cone. P3 sometimes has a weak indentation in the lingual cone. A weak lingual cingulum is sometimes present. Entostyles are present on all upper molars. Protocone folds and metaconule folds are only rarely present.

There is no evidence for upper canines.

Rusa kendengensis Dubois 1908

Pedicles are relatively long. Antlers are moderately furrowed; the first bifurcation is close to the burr. The beam has got at least one more distal bifurcation.

The p4 has an anterior conid and stylid with a diagonal orientation; the transverse cristid is zigzagging, mesolingual cristids are present. The anterior valley is open; posterior elements are transversely oriented. There is a shallow labial incision. The lower molars have indentations on the labial walls; the metastylids are partly strongly developed. An anterior cingulid is present on at least m3. Ectostylids are present on one or more molars.

P2 and P3 either have clearly separate antero- and posterolingual cones or an indenta-

tion between them. The posterolingual part of the cone protrudes much more lingual than the anterolingual part. P4 has only one cone and an lingual cingulum. All premolars have one central fold. Upper molars have indentations on their lingual walls, and pronounced parastyles and mesostyles. Entostyles are present on at least two molars. They resemble the upper molars of *Rusa* and especially *Rucervus*.

Axis lydekkeri Dubois 1908

The mandible has a robust, minimally posteriad inclined ramus. The angulus mandibulae is wide and round with shallow indentations on the ventral and dorsal side.

The skull is slender in dorsal view, low and intermediate in length in lateral view. The lacrimal fossa is shallow, but clearly present. The orbit rims were often destroyed or reconstructed. The supraorbital foramina are large and round, sulci are absent. The cristae nuchae and protuberantia nuchae are prominent, partly extending posteriad. Auditory bullae are large and round. The anterior tuberosities on the rectangular basioccipital are strong with a clear groove between them.

Pedicles are relatively long and slender and inclined. The antlers are always three-tined, slender, and strongly curved. The antler morphology resembles *Axis axis*. The second tine of the main beam looks like a 'back tine'.

Generally, the dentition available for scrutiny was heavily worn.

The p2 was only fragmentarily preserved. On the p3 an anterior stylid is variably and weakly present; the mesolabial conid is prominent, the transverse cristid originates from the posterior side of the mesolabial conid. There are no mesolingual cristids. In two specimens (RGM 13796, RGM 1957) the mesolingual conid fuses with the posterior cristid, via a short mesolingual cristid. The posterior elements are relatively long and transversely orientated. The p4 has a weak labial incision; the anterior conid and stylid are transversely oriented. The posterior elements are long, mesolingual cristids are present. The transverse cristid is straight, sometimes slightly diagonal. The anterolingual cristid may fuse with the anterior conid. All lower molars have a strong anterior cingulid, Ectostylids are present on at least two molars. The third lobe of m3 is crescent-shaped.

A central fold is present in all premolars. P2 has an indentation between the antero- and posterolingual cone. P2 is longer than P3, and P3 is longer than P4. On P2 and P3 the posterolabial cone is more prominent. A metaconule fold is present in all molars, whereas a protocone fold could not be observed. Entostyle are weakly present on one or more molars. Rarely a weak lingual cingulum is present in the upper molars.

Alveoli for upper canines are clearly present.

Metacervocerus rhenanus Dubois 1904

Left antler figured by Dubois in 1904, p. 219, fig. 2, same antler

The mandible is slender with a slightly posteriad inclined ramus and processus coronoideus. The angulus mandibulae is round and broad with a weak ventral indentation.

The skull fragment is slender in dorsal view. The pedicles are relatively long and inclined. Antlers are slender, three-tined, and weakly ornamented; there is a strong burr.

The p2 is simple with a transversely orientated anterior conid, a diagonally oriented transverse cristid, and prominent posterior elements. On the p3 the anterior stylid and conid are longitudinally orientated. The anterior valley is wide. The transverse cristid

originates far posterior, there are weak labial incision, no mesolingual cristids, posterior elements are long. The p4 has an anterior conid and stylid, which are sometimes fused forming a fossetta; the transverse cristid is zigzagging, mesolingual cristids are present. The posterolingual conid has a kink. there is a weak labial incision. All lower molars have a weak anterior cingulid. The third lobe on m3 is crescent-shaped. Ectostylids are present on at least one molar.

All upper premolars have an indentation between the antero- and posterolingual cone, which is often separated in P2. A prominent central fold is present in all premolars. P3 and P4 have prominent anterior styles. On P3 the central fold may connect with the posterolingual crista. P4 is the shortest premolar. All upper molars have prominent para- and mesostyles and a metaconule fold. The protocone fold is absent on all molars. A very weak lingual cingulum is variably present. The posterior lobe of M3 is distinctively smaller.

Megaloceros giganteus (Blumenbach 1803)

The corpus mandibulae is strongly thickened on the lateral and medial sides, the ramus is robust and upright with a long and slender, slightly posteriad curving processus coronoideus. The angulus mandibulae is stronger indented on the dorsal side than on the ventral side. There are clear tuber on the lateral sides of the mandibles.

The skull is long and low with a strongly concave dorsal outline between the orbits in lateral view. Most sutures around the cranium are fused. The praeorbital vacuity is tiny, nearly closed in some specimens, the lacrimal pit is shallow. Both lacrimal foramina are situated on the thick orbit rim. The praemaxillary has a far posteriad extending processus nasalis. There are small mediad pointing processi on the most anterior part of the praemaxillaries. The ‘vomer kite’ is present at the ventral praemaxillary-maxillary contact, the fissura palatina is half-moon-shaped. The processi rostralis on the nasals are short and of equal length. Supraorbital foramina are very large; the fossa temporalis is prominent. There is a bulge above the temporal fossa in middle of cranium. Auditory bullae are relatively small. There is a prominent process on the medial side of the mandibular fossa. The occipital condyles are broad and strong with a fossa anterior to them. The basioccipital is prominent with well-developed tuberosities and a groove between the anterior tuberosities (even in females).

The pedicles are short and strong with a large diameter. Burrs are prominent on the antlers. The first bifurcation is directly above the burr and splits into a flattened brow tine and a massive, extremely long, palmated, and multi-tined main beam.

The p2 has a longitudinal anterior conid, a short transverse cristid, and transversely oriented, long posterior elements. The posterolabial conid is the most prominent. The p3 has an anterior conid and stylid, a short diagonally oriented transverse cristid without mesolingual cristids. A weak labial incision is variably present. The posterior elements are long and transversely oriented. The p4 has a deep labial incision; the posterior elements are very long and transversely oriented. In some specimens the anterior conid is fused with the mesolingual cristid, closing the anterior valley, sometimes the anterior conid and stylid are separate; in that case the mesolingual conid and associated cristids form a lingual wall, which is separated from the transverse cristid. All lower molars have ectostylids. Anterior cingulids are variably present. The third lobe on m3 is crescent-shaped and sometimes

forms a circle in later wear.

All upper teeth have a lingual cingulum, partly including cusps. All upper premolars have one central fold. The P2 has an indentation between the antero- and posterolingual cone and is longer than P3 and P4. The anterior styles are prominent on P3 and P4. Upper molars have prominent para- and mesostyles, a small metaconule fold is commonly present. Entostyles are present on all molars.

***Muntiacus muntjak* RGM** The corpus mandibulae is slender, the ramus was missing in the examined specimen. The angulus mandibulae is indented and elongated. The cristae on the anterior part of the diastema extend dorsally.

No cranial remains were available to investigate.

Antlers have a burr and are two-tined (similar morphology as in *Muntiacus*). There are ridges covering the whole antler surface.

The elements on p2 are short and consist of an anterior conid, a transverse cristid, and transversely oriented posterior elements. p2 has a weak, p3 and p4 a deep labial incision. p3 has an anterior conid, a transverse cristid, and diagonally orientated posterior elements. Mesolingual cristids are absent. On the p4 an anterior conid and stylid are present, a diagonally oriented transverse cristid, and more transversely oriented posterior elements. The anterior valley is open; there are no mesolingual cristids. All lower molars have a strongly developed anterior cingulid and ectostylids. The third lobe of m3 is crescent-shaped forming a circle in later wear.

The upper dentition is heavily worn, fragmentary and in bad condition. P2 has a separate antero- and posterolingual cone. The P3 has two short central folds and a weak indentation between the antero- and posterolingual cone. The P4 has one anterior oriented central fold. M1 and M2 have anterior and posterior cingula. The lingual walls are indented. An entostyle is clearly present on M1, and probably was present on M2 as well. There are no metaconule or protocone folds.

The upper canine is elongated and strong with typical *Muntiacus*-like morphology.

Odocoileus The individuals scrutinised at the NHM consist of several isolated specimens, all but one from Brazil, one from Florida.

Florida specimen: The mandible lacks the anterior-most part; the processus coronoideus is slender and slightly curving posteriorly. The angulus mandibulae is wide and round and indented. The corpus mandibulae is slender. p2 is short, the anterior conid barely present. The transverse cristid and posterior elements are short. p3 has an anterior stylid and conid, the transverse cristid is diagonal, originating on the posterior end of the mesolabial conid. The posterior elements are transverse and long. On p4 the anterior stylid and conid are present despite fusion of the anterior conid with the mesolingual cristid. The transverse cristid is disconnected from the mesolingual conid. There are long mesolingual cristids and a very deep labial incision. The posterolingual conid/posterior cristid are diagonal, the posterior stylid is transverse. Ectostylids are present on at least one molar. The third lobe of m3 is crescent-shaped with a tendency for a tripartite hypoconulid. m3 has a weak anterior cingulid.

The other three mandible specimens show a similar morphology with a closed anterior valley on p4 and a disconnection of the transverse cristid from the lingual elements. In the

latter case the anterior stylid is often missing.

The upper dentition is highly fragmentary, only P4-M3 are present; there are two large central folds on P4. All upper molars have protocone and metaconule folds. Entostyles are present on two or more molars.

All skull specimens are female, some of them might be juvenile or of the small sized morphotype. The supraorbital foramina are moderately sized, embedded in weak sulci. The cristae and protuberantia nuchae are weak, the foramina ovale are large. The tuberosities on basioccipital are weak; the bony bar posterior to the fossa mandibularis is open; the process posterior to the fossa mandibularis is two-humped.

BSPG specimen:

The female skull lacks most of the praemaxillae and nasals. It is moderately long and low. The tuber maxillae are broken, but presumably were elongated. Orbits are large and round. Both lacrimal foramina are situated on top of each other on the orbit rim. The praeorbital vacuity is large, the lacrimal fossa is well-developed. The infraorbital foramen is dorsal to the P2/P3 border. The process on the mandibular fossa is two-humped. The protuberantia and cristae nuchae are prominent. The supraorbital foramina are large embedded in deep sulci. The foramina ovale are large; auditory bullae have a median process. The posterior tuberosities on the basioccipital are weakly present.

The dentition is heavily worn. P2 is longer than P3 and P4 teeth worn with one or two tiny central folds. P3 has one or two tiny central folds. P4 with one small central fold. The anterior styles on P3 and P4 are bent posteriad. The labial walls of the premolars are tilted against the jaw axis. Entostyles are present on all molars. Molars have a fossetta in the anterior lobe, presumably caused by the fusion of the protocone fold with the postprotocrista. Tiny metaconule folds are present in all molars. The posterior lobe of M3 is distinctively smaller.

F Adam's Consensus Trees of Chapter 3

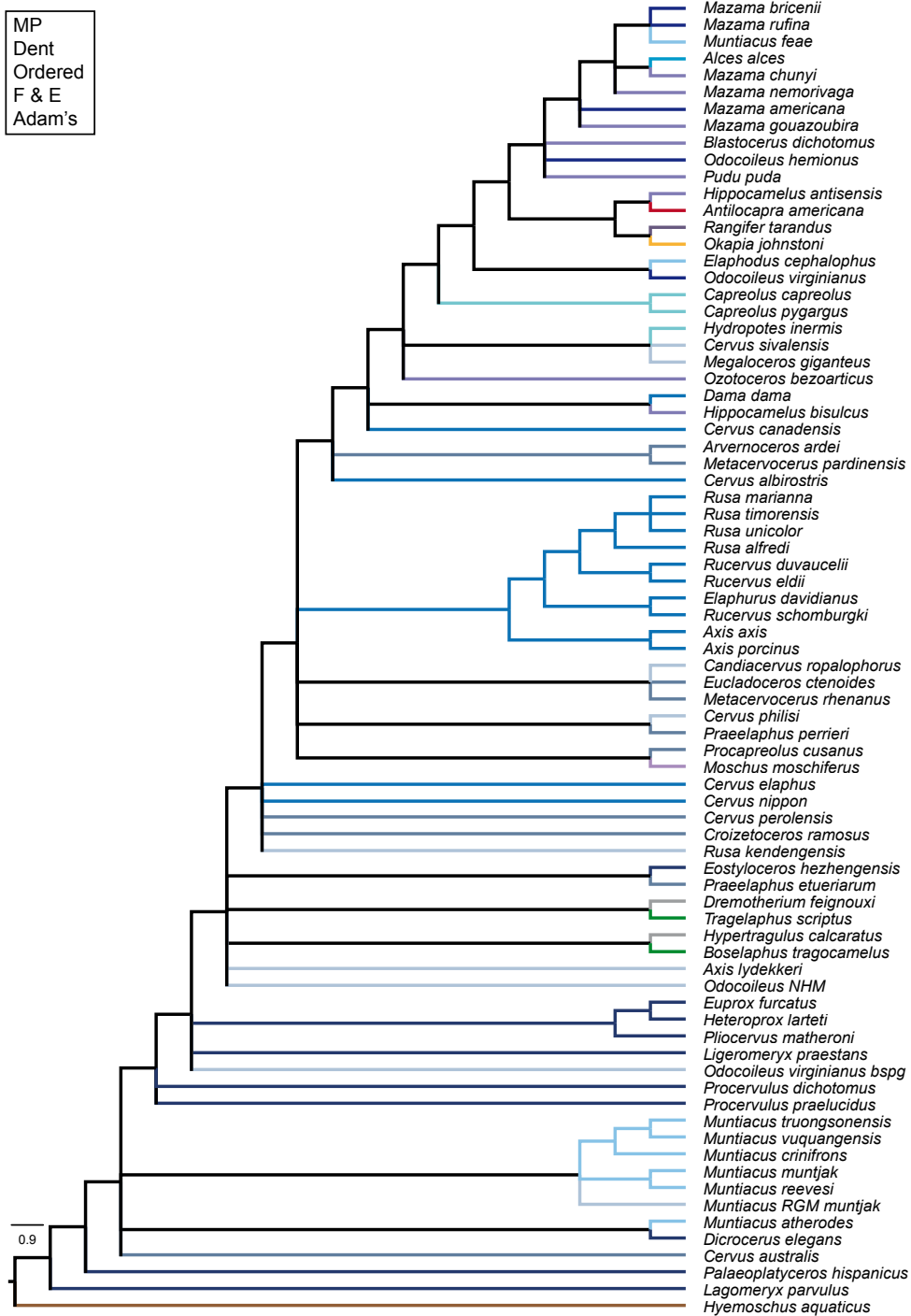


Figure F.1: Adam's consensus topology of the maximum parsimony analysis based on the ordered dental character set for fossil and extant taxa.

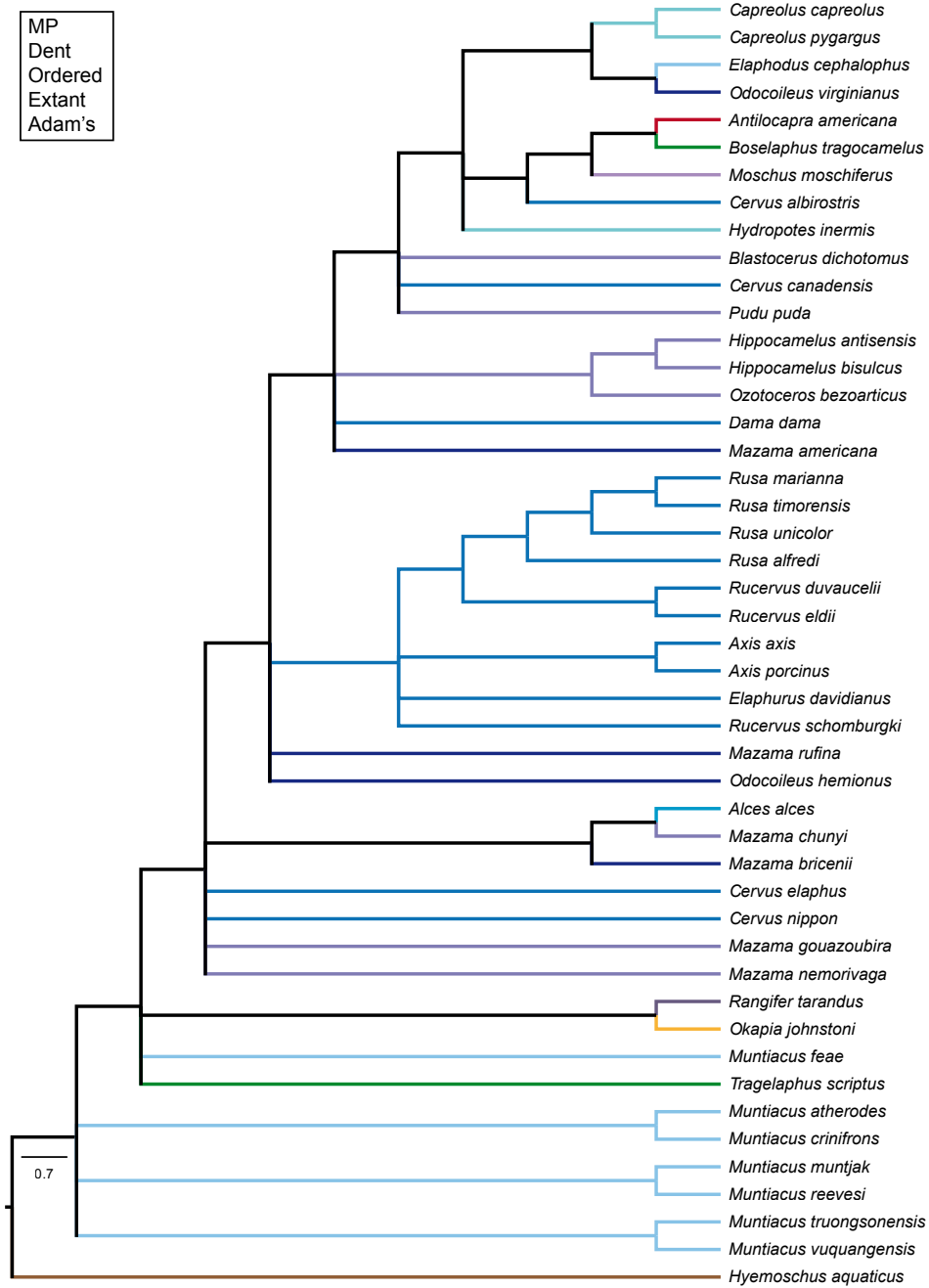


Figure F.2: Consensus topology of the maximum parsimony analysis based on the ordered dental character set for extant taxa.

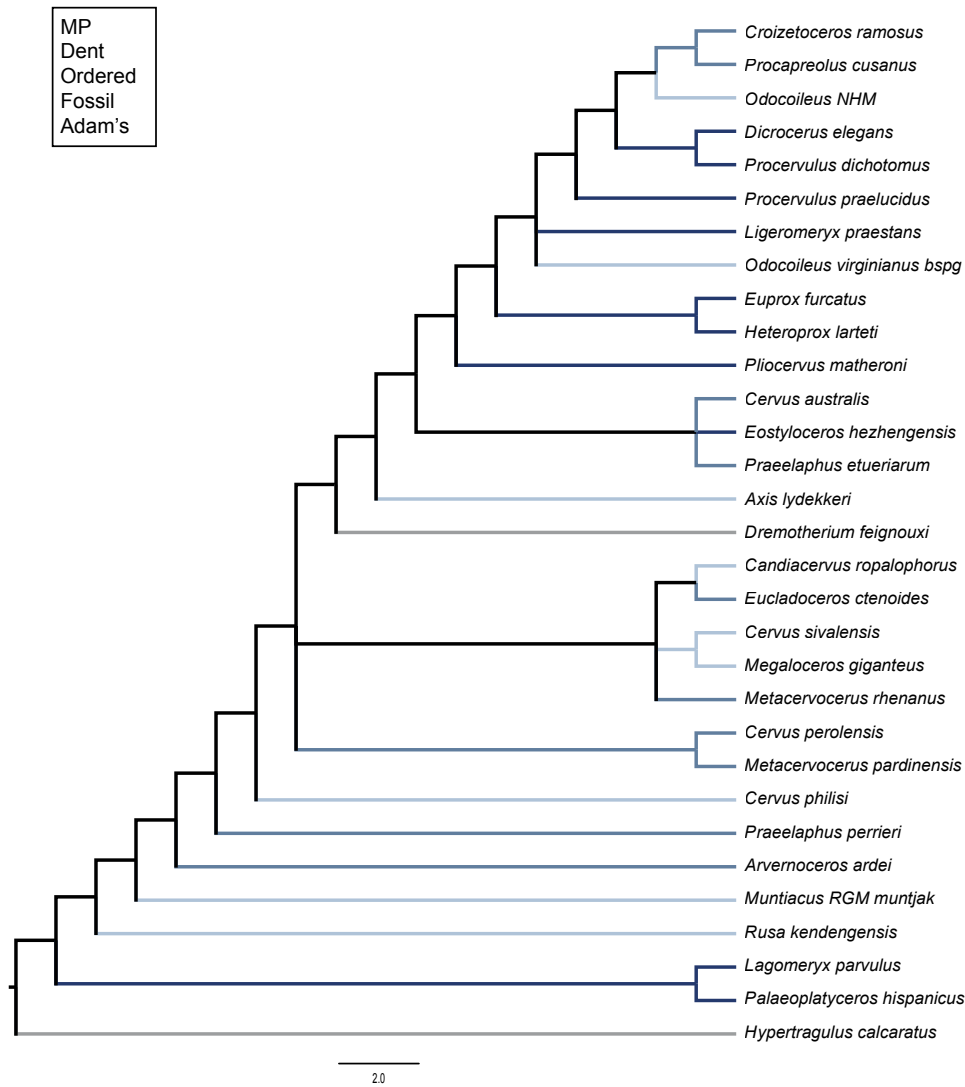


Figure F.3: Adam's consensus topology of the maximum parsimony analysis based on the ordered dental character set for fossil taxa.

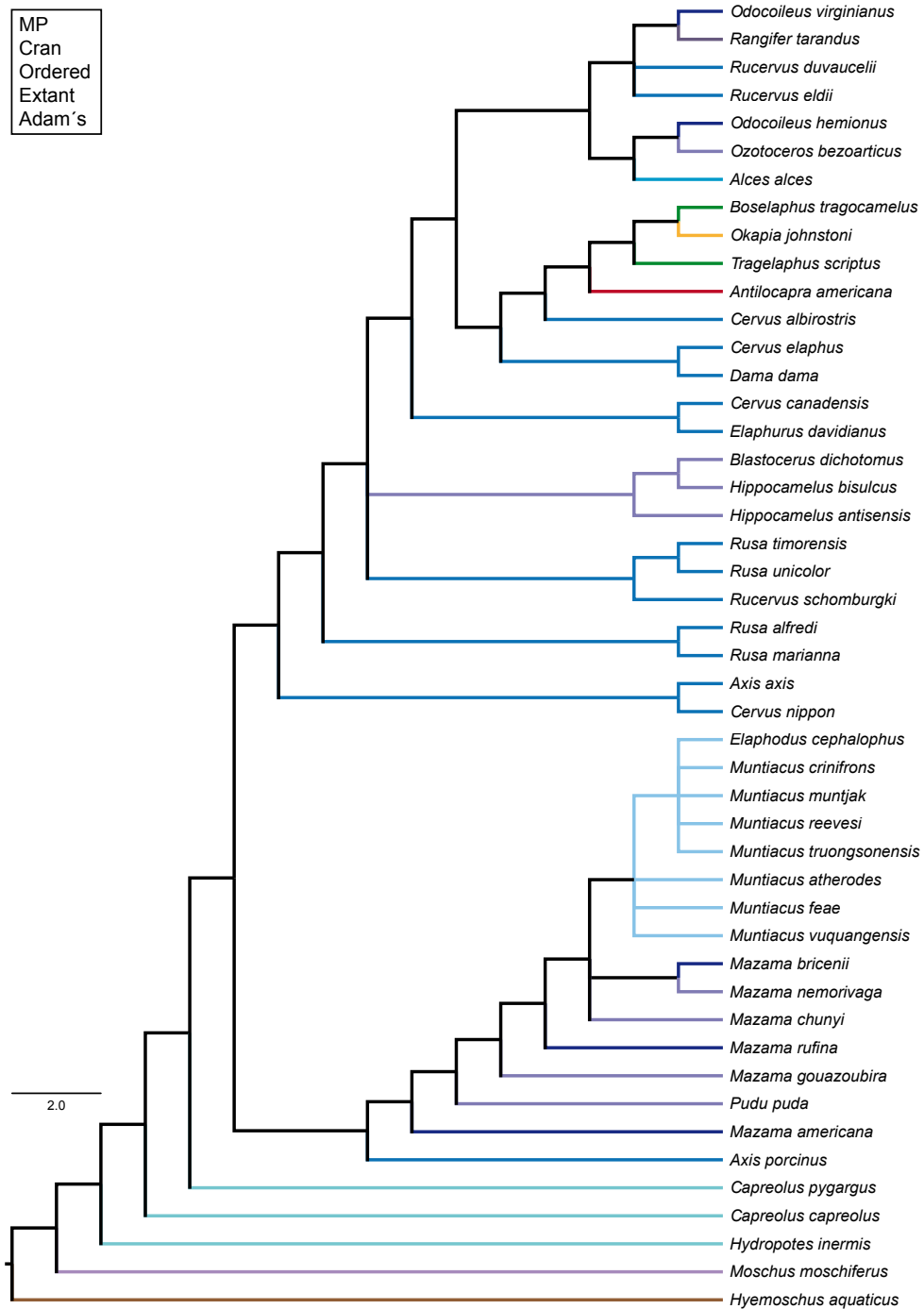


Figure F.4: Adam's consensus topology of the maximum parsimony analysis based on the ordered cranial character set for extant taxa.

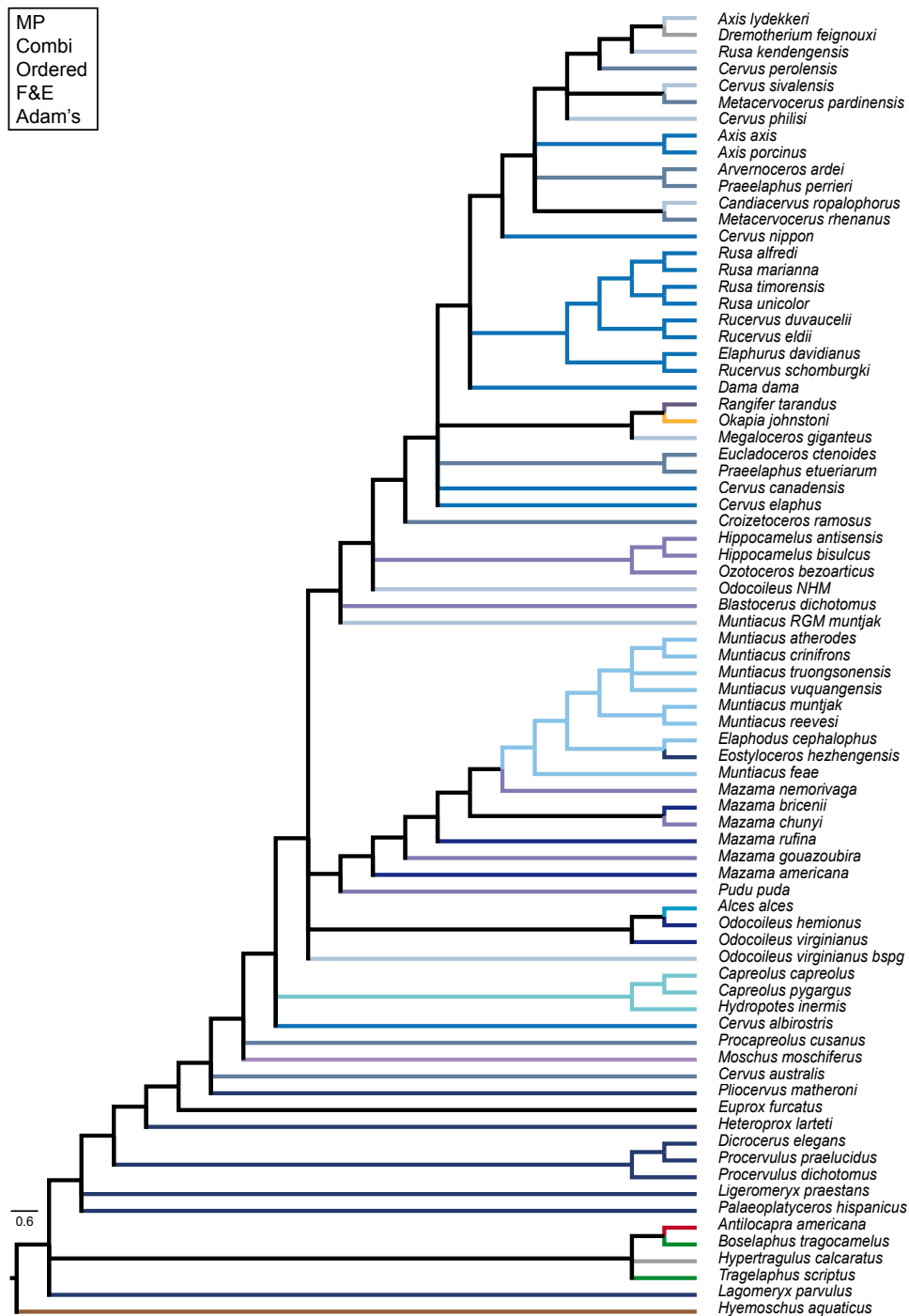


Figure F.5: Adam's consensus topology of the maximum parsimony analysis based on the ordered combined character set for fossil and extant taxa.

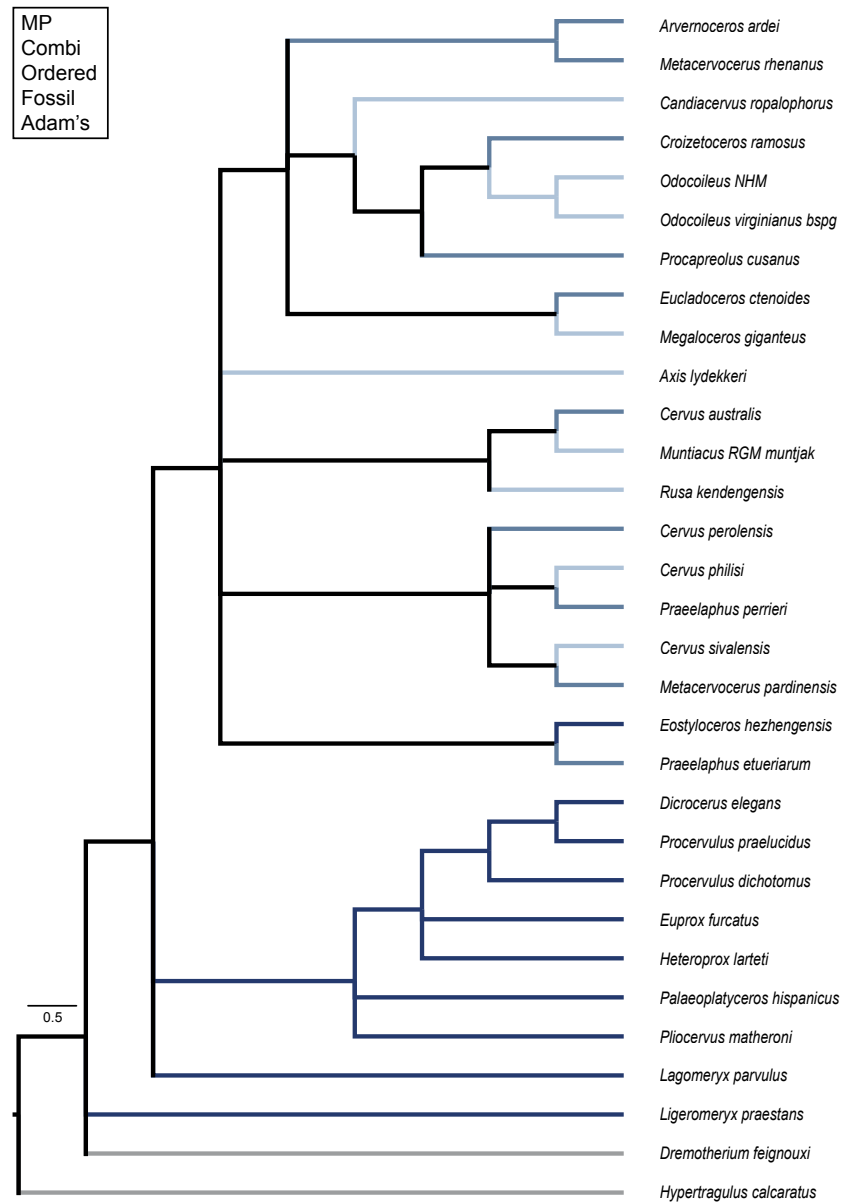


Figure F.6: Adam's consensus topology of the maximum parsimony analysis based on the ordered combined character set for fossil taxa.

G Topologies from SFA Chapter 3



Figure G.1: Overview of the three single fossil analyses for *Arvernoceros ardei*, *Axis lydekkeri*, and *Cervus australis*. From left to right: topology based on the combined matrix of the complete mitochondrial genome and the combined morphological data set including outgroup taxa, topology based on the the same data set, but excluding outgroup taxa except for *Hyemoschus aquaticus*, topology using a constraint topology as a backbone with Capreolinae, Muntiacini and Cervini as monophyletic polytomies.



Figure G.2: Overview of the three single fossil analyses for *'Cervus' perolensis*, *'Cervus' philisi*, and *Croizetoceros ramosus*. From left to right: topology based on the combined matrix of the complete mitochondrial genome and the combined morphological data set including outgroup taxa, topology based on the the same data set, but excluding outgroup taxa except for *Hyemoschus aquaticus*, topology using a constraint topology as a backbone with Capreolinae, Muntiacini and Cervini as monophyletic polytomies.

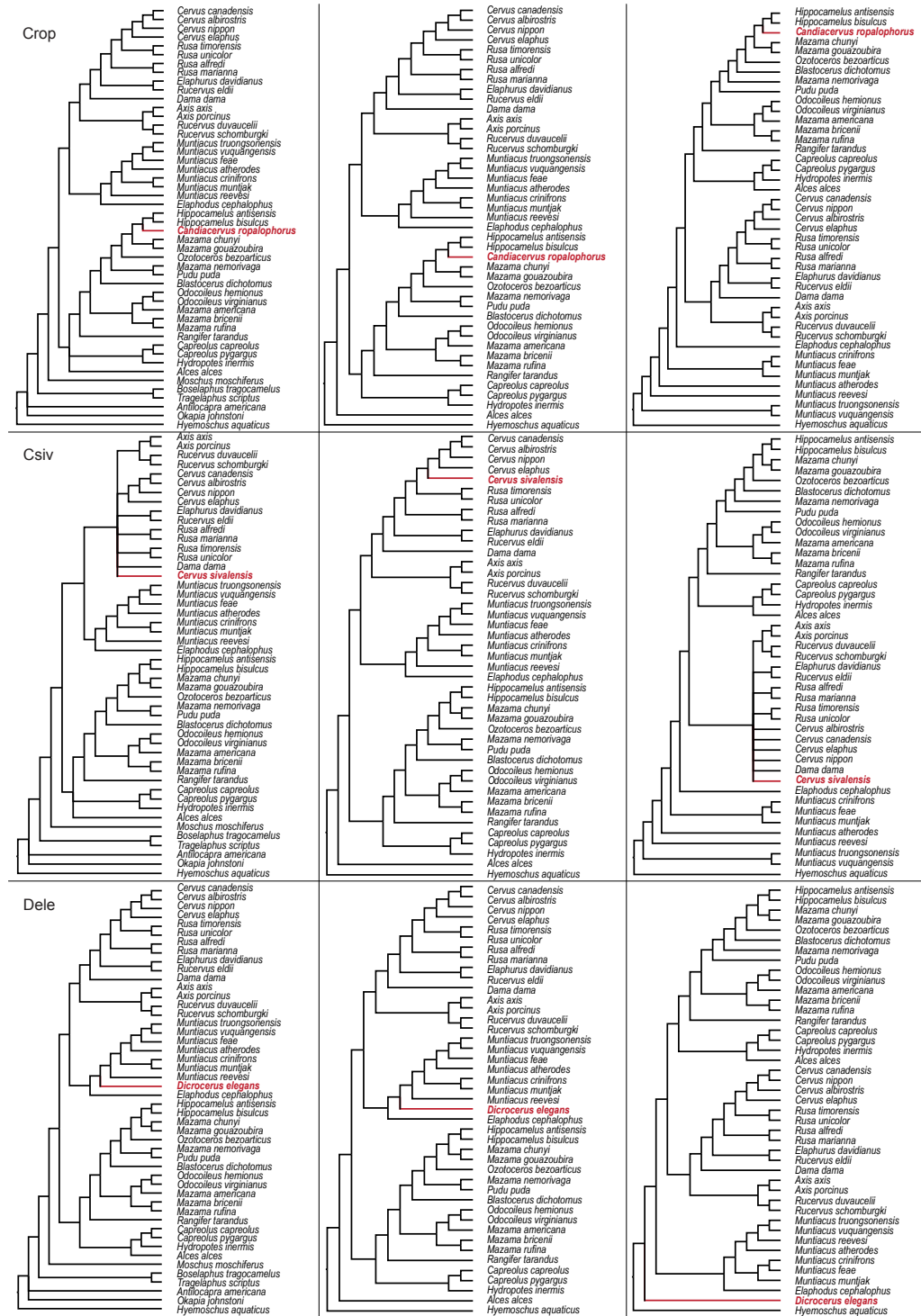


Figure G.3: Overview of the three single fossil analyses for *Candiacerus ropalophorus*, '*Cervus*' *sivalensis*, and *Dicrocerus elegans*. From left to right: topology based on the combined matrix of the complete mitochondrial genome and the combined morphological data set including outgroup taxa, topology based on the the same data set, but excluding outgroup taxa except for *Hyemoschus aquaticus*, topology using a constraint topology as a backbone with Capreolinae, Muntiacini and Cervini as monophyletic polytomies.

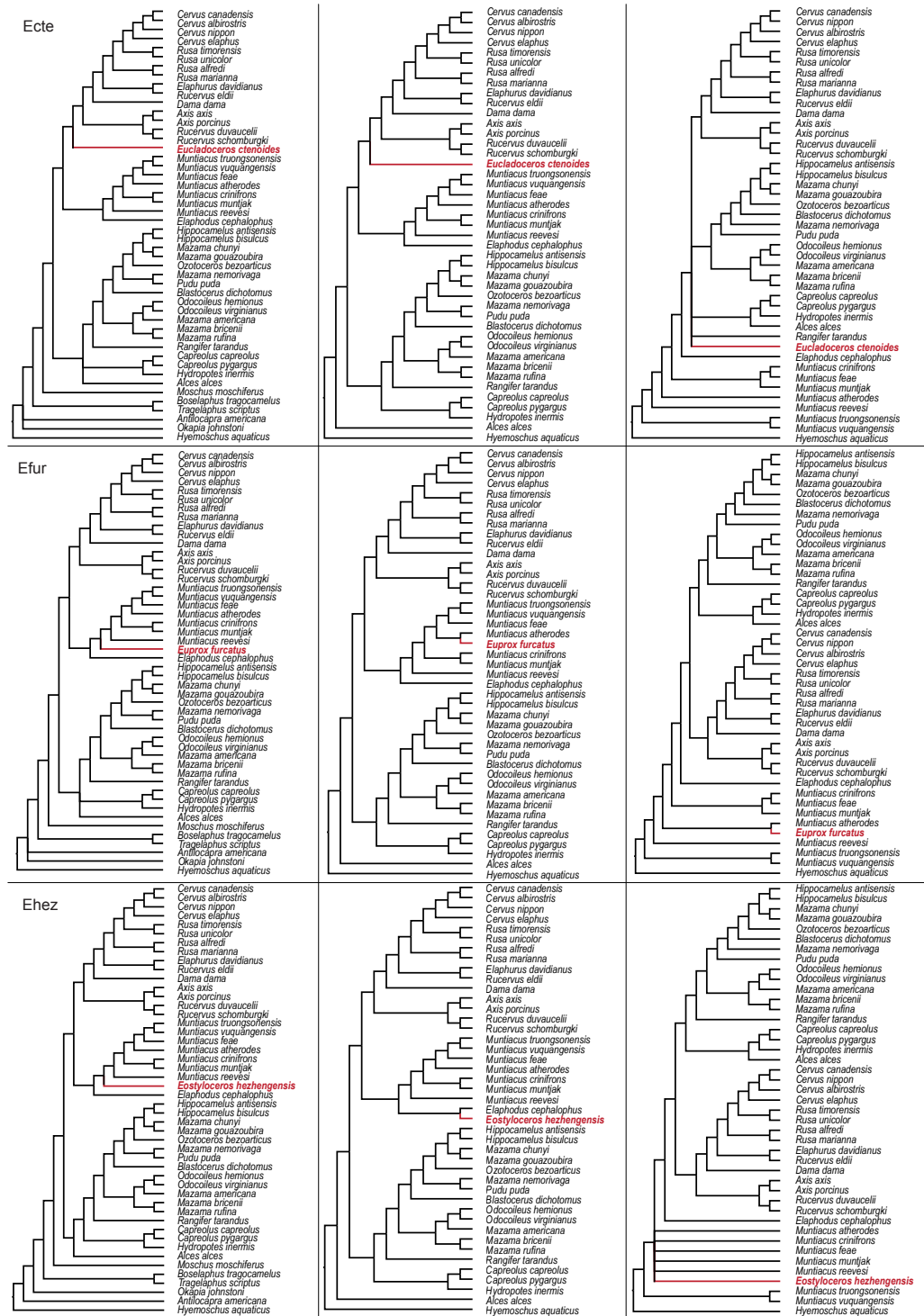


Figure G.4: Overview of the three single fossil analyses for *Eucladoceros ctenoides*, *Euprox furcatus*, and *Eostyloceros hezhengensis*. From left to right: topology based on the combined matrix of the complete mitochondrial genome and the combined morphological data set including outgroup taxa, topology based on the the same data set, but excluding outgroup taxa except for *Hyemoschus aquaticus*, topology using a constraint topology as a backbone with Capreolinae, Muntiacini and Cervini as monophyletic polytomies.

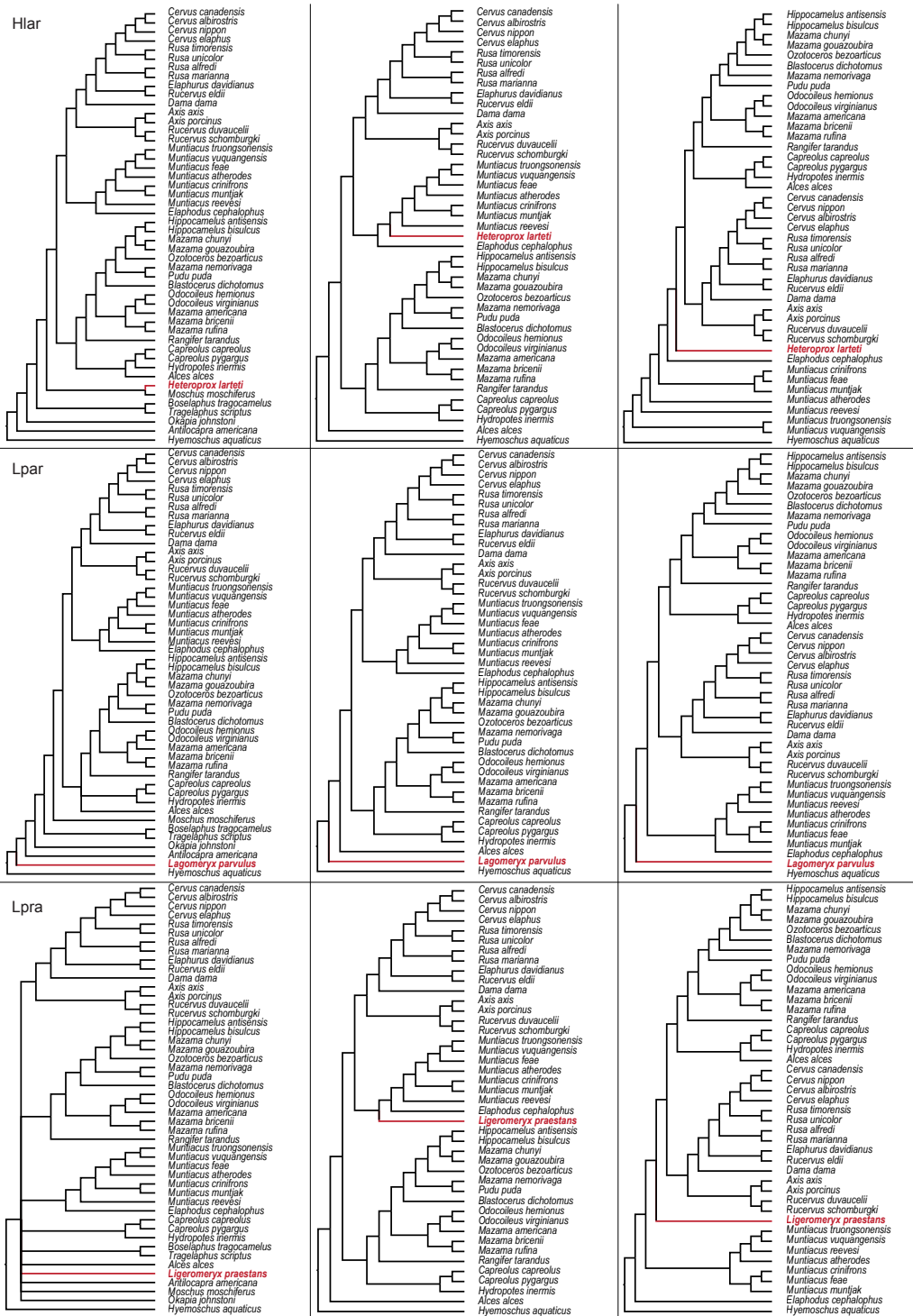


Figure G.5: Overview of the three single fossil analyses for *Heteroprox larteti*, *Lagomeryx parvulus*, and *Ligeromeryx praestans*. From left to right: topology based on the combined matrix of the complete mitochondrial genome and the combined morphological data set including outgroup taxa, topology based on the the same data set, but excluding outgroup taxa except for *Hyemoschus aquaticus*, topology using a constraint topology as a backbone with Capreolinae, Muntiacini and Cervini as monophyletic polytomies.

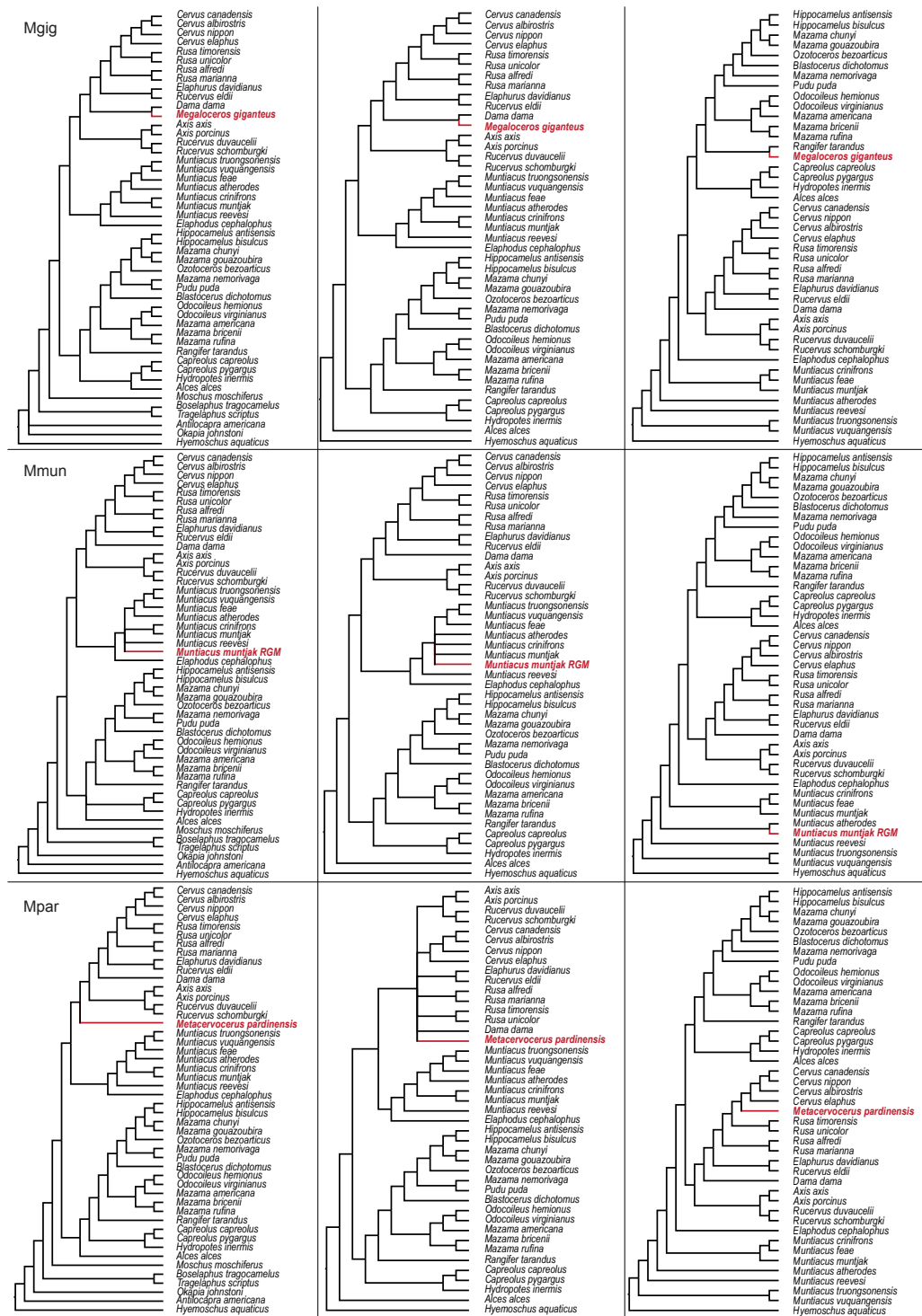


Figure G.6: Overview of the three single fossil analyses for *Megaloceros giganteus*, *Muntiacus muntjak*, and *Metacervocerus pardinensis*. From left to right: topology based on the combined matrix of the complete mitochondrial genome and the combined morphological data set including outgroup taxa, topology based on the the same data set, but excluding outgroup taxa except for *Hyemoschus aquaticus*, topology using a constraint topology as a backbone with Capreolinae, Muntiacini and Cervini as monophyletic polytomies.

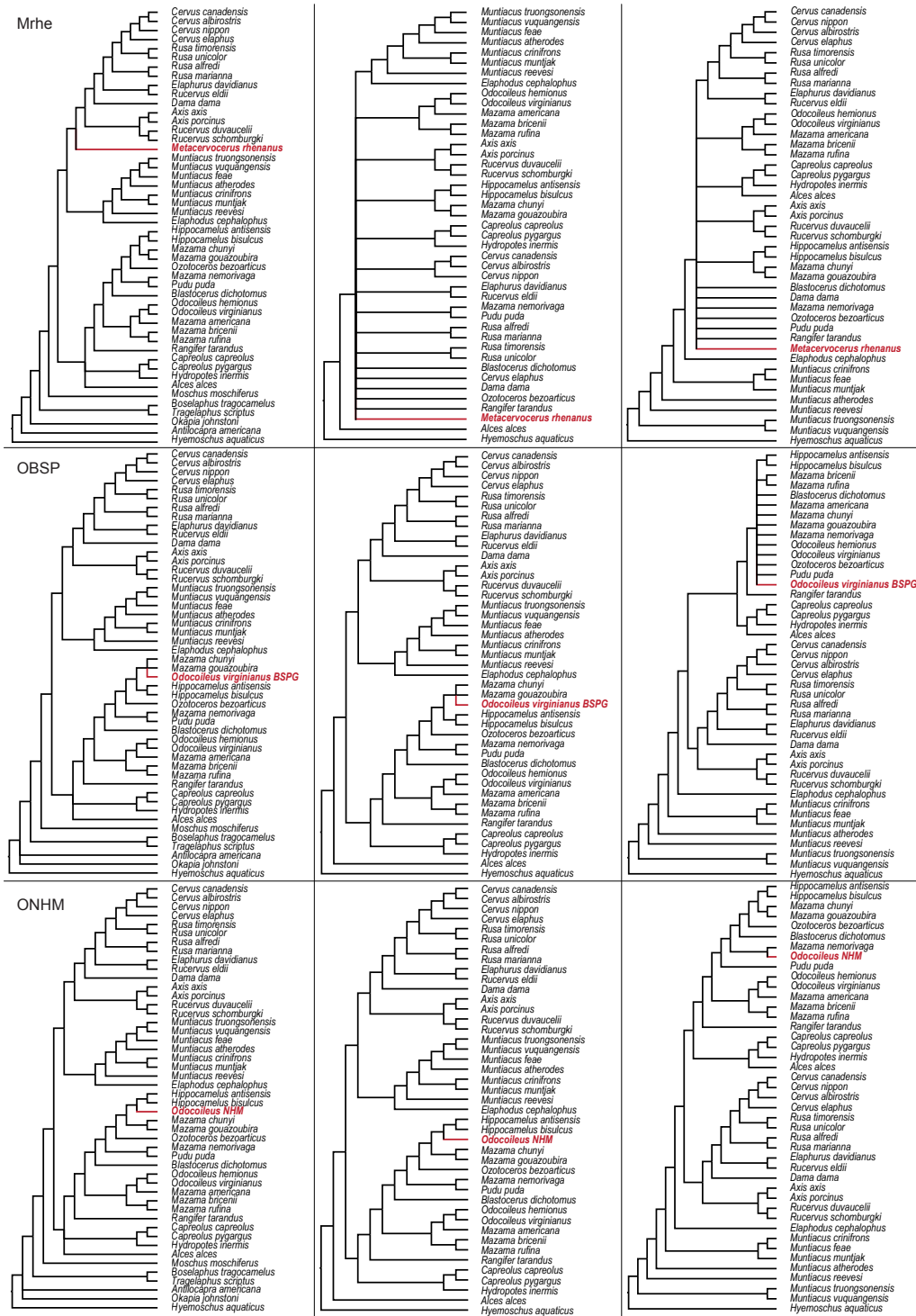


Figure G.7: Overview of the three single fossil analyses for *Metacervocerus rhenanus*, *Odocoileus* (BSPG), and *Odocoileus* (NHM). From left to right: topology based on the combined matrix of the complete mitochondrial genome and the combined morphological data set including outgroup taxa, topology based on the the same data set, but excluding outgroup taxa except for *Hyemoschus aquaticus*, topology using a constraint topology as a backbone with Capreolinae, Muntiacini and Cervini as monophyletic polytomies.

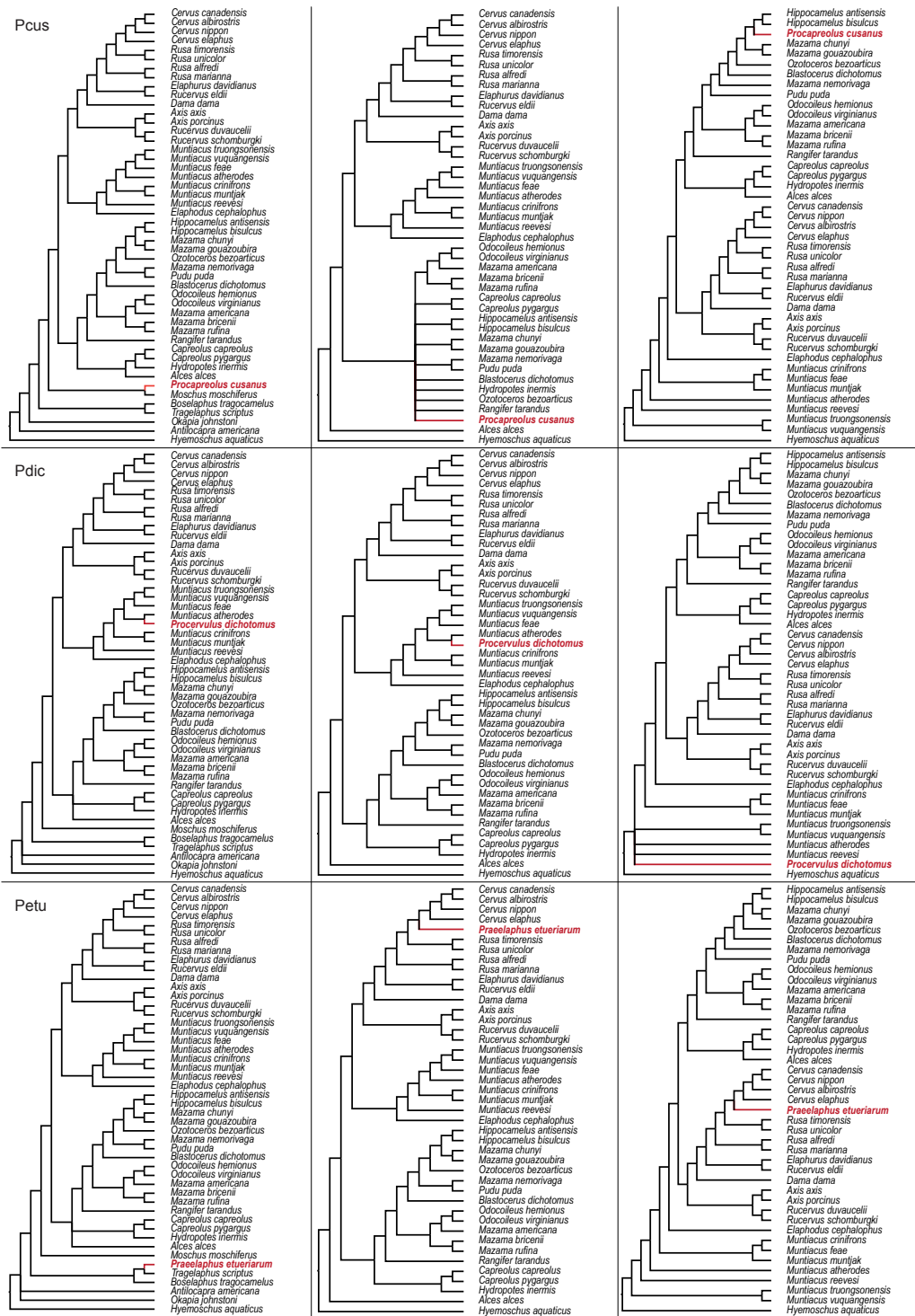


Figure G.8: Overview of the three single fossil analyses for *Procaptiveolus cusanus*, *Procervulus dichotomus*, and *Praelaphus etueriarum*. From left to right: topology based on the combined matrix of the complete mitochondrial genome and the combined morphological data set including outgroup taxa, topology based on the the same data set, but excluding outgroup taxa except for *Hyemoschus aquaticus*, topology using a constraint topology as a backbone with Capreolinae, Muntiacini and Cervini as monophyletic polytomies.

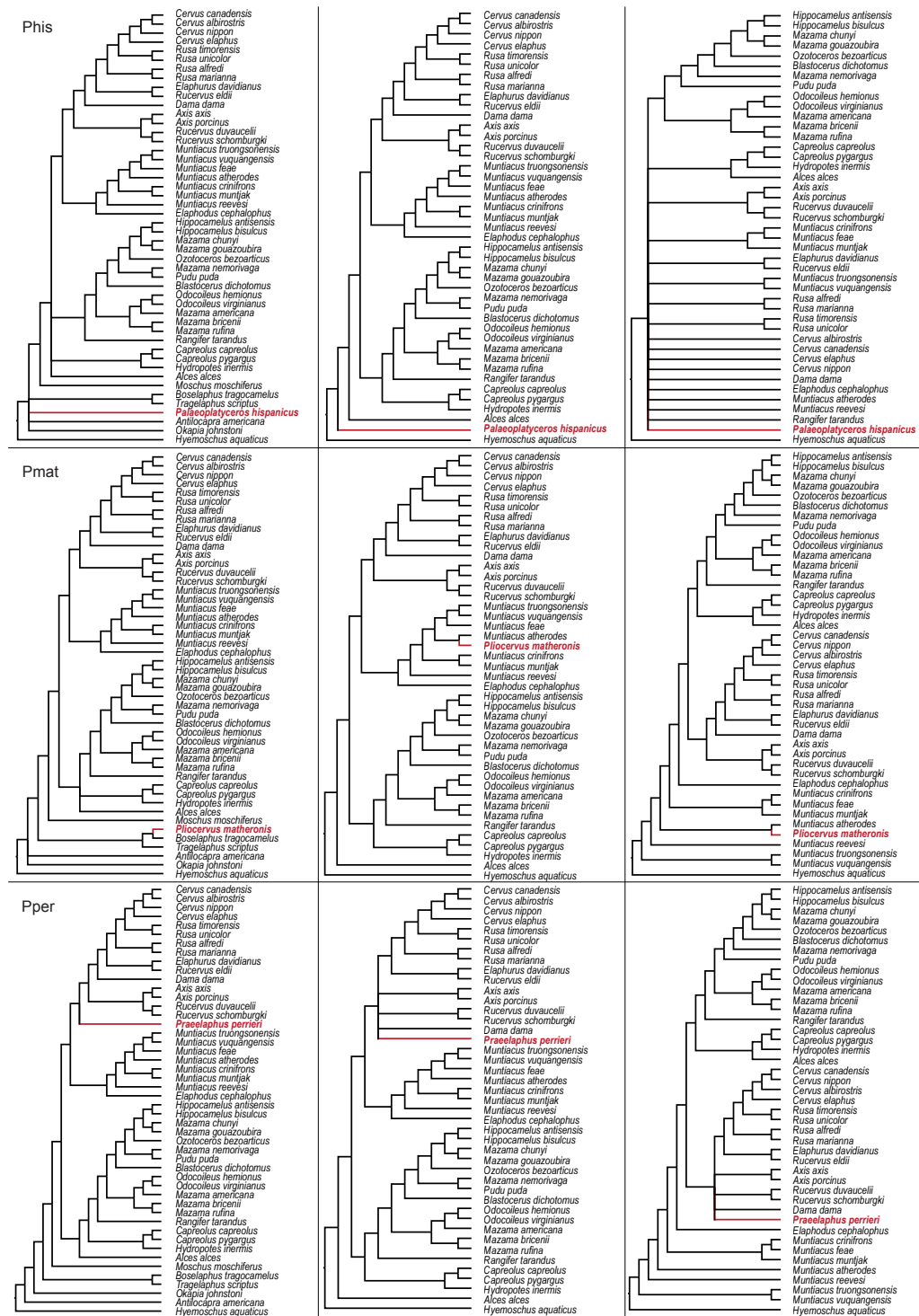


Figure G.9: Overview of the three single fossil analyses for *Palaeoplatyceros hispanicus*, *Pliocervus matheronis*, and *Praelaphus perrieri*. From left to right: topology based on the combined matrix of the complete mitochondrial genome and the combined morphological data set including outgroup taxa, topology based on the the same data set, but excluding outgroup taxa except for *Hyemoschus aquaticus*, topology using a constraint topology as a backbone with Capreolinae, Muntiacini and Cervini as monophyletic polytomies.

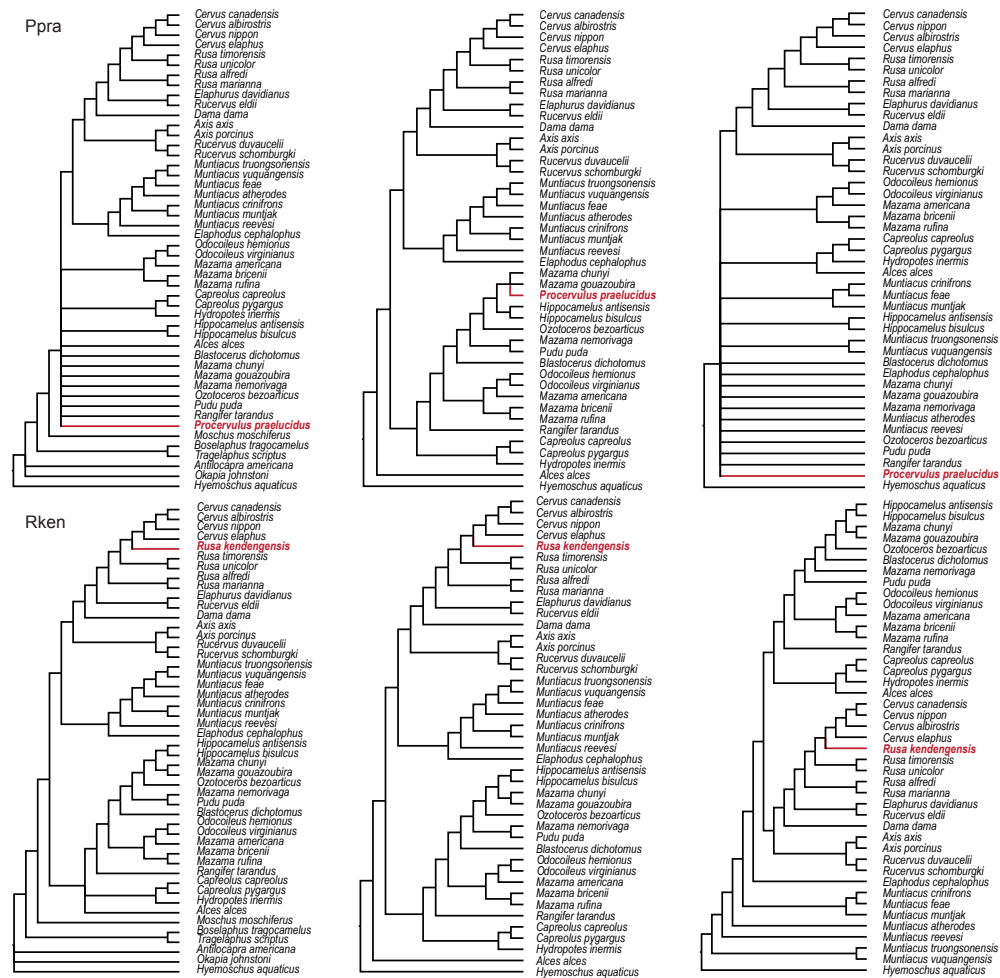


Figure G.10: Overview of the three single fossil analyses for *Procervulus praelucidus* and *Rusa kendagensis*. From left to right: topology based on the combined matrix of the complete mitochondrial genome and the combined morphological data set including outgroup taxa, topology based on the the same data set, but excluding outgroup taxa except for *Hyemoschus aquaticus*, topology using a constraint topology as a backbone with Capreolinae, Muntiacini and Cervini as monophyletic polytomies.

H Supplementary Information of Chapter 4

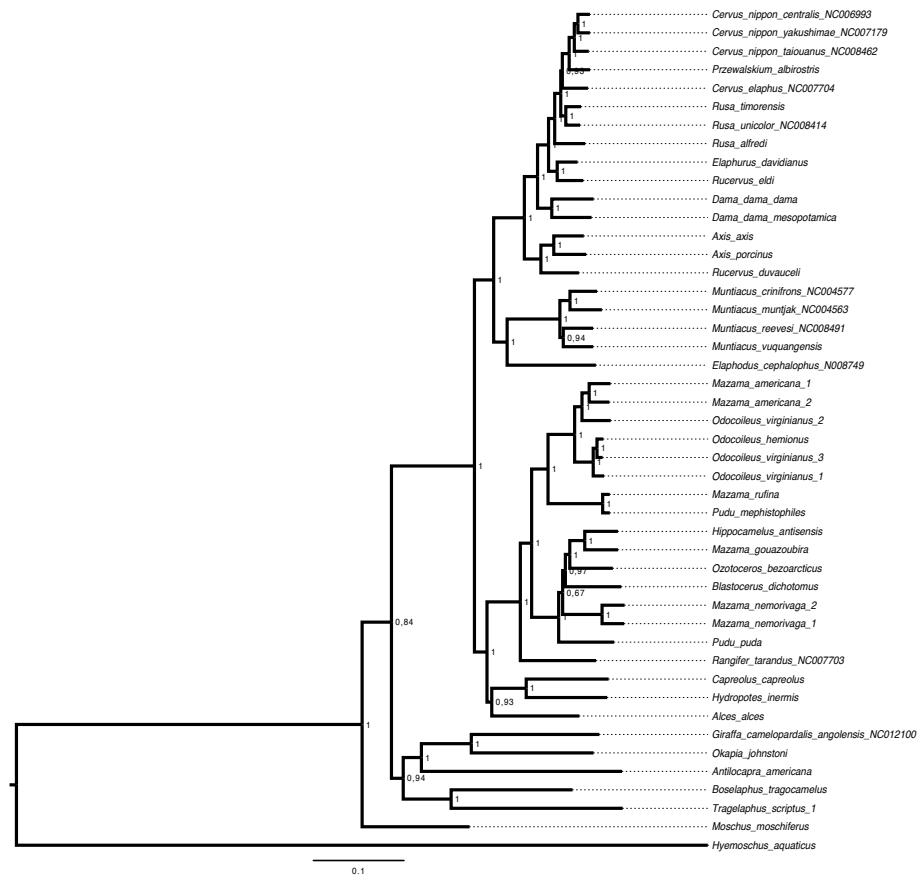


Figure H.1: Bayesian topology of the re-analysis of the complete mitochondrial genome data set published by Hassanin et al. (2012) using their partitioning and model scheme.

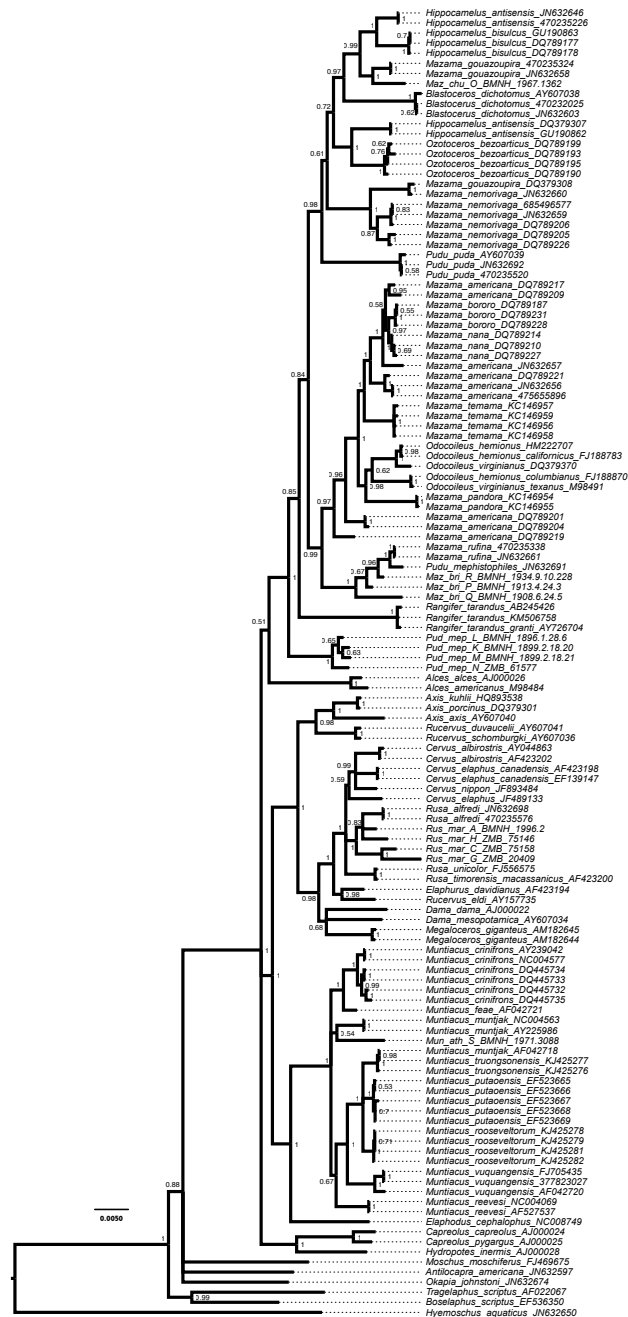


Figure H.2: Bayesian Inference topology based on the unpartitioned data set of the complete cytochrome b sequence (1140 bp) using GTR+ Γ . This is the detailed view of the tree in the main text Figure 4.4.

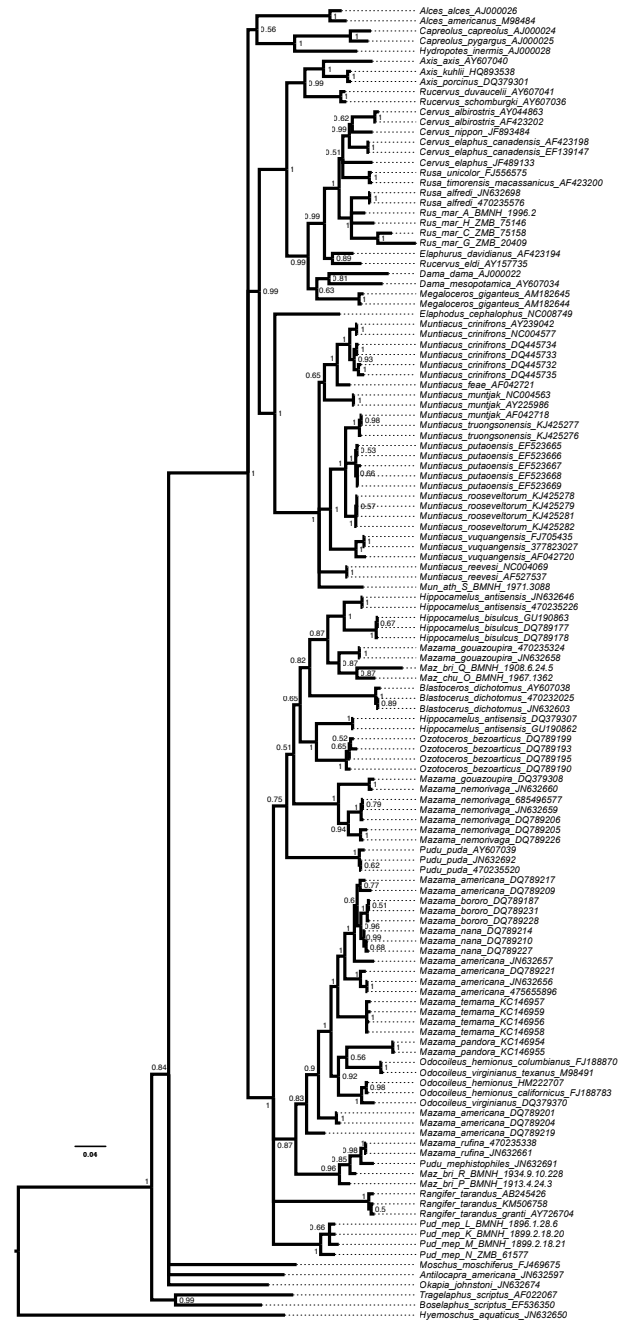


Figure H.3: Bayesian topology based on the partitioned data set of the complete cytochrome b sequence (1140 bp) using SYM, HKY, and GTR for the 1st, 2nd, 3rd codon position, all with the Γ -distribution.

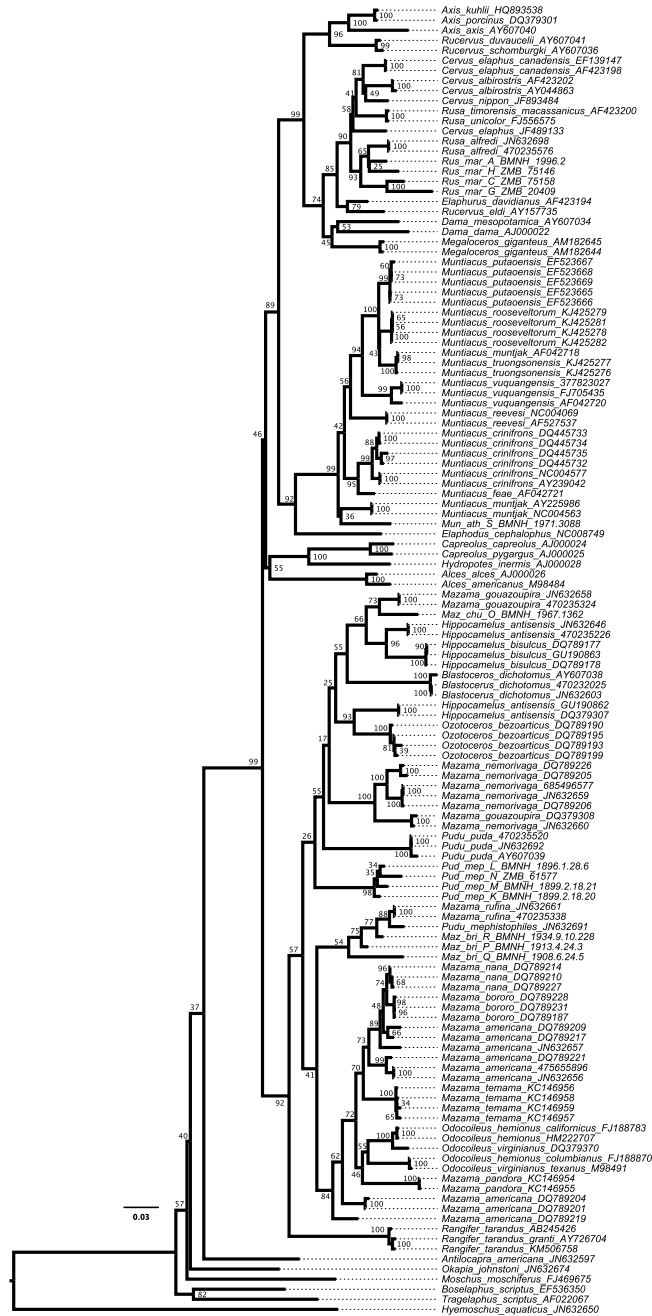


Figure H.4: Maximum Likelihood topology based on the partitioned data set (per codon position) of the complete cytochrome b sequence (1140 bp) using GTR+ Γ

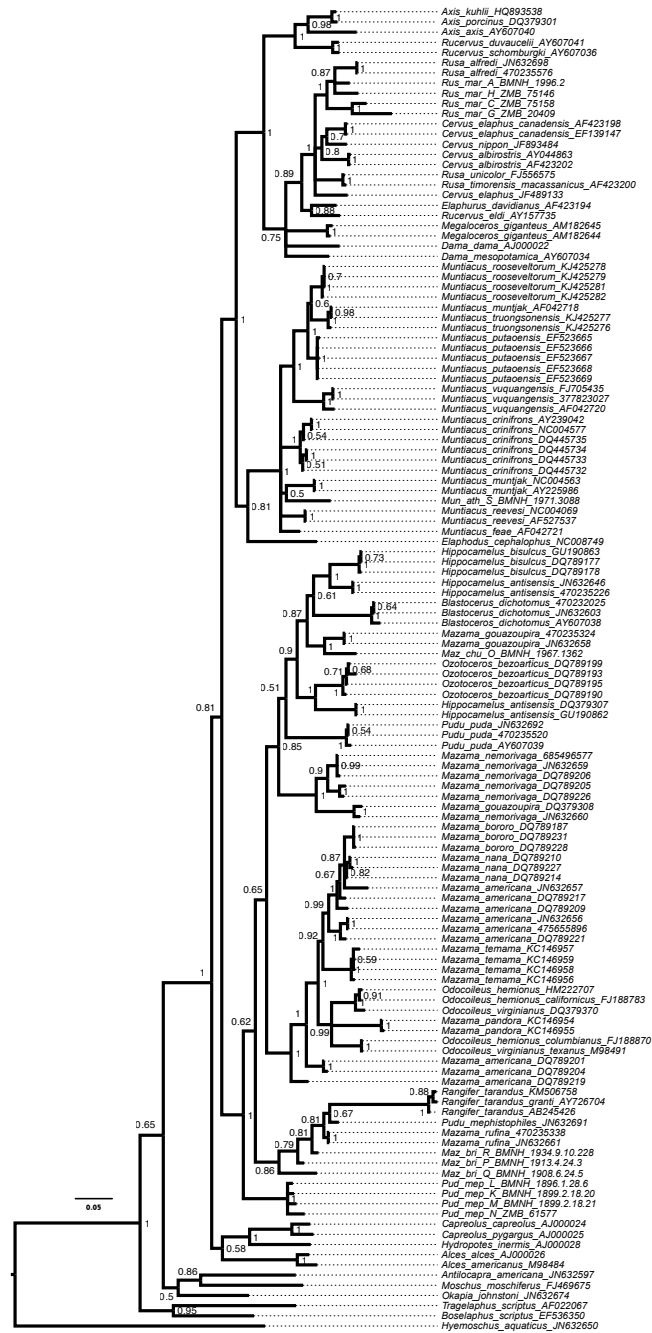


Figure H.5: Bayesian topology of the unpartitioned data set of 747 bp long cytochrome b sequence using GTR for all three codon position, all with the Γ -distribution.

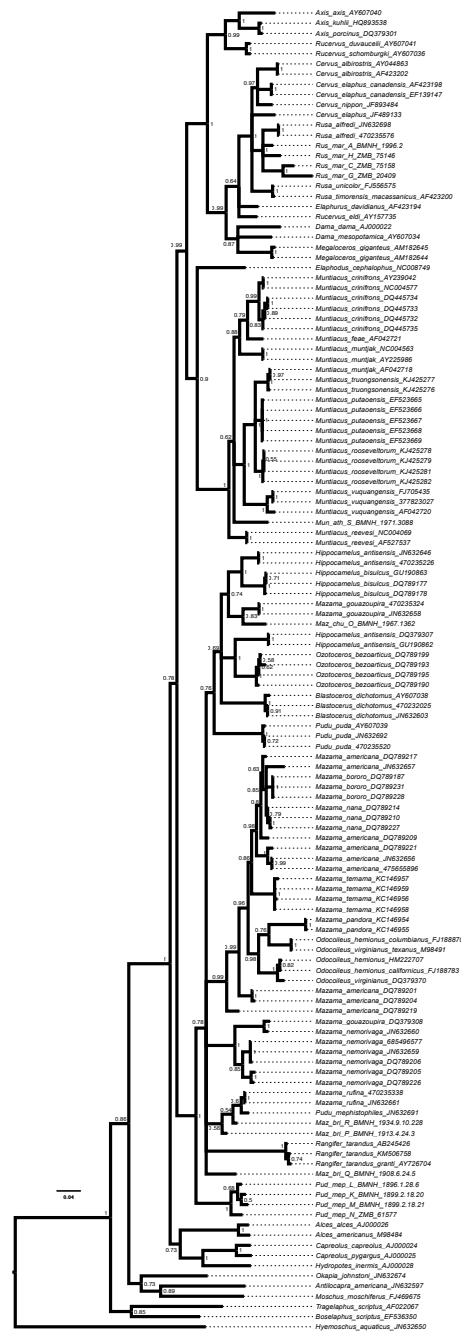


Figure H.6: Bayesian topology of the partitioned data set of 747 bp long cytochrome b sequence using SYM, HKY, and GTR for the 1st, 2nd, 3rd codon position, all with the Γ -distribution.

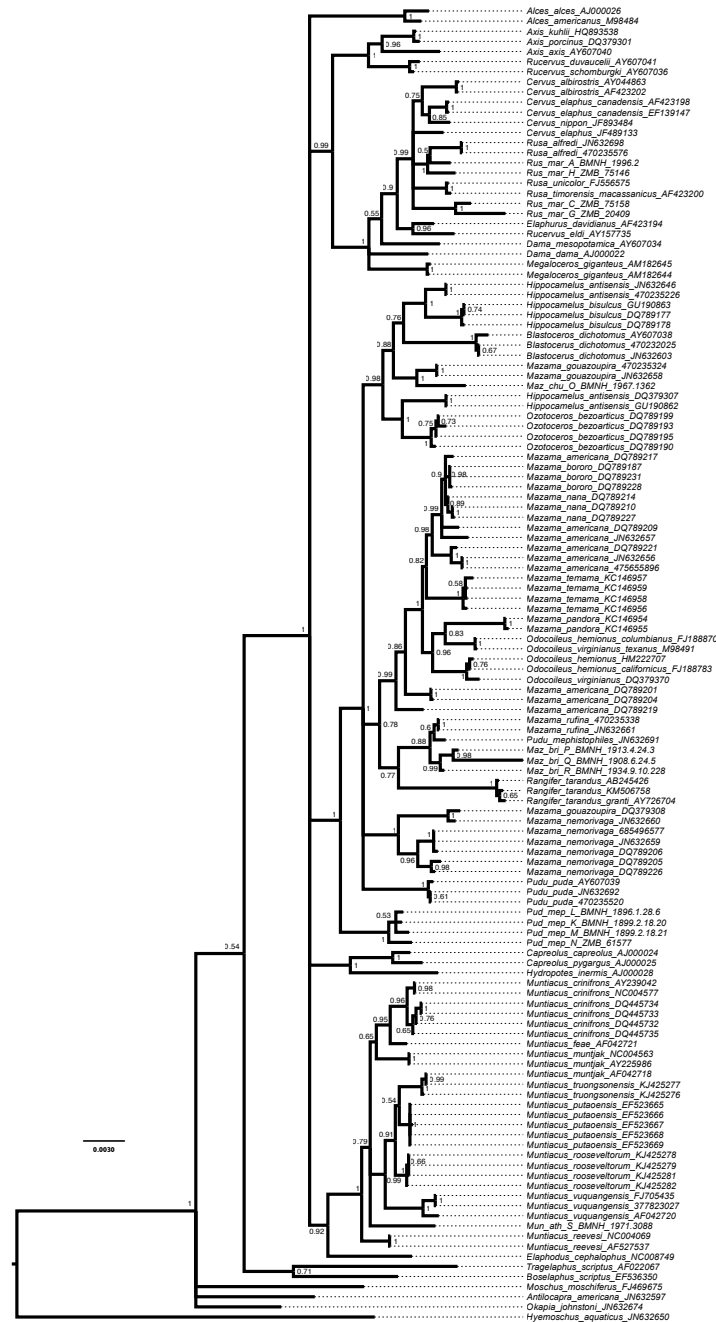


Figure H.7: Bayesian topology of the unpartitioned data set of the cytochrome b sequence reduced to 569 bp using GTR+Γ.

H.1 Comments about Ancient DNA Sequencing

For the sequencing of the *Cytb* fragment 20 specimens were sampled, 10 *Rusa marianna*, 4 *Pudu mephistophiles*, 1 *Mazama chunyi*, 3 *Mazama bricenii*, and 2 *Muntiacus atherodes*, from the BMNH (London) and the ZMB (Berlin). The procedure of extracting the DNA is described in detail in the Material and Method section of Chapter 4. With 8 cervid-specific *Cytb* primers (Lister et al., 2005) a 747 base-pair-long region from the 1140-base-pair-long mitochondrial *Cytb* was amplified, ranging from nucleotide position 64 to 810. Each primer pair amplified a 100–140-base-pair-long sequence with overlap to adjacent sequences (Lister et al., 2005). Details on how the PCR were performed and the sequencing process of successfully amplified PCR products are described in the Material and Method section of Chapter 4.

To ensure that a genuine cervid *Cytb* fragment has been amplified, the forward and reverse pre-assembly sequences from each primer (excluding the primers), the individual contigs of forward and reverse strands and the final 747-base-pair-long concatenated contigs were each BLASTed against NCBI GenBank entries. Only fragments returning a cervid in the first 50 BLAST search results were used. In almost all cases, where the BLAST result was different from the cervid result, the sequences were found to be most similar to *Bos taurus*. This contamination is possibly caused by the BSA added to enhance PCR outcomes. For some sequences, especially those, which were difficult to obtain, hits of cervids AND other ruminants were tolerated.

In the end, of the 20 sampled specimens, 13 specimens had enough successfully amplified and sequenced fragments to be further processed. For some of the eight *Cytb* fragments of these 13 specimens, DNA amplification was not sufficient, which resulted in gaps in the sequence for a few specimens. Out of the 570 individual sequences, only 276 were used for the concatenated sequences of the final 13 specimens (Table E1). Only for one project undertaken in 2011 samples of mammals (antelopes) were extracted and amplified in the Molecular Palaeobiology Lab. The other research focuses on invertebrates. Contamination of these invertebrates in my own samples was not observed. Therefore, cross-chemical contamination can be excluded. My research used different primers and of course different equipment from those used in 2011. Cross-contamination from this project is therefore highly unlikely.

The only abnormality observed in the sequences was that Y (C or T; $n = 50$) and R (G or A; $n = 19$) were the most common ambiguities. These nucleotide substitutions are most likely caused by hydrolytic deamination and are briefly explained in the Results section of Chapter 4 and in more detail in the literature (Hofreiter et al., 2001a; Pääbo et al., 2004; Briggs et al., 2007, 2010). I tested the impact of the ambiguities on the reconstruction and found that the ambiguities did not tremendously influence the phylogenetic signal of the samples. However, these ambiguities represent an additional uncertainty in the analyses. Additionally, the impact of the variability of sites on the phylogenetic signal has been tested in three analyses, one analysing codon position 1, the other analysing codon position 2, and the third analysing codon position 3.

Critical views on (ancient) DNA extraction and occurring problems can be found in the literature (e.g., Olson & Hassanin, 2003; Gilbert et al., 2005; Hassanin et al., 2010) and new insights into palaeogenomics are given in Shapiro & Hofreiter (2014).

Table H.1: List of individual sequence fragments with BLAST search results. Only the genera of the five most frequent hits are listed. If the BLAST search of the forward and reverse sequence had the same results, it is stated only once.

Sequencing No.	Collection	ID	PCR	Primer	BLAST Result
NH0043	BMNH	1996.2_R_mar_1AF	5	1285	<i>Cervus, Rusa</i>
NH0044	BMNH	1996.2_R_mar_1AR	5	1286	
NH0063	BMNH	1996.2_R_mar_2AF	5	1287	<i>Cervus, Rusa</i>
NH0064	BMNH	1996.2_R_mar_2AR	5	1288	<i>Cervus, Rusa</i>
NH0083	BMNH	1996.2_R_mar_3AF	5	1289	<i>Cervus, Rusa, Cervidae</i>
NH0084	BMNH	1996.2_R_mar_3AR	5	1290	
NH0349	BMNH	1996.2_R_mar_4AF	8	1291	<i>Cervus, Rusa</i>
NH0350	BMNH	1996.2_R_mar_4AR	8	1292	
NH0391	BMNH	1996.2_R_mar_5AF	9	1293	<i>Axis, Cervus, Odocoileus</i>
NH0392	BMNH	1996.2_R_mar_5AR	9	1294	
NH0101	BMNH	1996.2_R_mar_6AF	5	1295	<i>Cervus, Rusa, Cervidae</i>
NH0102	BMNH	1996.2_R_mar_6AR	5	1296	
NH0109	BMNH	1996.2_R_mar_7AF	5	1297	<i>Cervus, Rusa</i>
NH0110	BMNH	1996.2_R_mar_7AR	5	1298	
NH0117	BMNH	1996.2_R_mar_8AF	5	1299	<i>Cervus, Rusa</i>
NH0118	BMNH	1996.2_R_mar_8AR	5	1300	
NH0047	ZMB	75158_R_mar_1CF	5	1285	<i>Capreolus, Hydropotes</i>
NH0048	ZMB	75158_R_mar_1CR	5	1286	
NH0547	ZMB	75158_R_mar_2CF	15	1287	<i>Cervus</i>
NH0548	ZMB	75158_R_mar_2CR	15	1288	
NH0085	ZMB	75158_R_mar_3CF	5	1289	<i>Cervus, Rusa</i>
NH0086	ZMB	75158_R_mar_3CR	5	1290	
NH0595	ZMB	75158_R_mar_4CF	18	1291	<i>Cervus, Rusa, Odocoileus, Hippocamelus, Pudu</i>
NH0596	ZMB	75158_R_mar_4CR	18	1292	
NH0551	ZMB	75158_R_mar_5CF	15	1293	<i>Cervus, Rusa</i>
NH0103	ZMB	75158_R_mar_6CF	5	1295	<i>Cervus, Rusa</i>
NH0104	ZMB	75158_R_mar_6CR	5	1296	
NH0111	ZMB	75158_R_mar_7CF	5	1297	<i>Cervus, Rusa</i>
NH0112	ZMB	75158_R_mar_7CR	5	1298	
NH0293	ZMB	75158_R_mar_7CF	5	1297	<i>Cervus, Rusa</i>
NH0294	ZMB	75158_R_mar_7CR	5	1298	
NH0121	ZMB	75158_R_mar_8CF	5	1299	<i>Rusa</i>
NH0297	ZMB	75158_R_mar_8CF	5	1299	<i>Cervus, Rusa</i>
NH0406	ZMB	75158_R_mar_8CR	11	1300	<i>Mazama, Bubalus (bovid)</i>
NH0055	ZMB	20409_R_mar_1GF	5	1285	<i>Capreolus, Hydropotes</i>
NH0056	ZMB	20409_R_mar_1GR	5	1286	
NH0561	ZMB	20409_R_mar_2GF	16	1287	<i>Cervidae</i>
NH0562	ZMB	20409_R_mar_2GR	16	1288	
NH0093	ZMB	20409_R_mar_3GF	5	1289	<i>Cervus, Rusa</i>
NH0094	ZMB	20409_R_mar_3GR	5	1290	
NH0597	ZMB	20409_R_mar_4GF	18	1291	<i>Cervus, Hippocamelus, Pudu</i>
NH0598	ZMB	20409_R_mar_4GR	18	1292	
NH0393	ZMB	20409_R_mar_5GF	9	1293	<i>Cervus, Rusa</i>
NH0394	ZMB	20409_R_mar_5GR	9	1294	
NH0105	ZMB	20409_R_mar_6GF	5	1295	<i>Cervus, Rusa</i>
NH0106	ZMB	20409_R_mar_6GR	5	1296	
NH0289	ZMB	20409_R_mar_6GF	5	1295	<i>Cervus</i>
NH0290	ZMB	20409_R_mar_6GR	5	1296	
NH0113	ZMB	20409_R_mar_7GF	5	1297	<i>Cervus, Rusa, Rucervus, Megaloceros</i>
NH0114	ZMB	20409_R_mar_7GR	5	1298	
NH0295	ZMB	20409_R_mar_7GF	5	1297	<i>Cervus, Rusa</i>
NH0296	ZMB	20409_R_mar_7GR	5	1298	
NH0411	ZMB	20409_R_mar_8GF	11	1299	<i>Mazama</i>
NH0412	ZMB	20409_R_mar_8GR	11	1300	
NH0057	ZMB	75146_R_mar_1HF	5	1285	<i>Rusa, Cervidae</i>
NH0058	ZMB	75146_R_mar_1HR	5	1286	
NH0437	ZMB	75146_R_mar_23HF	12	1287	<i>Cervus, Rusa</i>
NH0438	ZMB	75146_R_mar_23HR	12	1290	
NH0095	ZMB	75146_R_mar_3HF	5	1289	<i>Cervus, Rusa</i>
NH0096	ZMB	75146_R_mar_3HR	5	1290	
NH0557	ZMB	75146_R_mar_5HF	15	1293	<i>Rusa, Rucervus, Cervus, Axis</i>
NH0558	ZMB	75146_R_mar_5HR	15	1294	
NH0107	ZMB	75146_R_mar_6HF	5	1295	<i>Cervus, Rusa, ruminants</i>
NH0108	ZMB	75146_R_mar_6HR	5	1296	
NH0291	ZMB	75146_R_mar_6HF	5	1295	<i>Cervus, Rusa</i>
NH0292	ZMB	75146_R_mar_6HR	5	1296	
NH0115	ZMB	75146_R_mar_7HF	5	1297	<i>Cervus, Rusa</i>
NH0116	ZMB	75146_R_mar_7HR	5	1298	
NH0375	ZMB	75146_R_mar_8HF	8	1299	<i>Cervus, Rusa</i>

Table H.1: Continued

NH0145	BMNH	1899.2.18.20_Pud_mep.1KF	6	1285	<i>Capreolus, Hydropotes</i>
NH0146	BMNH	1899.2.18.20_Pud_mep.1KR	6	1286	
NH0269	BMNH	1899.2.18.20_Pud_mep.1KF	6	1285	<i>Capreolus</i>
NH0443	BMNH	1899.2.18.20_Pud_mep.23KF	12	1287	<i>Ozotoceros, Mazama, Hippocamelus, Rusa, Cervus</i>
NH0444	BMNH	1899.2.18.20_Pud_mep.23KR	12	1290	
NH0161	BMNH	1899.2.18.20_Pud_mep.3KF	6	1289	<i>Ozotoceros, Mazama, Hippocamelus, Cervidae</i>
NH0162	BMNH	1899.2.18.20_Pud_mep.3KR	6	1290	
NH0313	BMNH	1899.2.18.20_Pud_mep.3KF	6	1289	<i>Ozotoceros, Mazama, Hippocamelus, Cervidae</i>
NH0314	BMNH	1899.2.18.20_Pud_mep.3KR	6	1290	
NH0463	BMNH	1899.2.18.20_Pud_mep.34KF	12	1289	<i>Ozotoceros, Hippocamelus, Mazama, Cervus, Rucervus</i>
NH0464	BMNH	1899.2.18.20_Pud_mep.34KR	12	1292	
NH0503	BMNH	1899.2.18.20_Pud_mep.4KF	14	1291	<i>Hippocamelus, Pudu, Cervus</i>
NH0504	BMNH	1899.2.18.20_Pud_mep.4KR	14	1292	
NH0299	BMNH	1899.2.18.20_Pud_mep.4KF	8	1291	<i>Mazama, Pudu, Odocoileus, Hippocamelus, Cervus</i>
NH0300	BMNH	1899.2.18.20_Pud_mep.4KR	8	1292	
NH0469	BMNH	1899.2.18.20_Pud_mep.45KF	12	1291	<i>Mazama, Pudu, Cervus, Hippocamelus, Ozotoceros</i>
NH0470	BMNH	1899.2.18.20_Pud_mep.45KR	12	1294	
NH0169	BMNH	1899.2.18.20_Pud_mep.5KF	6	1293	<i>Mazama, Pudu, Ozotoceros, Odocoileus, Cervidae</i>
NH0170	BMNH	1899.2.18.20_Pud_mep.5KR	6	1294	
NH0333	BMNH	1899.2.18.20_Pud_mep.5KF	6	1293	<i>Mazama, Pudu, Muntiacus, Cervidae</i>
NH0334	BMNH	1899.2.18.20_Pud_mep.5KR	6	1294	
NH0475	BMNH	1899.2.18.20_Pud_mep.56KF	13	1293	<i>Ozotoceros, Odocoileus</i>
NH0476	BMNH	1899.2.18.20_Pud_mep.56KR	13	1296	
NH0517	BMNH	1899.2.18.20_Pud_mep.6KF	14	1295	<i>Alces, Odocoileus, Ozotoceros, Mazama, Capreolus</i>
NH0518	BMNH	1899.2.18.20_Pud_mep.6KR	14	1296	
NH0357	BMNH	1899.2.18.20_Pud_mep.6KF	8	1295	<i>Mazama, Alces, Ozotoceros, Odocoileus, Rangifer</i>
NH0358	BMNH	1899.2.18.20_Pud_mep.6KR	8	1296	
NH0179	BMNH	1899.2.18.20_Pud_mep.7KF	6	1297	<i>Mazama, Hydropotes, Hippocamelus, Alces, Axis</i>
NH0180	BMNH	1899.2.18.20_Pud_mep.7KR	6	1298	
NH0337	BMNH	1899.2.18.20_Pud_mep.7KF	6	1297	<i>Mazama, Pudu, Hippocamelus, Cervidae</i>
NH0338	BMNH	1899.2.18.20_Pud_mep.7KR	6	1298	
NH0183	BMNH	1899.2.18.20_Pud_mep.8KF	6	1299	<i>Blastocerus, Ozotoceros, Mazama, Pudu, Rangifer</i>
NH0184	BMNH	1899.2.18.20_Pud_mep.8KR	6	1300	
NH0341	BMNH	1899.2.18.20_Pud_mep.8KF	6	1299	<i>Mazama</i>
NH0342	BMNH	1899.2.18.20_Pud_mep.8KR	6	1300	
NH0147	BMNH	1896.1.28.6_Pud_mep.1LF	6	1285	<i>Capreolus, Hydropotes</i>
NH0148	BMNH	1896.1.28.6_Pud_mep.1LR	6	1286	
NH0271	BMNH	1896.1.28.6_Pud_mep.1LF	6	1285	<i>Capreolus</i>
NH0272	BMNH	1896.1.28.6_Pud_mep.1LR	6	1286	
NH0445	BMNH	1896.1.28.6_Pud_mep.23LF	12	1287	<i>Ozotoceros, Hippocamelus, Mazama, Cervus, Axis</i>
NH0446	BMNH	1896.1.28.6_Pud_mep.23LR	12	1290	
NH0163	BMNH	1896.1.28.6_Pud_mep.3LF	6	1289	<i>Ozotoceros, Hippocamelus, Mazama</i>
NH0164	BMNH	1896.1.28.6_Pud_mep.3LR	6	1290	
NH0315	BMNH	1896.1.28.6_Pud_mep.3LF	6	1289	<i>Cervidae</i>
NH0316	BMNH	1896.1.28.6_Pud_mep.3LR	6	1290	
NH0465	BMNH	1896.1.28.6_Pud_mep.34LF	12	1289	<i>Hippocamelus, Mazama, Pudu, Cervus, Elaphurus</i>
NH0466	BMNH	1896.1.28.6_Pud_mep.34LR	12	1292	
NH0301	BMNH	1896.1.28.6_Pud_mep.4LF	8	1291	<i>Mazama, Hippocamelus, Odocoileus, Pudu, Cervus</i>
NH0302	BMNH	1896.1.28.6_Pud_mep.4LR	8	1292	
NH0505	BMNH	1896.1.28.6_Pud_mep.4LF	14	1291	<i>Hippocamelus, Pudu, Cervus</i>
NH0506	BMNH	1896.1.28.6_Pud_mep.4LR	14	1292	
NH0471	BMNH	1896.1.28.6_Pud_mep.45LF	12	1291	<i>Mazama, Pudu, Ozotoceros, Hippocamelus, Rusa</i>
NH0472	BMNH	1896.1.28.6_Pud_mep.45LR	12	1294	
NH0395	BMNH	1896.1.28.6_Pud_mep.5LF	9	1293	<i>Mazama, Pudu, Ozotoceros, Odocoileus</i>
NH0396	BMNH	1896.1.28.6_Pud_mep.5LR	9	1294	
NH0360	BMNH	1896.1.28.6_Pud_mep.6LR	8	1296	<i>Capreolus</i>
NH0519	BMNH	1896.1.28.6_Pud_mep.6LF	14	1295	<i>Ozotoceros, Odocoileus, Mazama, Alces, Capreolus</i>
NH0520	BMNH	1896.1.28.6_Pud_mep.6LR	14	1296	
NH0366	BMNH	1896.1.28.6_Pud_mep.7LR	8	1298	<i>Mazama, Pudu, Muntiacus, Axis</i>
NH0537	BMNH	1896.1.28.6_Pud_mep.7LF	14	1297	<i>Pudu, Mazama, Cervus, Elaphodus, Rucervus</i>
NH0483	BMNH	1896.1.28.6_Pud_mep.78LF	13	1297	<i>Mazama, Blastocerus, Ozotoceros, Odocoileus, Megaloceros</i>
NH0484	BMNH	1896.1.28.6_Pud_mep.78LR	13	1300	
NH0185	BMNH	1896.1.28.6_Pud_mep.8LF	6	1299	<i>Blastocerus, Mazama, Pudu, Rangifer, Elaphurus</i>
NH0186	BMNH	1896.1.28.6_Pud_mep.8LR	6	1300	
NH0343	BMNH	1896.1.28.6_Pud_mep.8LF	6	1299	<i>Mazama, Blastocerus, Ozotoceros, Odocoileus, Hippocamelus</i>
NH0344	BMNH	1896.1.28.6_Pud_mep.8LR	6	1300	

Table H.1: Continued

NH0149	BMNH	1899.2.18.21.Pud_mep_1MF	6	1285	<i>Capreolus, Philantomba</i> (bovid)
NH0150	BMNH	1899.2.18.21.Pud_mep_1MR	6	1286	
NH0273	BMNH	1899.2.18.21.Pud_mep_1MF	6	1285	<i>Capreolus</i>
NH0274	BMNH	1899.2.18.21.Pud_mep_1MR	6	1286	
NH0563	BMNH	1899.2.18.21.Pud_mep_2MF	16	1287	Cervidae
NH0564	BMNH	1899.2.18.21.Pud_mep_2MR	16	1288	
NH0581	BMNH	1899.2.18.21.Pud_mep_2MF	17	1287	Cervidae
NH0582	BMNH	1899.2.18.21.Pud_mep_2MR	17	1288	
NH0165	BMNH	1899.2.18.21.Pud_mep_3MF	6	1289	<i>Ozotoceros</i> , Cervidae, Bovidae
NH0166	BMNH	1899.2.18.21.Pud_mep_3MR	6	1290	
NH0317	BMNH	1899.2.18.21.Pud_mep_3MF	6	1289	<i>Cervus</i> , <i>Mazama</i>
NH0318	BMNH	1899.2.18.21.Pud_mep_3MR	6	1290	
NH0303	BMNH	1899.2.18.21.Pud_mep_4MF	8	1291	<i>Hippocamelus</i> , <i>Pudu</i>
NH0304	BMNH	1899.2.18.21.Pud_mep_4MR	8	1292	
NH0173	BMNH	1899.2.18.21.Pud_mep_5MF	6	1293	<i>Mazama</i> , <i>Ozotoceros</i> , <i>Dama</i> , <i>Muntiacus</i> , <i>Cervus</i>
NH0511	BMNH	1899.2.18.21.Pud_mep_5MF	14	1293	<i>Mazama</i> , <i>Pudu</i> , <i>Odocoileus</i>
NH0512	BMNH	1899.2.18.21.Pud_mep_5MR	14	1294	
NH0521	BMNH	1899.2.18.21.Pud_mep_6MF	14	1295	<i>Capreolus</i> , <i>Cervus</i> , <i>Dama</i> , <i>Antilocapra</i> (antilocaprid)
NH0522	BMNH	1899.2.18.21.Pud_mep_6MR	14	1296	
NH0539	BMNH	1899.2.18.21.Pud_mep_7MF	14	1297	<i>Mazama</i> , <i>Pudu</i> , <i>Hippocamelus</i> , <i>Elaphodus</i> , <i>Rucervus</i>
NH0187	BMNH	1899.2.18.21.Pud_mep_8MF	6	1299	<i>Mazama</i> , <i>Hippocamelus</i> , <i>Ozotoceros</i> , <i>Pudu</i> , <i>Rangifer</i>
NH0188	BMNH	1899.2.18.21.Pud_mep_8MR	6	1300	
NH0151	ZMB	61577.Pud_mep_1NF	6	1285	<i>Capreolus, Philantomba</i> (bovid)
NH0152	ZMB	61577.Pud_mep_1NR	6	1286	<i>Pudu</i> , <i>Rangifer</i> , <i>Dama</i> , <i>Muntiacus</i>
NH0275	ZMB	61577.Pud_mep_1NF	6	1285	<i>Mazama</i> , <i>Odocoileus</i> , <i>Muntiacus</i> , <i>Axis</i>
NH0276	ZMB	61577.Pud_mep_1NR	6	1286	
NH0383	ZMB	61577.Pud_mep_2NF	9	1287	Cervidae, Bovidae
NH0384	ZMB	61577.Pud_mep_2NR	9	1288	
NH0167	ZMB	61577.Pud_mep_3NF	6	1289	<i>Rucervus</i> , <i>Odocoileus</i> , <i>Budorcas</i>
NH0168	ZMB	61577.Pud_mep_3NR	6	1290	
NH0319	ZMB	61577.Pud_mep_3NF	6	1289	<i>Ozotoceros</i> , Cervidae
NH0320	ZMB	61577.Pud_mep_3NR	6	1290	
NH0305	ZMB	61577.Pud_mep_4NF	8	1291	<i>Hippocamelus</i> , <i>Pudu</i> , <i>Cervus</i>
NH0306	ZMB	61577.Pud_mep_4NR	8	1292	
NH0397	ZMB	61577.Pud_mep_5NF	9	1293	<i>Mazama</i> , <i>Blastocerus</i> , <i>Rusa</i> , <i>Muntiacus</i>
NH0398	ZMB	61577.Pud_mep_5NR	9	1294	
NH0177	ZMB	61577.Pud_mep_6NF	6	1295	<i>Odocoileus</i> , <i>Alces</i> , <i>Dama</i>
NH0178	ZMB	61577.Pud_mep_6NR	6	1296	
NH0181	ZMB	61577.Pud_mep_7NF	6	1297	<i>Mazama</i> , <i>Hippocamelus</i> , <i>Alces</i> , <i>Hydropotes</i> , <i>Axis</i>
NH0339	ZMB	61577.Pud_mep_7NF	6	1297	<i>Mazama</i> , <i>Blastocerus</i> , <i>Ozotoceros</i> , <i>Odocoileus</i> , <i>Hippocamelus</i>
NH0340	ZMB	61577.Pud_mep_7NR	6	1298	
NH0189	ZMB	61577.Pud_mep_8NF	6	1299	<i>Mazama</i> , <i>Odocoileus</i> , <i>Gazella</i>
NH0190	ZMB	61577.Pud_mep_8NR	6	1300	
NH0347	ZMB	61577.Pud_mep_8NF	6	1299	<i>Blastocerus</i> , <i>Mazama</i> , <i>Hippocamelus</i> , <i>Odocoileus</i>
NH0348	ZMB	61577.Pud_mep_8NR	6	1300	
NH0599	BMNH	1967.1362.Maz.chu_1OF	19	1285	Cervidae, Bovidae
NH0600	BMNH	1967.1362.Maz.chu_1OR	19	1286	
NH0607	BMNH	1967.1362.Maz.chu_1OF	7	1285	Cervidae, Bovidae
NH0608	BMNH	1967.1362.Maz.chu_1OR	7	1286	
NH0203	BMNH	1967.1362.Maz.chu_2OF	7	1287	<i>Mazama</i> , <i>Hippocamelus</i> , <i>Capreolus</i> , <i>Alces</i> , <i>Rangifer</i>
NH0204	BMNH	1967.1362.Maz.chu_2OR	7	1288	
NH0321	BMNH	1967.1362.Maz.chu_3OF	8	1289	<i>Mazama</i> , <i>Hippocamelus</i> , Cervidae
NH0322	BMNH	1967.1362.Maz.chu_3OR	8	1290	
NH0389	BMNH	1967.1362.Maz.chu_4OF	9	1291	<i>Mazama</i> , <i>Pudu</i> , <i>Hippocamelus</i>
NH0390	BMNH	1967.1362.Maz.chu_4OR	9	1292	
NH0223	BMNH	1967.1362.Maz.chu_5OF	7	1293	<i>Capreolus</i> , <i>Blastocerus</i> , <i>Axis</i> , <i>Muntiacus</i> , <i>Rucervus</i>
NH0224	BMNH	1967.1362.Maz.chu_5OR	7	1294	
NH0477	BMNH	1967.1362.Maz.chu_56OF	13	1293	<i>Mazama</i> , <i>Odocoileus</i>
NH0241	BMNH	1967.1362.Maz.chu_7OF	7	1297	<i>Mazama</i>
NH0242	BMNH	1967.1362.Maz.chu_7OR	7	1298	
NH0249	BMNH	1967.1362.Maz.chu_8OF	7	1299	<i>Mazama</i> , <i>Hippocamelus</i> , <i>Alces</i> , Bovidae
NH0250	BMNH	1967.1362.Maz.chu_8OR	7	1300	
NH0193	BMNH	1913.4.24.3.Maz_bri_1PF	7	1285	<i>Mazama</i> , <i>Pudu</i>
NH0194	BMNH	1913.4.24.3.Maz_bri_1PR	7	1286	
NH0279	BMNH	1913.4.24.3.Maz_bri_1PF	7	1285	<i>Mazama</i> , <i>Pudu</i> , <i>Capreolus</i> , Cervidae
NH0280	BMNH	1913.4.24.3.Maz_bri_1PR	7	1286	
NH0205	BMNH	1913.4.24.3.Maz_bri_2PF	7	1287	<i>Pudu</i> , <i>Mazama</i> , <i>Capreolus</i> , <i>Rangifer</i> , Cervidae
NH0206	BMNH	1913.4.24.3.Maz_bri_2PR	7	1288	
NH0323	BMNH	1913.4.24.3.Maz_bri_3PF	8	1289	<i>Mazama</i> , <i>Cervus</i>
NH0324	BMNH	1913.4.24.3.Maz_bri_3PR	8	1290	
NH0219	BMNH	1913.4.24.3.Maz_bri_4PF	7	1291	<i>Mazama</i> , <i>Pudu</i> , <i>Hippocamelus</i> , <i>Cervus</i> , <i>Megaloceros</i>
NH0220	BMNH	1913.4.24.3.Maz_bri_4PR	7	1292	
NH0225	BMNH	1913.4.24.3.Maz_bri_5PF	7	1293	<i>Mazama</i> , <i>Pudu</i> , <i>Odocoileus</i> , <i>Rusa</i>
NH0226	BMNH	1913.4.24.3.Maz_bri_5PR	7	1294	
NH0479	BMNH	1913.4.24.3.Maz_bri_56PF	13	1293	<i>Mazama</i> , <i>Pudu</i> , <i>Ozotoceros</i> , <i>Odocoileus</i>
NH0480	BMNH	1913.4.24.3.Maz_bri_56PR	13	1296	
NH0525	BMNH	1913.4.24.3.Maz_bri_6PF	14	1295	<i>Mazama</i> , <i>Pudu</i> , <i>Hippocamelus</i> , <i>Ozotoceros</i> , <i>Odocoileus</i>
NH0526	BMNH	1913.4.24.3.Maz_bri_6PR	14	1296	
NH0243	BMNH	1913.4.24.3.Maz_bri_7PF	7	1297	<i>Mazama</i> , <i>Pudu</i>
NH0244	BMNH	1913.4.24.3.Maz_bri_7PR	7	1298	
NH0417	BMNH	1913.4.24.3.Maz_bri_8PF	11	1299	<i>Mazama</i> , <i>Hippocamelus</i> , <i>Alces</i>
NH0418	BMNH	1913.4.24.3.Maz_bri_8PR	11	1300	

Table H.1: Continued

NH0195	BMNH	1908.6.24.5_Maz_bri.1QF	7	1285	<i>Capreolus</i>
NH0196	BMNH	1908.6.24.5_Maz_bri.1QR	7	1286	
NH0281	BMNH	1908.6.24.5_Maz_bri.1QF	7	1285	<i>Capreolus</i>
NH0282	BMNH	1908.6.24.5_Maz_bri.1QR	7	1286	
NH0565	BMNH	1908.6.24.5_Maz_bri.2QF	16	1287	<i>Pudu, Mazama, Hippocamelus, Alces, Rucervus</i>
NH0566	BMNH	1908.6.24.5_Maz_bri.2QR	16	1288	<i>Blastocerus, Hippocamelus, Rucervus</i>
NH0583	BMNH	1908.6.24.5_Maz_bri.2QF	17	1287	<i>Mazama, Pudu, Elaphurus, Budorcas</i> (bovid)
NH0584	BMNH	1908.6.24.5_Maz_bri.2QR	17	1288	
NH0351	BMNH	1908.6.24.5_Maz_bri.4QF	8	1291	<i>Mazama, Pudu, Hippocamelus, Cervus</i>
NH0352	BMNH	1908.6.24.5_Maz_bri.4QR	8	1292	
NH0227	BMNH	1908.6.24.5_Maz_bri.5QF	7	1293	<i>Mazama, Odocoileus, Pudu</i>
NH0265	BMNH	1908.6.24.5_Maz_bri.5QF	7	1293	<i>Mazama, Odocoileus, Pudu</i>
NH0266	BMNH	1908.6.24.5_Maz_bri.5QR	7	1294	
NH0419	BMNH	1908.6.24.5_Maz_bri.8QF	11	1299	<i>Mazama, Bubalus</i> (bovid)
NH0420	BMNH	1908.6.24.5_Maz_bri.8QR	11	1300	
NH0197	BMNH	1934.9.10.228_Maz_bri.1RF	7	1285	<i>Pudu, Mazama, Cervidae</i>
NH0198	BMNH	1934.9.10.228_Maz_bri.1RR	7	1286	
NH0283	BMNH	1934.9.10.228_Maz_bri.1RF	7	1285	<i>Pudu, Mazama, Capreolus, Cervus</i>
NH0284	BMNH	1934.9.10.228_Maz_bri.1RR	7	1286	
NH0209	BMNH	1934.9.10.228_Maz_bri.2RF	7	1287	<i>Mazama, Pudu, Cervidae</i>
NH0210	BMNH	1934.9.10.228_Maz_bri.2RR	7	1288	
NH0327	BMNH	1934.9.10.228_Maz_bri.3RF	8	1289	<i>Mazama, Pudu, Cervidae</i>
NH0328	BMNH	1934.9.10.228_Maz_bri.3RR	8	1290	
NH0221	BMNH	1934.9.10.228_Maz_bri.4RF	7	1291	<i>Mazama, Pudu, Hippocamelus, Odocoileus, Axis</i>
NH0222	BMNH	1934.9.10.228_Maz_bri.4RR	7	1292	
NH0229	BMNH	1934.9.10.228_Maz_bri.5RF	7	1293	<i>Mazama, Pudu, Odocoileus</i>
NH0230	BMNH	1934.9.10.228_Maz_bri.5RR	7	1294	
NH0481	BMNH	1934.9.10.228_Maz_bri.56RF	13	1293	<i>Mazama, Pudu, Odocoileus, Ozotoceros</i>
NH0482	BMNH	1934.9.10.228_Maz_bri.56RR	13	1296	
NH0529	BMNH	1934.9.10.228_Maz_bri.6RF	14	1295	<i>Pudu, Mazama, Ozotoceros, Odocoileus, Megaloceros</i>
NH0530	BMNH	1934.9.10.228_Maz_bri.6RR	14	1296	
NH0245	BMNH	1934.9.10.228_Maz_bri.7RF	7	1297	<i>Mazama, Pudu, Cervus, Muntiacus</i>
NH0246	BMNH	1934.9.10.228_Maz_bri.7RR	7	1298	
NH0543	BMNH	1934.9.10.228_Maz_bri.7RF	14	1297	<i>Mazama, Pudu</i>
NH0544	BMNH	1934.9.10.228_Maz_bri.7RR	14	1298	
NH0485	BMNH	1934.9.10.228_Maz_bri.78RF	13	1297	<i>Axis, Megaloceros, Rucervus, Muntiacus, Bovidae</i>
NH0486	BMNH	1934.9.10.228_Maz_bri.78RR	13	1300	
NH0253	BMNH	1934.9.10.228_Maz_bri.8RF	7	1299	<i>Mazama, Odocoileus, Pudu, Elaphodus</i>
NH0254	BMNH	1934.9.10.228_Maz_bri.8RR	7	1300	
NH0421	BMNH	1934.9.10.228_Maz_bri.8RF	11	1299	<i>Mazama, Hippocamelus</i>
NH0422	BMNH	1934.9.10.228_Maz_bri.8RR	11	1300	
NH0199	BMNH	1971.3088_Mun_ath.1SF	7	1285	<i>Muntiacus</i>
NH0200	BMNH	1971.3088_Mun_ath.1SR	7	1286	
NH0285	BMNH	1971.3088_Mun_ath.1SF	7	1285	<i>Muntiacus, Mazama, Capreolus</i>
NH0286	BMNH	1971.3088_Mun_ath.1SR	7	1286	
NH0451	BMNH	1971.3088_Mun_ath.23SF	12	1287	<i>Muntiacus</i>
NH0452	BMNH	1971.3088_Mun_ath.23SR	12	1290	
NH0215	BMNH	1971.3088_Mun_ath.3SF	7	1289	<i>Muntiacus</i>
NH0216	BMNH	1971.3088_Mun_ath.3SR	7	1290	
NH0354	BMNH	1971.3088_Mun_ath.4SR	8	1292	<i>Muntiacus, Cervus</i>
NH0507	BMNH	1971.3088_Mun_ath.4SF	14	1291	<i>Muntiacus</i>
NH0508	BMNH	1971.3088_Mun_ath.4SR	14	1292	
NH0473	BMNH	1971.3088_Mun_ath.45SF	12	1291	<i>Muntiacus, Cervus, Rusa</i>
NH0577	BMNH	1971.3088_Mun_ath.6SF	16	1295	<i>Cervus</i>
NH0604	BMNH	1971.3088_Mun_ath.67SR	19	1298	<i>Muntiacus, Hydropotes, Axis</i>
NH0247	BMNH	1971.3088_Mun_ath.7SF	7	1297	<i>Muntiacus, Cervidae</i>
NH0248	BMNH	1971.3088_Mun_ath.7SR	7	1298	
NH0255	BMNH	1971.3088_Mun_ath.8SF	7	1299	<i>Muntiacus</i>
NH0256	BMNH	1971.3088_Mun_ath.8SR	7	1300	

I Molecular Data of Chapter 5

Table I.1: Statistical data for all molecular markers

Gene	Abbr.	Total Length	Excluded Length	Final Lengthing	Cod-#	in- up	out- up	Identical gro- sites*	Pair- wise Ident- ity	Un- gapped lengths [†]	GC	A	C	G	T	Other	Gaps [-]
kappa-casein	Csn	714	1-349	369	Y	20	13	7	263 (71.3%)	93.4% ±90.4; 156; 369	2,864 (45.9%)	1,908 (30.6%)	1,837 (29.4%)	1,027 (16.5%)	1,466 (23.5%)	Y:1	0 (0.0%)
alpha-lactalbumin	Lalba	525	1-16, 227-235, 389-404, 505-525	465	N	25	19	6	282 (60.6%)	93.1% ±38.5; 269; 464	4,528 (40.2%)	2,813 (25.4%)	2,271 (20.5%)	2,257 (20.4%)	3,722 (33.6%)	Y:1	195 (1.7%)
protein kinase C iota	Prkci	578	1-28, 169-183, 292-306, 570-578	513	N	29	23	6	348 (67.8%)	95.8% ±19.6; 415; 509	4,014 (27.4%)	4,829 (33.4%)	1,677 (11.6%)	2,337 (16.2%)	5,596 (38.7%)	Y:4; W:3; R:2	189 (1.3%)
prion protein	Prnp	863	1-37, 254-277, 351-353, 831-863	768	Y	21	15	6	631 (82.2%)	97.2% ±97.3; 315; 768	8,556 (54.9%)	3,939 (25.3%)	3,868 (24.8%)	4,688 (30.1%)	3,073 (19.7%)	Y:11; W:2; S:1; R:6; M:1	0 (0.0%)
sex determining region on y-chromosome	Sry	690	-	690	Y	70	66	4	510 (73.9%)	97.2% ±90.7; 146; 690	20,849 (47.3%)	14,032 (31.8%)	10,677 (24.2%)	10,172 (23.1%)	9,193 (20.9%)	-	18 (0.0%)
mitochondrial genome	mtG	14904	-	14904	Y	46	39	7	8,748 (58.8%)	88.9% ±2.2; 14861; 14878	259,297 (37.8%)	226,307 (33.1%)	167,043 (24.4%)	92,254 (13.5%)	198,332 (29.0%)	Y:9; S:2; R:5; N:1; M:2; K:2	1,627 (0.2%)
cytochrome b	Cytb	1140	-	1140	Y	130	124	6	583 (51.1%)	87.9% na	52,573 (35.5%)	41,340 (27.9%)	35,444 (23.9%)	17,129 (11.6%)	39,088 (26.4%)	Y:52; W:15; S:3; R:22; M:5; K:2; D:1	15,099 (10.2%)

Notes. *positions refer to final length sequence; [†]values are provided as [mean ±Stdv; min; max]; columns ‘GC’ to ‘T’ and ‘Gaps’: Frequency (%) of non-gaps